Nova Biomedical

Clinical Chemistry Research

Brian H. Mitchem
Charles L. Sharnham
Editors

NOVA

CLINICAL CHEMISTRY RESEARCH

CLINICAL CHEMISTRY RESEARCH

BRIAN H. MITCHEM
AND
CHARLES L. SHARNHAM
EDITORS

Nova Biomedical Books
New York

Library of Congress Cataloging-in-Publication Data

Clinical chemistry research / [edited by] Brian H. Mitchem and Charles L. Sharnham.
p. ; cm.
Includes bibliographical references and index.
ISBN 978-1-61209-884-5 (eBook)
1. Pharmaceutical chemistry. 2. Clinical chemistry. 3. Clinical biochemistry. I. Mitchem, Brian H. II. Sharnham, Charles L.
[DNLM: 1. Chemistry, Clinical--methods. QY 90 C64137 2009]
RS403.C65 2009
615'.19--dc22 2009000606

Published by Nova Science Publishers, Inc.✣New York

Contents

Preface

Among many research topics, this book considers phytoestrogens, natural compounds found in plants that possess estrogen-like activity. Despite the growing evidence of the health benefits of phytoestrogens, further investigation is needed to better understand their mechanism of actions, the biological outcomes and possible adverse effects. This book chapter summarizes the most recent developments of lanthanide nanorods in the field of biomedical nanotechnology. The cellular uptake of nanoparticles as a function of several parameters, such as polymeric material and surfactant type are considered. Camptothecins (CPTs) are regarded as one of the most promising anticancer drugs of the twenty-first century. A further chapter describes SAR, QSAR, and the clinical chemistry of CPT derivatives to understand their chemical–biological interactions and side effects. This book addresses the biological and pharmacological significances of identification and analysis of effective components of natural medicines and describes methods and procedures for identification and analysis. Potential future prospects in the field are provided. The porphyrazines are an emerging class of compounds exhibiting tremendous potential for use as anti-tumor therapeutic agents and in imaging applications. This book reviews the initial structure-function studies that have been carried out to date on this little-studied class of compounds. A further study hypothesizes that the differences in the biology of breast cancers observed in women of different races are partially related to differences in the secretory activity of adipocytes in the breast tissue. The possible role of adipokines in breast malignancies of women of various races is reviewed.

Chapter I - Phytoestrogens are natural compounds found in plants that possess estrogen-like activity. The major classes of phytoestrogens are isoflavones, lignans and coumestans. Isoflavones are structurally similar to mammalian estrogen and are found in large amounts in soybean and soy products. Lignans are found in flaxseed, whole grain cereals, teas and some vegetables, and coumestans are mainly present in clover and alfalfa sprouts. The major isoflavones are genistein, daidzein and glycitein. These compounds are hydrolysis products of glycosides in plants, termed genistin, daidzin and glycitin, which, after oral ingestion, are metabolized by intestinal flora. In lignans, the plant precursors are matairesinol and secoisolariciresinol, which are also metabolized by the intestinal microflora to enterolactone and enterodiol, respectively. Phytoestrogens have been largely used throughout the world and during various time periods, and it has been observed that the incidence of hormone-

dependent disease is reduced in countries, especially Asian countries, with a high dietary content of phytoestrogens. Animal models and clinical investigations have shown that phytoestrogens are protective in the prevention of hormone-dependent cancers—primarily breast and prostate cancers, cardiovascular disease and osteoporosis, and to alleviate the symptoms of menopause. The estrogenic effects of the phytoestrogens are mediated through the estrogen receptors ERα and ERβ, which function as ligand-inducible transcription factors for genes involved in cell growth, proliferation, and differentiation. Many mechanisms of action have been identified for phytoestrogen prevention of diseases, including estrogenic/antiestrogenic activity, antiproliferation, induction of cell cycle arrest and apoptosis, antioxidation activity, induction of detoxification enzymes, regulation of the host immune system, and changes in cell signaling. Despite the growing evidence of the health benefits of phytoestrogens, it is important to investigate further their mechanism of actions for a better understanding of the biological outcomes and possible adverse effects.

Chapter II - Camptothecins (CPTs) are regarded as one of the most promising anticancer drugs of the twenty-first century. The structure–activity relationships (SAR) provide insight into the mechanism of topo I inhibition and helped in the synthesis of various CPT analogues by modifying the different rings of the original CPT molecule, giving each analogue a unique property. These modifications have resulted in various improvements in the parent molecule, including changes in bioavailability, stabilization of the lactone ring, and/or a decrease in the substrate recognition by drug-resistant proteins as well as improvements in the toxicity profile in preclinical studies. The quantitative structure–activity relationships (QSAR) have suggested that the hydrophobic and steric descriptors of CPT analogues are the two most important determinants for their activity. Currently, two anticancer CPT derivatives, topotecan and irinotecan are in clinical use. These analogues have shown tremendous promise as solid tumor drugs and become a part of the multi-million dollar industry, but suffer from low tumor response rates and dose-limiting toxicity. At present, the extensive clinical trials are continuing to describe the better picture of clinical chemistry of topotecan, irinotecan, and some other new CPT derivatives (which are in various stages of clinical trials) to determine their optimal dose, route of administration, schedules, and the possibility in the combination with other chemotherapeutic agents. In this chapter, we describe SAR, QSAR, and the clinical chemistry of CPT derivatives to understand their chemical–biological interactions and side effects, which may provide strategies that might aid in the development of outstanding antitumor agents belonging to this family.

Chapter III - Lanthanides [especially Europium (Eu) and Terbium (Tb)] are not biometals, however lanthanide nanomaterials play an appreciable role in biology and medicine. Nanoparticles are at the leading edge of the rapidly developing field of nanomedicine and nanobiotechnology. Their unique size-dependent properties make these nanomaterials superior and indispensable in many biological and medicinal areas of human activity. Nanomedicine/nanobiotechnology is the medical/biological application of nanotechnology that will hopefully lead to useful research tools, advanced drug delivery systems, and new ways to detect and treat disease or repair damaged tissues and cells. In this particular chapter, we have discussed the most recent developments of lanthanide (especially europium & terbium) nanorods/nanoparticles in the field of fluorescent labeling and angiogenesis (the budding of capillaries that leads to the formation of new microvessels from

pre-existing vascular structures) in biology and medicine. Firstly, we have discussed the synthesis, characterization and application of these non-toxic inorganic lanthanide (europium and terbium) nanorods as a fluorescent label (a novel alternative to conventional organic dyes) in biomedical research due to their unique optical and electronic properties. It is important to point out that fluorescence labeling of molecules is a standard technique in biomedical application. Therefore, these lanthanide nanorods offer useful and alternative inorganic fluorescent probes for targeting various molecules in living cells. Secondly, we have demonstrated the pro-angiogenic properties of europium(III) hydroxide nanorods which could be used to develop new treatment strategies for cardiovascular ischemic and peripheral vascular diseases where the most important objective of angiogenesis is to induce or stimulate vessel growth in patients with conditions characterized by insufficient blood flow. In addition to that we have also discussed the diagnostic and therapeutic applications of lanthanide compounds. This book chapter tries to summarize the most recent developments of lanthanide (especially europium and terbium) nanorods in the field of biomedical nanotechnology, and discusses the current standing with respect to nanotechnology.

Chapter IV - Natural medicines play their biological and pharmacological roles after orally administered, based upon their effective substances including both the original components in the natural medicines absorbed and their metabolites. These effective substances can only be identified when chemical structures of these components and their metabolites are revealed, and corresponding pharmacological experiments have been carried out. Identification and analysis of the effective components following oral administration of natural medicines in animal biofluids are of great importance both to understand how these natural medicines exert their biological effects, and to improve methods for quality control in production of natural medicines. However, advances in the field have seldom been reviewed. Based on research experience of our group for dozens of years and corresponding literature, we will review on the identification and analysis of effective components following orally administration of natural medicines in animal biolfuids, mainly in blood and urine. First, we will address the biological and pharmacological significances of identification and analysis of effective components of natural medicines. Then, we will describe, in detail, the commonly used methods and procedures for identification and analysis of effective components of natural medicines. These methods and procedures include how to prepare natural medicines for oral administration, how to choose appropriate animals, how to administer natural medicines, how to collect blood and urine samples of animals, how to prepare samples for identification, and how to identify and analyse chemical structures of effective components. Finally, we wish to provide the potential future prospects in the field.

Chapter V - Current methods of prenatal diagnosis for chromosomal and single gene disorders involve invasive procedures such as amniocentesis, chorion villus sampling or fetal blood sampling to obtain fetal genetic material for cytogenetic and/or molecular analysis. These procedures involve a 1-4% risk of miscarriage that is unacceptable to some couples. Invasive prenatal diagnosis can cause a psychological burden on pregnant women. The anxiety about the invasive nature of the procedure and the attendant risk of fetal loss of a wanted pregnancy can cause emotional stress (Beeson and Golbus, 1979; Weinman and Johnston, 1988; Kowalcek, 2007). Missed diagnosis of handicapping congenital diseases occurs in at-risk women who reject invasive prenatal diagnosis due to the risk of fetal loss or

morbidity (Chitty, 1998). Noninvasive and accurate prenatal diagnosis that does not carry any risk of procedural-related fetal loss is therefore desirable to at-risk pregnant women. The presence of cell-free fetal DNA/RNA circulating in the maternal blood offers an alternative source of fetal genetic material for prenatal diagnosis. Fetal DNA is readily detected in maternal plasma and serum (Bianchi and Lo 2001; Lo and Poon 2003; Birch et al., 2005; Galbiati et al., 2005). The estimated 3-6% fetal DNA in maternal plasma (Lo et al., 1997) can be detected in as early as 5 gestational weeks (Rijnders et al., 2003). In theory, fetal DNA sequences that differ from maternal DNA sequences can be identified in maternal plasma, thus allowing noninvasive prenatal testing of paternally-inherited genetic diseases. However, enrichment and detection of fetal sequences is hindered by the high amounts of background maternal sequences. The detection of fetal DNA sequences is therefore, dependent on the sensitivity of the assay and the amount of fetal sequences. Using innovative strategies and state-of-the-art technologies, researchers had overcome many technical challenges by the development of many potential noninvasive tests with significant clinical applications.

Chapter VI - In recent years, polymeric nanoparticles have emerged as a powerful tool in bio-related fields. Their application in the diagnostics and drug delivery systems is a rapidly advancing research area. A detailed understanding of particle-cell interaction is essential and of immense interest in order to create a specific carrier for each particular application need. Changes in the structural and functional properties of the particle, namely chemical composition, surface charge and morphology, can significantly affect particle-cell interaction. In this chapter, we consider the cellular uptake of nanoparticles as a function of several parameters, such as polymeric material (polystyrene- or polyester-based), surfactant type (nonionic versus ionic), surface charge sign (cationic versus anionic), surface groups' density, and type of cell line. Furthermore, the influence of surface charge sign on the uptake mechanism of polystyrene particles was studied on the example of HeLa cells. The particle uptake efficiency was evaluated as a function of different factors (e.g. temperature, presence of drugs, etc.) known to inhibit the endocytosis.

Chapter VII - Cells of the monocyte/macrophage and lymphoid lineages express receptors for 1, 25-dihydroxy-vitamin D3 (calcitriol). While this vitamin has been shown to promote differentiation of monocyte precursors to monocytes/macrophages and formation of antimicrobial peptides by this cell population, it has been shown to inhibit effector function of both T-and B lymphocytes. This is related to a reduction of accumulation of mRNA for IL-1 alpha, tumor necrosis factor alpha, IL-2 and IFN gamma, interference with T helper cell function reducing induction of immunoglobulin production by B cells and promotion of T-suppressor cells. In HIV infection in vitro studies suggest promotion of HIV replication by calcitriol, while genetic linkage studies suggest an association of dysfunctional vitamin D receptor genotypes and progression of HIV related immunodeficiency. Immunological effects cannot explain the higher risk of active tuberculosis in patients with low serum vitamin D levels evident from a meta-analysis of observational studies and the higher risk may be related to the reduction in production of antimycobacterial peptides. Future studies need to explore the potential of vitamin D supplementation in treatment and prevention of mycobacterium tuberculosis infection and its impact on the course of HIV infection and on the immunological and related functional long-term impact of viral lower respiratory tract infections.

Chapter VIII - Animal models are required for studying the pathobiology of diseases as well as for the development and evaluation of therapeutic strategies. Specific mouse models for known genetic diseases are generated by reverse genetics strategies using genetic engineering techniques which result in defined alterations of the mouse genome. Standardized clinical chemical analysis contributes to the determination of the exact phenotype of the animal models. However, the resulting phenotypes of the mutant mice cannot be predicted and do not always mirror the respective human disease. A complementary strategy is to generate new alleles by random mutagenesis and to screen for clinically relevant phenotypes. The underlying mutations are then identified by forward genetics strategies and lead to the identification of genes/alleles which may have counterparts relevant for human diseases. Novel disease models were derived from phenotype-driven large-scale ethylnitrosourea (ENU) mouse mutagenesis projects which started a decade ago by using clinical chemical parameters in high-throughput screens. Offspring of chemically mutagenized mice were analyzed in order to detect phenotypic variants with defects of various organ systems or changes in metabolic pathways. Breeding of the affected mice and screening of the offspring confirmed the transmission of the altered phenotype to subsequent generations, thereby revealing a mutation as cause for the aberrant phenotype. The subsequent in-depth genotypic and phenotypic analysis of mutant lines showing alterations in clinical chemical parameters produced novel models for the biomedical research.

Chapter IX - Congenital diseases refer to the pathologic changes that ascribe to the solitude or cooperative factors of heredity, poison or drugs, infection and environment, before or at birth. The onset of congenital diseases can either be found immediately after birth, or in the growth process of children, or even after adult. There are several kinds of pathologic changes of congenital diseases: malformation, chromosomal abnormality and genic abnormality, etc. Gene therapy is a new technology developed in last two decades, and traditional gene therapy is to introduce exogenous DNA or RNA segments into target cells or tissues, or to retrieve and repair gene defects. In recent years, this technology, besides above-mentioned, has expanded to skipping or silencing virulence genes, enhancement of antivirulence genes, and regulation of cell functions by using cytokine genes, etc. Although still in a primitive stage, now gene therapy is widely used in the management of congenital diseases. In this article, we reviewed some representative preclinical and clinical gene therapies, in the aspects of gene targets, vectors, routes and opportunity of administration, as well as side-effects, to analyze the key points and research highlights in gene therapy of congenital diseases and prospect for possible approaches and potential applications in future.

Chapter X - The tetraazaporphyrins, or porphyrazines (pzs), are an emerging class of compounds exhibiting tremendous potential for use as anti-tumor therapeutic agents and in imaging applications. Pzs are related to the porphyrins, a class of compounds widely known for the clinically used photodynamic therapy agent Photofrin. Thus, like the porphyrins, it is anticipated that the pzs will be useful as anti-tumor agents. However, while similar in structure to the porphyrins, pzs are prepared via a different synthetic route—the macrocyclization of dinitrile derivatives—that results in greater synthetic flexibility, and they have improved optical properties compared to the porphyrins. The improved chemical and physical features of the pzs gives rise to differences in their biological behavior when compared to those of the porphyrins. Therefore, the initial work in this field has focused on

elucidating the structure-function relationships of the pzs. As these relationships become more clearly defined, future work will involve tailoring the structure of the pzs and/or the delivery mechanisms to more selectively target tumor cells. Herein we review the initial structure-function studies that have been carried out to date on this little-studied class of compounds and discuss possible methods for maximizing their promising biomedical potential.

Expert Commentary - Mass spectrometry (MS) can be viewed as the universal “balance” of the natural sciences. By measuring atomic and molecular weights it has become an essential tool for composition and structural analysis. In fact, the discovery of soft ionization techniques some 20 years ago has introduced MS to the biosciences and ultimately to clinic-associated facilities. Electrospray (ESI) and MALDI (matrix-assisted laser desorption) ionization leave biomolecules intact and allow their measurement up to very high masses. As the 2002 Nobel Price Winner John Fenn of Virginia Commonwealth University put it – elephants learned to fly. Nevertheless, MS had its place in the clinical laboratory before those discoveries with the long established coupling of gas chromatography (GC)-MS for the detection of small organic acids and metabolites. Especially for the “General-Unknown-Screening” in cases of intoxication the method has proven very useful. It is limited, however, to volatile compounds or such samples which can be derivatized to achieve that effect. The mass range of the instruments ends mostly well below 1000 Da. Therefore, liquid chromatography (LC)-MS couplings soon moved in to complement GC-MS for water-soluble and higher-molecular-weight compounds. Those two coupling techniques remain the only MS-based methods with some impact in the clinical laboratory so far. The new possibilities of investigating whole proteins or other macromolecules using MS technology have not yet found their way into clinical diagnostics. Attempts were made trying to apply SELDI (surface-enhanced laser desorption ionization) to comparative biomarker profiling of body liquids such as serum. To that end, biochips were covered with various chromatographic surfaces with the goal to simplify as well as standardize sample preparation. While some interesting reports can be found in the literature, reproducibility seems to be a major problem which has so far effectively prevented SELDI from becoming a diagnostic tool. Reasons may be the biochips themselves whose production is an art. In addition, the biological variation introduced by the study subjects is difficult to control. A blood sample, e.g., will vary depending on the time of day it is taken, the gender and age of the person, monthly or age-dependent hormone changes, or food and drink which was consumed on a regular basis or shortly before sampling. Therefore, only drastic reproducible biological effects can be monitored in diagnostics and even then, some diagnostic markers are not very reliable as, e.g., PSA for prostate cancer. A third reason for the difficulties SELDI was experiencing was ion suppression during ionization. The effect molecules have on each other hunting for protons in the ion cloud depends on the respective make-up of the analyte and surrounding solvent system and is difficult to control. In case of large concentration differences – one major component in a bulk of minor components - this is hardly an issue for the main analyte. Minor components, however, may be effectively suppressed and become invisible in the spectrum.

Short Communication A - The Mass Spectra (MS) of blood human proteome can be of great help in detecting diseases. In Prostate Cancer (PCa), prognostic (predictive) factors are

particularly important given the marked heterogeneity of this disease at clinical, morphologic and biomolecular levels. Blood contains a treasure of previously unstudied biomarkers that could reflect the ongoing physiological state of all tissue. The serum Prostate-Specific Antigen (PSA) measurement is a very good biomarker for PCa, but the Sensitivity is somewhat low (above 62%). In this paper we propose a general strategy, based on Computational Chemistry techniques, which should improve the predictive power of PSA. Our group adapted the Shining Star graph to represent human serum-plasma-proteome MS for healthy and PCa patients. In this work we calculated different Spectral Moments of the Markov Matrix associated to the Star graph for a sample of patients. These indices are similar to other graph parameters such as Topological Indices (TIs) or Connectivity Indices (CIs). We used these indices to create Quantitative Proteome-Disease Relationships QPDRs models in analogy to QSAR models of small drugs. The best QPDRs found model showed a sensitivity value of 89.9%. This methodology might be useful in several Bioinformatics applications based on Translational Medicine.

Short Communication B - Breast cancer is one of the most frequent malignancies in women and ranks second only to lung carcinoma among cancer deaths in adult female patients. Breast cancer is a heterogenous disease that encompasses a number of pathological entities with distinct clinical behavior. Racial differences in the biology and treatment of breast cancer are also well documented. A positive correlation between obesity and breast cancer has been established. Indeed, deregulated adipokine production from fat cells represents an important molecular basis underlying obesity-related carcinogenesis. Thus, the growth and progression of breast tumor cells is dependent both on their intrinsic malignant potential and the microenvironment they interact with.

The circulating concentrations of adiponectin, an insulin-sensitizing adipokine, correlate inversely with breast cancer development since adiponectin could potently inhibit the proliferation of both estrogen receptor-positive and estrogen receptor-negative human breast carcinoma cells.

We hypothesize that the differences in the biology of breast cancers observed in women of different races are at least partially related to differences in the secretory activity of adipocytes in the breast tissue. We review the possible role of adipokines in breast malignancies of women of various races. It is hoped that these biomarkers could identify those women who are at increased risk for developing aggressive breast carcinomas and thus may benefit from increased surveillance and/or prophylactic intervention.

Short Communication C - In primates, including man, purine catabolism terminates with the formation of uric acid. This is due to a lack of uricase, which catalyzes the conversion of uric acid into allantoin in most other mammals. A nonsense mutation during evolution inactivated uricase activity in humans, resulting in enhanced protection against reactive oxygen species. The loss of uric acid degradation in purine catabolism is believed to compensate for the inability of humans to synthesize vitamin C, which is a powerful antioxidant. Blood in humans contains a very low concentration of allantoin produced from the elimination of reactive oxygen species by uric acid. Therefore, the measurement of serum allantoin is a good marker for judging the degree of reactive oxygen species generation in the body. In recent years, serum allantoin has been extensively used as a marker of oxidative stress. Serum allantoin levels are reportedly increased in Down syndrome, Behçet's

syndrome, Wilson disease, neonatal chronic lung disease, chronic rheumatoid arthritis, and patients undergoing hemodialysis. In this review, we will describe the analytical methods of serum allantoin measurement and their clinical significance.

Short Communication D - Background: Patients with markedly elevated serum creatine kinase (CK) activity due to muscle damage often also have increased serum aminotransferase activity (AST, ALT). However, the expected ratio of serum CK to aminotransferase activity in patients with severe muscle damage is uncertain.

Methods: We evaluated consecutive patients seen during a 6-month period who had markedly increased serum CK activity (≥ 1,000 U/L). Only patients with simultaneous measurements of CK, ALT and AST activity were included. One hundred eight patients ages of 17 to 93 years met these inclusion criteria. Their records were reviewed to ascertain the cause of the elevated CK activity.

Results: Eighty five of the study patients had rhabdomyolysis from a variety of causes to explain their marked CK elevation, while 23 had myocardial necrosis, usually from acute myocardial infarction. The median ratio of serum CK to AST activity in these 108 high-CK patients was 25:1 (interquartile range, 13 to 37:1). The median ratio of serum CK to ALT activity was 41:1 (interquartile range, 24 to 80:1). Patients with high CK activity due to rhabdomyolysis or myocardial necrosis had similar CK/AST and CK/ALT ratios.

Conclusions: In patients with a serum CK activity above 1,000 U/L, the serum CK activity should be expected to be approximately 25 times the AST activity and to be 40 times the ALT activity. These ratios can serve as guidelines when assessing high-CK patients who also have elevated serum aminotransferase activity.

In: Clinical Chemistry Research ISBN 978-1-60692-517-1
Editors: Brian H. Mitchem and Charles L. Sharnham

Chapter I

Phytoestrogens: Biochemical Aspects and Biological Activities

Rita de Cássia da Silveira e Sá[1] and Luciana Valente Borges[2]
[1]Reproduction Biology Center/Biology Department,
Federal University of Juiz de Fora, Juiz de Fora, MG, Brazil
[2]Reproduction Biology Center, Federal University of Juiz de Fora,
Juiz de Fora, MG, Brazil

Abstract

Phytoestrogens are natural compounds found in plants that possess estrogen-like activity. The major classes of phytoestrogens are isoflavones, lignans and coumestans. Isoflavones are structurally similar to mammalian estrogen and are found in large amounts in soybean and soy products. Lignans are found in flaxseed, whole grain cereals, teas and some vegetables, and coumestans are mainly present in clover and alfalfa sprouts. The major isoflavones are genistein, daidzein and glycitein. These compounds are hydrolysis products of glycosides in plants, termed genistin, daidzin and glycitin, which, after oral ingestion, are metabolized by intestinal flora. In lignans, the plant precursors are matairesinol and secoisolariciresinol, which are also metabolized by the intestinal microflora to enterolactone and enterodiol, respectively. Phytoestrogens have been largely used throughout the world and during various time periods, and it has been observed that the incidence of hormone-dependent disease is reduced in countries, especially Asian countries, with a high dietary content of phytoestrogens. Animal models and clinical investigations have shown that phytoestrogens are protective in the prevention of hormone-dependent cancers—primarily breast and prostate cancers, cardiovascular disease and osteoporosis, and to alleviate the symptoms of menopause. The estrogenic effects of the phytoestrogens are mediated through the estrogen receptors ERα and ERβ, which function as ligand-inducible transcription factors for genes involved in cell growth, proliferation, and differentiation. Many mechanisms of action have been identified for phytoestrogen prevention of diseases, including estrogenic/antiestrogenic activity, antiproliferation, induction of cell cycle arrest and

apoptosis, antioxidation activity, induction of detoxification enzymes, regulation of the host immune system, and changes in cell signaling. Despite the growing evidence of the health benefits of phytoestrogens, it is important to investigate further their mechanism of actions for a better understanding of the biological outcomes and possible adverse effects.

Introduction

Numerous epidemiological studies have shown possible associations between diet and many common diseases. It is now generally accepted that many of these diseases, more prevalently found in Western cultures, are diet related [1] and could be avoided with a thorough dietary intervention. Populations and case-control studies have provided a large body of information that correlates diets low in fat and rich in complex carbohydrates from vegetables, fruits and grains to a decreased risk of chronic diseases [1,2,3,4,]. In addition to the essential nutrients, the human diet contains naturally-occurring plant-derived bioactive constituents known as phytochemicals. Among these biologically active substances are carotenoids, sulphides, coumarins, terpens, saponins, glucosinolates, flavonoids, protease inhibitors, phenolic acids and plant sterols which, if consumed either naturally as an integral part of the food or as a food supplement, may provide long-term health benefits, such as prevention of degenerative diseases [1,5].

One class of phytochemicals, named phytoestrogens, comprises a group of natural compounds found in plants (e.g., vegetables, legumes, fruits, whole grains, and, especially, soy food products) to varying degrees. Phytoestrogens are classically defined as non-steroidal polyphenolic compounds that have chemical and structural properties similary to that of estrogens [5,6,7,8]. Hundreds of molecules fall under this classification and they can be divided into two main groups: the flavonoids, which are further subdivided into isoflavones, coumestans and prenyl flavonoids; and non-flavonoids, comprising the lignans and stillbenes [9] (Figure 1).

The three main classes of phytoestrogens of clinical interest are isoflavones (derived mainly from soy beans and clover), lignans (found in flaxseed in large quantities) and coumestans (derived from sprouting plants like alfalfa) [10]. Of these classes, isoflavones play a major role in human consumption, being found in a variety of foodstuffs, and because of the use of nutritional supplements rich in soy. A fourth class of compounds, referred to as resorcylic acid lactones, are better classified as myco-estrogens, which are estrogenic fungal products that are not plant-derived but are found in pasture grasses and legumes infected by the fungal genus *Fusarium* [11,12].

Investigations developed in animal models and clinical trials have shown that phytoestrogens can function as protective agents against age-related diseases (cardiovascular and osteoporosis) and hormone-dependent cancers (e.g., breast and prostate cancers). They also alleviate the symptoms of menopause, such as hot flushes [5,6,7,8,13,14,15,1,6]. The cancer chemopreventive effects of phytoestrogens are apparently related to several possible mechanisms, including their ability to inhibit growth factors, DNA topoisomerase, steroidogenic, and enzymes tyrosine kinase(s), which inhibits cell growth due to non-

phosphorylation of proteins required for cell division. Other mechanisms are related to their ability to act as antioxidant and antiangiogenic agents [5,17].

Phytoestrogens bind to estrogen receptors and within each class of compounds, they affect the estrogen-mediated response in different ways. For instance, they may act as estrogen agonists at some tissue-specific targets, whereas in others, they may act as antagonistic agents [16,18,19].

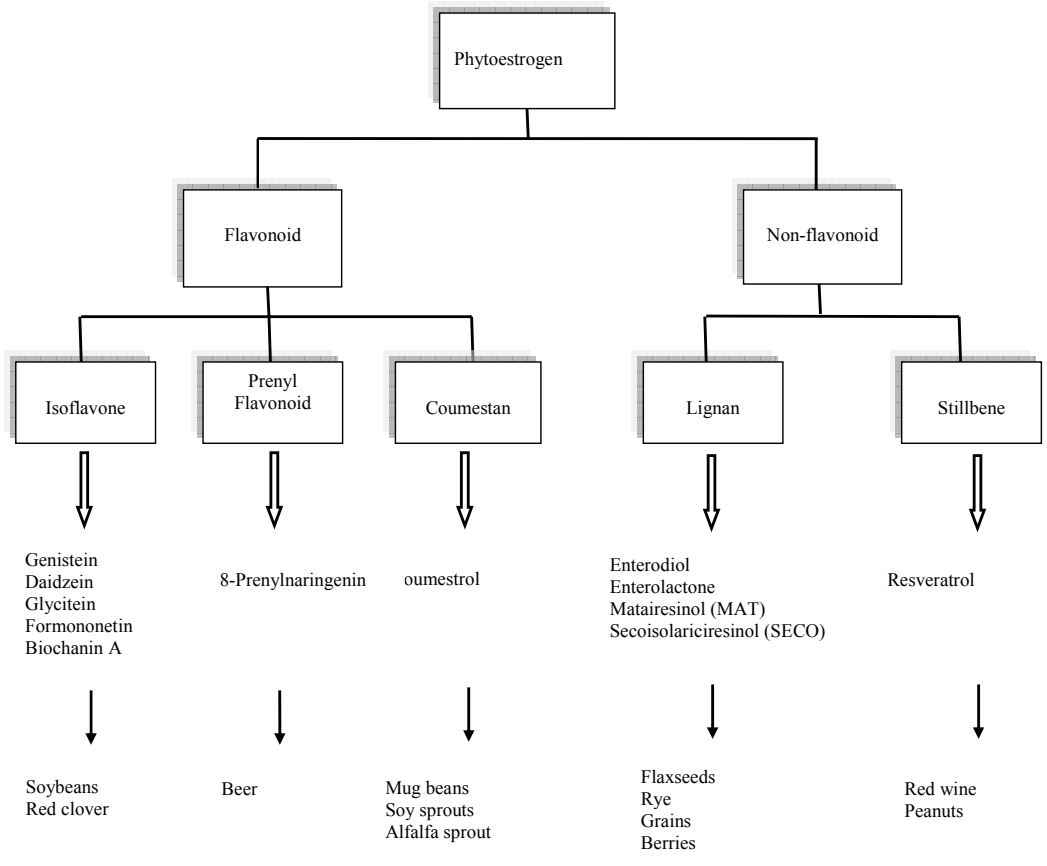

Figure 1. Schematic presentation of the different classes of phytoestrogens. (Based on references 9 and 18.)

Signal Transduction by Estrogens

General Aspects

Estrogens are hydrophobic steroid hormones produced in the ovaries and testis that are involved in the development, differentiation, growth, normal functioning, and malignancies of the organs and tissues of the mammalian reproductive systems, such as the mammary gland, ovary, uterus, vagina, testis, epididymis, and prostate [20,21,22]. In addition to these effects, they exert many biological effects in the body beyond the reproductive system, including the cardiovascular system, where estrogens have certain cardioprotective effects,

bone maintenance and brain [23,24]. Estrogen action in the brain affects the activity and connectivity of certain neuronal cells and, consequently, may interfere with important physiological parameters that regulate animal reproduction, including mood and behavior, gonadotropin production and release from the pituitary, and locomotor activity [25]. It is also believed that estrogens may interfere with nonreproductive events in the brain, such as learning and memory [26,27]. In rodents, they are negative regulators of lymphopoiesis, causing transient involution of the thymus during pregnancy and atrophy during estrogen treatment [28]. They are also responsible for promoting the development of certain types of breast cancer and the understanding of the relationship between estrogen dependency and breast tumors is the key for therapeutic intervention with antiestrogens such as tamoxifen [26] and plant-derived compounds such as phytoestrogens [19].

In the hypothalamic-anterior pituitary-gonad axis (Figure 2), the release of the gonadotropin-releasing hormone (GnRH) by the hypothalamus triggers the secretion of the follicle-stimulating hormone (FSH) and luteinizing hormone (LH) in the anterior pituitary to stimulate the granulosa cells in the ovaries to produce estrogen and progesterone. In the testis, FSH and LH stimulate the Sertoli cells or Leydig cells to produce androgen binding protein (ABP) and testosterone, respectively [29]. Following their synthesis and release, estrogens bind primarily to sex hormone-binding globulin (SHBG) in the plasma and, secondarily, to plasma albumin. Owing to their hydrophobic nature, estrogens cross the plasma membrane of the target cells by simple diffusion; however, before doing so, they first dissociate from the plasma-bound proteins. Once inside the cells, estrogens bind with high affinity and specificity to an intranuclear binding protein, termed estrogen receptor, which functions as ligand-inducible transcription factors for genes involved in cell growth, proliferation and differentiation [30,31,32]. The estrogen-receptor interaction results in conformational changes, enabling the estrogen-receptor complex to bind to specific transcriptional enhancer DNA sequences, also known as estrogen-responsive elements (ERE) [32,33,34]. The dominant form of estrogen in the body is 17β estradiol, however, any compound capable of inducing receptor dimerization and subsequent binding to ERE, can be considered an estrogen [35].

The activation process of the estrogen-receptor complex involves the dislocation of heat shock proteins, such as hsp 90, which were blocking the DNA binding site on the receptor [32,34]. Following activation, the estrogen-receptor complex dimer binds to the ERE in the regulating region of the target gene promoters resulting in activation of specific genes, transcription, accumulation of mature mRNAs, and their subsequent translocation into the cytoplasm. In the cytoplasm, mRNAs are translated on the ribosomes and, as a consequence, several specific proteins are synthesized producing various metabolic and physiologic functions [32,33,34] (Figure 3).

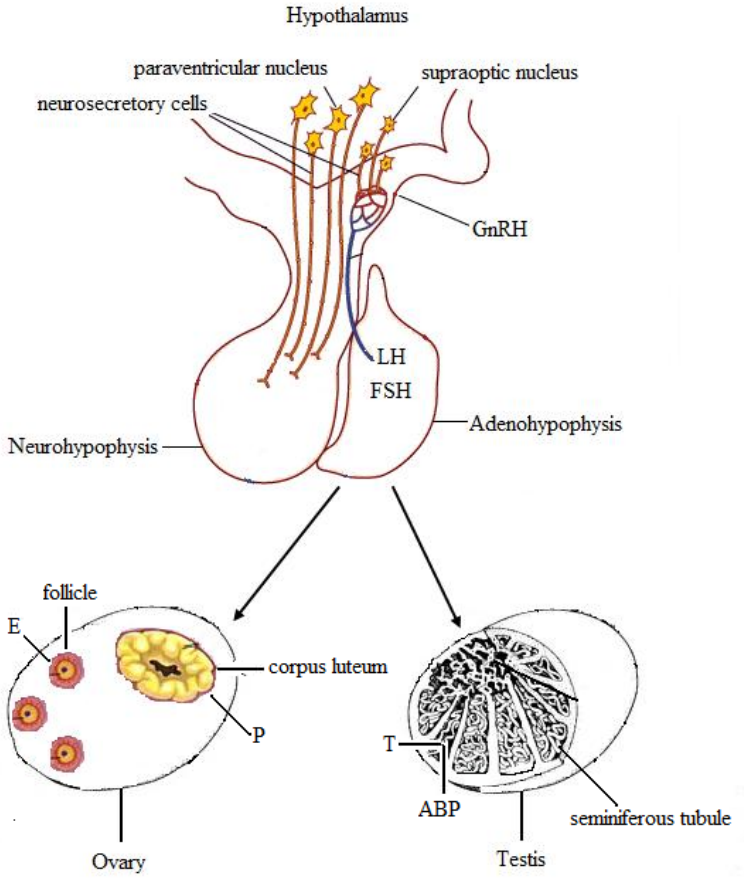

Figure 2. Schematic presentation of the hypothalamus-pituitary-gonads axis. GnRH is released by the hypothalamus to stimulate the adenohypophysis (= anterior hypophysis) to secrete FSH and LH. These hormones stimulate the granulosa cells in the ovaries and the Sertoli cells or Leydig cells in the testis to produce the sex steroid hormones. GnRH = gonadrotopin-releasing hormone; FSH = follicle-stimulating hormone; LH = luteinizing hormone; ABP = androgen binding protein; E = estrogen; P = progesterone; T = testosterone.

The receptor numbers vary greatly in different cell types. For example, reproductive tissues have approximately 100–1000 fold greater numbers than bone cells and most of other cells in the body [36]. A small percentage (2–3%) of estrogen receptor are found on the cell membrane [37,38], representing an alternative nongenomic pathway. This pathway has been proposed as an explanation for the fast effects of estrogen in the brain and in the reproductive system [26,39,40,41].

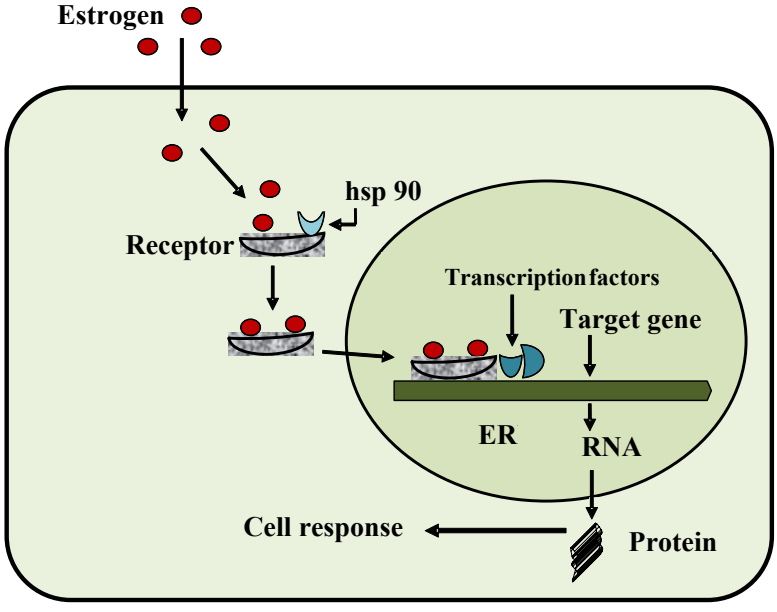

Figure 3. Scheme of a model of estrogen receptor action. Estrogens cross cell membrane by simple or facilitated diffusion and bind to specific receptors. The estrogen receptor is, in fact, a transcription factor that can be found either in the cytoplasm or the nucleus in an inactive state due to blockage by heat shock proteins (e.g., hsp 90). Upon hsp 90 exits and estrogen binding, the estrogen receptor undergoes activation which enables its effective binding to the estrogen responsive element (ER) in target gene promoters and activation of transcription of that gene. (Based on reference 24.)

Receptor Structure and Function

The estrogen receptor (ER) is a member of the steroid hormone receptor superfamily of genes which also includes receptors for progestins, glucocorticoids, mineralocorticoids, and androgens [42]. Steroid hormone receptors can be subdivided into several functional domains: 1. a highly variable N-terminal domain (A/B region) that contains a transactivation domain, which interacts with components of the core transcriptional complex; 2. a highly conserved central domain, with a C-region that contains two type II zinc clusters and is responsible for showing specific DNA binding and receptor dimerization [43]; 3. a C-terminal domain (E/F region) which is a functionally complex domain involved in ligand binding and receptor dimerization, nuclear localization, and interactions with transcriptional coactivators and corepressors [44,45].

There are two known estrogen receptor, ERα and ERβ [35]. Although these receptors can be localized within the same cell, they vary in tissue distributions and many have different effects on mixed agonists and antagonists [46]. Upon binding to the receptor, some compounds act as estrogen agonists or antagonists and are referred to as selective estrogen modulators (SERMs) [46]. For example, the antiestrogen tamoxifen is an estrogen antagonist in breast tissue but act as an agonist in the uterus, bone and vascular system [47]. When a compound binds to the receptor in a target cell and antagonistic effects are produced, it is

either because dimerization failed to occur or the correct configuration to activate ERE was not attained [35].

The physiological effects of estrogens are mediated predominantly by ERα [48], whereas ERβ may counteract ERα action [49]. However, even though ERβ has lower binding affinity for and activation by endogenous estrogens, some xenoestrogens preferentially bind and activate ERβ [50]. The presence of ERs has been identified in numerous normal and pathological tissues. Both ERα and ERβ are active in normal ovarian follicular development, vascular endothelia cells, myocardial cells, smooth muscle, and breast tissue [46]. ERα acts in bone maturation in males and females, but only ERβ is involved in bone maintenance in females [46]. ERα is more functional in maintaining follicle-stimulating hormone (FSH) and lutenizing hormone (LH) concentrations in blood, whereas ERβ is more active in frontal lobe mediated learning and memory [46]. The ERβ expression was detected in various brain regions (hypothalamus, cerebellum, olfactory lobe, brain stem) and the spinal cord, as well as in the prostate, testis, epididymis, bladder, uterus, lung and pituitary [25].

Gonadal hormones have an important effect on bone maintenance. Ovariectomized adult rats and monkeys showed a decrease in bone ash weight and bone mineral density. In the menopause, estrogen deficiency is the cause of the most rapid phase of bone loss in women. In both cases, the use of exogenous estrogens can prevent these bone changes from happening and can prevent the fractures associated with low bone mass [51]. In men, associations between plasma estrogen levels and bone mineral density have been observed, suggesting that estrogen is involved in maintaining male skeleton as well. Bone loss and fractures associated with low bone mass also occur in men, although at a lower rate than observed in women [51]. The expression of ERα and ERβ has been detected in osteoblastic cells. It was revealed that osteoblastic cells isolated from the bone of neonatal rats expressed a much higher level ERβ mRNA than that of ERα mRNA [52].

Chemically diverse compounds, for instance, estrogens, some androgens, antiestrogens, and xenoestrogens, have estrogenizing activity and interact with the ER. Phytoestrogens also bind to the estrogen receptors; however, the different classes of phytoestrogens show distinct affinity to ERα and ERβ. This differential affinity is probably functionally related to differences in tissue distribution of these two receptor sub-types and possibly to differences in biological activity [50]. Phytoestrogens compete with estrogen for receptor binding at nanomolar (10^{-9} M) concentrations and in higher macromolar (10^{-6} M) concentrations. Depending on the affinity of the phytoestrogen molecule for the estrogen receptor, the binding of a phytoestrogen to the receptor may result in partial activation of the receptor (weak agonistic effect) or the displacement of an estrogen molecule, which may reduce receptor activation (antagonistic or anti-estrogenic effect).

Phytoestrogens: Biology, Structure, Distribution and Metabolism

The phytoestrogens are naturally-occurring compounds with a chemical structure possessing a phenolic ring similar to that of estradiol and two hydroxyl groups at positions that allow the correct distance between them to facilitate binding to the estrogen receptor.

Because they can act as estrogen agonists or antagonists, phytoestrogens also act like natural SERMs at various tissues throughout the body [50,53,54]. Their ability to behave like estrogen mimics at some tissue-specific targets apparently plays an important part in their health-promoting effects, whereas, in other target tissues, the antagonistic characteristics displayed is comparable to that of tamoxifen or raloxifene, suggesting that SERM activity is sex hormone and gender dependent [55]. Phytoestrogen actions at the cellular and molecular level are influenced by many factors, such as concentration dependency, receptor status, presence or absence of endogenous estrogens, and the type of target organ or cell [1] (Figure 4).

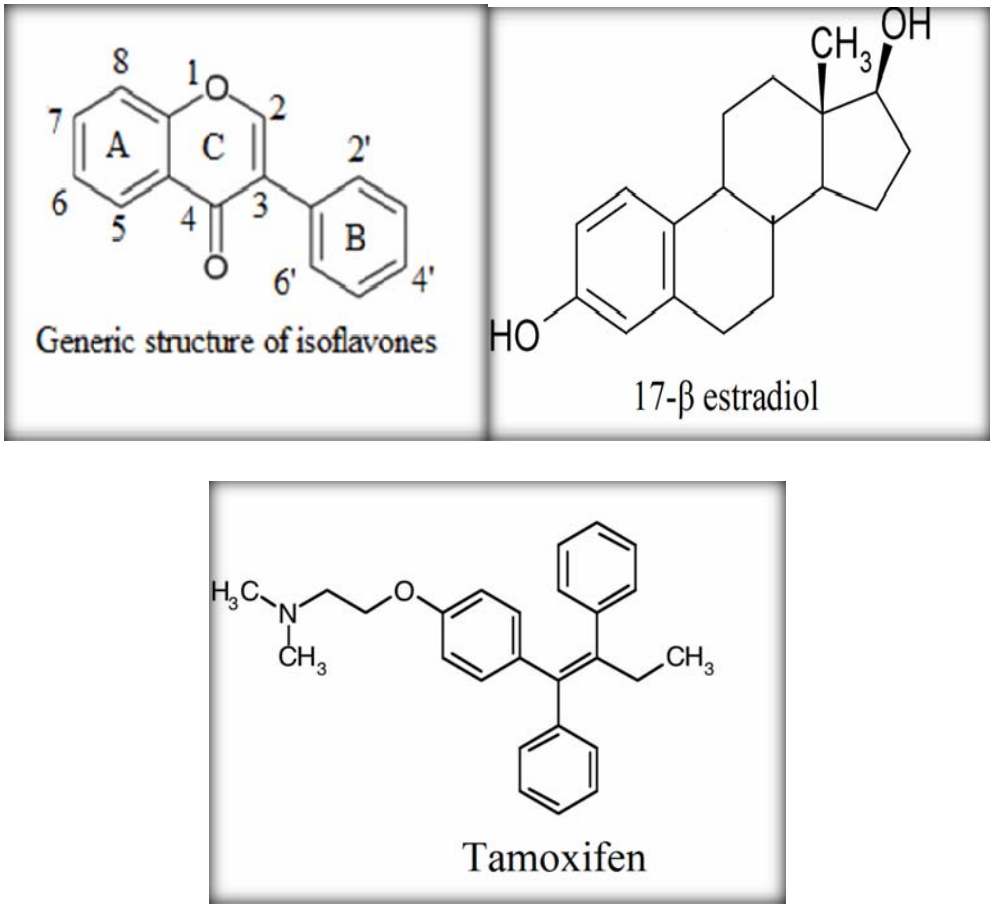

Figure 4. Chemical structure of isoflavones, 17β-estradiol and tamoxifen.

The three major classes of phytoestrogens—isoflavones, lignans and coumestans—are represented by different compounds, which can be found in many foods, particularly leguminous plants, seeds, nuts and berries. Usually, single plants contain more than one type of phytoestrogen, and different plants contain different concentrations of the several phytoestrogen types [18].

In plants, the phytoestrogens function primarily as antioxidants and phytoalexins. Many isoflavones exhibit antimicrobial activity and are believed to play an important role on plant fight microbial disease. Antimicrobial isoflavones can be classified as pre-formed "phytoanticipins" or inducible "phytoalexins" [36]. Different kinds of lignans have been discovered in many plant species and parts, including the roots, leaves, flowers, fruits, seeds and wooden parts. The accumulation of lignans in the core of trees is important for their durability and longevity. Moreover, they also may function as phytoalexins, providing protection for the plant against diseases and pests, and may participate in controlling plant growth [56].

The estrogenic properties of the phytoestrogens were observed in the 1940s, when Australian sheep farmers noticed that their sheep were infertile. The ewes grazed on subterranean or red clover and their infertility was attributed to the presence of isoflavones like genistein and daidzein, along with their precursors, biochanin A and formononetin. Several estrogenic effects were found on different tissues including altered cell differentiation in the cervix leading to abnormal glands that produced a more hostile cervical mucus; weight gain of the uterus; ovulation abnormalities due to inhibition of follicular development or follicular degeneration; altered central nervous system/pituitary function, and altered sexual behavior [57]. Isoflavone consumption has also been associated with infertility in cattle [58], California quail [59], and captive cheetahs fed commercial diets that contained high levels of genistein and daidzein, suggesting that the presence of dietary isoflavones were responsible for their infertility [60,61].

Isoflavones

Isoflavones, or isoflavonoids, are the most common type of phytoestrogens although with a restricted distribution in the plant kingdom. They are mostly limited to the subfamily Papilionoideae of the Leguminosae [62] and are found in highest amounts in soybeans and soyfoods (like miso and tofu), being also present albeit at lower concentrations in other beans, fruits, vegetables and legumes [63,64]. Soy foods generally contain 1.2–3.3 mg isoflavones/g dry weight, with the precise amount depending on a number of factors that include the type of soy food as well as soybean variety, harvest year, geographical location, environmental conditions, and extent of industrial processing of the soybeans [65,66].

The major isoflavones present in soy foods are genistein, daidzein and, to a lesser extent, glycitein. These compounds are, in fact, hydrolysis products of glycosides in plants, termed genistin, daidzin and glycitin, which, after oral ingestion, are extensively biotransformed in the intestine by the action of bacterial enzymes [5]. The extent of intestinal bacterial metabolism will therefore have an effect on the bioavailability of dietary estrogens and, consequently, be expected to influence the potential for physiologic effects [5]. Another source of isoflavones is clover. It contains high concentrations of formononetin, which is a precursor of daidzein, and biochanin A, which is a precursor of genistein [63].

The flavonoids are a large chemical class of substances, in which the isoflavones are included, that are formed through the prenylpropanoid-acetate biodemal pathway via chalcone synthase and condensation reactions with malonyl CoA. The first step in flavonoid

biosynthesis is the condensation of *p*-coumaroy CoA with three molecules of malonyl CoA to give chalconaringenin (= naringenin chalcone), a reaction catalyzed by chalcone synthase [67] (Figure 5).

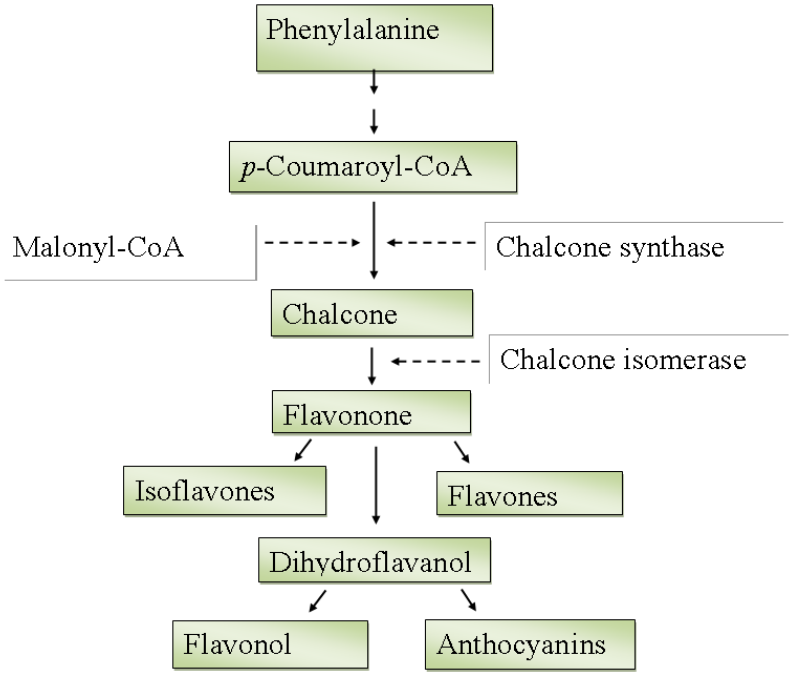

Figure 5. Scheme of general flavonoid pathway.

The isoflavones possess a 3-prenylchroman skeleton that is biogenetically derived from the 2-prenylchroman skeleton of the flavonoids [68]. The compounds of the isoflavones share a common structure, with genistein (4′, 5, 7 – trihydroxyisoflavone) having the important –OH groups at positions 7 and 4′, and biochantin A, a methoxy group at position 4' [9]. Small differences in the structure of the isoflavones may affect their activity. For example, daidzein differs from genistein only by the absence of a hydroxyl group on the A ring, but this difference greatly affects the functions of these two molecules [36].

The chemical composition of the dietary isoflavone may be a key determinant of its bioavailability and extent of biotransformation. The absence of isoflavones in plasma occurs 24 hours after oral intake [5]. The peak concentration range in women was 300–3200 nmol/L (80–800 ng/mL), but the time to reach this concentration was between 6 and 8 h after ingestion, and the half-life of plasma disappearance was at 7.9 h. Similar pharmacokinetics were obtained for adult men. These are quite high concentrations of isoflavones when compared with the endogenous plasma concentrations of estradiol throughout life, and despite the relatively weaker estrogenic activity, it is probable that the concentrations are sufficient to account for the many in vivo and in vitro biological effects that have been attributed to isoflavones [5].

The large number of phytoestrogens is introduced into the diet as inactive compounds. After their ingestion, a complex enzymatic conversion occurs in the gastrointestinal tract

resulting in the formation of compounds with a steroidal structure similar to estrogens [18]. Considering the isoflavone, they can be found as glucosides or as aglycones. The glucosides are readily hydrolyzed in the gut to their aglycones, which are then easily transported across intestinal epithelial cells [69]. In the intestine, bacteria take an important part in the absorption and metabolism of isoflavones by producing the enzymes, termed glucosidases, which are responsible for metabolizing the glycosidic isoflavones (genistin, daidzin and glycitin) to their corresponding aglycones (genistein, daidzein and glycitein) [5,17] (Figure 6). However, before absorption occurs, intestinal bacteria may further metabolize the isoflavone aglycones to isoflavone metabolites. This metabolic process particularly involves genistein conversion to *p*-ethyl phenol in the colon (Figure 7), and daidzein to dihydrodaidzein, equol and/or O-desmethylangolensin (O-DMA) (Figure 8), all of which may also be absorbed [5,17]. The physiological effects of these metabolites may differ from those of the primary isoflavones, like equol and O-DMA, which are more powerful antioxidants than genistein and daidzein [70]. Daidzein, genistein, equol and O-DMA are the major isoflavones detected in blood and urine of animals and humans. In addition, dihydrodaidzein, *p*-ethyl phenol and glycitein (Figure 9) have been detected in human plasma and urine [71,72].

After absorption, isoflavones go through hepatic conjugation to glucuronic acid or sulphate to produce forms that are measured in biological fluids [5,17,73]. Similar to endogenous steroids, they undergo enterohepatic circulation following deconjugation in the intestine and re-absorption or excretion in the feces [5,17]; or after enterohepatic circulation, they may be excreted in bile or deconjugated, reabsorbed, reconjugated, and excreted in the urine. The efficiency of conjugation of isoflavones is high and consequently the proportion of circulating free isoflavones is small [5]. Studies in humans have shown that serum and urinary concentrations of isoflavones increase in accordance with the amount consumed, indicating that absorption occurs in a dose-dependent manner [74]. Moreover, studies using a controlled quantity of soy have shown a variable individual metabolic response with up to a 1000-fold variation in isoflavone excretion [16]. It is supposed that the composition of the intestinal flora, intestinal transit time, and variation in redox potential of the colon might influence the variability observed in humans [75]. This metabolic variability of the phytoestrogens is clinically important as it may influence biological responses. In healthy humans, plasma concentrations of isoflavones are usually less than 40 nmol/L [76] when consuming soy-free diets. On the other hand, plasma concentrations of isoflavones increase markedly in the micromolar range after single ingestion of soybean milk [77], a soy meal [78] or baked soybean powder [79].

In non-fermented soy foods, the isoflavones are mostly present as betaglucosides, some of which are esterified with malonic [80,81] or acetic acid [81,82]. In fermented soy foods, such as miso, soybean paste or tempeh, the isoflavones are largely unconjugated [83]. These chemical differences have been shown to alter the isoflavones` pharmacokinetics in the rat [84] and therefore probably in humans. The unconjugated isoflavones, like many common drugs, are absorbed from the upper small intestine in the rat [85], whereas the isoflavone glycoside conjugates are absorbed more slowly, indicating that their hydrolysis occurs at more distal sites in the intestine in relation to the unconjugated isoflavones [78,84].

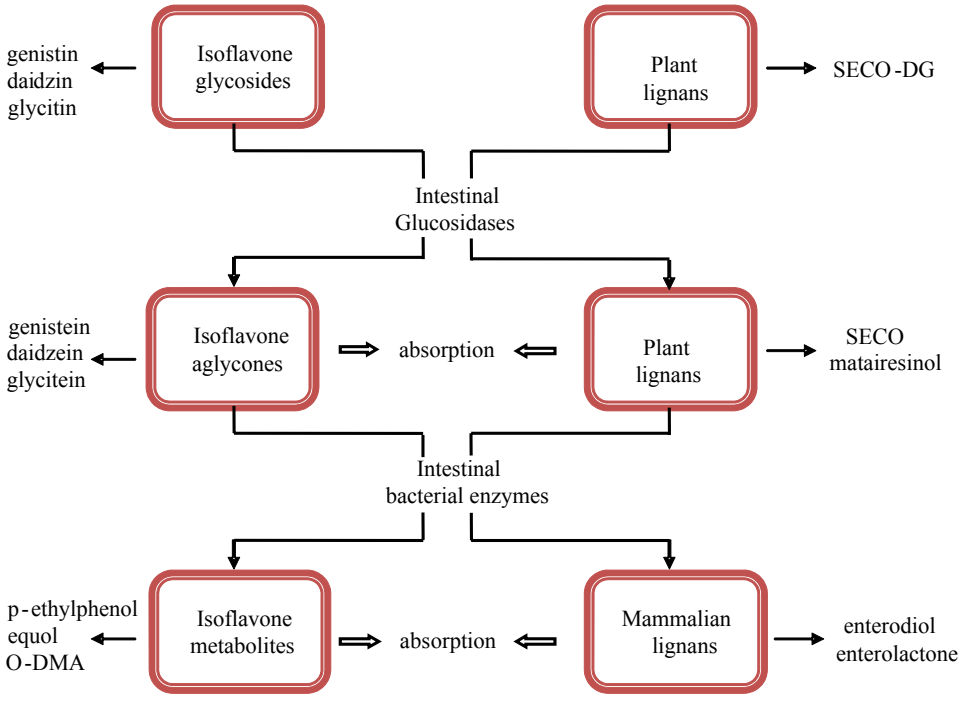

Figure 6. Schematic presentation of the absorption and metabolism of isoflavones and lignans. O-DMA = O-desmethylangolensin; SECO-DG = secoisalariciresinol-diglucoside; SECO = secoisalariciresinol. (Based on reference 110.)

Dietary phytoestrogens are weakly estrogenic (10^{-2} to 10^{-3}-fold, depending on the system examined) when compared with estradiol (E_2) or estrone, the main circulating estrogens of most mammals [86,87,88]. The preferential binding of nonsteroidal estrogen to the ERβ receptor suggests that they may exert their actions through distinct pathways from those of classical steroidal estrogens [5]. In addition, the lower binding rate of several phytoestrogens to serum proteins would indicate an increase in the numbers of molecules available for receptor occupancy [89]. Of the isoflavones, genistein and daidzein are thought to exert the most potent estrogenic effect. Numerous studies have shown that the isoflavones, as well as the lignans and the fungal estrogens, compete effectively with E_2 for binding ER-rich cells [12]. The phenolic B-ring of the isoflavones confers binding to estrogen receptors (ERβ > ERα, although at a lower affinity relative to estradiol) and acts like SERMS [25,53,90]. Genistein has one-third the potency of E_2 when it binds to ERβ, and one thousandth of the potency of E_2 when it binds to ERα as determined by expression of luciferase reporter gene construct in kidney cells cotransfected with ERα and ERβ [58].

Genistein can induce similar responses in prostate, endometrial, ovarian, breast, bone tissues and cell lines as estradiol [91,92,93,94], but it can also act as an estrogen antagonist in some tissues. When neonatal prepubertal Sprague-Dawley rats were treated with estrogens, an increase in the number of terminal end buds and cell proliferation in mammary tissue was observed [72]; however, after treatment with genistein, a reduction in the number of terminal end buds and cell proliferation was observed [95]. Other studies showed that genistein inhibited the development and growth of chemically induced tumors in the breast [96] and

prostate [97] of mice and rats. It is believed that genistein and other isoflavones exert this effect through induction of a signal transduction pathway leading to apoptosis [98]. In the rat uterus, genistein down-regulated ERα and up-regulated progesterone receptor, suggesting signaling via ER [99], while in castrated mice, it up-regulated the estrogen-responsive gene (c-fos), in the prostate, suggesting an estrogenic mechanism [100,101].

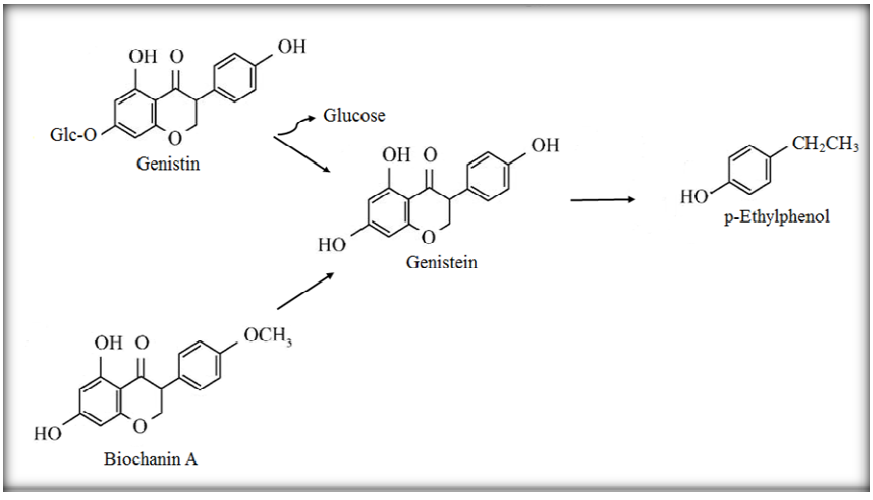

Figure 7. The metabolic pathway of genistin to its aglycone and metabolic product.

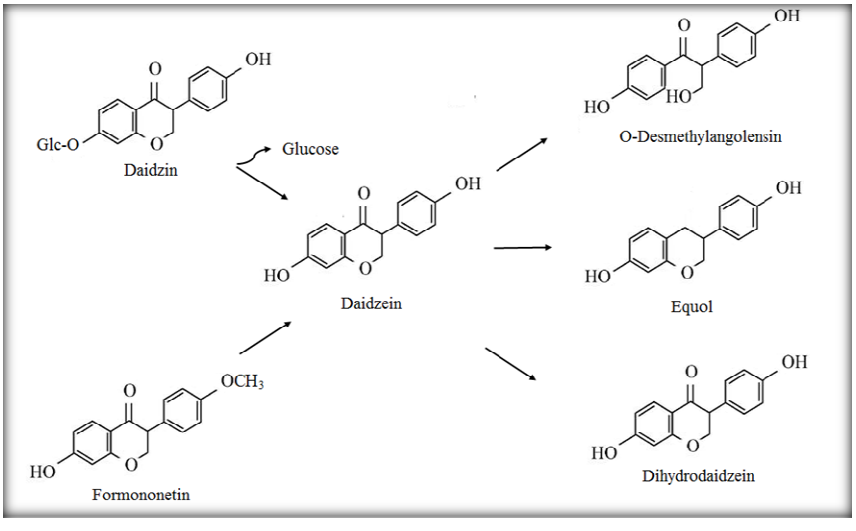

Figure 8. The metabolic pathway of daidzin to its aglycone and metabolic products.

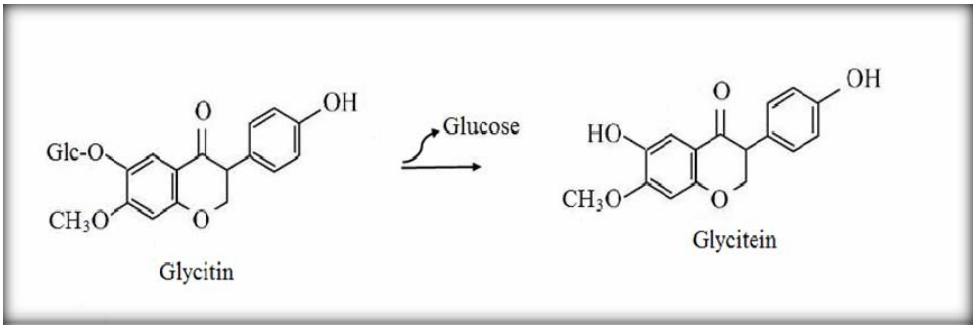

Figure 9. The metabolic pathway of glycitin to its aglycone.

Lignans

Lignans are more widely distributed in plants, being highly concentrated in flaxseed, but also found in oilseeds, seaweed, legumes, seeds, vegetables (especially carrots, spinach, broccoli and cauliflower), whole grains and tea. Fruits have low levels of lignans with the exception of strawberries and cranberries [102]. Flaxseed generally contains 0.96 – 3.15 μmol lignans/g, with the precise amount depending on factors such as variety, growing location and harvest year [103]. The term lignan is used for a diverse class of phenylpropanoid dimers and oligomers. The two main lignan dimers, that are not estrogenic by themselves, are termed secoisolariciresinol-diglucoside (SECO-DG) and matairesinol (MAT), which serve as precursors to the mammalian lignans, enterodiol (2,3-bis(3-hydroxybenzyl)-butane-1,4-diol) and enterolactone (trans-3,4-bis(3-hydroxybenzyl)-dihydro-2-furanone) respectively [5,103] (Figure 10). Lignans` precursors occur in grains close to the outer fiber-containing layer, a part that modern Western milling techniques usually eliminate. As a result, phytoestrogens are seldom present in cereal diets in Western countries [18]. Other recently discovered lignans are pinoresinol and lariciresinol [104].

Lignans present different biological activities in animal and *in vitro* systems, including anticarcinogenic, antioxidant, weakly estrogenic and antiestrogenic properties, and inhibition of enzymes involved in sex hormones metabolism [56,105,106]. For instance, enterodiol inhibits 5α-reductase and 17β-hydroxysteroid dehydrogenase in human tissues. Therefore it is suspected that lignans may reduce the plasma levels of free estradiol and testosterone and may affect the development of hormone dependent diseases. The two major mammalian lignans (enterodiol and enterolactone) have been found in human plasma, saliva, feces, semen and prostatic fluid [56].

The absorption and metabolism of lignans are similar to that of isoflavones. The conversion occurs by gut microflora and the mammalian lignans are readily absorbed. After oral ingestion, the lignan SECO-DG is metabolized to SECO through hydrolysis of the sugar moieties by intestinal bacteria, followed by dehydroxylation and demethylation to enterodiol, reactions which are also catalyzed by bacterial enzymes. Enterodiol may be absorbed or further oxidized irreversibly to enterolactone, which is then absorbed. Intestinal bacterial enzymes also catalyze dehydroxylation and demethylation reactions to convert MAT to enterolactone, which can then be absorbed. Once mammalian lignans are absorbed, they

undergo conjugation to glucuronic acid or sulphate and enter the circulation. After this, they may be excreted in the urine or undergo enterohepatic circulation [107]. Studies have shown that urinary and plasma concentrations of the mammalian lignans increase significantly in a dose-dependent manner following consumption of lignan-rich flaxseed [108,109]. A cross-sectional study reported a positive association between plasma enterolactone and consumption of vegetables and fibers, however, positive associations were also observed with alcohol and caffeine intake, raising concern regarding the specificity of plasma enterolactone as a biomarker for exposure to lignan-containing foods [110,111].

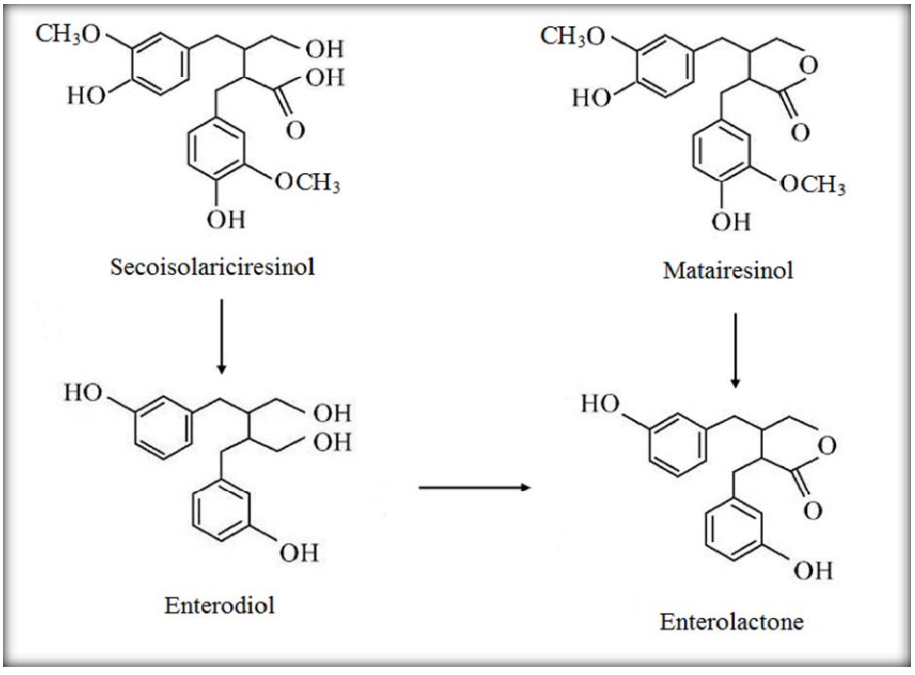

Figure 10. Chemical structure of lignans.

Coumestans

Coumestans are found in large quantities in plants, but only a small number have shown estrogenic activity, namely coumestrol (Figure 11) and 4' methoxy coumestrol [35]. Although they are much less commonly consumed, coumestrol is mainly found in legumes and vegetables, particularly soy sprouts and alfalfa sprouts [112]. Clover and soybean sprouts are reported to have the highest concentration, 28 and 7 mg/ 100 g dry weight, respectively, whereas mature soybeans only have 0.12 mg/100 g dry weight [113,114]. The estimated daily intake of coumestrol by US women is 0.6 μg/day, a much lower value than that of isoflavone intake (154 μg/day) [115]. Coumestrol binds twice as well to ERβ than to ERα and binds to ERβ with twice the affinity of estradiol [56,116].

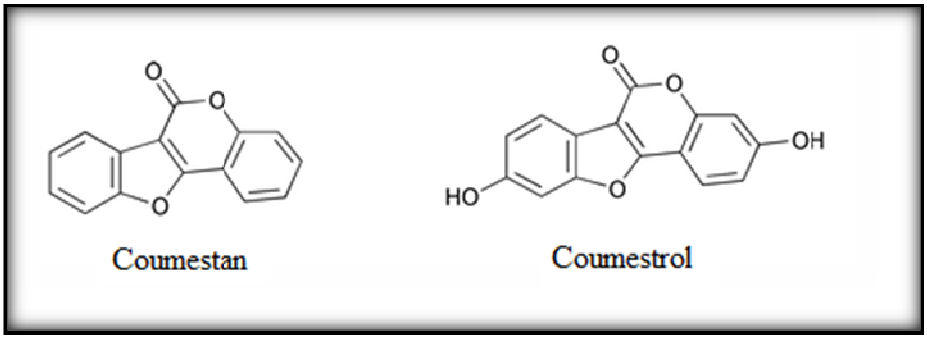

Figure 11. Chemical structure of coumestan and coumestrol.

Prenylflavonoids

The prenyflavonoids are primarily represented by 8-prenylnaringenin, which is known to be the most potent phytoestrogen (Figure 12). Beer is the most important dietary source of 8-prenylnaringenin, and its presence in this beverage is due to isomerization of desmethylxanthohumol in the brew kettle. Other prenylated flavonoids are xanthohumol and isoxanthohumol, also found in beer [67].

Although it is a much weaker estrogen than 17β estradiol (< 1%), the presence of 8-prenylnaringenin in beer has resulted in concerns as to the estrogenic effects of beer consumption. Most hopped beers contain less than 100 μg of 8-prenylnaringenin/L, and the highest amount concentration measured in microbrew beer was 240 μg/L [67]. In ovariectomized mice treated with 8-prenylnaringenin, the minimal concentration to cause estrogenic effect, i.e. to produce a significant increase in vaginal mitosis was 100 μg/mL drinking water. No effect on uterine growth was observed at this concentration [117], which is about 400 – 1000-fold higher than the 8-prenylnaringenin concentration in beer. Based on this information, it seems that it is safe to assume that human exposure to phytoestrogens through beer consumption is not a health threat.

The daily intake of prenylflavonoids, approximately 0.14 mg, is relatively small compared to total polyphenols from beer (42 mg as catechin equivalents per day) [118], indicating that the prenyflavonoids play a minor role to the antioxidant properties of beer. Prenylflavonoids differ from other polyphenols, such as flavonol glycosides and phenolic acids, in that they are more lipophilic and, consequently, may be more effective antioxidants at lipophilic surfaces such as membranes and low-density lipoprotein [119].

A competition assay with recombinant human ERα and ERβ from cytosolic SF-9 cell extracts has shown that 8-prenylnaringenin has a high affinity and strong selectivity for the ERα. In comparison with genistein, 8-prenylnaringenin was 100 times more potent ERα agonist but a much weaker agonist of ERβ in the estradiol-competition assay for receptor binding. It is believed that, to date, 8-prenylnaringenin is the strongest plant-derived ERα receptor agonist identified. An *in vivo* study has shown that the estrogenic potency of 8-prenylnaringenin was about 20.000-fold lower when compared to 17β estradiol using uterine and vagina growth assays [120].

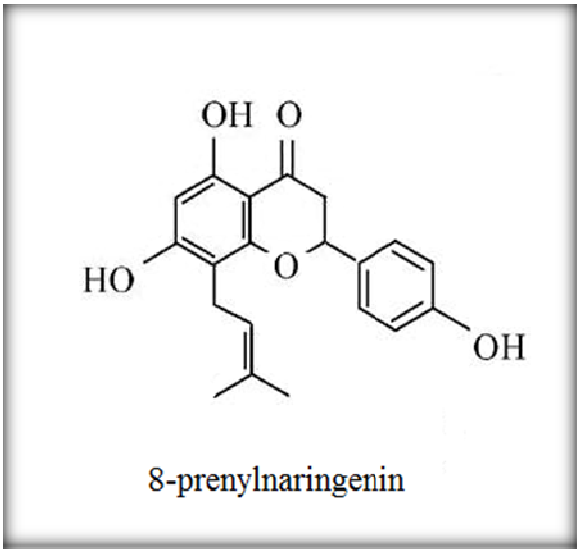

Figure 12. Chemical structure of 8-prenylnaringenin.

Stillbenes

Stillbenes, like the flavonoids, are produced through the prenypropanoid-acetate pathway. The main dietary source of stillbenes is resveratrol (Figure 13) found in red wine and peanuts although it is also synthesized by a variety of plant species in response to injury, ultra-violet irradiation and fungal attack [121]. There are two isomers of resveratrol, *cis* and *trans*, but only the *trans* form is estrogenic [122]. Resveratrol is only found in the skin of the grape, resulting in low levels of *trans*-resveratrol in white wine. Its content in wine depends on cultivar, geographic location, season, oenological practices and presence of Botrital fungus [123,124,125]. The longer the fermentation time the more *trans*-resveratrol will be in the wine. The level of *trans*-resveratrol in red wines, fermented with skins, can be as high as 14.5 mg/ L [126], but the type of post harvest processing has a large effect on the resveratrol content. For instance, the hot extraction method used for obtaining purple grape juice, as opposed to the cold pressing of grapes for obtaining the white grape juice, provide a higher concentration of resveratrol [124]. This is also true for peanuts, with boiled peanuts containing more resveratrol than peanut butter and roasted peanuts [127]. In peanuts, resveratrol is found throughout the nut; however, on a weight basis the seed-coat has the highest levels [128]. The smaller peanuts show higher resveratrol content, but as the peanuts mature the resveratrol content in the nut declines [127].

Other sources of stillbene have been reported in the literature. They include the roots of *Polygonum cuspidatum* (Japonese knotweed or Mexican bamboo) used in China for its therapeutic properties, with resveratrol levels in the dried roots being as high as 377 mg/100 g dry weight [129]. Resveratrol has also been isolated from several grass species [130], pine bark [131], ivy and lilies [124].

Resveratrol physiological levels can be obtained through drinking red wine. It shows a greater capacity to activate the ERβ than ERα [132]. Its agonistic and antagonistic activity

has been shown in MCF-7 cells and the hamster ovarian cell line (CHO-K1) transfected with human ERα and ERβ [133,134]. Resveratrol is considered to be an effective radical-scavenger, suggesting that it acts as a natural antioxidant against oxidative DNA damage [135,136]. It also exhibits anti-inflammatory effects and antimutagenic and anticarcinogenic activity [121]

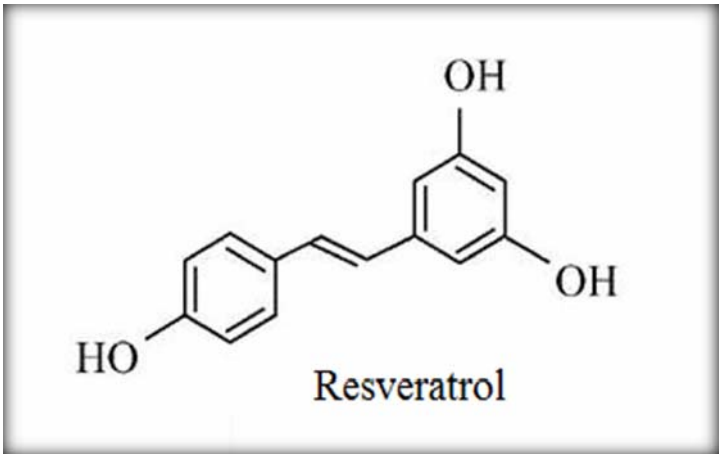

Figure 13. Chemical structure of stilbene resveratrol.

Effects on Human Health

Owing to the ability of the phytoestrogens to exert estrogenic activity, there has been considerable scientific interest on their potential beneficial health effects, particularly as anticarcinogens, cardioprotectants, in osteoporosis, and as alternatives to hormone replacement therapy in menopause. The incidence and mortality of hormone-related cancers such as breast, endometrial and prostate cancer vary around the world, being higher in the Western countries than in Asian countries. These differences are being related to variations in the diet, and one such example is the intake of phytoestrogens.

Cancer

Numerous epidemiological studies have shown that people who consume high amounts of isoflavones in their diet have lower rates of several cancers, including breast, prostate and colon cancer. The idea that soy may have a preventive role in cancer came from a broader research of the reasons for the large worldwide variation in cancer incidence and death. Americans and western Europeans are at much higher risk of breast cancer and prostate cancer than are peoples from the Asian countries (137). In Asia, where the consumption of phytoestrogen is much higher than that of the Western countries, the rates of these cancers are low (Figure 14). It is estimated that the average American diet contains less than 1–3g per day of isoflavone, whereas the average Japanese diet contains 30–50 g per day [138].

Immigrants from Asia living in the US have an increased risk of cancer compared with the length of stay in the US and the exposure to the North American diet [139]. For women, this change occurs mostly in the next generation, whereas for men, the increase in prostate cancer risk occurs in the same generation [140].

	Genistein	Daidzein	Biochanin A	Formono netine	Coumestrol	SECO	MAT
Whole grain	---	---	---	---	---	32.9	2.6
Barley	7.7	14.0	---	---	---	58.0	0
Wheat bran	6.9	3.5	---	---	---	110	---
Soy flower	93 900	67 400	70	30	---	130	---
Soybean	26 800 – 102 500	10 500 – 85 000	---	18.0 – 121.0	---	13.0 – 273.0	tr
Tofu	21 300	7 600	---	---	---	---	---
Miso	14 500	7 300	---	---	---	---	---
Soy drink	2 100	700	---	---	---	---	---
Soy Milk	310	30	---	---	---	---	---
Bean	365	9.7	14	7.5	1.8	172	0.25
Chick peas	69.0 – 214.0	11.0 – 192.0	838	215	5	7.0 – 8.0	0
Flaxseed	---	---	---	---	---	369 900	1087
Sunflower seed	13.9	8.0	---	---	---	610	0
Clover seed	323	178	381	1270	5.3	13	3.8
Alfalfa sprouts	5.0	62.0	124.0	4090	45.0	33.0	0
Peanut	64.0	58.0	31	---	---	298.0	tr
Strawberry	tr	tr	---	---	---	3718	22.5
Apple	tr	12.4	---	---	---	5.0	0
Banana	0	0	---	---	---	10.0	0
Orange	0	0	---	---	---	76.8	0
Avocado	0	0	---	---	---	76.7	16.0
Guava	0	0	---	---	---	699.7	tr
Broccoli	8.0	6.0	---	---	---	414.0	23.0
Cauliflower	9.0	5.0	---	---	---	97.0	tr
Garlic	tr	tr	---	---	---	379.0	3.6
Carrot	0	0	---	---	---	192.0	3.0
China Green tea*	tr	tr	---	---	---	2890	195.0
China Black tea*	0	0	---	---	---	1050	90.0

Figure 14. Phytoestrogen content in selected food items. Data expressed in µg/100g dry weight. SECO = Secoisolariciresinol; MAT = Matairesinol; tr = trace amounts. * brewed tea. (Based on references 1, 6, 18, 353).

The antiproliferative properties of isoflavones suggest that these compounds may inhibit the cell cycle or induce apoptosis. It has been reported that concentrations of 5–20 µg/mL genistein caused cell cycle arrest at the G1/S and G2/M phases in the human myelogenous leukemia HL-60 and the lymphocytic leukemia MOLT-4 cell line [141], and concentrations of up to 60µM genistein arrested human gastric cancer cells at G2/M [142]. In addition to genistein, genistin, daidzein and biochanin A at 0–50 µM inhibited murine and human cancer cells growth by inducing cell cycle arrest and apoptosis [143].

Apoptosis is an effective beneficial antitumor process since it removes damaged or abnormally functioning cells from tissues. At high concentrations, genistein is reported to induce apoptosis through mitochondrial dependent pathways. For example, 50 μM (24 h) genistein induced cytochrome c release, caspase-3 activation, nuclear condensation and DNA fragmentation by reducing the mitochondrial membrane potential [144]. Lower concentrations of genistein (15–60 μM, 24 h) induced apoptosis in murine T-cell lymphoma cell lines via mitochondrial depolarization and activation of caspases 3 and 9 [145]. Genistein has also been suggested to induce apoptosis by inhibiting DNA topoisomerase II, thereby preventing ligation of DNA double strand breaks [146].

The isoflavones might protect against cancer and/or heart disease through inhibition of oxidative damage [147], as DNA oxidation is probably an important cause of mutations that potentially can be reduced by dietary antioxidants. The isoflavones serve as derivatives of conjugated ring structures and hydroxyl groups that may function as antioxidants in in vitro cell culture or cell free systems by scavenging superoxide anion [148], lipid peroxy-radicals [149], singlet oxygen [150], and/or stabilizing free radicals involved in oxidative processes through hydrogenation or complexing with oxidizing species [151].

Breast Cancer

Cancer chemoprevention is different from cancer treatment because it is aimed at modulation of pathways that are relevant to carcinogenesis with the purpose of inhibiting, reversing, or retarding cellular hyperproliferation. It is targeted at the initiation, promotion and progression stages of carcinogenesis and requires long-term exposure to non-toxic nutrients, food supplements or pharmacological agents in order to prevent the development of malignancies [67,68].

There are two basic ways of cancer prevention—primary and secondary. In primary prevention, tumors do not appear clinically as a result of preventive measures that reduce the risk of genetic damage, the precursor to cancer at the initiation stage later in life, or stop the mutated cancer cell from growing abnormally and becoming an observable tumor. The secondary prevention aims at the prevention of another cancer from occurring, as after the removal of a breast tumor, a patient may develop a new primary tumor at a site different from that of the first one, usually the other breast. Since most breast tumors express functional estrogen receptors, a strategy for preventing the growth of tumor cells remaining after surgical removal of the mammary tumor is the anti-estrogen tamoxifen. As tamoxifen is tumouristatic rather than tumouricidal, it was later realized that it had a potential role as a prophylactic, primary and/or secondary prevention agent for breast cancer [152]. In relation to the natural occurring substances, one hypothesis regarding the breast cancer protective effect of phytoestrogens was associated with the prolonged follicular phase. In breast epithelial cells, proliferation is low during the follicular phase and increased two fold in the luteal phase. Women with longer cycles secondary to increased follicular phase therefore have decreased cell division. Less breast cell proliferation reduces the risk of dysplasia resulting in breast cancer [57,153].

The protective effect of phytoestrogens on cancer may also be due to their role in lowering circulating levels of unconjugated sex hormones. As mentioned earlier, estrogens primarily circulate as inactive conjugates of sex hormone binding globulin (SHBG) or albumin [35]. In postmenopausal women, dietary supplementation with soy isoflavones or lignans increased the levels of SHBG [154,155,156,157], and thereby lowered the serum levels of free estradiol [157,158]. In menstruating women, however, the effect of phytoestrogens on estrogen levels is inconsistent because most supplementation studies failed to report any difference in menstrual cycle length or hormone levels with soy supplementation [159,160,161,162].

The consumption of isoflavone and flaxseed significantly changed the urinary excretion of genotoxic estrogen metabolites related to decreased breast cancer risk. Three major pathways, leading to different metabolites, can metabolize estradiol and estrone. Two of these pathways produce 16α-hydroxyestrogens and 4-hydroxyestrogens, which are known to be genotoxic [163], whereas the 2-hydroxyestrogen metabolites are believed to play a protective role on breast cancer. Following high ingestion of soy and flax, it was observed that the ratio of 2-hydroxyestrogens to 16α-hydroxyestrogens increased and this is considered to be an important breast cancer biomarker [164]. In addition, the level of serum SHBG has been negatively correlated with the urinary excretion of 16α-hydroxyestrogens [154]. Other potential mechanisms by which phytoestrogens may protect against breast cancer risk are independent of the estrogen receptor and include inhibition of enzymes involved in the synthesis of steroid hormones, including aromatase and 17β-hydroxysteroid dehydrogenase [165,166].

Urinary excretion of phytoestrogen metabolites can be used as a biomarker for the intake and bioavailability of the phytoestrogens. The data available indicates a lower risk of breast cancer in women with increased excretion of phytoestrogens, and, in case control study, breast cancer patients had significantly lower excretion of isoflavones and lignans than healthy subjects [167].

Neonatal exposure to genistein has been shown to prevent mammary cell tumor in rats, possibly through nonestrogenic mechanisms. The mechanisms proposed to explain the protective effect of genistein against cancer include induction of differentiation, inhibition of DNA topoisomerases, inhibition of specific cell cycle events, induction of apoptosis, inhibition of angiogenesis, antioxidant activity (due to the phenolic ring structures), inhibiting production of hydrogen peroxidase, and inhibition of protein tyrosine kinase (PTK), which is associated with cellular receptors for several growth factors such as epidermal growth factor (EGF), platelet-derived growth factor (PDGF), fibroblast growth factor (FGF) and mononuclear phagocyte growth factor [168,169].

Soybeans have been shown to contain protease inhibitors and there are at least two different inhibitors measurable in soybeans: Kunitz trypsin inhibitor and Bowman-Birk protease inhibitor (BBI). These may help to prevent conversion of normal cells to malignant ones, even very late in the process of carcinogenesis, but have no effect on cancer cells. BBI has been shown to prevent experimentally induced colon, oral, lung, liver, and esophageal cancer in animals. It is thought that this anticarcinogenic effect comes from its inhibition of chymotrypsin; however, there are conflicting data on the heat stability of these protease inhibitors and thus on their activity in foods [170]. Another mechanism of action of

isoflavones is through modulation of gene transcription. For example, genistein modulates transcriptional regulation of transforming growth factor-β1 (TGF-β1), a multifunctional cytokine involved in cell proliferation and differentiation and extracellular matrix (ECM) synthesis [171]. Isoflavones may also inhibit PTK-dependent activation of transcription factors, such as nuclear factor-KB (NF-KB) and activator protein-l which are important signaling molecules involved in the response of cells to inflammation and oxidative stress [172,173,174,175]

The timing of exposure to the anticancer components of soy may be crucial. In an experimental model of induced breast cancer using neonatal and pre-pubertal rats, genistein not only suppressed by 50% the number of mammary tumors observed over a 6-month period [95,176], but it also delayed the appearance of the tumors. Genistein was initially administered in high doses by injection; however, similar degrees of protection were later obtained by placing genistein in the feed (0.25 g/kg) of the mother, whereby the offspring were exposed to genistein from the diet from conception through to day 21 postpartum [96].

In addition to the isoflavones, lignans and prenylflavonoids have also been shown to contribute towards reducing breast cancer risk. Vegetarians, who have a low risk of breast cancer relative to that of the omnivores, also have a significantly higher dietary intake and urinary excretion of lignans [177]. High plasma concentration of the mammalian lignan enterolactone is correlated with a reduced risk of breast cancer [178,179]. Furthermore, urinary enterodiol [180] and enterolactone [180,181] are significantly lower in post-menopausal breast cancer patients relative to controls. Consistent with these data are studies showing that consumption of flax or purified lignans reduces the risk of mammary cancer in rodents [182]. Experimental data have indicated that hop prenylflavonoids have potential as cancer chemopreventive agents by interfering with a variety of cellular mechanisms at low micromolar concentrations, such as inhibition of metabolic activation of procarcinogens, induction of carcinogen-detoxifying enzymes, and inhibition of tumor growth by inhibiting inflammatory signals and angiogenesis.

Despite the supportive data regarding cancer chemoprevention of the phytoestrogens, the epidemiological studies relating breast cancer risk to intake and/or urinary excretion of these compounds have not been consistent. For instance, there was no observed relationship between consumption of soy foods and breast cancer risk in a diet and cancer case–control study in Chinese and Japanese women [183,184]. Similarly, in a case–control study involving multiethnic American women, breast cancer risk was also not affected by either isoflavone or lignan intake [185], and no significant associations were observed between urinary genistein or enterolactone and breast cancer risk in a prospective study of post-menopausal Dutch women [186]. Finally, in Finland, a case control study found no correlation between serum enterolactone concentration and the risk of developing breast cancer in pre- or post-menopausal women [187].

Prostate Cancer

Prostate cancer is the most commonly diagnosed malignancy in man in the world, with incidence rates varying considerably between populations and countries. The lowest rates,

however, are usually observed in Asia, and some migration studies have shown that Japanese migrants to the US present increased incidence of prostate cancer [140]. The high intake of isoflavones by Asian men is evident by the high concentrations of soy isoflavones found in their blood, urine and prostatic fluid, compared with their European and Western counterparts [110].

Prostate cancer is a major health concern and treatment is principally based on its hormone dependence, as this type of cancer is dependent on androgen for development, growth, and survival [188]. Therefore, substances that alter hormone action can have substantial biological effects on prostate cancer development and progression.

The biological activity of androgens is triggered by the activation of the androgen receptor (AR) when binding to its specific ligand [188,189]. Like the estrogen receptors, AR is a member of the nuclear receptor superfamily that functions as a ligand-dependent transcription factor, which, before ligand activation, is present in the cell in an inactive state through association with inhibitory heat shock proteins. Testosterone is the primary AR ligand in serum, but is converted to the more potent dihydrotestosterone (DHT) in prostatic epithelial or adenocarcinoma cells through the action of the enzyme 5α reductase, [190,191]. DHT is a high-affinity ligand for AR, and following DHT binding, a series of events occur, including displacement of heat shock proteins, receptor homodimerization, and rapid translocation to the nucleus. Upon activation, AR then binds to specific DNA sequences, termed androgen responsive elements (AREs), and initiate gene transcription [188]. This results in a myriad of biological response that may involve differentiation, secretion, and cellular proliferation. In prostate cancer, the AR function is required for the development and survival of the tumor [188,192], and the androgen depravation therapy is designed to block AR function [193] either through preventing androgen synthesis or through the use of direct AR antagonists. At the cellular level, the androgen depravation therapy triggers a cascade of events leading to either programmed cell death or cell cycle arrest [193,194].

A group of environmental and industrial substances are classified as endocrine disrupting compounds (EDCs) due to their ability to simulate, alter, or block endogenous hormone action. Some of these compounds may act through the activation of nuclear hormone receptors and may present estrogenic activity, being referred to as estrogenic endocrine disrupting compounds (EEDCs) [195]. Similar to endogenous estrogens, several EEDCs have been hypothesized to alter androgen action or prostate growth and development [196]. These agents can be classified into naturally occurring compounds such as phytoestrogens or synthetically generated agents.

A considerable amount of evidence has revealed the potential beneficial effects of phytoestrogens on prostate cancer development. However, these effects may be influenced by the discrete biological activities of metabolites and by variations in the metabolic profiles of different individuals. Several studies have pointed out that phytoestrogens do not act via a single mechanism of action, nor do different phytoestrogens produce the same profile of biological responses. The protective effect of phytoestrogens has been investigated in animal models and in humans. Studies in humans have described an association between diets rich in soy, lignan, or rye and decreased prostate cancer risk [197]. In rats or mice, a diet rich in phytoestrogens resulted in reduced incidence of prostate tumors [198,199], and the inhibition of prostate tumor development was observed in rats fed an isoflavone-rich diet [200]. In a

transgenic mouse model of prostate cancer, growth and metastatic potential of tumors was reduced as a result of genistein exposure [201]. The developing rat dorsolateral prostate showed reduced expression of AR, ERα and ERβ after oral exposure to genistein [202], revealing one possible mechanism behind the lower incidence of prostate cancer in populations consuming high levels of phytoestrogens. Resveratrol has also been examined in animal models of prostate cancer and has showed a chemopreventive activity [203].

Most prostate cancer studies have been conducted in animals fed with soy, pure isoflavones, or rye-bran. In particular, genistein has been shown to inhibit the growth of cancer cells through modulation of genes involved in the homeostatic control of the cell cycle and apoptosis. In this case, genistein inhibited activation of nuclear transcription factor, NF-kappaB and the Akt signaling pathway, both of which are known to maintain balance between cell survival and programmed cell death [204,205,206,207,208].

The consumption of phytoestrogen has also been implicated in the improvement of patients being treated for prostate cancer. Intake of an isoflavone-supplemented diet for a minimum of 3 months was shown to decrease the rise of PSA levels in both ADT-sensitive and ADT-refractory prostate cancers [209]. Phytoestrogens have also been shown to influence the steroid hormone axis, including the production, metabolism and biological activity of sex hormones, and the regulation of numerous intracellular steroid-metabolizing enzymes, including aromatase and 17β-hydroxysteroid dehydrogenase [6,8,165,166,210]. They may prevent prostate cancer via a dose dependent reduction of serum 17β estradiol and testosterone levels, as reported in Japanese men [211]. The presence of estrogen receptor β in the prostate [212], which binds genistein with an affinity similar to that of 17β estradiol, suggests that the effect of phytoestrogens may be mediated by this target [213]. In a pilot study, prostate cancer patients in a low-fat, phytoestrogen supplemented diet, presented a reduced testosterone and androgen levels [214]. In rats, soy-based diets significantly decreased circulating testosterone levels and prostate weights [215]. In vitro studies have also revealed that high concentrations of isoflavones and lignans inhibited the growth of prostate cancer cells in a dose dependant manner regardless of AR expression or hormone dependency [216,217,218].

Although a large number of evidence has suggested the protective action of phytoestrogens on prostate cancer, some studies have not been entirely supportive and information is still inconsistent. For instance, two case–control [219,220] and one prospective study [221] conducted in Asian countries were unable to detect significant associations between soy consumption and prostate cancer risk.

Menopause

Some women experience a decrease in the quality of life during menopause especially because of sleep deprivation, hot flushes, mood swings, forgetfulness and difficulty concentrating. In postmenopausal women, studies have tried to analyze whether dietary supplementation can alleviate menopausal symptoms, but the results have been inconclusive. Several clinical studies have indicated that a dietary increase in phytoestrogens in addition to a regular diet [222] and phytoestrogen supplementation are associated with an increase in

quality of life as well as a significant amelioration of the signs and symptoms of the climacteric syndrome [18,223]. However, several other studies could not demonstrate any clinical effects, especially with regard to hot flushes [224]. Many reasons may account for these discrepancies found in the various studies, which include differences in patient selection, phytoestrogen content, and symptom assessment, and variations in endogenous estrogen production, intestinal resorption, and activation of orally ingested isoflavones [225].

In regard to the climacteric syndrome, a large number of clinical and experimental data on the use of phytoestrogens for the alleviation of signs and symptoms of this condition have indicated that the efficacy of isoflavones is reduced in women with idiopathic premature ovarian failure, premature ovarian failure after cancer treatment, after long-term hormone therapy, and when isoflavone treatment is initiated more than 3 years after menopause [226]. On the other hand, phytoestrogens were found to be most effectively in early postmenopausal women with a natural menopause and mild to moderate climacteric syndrome. The literature indicates that phytoestrogen compounds used to treat women with climacteric syndrome should contain 40 to 100 mg of isoflavones consisting of variable combinations of different aglycans (i.e., genistein, daidzein, glycitein, formononetin, and biochanin A). A daily dose of 40–100 mg of isoflavones is toxicologically safe and is consistent with the dietary content of isoflavones in Asian countries [227].

Another factor that may partially interfere with the effect of a phytoestrogen diet is the individual age of the woman when starting the diet. Asian women usually begin consumption of phytoestrogens early in childhood, whereas the Western women tend to adopt a phytoestrogen-rich diet or phytoestrogen supplementation during perimenopause or postmenopause. This late consumption may then be too late to exert a protective effect on the breast. Phytoestrogens may induce differentiation of breast epithelium during early childhood and puberty, thus making the breast epithelium less sensitive to noxious agents such as chemical carcinogens [228].

Overall, it appears that there is some evidence to support a role for soy isoflavones in the management of menopausal hot flushes, but the effects specifically due to soy isoflavones are still considered modest. The use 60 g of isolated soy protein powder containing 40 g of proteins and 76 mg phytoestrogens, in the aglycone-active form, has been shown to halve the number of hot flushes in postmenopausal women in a double-blind, placebo-controlled trial [229]. Other studies in peri and postmenopausal women have reported decreased hot flushes following consumption of soy; however, in many studies, the results were not significantly greater than the decrease observed for the control group [230,231]. Despite this, a few studies have found significant decreases in number [229] or severity [232] of hot flushes within the soy treatment group beyond placebo.

The effect of lignans on hot flushes has not been widely investigated and the median daily intake of lignans has been estimated at 578 μg in American postmenopausal women [115]. A study using flaxseed as a treatment group found that it reduced the frequency of hot flushes; however the results were not significantly different from the soy or wheat groups [230].

A few studies have investigated the effect of phytoestrogen supplementation on the endometrium of postmenopausal women. No effects were observed in the endometrial

thickness as measured with transvaginal ultrasound [233,234], or in uterine artery pulsatility index [234]

Osteoporosis

Bone health and osteoporosis are two major concerns to postmenopausal women, considering that the decline in estrogen production that occurs during menopause is an important contributing factor. Estrogen is important for maintaining bone density because it regulates the formation and resorption of bone [46].

During menopause, the circulating levels of estradiol is lower, thereby more calcium is lost from the bone into blood plasma, leading to osteoporosis [235]. The hormone replacement therapy (HRT) was designed to prevent or lower the incidence of osteoporosis in postmenopausal women, however, due to the relatively few benefits of the hormone replacement therapy for quality of life reported by the Women`s Health Institute [236], other alternatives, such as a dietary alternative, are being searched. It is in this regard that the phytoestrogens are being investigated in relation to bone health. Observations of significantly lower numbers of hip fractures in Asian women, when compared to Western women, generated this interest in the potential relation between phytoestrogens and osteoporosis risk [237].

Several in vitro, animal and clinical studies have suggested that phytoestrogens, particularly the isoflavones, are somewhat effective in maintaining bone mineral density (BMD) in postmenopausal women [230,238,239,240]. Results from ovariectomized rodent models have demonstrated a beneficial effect of phytoestrogens on the retention of bone mass. Furthermore, they have indicated that a threshold dose of isoflavones needs to be consumed for a sufficiently long period of time, i.e., approximately one month to years depending on the species, before any measurable effects on bone mass and density can be observed. When animals consumed higher doses of isoflavones, the effect was no greater than that of the minimal threshold dose, and the higher doses may be less effective.

Isoflavones have been demonstrated to increase the synthesis of vitamin D in a number of nonrenal cell types, and, due to this mechanism, they are thought to contribute to bone mineral density [228,241]. In a double blind placebo controlled study of postmenopausal women, the daily administration of 54 mg genistein for a period of 12 months showed a significant increase in BMD [240], while in a 24-week study comparing isoflavone rich soy protein (80.4 mg aglycone isoflavones/ day) and isoflavone poor soy protein (4.4 mg aglycone isoflavones/day) in perimenopausal women, both BMD and bone mineral content (BMC) were significantly higher with the diet high in isoflavones [238]. The lumbar spine seems to benefit the most from consumption of soy phytoestrogens. A 24-week long study with postmenopausal women consuming soy protein with 90mg isoflavones/day showed a significant increase in BMD of the lumbar spine, with no effect on the femoral neck or total body BMD [242].

Still in relation to isoflavones, studies have shown that ipriflavone, a synthetic isoflavone, effectively reduces bone loss in postmenopausal women [243]. This synthetic isoflavone undergoes intensive intestinal bacteria biotransformation to many metabolites,

including daidzein [244]. It is believed that its action is exerted by interfering with bone resorption, and this is done by controlling preosteoclast recruitment, which decreases the number of osteoclasts and mononuclear cells. It is also believed that ipriflavone stimulates collagen synthesis, probably due to the activation of proline hydroxylase [245].

In addition to isoflavones, the effects of coumestans have also been investigated. An in vitro study using bone tissue in organ culture, reported that the exposure of 9-day old chick embryonic femurs to coumestrol inhibited bone resorption and stimulated bone mineralization. Both coumestrol and 17β estradiol inhibited the increased bone resorption induced by treatment with either parathyroid hormone, the hormonal form of vitamin D or prostaglandin E_2 [246].

The beneficial effects of soy isoflavones on bone tissue can result from either increased bone formation by osteoblasts or decreased bone resorption by osteoclasts. These mechanisms could increase bone mass, helping to prevent the development of osteoporosis. It has been suggested that osteoblasts and osteoclasts are target cells for the phytoestrogens. While estrogen receptors are present in relatively low numbers in osteoblasts, mammalian osteoclasts are not believed to express these receptors. Phytoestrogens may act directly on osteoblasts by genomic mechanisms, involving the activation or inhibition of the nuclear estrogen receptor, or, alternatively, may use non-genomic mechanisms, including the inhibition of tyrosine kinase [247], the inhibition of topoisomerase II [248] or the activation of a putative membrane-bound receptor for estrogenic molecules [249]. On the other hand, the inhibition of osteoclastic bone resorption may result from a direct action of phytoestrogens [250], presumably via non-genomic mechanisms, or from an indirect action mediated by inhibitory cytokines released by osteoblasts in response to the actions of phytoestrogens.

Despite the supportive studies regarding the benefits of a phytoestrogen rich diet on prevention of osteoporosis or bone fracture, several other studies have been unable to show the efficacy of phytoestrogen consumption on bone health. For instance, a study of 202 postmenopausal women found no benefit after 12 months of daily 99-mg isoflavone supplementation (52 mg of genistein, 41 mg of daidzein, and 6 mg of glycitein), which does not support the hypothesis that the use of a soy protein supplement containing isoflavones improves cognitive function, bone mineral density, or plasma lipids in healthy postmenopausal women when started at the age of 60 years or later [228,251].

Cardiovascular Disease

Several epidemiologic reports have linked the dietary intake of soy-based foods with the reduction of coronary heart disease [252]. In postmenopausal women, cardiovascular disease is the leading cause of death in many Western countries and it is known that estrogen can directly or indirectly affect the vascular system. In the first case, it acts through ERs located in vascular tissue; in the second case, it acts through altering the lipoprotein profile [253]. There are several clinical studies that have examined the effect that dietary phytoestrogens have on cardiovascular disease. Isoflavones or soy/soy protein and flaxseed have the ability to lower total cholesterol [242,254,255,256], low-density lipoprotein (LDL) cholesterol

[242,255,256] and to raise high-density lipoprotein (HDL) [128,242]. Soy may affect the synthesis of cholesterol even in newborns, as male infants fed soybased formula had lower cholesterol fractional synthesis rates than infants fed breast milk or cow milk-based formula [257].

The improvement on LDL cholesterol levels in humans is directly related to the initial cholesterol concentration and depends on the amount of soy intake [258]. Improvement of HDL cholesterol is also directly proportional to the initial plasma HDL cholesterol concentration [259] and to gender [260]. A study assessing the effects of isoflavone-rich soy protein on blood lipids reported overall reductions in total cholesterol by 9.3%, triglycerides concentration by 10.5%, plasma LDL cholesterol concentration by 12.9% and increase in HDL cholesterol by 2% following an average daily consumption of 47 g of soy protein per day. The effects of dietary soy supplementation in lowering the lipid profile was found to be dose-related and more robust the highest the plasma cholesterol was at baseline [258]. Furthermore, isolated soy protein, rich in phytoestrogen, was found to enhance vascular reactivity in female monkeys with atherosclerosis, an effect similar to that observed with estrogen replacement therapy [18].

The effects of flaxseed on cardiovascular disease have also been linked to reductions in serum lipids. Several studies have reported a significant reduction in serum lipids, including total cholesterol and non-high density lipoprotein (non-HDL) cholesterol, apolipoprotein B and apolipoprotein A-I, as a result of flaxseed consumption [256,261].

Oxidized LDL particles are considered to be important in enhancing atherogenesis [262]. Due to the reported antioxidant property of phytoestrogens, several studies have evaluated the relative efficacy of isoflavones in inhibiting lipoprotein oxidation. For instance, in one study, equol and O-DMA were found to be more potent inhibitors of lipoprotein oxidation than genistein and daidzein, while, in another study, the relative antioxidant activity of the phytoestrogens was shown to be: genistein > daidzein = genistein = biochanin A = daidzin > formononetin.

Endothelium-derived nitric oxide (NO) is a potent vasodilator and mediates the effects of antihypertensive drugs such as nitroglycerin. Isoflavones have been shown to stimulate the activity of the endothelial NO synthase (NOS3), thus inducing vasodilation via NO [263,264]. Isoflavones have also been reported to have antithrombotic and antiatherogenic effects. For example, genistein and daidzein decrease monocyte chemoattractant protein-1 and collagen-induced platelet aggregation in a dose-dependent manner (264).

Several studies, however, showed no effect of isoflavones derived from soy or red clover on serum cholesterol levels [265] or plasma lipids [266]. Two studies that examined the dietary intake of lignans and isoflavones containing foods in postmenopausal women showed that the quartile with the highest intake had a more favorable waist to hip ratio, triglyceride levels, metabolic score [267] and aortic stiffness [268] than women with the lowest intake. No correlation was found between the intake of phytoestrogens and blood pressure, total, LDL and HDL cholesterol [267].

Inhibition of Angiogenesis

Angiogenesis is the generation of new capillaries from pre-existing vessels. This process is absent in the healthy adult organism, being restricted to a few situations including wound healing and the formation of corpus luteum, endometrium and placenta [269]. In certain pathological conditions, angiogenesis increases and loses its self-limiting capacity [270], and this is particularly true for solid tumors [271]. Well-vascularized tumours expand both locally and by metastasis, while avascular tumours do not grow beyond a diameter of 1–2 mm [269].

The formation of new capillaries begins with a localized breakdown of the basement membrane of the parent vessel [272]. This is followed by a series of events that includes migration of endothelial cells and invasion of the surrounding matrix, elongation of the initial sprout, lumen formation and fusion of the capillary with the tip of another maturing sprout, forming a functional capillary loop [273]. Proteolytic degradation of the extracellular matrix by endothelial cells is controlled by angiogenic factors. For example, the basic fibroblast gowth factor (bFGF) induces the production of urokinase-type plasminogen activator [274] and its physiological inhibitor, plasminogen activator inhibitor-1 [272]. Studies using bovine microvascular endothelial cells have shown that genistein reduced both bFGF-stimulated and basal levels of both plasminogen activator and plasminogen activator inhibitor-1 activity in these cells [275]. This information suggests that phytoestrogens may contribute to the prevention of pathological neovascularization that is often seen during the development and progression of many diseases, including solid malignant tumors.

Reproductive Actions

Female Reproductive System

Phytoestrogens may alter ovarian cycles through ovarian, pituitary or hypothalamic actions. As mentioned earlier, genistein and coumestrol have a high affinity for ERβ [50], and this type of receptor is widely found in granulosa cells in the early stages of follicular development [276]. Therefore, phytoestrogens could inhibit estradiol action in the early stages of follicular development or augment it in the luteal phase. Clinical studies using vegetarian or Asian diets provided evidence for phytoestrogen influences on the human menstrual cycle although the results obtained were considerably varied. Both reductions and increases in estradiol secretion have been reported, along with lengthening or shortening of the menstrual cycle [116].

Indirect effects of phytoestrogens could also occur through the augmentation or suppression of estrogen negative feedback in the anterior pituitary or hypothalamus. Experimental studies have shown that genistein inhibited gonadotropin releasing hormone (GnRH)-stimulated LH release, suggesting an action at the level of the pituitary rather than the hypothalamus. On the other hand, genistein increased plasma prolactin, an estrogenic action caused by the inhibition of hypothalamic dopamine secretion [277,278]. Clinical studies have provided some evidence for the phytoestrogen regulation of gonadotropin release, but the results also were variable [279]. For example, in premenopausal women,

reductions in midcycle LH and FSH were observed during a 1-month treatment with 0.8 mg/kg soy isoflavones [280], whereas in postmenopausal women, the same amount reduced LH levels over a 4-week period [281].

The effects of phytoestrogens on the uterine and vaginal epithelium have been reported in a variety of mammalian species. Epithelial cell proliferation in the uterus and vagina is a classical estrogen response, and isoflavones have been shown to induce uterine growth at oral doses of 100–800 mg/kg in mice [281], 10–40 mg/kg in rats [278,282]; and 100 mg/kg in cows [283]. However, a soy-based diet failed to induce uterine growth in ovariectomized rats [284] or rhesus macaques [285]. In addition, a soy-based diet with 10 mg/kg isoflavones did not induce maturation of the vaginal epithelium in ovariectomized rhesus monkeys [286] and also failed to alter vaginal cytology in ovariectomized rats [284].

Male Reproductive System

The effects of phytoestrogens on testicular function have been investigated in a few nonclinical trails with somewhat contradictory results. Micromolar concentrations of coumestrol (15μM) and genistein (7μM) reduced gonadotropin-induced testosterone production by cultured Leydig cells [287]. In pre-pubertal mice fed orally with 900–3600 mg/kg body weight for 6 weeks, genistin suppressed testicular weight and spermatogenesis, whereas oral doses of 300–1000 mg/kg genistein or genistin failed to alter testis weight over a 4-week period in adult male rats. Diets containing 7% soymeal increased testicular size when fed to pre-pubertal rats from weaning to 10 months of age and when fed to mice from fertilization to old age [116]. No significant differences in testosterone or testicular weight were found in rhesus monkeys treated with 1 mg/kg and 9 mg/kg soy isoflavones, respectively, for six months. In a similar dietary comparison, no effects of a higher isoflavone intake [288] on testicular weight were seen in juvenile rhesus monkey males ranging from 0.7 to 1.8 years of age [289].

Developmental Actions

The differentiation and development of the brain and reproductive tract is regulated by endogenous steroids, particularly in the early stages development [290,291,292], when their actions can permanently alter organ organization and subsequent cellular responsiveness. The action of non-steroidal estrogens during early development may be of some concern because they generally bind less well to the binding proteins that protect the developing offspring from maternal steroids and therefore have access to these tissues.

Although isoflavones concentrations in breast milk are generally lower than those found in adult plasma, concentrations in infant formula are high. Soy-based infant formulae contain concentrations at final dilution as high as 100–150 μM [293,294], and an infant nursed on human breast milk consumes no more than 4 μg/kg body weight per day. An infant on soy formula consumes as much as 6–9 mg/kg per day [294], a dose substantially higher than the 0.3–1.2 mg/kg dose received on a typical vegetarian or Asian diet [295]. Like other

estrogenic substances, the isoflavones are effective differentiating agents in rodent models of development. For example, the prenatal administration of 20–100 mg/kg genistein to pregnant female rats showed reduced male anogenital distance and delayed vaginal opening in females [296,297]. Additionally, coumestrol and equol, at subcutaneous doses of 10–100 mg/kg, inhibited the development of uterine glands in female rats [298] and neonatal coumestrol induced precocious sexual maturation and premature anovulation following the treatment of lactating dams with oral doses of 16 mg/kg [299]. In mice, neonatal exposures to subcutaneous doses of 2–5 mg/kg coumestrol are associated with persistent vaginal cornification, haemorrhagic and polyovular follicles, uterine squamous metaplasia and cervicovaginal adenosis [300].

Early exposure to estrogen may also influence susceptibility to mammary cancer by enhancing or reducing the differentiation of terminal end-buds, the site of neoplastic transformation in the rodent mammary gland [301], thereby influencing susceptibility to carcinogenesis [302]. Similar effects have been observed with phytoestrogens. It has been reported that genistein enhances terminal duct differentiation and reduces the susceptibility to induced mammary cancer [303,304]. However, the high-dose treatments required for genistein action were also associated with precocious vaginal opening, atretic antral follicles and fewer corpora lutea [176].

Neurobehavioral Actions

In reference to brain, the majority of studies support the concept that isoflavones are neuroprotective [10]. The literature reports that soy phytoestrogens regulate choline acetyltransferase, nerve growth factor and brain-derived neurotrophic factor in brain areas such as the frontal cortex and hippocampus of female rats [305,306]. They have also been found to attenuate tau protein phosphorylations associated with Alzheimer's disease [307].

The presence of phytoestrogen in the brain was detected in adult Sprague–Dawley rats after intraperitoneal injection of genistein and daidzein [308]. Two well known hypothalamic brain regions are sexually dimorphic in rats. These two regions are the sexually dimorphic nucleus of the preoptic area (SDN-POA), which is normally two to five times larger in male than female rats, and the anteroventral periventricular (AVPV) nucleus, both under the influence of steroid hormones and/or estrogen-like molecules [309,310,311]. The SDN-POA is thought to regulate sexual behavior and gonadotropin levels [309,312], while the AVPV region regulates luteinizing hormone-releasing hormone via receptors for ovarian steroid hormones [311]. Studies have demonstrated that the perinatal administration of genistein significantly affected SDN-POA. In ovariectomized female rats, the injection of genistein significantly increased SDN-POA volumes [313,314], whereas in non-ovariectomized female rats, the administration of genistein resulted in a non-significant numerical decrease in SDN-POA volumes [296]. This suggests that isoflavones influence SDN-POA volumes that are dependent on the basal estrogen hormonal status of the organism [19,315].

The two major pathways of steroid metabolism in brain are the aromatization of androgens and the 5α-reduction of progesterone and androgens [316,317,318,319]. The aromatase cytochrome P450 (P450aro) is the enzyme that catalyzes the conversion of

androgens to estrogens in specific brain regions [319,320,321], whereas, the 5α-reductase enzymes convert androgens, progestagens and glucocorticoids to their 5α-reduced metabolites throughout the brain [316,317,318]. The aromatase and 5α-reductase pathways are important mechanisms of seroid hormonal action in the central nervous system, especially in the hypoyhalamic region during perinatal and postnatal development. They also regulate neuroendocrine functions, reproductive endocrine physiology and sexual behavior [316,319,322,323].

The estrogen product of brain aromatase is known to stimulate neurite growth, migration and regulate neuronal plasticity in various brain regions; protect against neurodegenerative disease such as Alzheimer`s disease and stroke [324,325]; and influence learning, memory, stress, mood, reproductive endocrine function and sexual behavior [319,326,327]. The products of brain 5α-reductase are known to stimulate neurite growth [317,318,326,328]; promote neuroprotection in the spinal cord [330]; influence learning and memory [316,326,328]; inhibit epileptic seizures, and alters mood, fatigue and locomotor activity [318,328,331]. Phytoestrogens are mild inhibitors of the P450aro and 5α-reductase enzymes in peripheral tissues. In the brain, experiments using animal models have shown that treatment with low phytoestrogen diets displayed varying levels of brain 5α-reductase, whereas administration of moderate (200 μg/g) or high (600 μg/g) phytoestrogen diets displayed stable brain 5α-reductase enzyme activities [332].

Calbindin-D28k (CALB) is a calcium-binding protein found in neurons thought to be responsible for sequestering/regulating intracellular calcium levels within homeostatic range and protecting neurons against apoptosis [333,334]. Decreased levels of CALCB may weaken calcium sequestration by the nerve cells leading to apoptosis as seen in neurodegenerative diseases such as Huntington's and Parkinson's diseases [333]. Several studies have shown that CALB levels were significantly decreased in the hypothalamus and amygdale of animals fed in a high phytoestrogen diet [334,335], suggesting a potential lack of neuroprotection.

Renal Disease

The mechanisms by which phytoestrogens may exert their renal protective effects are not completely elucidated. However, the available data suggests that diets rich in isoflavones and lignans, namely soy protein and flaxseed, can slow the development and progression of renal disease as observed in various types of chronic renal disease in both animals and humans. Several mechanisms have been proposed to explain the renal protective effects of isoflavones and lignans They include inhibition of cell growth and proliferation through ER-mediated mechanisms, especially ERβ, or through non-ER-mediated pathways; inhibition of tyrosine kinases and DNA topoisomerases I and II; inhibition of angiogenesis; modulation of TGF-β1 and other growth factors; inhibition of cytokine-mediated activation of transcription factors; and inhibition of platelet-activating factor (PAF) [168]. In humans, the consumption of a vegetarian diet with 52% soybean protein during eight weeks reduced proteinuria, serum lipids and serum lipoproteins in cases of chronic glomerular disease with nephritic syndrome [336], and reduced proteinuria and hyperlidemia in cases of chronic glomerulonephritis with

nephritic-range proteinuria [337]. In cases of lupus nephritis, decreased serum lipids, proteinuria, increased creatinine clearance and inhibition of PAF were observed after a 12-week ingestion of 15, 30 and 45 g/d of flaxseed sequentially at 4-week intervals [338].

Anti-Viral Activity

In addition to all beneficial effects already mentioned, phytoestrogens have also been found to exert anti-viral properties. Viruses enter cells in order to carry out replication and they do so by a variety of mechanisms, such as clathrin-mediated endocytosis and caveolae-mediated endocytosis, which have been shown to be influenced by phytoestrogens [339,340]. In caveolae-mediated endocytosis, some viruses, before internalization, firstly attach to major histocompatibility complex class I molecules on the cell surface, move laterally along the plasma membrane and eventually become trapped in a caveola, which is an invagination of the plasma membrane lined with a protein coat of caveolin-1. This is followed by activation of tyrosine kinases and since phytoestrogens are known to be tyrosine kinase inhibitors, it is believed that they inhibit the phosphorylation events important for viral entry and infection [49,247]. For example, in kidney fibroblast cells treated with genistein, simian virus 40 (SV-40) (associated with pleural mesothelioma and osteosarcome) were unable to enter the cells due to inhibition of virus-induced signals that are necessary for its entry. Evidence suggests that genistein may block tyrosine phosphorylation of caveolin-1 resulting in inhibition of SV-40 entry into the cells [341,342]. Following internalization, the virus is transported from the caveosome to the endoplasmic reticulum. Genistein have also been found to block the downstream signals that enable the SV-40 virus to reach the endoplasmic reticulum [343] (Figure 15).

In another study, 50μM genistein was capable of suppressing replication of encephalomyocarditis virus in L929 cells to 0.5% of control level by a mechanism involving inhibition of viral protein synthesis [344]. When dengue virus infects cells, a series of events occur leading to alteration in cellular permeability with associated actin cytoskeleton rearrangements. Human dermal microvascular endothelial cells treated with genistein showed inhibition of phosphorylation of proteins involved with actin reorganization causing a reduction in stress fibers and focal adhesions during dengue virus infection [345]. Biochanin A has also been shown to exert anti-viral activity. In HSB-2 cells exposed to human herpesvirus 6, biochanin A blocked infection by inhibiting the expression of early and late viral antigens and syncytium formation [346].

Few animal studies have provided evidence to corroborate the in vitro findings. In pigs, it has been shown that a soy genistein enriched diet reduced replication of porcine reproductive and respiratory syndrome virus when virally challenged [347]. Although genistein is the best characterized phytoestrogen in regard to its anti-viral activity, other types of phytoestrogens are expected to exert similar function and this further supports the health benefits of a phytoestrogen-rich diet in humans.

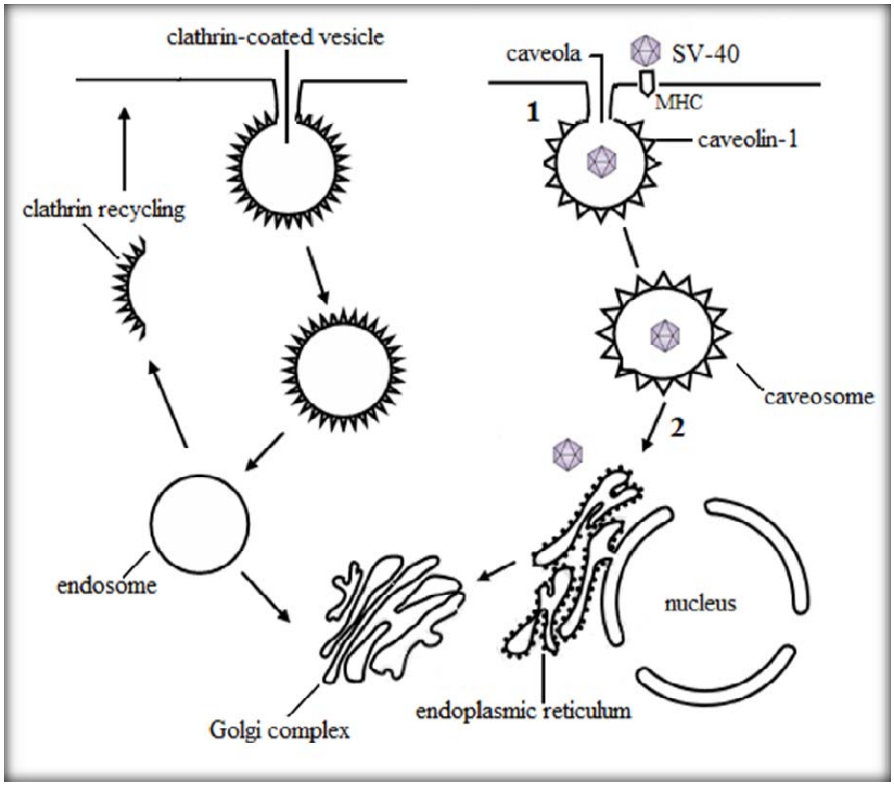

Figure 15. Schematic presentation of clathrin-mediated endocytosis and caveola-mediated endocytosis. It is suggested that genistein may block tyrosine phosphorylation of caveolin -1 resulting in inhibition of SV-40 entry into the cells (**1**) [342]. Following internalization, the virus is transported from the caveosome to the endoplasmic reticulum. Genistein have also been found to block the downstream signals that enable the SV-40 virus to reach the endoplasmic reticulum (**2**) [343]. (Based on reference 9.)

Phytoestrogen Toxicity

Although most phytoestrogens exert pleiotropic effects involving kinase inhibition, cell cycle regulation and antioxidative properties that are likely to contribute to the their beneficial effects, estrogenic and/or anti-estrogenic activities may reduce but also may stimulate estrogen-dependent tumor growth depending on dose and timing of exposure. Other adverse effects have been reported in relation to the action of phytoestrogens. For example, in mice neonates exposed to genistein at dose levels comparable to serum levels of 1–5 μM in human infants, a variety of adverse reproductive effects were noted later in life, including altered mammary gland morphology, abnormal estrous cycle, altered ovarian function and infertility [348]. In vitro cell culture studies have reported genistein to be clastogenic (chromosome breaking), DNA damaging and even mutagenic, in contrast to *in vivo* studies that generally have shown negative genotoxicity results [349]. In Chinese hamster V79 cells, 50–150 μM genistein was found to induce micronucleus formation, indicative of chromosome breakage [350].

Another situation which deserves attention is the feeding of neonates with soy-products. Soy infant formula contains high levels of the isoflavones genistein and daidzein that are well absorbed by infants and circulate at concentrations that are greater than levels which have been shown to produce physiological effects in adult women consuming a high soy diet, generating considerable concern regarding their long-term health effects, particularly on endocrinological and reproductive outcomes. The existing data indicate no adverse effect on human growth, development or reproduction [351], however there is very little research on the effects of consumption of soy phytoestrogens by human neonates and this requires a cautious approach in situations where there are potential developmental effects from the consumption of pharmacologically active compounds in infancy and childhood [352].

Conclusion

In vitro and in vivo studies indicate that phytoestrogens exhibit a broad spectrum of biological activities and resemble other estrogens in their ability to regulate cell proliferation and differentiation. Phytoestrogens also exhibit anti-proliferative and anti-estrogenic actions that are thought to provide protection against carcinogenesis. Initially, it was thought that phytoestrogen actions were predominantly hormonal, but it is now clear that they display a diversity of properties that enable them to exert multiple effects in the organism, and this is consistent with steroid action in general. Differences in the amounts and distribution of α and β estrogen receptors reflect different responses in the cell, since phytoestrogens have preferential actions on either receptor. The discrepancies observed in the many studies available are probably related to expected limitations of dietary assessments. This is particularly true in that they may fail to consider variations in the bioavailability of phytoestrogens due to, for example, intestinal microflora, sex, genetics, diet and antibiotic use. Human responses to phytoestrogens were shown to be highly variable in both quality and incidence of response as well as in the nature of the hormonal response, as both estrogenic and anti-estrogenic responses have been observed. Phytoestrogens preparations, as pharmaceuticals and herbal medicines or as food supplements, require quality standards regarding manufacturing, and special attention should be given to isoflavone content. The growing availability and popularity of purified phytoestrogen makes it especially important to investigate even further the possibility of their beneficial or adverse effects.

References

[1] Mazur, W. Phytoestrogen content in foods. *Bail. Clin. Endocrinol. Metab.*, 1998 12, 729-742.

[2] Steinmetz, KA; Potter, JD. Vegetables, fruit and cancer. I, *Epidemiology.* Cancer Causes and Control, 1991a 2, 325-357.

[3] Steinmetz, KA; Potter, JD. Vegetables, fruit and cancer. II, *Mechanisms.* Cancer Causes and Control*,* 1991b 2, 427-442.

[4] Dragsted, LO; Strube, M; Larsen, JC. Cancer-protective factors in fruits and vegetables, biochemical and biological background. *Pharmacol. Toxicol.*, 1993 suppl. 72, 116-135.

[5] Setchell, KDR. Phytoestrogens, biochemistry, physiology and implications for human health of soy isoflavones. *Am. J. Clin. Nutr.*, 1998 129, 1333S–1346S.

[6] Adlercreutz, H; Mazur, W. Phyto-estrogens and western diseases. *Ann. Med*., 1997 29, 95–120.

[7] Barnes, S. Evolution of the health benefits of soy isoflavones. *Proc. Soc. Exp. Biol. Med*., 1998 217, 386–392.

[8] Kurzer, MS; Xu, X. Dietary phytoestrogens. *Ann. Rev. Nutr.*, 1997 17, 353–381.

[9] Martin, JHJ; Crotty, S; Warren, P; Nelson, PN. Does an apple a day keep the doctor away because a pytoestrogen a day keeps the virus at bay? A review of the anti-viral properties of phytoestrogens. *Phytochemistry*, 2007 68, 266-274.

[10] Lephart, ED; Setchell, KDR; Lund, TD. Phytoestrogens: hormonal action and brain plasticity. *Brain Res. Bull*., 2005 65, 193-198.

[11] Adlercreutz, H. Phyto-oestrogens and cancer. *Lancet Oncology,* 2002 3, 364–373.

[12] Whitten, PL; Patisaul, HB. Cross-species and interassay comparisons of phytoestrogen action. *Environ. Health Perspect.*, 2001 suppl. 109, 5–20.

[13] Glazier, MG; Bowman, MA. A review of the evidence for the use of phytoestrogens as a replacement for traditional estrogen replacement therapy. *Arch. Intern. Med.*, 2001 161, 1161– 1172.

[14] Knight, DC; Eden, JA. A review of the clinical effects of phytoestrogens. *Obstet. Gynecol.*, 1996 87, 897– 904.

[15] Mazur, W; Adlercreutz, H. Overview of naturally occurring endocrineactive substances in the human diet in relation to human health. *Nutrition,* 2000 16, 654–658.

[16] Murkies, AL; Wilcox, G; Davis, SR. Phytoestrogens—review. *J. Clin. Endocrinol. Metab.*, 1998 83, 297–303.

[17] Setchell, KDR. A. Cassidy, Dietary isoflavones—biological effects and relevance to human health. *J. Nutr*., 1999 129, 758S– 767S.

[18] Albertazzi, P; Purdie, D. The nature and utility of the phytoestrogens, a review of the evidence. *Maturitas,* 2002 42, 173–185.

[19] Lephart, ED; West, TW; Weber, KS; Rhees, RW; Setchell, KD; Adlercreutz, H; Lund, TD. Neurobehavioral effects of dietary soy phytoestrogens. *Neurotox. Terat.*, 2002 24, 5–16.

[20] Kalimi, M; Dave, JR. Mechanisms of action of hormones associated with reproduction. In: Witorsch, RJ, editor. *Reproductive Biology.* New York: Raven Press, 1995, 61-72.

[21] Hess, RA; Bunick, D; Lee, K-H; Bahr, J; Taylor, JA; Korach, KS; Lubahn, DB. A role for oestrogens in the male reproductive system. *Nature,* 1997 390**,** 509–512.

[22] Sharpe, RM. Do males rely on female hormones? *Nature,* 1997 390**,** 447–448.

[23] Farhat, MY; Lavigne, MC; Ramwell, PW. The vascular protective effects of estrogen. *FASEB J.*, 1996 10, 615–624.

[24] Turner, RT; Riggs, BL; Spelsberg, TC. Skeletal effects of estrogen. *Endocrine Rev*., 1994; 15, 275–296.

[25] Kuiper, GGJM; Shughrue, PJ; Merchenthaler, I; Gustafsson, J-Å. The estrogen receptor β subtype: a novel mediator of estrogen action in neuroendocrine systems. Front. *Neuroendocrinol.*, 1998 19, 253-286.

[26] Joels, M. Steroid hormones and excitability in the mammalian brain. Front. *Neuroendocrinol.,* 1997 18, 2–48.

[27] Wickelgren, I. Estrogen stakes claim to cognition. *Science,* 1997 276**,** 675–678.

[28] Kincade, PW; Medina, KL; Smithson, G. Sex hormones as negative regulators of lymphopoiesis. *Immunological Rev*., 1994 137**,** 119–134.

[29] Herbert, DC; Supakar, PC; Roy, AK. Male reproduction. In: Witorsch, RJ, editor. *Reproductive Biology.* New York: Raven Press, 1995, 3-21.

[30] Hall, JM; Couse, JF; Korach, KS. The multifaceted mechanisms of estradiol and estrogen receptor signaling. *J. Biol. Chem.*, 2001 276, 36869–36872.

[31] Evans, R. The steroid and thyroid hormone receptor superfamily. *Science,* 1988 240, 889-895.

[32] Carson-Jurica, M; Schrader, W; O`Malley, B. Steroid receptor family: structure and function. *Endocrine Rev.*, 1990 11, 201-220.

[33] Wahli, W; Martinez, E. Superfamily of steroid nuclear receptor: positive abd negative regulators of gene expression. *FASEB J.,* 1991 5, 2243-2249.

[34] Fuller, P. The steroid receptor superfamily: mechanism of diversity. *FASEB J.*, 1991 5, 3092-3099.

[35] Cornwell, T; Cohick, W; Raskin, I. Dietary phytoestrogens and health. *Phytochemistry*, 2004 65, 995-1016.

[36] Anderson, JJB; Garner, SC. Phytoestrogens and bone. *Bail. Clin. Endocrinol. Metab*., 1998 12, 543-557.

[37] Xu, YJ; Traystman, RD; Hurn, P; Wang, M. Neuritelocalized estrogen receptor—a mediates rapid signaling by estrogen. *J. Neurosci. Res.*, 2003 74, 1–11.

[38] Chen, D-B; Bird, IM; Zheng, J; Magness, RR. Membrane estrogen receptor-dependent extracellular signal-regulated kinase pathway mediates acute activation of endothelial nitric oxide synthase by estrogen in uterine artery endothelial cells. *Endocrinology,* 2004 145, 113–125.

[39] Brann, DW; Hendry, LB; Mahesh, VB. Emerging diversities in the mechanism of action of steroid hormones. *J. Steroid. Biochem. Mol. Biol.*, 1995 52**,** 113–133.

[40] Revelli, A; Massobrio, M; Tesarik, J. Non-genomic actions of steroid hormones in reproductive tissues. Endocrine Rev., 1998 19**,** 3–17.

[41] Wehling, M. Specific, nongenomic actions of steroid hormones. *Annu. Rev. Physiol*., 1997 59**,** 365–393.

[42] Beato, M; Herrlich P; Schutz, G. Steroid hormone receptors, Many actors in search of a plot. *Cell,* 1995 83, 851–857.

[43] Zilliacus, J; Carlstedt-Duke, J; Gustafsson, J-Å; Wright, APH. Evolution of distinct DNA binding specificities within the nuclear receptor family of transcription factors. *Proc. Natl. Acad. Sci. USA*, 1994 91, 4175–4179.

[44] Horwitz, KB; Jackson, TA; Bain, DL; Richer, JK; Takimoto, GS; Tung, L. Nuclear receptor coactivators and corepressors. *Mol. Endocrinol.,* 1996 10**,** 1167–1177.

[45] Tsai, M-J; O'Malley, BW. Molecular mechanisms of action of steroid/thyroid receptor superfamily members. *Annu. Rev. Biochem.,* 1994 63**,** 451–486.

[46] Nilsson, S; Gustafsson, JA. Biological role of estrogen and estrogen receptors. Crit. Rev. Biochem. Mol. Biol., 2002 37, 1–28.

[47] Macgregor, JI; Jordan, VC. Basic guide to the mechanisms of antiestrogen action. *Pharmacol. Rev*., 1998 50, 151–196.

[48] Couse, JF; Hewitt, SC; Bunch, DO; Sar, M; Walker, VR; Davis, BJ; Korach, KS. Postnatal sex reversal of the ovaries in mice lacking estrogen receptors α and β. *Science*. 1999 286, 2328–2331.

[49] Liu, MM; Albanese, C; Anderson, CM; Hilty, K; Webb, P; Uht, RM; Price, RH; Pestell, RG; Kushner, PJ. Opposing action of estrogen receptors α and β on cyclin D1 gene expression. *J. Biol. Chem.,* 2002 277, 24353–24360.

[50] Kuiper, GGJM; Carlsson, B; Grandien, K; Enmark, E; Haggblad, J;., Nilsson, S; Gustafsson, JA. Comparison of the ligand binding specificity and transcript tissue distribution of estrogen receptors α and β. *Endocrinology,* 1997 138, 863–870.

[51] Turner, RT; Riggs, BL; Spelsberg, TC. Skeletal effects of estrogen. *Endocrine Rev.*, 1994 15, 275–296.

[52] Onoe, Y; Miyaura, C; Ohta, H; Nozawa, S; Suda, T. Expression of estrogen receptor β in rat bone. *Endocrinology,* 1997 138, 4509–4512.

[53] Kuiper, GG; Lemmen, JG; Carlsson, B; Corton, JC; Safe, SH; van der Saag, PT; van der Burg, B; Gustafsson, JA. Interaction of estrogenic chemicals and phytoestrogens with estrogen receptor beta. *Neuroendocrinology*, 1998 139, 4252–4263.

[54] Setchell, KDR. Soy isoflavones-benefits and risks from nature's selective estrogen receptor modulators (SERMs). *J. Am. Coll. Nutr*., 2001 20, 354S–383S.

[55] Halbreich, U; Kahn, LS. Selective oestrogen receptor modulators–current and future brain and behaviour applications. Expert. Opin. *Pharmacother.,* 2000 1, 1385–1398.

[56] Raffaeli, B; Hoikkala, E; Leppä lä , E; Wä hä lä , K. Enterolignans. *J. Chromatr*., 2002 777, 29-43.

[57] Lotke, PS. Phytoestrogens: a potential role in hormone replacement therapy. *Prim. Care Update Ob/Gyns*., 1998 5, 290-295.

[58] Adams, NRJ. A changed responsiveness to oestrogens in ewes with clover disease. *Reprod. Fertil.,* 1981 suppl. 30, 223-230.

[59] Leopold, AS; Erwin, M; Oh, J; Browning, B. Phytoestrogens, adverse effects on reproduction in California quail. *Science,* 1976 191, 98–99.

[60] Setchell, KD; Gosselin, SJ; Welsh, MB; Johnston, JO; Balistreri, WF; Kramer, LW; Dresser, BL; Tarr, M. Dietary estrogens-a probable cause of infertility and liver disease in captive cheetahs. *Gastroenterology,* 1987a 93, 225–233.

[61] Setchell, KD; Gosselin, SJ; Welsh, MB; Johnston, JO; Balistreri, WF; Kramer, LW; Dresser, BL; Tarr, MJ. Dietary estrogens – a probable cause of infertility and liver disease in captive cheetahs. *Gastroenterology,* 1987b 93, 225–233.

[62] Dixon, RA; Ferreira, D. Genistein. *Phytochemistry,* 2002 60, 205-211.

[63] Reinli, K; Block, G. Phytoestrogen content of foods—a compendium of literature values. *Nutr. Cancer*, 1996 26, 123–148.

[64] Boker, LK; Van der Schouw, YT; De Kleijn, MJ; Jacques, PF; Grobbee, DE; Peeters, PH. Intake of dietary phytoestrogens by Dutch women. J. Nutr., 2002 132, 1319–1328.

[65] Wang, HJ; Murphy, PA. Isoflavone content in commercial soybean foods. *J. Agric. Food Chem*., 1994 42, 1666–1673.

[66] Wang, HJ; Murphy, PA. Isoflavone composition of American and Japanese soybeans in Iowa, effects of variety, crop year, and location. *J. Agric. Food Chem*., 1994 42, 1674–1677.

[67] Stevens, JF; Page, JE. Xanthumol and related prenylflavonoids from hops and beer: to your good health! *Phytochemistry,* 2004 65, 1317-1330.

[68] Birt, DF; Hendrich, S; Wang, W. Dietary agents in cancer prevention: flavonoids and isoflavonoids. *Pharmacol. Ther.,* 2001 90, 157-177.

[69] Dixon, RA; Ferreira, D. Genistein. Phytochemistry, 2002 60, 205– 211.

[70] Hodgson, JM; Croft, KD; Puddey, IB et al. Soybean isoflavonoids and their metabolic products inhibit in vitro lipoprotein oxidation in serum. *J. Nutr. Biochem.,* 1996 7, 664-669.

[71] Zhang, Y; Wang, G-J; Song, TT; Murphy, PA; Hendrich, S. Urinary disposition of the soybean isoflavones, daidzein, genistein and glycitein differs among humans with moderate fecal isoflavone degradation activity. *J. Nutr.*, 1999 129, 957-962.

[72] Adlercreutz, H; Fotsis, T; Kurzer, MS; Wahala, K; Makela, T; Brunow, G; Hase, T. Isotope dilution gas chromatographic- mass spectrometric method for the determination of unconjugated lignans and isoflavonoids in human feces, with preliminary results in omnivorous and vegetarian women. Anal. *Biochem.,* 1995 225, 101-108,

[73] Adlercreutz, H; Fotsis ,T; Lampe, J et al. Quantitative determination of lignans and isoflavonoids in plasma of omnivorous and vegetarian women by isotope dilution gas chromatography-mass spectrometry. *Scandinavian J. Clin. Lab. Invest.*, 1993 215, 5–18.

[74] Karr, SC; Lampe, JW; Hutchins, AM; Slavil, JL. Urinary isoflavonoid excretion in humans is dose dependent at low to moderate levels of soy-protein consumption. *Am. J. Clin. Nutr.,* 1997 66, 46–51.

[75] Setchel, KDR; Borriello, SP; Hulme, P; Kirk, DN; Axelson, M. Non-steroidal estrogens of dietary origin, a possible role in gut hormone metabolism. *Am. J. Clin. Nutr.*, 1984 40, 569–578.

[76] Morton, MS; Wilcox, G; Wahlgvist, ML; Griffitts, K. Determination of lignans and isoflavonoids in human female plasma following dietary supplementation. *J. Endocrinol.*, 1994 142, 251-259.

[77] Xu, X; Wang, H-J; Murphy, PA; Cook, L; Hendrich, S. Daidzein is a more bioavailable soymilk isoflavone than is genistein in adult women. *J. Nutr.,* 1994 124, 825-832,

[78] King, RA; Bursill, DB. Plasma and urinary kinetics of the isoflavones daidzein and genistein after a single soy meal in humans. *Am. J. Clin. Nutr.*, 1998 67, 867-872.

[79] Watanabe, S; Yamaguchi, M; Sobue, T; Miura, T; Arai, Y; Mazur, W, Wahala, K; Adlercreutz, H. Pharmacokinetics of soybean isoflavones in plasma, urine, and feces of men after ingestion of 60 g baked soybean powder (kinako). *J. Nutr.*, 1998 128, 1710-1715.

[80] Kudou, S; Fleury, Y; Welti, D et al. Malonyl isoflavone glycosides in soybean seeds (Glycine max MERRILL). Agric. Biol. Chem., 1991 55, 2227-2233.

[81] Barnes, S; Kirk, M; Coward L. Isoflavones and their conjugates in soy foods, extraction conditions and analysis by HPLC-mass spectrometry. *J. Agric. Food Chem.*, 1994 42, 2466-2474.

[82] Farmakalidis, E; Murphy, PA. Isolation of 6"-O-acetyldaidzein and 6"-O-acetylgenistein from toasted defatted soy flakes. J. Agric. Food Chem., 1985 33, 385-389.

[83] Coward, L; Barnes, NC; Setchell, KDR; Barnes, S. The antitumor isoflavones, genistein and daidzein, in soybean foods of American and Asian diets. *J. Agric. Food Chem.*, 1993 41, 1961-1967.

[84] King, RA; Broadbent, JL; Head, RJ. Absorption and excretion of the soy isoflavone genisteinin rats. *J. Nutr.,* 1996 126, 176-182.

[85] Sfakianos, J; Coward, L; Kirk, M; Barnes, S. Intestinal uptake and biliary excretion of the isoflavone genistein in the rat. J. Nutr., 1997 127, 1260-1268.

[86] Farmakalidis, E; Hathcock, JN; Murphy, PA. Oestrogenic potency of genistin and daidzin in mice. Food Chem. *Toxicol.,* 1985 23, 741–745.

[87] Markiewicz, L; Garey, J; Adlercreutz, H; Gurpide, E. In vitro bioassays of non-steroidal phytoestrogens. *J. Steroid Biochem. Mol. Biol.,* 1993 45, 399–405.

[88] Molteni, A; Brizio-Molteni, L; Persky, V. In vitro hormonal effects of soybean isoflavones. *J. Nutr.,* 1995 125, 751S–756S.

[89] Nagel, SE; vonSaal, FF; Welshons, WV. The effective free fraction of estradiol and xenoestrogens in human serum measured by whole cell uptake assays; physiology of delivery modifies estrogenic activity. Proc. Soc. Exp. Biol. Med., 1998 217, 300–309.

[90] Hol, T; Cox, MB; Bryant, HU; Draper, MW. Selective estrogen receptor modulators and postmenopausal women's health. *J. Women's Health,* 1997 6, 523– 531.

[91] Liu, J; Burdette, JE; Xu, H; Gu, C; van Breemen, RB; Bhat, KP; Booth, N; Constantinou, AI; Pezzuto, JM; Fong, HH; Farnsworth, NR; Bolton, JL. Evaluation of estrogenic activity of plant extracts for the potential treatment of menopausal symptoms. *J. Agric. Food Chem.,* 2001 49, 2472–2479.

[92] Davis, JN; Kucuk, O; Sarkar, FH. Expression of prostatespecific antigen is transcriptionally regulated by genistein in prostatecancer cells. Mol. Carcinog., 2002 34, 91–101.

[93] Wang, D; Gutkowska, J; Marcinkiewicz, M; Rachelska, G; Jankowski, M. Genistein supplementation stimulates the oxytocin system in the aorta of ovariectomized rats. *Cardiovasc. Res.,* 2003. 57, 186–194.

[94] Zhou, S; Turgeman, G; Harris Stephen, E; Leitman Dale, C., Komm Barry, S; Bodine Peter, V.N; Gazit, D. Estrogens activate bone morphogenetic protein-2 gene transcription in mouse mesenchymal stem cells. *Mol. Endocrinol.,* 2003 17, 56–66.

[95] Murrill, W; Brown, N; Zhang, J; Manzolillo, P; Barnes, S; Lamartiniere, CA. Prepubertal genistein exposure suppresses mammary cancer and enhances gland differentiation in rats. *Carcinogenesis,* 1996 17, 1451–1457.

[96] Fritz, WA; Wang, J; Lamartiniere, CA. Dietary genistein, perinatal mammary cancer prevention, bioavailability and toxicity testing in the rat. *Carcinogenesis,* 1998 19, 2151–2158.

[97] Fritz, WA; Eltoum, I-E; Cotroneo, MS; Lamartiniere, CA. Genistein alters growth but is not toxic to the rat prostate. *J. Nutr.,* 2002 132, 3007–3011.

[98] Yanagihara, K; Ito, A; Toge, T; Numoto, M. Antiproliferative effects of isoflavones on human cancer cell lines established from the gastrointestinal tract. *Cancer. Res.,* 1993 53, 5815–5821.

[99] Cotroneo, MS; Wang, W; Eltoum, IE; Lamartiniere, CA. Sex steroid receptor regulation by genistein in the prepubertal rat uterus. *Mol. Cell. Endocrinol.,* 2001 173, 135–145.

[100] Strauss, L; Makela, S; Joshi, S; Huhtaniemi, I; Santti, R; Genistein exerts estrogen-like effects in male mouse reproductive tract. *Mol. Cell. Endocrinol.,* 1998 144, 83–93.

[101] Fritz, WA; Wang, J; Eltoum, I-E; Lamartiniere, CA. Dietary genistein down-regulates androgen and estrogen receptor expression in the rat prostate. *Mol. Cell. Endocrinol.*, 2002 186, 89-99.

[102] Thompson, LU; Robb, P; Serraino, M; Cheung F. Mammalian lignan production from various foods. *Nutr.Cancer,* 1991 16, 43–52.

[103] Thompson, LU; Rickard, SE; Cheung, F et al. Variability in anticancer lignan levels in flaxseed. *Nutr. Cancer,* 1997 27, 26–30.

[104] Heinonen, S; Nurmi, T; Liukkonen, K; Poutanen, K; Wahala, K; Deyama T et al. In vitro metabolism of plant lignans, new precursors of mammalian lignans enterolactone and enterodiol. *J. Agric. Food Chem.*, 2001 49, 3178- 3186.

[105] Adlercreutz, H; Wang, GJ; Lapcik, O; Hampl, R; Wahala, K; Makela, T; Lusa, K; Talme, M; Mikola, H. Time-resolved fluoroimmunoassay for plasma enterolactone. *Anal. Biochem.*, 1998 265, 208–215.

[106] Dean, B; Chang, S; Doss, GA; King, C; Thomas, PE. Glucuronidation, oxidative metabolism, and bioactivation of enterolactone in rhesus monkeys. *Arch. Biochem. Biophys.,* 2004 429, 244-251.

[107] Setchell, KDR; Adlercreutz H. Mammalian lignans and phyto-estrogens. Recent studies on their formation, metabolism and biological role in health and disease. In: Rowland, IR, editor. Role of the Gut Flora in Toxicity and Cancer. *London: Academic Press,* 1988.

[108] Lampe, JW; Martini, MC; Kurzer, MS et al. Urinary lignan and isoflavonoid excretion in premenopausal women consuming flaxseed powder. *Am. J. Clin. Nutr.*, 1994 60, 122–128.

[109] Nesbitt, PD; Lam, Y; Thompson, LU. Human metabolism of mammalian lignan precursors in raw and processed flaxseed. *Am. J. Clin. Nutr,* 1999 69, 549–555.

[110] Duncun, AM; Phipps, WR; Kurzer, MS. Phyto-oestrogens. Best Pract. Res. Clin. *Endocrinol. Metab*., 2003 17, 273-271.

[111] Horner, NK; Kristal, AR; Prunty, J et al. Dietary determinants of plasma enterolactone. *Cancer Epidemiol. Biomarkers Prev.*, 2002 11, 121–126.

[112] Murphy, PA; Song, T., Buseman, G; Barua, K; Beecher, GR; Trainer, D; Holden, J. Isoflavones in retail and institutional soy foods. *J. Agric. Food Chem.*, 1999 47, 2697–2704.

[113] Wang, GS; Kuan, S; Francis, OJ; Ware, GM; Carman, AS. A simplified HPLC method for the determination of phytoestrogens in soybean and its processed products. *J. Agric. Food Chem.*, 1990 38, 185–190.

[114] Franke, AA; Custer, LJ; Cerna, CM; Narala, KK. Quantitation of phytoestrogens in legumes by HPLC. *J. Agric. Food Chem.*, 1994 42, 1905–1913.

[115] de Kleijn, MJ; van der Schouw, YT; Wilson, PW; Adlercreutz, H; Mazur, W; Grobbee, DE; Jacques, PF. Intake of dietary phytoestrogens is low in postmenopausal women in the United States. The Framingham study. *J. Nutr.,* 2001 131, 1826–1832.

[116] Whitten, PL; Naftolin, F. reproductive actions of phytoestrogens. *Bail. Clin. Endocrinol. Metab.*, 1998 12, 667-690.

[117] Milligan, S; Kalita, J; Pocock, V; Heyerick, A; De Cooman, L; Rong, H; De Keukeleire, D. Oestrogenic activity of the hop phyto-oestrogen, 8-prenylnaringenin. *Reproduction Bristol UK,* 2002 123, 235–242.

[118] Vinson, JA; Mandarano, M; Hirst, M; Trevithick, JR; Bose, P. Phenol antioxidant quantity and quality in foods, beers and the effect of two types of beer on an animal model of atherosclerosis. *J. Agric. Food Chem.*, 2003 51, 5528–5533.

[119] Stevens, JF; Miranda, CL; Frei, B; Buhler, DR. Inhibition of peroxynitrite-mediated LDL oxidation by prenylated flavonoids, the alpha, beta-unsaturated keto functionality of 20-hydroxychalcones as a novel antioxidant pharmacophore. *Chem. Res. Toxicol.*, 2003 16, 1277–1286.

[120] Schaefer, O; Humpel, M; Fritzemeier, KH; Bohlmann, R., Schleuning, WD. 8-Prenylnaringenin is a potent ERalpha selective phytoestrogen present in hops and beer. J. Steroid Biochem. Mol. Biol., 2003 84, 359–360.

[121] Schmitt, E; Lehmann, L; Metzler, M; Stopper, H. Hormonal and genotoxic activity of resveratrol. *Toxicol. Let.,* 2002 136, 133-142.

[122] Gehm, BD; McAndrews, JM; Chien, PY; Jameson, JL. Resveratrol, a polyphenolic compound found in grapes and wine, is an agonist for the estrogen receptor. *PNAS,* 1997 94, 14138–14143.

[123] Frankel, EN; Waterhouse, AL; Teissedre, PL. Principal phenolic phytochemicals in selected California wines and their antioxidant activity in inhibiting oxidation of human low-density lipoproteins. *J. Agric. Food Chem.,* 1995 43, 890–894.

[124] Creasy, LL; Creasy, MT. Grape chemistry and the significance of resveratrol, An Overview. *Pharm. Biol.,* 1998 36, 8–14.

[125] Fremont, L. Biological effects of resveratrol. *Life Sci.*, 2000 66, 663– 673,

[126] Lamikanra, O; Grimm, CC; Rodin, JB; Inyang, ID. Hydroxylated stilbenes in selected american wines. *J. Agric. Food Chem.,* 1996 44, 1111–1115.

[127] Sobolev, VS; Cole, RJ. trans-Resveratrol content in commercial peanuts and peanut products. *J. Agric. Food Chem.*, 1999 47, 1435–1439.

[128] Sanders, TAB; Dean, TS; Grainger, D; Miller, GJ; Wiseman, H. Moderate intakes of intact soy protein rich in isoflavones compared with ethanol-extracted soy protein increase HDL but do not influence transforming growth factor beta(1) concentrations

and hemostatic risk factors for coronary heart disease in healthy subjects. *Am. J. Clin. Nutr.,* 2002 76, 373–377.

[129] Vastano, BC; Chen, Y; Zhu, N; Ho, C-T; Zhou, Z; Rosen, RT. Isolation and identification of stilbenes in two varieties of *Polygonum cuspidatum*. J. Agric. Food Chem., 2000 48, 253–256.

[130] Powell, RG; TePaske, MR; Plattner, RD; White, JF; Clement, SL. Isolation of resveratrol from *Festuca versuta* and evidence for the widespread occurrence of this stilbene in the poaceae. *Phytochemistry*, 1994 35, 335–338.

[131] Mannila, E; Talvitie, A. Stilbenes from Picea abies bark. *Phytochemistry,* 1992 31, 3288–3289.

[132] Klinge, CM; Risinger, KE; Watts, MB; Beck, V; Eder, R; Jungbauer, A. Estrogenic activity in white and red wine extracts. J. Agric. Food Chem., 2003 51, 1850–1857.

[133] Bowers, JL; Tyulmenkov, VV; Jernigan, S.C; Klinge, CM. Resveratrol acts as a mixed agonist/antagonist for estrogen receptors alpha and beta. *Endocrinology*, 2000 141, 3657–3667.

[134] Brownson, DM; Azios, NG; Fuqua, BK; Dharmawardhane, SF; Mabry, TJ. Flavonoid effects relevant to cancer. *J. Nutr.*, 2002 132, 3482S–3489S.

[135] Cadenas, S; Barja, G. Resveratrol, melatonin, vitamin E, and PBN protect against renal oxidative DNA damage induced by the kidney carcinogen KBrO3. *Free Radical Biol. Med.*, 1999 26, 1531-1537.

[136] Lin, JK; Tsai, S.H. Chemoprevention of cancer and cardiovascular disease by resveratrol. *Proc. Natl. Sci. Counc. Repub. China*, 1999 B23, 99-106.

[137] Tominaga, S. Cancer incidence in Japanese in Japan, Hawaii, and western United States. *National Cancer Institute Monograph*, 1969 19, 83-92.

[138] Knight, DC; Eden, JA. A review of the clinical effects of phytoestrogens. *Obstet. Gynecol.*, 1996 87, 897–904.

[139] Ziegler, R; Hoover, R; Pike, M; Hildesheim, A; Nomura, A; West, D; Wu-Williams, A; Kolonel, L; Horn-Ross, P; Rosenthal, J. Migration patterns and breast cancer risk in Asian–American women. *J. Natl. Cancer Inst.*, 1993 85, 1819–1827.

[140] Shimizu, H; Ross, RK; Bernstein, L et al. Cancers of the prostate and breast among Japanese and white immigrants in Los Angeles County. Br. *J. Cancer,* 1991 63, 963-966.

[141] Traganos, F; Ardelt, B; Halko, N; Bruno, S; Darzynkiewicz, Z. Effects of genistein on the growth and cell cycle progression of normal human lymphocytes and human leukemic MOLT-4 and HL-60 cells. *Cancer Res*., 1992 52, 6200– 6208.

[142] Matsukawa, Y; Marui, N; Sakai, T; Satomi, Y; Yoshida, M;Matsumoto, K;Nishino, H; Aoike, A. Genistein arrests cell cycle progression at G2-M. *Cancer Res.,* 1993 53, 1328– 1331.

[143] Zhou, JR; Mukherjee, P; Gugger, ET; Tanaka, T; Blackbum, GL; Clinton, SK. Inhibition of murine bladder tumorigenesis by soy isoflavones via alterations in the cell cycle, apoptosis, and angiogenesis. *Cancer Res.*, 1998 58, 5231– 5238.

[144] Yoon, HS; Moon, SC; Kim, ND; Park, BS; Jeong, MH; Yoo, YH. Genistein induces apoptosis of RPE-J cells by opening mitochondrial PTP. *Biochem. Biophys. Res. Commun.*, 2000 276, 151–156.

[145] Baxa, DM; Luo, X; Yoshimura, FK. Genistein induces apoptosis in T lymphoma cells via mitochondrial damage. *Nutr. Cancer,* 2005 51, 93–101.

[146] Klein, CB; King, AA. Gensitein genotoxicity: Critical considerations of *in vivo* exposure dose. Toxicol. *Appl. Pharmacol.,* 2007 224, 1-11.

[147] Omenn, GS. What accounts for the association of vegetables and fruits with lower incidence of cancers and coronary heart diseases. *Ann. Epidemiol.,* 1995 5, 333– 335.

[148] Robak, J; Gryglewski, RJ. Flavonoids are scavengers of superoxide anion. *Biochem. Pharmacol.*, 1988 37, 83– 88.

[149] Torel, J; Cillard, J; Cillard, P. Antioxidant activity of flavonoids and reactivity with peroxy radical. Phytochemistry, 1986 25, 383–385.

[150] Husain, SR; Cillard, J; Cillard, P. Hydroxyl radical scavenging activity of flavonoids. *Phytochemistry*, 1987 26, 2489– 2491.

[151] Shahidi, F; Janitha, PK; Wanasundara, PD. Phenolic antioxidants. *Crit. Rev. Food Sc*i. *Nutr.*, 1992 32, 67– 103.

[152] Barnes, S. Phytoestrogens and breast cancer. *Bail. Clin. Endocrinol. Metab.,* 1998 12, 559-666.

[153] Cassidy, A; Bingham S; Setchell, KDR. Biological effects of isoflavones in young women, importance of the chemical composition of soyabean products. *Br. J. Nutr.*, 1995 74, 587–601.

[154] Adlercreutz, H; Mousavi, Y; Clark, J; Hockerstedt, K; Hamalainen, E; Wahala, K; Makela, TH; Hase, T. Dietary phytoestrogens and cancer, in vitro and in vivo studies. *J. Steroid Biochem. Mol. Biol.*, 1992 41, 331–337.

[155] Pino, AM; Valladares, LE; Palma, MA; Mancilla, AM; Yanez, M; Albala, C. Dietary isoflavones affect sex hormone-binding globulin levels in postmenopausal women. *J. Clin. Endocrinol. Metab.*, 2000 85, 2797–2800.

[156] Berrino, F; Bellati, C; Secreto, G; Camerini, E; Pala, V; Panico, S;Allegro, G; Kaaks, R. Reducing bioavailable sex hormones through a comprehensive change in diet, the diet and androgens (DIANA) randomized trial. *Cancer Epidemiol. Biomarkers Prev*., 2001 10, 25–33.

[157] Hutchins, AM; Martini, MC; Olson, BA; Thomas, W; Slavin, JL. Flaxseed consumption influences endogenous hormone concentrations in postmenopausal women. *Nutr. Cancer,* 2001 39, 58–65.

[158] Xu, X; Duncan, AM; Wangen, KE; Kurzer, MS. Soy consumption alters endogenous estrogen metabolism in postmenopausal women. *Cancer Epidemiol. Biomarkers Prev.*, 2000 9, 781–786.

[159] Nagata, C; Takatsuka, N; Inaba, S; Kawakami, N; Shimizu, H. Effect of soymilk consumption on serum estrogen concentrations in premenopausal Japanese women. *J. Natl. Cancer Inst.*, 1998 90, 1830–1835.

[160] Martini, MC; Dancisak, BB; Haggans, CJ; Thomas, W; Slavin, JL. Effects of soy intake on sex hormone metabolism in premenopausal women. *Nutr. Cancer,* 1999 34, 133–139.

[161] Maskarinec, G; Williams, AE; Inouye, JS; Stanczyk, FZ; Franke, AA. A randomized isoflavone intervention among premenopausal women. *Cancer Epidemiol. Biomarkers Prev.*, 2002 11, 195–201.

[162] Nicholls, J; Lasley Bill, L; Nakajima Steven, T; Setchell, KDR; Schneeman Barbara, O. Effects of soy consumption on gonadotropin secretion and acute pituitary responses to gonadotropin-releasing hormone in women. *J. Nutr.,* 2002 132, 708–714.

[163] Xu, X; Duncan, AM; Merz, BE; Kurzer, MS. Effects of soy isoflavones on estrogen and phytoestrogen metabolism in premenopausal women. *Cancer Epidemiol. Biomarkers Prev.*, 1998 7, 1101–1108.

[164] Haggans, CJ; Hutchins, AM; Olson, BA; Thomas, W; Martini, MC; Slavin, JL. Effect of flaxseed consumption on urinary estrogen metabolites in postmenopausal women. *Nutr. Cancer,* 1999 33, 188–195.

[165] Adlercreutz, H; Bannwart, C; Wahala, K et al. Inhibition of human aromatase by mammalian lignans and isoflavonoid phytoestrogens. *J. Steroid Biochem. Mol. Biol.*, 1993 44, 147–153.

[166] Krazeisen, A; Breitling, R; Moller, G; Adamski, J. Phytoestrogens inhibit human 17beta-hydroxysteroid dehydrogenase type 5. Mol. *Cell Endocrinol.*, 2001 171, 151–162.

[167] Dai, Q; Franke, AA; Jin, F., Shu, X-O; Hebert, JR; Custer, LJ; Cheng, J; Gao, Y-T; Zheng, W. Urinary excretion of phytoestrogens and risk of breast cancer among Chinese women in Shanghai. *Cancer Epidemiol. Biomarkers Prev.*, 2002 11, 815–821.

[168] Velasquez, MT; Bhathena, SJ. Dietary phytoestrogens: a possible role in renal disease protection. *Am. J. Kidney Disease,* 2001 37, 1056-1068.

[169] Barnes, S; Peterson, G; Coward, L. Rationale for the use of genistein containing soy matrices in chemoprevention trials for breast and prostate cancer. *J. Cell Biochem.*, 1995 22, 181–187.

[170] Messina, M; Barnes, S. The role of soy products in reducing risk of cancer. *J. Natl. Cancer Inst.*, 1991 83, 541–546.

[171] Kim, H; Peterson, TG; Barnes, S. Mechanisms of action of the soy isoflavone genistein, Emerging role for its effects via transforming growth factor-β signaling pathways. *Am. J. Clin. Nutr.*, 1998 68 (suppl 6), S1418-S1425.

[172] Zhu, Y; Lin, JH-C; Liao, H-L; Verna, L; Stemerman, MB. Activation of ICAM-I promoter by lysophosphatidylcholine, Possible involvement of protein tyrosine kinases. *Biochim. Biophys. Acta.*, 1997 1345, 93-98.

[173] Zhu, Y; Lin, JH-C; Liao, H-L; Friedli, O Jr; Verna, L; Marten, NW; Straus, DS; Stemerman, MB. LDL induces transcription factor activator protein-I in human endothelial cells. *Arterioscler. Thromb. Vasc. Biol.*, 1998 18, 473-480.

[174] Barnes, PJ; Karin, M. Nuclear factor-KB, A pivotal transcription factor in chronic inflammatory diseases. *N. Engl. J. Med.*, 1997 336, 1066-1071.

[175] Lan, Q; Mercurius, KO; Davies, PF. Stimulation of transcription factor NF-KB and AP-I in endothelial cells subjected to shear stress. *Biochem. Biophys. Res. Commun.,* 1994 201, 950-956,

[176] Lamartiniere, CA; Moore, JB; Brown, NA et al. Genistein suppresses mammary cancer in rats. *Carcinogenesis,* 1995 16, 2833-2840.

[177] Adlercreutz, H; Fotsis, T; Bannwart, C et al. Determination of urinary lignans and phytoestrogen metabolites, potential antioestrogens and anticarcinogens in urine of women on various habitual diets. *J. Steroid Biochem.,* 1986 25, 791–797.

[178] Pietinen, P; Stumpf, K; Mannisto, S; Kataja, V; Uusitupa, M; Adlercreutz, H. Serum enterolactone and risk of breast cancer, a case-control study in Eastern Finland. *Cancer Epidemiol. Biomarkers Prev.*, 2001 10, 339–344.

[179] Boccardo, F; Lunardi, G; Guglielmini, P; Parodi, M; Murialdo, R; Schettini, G; Rubagotti, A. Serum enterolactone levels and the risk of breast cancer in women with palpable cysts. Eur. *J. Cancer,* 2004 40, 84–89.

[180] Adlercreutz, H; Fotsis, T; Heikkinen, R et al. Excretion of the lignans enterolactone and enterodiol and of equol in omnivorous and vegetarian post-menopausal women and in women with breast cancer. *Lancet,* 1982 ii, 1295–1299.

[181] Ingram, D; Sanders, K; Kolybaba, M; Lopez, D. Case–control study of phyto-oestrogens and breast cancer. *Lancet,* 1997 350, 990–994.

[182] Thompson, LU. Experimental studies on lignans and cancer. *Bail. Clin. Endocrinol. Metab*., 1998 12, 691–705.

[183] Yuan, JM; Wang, QS; Ross, RK et al. Diet and breast cancer in Shanghai and Tianjin, China. *Br. J. Cancer*, 1995 71, 1353–1358.

[184] Key, TJ; Sharp, GB; Appleby, PN et al. Soya foods and breast cancer risk, a prospective study in Hiroshima and Nagasaki, Japan. *Br. J. Cancer,* 1999 81, 1248–1256.

[185] Horn-Ross, PL; John, EM; Lee, M et al. Phytoestrogen consumption and breast cancer risk in a multiethnic population, the Bay Area Breast Cancer Study. *Am. J. Epidemiol.*, 2001 154, 434–441.

[186] den Tonkelaar, I; Keinan-Boker, L; Veer, PV et al. Urinary phytoestrogens and postmenopausal breast cancer risk. Cancer Epidemiol. Biomarkers Prev., 2001 10, 223–228.

[187] Kilkkinen, A; Virtamo, J; Vartiainen, E; Sankila, R; Virtanen, MJ; Adlercreutz, H; Pietinen, P. Serum enterolactone concentration is not associated with breast cancer risk in a nested casecontrol study. Int. J. Cancer, 2004 108, 277–280.

[188] Trapman, J; Brinkmann, OA. The androgen receptor in prostate cancer. *Pathol. Res. Pract.*, 1996 192, 752–760.

[189] Lee, C; Sutkowski, DM; Sensibar, JA; Zelner, D; Kim, I; Amsel, I et al. Regulation of proliferation and production of prostate-specific antigen in androgen-sensitive prostatic cancer cells, LNCaP, by dihydrotestosterone. *Endocrinology*, 1995 136, 796–803.

[190] Russell, DW; Wilson, JD. Steroid 5 alpha-reductase, two genes/two enzymes. *Annu. Rev. Biochem*., 1994 63, 25–61.

[191] Russell, DW; Berman, DM; Bryant, JT; Cala, KM; Davis, D.L; Landrum CP et al. The molecular genetics of steroid 5 alpha-reductases. *Recent Prog. Horm. Res.*, 1994 49, 275–284.

[192] Feldman, BJ; Feldman, D. The development of androgen independent prostate cancer. *Nat. Rev. Cancer,* 2001 1, 34– 45.

[193] Reid, P; Kantoff, P; Oh, W. Antiandrogens in prostate cancer. *Invest. New Drugs*, 1999 17, 271–284.

[194] Klotz, L. Hormone therapy for patients with prostate carcinoma. *Cancer*, 2000 88, 3009–3014.

[195] Welshons, WV; Thayer, KA; Judy, BM; Taylor, JA; Curran, EM; vom Saal, FS. Large effects from small exposures. I. Mechanisms for endocrine-disrupting chemicals with estrogenic activity. *Environ. Health Perspect*., 2003 111, 994–1006.

[196] Jarred, RA; Cancilla, B; Prins, GS; Thayer, KA; Cunha, GR; Risbridger, GP. Evidence that estrogens directly alter androgen-regulated prostate development. *Endocrinology*, 2000 141, 3471–3477.

[197] Hirayama, T. Nutrition and cancer – a large scale cohort study. *Prog. Clin. Biol. Res*., 1986 206, 299–311.

[198] Onozawa, M; Kawamori, T; Baba, M; Fukuda, K; Toda, T; Sato H et al. Effects of a soybean isoflavone mixture on carcinogenesis in prostate and seminal vesicles of F344 rats. Jpn. *J. Cancer Res*., 1999 90, 393–398.

[199] Landstrom, M; Zhang, JX; Hallmans, G; Aman, P; Bergh, A; Damber JE et al. Inhibitory effects of soy and rye diets on the development of dunning R3327 prostate adenocarcinoma in rats. *Prostate,* 1998 36, 151–161.

[200] Pollard, M; Wolter, W. Prevention of spontaneous prostate related cancer in lobund-wistar rats by a soy protein isolate/isoflavone diet. *Prostate,* 2000 45, 101–105.

[201] Mentor-Marcel, R; Lamartiniere, CA; Eltoum, IE; Greenberg, NM; Elgavish, A. Genistein in the diet reduces the incidence of poorly differentiated prostatic adenocarcinoma in transgenic mice (TRAMP). *Cancer Res.*, 2001 61, 6777–6782.

[202] Fritz, WA; Wang, J; Eltoum, IE; Lamartiniere, CA. Dietary genistein down-regulates androgen and estrogen receptor expression in the rat prostate. Mol. Cell. *Endocrinol.*, 2002 186, 89–99.

[203] Jang, M; Pezzuto, JM. Cancer chemopreventive activity of resveratrol. Drugs Exp. *Clin. Res.*, 1999 25, 65–77.

[204] Landstrom, M; Zhang, JX; Hallmans, G; Aman, P; Bergh, A; Damber, JE et al. Inhibitory effects of soy and rye diets on the development of Dunning R3327 prostate adenocarcinoma in rats. *Prostate*, 1998 1–36, 151–161.

[205] Bylund, A; Zhang, JX; Bergh, A; Damber, JE; Widmark, A; Johansson, A et al. Rye bran and soy protein delay growth and increase apoptosis of human LNCaP prostate adenocarcinoma in nude mice. *Prostate,* 2000 42, 304–314.

[206] Sarkar, FH; Li, Y. Mechanisms of cancer chemoprevention by soy isoflavone genistein. *Cancer Metastasis Rev.*, 2002 21, 265–280.

[207] Castle, EP; Thrasher, JB. The role of soy phytoestrogens in prostate cancer. *Urol. Clin. North Am*., 2002 297, 1–81.

[208] Adlercreutz, H; Mazur, W; Bartels, P; Elomaa, V; Watanabe, S; Wahala, K et al. Phytoestrogens and prostate disease. *J. Nutr.*, 2000 130, 658S–659S.

[209] Hussain, M; Banerjee, M; Sarkar, FH; Djuric, Z; Pollak, MN; Doerge D et al. Soy isoflavones in the treatment of prostate cancer. *Nutr. Cancer,* 2003 47, 111–117.

[210] Hess-Wilson, JK; Knudsen, KE. Endocrine disrupting compounds and prostate cancer. *Cancer Let.*, 2006 241, 1-12.

[211] Nagata, C; Inaba, S; Kawakami, N. Inverse association of soy product intake with serum androgen and estrogen concentrations in Japanese men. *Nutr. Cancer,* 2000 36, 14–18.

[212] Kuiper, GG; Carlsson, B; Grandien, K. Cloning of a novel estrogen receptor expressed in a rat prostate and ovary. *Proc. Natl. Acad. Sci.*, 1996 93, 5925–5930.

[213] Barnes, S. Role of phytochemicals in prevention and treatment of prostate cancer. *Epidemiol. Rev.*, 2001 23, 102–105.

[214] Demark-Wahnefried, W; Price, DT; Polascik, TJ; Robertson, CN; Anderson, EE; Paulson, DF et al. Pilot study of dietary fat restriction and flaxseed supplementation in men with prostate cancer before surgery, exploring the effects on hormonal levels, prostate-specific antigen, and histopathologic features. *Urology,* 2001 58, 47–52.

[215] Weber, KS; Setchell, KD; Stocco, DM; Lephart, ED. Dietary soy-phytoestrogens decrease testosterone levels and prostate weight without altering LH, prostate 5 alpha-reductase or testicular steroidogenic acute regulatory peptide levels in adult male sprague-dawley rats. *J. Endocrinol.*, 2001 170, 591–599.

[216] Kato, K; Takahashi, S; Cui, L; Toda, T; Suzuki, S; Futakuchi M et al. Suppressive effects of dietary genistin and daidzin on rat prostate carcinogenesis. Jpn. *J. Cancer Res.*, 2000 91, 786–791.

[217] Hempstock, J; Kavanagh, JP; George, NJ. Growth inhibition of prostate cell lines in vitro by phyto-oestrogens. Br. *J. Urol.,* 1998 82, 560–563.

[218] Santibanez, JF; Navarro, A; Martinez, J. Genistein inhibits proliferation and in vitro invasive potential of human prostatic cancer cell lines. *Anticancer Res.*, 1997 17, 1199–1204.

[219] Lee, MM; Wang, RT; Hsing, AW et al. Case–control study of diet and prostate cancer in China. *Cancer Causes Control*, 1998 9, 545–552.

[220] Oishi, K; Okada, K; Yoshida, O et al. A case–control study of prostatic cancer with reference to dietary habits. *Prostate,* 1988 12, 179–190.

[221] Hirayama, T. Epidemiology of prostate cancer with special reference to the role of diet. *National Cancer Institute Monograph,* 1979 53, 149–155.

[222] Nagata, C; Shimizu, H; Takami, R; Hayashi, M; Takeda, N; Yasuda, K. Soy product intake and hot flashes in Japanese women. *Am. J. Epidemiol.*, 2001 153, 790–793.

[223] Han, KK; Soares, JM Jr; Haidar, MA; de Lima, GR; Baracat, EC. Benefits of soy isoflavone therapeutic regimen on menopausal symptoms. *Obstet. Gynecol.,* 2002 99, 389–394.

[224] Krebs, EE; Ensrud, KE; MacDonald, R; Wilt, TJ. Phytoestrogens for treatment of menopausal symptoms, a systematic review. *Obstet. Gynecol*., 2004 104, 824–836.

[225] Baber, RJ; Templeman, C; Morton, T; Kelly, GE; West, L. Randomized placebo-controlled trial of an isoflavone supplement and menopausal symptoms in women. *Climacteric,* 1999 2, 85–92.

[226] Messina, M; Hughes, C. Efficacy of soyfoods and soybean isoflavone supplements for alleviating menopausal symptoms is positively related to initial hot flush frequency. *J. Med. Food,* 2003 6, 1–11.

[227] Barnes S. Phyto-oestrogens and osteoporosis, what is a safe dose? Br. *J. Nutr*. 2003 89, 101–108.

[228] Tempfer, CB; Bentz, E-K; Leodolter, S; Tscherne, G; Reuss, F; Cross, HS; Huber, JC. Phytoestrogens in clinical practice: a review of the literature. Fertil. *Steril.,* 2007 87, 1243-1249.

[229] Albertazzi, P; Pansini, F; Bonaccorsi, G; Zanotti, L; Forini, E; De Aloysio, D. The effects of soy supplementation on hot flushes. Obstet. Gynecol., 1998 91, 6 –11.

[230] Dalais, FS; Rice, GE; Wahlqvist, ML et al. Effects of dietary phytoestrogens in post-menopausal women. *Climacteric*, 1998 1, 124–129.

[231] van Patten, CL; Olivotto, IA; Chambers, GK et al. Effect of soy phytoestrogens on hot flushes in postmenopausal women with breast cancer, a randomized, controlled clinical trial. *J. Clin. Oncol.*, 2002 20, 1449–1455.

[232] Brzezinski, A; Adlercreutz, H; Shaoul, R et al. Short-term Effects of phytoestrogen-rich diet on postmenopausal women. *J. bNorth Am. Menopause Soc*., 1997 4, 89–94.

[233] Scambia, G; Mango, D; Signorile, PG et al. Clinical effects of a standardazided soy extract in postmenopausal women, a pilot study. *Menopause*, 2000 2, 150–151.

[234] Baber, RJ; Templeman, C; Morton, T; Kelly, GE; West L. Randomised placebo-controlled trial of an isoflavone supplement and menopausal symptom in women. *Climacteric*, 1999 2, 85–92.

[235] Yamaguchi, M. Isoflavone and bone metabolism, its cellular mechanism and preventive role in bone loss. *J. Health Sci.*, 2002 48, 209–222.

[236] Hays, J; Ockene, JK; Brunner, RL; Kotchen, JM; Manson, JE; Patterson, RE; Aragaki, AK; Shumaker, SA; Brzyski, RG; LaCroix, AZ; Granek, IA; Valanis, BG., Women's Health Initiative Investigators. Effects of estrogen plus progestin on health related quality of life. N. Engl. *J. Med.,* 2003 348, 1835–1837.

[237] Lauderdale, DS; Jacobsen, SJ; Furner, SE et al. Hip fracture incidence among elderly Asian–American populations. *Am. J. Epidemiol.*, 1997 146, 502–509.

[238] Alekel, DL; Germain, AS; Peterson, CT; Hanson, KB; Stewart, JW; Toda, T. Isoflavone-rich soy protein isolate attenuates bone loss in the lumbar spine of perimenopausal women. *Am. J. Clin. Nutr.*, 2000 72, 844–852.

[239] Mei, J; Yeung, SS; Kung, A.W. High dietary phytoestrogen intake is associated with higher bone mineral density in postmenopausal but not premenopausal women. *J. Clin. Endocrinol. Metab.,* 2001 86, 5217–5221.

[240] Morabito, N; Crisafulli, A; Vergara, C; Gaudio, A; Lasco, A; Frisina, N; D'Anna, R; Corrado, F; Pizzoleo, MA; Cincotta, M; Altavilla, D; Ientile, R; Squadrito, F. Effects of genistein and hormone-replacement therapy on bone loss in early postmenopausal women, a randomized double-blind placebo-controlled study. *J. Bone Mineral Res*., 2002 17, 1904–1912.

[241] Potter, S; Baum, J; Teng, H; Stillman, R; Shay, N; Erdman Jr, J. Soy protein and isoflavones, their effects on blood lipids and bone density in postmenopausal women. *Am. J. Clin. Nutr.,* 1998 68, 1375-1379.

[242] Cross, HS; Kallay, E; Lechner, D; Gerdenitsch, W; Adlercreutz, H; Armbrecht, HJ. Phytoestrogens and vitamin D metabolism, a new concept for the prevention and therapy of colorectal, prostate and mammary carcinomas. *J. Nutr.,* 2004 134, 1207–1212.

[243] Gennari, C; Agnusdei, D; Crepaldi, G et al. Effect of ipriflavone—a synthetic derivative of natural isoflavones—on bone mass loss in the early years after menopause. *Menopause,* 1998 5, 9–15.

[244] Yoshida, K; Tsukamoto, T; Torii, H et al. Metabolism of ipriflavone (TC-80) in rats. Radioisotopes, 1985 34, 612–617.

[245] Gambacciani, M; Spinetti, A; Piaggesi, L et al. Ipriflavone prevents the bone mass reduction in premenopausal women treated with gonadotropin hormone-releasing hormone agonists. Bone Mineral, 1994 26, 19–26.

[246] Tsutsumi, N. Effect of coumestrol on bone metabolism in organ culture. *Biol. Pharm. Bull.*, 1995 18, 1012-1015.

[247] Akiyama, T; Ishida, J; Nakagawa, S et al. Genistein, a specific inhibitor of tyrosine-specific protein kinases. *J. Biol. Chem.*, 1987 262, 5592-5595.

[248] Okura, A; Arakawa, H; Oka, H et al. Effect of genistein on topoisomerase activity and the growth of val 12 H-ras-transformed NIH3T3 cells. *Biochem. Biophy. Res. Comm.*, 1988 157, 183-189.

[249] Watson, CS; Pappas, TC; Gametchu, B. The other estrogen receptor in the plasma membrane, implications for the actions of environmental estrogens. *Environ. Health Persp.,* 1995 103 (suppl. 7), 41-50.

[250] Williams, JE; Jordan, SE; Barnes, S; Blair, HC. Tyrosine kinase inhibitor effects on osteoclastic acid transport. *Am. J.Clin. Nutr.*, 1998 68, 13 695 13 745.

[251] Kreijkamp-Kaspers, S; Kok, L; Grobbee, DE; de Haan, EH; Aleman, A; Lampe, JW; van der Schouw, YT. Effect of soy protein containing isoflavones on cognitive function, bone mineral density, and plasma lipids in postmenopausal women, a randomized controlled trial. *JAMA*, 2004 292, 65–74.

[252] Beaglehole, R. International treands in coronary heart disease mortality, morbidity and risk factors. Epidemiol. Rev., 1990 12, 1–15.

[253] Rubanyi, GM; Johns, A; Kauser, K. Effect of estrogen on endothelial function and angiogenesis. *Vasc. Pharmacol.,* 2002 38, 89–98.

[254] Washburn, S; Burke, GL; Morgan, T; Anthony, M. Effect of soy protein supplementation on serum lipoproteins, blood pressure, and menopausal symptoms in perimenopausal women. *Menopause,* 1999 6, 7–13.

[255] Merz-Demlow, BE; Duncan, AM; Wangen, KE; Xu, X; Carr, TP; Phipps, WR; Kurzer, MS. Soy isoflavones improve plasma lipids in normocholesterolemic, premenopausal women. *Am. J. Clin. Nutr.*, 2000 71, 1462–1469.

[256] Lucas, EA; Wild, RD; Hammond, LJ; Khalil, DA; Juma, S; Daggy, BP; Stoecker, BJ; Arjmandi, BH. Flaxseed improves lipid profile without altering biomarkers of bone metabolism in postmenopausal women. J. Clin. Endocrinol. *Metab.,* 2002 87, 1527–1532.

[257] Cruz, ML; Wong, WW; Mimouni, F; Hachey, DL; Setchell, KD; Klein, PD; Tsang, RC. Effects of infant nutrition on cholesterol synthesis rates. *Pediatr. Res.,* 1994 35, 135–140.

[258] Anderson, JW; Johnstone, BM; Cook-Newell, ME. Metaanalysis of the effects of soy protein intake on serum lipids. New Engl. *J. Med.*, 1995 333, 276–282.

[259] Sirtori, CR; Galli, G; Lovati, MR; Cxarrara, P; Bosisio, E; Kienle, MG. Effects of dietary proteins on regulation of liver lipoprotein receptors in rats. *J. Clin. Nutr.,* 1998 114, 1493–1500.

[260] Baum, JA; Teng, H; Erdman, JW et al. Long-term intake of soy protein improves blood lipids profiles and increases mononuclear cell LDL receptor mRNA in hypocholesterolemic postmenopausal women. *Am. J. Clin. Nutr.*, 1998 68, 545–551.

[261] Jenkins, DJ; Kendall, CW; Vidgen, E et al. Health aspects of partially defatted flaxseed, including effects on serum lipids, oxidative measures, and in vivo androgen and progestin activity, a controlled crossover trial. *Am. J. Clin. Nutr.*, 1999 69, 395–402.

[262] Witztum, JL; Steinberg, D. Role of oxidized low density lipoprotein in atherogenesis. *J. Clin. Inv.*, 1991 88, 1785-1792.

[263] Simoncini, T; Fornari, L; Mannella, P; Caruso, A; Garibaldi, S; Baldacci, C; Genazzani AR. Activation of nitric oxide synthesis in human endothelial cells by red clover extracts. *Menopause*, 2005 12, 69–77.

[264] Gottstein, N; Ewins, BA; Eccleston, C; Hubbard, GP; Kavanagh, IC; Minihane, AM et al. Effect of genistein and daidzein on platelet aggregation and monocyte and endothelial function. Br. *J. Nutr.,* 2003 89, 607–616.

[265] Howes, JB; Sullivan, D; Lai, N; Nestel, P; Pomeroy, S; West, L; Eden, JA; Howes, LG. The effects of dietary supplementation with isoflavones from red clover on the lipoprotein profiles of post menopausal women with mild to moderate hypercholesterolaemia. *Atherosclerosis,* 2000 152, 143–147.

[266] Dewell, A; Hollenbeck Clarie, B; Bruce, B. The effects of soy-derived phytoestrogens on serum lipids and lipoproteins in moderately hypercholesterolemic postmenopausal women. J. Clin. Endocrinol. *Metab.,* 2002 87, 118–121.

[267] De Kleijn, MJJ; Van der Schouw, YT; Wilson, PWF; Grobbee, DE; Jacques, PF. Dietary intake of phytoestrogens is associated with a favorable metabolic cardiovascular risk profile in postmenopausal US. women, the Framingham Study. *J. Nutr.*, 2002 132, 276–282.

[268] Van der Schouw, YT; Pijpe, A; Lebrun, CEI; Bots, ML; Peeters, PHM; Van Straveren, WA; Lamberts, SWJ; Grobbee, DE. Higher usual dietary intake of phytoestrogens is associated with lower aortic stiffness in postmenopausal women. Arterioscler. Thromb. *Vasc. Biol.*, 2002 22, 1316–1322.

[269] Fotsis, T; Pepper, MS; Montesano, R; Aktas, E; Breit, S; Schweigerer, L; Rasku, S; Wä hä lä , K; Adlercreutz, H. Phtoestrogens and inhibition of angiogenesis. Bail. Clin. Endocrinol. *Metab.,* 1998 12, 649-666.

[270] Denekamp, J. Vascular attack as a therapeutic strategy for cancer. *Cancer Metab. Rev.*, 1990 9, 267-282.

[271] Folkman, J. Tumor angiogenesis. *Adv. Cancer Res.*, 1985 43, 175-203.

[272] Pepper, MS; Montesano, R. Proteolytic balance and capillary morphogenesis. Cell Differentiation and Development, 1990 32, 319-328.

[273] Folkman, J; Klagsbrun, M. Angiogenic factors. *Science,* 1987 235, 442-447.

[274] Montesano, R; Vassalli, J-D; Baird, A et al. Basic fibroblast growth factor induces angiogenesis in vitro. *Proc. Nat. Acad. Sci. USA,* 1986 83, 7297-7301.

[275] Fotsis, T; Pepper, M; Adlercreutz, H et al. Genistein a dietary-derived inhibitor of *in vitro* angiogenesis. *Proc. Nat. Acad. Sci. USA,* 1993 90, 2690-2694.

[276] Byers, M; Kuiper, GGJM; Gustafsson, JA; Park-Sarge, OK. Estrogen receptor-mRNA expression in rat ovary, down-regulation by gonadotropins. Mol. *Endocrinol.*, 1997 11, 172-182.

[277] Wang, W; Tanaka, Y; Hau, Z; Higuchi, CM. Proliferative response of mammary glandular tissue to formononetin. *Nutr. Cancer,* 1995 23, 131-140.

[278] Santell, RC; Chang, YC; Nair, MG; Helferich, WG. Dietary genistein exerts estrogenic effects upon the uterus, mammary gland, and the hypothalamic/pituitary axis in rats. *J. Nutr.*, 1997 127, 263-269.

[279] Cassidy, A. Phytoestrogens, a possible alternative to HRT? *J. Br. Menopause Soc*., 1998 suppl. SI, 10-11.

[280] Cassidy, A; Bingham, S; Setchell, KDR. Biological effects of a diet of soy protein rich in isoflavones on the menstrual cycle of premenopausal women. Am. *J. Clin. Nutr.*, 1994 60, 333-340.

[281] Coldham, NG; Dave, M; Sivapathasundaram, S et al. Evaluation of a recombinant yeast cell estrogen screening assay. Environ. *Health Perspectives,* 1997 105, 734-742.

[282] Dodge, JA; Glasebrook, AL; Magee, DE et al. Environmental estrogens, effects on cholesterol lowering and bone in the ovariectomized rat. *J. Steroid Biochem. Mol. Biol.*, 1996 59, 155-161.

[283] Nwannenna, AI; Madej, A; Lundh, TJO; Fredriksson, G. Effects of oestrogenic silage on some clinical and endocrinological parameters in ovariectomized heifers. *Acta Veterinaria Scandinavica*, 1994 35, 173.

[284] Tansey, G; Hughes, CLJ; Cline, JM et al. Effects of dietary soybean estrogens on the reproductive tract in female rats. *Proc. Soc. Exp. Biol. Med*., 1998 217, 340-344.

[285] Clarkson, TB; Anthony, MS; Williams, JK et al. The potential of soybean phytoestrogens for postmenopausal hormone replacement therapy. *Proc. Soc. Exp. Biol. Med.,* 1998 217, 365-368.

[286] Cline, JM; Paschold, JC; Adams, MS et al. Effects of hormonal therapies and dietary soy phytoestrogens on vaginal cytology in surgically postmenopausal macaques. *Fertil. Steril.,* 1996 65, 1031-1035.

[287] Stammel, W; Thomas, H; Staib, W; Kuhn-Velten, WN. Tetrahydroisoquinoline alkaloids mimic direct but not receptor-mediated inhibitory effects of estrogens and phytoestrogens on testicular endocrine function. Possible significance for Leydig insufficiency in alcohol addiction. *Life Sciences*, 1991 49, 1319-1329.

[288] Anthony, MS; Clarkson, TB; Bullock, BC; Wagner, JD. Soy protein versus soy phyotestrogens in the prevention of diet-induced coronary artery atherosclerosis of male cynomologus monkeys. Arterioscler. Thromb. *Vasc. Biol.*, 1997 17, 2524-2531.

[289] Anthony, MS; Clarkson, TB; Hughes, CL Jr et al. Soybean isoflavones improve cardiovascular risk factors without affecting the reproductive system of peripubertal rhesus monkeys. *J. Nutr.*, 1996 126, 43-50.

[290] Whitten, PL; Naftolin, F. Xenoestrogens and neuroendocrine development. In: Needleman, HL; Bellinger, D, editor. Prenatal Exposure to Environmental Toxicants, Developmental Consequences. Baltimore: *Johns Hopkins University Press,* 1994, 269-293.

[291] Toppari, J; Larsen, JC; Christiansen, P et al. Male reproductive health and environmental xenoestrogens. *Environ. Health Perspectives,* 1996 104, 741-803.

[292] Gallo, D; Cantelmo, F; Distefano, M; Ferlini, C; Zannoni, GF; Riva, A; Morazzoni, P; Bombardelli, E; Mancuso, S; Scambia, G. Reproductive effects of dietary soy in female Wistar rats. Food Chem. *Toxicol.*, 1999 37, 493-502.

[293] Murphy, PA; Song, TT; Buseman, G; Barua, K. Isoflavones in soy-based infant formulas. J.Agric. *Food Chem.*, 1997 45, 4635-4638.

[294] Setchell, KDR; Zimmer-Nechemias, L; Cai, J; Heubi, JE. Exposure of infants to phytooestrogens from soy-based infant formula. *Lancet,* 1997 350, 23-27.

[295] Barnes, S. Effect of genistein on in vitro and in vivo models of cancer. *J. Nutr.;* 1995 125, S777.

[296] Levy, JR; Faber, KA; Ayyash, L; Hughes, CL Jr. The effect of prenatal exposure to the phytoestrogen genistein on sexual differentiation in rats. *Proc. Soc. Exp. Biol. Med*., 1995 208, 60-66.

[297] McClain, RM; Wolz, E; Davidovich, A; Edwards, J; Bausch, J. Reproductive safety studies with genistein in rats. Food Chem. *Toxicol.,* 2007 45, 1319-1332.

[298] Medlock, KL; Branham, WS; Sheehan, DM. Effects of coumestrol and equol on the developing reproductive tract of the rat. *Proc. Soc. Exp. Biol. Med.*, 1995 208, 67-71.

[299] Whitten, PL; Lewis, C; Naftolin, F. A phytoestrogen diet induces the premature anovulatory syndrome in lactationally exposed female rats. *Biol. Reprod.*, 1993 49, 1117-1121.

[300] Burroughs, CD. Long-term reproductive tract alterations in female mice treated neonatally with coumestrol. Proc. Soc. Exp. *Biol. Med.*, 1995 208, 78-81.

[301] Russo, J; Russo, IH. Biological and molecular bases of mammary carcinogenesis. *Lab. Investigations*, 1987 57, 112-137.

[302] Lopez, J; Ogren, L; Verjan, R; Talamantes, F. Effects of perinatal exposure to a synthetic estrogen and progestin on mammary tumorigenesis in mice. *Teratology,* 1988 38, 129-134.

[303] Murrill, WB; Brown, NM; Zhang, J et al. Prepubertal genistein exposure suppresses mammary cancer and enhances gland differentiation in rats. *Carcinogenesis,* 1997 17, 1451.

[304] Lamartiniere, CA; Murrill, WB; Manzolillo, PA et al. Genistein alters the ontogeny of mammary gland development and protects against chemically-induced mammary cancer in rats. Proc. Soc. Exp. *Biol. Med.*, 1998 217, 358-364.

[305] Pan, Y; Anthony, M; Clarkson, TB. Effect of estradiol and soy phytoestrogens on choline acetyltransferase and nerve growth factor mRNAs in the frontal cortex and hippocampus of female rats. Proc. Soc. Exp. *Biol. Med.*, 1999 221, 118–125.

[306] Pan, Y; Anthony, M; Clarkson, TB. Evidence for up-regulation of brain-derived neurotrophic factor mRNA by soy phytoestrogens in the frontal cortex of retired breeder female rats. *Neurosci. Lett.*, 1999 261, 17–20.

[307] Kim, H; Xia, H; Li, L; Gewin, J. Attenuation of neurodegeneration-relevant modifications of brain proteins by dietary soy. *Biofactors,* 2000 12, 243–250.

[308] Gamache, PH; Maher, TJ; Setchell, KDR; Wu, T-H; Acworth, IN. The transfer of non-steroidal dietary estrogens into brain. *Soc. Neurosci. Abstr.*, 1996 22, 1967.

[309] Arnold, AP; Gorski, RA. Gonadal steroid interaction of structural sex differences in the central nervous system. Annu. Rev. *Neurosci.*, 1984 7, 413–422.

[310] Davis, SR; Shryne, JE; Gorski, RA. A revised critical period for the sexual differentiation of the sexually dimorphic nucleus of the preoptic area in the rat. *Neuroendocrinology*, 1995 62, 579–585.

[311] Simerly, RB. Organization and regulation of sexually dimorphic neuroendocrine pathways. Behav. *Brain Res.*, 1998 92, 195–203.

[312] De Jonge, FH; Louwerse, AL; Ooms, P; Evers, MP; Endert, E; van de Poll, NE. Lesions of the SDN-POA inhibit sexual behavior of Wistar rats. *Brain Res. Bull.*, 1987 23, 483–492.

[313] Faber, KA; Hughes Jr., CL. The effect of neonatal exposure to diethylstilbestrol, genistein, and zearalenone on pituitary responsiveness and sexually dimorphic nucleus volume in the castrated adult rat. *Biol. Reprod.*, 1991 45, 649–653.

[314] Faber, KA; Hughes Jr., CL. Dose–response characteristics of neonatal exposure to genistein on pituitary responsiveness to gonadotropin releasing hormone and volume of the sexually dimorphic nucleus of the preoptic area (SDN-POA) in postpubertal castrated female rats. Reprod. *Toxicol.*, 1993 7, 35–39.

[315] Lephart, ED; Rhees, RW; Setchell, KDR; Bu, LH; Lund, TD. Estrogens and phytoestrogens, brain plasticity of sexually dimorphic brain volumes. *J. Steroid Biochem. Mol. Biol*., 2003 85, 299–309.

[316] Celotti, F; Melcangi, C; Martini, L. The 5a-reductase in the brain, Molecular aspects and relation to brain function. Front. *Neuroendocrinol.*, 1992 13, 163–215.

[317] Celotti, F; Negri-Cesi, P; Poletti, A. Steroid metabolism in the mammalian brain, 5 alpha-reduction and aromatization. Brain Res. *Bull.*, 1997 44, 365–375.

[318] Lephart, ED. A review of brain 5a-reductase: Cellular, enzymatic and molecular perspectives and implications for biological function. Mol. Cell *Neurosci.*, 1993 4, 473–484.

[319] Lephart, ED. A review of brain aromatase cytochrome P450. *Brain Res. Rev.*, 1996 22, 1–26.

[320] MacLusky, NJ; Naftolin, F. Sexual differentiation of the central nervous system. *Science*, 1981 211, 1294–1302.

[321] Roselli, CE; Horton, LE; Resko, JA. Distribution and regulation of aromatase activity in the rat hypothalamus and limbic system. *Endocrinology*, 1985 117, 2471–2476.

[322] Lephart, ED. A review of brain 5a-reductase, cellular, enzymatic, and molecular perspectives and implications for biological function. Mol. Cell. *Neurosci.,* 1993 4, 473–484.

[323] Naftolin, F. Brain aromatization of androgens. *J. Reprod. Med*., 1994 39, 257– 261.

[324] Garcia-Segura, LM; Azcoitia, I; DonCarlos, LL. Neuroprotection by estradiol. Prog. *Neurobiol.*, 2001 63, 29–60.

[325] Simpkins, JW; Green, PS; Gridley, KE; Singh, M; de Fiebre, NC; Rajakumar, G. Role of estrogen replacement therapy in memory enhancement and the prevention of neuronal loss associated with Alzheimer's disease. *Am. J. Med.*, 1997 103, 19S–25S.

[326] Fink, G; Sumner, BE; McQueen, JK; Wilson, H; Rosie, R. Sex steroid control of mood, mental state and memory. Clin. Exp. Pharmacol. *Physiol.*, 1998 25, 764–775.

[327] Sherwin, BB. Estrogen and cognitive function in women. *Proc. Soc. Exp. Biol. Med*., 1998 217, 17–22.

[328] Martini, L; Melcangi, RC; Maggi, R. Androgen and progesterone metabolism in the central and peripheral nervous system. J. Steroid Biochem. *Mol. Biol.*, 1993 47, 195–205.

[329] Negri-Cesi, P; Poletti, A; Celotti, F. Metabolism of steroids in the brain: a new insight into the role of 5 alpha-reductase and aromatase in brain differentiation and functions. J. Steroid Biochem. *Mol. Biol.*, 1996 58, 455–466.

[330] MacLusky, NJ; Clark, CR; Shanabrough, M; Naftolin, F. Metabolism and binding of androgens in the spinal cord of the rat. *Brain Res*., 1987 422, 83–91.

[331] Lephart, ED; Ladle, DR; Jacobson, NA; Rhees, RW. Inhibition of brain 5 alpha-reductase in pregnant rats, effects on enzymatic and behavioral activity. *Brain Res*., 1996 739, 356–360.

[332] Weber, KS; Jacobson, NA; Setchell, KDR; Lephart, ED. Brain aromatase and 5α-reductase, regulatory behaviors and testosterone levels in adult rats on phytoestrogen diets. *Proc. Soc. Exp. Biol. Med.*, 1999 22, 131–135.

[333] Iacopino, AM; Quintero, EM; Miller, EK. Calbindin-D a 28-K potential neuroprotective protein. *Neurodegeneration,* 1994 3, 1–20.

[334] Lephart, ED; Thompson, JM; Setchell, KDR; Adlercreutz, H; Weber, KS. Phytoestrogens decrease brain calbindin-binding proteins but do not alter hypothalamic androgen metabolizing enzymes in adult male rats. *Brain Res*., 2000 859, 123–131.

[335] Taylor, H; Quintero, EM; Iacopino, AM; Lephart, ED. Phytoestrogens alter hypothalamic calbindin-D28K levels during prenatal development. *Dev. Brain Res*., 1999 114, 277–281.

[336] D'Amico, G; Gentile, MG; Manna, G; Fellin, G; Ciceri, R; Cofano, F; Petrini, C; Lavarda, F; Perolini, S; Porrini, M. Effect of vegetarian soy diet on hyperlipidaemia in nephritic syndrome. *Lancet,* 1992 339, 1131-1134.

[337] Gentile, MG; Fellin, G; Cofano, E; Delle Fave, A; Manna, G; Ciceri, R; Petrini, C; Lavarda, E; Pozzi, F; D'Amico, G. Treatment of proteinuric patients with a vegetarian soy diet and fish. Clin. *Nephrol.,* 1993 40, 315-320.

[338] Clark, WE; Parbtani, A; Huff, MW; Spanner, E; de Salis, H; Chin-Yee, I; Philbrick, DJ; Holub, BJ. Flaxseed, A potential treatment for lupus nephritis. *Kidney Int.*, 1995 48, 475-480.

[339] Pelkmans, L; Helenius, A. Insider information, what viruses tell us about endocytosis. Curr. Opin. Cell. *Biol.*, 2003 15, 414–422.

[340] Smith, AE; Helenius, A. How viruses enter cells. *Science,* 2004 304, 237– 242.

[341] Pelkmans, L; Helenius, A. Endocytosis via caveolae. *Traffic,* 2002 3, 311–320.

[342] Pelkmans, L; Puntener, D; Helenius, A. Local actin polymerization and dynamin recruitment in SV40-induced internalization of caveolae. *Science,* 2002 296, 535–539.

[343] Dangoria, NS; Breau, WC; Anderson, HA; Cishek, DM; Norkin, LC. Extracellular simian virus 40 induces an ERK/MAP kinase-independent signaling pathway that activates primary response genes and promotes virus entry. *J. Gen. Virol.*, 1996 77, 2173–2182.

[344] Hirasawa, K; Kim, A; Han, HS; Han, J; Jun, HS; Yoon, JW. Effect of p38 mitogen-activated protein kinase on the replication of encephalomyocarditis virus. *J. Virol.*, 2003 77, 5649–5656.

[345] Talavera, D; Castillo, AM; Dominguez, MC; Gutierrez, AE; Meza, I. IL8 release, tight junction and cytoskeleton dynamic reorganization conducive to permeability increase are induced in dengue virus infection of microvascular endothelial monolayers. *J. Gen. Virol.,* 2004 85, 1801–1813.

[346] Cirone, M; Zompetta, C; Tarasi, D; Frati, L; Faggioni, A. Infection of human T lymphoid cells by human herpesvirus 6 blocked by two unrelated protein tyrosine kinase inhibitors, biochanin A and herbimycin. AIDS Res. *Hum. Retroviruses,* 1996 12, 1629–1634.

[347] Greiner, LL; Stahly, TS; Stabel, TJ. The effect of dietary soy genistein on pig growth and viral replication during a viral challenge. *J. Anim. Sci.*, 2001 79, 1272–1279.

[348] Padilla-Banks, E; Jefferson, WN; Newbold, RR. Neonatal exposure to the phytoestrogen genistein alters mammary gland growth and developmental programming of hormone receptor levels. *Endocrinology,* 2006 147, 4871–4882.

[349] McClain, RM; Wolz, E; Davidovich, A; Bausch, J. Genetic toxicity studies with genistein. Food Chem. *Toxicol.,* 2006 44, 42–55.

[350] Snyder, RD; Gillies, PJ. Reduction of genistein clastogenicity in Chinese hamster V79 cells by daidzein and other flavonoids. Food Chem. *Toxicol*., 2003 41, 1291–1298.

[351] Merritt, RJ; Jenks, BH. Safety of soy-based infant formulas containing isoflavones, the clinical evidence. *J. Nutr.*, 2004 134, 1220S–1224S.

[352] Tuohy, P. Soy infant formula and phytoestrogens (Review article). *J. Paediatr. Child Health,* 2003 39, 401–405.

[353] Mazur, WM; Adlercreutz, H. Naturally occurring oestrogens in food. *J. Pure Appl. Chem.*, 1998 70, 1759-1776.

In: Clinical Chemistry Research
Editors: Brian H. Mitchem and Charles L. Sharnham
ISBN 978-1-60692-517-1

Chapter II

(Q)SAR and Clinical Chemistry of Camptothecin Analogues

Rajeshwar P. Verma* and Corwin Hansch
Department of Chemistry, Pomona College
Claremont, California, USA

Abstract

Camptothecins (CPTs) are regarded as one of the most promising anticancer drugs of the twenty-first century. The structure–activity relationships (SAR) provide insight into the mechanism of topo I inhibition and helped in the synthesis of various CPT analogues by modifying the different rings of the original CPT molecule, giving each analogue a unique property. These modifications have resulted in various improvements in the parent molecule, including changes in bioavailability, stabilization of the lactone ring, and/or a decrease in the substrate recognition by drug-resistant proteins as well as improvements in the toxicity profile in preclinical studies. The quantitative structure–activity relationships (QSAR) have suggested that the hydrophobic and steric descriptors of CPT analogues are the two most important determinants for their activity. Currently, two anticancer CPT derivatives, topotecan and irinotecan are in clinical use. These analogues have shown tremendous promise as solid tumor drugs and become a part of the multi-million dollar industry, but suffer from low tumor response rates and dose-limiting toxicity. At present, the extensive clinical trials are continuing to describe the better picture of clinical chemistry of topotecan, irinotecan, and some other new CPT derivatives (which are in various stages of clinical trials) to determine their optimal dose, route of administration, schedules, and the possibility in the combination with other chemotherapeutic agents. In this chapter, we describe SAR, QSAR, and the clinical chemistry of CPT derivatives to understand their chemical–biological interactions and side effects, which may provide strategies that might aid in the development of outstanding antitumor agents belonging to this family.

∗ Phone: (909)607-4249, Fax: (909)607-7726, E-mail: rverma@pomona.edu

Keywords: Camptothecin, Clinical chemistry, Hydrophobicity, Molar refractivity, SAR, QSAR, Topoisomerase I

1. Introduction

Camptothecin (CPT, I), a naturally occurring quinoline alkaloid, was first isolated from the Chinese tree *Camptotheca acuminata* by Wall et al. in 1966. [1] It has shown remarkable promise as an anticancer agent, but its use has been limited by its poor water solubility and high in vivo hepatotoxicity. The important parameters for the anticancer activity of camptothecin derivatives have now been established, showing that the intact lactone form with an α-hydroxyl group at position 20 of the molecule with an *S*-configuration is required for the anticancer activity. [2] On the other hand, the discovery that the primary cellular target of CPT is DNA topoisomerase I (topo I) was the breakthrough that created renewed interest in this agent and led to synthesizing more water-soluble analogues with impressive activity. [3,4] Two of them, topotecan (II) for the clinical treatment of the ovarian and small-cell lung cancers, [5-7] and irinotecan (CPT-11, III) [8,9] for the metastatic colorectal cancers have already been approval by the FDA. [10-12] Irinotecan is a prodrug that is converted into their active metabolic form 10-hydroxy-7-ethylcamptothecin (SN-38, IV) (Fig. 1). These two drugs (topotecan and irinotecan) and other derivatives of CPT have become a part of the multi-million dollar industry that is dedicated to finding better chemotherapeutic agents with excellent antitumor activity and less normal tissue toxicity.

DNA topoisomerases are ubiquitous enzymes that can manipulate DNA by changing the number of topological links between two strands of the same or different DNA molecules. [13] These enzymes are involved in many cellular processes, such as replication, recombination, transcription, and chromosome segregation. There are two major classes of topoisomerases, topo I, which break and reseal one strand of DNA, and topo II that alter DNA topology by catalyzing the passage of an intact DNA double helix through a transient double-stranded break made in a second helix [14,15] Topo I produces a DNA single strand break allowing DNA relaxation for replication. This single strand break is then relegated, thus restoring the DNA double strands. Interestingly, there is no energy cofactor required to carry out this reaction suggesting that hydrolysis was not involved in the mechanism of the DNA cleavage; otherwise relegation would require a coupled reaction to balance the unfavorable free energy of dehydration in an aqueous medium. [16] It was therefore proposed that the enzymatic mechanism involves two sequential transesterification reactions. In the cleavage reaction, the active site tyrosine (Tyr 732 in human topo I) acts as a nucleophile. The phenolic oxygen attacks a DNA phosphodiester bond, forming an intermediate in which the 3′ end of the broken strand is covalently attached by an O^4-phosphodiester bond to the topo I tyrosine. [16,17]

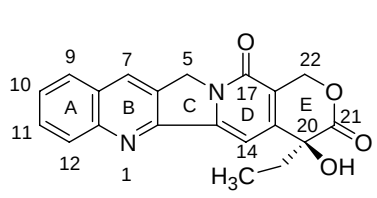

20(*S*)-Camptothecin (CPT, **I**)

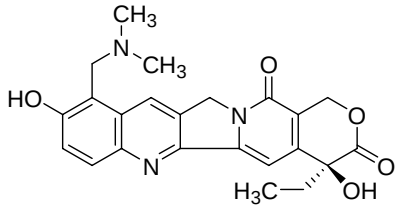

Topotecan (**II**)

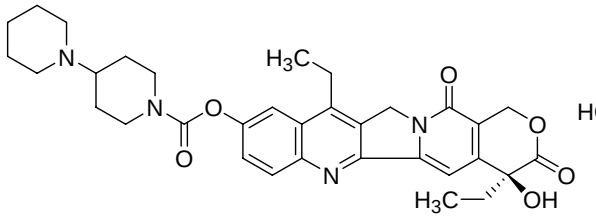

Irinotecan (CPT-11, **III**)

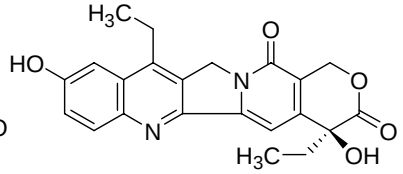

SN-38 (**IV**)

Figure 1. Structures of 20(*S*)-Camptothecin, Topotecan, Irinotecan and SN-38.

Human DNA topoisomerase I (topo I) is the sole target for the CPT family of anticancer compounds, which acts by stabilizing the covalent protein-DNA complex and enhancing apoptosis through blocking the advancement of replication forks. Once the CPT molecule has intercalated into the topo I-DNA cleavable complex, the collision between the complex and the replication fork during S-phase is thought to result in DNA double strand breaks (DSBs) that eventually lead to cell death. [10,18] It was also suggested that topo I cleaves DNA at multiple sites. The highest efficient sites exhibit significant sequence homology. Approximately 90% of topo I site have a tyrosine residue at position-1. However, sites of cleavage stabilized by CPT exhibit a strong preference for guanine at +1 position, while thymidine remains the preferred nucleobase at the –1 position. [19] The atomic force microscope (AFM) images have recently been used to investigate the mode of action of DNA topo I in the presence and absence of CPT. The AFM analysis revealed that the position of the enzyme in the topo I-DNA covalent complexes (in the presence of CPT) differed from its position in the absence of this drug. Topo I was attached to the double stranded relaxed DNA molecules in the absence of CPT, while in the presence of this drug the enzyme was located inside a relaxed DNA bubble. [20]

The exact mechanism for the stabilization of DNA–topo I covalent binary complex by CPTs is not fully understood because the drug acts as an uncompetitive inhibitor and binds only the transient binary complex. [21] It has been confirmed from the enzymatic studies that CPT does not interact with topo I alone, nor does it bind to DNA. [22] Although it has been reported that topotecan, which should be protonated at physiological pH, does bind to DNA at high concentration. [23] Despite the apparent lack of affinity of CPT to DNA or topo I alone, the binding of CPT to the covalent binary complex is suggested to be responsible for the observed stabilization. X-ray crystal structure of a ternary complex containing a human topo I covalently attached to a DNA duplex and bound to topotecan, suggests that topotecan intercalates at the site of DNA cleavage and is stabilized by base-stacking interactions with

both the upstream (–1) and downstream (+1) base pair. The intercalation resulted in a shift of the downstream base pairs and displacement of 5′-OH strand away from the phosphotyrosine bond thus blocking relegation. This binding occurred whether E ring of topotecan was in the closed lactone form or the open carboxylate form; however, a higher occupancy rate (63%) was seen with the lactone form. [24]

Another possible mechanism of cell death by CPT is by blocking angiogenesis. In an effort to investigate the antiangiogenic and antitumor activity of oral ST1481 (gimatecan) in human tumor xenografts, Petrangolini and co-workers [25] have suggested the possibility that the antiangiogenic properties of ST1481 contribute to its antitumor potential and that this effect might be enhanced by the continuous low-dose treatment. Recently, it has been demonstrated that the CPT-11 is an effective inhibitor of angiogenesis and providing strong implications for wider clinical application for colon cancer. [26] CPT is found to be effective in treating psoriasis by inhibiting the growth of keratinocytes in vitro by inducing apoptosis. CPT inhibited keratinocyte proliferation and telomerase activity as well as the induction of apoptosis. The inhibitory activity of CPT is well correlated with its concentration, suggesting concentration dependency. It is important to note that the down-regulation of telomerase activity was observed not only in cells treated at concentrations able to induce apoptosis, but also in cells treated at concentration insufficient to induce apoptosis, indicating that CPT-induced apoptosis may be preceded by down-regulation of telomerase activity. Thus, the antiproliferative activity of CPT and its inhibition of keratinocyte apoptosis through down-regulation of telomerase activity may explain the drug's therapeutic mechanism in psoriasis. [27]

The major clinical complication in cancer therapy is the resistance to chemotherapeutic agents. Studies on CPT resistance using yeast and mammalian cell culture models have suggested mainly three important mechanisms of resistance: (a) reduced cellular accumulation of CPTs, (b) alteration in the structure or location of topo I, and (c) alterations in the cellular response to CPT-DNA-ternary complex formation. The relevance of these mechanisms to clinical drug resistance is not yet known, but evaluation of these models in clinical specimens should enhance the use of CPTs both as single agents and in combination with other anticancer drugs. [28] Resistance to CPT has also been attributed to enhanced drug efflux by a novel ABC transporter, the BCRP/MXR/$ABCG_2$ transporter, which is widely expressed in normal human tissues. [29,30] The crystal structures of two CPT-resistant forms of human topo I (Phe361Ser at 2.6 Å resolution and Asn722Ser at 2.3 Å resolution) in ternary complexes with DNA and topotecan have suggested that the alteration of Asn722 to Ser leads to the elimination of a water-mediated contact between the enzyme and topotecan. [31] Further consideration of CPT-resistant mutations at seven additional sites in human topo I presented the structural evidence that explaining their possible impact on drug binding. These results provide better understanding towards the mechanism of cell poisoning by CPT and suggest specific modifications to the drug that may improve efficacy.

Scientific efforts are continued to develop new CPT analogues in order to improve their pharmacokinetics, drug resistance, clinical chemistry and toxicity profiles. At present, over a dozen new CPT derivatives are in various stages of clinical trials. [32] In the present chapter, we describe SAR, QSAR, and clinical chemistry of CPT derivatives to understand their chemical–biological interactions and side effects, which may provide strategies that might aid

in the development of outstanding antitumor agents belonging to this family. It is important to understand the difference between SAR and QSAR: SAR is qualitative in nature, often occurring in the form of structural alerts that include molecular substructures or fragment counts related to the presence or absence of biological activity; while QSAR is typically quantitative in nature, producing categorical or continuous prediction scales. [33,34]

2. Structure–Activity Relationships (SAR)

The design and development of novel CPT derivatives depend mainly on the following four factors:

(i) The essential structural features for the activity of CPT analogues are the 20(*S*)-hydroxyl, pyridone moiety (D-ring), lactone moiety (E-ring), and the planarity of the pentacyclic (A, B, C, D, and E) ring system. [35,36]
(ii) The modifications of quinoline ring (9, 10, and 11-positions of the A-ring and 7-position of the B-ring) are generally enhance the potency of the CPT derivatives. [36,37]
(iii) The development of homocamptothecins (hCPTs; CPT derivatives with seven-membered lactone E-ring) with enhanced activity necessitate a reevaluation of the E-ring lactone function. [11,24,38,39]
(iv) CPT derivatives must have to possess the following four criteria for the targeted enzymatic activation of tumor cells: (a) improved water solubility, (b) stability in blood, (c) decreased cytotoxicity, and (d) susceptibility to defined enzymatic cleavage. [11,40]

The details about the structure–activity relationships (SAR) of CPT derivatives with respect to their pentacyclic (A, B, C, D, and E) ring system are as follows:

2.1. Modification in the A Ring

Numerous reports indicated that CPT derivatives with substitutions at the A ring are regarded to be of great interest. The SAR for the modifications in the A ring (C-9, C-10, C-11, and C-12) of CPT derivatives includes the following:

(i) Monosubstitution by NH_2 or OH group at positions C-9, C-10, or C-11 of the A ring increases the antitumor activity, whereas substitution at position C-12 greatly reduces the activity. [41]
(ii) Substitution at C-9 and C-10 positions of the A ring by halides and other electron-rich groups (e.g. NH_2, OH, etc.) generally increases the DNA topo I inhibition. [42]
(iii) Addition of small substituents at C-10 position of the A ring generally increases the DNA topo I inhibition. Substitution at C-10 position with a hydroxyl group contributes to the increased activity of SN-38 and topotecan. [43]

(iv) The additional furan and dihydrofuran rings fused with C-9 and C-10 positions of camptothecin could improve the antitumor activity *in vitro* and *in vivo*, though the stability of the lactone ring did not increase. [44]

(v) Substitution at C-10 and C-11 positions of the A ring are generally unfavorable to the biological activity. [45] Exceptions are the 10,11-methylenedioxy or 10,11-ethylenedioxy functional group at the A ring substantially increases the DNA topo I inhibition. [42,46]

(vi) Modification at C-11 position of the A ring increases the DNA topo I inhibition e.g. 11-azacamptothecin has activity approximately twice that of CPT. [47]

(vii) 9-Amino camptothecin was shown in early studies to have very impressive preclinical study. By introducing various alkylidine groups (-CH=CR_1R_2) at C-9 position of the A ring, the cytotoxicity of the resulting CPTs increases/decreases depending on the nature of their R_1 and R_2 substituents. For example, 9-(CH=CH_2)-CPT [where, R_1 = R_2 = H] and 9-(CH=CHCOOCH_3)-CPT [where, R_1 = $COOCH_3$, R_2 = H] have shown enhanced cytotoxicity in comparison to 9-NH_2-CPT. On the other hand, 9-(CH=CHCONH_2)-CPT [where, R_1 = $CONH_2$, R_2 = H] and 9-(CH=C($COOCH_3$)NHCOCH_3)-CPT [where, R_1 = $COOCH_3$, R_2 = $NHCOCH_3$] have shown decreased cytotoxic activity with respect to 9-NH_2-CPT. The reduction of the alkylidine double bonds to afford the more flexible, non conjugated 9-alkylcamptothecins did not lead to relevant differences in cytotoxicity in respect to the parent compounds. [48]

(viii) In vitro experiments using three kinds of purified carboxylesterase isozymes from the liver microsomes of rat, pig, and human demonstrated that the long-chain fatty acid esters of 10-hydroxycamptothecins [10-OCO(CH_2)nCH_3-CPT; where n = 8, 10, 14, 16, and 18] were efficiently metabolized by enzymes compared with CPT-11. These results suggested that long-chain fatty acid esters of 10-hydroxycamptothecins could be useful as prodrugs anticancer property. [49]

2.2. Modification in the B Ring

A systematic study has revealed that the C-7 position of the CPT is a favorable site for the introduction of a hydrophobic group, since the antitumor activity is maintained or improved with proper substituents. The SAR for the modification in the B ring (C-7) of CPT derivatives includes the following:

(i) Substitution at the C-7 position of the B ring has been found to be more potent, and an increase in water solubility has been observed depending on the nature of the C-7 substituent. [42]

(ii) 7-*N*-isopropylaminoethyl-CPT has shown enhanced cytotoxicity and lower toxicity in comparison with CPT and topotecan. [50]

(iii) Camptothecin substituted at C-7 position of the B ring by an alkyl, alkenyl, cyano or carbethoxy groups showed potent cytotoxic activity *in vitro* against human non-small-cell lung carcinoma H460 cell-line, most of them exhibiting IC_{50} values in the

0.05-1μM range, and were more active than topotecan. In particular, 7-cyanocamptothecin showed high *in vitro* cytotoxicity against a topotecan-resistant H460 cell subline and cisplatin-resistant ovarian cancinoma subline. In an *in vivo* evaluation of the antitumor activity, 7-CN-CPT appeared significantly more effective than topotecan in the H460 tumor model and comparable with topotecan in small-cell lung carcinoma and colon carcinoma models. [51]

(iv) 7-Iminomethyl derivatives of camptothecin [7-(CH=NR)-CPT; where, R = C_6H_5, C_6H_{11}, $(CH_2)_2N(CH_3)_2$, $(CH_2)_4OH$, p-NO_2-C_6H_4, and $CH_2C_6H_5$] showed a marked increase of cytotoxicity (IC_{50} = 0.12-0.37μM) against non-small-cell lung carcinoma H460 cell-line, with respect to topotecan (IC_{50} = 1.38μM). [52] Similarly, 7-oxyiminomethyl derivatives of CPT had also been found to show improved efficacy. [53]

(v) Conjugates (Va-e) composed of a paclitaxel and a camptothecin derivatives joined by an imine linkage were found to be potent inhibitors of tumor cell replication with improved activity relative to CPT. Significantly, compounds (Va-c) were found to be more active than paclitaxel and CPT against HCT-8 (colon adenocarcinoma) cell replication. All of the conjugates (Va-e) were significantly less potent than CPT as inhibitors of human topo I in vitro. Based on the activity against drug-resistant cell line replication, one could conclude that the conjugates were simply acting as 'weak taxanes' but the spectrum of activity, particularly against MCF-7 and HCT-8, strongly suggests that a novel mechanism of action has been achieved through conjugation. [54]

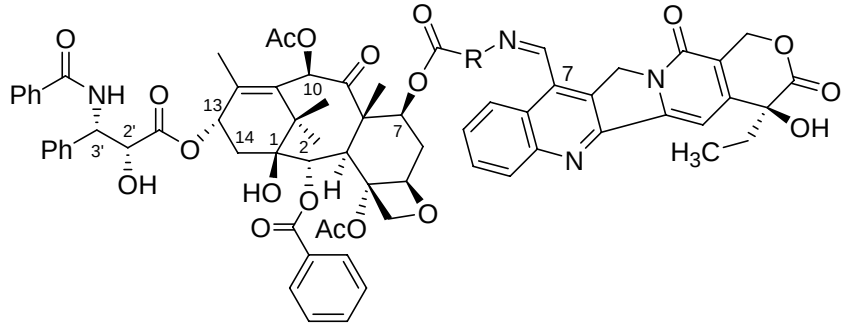

V

Va, R = $(CH_2)_2$; Vb, R = $(CH_2)_3$; Vc, R = $(CH_2)_5$;
Vd, R = $C_6H_4CH_2$; Ve, R = $(CH_2)_3C_6H_4$

2.3. Modification in the A/B Ring

It has already been demonstrated that the CPT analogues with modifications at quinoline (A/B) ring are of great interest. This is further supported by the fact that the only two CPT derivatives approved by FDA for the clinical use, that are, topotecan (II) and irinotecan (III), are the analogues of CPT with substitutions within the quinoline ring. The SAR for the quinoline (A/B) ring of the CPT derivatives includes the following:

(i) Substitutions at C-7 and C-9 positions of B and A rings do not affect the DNA topo I inhibitory activity, suggesting the absence of tight interaction with the receptor site and the regions around positions 7 and 9. [43]

(ii) The stability of the E-ring lactone in human plasma can also be affected by derivatization of the quinoline ring. [19]

(iii) 7-Ethylcamptothecin substituted at the C-11 position by fluorine or cyano group showed strong cytotoxicity to KB and L1210 cells as well as also exhibited strong inhibitory activity on DNA topo I. [55]

(iv) Comparison of the stability among CPT-, SN-38-, and 10-OH-CPT-induced cleavable complexes reveals that the OH group at position C-10 enhances stability of the cleavable complexes. The difference between SN-38- and 10-OH-CPT-induced cleavable complexes suggests that the ethyl group at the C-7 position is also important for stabilizing the interaction between CPT derivatives and topo I-DNA complex. [56]

(v) Substitution at C-7 and C-10 positions of B and A rings (where the substituent at position C-10 is a hydroxyl group) results in greatly improved drug stability in the presence of human albumin. This is due to the occurrence of a favorable, reversible binding between the lactone form of the drug and human serum albumin (HSA). SN-38 is one of the best examples with 7-alkyl-10-hydroxy substitution pattern. [57]

(vi) 7-*tert*-butyldimethylsilyl-10-hydroxycamptothecin (DB-67, VI) had displayed superior stability in human blood when compared with the clinically relevant CPT analogs. In human blood, VI displayed a $t_{1/2}$ of 130 min and a percent lactone at equilibrium value of 30%. The *t*-butyldimethylsilyl group rendered the new agent 25 times more hydrophobic than CPT. In addition, the dual 7-alkylsilyl and 10-hydroxy substitution in VI enhanced the drug stability in the presence of human serum albumin (HSA). Thus, the net hydrophobicity and the altered HSA interactions together function to promote the enhanced blood stability. The cytotoxic activity of VI against multiple different cell lines derived from eight distinct tumor types showed comparable or slightly enhanced potency relative to CPT, 10-OH-CPT, topotecan and CPT-11. The cell-free cleavage assays further revealed that VI was highly active and forms more stable topo I cleavage complexes than CPT or SN-38. [58]

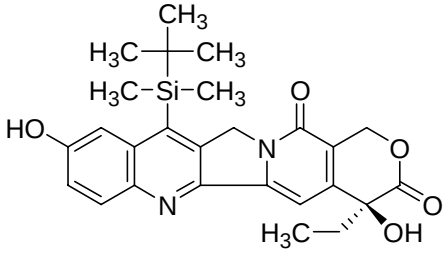

VI

(vii) Camptothecin substituted at C-10 position by -OCH_3 group and at C-7 position by -CH_2OCOCH_3, -CHO or -CN groups showed potent cytotoxic activities *in vitro*

against human non-small-cell lung carcinoma H460 cell-line, and exhibiting IC_{50} values 0.04, 0.18, and 0.66μM, respectively, and were more active than topotecan (IC_{50} = 1.38μM). [51]

(viii) Some of the derivatives with an additional ring combined with the positions C-10 and C-11, positions C-9 and C-10, or positions C-7 and C-9 were predicted to be superior antitumor activities to those original pentacyclic CPTs, such as lurtotecan and extatecan. [11]

(ix) CPT derivative (VII) containing a 1,4-oxazine ring combined with the position C-9 and C-10 showed about 2-fold more potent than topotecan and as potent as CPT toward six human cancer cell lines A549, H128, WiDr, MKN45, SK-OV-3, and SK-BR-3 *in vitro*, and was slightly less potent than SN-38. The stability of the lactone form of this compound in human plasma seemed to be much higher than that of CPT and similar to that of topotecan but lower than that of SN-38. Compound VII showed higher antitumor activity against human tumor xenograft, WiDr, in nude mice compared to that of SN-38. [59]

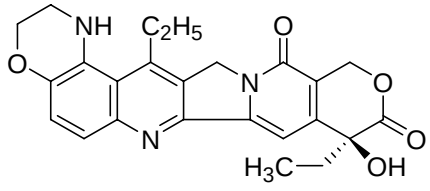

VII

(x) The cytotoxicity results of a series of 7-*N*-alkylaminoethyl-10,11-methylenedioxy- and ethylenedioxy-CPT against five human tumor cell lines revealed that the more bulky alkyl groups at position C-7 (higher than propyl) showed the less cytotoxicity. Generally, methylenedioxy derivatives showed higher cytotoxicity than the corresponding ethylenedioxy derivatives. It was thought that ethylenedioxy group can not hold the coplanarity with A, B, and C rings of CPT, which is required to interact with DNA and topo I complex. CPT derivatives VIIIa and VIIIb were found about 100 times more potent against ovarian cancer (CAOV-3) than CPT. [50]

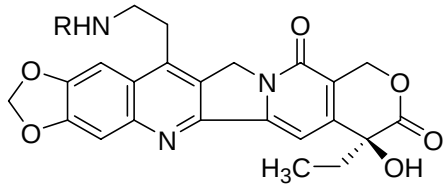

VIII

VIIIa**,** R = CH_2CH_3**;** VIIIb, R = $CH_2CH_2CH_3$

(xi) CPT derivative IX was twice as active as SN-38 against two cancer cell lines (P388, mouse leukemia and HOC-21, human ovarian cancer) suggesting that the conformational rigidity of the substituents at positions C-7 and C-9 is favorable for antitumor activity. [60]

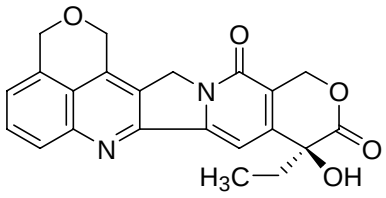

IX

2.4. Modification in the C Ring

There are few reports, which have focused on the modification of C ring of the CPT. It has generally been suggested that either the replacement or the substitution at C ring would reduce the activity. There is only one available site for the substituents i.e. C-5 in the C ring. The SAR for the C ring of the CPT derivatives includes the following:

(i) Substitution at C-5 position of the C ring by acetoxy, alkoxy, amino, or hydroxyl groups generally diminishes the antitumor activity. [19,61]

(ii) Substitutions of alkoxy or several other groups at C-5 of the C ring are reasonably well tolerated when either hydroxyl or nitro group is present to the A-ring. 9-OH-5-OEt-CPT is one of the best examples. [62,63] Exceptions are the CPT derivatives (X) and (XI), which contained no additional group within the quinoline ring and showed a good or maintain the same potency equivalent to CPT. [64,65]

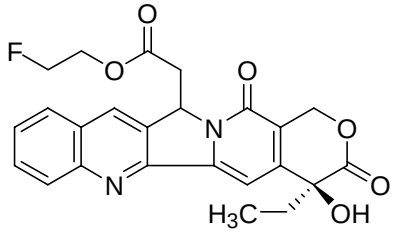

X

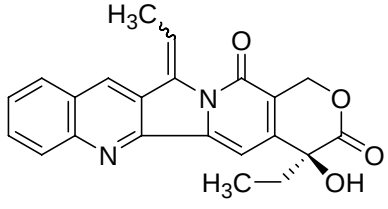

XI

2.5. Modification in the D Ring

Reports on D ring substituents have been limited, presumably due to the paucity of accessible carbons for substitution and more difficult synthetic routes leading to potential analogues. [19] There is only one available site for substituents i.e. C-14 in the D ring. The SAR for the D ring of the CPT derivatives includes the following:

(i) Steric factor at position C-14 of the D-ring is shown to be crucial for the activity. Substitution at C-14 by methyl ester group generally reduces the anti-tumor activity. [66]

(ii) The pyridone carbonyl of CPT is an important ring to stabilizing the enzyme-DNA-CPT ternary complex. The deaza derivative of CPT (XII) is the best example, which

should maintain quite similar shape and planarity relative to CPT, was found to be approximately 60-fold less efficient as a topo I inhibitor. [67]

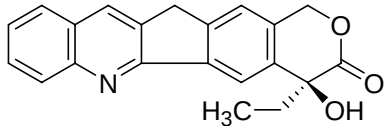

XII

(iii) 14-Azacamptothecin (XIII) had exhibited reasonable potency as a topo I poison and topo I dependent cytotoxicity, and stabilized enzyme-linked DNA breaks with the same sequence selectivity as CPT itself. [11,68,69] Interestingly, 14-aza CPT was found to inhibit the relaxation of super-coiled plasmid DNA more potently than CPT. Thus, it may modified structurally to further improve its properties as a topo I poison. [70]

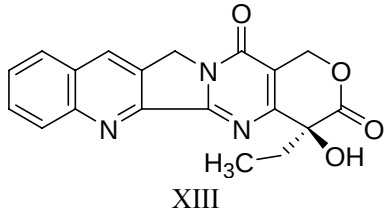

XIII

2.6. Modification in the E Ring

E-ring plays a key role in supporting both the efficient topo I inhibition and *in vivo* potency. Early studies demonstrated that the removal of the 20-OH group on the lactone (20-deoxy-CPT) or the conversion of the lactone into a lactum, or the conversion of the stereochemistry of the OH group (20-*S* to 20-*R* isomer) were detrimental both in topo I inhibition and *in vivo* assays. [71-73] The SAR for the E-ring of the CPT derivatives includes the following:

(i) The lactone (E-ring) with 20-*S* configuration is critical for both efficient topo I inhibition and *in vivo* potency. [73]
(ii) Under physiological conditions, the presence of α-OH group (20-*S* configuration) results in an equilibrium that favors the (inactive) open carboxylate over the (active) ring-closed lactone form. [11,19,57, 74-76]
(iii) Any changes in the E-ring, such as replacement of the lactone by a lactum group, reduction of the lactone, removal of the carbonyl oxygen, removal of the 20-hydroxyl group, or replacement of 20-OH group by other groups inactivate the molecule. [38,71]
(iv) There are mainly two possible reasons for the importance of α-OH group (20-*S* configuration) of the CPT for topo I inhibition: (a) the formation of a hydrogen bond between the hydroxyl group and the enzyme-DNA complex, and (b) the presence of

an intra-molecular hydrogen bond with the lactone carbonyl (C-21 position). Both interactions may facilitate the possible E-ring opening. [11,66,71] 20-OH group and C-21 carbonyl moiety of the CPT may act as H-bond donor and H-bond acceptor, respectively. [70]

(v) Replacement of 20-OH group by amino or halogens results in the significant diminished activity. [11,19] The 20-NH_2-CPT (XIV) has the same potential of H-bond donor capacity as that of CPT, which stabilized the covalent binary complex formed from DNA and human topo I, and also mediated topo I-dependent cytotoxicity toward a yeast strain lacking the homologous topo I, but expressing the human enzyme under the control of a galactose promoter. However, the compound (XIV) was much less potent than CPT. It is interesting to note here that the 20-NH_2 group would be expected to be protonated at the physiological pH. It would thus be capable of acting as H-bond acceptor and not H-bond donor. In the case of halogen derivatives i.e. 20-Cl-CPT and 20-Br-CPT, the chloro and bromo groups can only act as H-bond acceptors were also found to stabilize the ternary complex and to mediate topo I-dependent cytotoxicity toward yeast expressing the human enzyme, and to exhibit greater potency than 20-NH_2-CPT but lower than that of CPT. [35,70]

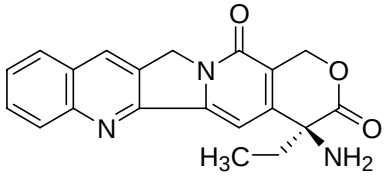

XIV

(vi) Esterification of 20-OH group, which can either eliminate the intra-molecular hydrogen bonding or increase the steric hindrance of the carbonyl group of E-ring, results in the stability of lactone ring *in vivo*. [11,77,78] A series of 20-*O*-linked nitrogen based camptothecin esters including ester (XV) was reported by Wang et al. [79] All these esters showed lower toxicity *in vitro* than CPT and topotecan. Compound (XV), among all the esters of the series, showed the best antitumor activity both in *in vitro* and *in vivo*.

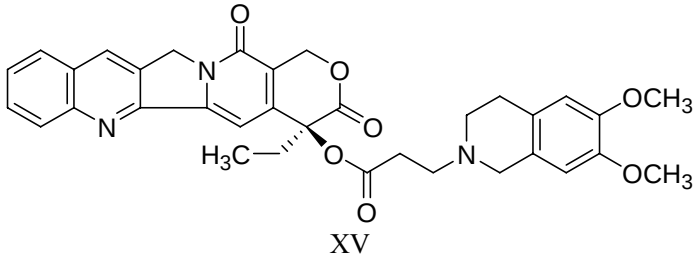

XV

(vii) In an effort to improve the water solubility of CPT, four 20-*O*-phosphate and its derivatives (XVI; R = OH, OCH_3, CH_3, C_6H_5) were synthesized by Rahier et al. [80] These compounds are freely water soluble, stable at physiological pH, and stabilize

the human topo I-DNA covalent binary complex with the same sequence selectivity as CPT itself. Thus, it may be regarded as the good examples for the comparison between α-OH (20-*S*) and α-OX (20-*S*) of CPTs in improving their water solubility and stabilizing topo I –DNA covalent binary complex. Among the derivatives, CPT phosphate monoester (XVI; R = OH) was the most cytotoxic, although its potency was much lower than that of CPT itself. Thus, the experimental evidence finally revealed that the esterification of 20-OH markedly reduced the toxicity of CPT analogues.

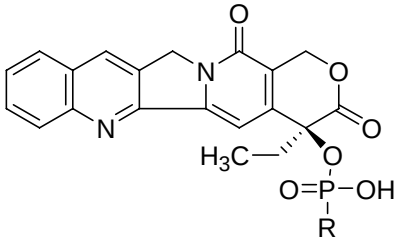

XVI

(R = OH, OCH_3, CH_3, C_6H_5)

(viii) Hertzberg et al. [71] replaced the 21-C of the CPT with other atom such as N and S to lactam (XVII) and thiolactam (XVIII), thereby reducing the tendency of the E-ring to open. However, the resulting CPT derivatives XVII and XVIII were essentially inactive. The lactam derivative (XVII) differed from CPT in two respect: (a) the lactam ring was more stable to hydrolysis than the lactone ring, and (b) the lactam NH was a hydrogen bond donor while the lactone oxygen was a hydrogen bond acceptor. In the case of thiolactam (XVIII) where E-ring more closely resemble to the lactone ring in CPT, was expected to be more reactive than a lactone, but sulfur is a poorer hydrogen bond acceptor than oxygen and also represents an increased steric bulk and size.

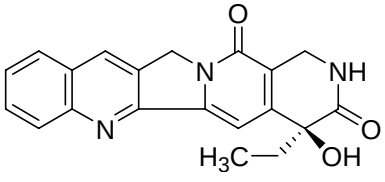

XVII

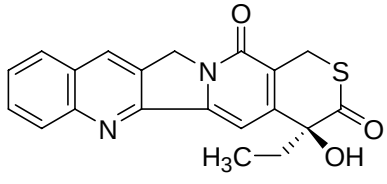

XVIII

(ix) The idea of reducing the electronic influence (via an inducible effect from the electronegative oxygen atom) of the OH group by increasing the distance between the C=O and OH functionalities, proved to be a full success. The one-carbon ring expansion of the E-ring of CPT afforded a family analogues designated hCPTs, hereafter referred to as hCPT or homoCPT. [81] It is important to note that homoCPT (XIX) obtained by the replacement of α-hydroxylactone moiety with β-hydroxy-lactone exerts potent inhibition of topo I, elevated levels of cytotoxicity, and stability of the lactone after 24 h at physiological pH. [82] These demonstrations

have prompted the synthesis and evaluation of numerous homoCPT derivatives. [38,82-86] Among them the most important homoCPT derivatives is 10,11-difluoro-homoCPT (XX) which exhibits strong antiproliferative activity against numerous cell lines and is currently in clinical trials. [8,84]

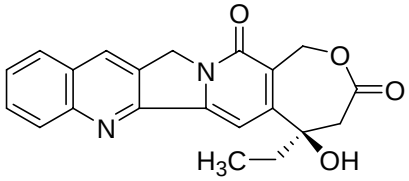

XIX

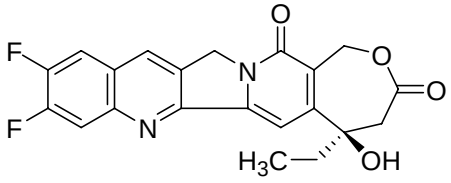

XX

(x) The 7-(*tert*-butyldimethylsilyl)homoCPT (XXI) with an increased hydrophobicity, was reported to display the highest level of lactone stability in both buffer systems and plasma. [87] It is interesting to note that Du1441 (XXII) an analogue similar to homoCPT, contains an α-hydroxyketo ether in place of β-hydroxylactone, was inactive as a topo I inhibitor and in inhibiting cellular proliferation. [88]

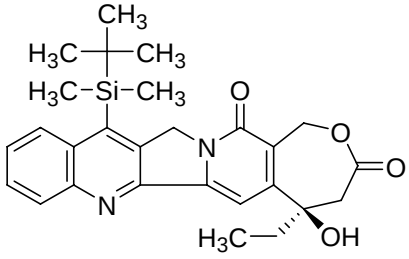

XXI

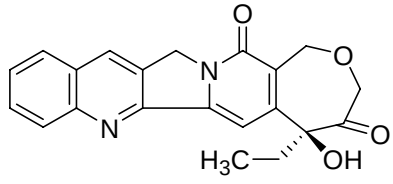

XXII

(xi) Recent report suggested that the pyrroloquinazolinoquinoline alkaloid luotonin A (XXIII) is a topo I poison, which has been shown to stabilize the human topo I-DNA covalent binary complex in the same fashion as that of CPT. [89] While this may seem to be unsurprising that luotonin A (XXIII) is less cytotoxic than CPT, and less potent in stabilizing the topo I-DNA covalent binary complex. [90] There are obvious structural similarities between CPT (I) and luotonin A (XXIII), notably in identical rings A–C. The greatest differences are in the ring E, which is known to be critical for CPT function as a topo I inhibitor. The E-ring of luotonin A (XXIII) is a simple benzene ring lacking any additional functionality cannot undergo (reversible) covalent attachment to the topo I-DNA binary complex as has been suggested for CPT. This finding might be thought to make it less likely that CPT binding to the topo I-DNA covalent binary complex. Thus, even in the absence of a group analogous to the 20-OH group in CPT, significant stabilization of the enzyme-DNA covalent complex could be achieved. To evaluate the nature of the interaction of luotonin A (XXIII) with the human topo I-DNA covalent binary complex, and explore possible commonalities with the binding of CPT, a number of derivatives of luotonin A (XXIII) were prepared and tested for their ability to stabilize the human

topo I-DNA covalent binary complex. The most effective compounds included are 17-fluoroluotonin A (XXIV) and 18-methylluotonin A (XXV), while 16-OH luotonin A (XXVI), having an OH group in the position analogous to position C-20 in CPT, was only very weakly active. Thus, the E-ring substitutions of the luotonin A (XXIII) conferred the most favorable properties as a topo I poison, were different than those found to support the activity of CPT as a topo I poison. [70,89-91]

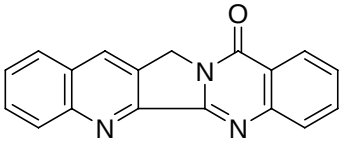

XXIII

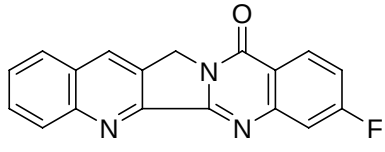

XXIV

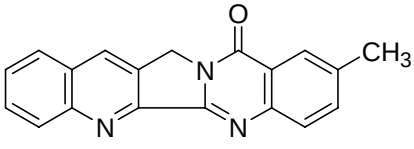

XXV

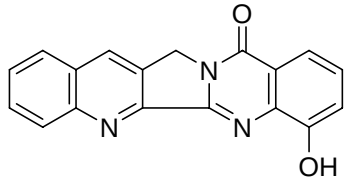

XXVI

3. Quantitative Structure–Activity Relationships (QSAR)

Quantitative structure–activity relationship (QSAR) is one of the well-developed areas in computational chemistry. The interest in the application of QSAR has steadily increased in recent decades because it has repeatedly proven itself to be a low-cost, high-return investment. Potential use of the QSAR models for screening of chemical databases or virtual libraries before their synthesis appears equally attractive to chemical manufacturers, pharmaceutical companies and government agencies.

The QSAR approach employs extra-thermodynamically derived and computational-based descriptors to correlate biological activity in isolated receptors, in cellular systems and *in vivo*. Four standard molecular descriptors are routinely used in QSAR analysis: electronic, hydrophobic, steric, and topological indices. These descriptors are invaluable in helping to delineate a large number of receptor–ligand interactions that are critical to biological processes. The quality of a QSAR model depends strictly on the type and quality of the data, and not on the hypotheses, and is valid only for the compound structure analogues to those used to build the model. QSAR models can stand alone to augment other computational approaches or can be examined in tandem with the equations of a similar mechanistic genre to establish their authenticity and reliability. [92]

In the past 45 years, the use of QSAR (since the advent of this methodology [93]) has become increasingly helpful in understanding many aspects of chemical–biological interactions in the drug-design process and pesticide research, as well as in the field of toxicology. [94,95] This method is useful in elucidating the mechanisms of chemical–

biological interactions in various biomolecules, particularly enzymes as well as membranes, organelles, cells, and in humans. [94,96-99] It has also been used for the evaluation of absorption, distribution, metabolism and excretion (ADME) phenomena in many organisms and whole animal studies. [100-103]

Over the past three decades, a major trend in the evolution of QSAR has been the development of 3D-QSAR, which is viewed as an extension of QSAR and addressed as three-dimensional (3D). The main reason for this trend is due to an in-depth understanding of protein-ligand interaction or binding to various receptors at the atomic level - supported by a wealth of experimental evidences. [104] The most popular method in 3D-QSAR studies is CoMFA that has been used to develop several QSAR models. However, despite the development of regression equations, the results are best mapped and visualized as 3D color-coded contour plots. Semi-quantitative generalizations are drawn from these graphics but clear-cut quantitative aspects of the models are minimized. Thus, rigorous and direct comparisons or extrapolations cannot be made between CoMFA models for different proteins/receptors, unlike 2D-QSAR. One of the attributes of CoMFA is its ability to combine diverse data sets and examine them as a whole. This operation can also be a weakness since it suggests that all the members of the set bind to a receptor/protein at the 'same' binding site and in the 'same' mode. [105] Other drawback is the increasing complexity of the models which requires 3D conformations, their alignment and a large number of variables. This can make it more difficult to reproduce a model or at least to apply it to new compounds if the alignment rules are too specific or are not suitable for other chemical classes, limiting the range of chemicals that can be analyzed. [106] In the presence of a sound knowledge of alignment and conformation of the individual molecules, it becomes necessary to examine numerous alignments and conformations to select the best combination that generates a CoMFA model with the highest predictive power (q^2). [107] On the other hand, 2D-QSAR allows for the direct comparison of the descriptors, their contributions, and other statistical terms. It has great utility in mechanistic interpretation as well as predictability within a congener series. It can also pinpoint molecules that behave in an anomalous fashion. A further aspect to be considered is that it can be easily and quickly used by non expert users. All the QSAR reported in this chapter are for 20-*S*-camptothecin derivatives.

3.1. QSAR for the Inhibition of DNA Topoisomerase I

Two QSAR models 1 and 2 were recently developed by Hansch and Verma [108] for the inhibition of DNA topo I by camptothecin derivatives XXVII and XXVIII, respectively. These QSAR models have suggested that the inhibitory activity of CPT analogues XXVII toward DNA topo I was mainly due to their hydrophobic and steric descriptors, whereas the same activity of 10,11-methylenedioxy-CPT analogues XXVIII was largely due to their hydrophilic descriptor of the substituents at position C-7.

Inhibition of DNA topo I by 7-X-9-Y-10-Z-camptothecins (XXVII) [108]

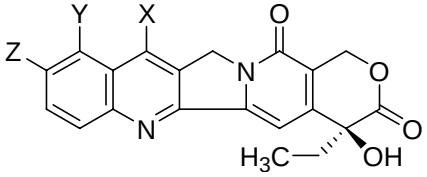

XXVII

$$\log 1/C = 0.84(\pm0.22)\text{Clog } P - 0.62(\pm0.14)B5_X - 0.59(\pm0.33)MR_Y - 0.45(\pm0.36)MR_Z + 0.88(\pm0.28)I_1 - 0.52(\pm0.28)I_2 + 6.37(\pm0.31) \quad (1)$$

$$n = 30,\ r^2 = 0.854,\quad s = 0.258,\ q^2 = 0.738,\quad Q = 3.581,\ F_{6,23} = 22.422$$

In this equation, C represents the minimum concentration (mol/L) of camptothecin analogues (XXVII) that inhibited the cleavable complex formation by 50%. n is the number of data points, r is the correlation coefficient between observed values of the dependent and the values calculated from the equation, r^2 is the square of the correlation coefficient and represents the goodness of fit, q^2 is the cross-validated r^2 (a measure of the quality of the QSAR model), and s is the standard deviation. Q is the quality factor ($Q = r/s$) and F is the Fischer statistics, for which $F = fr^2/[(1–r^2)m]$, where f is the number of degrees of freedom [$f = n–(m+1)$], n is the number of data points, and m is the number of variables. Clog P is the calculated partition coefficient in *n*-octanol/water and is a measure of hydrophobicity for the whole molecule. Positive coefficient of Clog P suggests that the highly hydrophobic molecules will be more active. $B5_X$ is a Verloop's sterimol descriptor, which measures the maximum width of the X-substituents. MR_Y and MR_Z are the calculated molar refractivities of Y and Z substituents, respectively. A negative sign associated with $B5_X$, MR_Y, and MR_Z brings out steric effect for these substituents. The indicator variable (I_1) takes the value of 1 and 0 for the presence and absence of hydroxyl group at position 10, respectively. Similarly, I_2 takes the value of 1 and 0 for the presence and absence of *n*-alkyl groups at position 7, respectively. The presence of the hydroxyl group at position 10 increases the activity as evidenced by the positive coefficient of the indicator variable (I_1). The negative coefficient of the indicator variable (I_2) suggests that the presence of branched alkyl groups at position 7 is preferred over *n*-alkyl groups. It is interesting to note that camptothecin derivatives (XXVII) fulfill all conditions of Lipinski's "rule of five". [109] Using QSAR model 1, two compounds (X = H, Y = Z = Br and X = H, Y = Z = OH) were suggested as potential synthetic target that also fulfill the conditions of the rule of five. The predicted log 1/C for these two compounds obtained from equation 1 is 7.29 and 7.58, respectively.

Inhibition of DNA topo I by 7-X-9-Y-10,11-methylenedioxycamptothecins (XXVIII) [108]

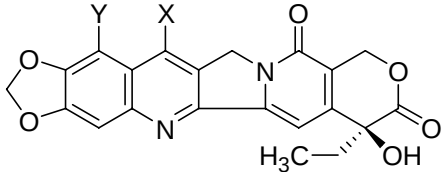

XXVIII

$$\log 1/C = -0.71(\pm 0.20)\pi_X - 0.88(\pm 0.39)I_3 + 0.73(\pm 0.44)I_4 + 7.19(\pm 0.22) \quad (2)$$

$n = 16,\ r^2 = 0.873,\ s = 0.215,\ q^2 = 0.788,\ Q = 4.349,\ F_{3,12} = 27.496$

In this equation, π_X is the calculated hydrophobic parameter for X-substituents, which is the most important parameter for this series of compounds. The negative coefficient associated with π_X suggests that molecules (XXVIII) with highly hydrophilic X-substituents would present better inhibitory activity. I_3 is an indicator variable that takes the value 1 and 0 for the presence and absence of aminomethyl group at position X, respectively. Similarly, I_4 takes the value 1 and 0 for the presence and absence of a cyclic group at position X, respectively. Negative coefficient of I_3 suggests that the presence of X = aminomethyl groups will be detrimental to the activity. On the other hand, the presence of X = cyclic groups will promote the inhibitory activity as shown by the positive coefficient of I_4. It is also important to note that all the camptothecin derivatives (XXVIII) except two fulfill all the conditions of Lipinski's "rule of five". [109] Based on QSAR model 2, three compounds [X = CH_2(–$NCH_2CH_2NHCH_2CH_2$–), Y = H; X = CH_2NHCH_3, Y = H; and X = Cyclo-C_4H_7, Y = H] were suggested as potential synthetic target that also fulfill all conditions of the rule of five. The predicted log 1/C for these three compounds obtained from equation 2 is 6.50, 6.75, and 7.01, respectively.

Inhibition of DNA topo I by X-camptothecins (XXIX) [110]

Using the published data of Wall et al. [46] for the inhibition of DNA topo I by X-camptothecins (XXIX), Eq. 3 was developed. [110]

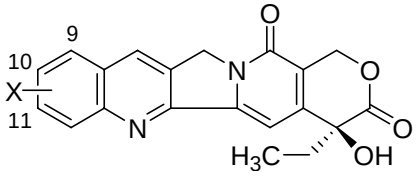

XXIX

$$\log 1/C = 0.43(\pm 0.29)\text{Clog } P - 0.43(\pm 0.22)\sigma^+_X - 0.89(\pm 0.40)MR_9 + 1.11(\pm 0.35)I + 6.37(\pm 0.19) \quad (3)$$

$n = 17,\ r^2 = 0.862,\ s = 0.226,\ q^2 = 0.681,\ Q = 4.108,\ F_{4,12} = 18.739$

In the above QSAR Eq. 3, *C* is the molar concentration of X-camptothecins (XXIX) that cause 50% inhibition of topo I cleavable complex formation, σ^{+}_{X} is the sum of the Hammett parameters of substituents at positions C-9, C-10, and C-11, while MR_9 is the molar refractivity for the substituents at only position C-9. The negative coefficient associated with σ^{+}_{X} (-0.43) implies that the highly electron releasing substituents at positions C-9, C-10, and C-11 may strengthen the inhibitory activity of these compounds against topo I. An unfavorable steric interaction at C-9 position has been detected by the presence of a negative coefficient of MR_9 (–0.89). The indicator variable *I* is assigned the value of 1 and 0 for the presence and absence of X = 10-OCH_2O-11 group, respectively. Its positive coefficient suggests that the presence of a 10, 11-methylenedioxy moiety increases the activity. The positive hydrophobic effect for the whole molecule is also suggested by the presence of a Clog *P* term in the equation. However, this QSAR model does not allow any clue for an adequate distinction between the σ^{+} responsiveness of topo I inhibition for C-9, C-10, and C-11 substituents. Considering these drawbacks of equation 3, QSAR model 4 was then developed using only 10-X-camptothecins (XXX) from the same data set, [46] which gave a very good correlation between the inhibitory activities of 10-X-camptothecins (XXX) towards topo I and the hydrophobic parameters of their X-substituents (π_X). [111]

Inhibition of DNA topo I by 10-X-camptothecins (XXX) [111]

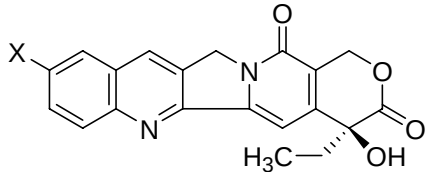

XXX

$$\log 1/C = 0.75(\pm 0.20)\pi_X + 6.24(\pm 0.10) \quad (4)$$

$n = 8,\ r^2 = 0.936,\ s = 0.110,\ q^2 = 0.890,\ Q = 8.795,\ F_{1,6} = 87.750$

The positive coefficient of π_X (+0.75) suggests that molecules (XXX) with highly hydrophobic substituents at position C-10 would present better inhibitory activity.

Three-dimensional quantitative structure–activity relationship (3D-QSAR) with a comparative molecular field analysis (CoMFA) was conducted by Carrigan et al. [42] on a series of 32 CPTs to correlate topo I inhibition with their steric and electrostatic properties. CoMFA model with predictive ability was obtained when both the *R*- and *S*-isomers were included in the data set. The cross-validated R^2 (r^2_{cv}) and non-cross-validated R^2 of this model were 0.758 and 0.916, respectively. In another study, a training set of 43 structurally diverse CPT analogues for their topo I inhibitory activities was used by Lu et al. [112] to construct a 3D-QSAR model with a comparative molecular field analysis. The CoMFA model gave a good cross-validated correlation in which q^2 was 0.495. Then, the analysis of the non-cross-validated PLS model in which r^2 was 0.935 was built and permitted demonstrations of high predictability for the activities of the 10 CPT analogs in the test set.

The CoMFA contour maps illustrated that more negative-charged groups at position C-9, C-10 and C-11 of CPT would increase activity, but excessively increasing the bulky group at position C-10 would be adverse to the activity; substituents that occupy position C-7 with the bulky positively-charged group will enhance the inhibition activity. A tuned 3D QSAR model was developed by the research group of Amat et al. [113] using molecular quantum similarity measures (MQSM) in order to predict the topo I inhibition for 12 CPT analogues. The best regression model was obtained with $r^2 = 0.928$ and $q^2 = 0.866$.

3.2. QSAR for the Inhibition of Various Cancer Cells

Three series of camptothecin analogues (XXXI-XXXIII) were used by Li et al. [114] in order to develop predictive QSAR models **5-7,** which represent the good correlations between biological activities of these compounds and their topological descriptors. The following topological descriptors were used for the development of QSAR models **5-7**: *Ax* = topological molecular descriptors; ${}^{m}\chi_{v}$ = Kier and Hall valence connectivity indices; ${}^{m}K$ = Kier shape indices; ${}^{m}\chi$ = Randic indices of different orders; ^{k}ACIC = average complementary information content index; ^{k}CIC = complementary information content index; ^{k}SIC = structure information content index; RPCG = relative positive charge; and *P* = polarity.

Cytotoxicities (pIC_{50}) of 7-oxyiminomethyl derivatives of camptothecin i.e. 7-X-camptothecins (XXXI) to H460 human NSCLS cell line [114]

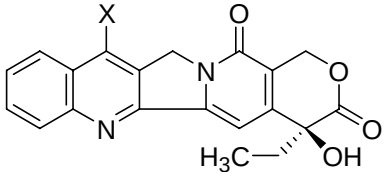

XXXI

$$pIC_{50} = 3.045\ {}^{1}\text{ACIC} - 8.347\ \text{RPCG} - 0.286\ {}^{2}K + 7.514 \quad (5)$$

$n = 23, \quad r^2 = 0.841, \quad s = 0.313, \quad F = 33.597$

On the basis of the above QSAR model 5, it was predicted by the authors [114] that lower the value of RPCG and larger the value of ^{1}ACIC of X-substituents would prefer to lead the higher cytotoxic activity.

Inhibition of HL-60 (human promyelocytic leukemic) cells by 7-silylcamptothecin derivatives with variable substitution at C-10 position i.e. 7-X-10-Y-camptothecins (XXXII) [114]

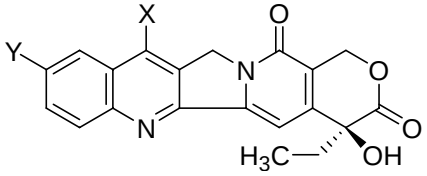

XXXII

$$pIC_{50} = -0.756\,X_1 - 1.493\,X_2 + 0.669\,X_3 - 1.981 \times 10^{-2}\,X_4 + 8.452 \quad (6)$$

$n = 15, \quad r^2 = 0.907, \quad s = 0.381, \quad F = 24.352$

Where, pIC_{50} is the biological activities (inhibition effects on the growth of HL-60) of CPTs (XXXII); X_1 is ^{2}ACIC of X; X_2 is ^3K_v of X; X_3 is $^2\chi$ of X; and X_4 is $Ax3$ of Y.

It was predicted from the above QSAR model that the lipophilicity of the substituents at C-7 position of the ring-B play an important role in increasing biological activity of camptothecin derivatives (XXXII). The steric factor of the substitutions at C-10 position of the ring-A also affects the activity. In most cases, more steric substituents at position C-10 lead to the compound with less biological activity (pIC_{50}).

Cytotoxic activities (IC_{50}) of 20-S-camptothecin alkanoic esters (XXXIII) on BRE-MCF-7 cells (a breast cancer cell line) [114]

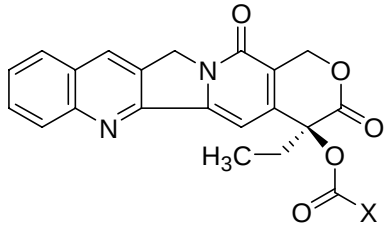

XXXIII

$$IC_{50} = 0.215\,{}^1\text{CIC} + 36.658\,P'' - 1.564\,{}^0\text{SIC} - 8.354 \times 10^{-3} \quad (7)$$

$n = 10, \quad r^2 = 0.907, \quad s = 1.542, \quad F = 19.544$

Based on of the above QSAR model, it was suggested that the polarity plays an important role in increasing the biological activities of CPT esters (XXXIII).

Inhibition of SKOV-3 human ovarian cancer cells by camptothecin derivatives (XXXIV) [115]

From the cytotoxicity data of camptothecin derivatives (XXXIV) against SKOV-3 human ovarian cancer cells, [59] QSAR model 8 was developed. [115]

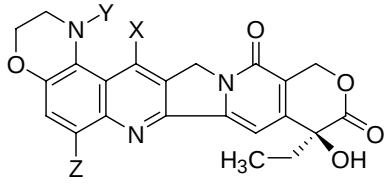

XXXIV

$$\log 1/C = 6.90\ \mathrm{CMR} - 0.33\ \mathrm{CMR}^2 - 28.31 \quad (8)$$

$n = 10$, $r^2 = 0.921$, $s = 0.278$, $q^2 = 0.723$, $F = 40.804$

optimum CMR = 10.50(9.65-10.90)

Where, C is the molar concentration of camptothecin derivatives (XXXIV) that causing 50% cell death (IC_{50}). QSAR 8 is a parabolic correlation in terms of CMR (calculated molar refractivity of the whole molecule), which suggests that the cytotoxic activities of camptothecin derivatives (XXXIV) against SKOV-3 cells first increases with an increase in molar refractivity up to an optimum CMR value of 10.50 and then decreases.

Cytotoxic activities (IC_{50}) of camptothecin derivatives (XXXV) against H460 human NSCLC cell line [53]

Using multiple linear regression (MLR) analysis, a QSAR model 9 was developed by Dallavalle et al. [53] in order to predict cytotoxic activities (IC_{50}) of camptothecin derivatives (XXXV) against H460 human NSCLC cell line, employing descriptors related to the lipophilicity.

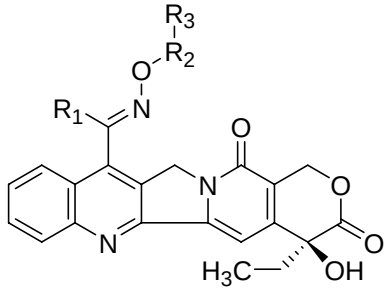

XXXV

$$Y = -0.039\ (\mathrm{X1}) - 0.020\ (\mathrm{X2}) + 0.332\ (\mathrm{X3}) + 6.939 \quad (9)$$

$n = 21$, $r^2 = 0.820$, $s = 0.441$, $F = 26.48$

In the above equation, Y represents pIC_{50}, where IC_{50} is the cytotoxic activities of CPT derivatives (XXXV) in molar concentration. X1 is the molecular volume ($Å^3$) of R_1, X2 is the molecular volume ($Å^3$) of R_2, and X3 is Clog *P* or log *D* (in case of ionizable groups). According to the above equation, it was suggested that the most important determinant for the *in vitro* cytotoxicity of the CPT derivatives (XXXV) is the lipophilicity.

QSAR studies for 58 structurally diverse CPT analogues were carried out by Fan et al. [116] using the mean 50% growth inhibitory concentrations (GI_{50}) for 60 cell lines as the dependent variables. Different statistical methods, including stepwise linear regression, principal component regression (PCR), partial least-squares regression (PLS), and fully cross-validated genetic function approximation (GFA) were applied to construct quantitative structure–activity relationship models. The best model was obtained from the GFA method in terms of correlation coefficients and cross-validation analysis. The cross-validated r^2 for the final GFA model was 0.783, indicating a predictive QSAR model. The most important descriptors for the QSAR models were partial atomic charges at the 11- and 12-positions of the A-ring and three inter-atomic distances that define the relative spatial dispositions of three significant atoms (the hydroxyl hydrogen of the E-ring, the lactone carbonyl oxygen of the E-ring, and the carbonyl oxygen of the D-ring).

Comparative molecular field analysis (CoMFA) and comparative molecular similarity index analysis (CoMSIA) were performed by Yoon et al. [117] to predict the biological activity of a 4-benzylpiperazine derivative of CPT-11 [7-ethyl-10-{4-(1-benzyl)-1-piperazino} carbonyl-oxycamptothecin; (BP-CPT)] in U373MG glioma cell lines transfected with plasmids encoding rabbit liver carboxylesterases (rCE) or human intestinal carboxylesterases (hiCE). BP-CPT has been proved to be activated more efficiently than CPT-11 by a rat serum esterase activity; however, 3D-QSAR studies (CoMFA and CoMSIA) predicted that rCE would activate BP-CPT less efficiently than CPT-11. The models of CoMFA and CoMSIA were based on the relative activity values of 10 compounds (CPT-11 plus nine analogues) for the training set and 4 compounds (CPT-11 derivatives including BP-CPT) for the test set. The SN-38 portions of all the 14 molecules were superimposed. CoMFA analysis was based on steric plus electrostatic properties, PLS analysis gave a cross-validated q^2 correlation coefficient of 0.528 and conventional non-cross-validated correlation coefficient of $r^2 = 1$. The steric parameter alone as the primary descriptor gave a higher cross-validated q^2 (0.583) than that observed when both steric and electrostatic properties were combined. As similar to CoMFA analysis, a primary descriptor of steric plus electrostatic parameters gave a lower q^2 value in CoMSIA analysis than that with steric properties alone. PLS analysis of the CoMSIA values for compounds in the training set resulted in q^2 value of 0.440 and r^2 value of 0.999 for both parameters and a q^2 value of 0.656 and r^2 value of 0.997 for the steric descriptor alone. The hydrophobic descriptor also produced an excellent q^2 value of 0.678 and r^2 value of 0.998. Thus, CoMFA and CoMSIA results suggest together that steric properties may most accurately predict the biological activity of this class of prodrugs, with the hydrophobicity of the compound also a possible contributing factor.

A data set of 7-substituted homocamptothecins (hCPTs) was used by Miao and cowerkers [118] to perform the CoMFA and CoMSIA analysis. The first five models, using a single CoMSIA field, indicated that the steric field, the electrostatic field, and the hydrophobic field were more important than the other two fields, the hydrogen-bond donor

and the hydrogen-bond acceptor. However, the addition of hydrogen-bond acceptor field generated the best CoMSIA model (q^2 = 0.717). The correlation coefficients of r^2 of 0.905 and 0.938, and the cross-validated coefficients of q^2 of 0.703 and 0.717 were obtained for the best CoMFA and CoMSIA models, respectively. To visualize the information content of the derived 3D-QSAR models, the CoMFA and CoMSIA contour maps were generated. The sterically favored regions were found mainly around the aromatic ring attached to the iminomethyl group of the C-7 side chain, which indicates that the larger substituents on the iminomethyl group are favorable for high cytotoxicity. From the CoMFA model, the contribution of electrostatic field (0.272) was lower than that of steric field (0.728). Negative charge favored regions were found around the C-2 and C-5 of the phenyl ring of 7-iminomethyl hCPTs and the positive charge favored regions were around the N atom of imino group and C-4 of the phenyl ring. These regions support the observation that the imino group is important for the antitumor activity. Furthermore, CoMSIA reveals that the hydrophobic favored regions are around the phenyl ring of the C-7 side chain. Except the *meta* position, the *ortho* and *para* positions of the phenyl ring are suitable to be substituted with hydrophobic groups.

4. Clinical Chemistry

There are currently two CPT derivatives in clinical use, topotecan (II) and irinotecan (III). These analogues have shown tremendous promise as solid tumor drugs, but suffer from low tumor response rates and dose-limiting toxicity. Toxicity caused by topotecan presents a less complex problem than toxicities induced by irinotecan. The dose-limiting toxicities of irinotecan include the following: diarrhea, myelosuppression, neutropenia, thrombocytopenia, anaemia, nausea, vomiting, fatigue, and alopecia. [119,120] The main dose-limiting toxicities of irinotecan is severe myelosuppression (grade 3 or 4) with an incidence of about 15-20%, and delayed-type severe diarrhea, which is characteristically seen in 20-25% of patients about 5 days after the start of the therapy. The occurrence of diarrhea, in particular, has significant clinical ramifications, as it affects the dose that can be safely administered, and is occasionally associated with life-threatening events. Although the mechanism by which irinotecan induces delayed-type diarrhea has not yet been elucidated. [121,122] Recently, it has been suggested that the polymorphic ABCC2 transporter may have a crucial role in the occurrence of irinotecan-related diarrhea, particularly in individuals who are not genetically predisposed because of impaired UGT1A1-mediated glucuronidation of the active metabolite, SN-38. [122] It has also been reported about the problem of central nervous system (CNS) toxicity induced by irinotecan. Although the mechanism by which CNS toxicity occurs after irinotecan infusion is not much clear. [123] A recent review provides evidence broadly linking neurotoxicity to electron transfer (ET), reactive oxygen species (ROS), and oxidative stress (OS). [124] Experimental work with CPT demonstrates a fit within the ET-ROS-OS framework, indicating that CPT could serve as a model. Irinotecan (CPT-11) is bioactivated by metabolism to the active form 7-ethyl-10-hydroxycamptothecin (SN-38). Mechanistically, SN-38 incorporates a phenolic precursor of ET quinone capable of generating ROS. [125]

The combination therapies of irinotecan with various regimens indicated that irinotecan/5-FU/folinic acid (leucovorin) combinations have superior anti-tumor activity in stage III colon cancer and improved response rate as well as the time to progression compared with 5-FU/folinic acid regimens alone. [126] Although this combination (irinotecan/5-FU/folinic acid) increased the neutropenia. Other toxic effects were manageable, noncumulative and reversible. [127] In the adjuvant setting, FOLFOX (5-FU/leucovorin (LV)/oxaliplatin) has improved 3-years disease-free survival in stage II/III colorectal cancer in the MOSAIC trial. Since, 5-FU/LV-based combination therapy with oxaliplatin or irinotecan has similar efficacy in metastatic disease in the first-line setting, the impact of irinotecan in the adjuvant setting deserves further randomized clinical trials. [128] Similarly, the combination of irinotecan and cisplatin was significantly active against small cell lung cancer (SCLC), with an acceptable toxicity profile. [129] A Phase III trial for the treatment of small cell lung cancer carried out in Japan clearly demonstrated a survival advantage of a combination of cisplatin and irinotecan over the standard regimen of cisplatin and etoposide. [130] This combination (irinotecan and cisplatin) was also active in untreated as well as previously treated patients with gastric or gastroesophageal junction carcinoma with a manageable profile. [131] A modification in doses and schedules may be warranted to make the regimen more tolerable to patients. The addition of other active drugs or radiation therapy to this regimen would be of great interest. [132] Irinotecan and etoposide was found as an active combination in the treatment of either previously treated or untreated SCLC. Neutropenia was the most commonly observed toxicity in this combination; there were no severe gastrointestinal toxicities, including diarrhea. [129] Recently, a phase I study was conducted in a cohort of lung cancer patients to determine the maximum tolerated dose (MTD) and toxicities of irinotecan (CPT-11), a topoisomerase I inhibitor, in combination with amrubicin (AMR), a topoisomerase II inhibitor, and to observe their antitumor activities. The observed data suggested that the combination of CPT-11 and AMR was not tolerated, as it mediates an unexpectedly strong myelosuppressive effect, and is inactive against both NSCLC and SCLC. [133]

The principal dose-limiting toxicity of topotecan is neutropenia, but thrombocytopenia and anemia occur as well, while the nonhematological toxicities are usually mild. Alopecia is frequently observed and some patients may suffer from pronounced fatigue. [134] The gastrointestinal adverse effects of topotecan, including diarrhea, nausea and vomiting, were successfully controlled with standard supportive care measures. [135] A randomized phase III trial of topotecan versus paclitaxel in ovarian cancer patients pretreated with cisplatin/cyclophosphamide has demonstrated that topotecan is as effective as paclitaxel in the second-line treatment of these patients. [134] Topotecan freely crosses the blood-brain barrier and may be clinically effective in both the therapeutic and prophylactic settings in patients with brain metastases. Recent studies have demonstrated that the antitumor activity of topotecan against brain metastases, with objective response rates ranging from 33%-63% in patients with various solid tumors. The antitumor response in the central nervous system was often greater and occurred more quickly than the systemic antitumor response to topotecan treatment. Early studies have also suggested that topotecan, an apparent radiosensitizer, may be particularly effective in combination with radiotherapy, the current

Table 1. Camptothecin derivatives in clinical use/trial with their side effects and physicochemical descriptors.

No.	CPTs	Status	Indications	Side Effects	Clog *P*[a]	CMR[a]	MW[a]	HBD[b]	HBA[b]	TPSA[b]	Ref.
1	Topotecan (Hycamtin)	FDA approved (GlaxoSmith Kline)	Metastatic ovarian and SCLC cancers (second line)	Neutropenia, anemia, thrombocytopenia, leukopenia (sever). Alopecia, fatigue, abdominal pain, diarrhea, nausea, vomiting, and fever (mild)	0.73	11.43	421.49	2	8	104.90	119, 134, 135, 139, 140
2	Irinotecan (Camptosar)	FDA approved (Pfizer)	Metastatic colorectal cancer (first line with 5FU/leucovorin)	Neutropenia, anemia, myelosuppression, leukopenia, fatigue, abdominal pain or cramping, diarrhea, nausea, vomiting, and thrombocytopenia (sever). Alopecia, anorexia, and fever (mild)	2.73	16.12	586.75	1	10	114.21	119, 120, 121, 139, 140
3	Rubitecan (9-NC)	Phase II/III (SuperGen)	Pancreatic cancer	Neutropenia, anemia, thrombocytopenia, nausea, vomiting, diarrhea, asthenia, alopecia, anorexia, and abdominal pain.	0.76	10.13	393.38	1	9	127.25	32, 119, 139, 141
4	IDEC-132 (9-AC)	Phase II	Ovarian cancer (intraparenteral)	Myelosuppression, Neutropenia, thrombocytopenia, nausea, vomiting, and diarrhea	0.35	9.89	363.40	3	7	107.45	43, 119, 139

Table 1. Continued

No.	CPTs	Status	Indications	Side Effects	Clog *P*[a]	CMR[a]	MW[a]	HBD[b]	HBA[b]	TPSA[b]	Ref.
5	BAY38-3441	Phase I	MX-1 breast, LXFL529 lung, CXF280 and HT29 colon cancers and advanced solid malignancies	Thrombocytopenia, neutropenia, diarrhea, vomiting, nausea, lethargy, and abdominal pain.	1.54	23.84	896.08	6	18	237.50	32, 142
6	Gimatecan (ST-1481)	Phase I/II	Glioblastoma, SCLC and solid tumors	Myelosuppression, mild diarrhea, and mucositis	2.23	12.49	447.53	1	8	103.03	32, 139
7	Karenitecin (BNP-1350)	Phase II	Glioblastomas, melanomas and NSCLC tumors	Thrombocytopenia, neutropenia, and myelosuppression	3.70	12.73	448.64	1	6	81.43	43, 139, 143
8	Silatecan (DB-67)	Preclinical	Glioblastomas	ND	4.36	13.34	478.67	2	7	101.66	139
9	CKD-602	Phase II	Various tumor cell lines	Thrombocytopenia, neutropenia, diarrhea, and vomiting	1.17	12.21	433.55	2	7	93.46	43
10	DRF-1042	Phase I	Osteosarcoma, renal cell and breast carcinomas	Myelosuppression, neutropenia, and diarrhea	0.29	10.76	408.44	2	8	110.89	32
11	Lurtotecan (GI-147211 NX 211)	Phase II	Ovarian and other carcinomas	Myelosuppression, thrombocytopenia, neutropenia, and anemia (sever). Nausea, vomiting, fatigue, alopecia and anorexia (mild)	1.56	13.92	518.62	1	10	106.37	43, 119, 139

Table 1. Continued

No.	CPTs	Status	Indications	Side Effects	Clog *P*[a]	CMR[a]	MW[a]	HBD[b]	HBA[b]	TPSA[b]	Ref.
12	Exatecan mesylate (DX-8591f; DE-310)	Phase II/III	Various carcinomas	Myelosuppression, thrombocytopenia, neutropenia, and anemia (sever). Nausea, vomiting, diarrhea, fatigue, dizziness, stomatitis, asthenia, and anorexia (mild)	0.95	11.58	435.49	3	7	107.45	32, 43 119, 139
13	Diflomo-tecan (BN 80915)	Phase II	Advanced metastatic cancers: colon, breast and prostate	Hematological toxicity and alopecia (sever). Fatigue and gastrointestinal toxicity (mild)	1.21	10.02	398.39	1	6	81.43	32, 139, 144
14	Prothecan (PEG-CPT)	Phase II (Enzon)	NSCLC and other solid tumors	Myelosuppression, thrombocytopenia, neutropenia, anemia, nausea, vomiting, diarrhea, fatigue, cystitis and alopecia	ND	ND	ND	ND	ND	ND	32, 139, 145, 146, 147
15	PNU-166148 (MAG-CPT)	Phase I Pharmacia/Pfizer	Malignant solid tumors	Cumulative bladder toxicity (sever), myelosuppression, neutropenic sepsis, and diarrhea	ND	ND	ND	ND	ND	ND	147, 148, 149, 150

[a]Determined by using the C-QSAR program (http://www.biobyte.com)
[b]Determined by using the JME molecular editor (http://www.molinspiration.com)
ND = Not determined
HBA = Number of hydrogen bond acceptors
HBD = Number of hydrogen bond donors
TPSA = Topological polar surface area

standard of care for patients with brain metastases. Synergistic antitumor activity against brain metastasis may be achieved when topotecan is combined with other cytotoxic agents with different mechanisms of action. However, the number of cytotoxic agents that can cross an intact blood-brain barrier (BBB) is limited. Preliminary data suggested that topotecan in combination with temozolomide (another cytotoxic agent, has an approximately 100% oral bioavailability, and it readily crosses the BBB) may have synergistic antitumor activity against brain metastases. [136]

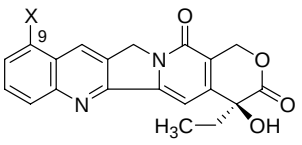

Rubitecan; X = NO_2
IDEC-132; X = NH_2

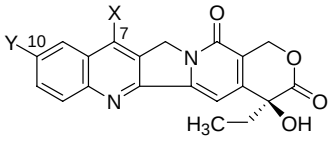

Gimatecan; X = $CH{=}NOC(CH_3)_3$, Y = H
Karenitecin; X = $CH_2CH_2Si(CH_3)_3$, Y = H
Silatecan; X = $Si(CH_3)_2C(CH_3)_3$, Y = OH
CKD-602; X = $CH_2CH_2NHCH(CH_3)_2$, Y = H

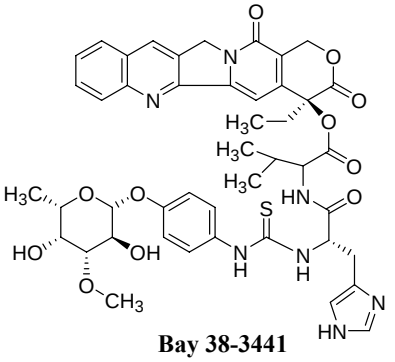

Bay 38-3441

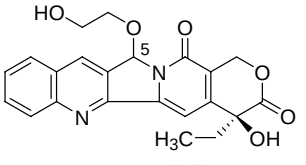

DRF-1042

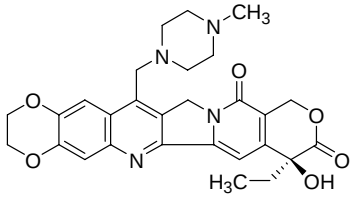

Lurtotecan

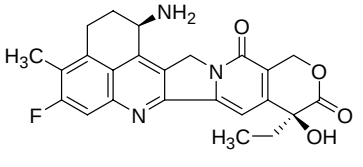

Exatecan

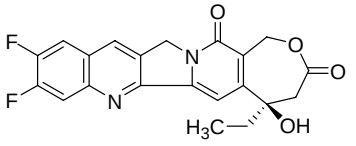

Diflomotecan

Prothecan

Figure 2. Continued on next page.

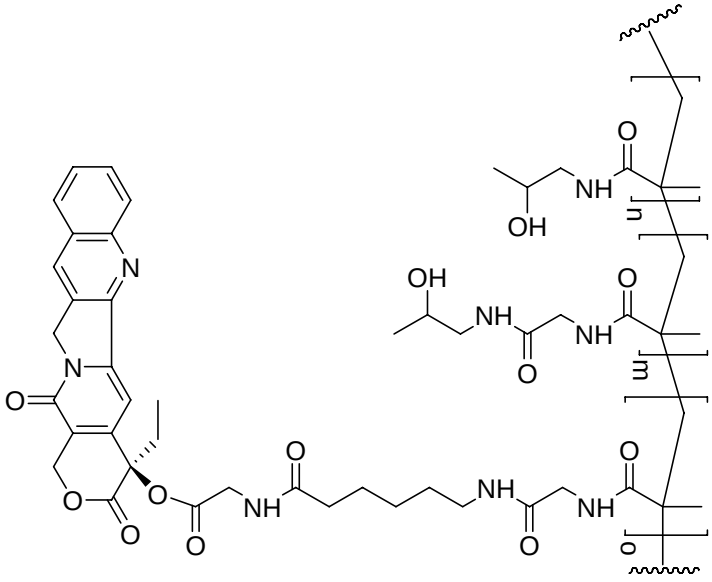

Figure 2. Structures of CPTs used in Table 1

The administration of topotecan (topo I inhibitor) and etoposide (topo II inhibitor) in patients with advanced solid malignancies did not provide substantial evidence that this combination is more advantageous than either topotecan or etoposide alone. [137] On the other hand, the combination of topotecan/cisplatin/paclitaxel with G-CSF support represented a well-tolerated and active therapeutic approach in both pre-treated and untreated patients with ovarian cancer or small cell lung cancer. [138]

At present, the extensive clinical trials are continuing to describe the better picture of clinical chemistry of topotecan, irinotecan, and some other new CPT derivatives (which are in various stages of clinical trials) to determine their optimal dose, route of administration, schedules, and the possibility in the combination with other chemotherapeutic agents. Details about the CPT derivatives (Figure 2) in clinical use/trial with their toxicities and physicochemical descriptors are listed in Table 1.

5. Conclusions

Camptothecins are regarded as one of the most promising anticancer drugs of the twenty-first century. The structure–activity relationships (SAR) provide insight into the mechanism of topo I inhibition and helped in the synthesis of various CPTs by modifying the different rings of the original CPT molecule, giving each analogue a unique property. These modifications have resulted in various improvements in the parent molecule, including changes in the bioavailability, stabilization of the lactone ring, and/or decrease in the substrate recognition by the drug-resistant proteins as well as improvements in the toxicity profile in preclinical studies. QSAR paradigm has already been proved to be useful in

understanding the requirements of physicochemical properties of the substituents in many key locations as well as molecules as a whole. An investigation on the QSAR results relative to the CPT derivatives has suggested that the hydrophobic and molar refractivity descriptors of the compound/substituents are the two most important determinants for their activity.

Although CPTs are therapeutically effective, they are not curative as single agents. The full curative/therapeutic potential of CPTs will not be realized without the development of approaches to compensate for their dose-limiting toxicities. Currently, two anticancer CPT derivatives, topotecan and irinotecan are in clinical use. These compounds have shown tremendous promise as solid tumor drugs and become a part of the multi-million dollar industry, but suffer from low tumor response rates and dose- limiting toxicity. At present, the extensive clinical trials are continuing to describe the better picture of the clinical chemistry of topotecan, irinotecan, and several new CPT derivatives (which are in various stages of clinical trials) to determine their optimal dose, route of administration, schedules, and their possibility to use in the combination with other chemotherapeutic agents to improve their antitumor activities and reduce their toxicities.

We hope that the knowledge of the clinical chemistry, together with the generation of SAR and QSAR, constitutes a large body of evidence that may assist in the development of new CPT with excellent antitumor activity and low dose-limiting toxicity.

References

[1] Wall, ME; Wani, MC; Cook, CE; Palmer, KH; McPhail, AT; Sim, GA. Plant antitumor agents. I. The isolation and structure of camptothecin, a novel alkaloidal leukemia and tumor inhibitor from *Camptotheca acuminate. J. Am. Chem. Soc.* 1966, 88, 3888-3890.

[2] Wall, ME; Wani, MC. Antineoplastic agents from plants. *Annu. Rev. Pharmacol Toxicol.* 1977, 17, 117-132.

[3] Hsiang, YH; Hertzberg, R; Hecht, S; Liu, LF. Camptothecin induces protein-linked DNA breaks via mammalian DNA topoisomerase I. *J. Biol. Chem*. 1985, 260, 14873-14878.

[4] Pommier, Y; Pourquier, P; Fan, Y; Strumberg, D. Mechanism of action of eukaryotic DNA topoisomerase I and drugs targeted to the enzyme. *Biochim. Biophys. Acta* 1998, 1400, 83-105.

[5] Kingsbury, WD; Boehm, JC; Jakas, DR; Holden, KG; Hecht, SM; Gallagher, G; Caranfa, MJ; McCabe, FL; Faucette, LF; Johnson, RK; Hertzberg, RP. Synthesis of water-soluble (aminoalkyl)camptothecin analogs: inhibition of topoisomerase I and antitumor activity. *J. Med. Chem.* 1991, 34, 98-107.

[6] Ormrod, D; Spencer, CM. Topotecan: a review of its efficacy in small-cell lung cancer. *Drugs* 1999, 58, 533-551.

[7] Markman, M. Topotecan as second-line therapy for ovarian cancer: Dosage versus toxicity. *Oncologist* 2005, 10, 695-697.

[8] Pavillard, V; Charasson, V; Laroche-Clary, A; Soubeyran, I; Robert, J. Cellular parameters predictive of the clinical response of colorectal cancers to irinotecan. A preliminary study. *Anticancer Res*. 2004, 24, 579-585.

[9] Fuchs, C; Mitchell, EP; Hoff, PM. Irinotecan in the treatment of colorectal cancer. *Cancer Treat. Rev*. 2006, 32, 491-503.

[10] Legarza, K; Yang, LX. New molecular mechanisms of action of camptothecin-type drugs. *Anticancer Res.* 2006, 26, 3301-3305.

[11] Li, QY; Zu, YG; Shi, RZ; Yao, LP. Review camptothecin: Current perspectives. *Curr. Med. Chem.* 2006, 13, 2021-2039.

[12] Oberlies, NH; Kroll, DJ. Camptothecin and taxol: Historic achievements in natural products research. *J. Nat. Prod.* 2004, 67, 129-135.

[13] Champoux, JJ. DNA topoisomerases: structure, function, and mechanism. *Annu. Rev. Biochem.* 2001, 70, 369-413.

[14] Corbett, A; Osheroff, N. When good enzymes go bad: Conversion of topoisomerase II to a cellular toxin by antineoplastic drugs. *Chem. Res. Toxicol.* 1993, 6, 585-597.

[15] Wang, JC. DNA topoisomerases. *Annu. Rev. Biochem.* 1996, 65, 635-692.

[16] Tse-Dinh, YC; Kirkegaard, K; Wang, JC. Covalent bonds between protein and DNA: Formation of phosphotyrosine linkage between certain DNA topoisomerases and DNA, *J. Biol. Chem.* 1980, 255, 5560–5565.

[17] Wang, JC. DNA Topoisomerases as targets of therapeutics: an overview. In: L.F. Liu, LF, editor, *Advances in pharmacology* (vol. 29A), New York: Academic Press; 1994; 1–19.

[18] Hsiang, YH; Lihou, MG; Liu, LF. Arrest of replication forks by drug-stabilized topoisomerase I-DNA cleavable complexes as a mechanism of cell killing by camptothecin. *Cancer Res.*. 1989, 49*,* 5077-5082.

[19] Thomas, CJ; Rahier, NJ; Hecht, SM. Camptothecin: current perspectives. *Bioorg. Med. Chem*. 2004, 12, 1585-1604.

[20] Argaman, M; Bendetz-Nezer, S; Matlis, S; Segal, S; Priel, E. Revealing the mode of action of DNA topoisomerase I and its inhibitors by atomic force microscopy. *Biochem. Biophys. Res. Commun.* 2003, 301, 789-797.

[21] Wang, X; Wang, LK; kingsbury, WD; Johnson, RK; Hecht, SM. Differential effects of camptothecin derivatives on topoisomerase I-mediated DNA structure modification. *Biochemistry* 1998, 37, 9399-9408.

[22] Hertzberg, RP; Caranfa, MJ; Hecht, SM. On the mechanism of topoisomerase I inhibition by camptothecin: evidence for binding to an enzyme-DNA complex. *Biochemistry* 1989, 28, 4629-4638.

[23] Miller, SE; Pilch, DS. A spectrophotometric study of the pH-dependent and DNA binding properties of topotecan. *Ann. N. Y. Acad. Sci.* 2000, 922, 309-313.

[24] Staker, BL; Hjerrild, K; Feese, MD; Behnke, CA; Burgin, AB, Jr.; Stewart, L. The mechanism of topoisomerase I poisoning by a camptothecin analog. *Proc. Natl. Aca. Sci.* 2002, 99, 15387-15392.

[25] Petrangolini, G; Pratesi, G; De Cesare, M; Supino, R; Pisano, C; Marcellini, M; Giordano, V; Laccabue, D; Lanzi, C; Zunino, F. Antiangiogenic effects of the novel camptothecin ST1481 (Gimatecan) in human tumor xenografts. *Mol. Cancer Res*. 2003, 1, 863-870.

[26] Ji, Y; Hayashi, K; Amoh, Y; Tsuji, K; Yamauchi, K; Yamamoto, N; Tsuchiya, H; Tomita, K; Bouvet, M; Hoffman, RM. The camptothecin derivative CPT-11 inhibits

angiogenesis in a dual-color imageable orthotopic metastatic nude mouse model of human colon cancer. Anticancer Res. 2007, 27, 713-718.

[27] Liu, X; Lin, J; Bao, Y; Lin, X; An, L. Camptothecin-mediated apoptosis and antiproliferation effect is accompanied by down-regulation of telomerase activity in HaCaT cells. *J. Dermatol. Sci*. 2006, 42, 262-264.

[28] Saleem, A; Edwards, TK; Rasheed, Z; Rubin, EH. Mechanisms of resistance to camptothecins. *Ann. N. Y. Acad. Sci.* 2000, 922, 46-55.

[29] Meng, LH; Liao, ZY; Pommier, Y. Non-camptothecin DNA topoisomerase I inhibitors in cancer therapy. *Curr. Top. Med. Chem*. 2003, 3, 305-320.

[30] Maliepaard, M; Van Gastelen, MA.; De Jong, LA.; Pluim, D; Van Waardenburg, RCAM; Ruevekamp-Helmers, MC; Floot, BGJ.; Schellens, JHM. Overexpression of the BCRP/MXR/ABCP gene in a topotecan-selected ovarian tumor cell line. Cancer Res. 1999, 59, 4559-4563.

[31] Chrencik, JE; Staker, BL; Burgin, AB; Pourquier, P; Pommier, Y; Stewart, L; Redinbo, MR. Mechanisms of camptothecin resistance by human topoisomerase I mutations. *J. Mol. Biol.* 2004, 339, 773-784.

[32] Legarza, K; Yang, LX. Novel camptothecin derivatives. *In Vivo* 2005, 19, 283-292.

[33] Eriksson, L; Jaworska, J; Worth, AP; Cronin, MTD; McDowell, RM; Gramatica, P. Methods for reliability and uncertainty assessment and for applicability evaluations of classification- and regression-based QSARs. *Environ. Health Perspect*. 2003, 111, 1361-1375.

[34] Verma, RP; Hansch, C. Matrix metalloproteinases (MMPs): Chemical-biological functions and QSARs. *Bioorg. Med. Chem.* 2007, 15, 2223-2268.

[35] Wang, X; Zhou, X; Hecht, SM. Role of the 20-hydroxyl group in camptothecin binding by the topoisomerase I-DNA binary complex. *Biochemistry* 1999, 38, 4374-4381.

[36] Lorence, A; Nessler, CL. Camptothecin: Over four decades of surprising findings. *Phytochemistry* 2004, 65, 2735-2749.

[37] Redinbo, MR; Stewart, L; Kuhn, P; Champoux, JJ; Hol, WGJ. Crystal structures of human topoisomerase I in covalent and noncovalent complexes with DNA. Science 1998, 279, 1504-1513.

[38] Bailly, C. Homocamptothecins: potent topoisomerase I inhibitors and promising anticancer drugs. *Crit. Rev. Oncol. Hematol*. 2003, 45, 91-108.

[39] Staker, BL; Feese, MD; Cushman, M; Pommier, Y; Zembower, D; Stewart, L; Burgin, AB. Structures of three classes of anticancer agents bound to the human topoisomerase I-DNA covalent complex. *J. Med. Chem*. 2005, 48, 2336-2345.

[40] Leu, YL; Roffler, SR; Chern, JW. Design and synthesis of water-soluble glucuronide derivatives of camptothecin for cancer prodrug monotherapy and antibody-directed enzyme prodrug therapy (ADEPT). J. Med. Chem. 1999, 42, 3623-3628.

[41] Wani, MC; Nicholas, AW; Wall, ME. Plant antitumor agents. 23. Synthesis and antileukemic activity of camptothecin analogs. *J. Med. Chem.* 1986, 29, 2358-2363.

[42] Carrigan, SW; Fox, PC; Wall, ME; Wani, M; Bowen, J. Comparative molecular field analysis and molecular modeling studies of 20-(S)-camptothecin analogs as inhibitors of DNA topoisomerase I and anticancer/antitumor agents. *J. Comput Aided Mol. Design* 1997, 11, 71-78.

[43] Kim, DK; Lee, N. Recent advances in topoisomerase I-targeting agents, camptothecin analogues. *Mini-Rev. Med. Chem.* 2002, 2, 611-619.

[44] Gao, H; Zhang, X; Chen, Y; Shen, H; Pang, T; Sun, J; Xu, C; Ding, J; Li, C; Lu, W. Synthesis and antitumor activity of the hexacyclic camptothecin derivatives. *Bioorg. Med. Chem. Lett*. 2005, 15, 3233-3236.

[45] Wani MC; Nicholas AW; Manikumar G; Wall ME. Plant antitumor agents. 25. Total synthesis and antileukemic activity of ring A substituted camptothecin analogues. Structure-activity correlations. *J. Med. Chem.* 1987, 30, 1774-1779.

[46] Wall ME; Wani MC; Nicholas AW; Manikumar G; Tele C; Moore L; Truesdale A; Leitner P; Besterman JM. Plant antitumor agents. 30. Synthesis and structure activity of novel camptothecin analogs. *J. Med. Chem.* 1993, 36, 2689-2700.

[47] Uehling, DE; Nanthakumar, SS; Croom, D; Emerson, DL; Leitner, PP; Luzzio, MJ; McIntyre, G; Morton, B; Profeta, S; Sisco, J; Sternbach, DD; Tong, WQ; Vuong, A; Besterman, JM. Synthesis, topoisomerase I inhibitory activity, and in vivo evaluation of 11-azacamptothecin analogs. *J. Med. Chem.* 1995, 38, 1106-1118.

[48] Candiani, I; Bedeschi, A; Cabri, W; Zarini, F; Visentin, G; Capolongo, L; Geroni, C; Ciomei, M. Synthesis and cytotoxic activity of alkylidene - and alkyl-substituted camptothecins. *Bioorg. Med. Chem. Lett*. 1997, 7, 847-850.

[49] Takayama H; Watanabe A; Hosokawa M; Chiba K; Satoh T; Aimi N. Synthesis of a new class of camptothecin derivatives, the long-chain fatty acid esters of 10-hydroxycamptothecin, as a potent prodrug candidate, and their in vitro metabolic conversion by carboxylesterases. *Bioorg. Med. Chem. Lett*. 1998, 8, 415-418.

[50] Jew, SS; Kim, HJ; Kim, MG; Roh, EY; Hong, CI; Kim, JK; Lee, JH; Lee, H; Park, HG. Synthesis and in vitro cytotoxicity of hexacyclic camptothecin analogs. *Bioorg. Med. Chem. Lett.* 1999, 9, 3203-3206.

[51] Dallavalle, S; Delsoldato, T; Ferrari, A; Merlini, L; Penco, S; Carenini, N; Perego, P; De Cesare, M; Pratesi, G; Zunino, F. Novel 7-Substituted Camptothecins with Potent Antitumor Activity. *J. Med. Chem.* 2000, 43, 3963-3969.

[52] Dallavalle, S; Ferrari, A; Merlini, L; Penco, S; Carenini, N; De Cesare, M; Perego, P; Pratesi, G; Zunino, F. Novel cytotoxic 7 -iminomethyl and 7 -aminomethyl derivatives of camptothecin. *Bioorg. Med. Chem. Lett.* 2001, 11, 291-294.

[53] Dallavalle, S; Ferrari, A; Biasotti, B; Merlini, L; Penco, S; Gallo, G; Marzi, M; Tinti, MO; Martinelli, R; Pisano, C; Carminati, P; Carenini, N; Beretta, G; Perego, P; De Cesare, M; Pratesi, G; Zunino, F. Novel 7-Oxyiminomethyl Derivatives of Camptothecin with Potent in Vitro and in Vivo Antitumor Activity. *J. Med. Chem*. 2001, 44, 3264-3274.

[54] Ohtsu, H; Nakanishi, Y; Bastow, KF; Lee, FY; Lee, KH. Antitumor agents 216. Synthesis and evaluation of paclitaxel-camptothecin conjugates as novel cytotoxic agents. *Bioorg. Med. Chem*. 2003, 11, 1851-1857.

[55] Yaegashi, T; Sawada, S; Nagata, H; Furuta, T; Yokokura, T; Miyasaka, T. Synthesis and antitumor activity of 20(S)-camptothecin derivatives. A-ring-substituted 7-ethylcamptothecins and their E-ring-modified water-soluble derivatives. *Chem. Pharm. Bull.* 1994, 42, 2518-2525.

[56] Tanizawa, A; Kohn, KW; Kohlhagen, G; Leteurtre, F; Pommier, Y. Differential stabilization of eukaryotic DNA topoisomerase I cleavable complexes by camptothecin derivatives. *Biochemistry* 1995, 34, 7200-7206.

[57] Burke, TG; Mi, Z. Ethyl substitution at the 7 position extends the half-life of 10-hydroxycamptothecin in the presence of human serum albumin. *J. Med. Chem*. 1993, 36, 2580-2582.

[58] Bom, D; Curran, DP; Kruszewski, S; Zimmer, SG; Strode, JT; Kohlhagen, G; Du, W; Chavan, AJ; Fraley, KA; Bingcang, AL; Latus, LJ; Pommier, Y; Burke, TG. The Novel Silatecan 7-tert-butyldimethylsilyl-10-hydroxycamptothecin displays high lipophilicity, improved human blood stability, and potent anticancer activity. *J. Med. Chem*. 2000, 43, 3970-3980.

[59] Kim, DK; Ryu, DH; Lee, JY; Lee, N; Kim, YW; Kim, JS; Chang, K; Im, GJ; Kim, TK; Choi, WS. Synthesis and biological evaluation of novel A-ring modified hexacyclic camptothecin analogues. J. Med. Chem. 2001, 44, 1594-1602.

[60] Sugimori, M; Ejima, A; Ohsuki, S; Uoto, K; Mitsui, I; Matsumoto, K; Kawato, Y; Yasuoka, M; Sato, K; Tagawa, H; Terasawa, H. Antitumor Agents. 7. Synthesis and antitumor activity of novel hexacyclic camptothecin analogs. J. Med. Chem. 1994, 37, 3033-3039.

[61] Subrahmanyam, D; Sarma, VM; Venkateswarlu, A; Sastry, TVRS; Kulakarni, AP; Srinivasa, RD; Krishna Reddy, KVSR. In vitro cytotoxicity of 5-aminosubstituted 20(S)-camptothecins. Part 1. *Bioorg. Med. Chem*. 1999, 7, 2013-2020.

[62] Sriram, D; Yogeeswari, P; Thirumurugan, R; Bal, TR. Camptothecin and its analogues: a review on their chemotherapeutic potential. *Nat. prod. Res*. 2005, 19, 393-412.

[63] Subrahmanyam, D; Sarma, VM; Venkateswarlu, A; Sastry, TV; Srinivas, AS; Krishna, CV; Deevi, DS; Kumar, SA; Babu, MJ; Damodaran, NK. Novel C-ring analogues of 20(S)- camptothecin. Part 3: synthesis and their in vitro cytotoxicity of A-, B- and C-ring analogues. *Bioorg. Med. Chem. Lett.* 2000, 10, 369-371.

[64] Subrahmanyam, D; Venkateswarlu, A; Rao, KV; Sastry, TVRS; Vandana, G; Kumar, SA. Novel C-ring analogues of 20(S)- camptothecin. Part-2: synthesis and in vitro cytotoxicity of 5-C-substituted 20(S)- camptothecin analogues. *Bioorg. Med. Chem. Lett.* 1999, 9, 1633-1638.

[65] Sugimori, M; Ejima, A; Ohsuki, S; Matsumoto, K; Kawato, Y; Yasuoka, M; Tagawa, H; Terasawa, H. Antitumor agents. VI. Synthesis and antitumor activity of ring A-, ring B-, and ring C-modified derivatives of camptothecin. *Heterocycles* 1994, 38, 81-94.

[66] Crow, RT; Crothers, DM. Structural modifications of camptothecin and effects on topoisomerase I inhibition. J. Med. Chem. 1992, 35, 4160-4164.

[67] Nicholas, AW; Wani, MC; Manikumar, G; Wall, ME; Kohn, KW; Pommier, Y. Plant antitumor agents. 29. Synthesis and biological activity of ring D and ring E modified analogs of camptothecin. *J. Med. Chem*. 1990, 33, 972-978.

[68] Rahier, NJ; Cheng, K; Gao, R; Eisenhauer, BM; Hecht, SM. Synthesis of 14-azacamptothecin, a water-soluble topoisomerase I poison. *Org. Lett.* 2005, 7, 835-837.

[69] Cheng, K; Rahier, NJ; Eisenhauer, BM; Gao, R; Thomas, SJ; Hecht, SM. 14 -azacamptothecin: a potent water-soluble topoisomerase I poison. *J. Am. Chem. Soc.* 2005, 127, 838-839.

[70] Hecht, SM. Camptothecin: Role of the D and E rings in binding to the topoisomerase I-DNA covalent binary complex. *Curr. Med. Chem. – Anti-Cancer Agents* 2005, 5, 353-362.

[71] Hertzberg, RP; Caranfa, MJ; Holden, KG; Jakas, DR; Gallagher, G; Mattern, MR; Mong, SM; Bartus, JO; Johnson, RK; Kingsbury, WD. Modification of the hydroxylactone ring of camptothecin: inhibition of mammalian topoisomerase I and biological activity. *J. Med. Chem*. 1989, 32, 715-720.

[72] Jaxel, C; Kohn, KW; Wani, MC; Wall, ME; Pommier, Y. Structure-activity study of the actions of camptothecin derivatives on mammalian topoisomerase I: evidence for a specific receptor site and a relation to antitumor activity. *Cancer Res.* 1989, 49, 1465-1469.

[73] Wani, MC; Nicholas, AW; Wall, ME. Plant antitumor agents. 28. Resolution of a key tricyclic synthon, 5'(RS)-1,5-dioxo-5'-ethyl-5'-hydroxy-2'H,5'H,6'H-6'-oxopyrano[3',4'-f]Δ6,8-tetrahydroindolizine: total synthesis and antitumor activity of 20(S)- and 20(R)-camptothecin. *J. Med. Chem.* 1987, 30, 2317-2319.

[74] Hatefi A; Amsden B. Camptothecin delivery methods. *Pharm. Res.* 2002, 19, 1389-1399.

[75] Burke, TG; Munshi, CB; Mi, Z; Jiang, Y. The important role of albumin in determining the relative human blood stabilities of the camptothecin anticancer drugs. *J. Pharm. Sci.* 1995, 84, 518-519.

[76] Mi, Z; Burke, TG. Differential interactions of camptothecin lactone and carboxylate forms with human blood components. *Biochemistry* 1994, 33, 10325-10336.

[77] Cao, Z; Harris, N; Kozielski, A; Vardeman, D; Stehlin, JS; Giovanella, B. Alkyl esters of camptothecin and 9-nitrocamptothecin: synthesis, in vitro pharmacokinetics, toxicity, and antitumor activity. *J. Med. Chem*. 1998, 41, 31-37.

[78] Cao, Z; Pantazis, P; Mendoza, J; Early, J; Kozielski, A; Harris, N; Vardeman, D; Liehr, J; Stehlin, JS; Giovanella, B. Structure-activity relationship of alkyl camptothecin esters. *Ann. N. Y. Acad. Sci.* 2000, 922, 122-135.

[79] Wang, CY; Pan, XD; Liu, HY; Fu, ZD; Wei, XY; Yang, LX. Synthesis and antitumor activity of 20-O-linked nitrogen-based camptothecin ester derivatives. *Bioorg. Med. Chem.* 2004, 12, 3657-3662.

[80] Rahier, NJ; Eisenhauer, BM; Gao, R;Jones, SH; Hecht, SM. Water-soluble camptothecin derivatives that are intrinsic topoisomerase I poisons. *Org. Lett.* 2004, 6, 321-324.

[81] Lavergne, O; Demarquay, D; Kasprzyk, PG; Bigg, Dennis, CH. Homocamptothecins: E-ring modified CPT analogues. *Ann. New York Acad. Sci.* 2000, 922, 100-111.

[82] Lavergne, O; Lesueur-Ginot, L; Rodas, FP; Bigg, DCH. BN 80245: an E-ring modified camptothecin with potent antiproliferative and topoisomerase I inhibitory activities. *Bioorg. Med. Chem. Lett.* 1997, 7, 2235-2238.

[83] Lavergne, O; Lesueur-Ginot, L; Rodas, FP; Kasprzyk, PG; Pommier, J; Demarquay, D; Prevost, G; Ulibarri, G; Rolland, A; Schiano-Liberatore, AM; Harnett, J; Pons, D; Camara, J; Bigg, DCH. Homocamptothecins: Synthesis and antitumor activity of novel E-ring-modified camptothecin analogs. *J. Med. Chem.* 1998, 41, 5410-5419.

[84] Lavergne, O; Harnett, J; Rolland, A; Lanco, C; Lesueur-Ginot, L; Demarquay, D; Huchet, M; Coulomb, H; Bigg, DCH. BN 80927: a novel homocamptothecin with inhibitory activities on both topoisomerase I and topoisomerase II. *Bioorg. Med. Chem. Lett*. 1999, 9, 2599-2602.

[85] Lavergne, O; Demarquay, D; Bailly, C; Lanco, C; Rolland, A; Huchet, M; Coulomb, H; Muller, N; Baroggi, N; Camara, J; Le Breton, C; Manginot, E; Cazaux, JB; Bigg, DCH. Topoisomerase I-Mediated antiproliferative activity of enantiomerically pure fluorinated homocamptothecins. *J. Med. Chem*. 2000, 43, 2285-2289.

[86] Larsen, AK; Gilbert, C; Chyzak, G; Plisov, SY; Naguibneva, I; Lavergne, O; Lesueur-Ginot, L; Bigg, DCH. Unusual potency of BN 80915, a novel fluorinated E-ring modified camptothecin, toward human colon carcinoma cells. *Cancer Res*. 2001, 61, 2961-2967.

[87] Bom, D; Curran, DP; Chavan, AJ; Kruszewski, S; Zimmer, SG; Fraley, KA; Burke, TG. Novel A, B, E-ring-modified camptothecins displaying high lipophilicity and markedly improved human blood stabilities. *J. Med. Chem*. 1999, 42, 3018-3022.

[88] Du, W; Curran, DP; Bevins, RL; Zimmer, SG; Zhang, J; Burke, TG. Synthesis and evaluation of a novel E-ring modified alpha-hydroxy keto ether analogue of camptothecin. *Bioorg. Med. Chem*. 2002, 10, 103-110.

[89] Cagir, A; Jones, SH; Gao, R; Eisenhauer, BM; Hecht, SM. Luotonin A. A Naturally occurring human DNA topoisomerase I poison. *J. Am. Chem. Soc*. 2003, 125, 13628-13629.

[90] Cagir, A; Jones, SH; Eisenhauer, BM; Gao, R; Hecht, SM. Synthesis and biochemical properties of E-ring modified luotonin A derivatives. *Bioorg. Med. Chem. Lett.* 2004, 14, 2051-2054.

[91] Cagir A; Eisenhauer BM; Gao R; Thomas SJ; Hecht SM. Synthesis and topoisomerase I inhibitory properties of luotonin A analogues. *Bioorg. Med. Chem.* 2004, 12, 6287-6299.

[92] Selassie, CD; Mekapati, SB; Verma, RP. QSAR: then and now. *Curr. Top. Med. Chem.* 2002, 2, 1357–1379.

[93] Hansch, C; Maloney, PP; Fujita, T; Muir, RM. Correlation of biological activity of phenoxyacetic acids with Hammett substituent constants and partition coefficients. *Nature* 1962, 194, 178–180.

[94] Hansch, C; Leo, A. *In Exploring QSAR: Fundamentals and Applications in Chemistry and Biology;* American Chemical Society; Washington, D.C. 1995.

[95] Schultz, TW; Hewitt, M; Netzeva, TI; Cronin, MTD. Assessing applicability domains of toxicological QSARs: definition, confidence in predicted values, and the role of mechanisms of action. *QSAR & Combinatorial Sci.* 2007, 26, 238-254.

[96] Selassie, CD; Garg, R; Kapur, S; Kurup, A; Verma, RP; Mekapati, SB; Hansch, C. Comparative QSAR and the radical toxicity of various functional groups. *Chem. Rev.* 2002, 102, 2585–2605.

[97] Hall, LH; Hall, LM. QSAR modeling based on structure-information for properties of interest in human health. *SAR & QSAR Environ. Res.* 2005, 16, 13-41.

[98] Verma, RP; Kurup, A; Mekapati, SB; Hansch, C. Chemical–biological interactions in human. *Bioorg. Med. Chem*. 2005, 13, 933–948.

[99] Winkler, DA. The role of quantitative structure-activity relationships (QSAR) in biomolecular discovery. *Brief. Bioinformatics* 2002, *3*, 73-86.

[100] Hansch, C; Leo, A; Mekapati, SB; Kurup, A. QSAR and ADME. *Bioorg. Med. Chem.* 2004, 12, 3391–3400.

[101] Khan, MTH; Sylte, I. Predictive QSAR modeling for the successful predictions of the ADMET properties of candidate drug molecules. *Curr. Drug. Discov. Tech.* 2007, 4, 141-149.

[102] Verma, RP; Hansch, C; Selassie, CD. Comparative QSAR studies on PAMPA/modified PAMPA for high throughput profiling of drug absorption potential with respect to caco-2 cells and human intestinal absorption. *J. Comput. Aided Mol. Des.* 2007, 21, 3–22.

[103] Hou, TJ; Zhang, W; Xia, K; Qiao, XB; Xu, XJ. ADME evaluation in Drug Discovery. 5. Correlation of caco-2 permeation with simple molecular properties. *J. Chem. Inf. Compt. Sci.* 2004, 44, 1585-1600.

[104] Verma, RP; Hansch, C. Taxane analogues against breast cancer: A quantitative structure–activity relationship study. *ChemMedChem* 2008, 3, 642-652.

[105] Selassie, CD; Garg, R; Mekapati, S. Mechanism-based QSAR approach to the study of the toxicity of endocrine active substances. *Pure Appl. Chem.* 2003, 75, 2363–2373.

[106] Roncaglioni, A; Benfenati, E. In silico-aided prediction of biological properties of chemicals: oestrogen receptor-mediated effects. *Chem. Soc. Rev*. 2008, 37, 441–450.

[107] Hughes, RA; Harris, T; Altmann, E; McAllister, D; Vlahos, R; Robertson, A; Cushman, M; Wang, Z; Stewart, AG. 2-Methoxyestradiol and analogs as novel antiproliferative agents: Analysis of three-dimensional quantitative structure-activity relationships for DNA synthesis inhibition and estrogen receptor binding. *Mol. Pharmacol.* 2002, 61, 1053–1069.

[108] Hansch, C; Verma, RP. 20-(*S*)-Camptothecin analogues as DNA topoisomerase I inhibitors: A QSAR study. *ChemMedChem* 2007, 2, 1807–1813.

[109] Lipinski, CA; Lombardo, F; Dominy, BW; Feeney, PJ. Experimental and computational approaches to estimate solubility and permeability in drug discovery and development settings. *Adv. Drug Delivery Rev*. 1997, 23, 3-25.

[110] Verma, RP. Understanding topoisomerase I and II in terms of QSAR. *Bioorg. Med. Chem.* 2005, 13, 1059-1067.

[111] Hansch, C; Verma, RP. Quantitative structure-activity relationships of heterocyclic topoisomerase I and II inhibitors. *Top. Heterocycl. Chem*. 2007, 10, 43-73.

[112] Lu, AJ; Zhang, ZS; Zheng, MY; Zou, HJ; Luo, XM; Jiang, HL. 3D-QSAR study of 20(*S*)-camptothecin analogs. *Acta Pharmacol. Sin.* 2007, 28, 307-314.

[113] Amat, L; Robert, D; Besalú, E; Carbó-Dorca, R. Molecular quantum similarity measures tuned 3D QSAR: An antitumoral family validation study. *J. Chem. Inf. Comput. Sci.* 1998, 38, 624-631.

[114] Li, MJ; Jiang, C; Li, MZ; You, TP. QSAR studies of 20(*S*)-camptothecin analogues as antitumor agents. *J. Mol. Structure (Theochem)* 2005, 723, 165-170.

[115] Verma, RP; Hansch, C. Cytotoxicity of organic compounds against ovarian cancer cells: A quantitative structure–activity relationship study. *Mol. Pharm.* 2006, 3, 441-450.

[116] Fan, Y; Shi, LM; Kohn, KW; Pommier, Y; Weinstein, JN. Quantitative structure–antitumor activity relationships of camptothecin analogues: Cluster analysis and genetic algorithm-based studies. *J. Med. Chem*. 2001, *44*, 3254-3263.

[117] Yoon, KJP; Krull, EJ; Morton, CL; Bornmann, WG; Lee, RE; Potter, PM; Danks, MK. Activation of a camptothecin prodrug by specific carboxylesterases as predicted by quantitative structure–activity relationship and molecular docking studies. *Mol. Cancer Ther*. 2003, 2, 1171-1181.

[118] Miao, Z; Sheng, C; Zhang, W; Ji, H; Zhang, J; Shao, L; You, L; Zhang, M; Yao, J; Che, X. New homocamptothecins: Synthesis, antitumor activity, and molecular modeling. *Bioorg. Med. Chem*. 2008, 16, 1493-1510.

[119] Ulukan, H.; Swaan, P. W. Camptothecins: a review of their chemotherapeutic potential. *Drugs* 2002, 62, 2039-2057.

[120] Thompson, J; Stewart, CF; Houghton, PJ. Animal models for studing the action of topoisomerase I targeted drugs. *Biochem. Biophys. Acta* 1998, 1400, 301-319.

[121] Kawahara, M. Irinotecan in the treatment of small cell lung cancer: a review of patient safety considerations. *Expert. Opin. Drug Saf.* 2006, 5, 303-312.

[122] de Jong, FA; Scott-Horton, TJ; Kroetz, DL; McLeod, HL; Friberg, LE; Mathijssen, RH; Verweij, J; Marsh, S; Sparreboom, A. Irinotecan-induced diarrhea: Functional significance of the polymorphic ABCC2 transporter protein. *Clin. Pharmacol. Therapeut.* 2007, 81, 42-49.

[123] Hamberg, P; Donders RCJM.; ten Bokkel Huinink, D. Central nervous system toxicity induced by irinotecan. *J. Natl. Cancer Inst*. 2006, 98, 219.

[124] Kovacic, P; Somanathan, R. Neurotoxicity: The broad framework of electron transfer, oxidative stress and protection by antioxidants. *Curr. Med. Chem.-CNS Agents* 2005, 5, 249-258.

[125] Kovacic, P. Mechanism of central nervous system toxicity by irinotecan. *Medical Hypotheses* 2006, 67, 997.

[126] Saltz, L. Irinotecan-based combinations for the adjuvant treatment of stage III colon cancer. *Oncology* 2000, 14(Suppl), 47-50.

[127] Douillard, JY. Irinotecan and high-dose fluorouracil/leucovorin for metastatic colorectal cancer. *Oncology* 2000, 14(Suppl), 51-55.

[128] Douillard, JY. Irinotecan-based regimens in the adjuvant therapy of colorectal cancer. *Clin. Colorectal Cancer* 2005, 5(Suppl.), S34-S37.

[129] Fukuoka, M; Masuda, N; Kudoh, S; Negoro, S. Irinotecan in small-cell lung cancer-Japanese trials. *Oncology* 2000, 14(Suppl), 57-62.

[130] Masuda, N; Fukuoka, M. Irinotecan in the treatment of small cell lung cancer. *Expert Rev. Anticancer Therapy* 2001, *1*, 187-195.

[131] Ajani, JA; Fairweather, J; Pisters, PW; Charnsangavej, C. Irinotecan and cisplatin in advanced gastric or gastroesophageal junction carcinoma. *Oncology* 2000, 14(Suppl), 19-21.

[132] Ajani, JA; Baker, J; Pisters, PWT.; Ho, L; Mansfield, PF; Feig, BW; Charnsangavej, C. CPT-11 plus cisplatin in patients with advanced, untreated gastric or gastroesophageal junction carcinoma: results of a phase II study. *Cancer* 2002, 94, 641-646.

[133] Kaneda, H; Kurata, T; Tamura, K; Uejima, H; Nakagawa, K; Fukuoka, M. A phase I study of irinotecan in combination with amrubicin for advanced lung cancer patients. *Anticancer Res.* 2006, 26, 2479-2486.

[134] Kollmannsberger, C; Mross, K; Jakob, A; Kanz, L; Bokemeyer, C. Topotecan, a novel topoisomerase I inhibitor. Pharmacology and clinical experience. *Oncology* 1999, 56, 1-12.

[135] Costin, D; Potmesil, M. Preclinical and clinical development of camptothecins. *Adv. Pharmacol*. 1994, 29B, 51-72.

[136] Wong, ET; Berkenblit, A. The role of topotecan in the treatment of brain metastases. *Oncologist* 2004, 9, 68-79.

[137] Hammond, LA; Eckardt, JR; Ganapathi, R; Burris, HA; Rodriguez, GA; Eckhardt, SG; Rothenberg, ML; Weiss, GR; Kuhn, JG; Hodges, S; Von Hoff, DD; Rowinsky, EK. A phase I and translational study of sequential administration of the topoisomerase I and II inhibitors topotecan and etoposide. *Clin. Cancer Res*. 1998, 4, 1459-1467.

[138] Frasci, G; Panza, N; Comella, P; Carteni, G; Guida, T; Nicolella, GP; Natale, M; Lombardi, R; Apicella, A; Pacilio, C; Gravina, A; Lapenta, L; Comella, G. Cisplatin-topotecan-paclitaxel weekly administration with G-CSF support for ovarian and small-cell lung cancer patients: a dose-finding study. *Ann Oncol*. 1999, 10, 355-358.

[139] Pommier, Y. Topoisomerase I inhibitors: camptothecins and beyond. *Nature Rev. Cancer* 2006, 6, 789-801.

[140] BCCA Cancer Drug Manual 2001 (freely available at http://www.bccancer.bc.ca/HPI/DrugDatabase/DrugIndexPro/default.htm)

[141] Burris, HA, III; Rivkin, S; Reynolds, R; Harris, J; Wax, A; Gerstein, H; Mettinger, KL; Staddon, A. Phase II trial of oral rubitecan in previously treated pancreatic cancer patients. *Oncologist* 2005, 10, 183-190.

[142] Chen, EX; Batist, G; Siu, LL; Bangash, N; Maclean, M; McIntosh, L; Miller, WH, Jr.; Oza, AM; Lathia, C; Petrenciuc, O; Seymour, L. Phase I and pharmacokinetic study of Bay 38-3441, a camptothecin glycoconjugate, administered as a 30-minute infusion daily for five days every 3 weeks in patients with advanced solid malignancies. *Investig. New Drugs* 2005, 23, 455-465.

[143] Daud, A; Valkov, N; Centeno, B; Derderian, J; Sullivan, P; Munster, P; Urbas, P; DeConti, RC; Berghorn, E; Liu, Z; Hausheer, F; Sullivan, D. Phase II trial of karenitecin in patients with malignant melanoma: Clinical and translational study. *Clin. Cancer Res*. 2005, 11, 3009-3016.

[144] Gelderblom, H; Salazar, R; Verweij, J; Pentheroudakis, G; de Jonge, MJA; Devlin, M; van Hooije, C; Seguy, F; Obach, R; Prunonosa, J; Principe, P; Twelves, C. Phase I pharmacological and bioavailability study of oral diflomotecan (BN80915), a novel E-ring-modified camptothecin analogue in adults with solid tumors. *Clin. Cancer Res.* 2003, 9, 4101-4107.

[145] Rowinsky, EK; Rizzo, J; Ochoa, L; Takimota, CH; Forouzesh, B; Schwartz, G; Hammond, LA; Patnaik, A; Kwiatek, J; Goetz, A; Denis, L; McGuire, J; Tolcher, AW. A phase I and pharmacokinetic study of pegylated camptothecin as a 1-hour infusion every 3 weeks in patients with advanced solid malignancies. *J. Clin. Oncology* 2003, 21, 148-157.

[146] Posey, JA, III; Saif, MW; Carlisle, R; Goetz, A; Rizzo, J; Stevenson, S; Rudoltz, MS; Kwiatek, J; Simmons, P; Rowinsky, EK; Takimoto, CH; Tolcher, AW. Phase 1 study of weekly polyethylene glycol-camptothecin in patients with advanced solid tumors and lymphomas. *Clin. Cancer Res.* 2005, 11, 7866-7871.

[147] Kratz, F; Mueller, IA; Ryppa, C; Warnecke, A. Prodrug strategies in anticancer chemotherapy. *ChemMedChem* 2008, 3, 20-53.

[148] Schoemaker, NE; van Kesteren, C; Rosing, H; Jansen, S; Swart, M; Lieverst, J; Fraier, D; Breda, M; Pellizzoni, C; Spinelli, R; Grazia Porro, M; Beijnen, JH; Schellens, JHM; ten Bokkel Huinink, WW. A phase I and pharmacokinetic study of MAG-CPT, a water-soluble polymer conjugate of camptothecin. *Br. J. Cancer* 2002, 87, 608-614.

[149] Wachters, FM; Groen, HJM; Maring, JG; Gietema, JA; Porro, M; Dumez, H; de Vries, EGE; van Oosterom, AT. A phase I study with MAG-camptothecin intravenously administered weekly for 3 weeks in a 4-week cycle in adult patients with solid tumours. *Br. J. Cancer* 2004, 90, 2261-2267.

[150] Bissett, D; Cassidy, J; De Bono, JS; Muirhead, F; Main, M; Robson, L; Fraier, D; Magne, ML; Pellizzoni, C; Porro, MG; Spinelli, R; Speed, W; Twelves, C. Phase I and pharmacokinetic (PK) study of MAG-CPT (PNU 166148): a polymeric derivative of camptothecin (CPT). *Br. J. Cancer* 2004, 91, 50-55.

In: Clinical Chemistry Research
Editors: Brian H. Mitchem and Charles L. Charnham
ISBN 978-1-60692-517-1

Chapter III

Application of Lanthanide (Ln = Eu & Tb) Nanoparticles in Biology and Medicine

Chitta Ranjan Patra[1*], Priyabrata Mukherjee[1,2] and Debabrata Mukhopadhyay[1,2]

[1]Department of Biochemistry and Molecular Biology,
Mayo Clinic College of Medicine, Mayo Foundation, Rochester, MN, USA
[2]Department of Biomedical Engineering, Mayo Clinic College of Medicine,
Mayo Foundation, Rochester, MN, USA

Abstract

Lanthanides [especially Europium (Eu) and Terbium (Tb)] are not biometals, however lanthanide nanomaterials play an appreciable role in biology and medicine. Nanoparticles are at the leading edge of the rapidly developing field of nanomedicine and nanobiotechnology. Their unique size-dependent properties make these nanomaterials superior and indispensable in many biological and medicinal areas of human activity. Nanomedicine/nanobiotechnology is the medical/biological application of nanotechnology that will hopefully lead to useful research tools, advanced drug delivery systems, and new ways to detect and treat disease or repair damaged tissues and cells. In this particular chapter, we have discussed the most recent developments of lanthanide (especially europium & terbium) nanorods/nanoparticles in the field of fluorescent labeling and angiogenesis (the budding of capillaries that leads to the formation of new microvessels from pre-existing vascular structures) in biology and medicine. Firstly, we have discussed the synthesis, characterization and application of these non-toxic inorganic lanthanide (europium and terbium) nanorods as a fluorescent label (a novel alternative to conventional organic dyes) in biomedical research due to their unique

∗ Chittaranjan Patra, Ph.D. Assistant Professor, 200 First Street S.W, Guggenheim 1494, Mayo Clinic College of Medicine, Mayo Foundation, Rochester, MN 55905, USA. E-Mail: patra.chittaranjan@mayo.edu. Alternate e-mail: patra.chitta@gmail.com. Phone: +1-507-284-9116, Fax:+1-507-284-1767

optical and electronic properties. It is important to point out that fluorescence labeling of molecules is a standard technique in biomedical application. Therefore, these lanthanide nanorods offer useful and alternative inorganic fluorescent probes for targeting various molecules in living cells. Secondly, we have demonstrated the pro-angiogenic properties of europium(III) hydroxide nanorods which could be used to develop new treatment strategies for cardiovascular ischemic and peripheral vascular diseases where the most important objective of angiogenesis is to induce or stimulate vessel growth in patients with conditions characterized by insufficient blood flow. In addition to that we have also discussed the diagnostic and therapeutic applications of lanthanide compounds. This book chapter tries to summarize the most recent developments of lanthanide (especially europium and terbium) nanorods in the field of biomedical nanotechnology, and discusses the current standing with respect to nanotechnology.

Keywords: Rare earth, Lanthanides, Europium, Terbium, Nanoparticles, Nanorods, Synthesis, Fluorescent, nanomedicine, Angiogenesis & Cardiovascular Disease.

1. Introduction

Lanthanides [especially Europium (Eu) and Terbium (Tb)] are not biometals (the role of metal ions in biology, biochemistry and medicine), however lanthanide compounds and their chelates play an appreciable role in biology and medicine due to their unique optical, electronic, physical and chemical characteristics arising from their 4f electrons[1]. Among lanthanide elements, the luminescence of Eu^{3+} and Tb^{3+} are particularly interesting because of their high color purity and high luminescence efficiency. Again the major emission band centered of Eu^{3+} is near 612 nm, which is one of the three primary colors [2]. Therefore, lanthanides especially Eu^{3+} and Tb^{3+} have been studied as luminescent activator in host lattices and as luminescent label in biomedical application[2]. Again, europium (Eu) and terbium (Tb) salts and their chelates have been used in diverse biomedical applications, namely time-resolved fluorometric assays and immunoassays [3-12] due to their better optical properties-enhanced photostability and large Stokes shift compared to conventional organic fluorophores. In order to enhance the luminescence intensity of lanthanide ions, scientists are developing new approaches. In this context, nanotechnology, the creation of new objects in nanoscale dimensions, is a cutting edge technology having important applications in modern biomedical research [13-21]. Because the dimension of nanoscale devices is similar to cellular components such as DNA and proteins [22-26], tools developed through nanotechnology may be utilized to detect or monitor several diseases at the molecular level [15, 27, 28]. Bio-imaging with inorganic fluorescent nanopartcles probes have recently attracted widespread interest in biology and medicine [13-17, 29-31]. Recently, nanoparticles, such as quantum dots (CdSe, ZnS, PbSe, ZnSe, and ZnS), have attracted a great deal of attention in biology due to presence of strong optical emission that exhibits a sharper spectral peak than typical organic dyes [17, 32-37]. However, these compounds are toxic to the cells [17, 36, 37]. In this context, several groups including our group have observed that lanthanide nanomaterials are not toxic to endothelial cells [38-44]. Again lanthanide compounds in the nanometer range have several better unique properties such as

(i) size dependent emission wavelengths, (ii) fluorescent peak profiles are sharp (the half-widths are 10 nm – 20 nm), (iii) photostability, (iv) large stokes shift, (v) simultaneous excitation of multiple fluorescence colors, (vi) Improved signal brightness, (vii) long life time (several hundreds microseconds) compared to conventional fluorescent organic dyes and inorganic bulk materials. In this context, lanthanide-based inorganic fluorescents, especially Eu- and Tb-phosphate/oxide/hydroxide nanoparticles/nanorods, have attracted a great deal of attention in cell biology and medicine due their non-toxic effect [38-40]. Moreover, recently we have observed the pro-angiogenic properties of lanthanide (especially europium) nanomaterials[40]. In the following sections, we focus the application of lanthanide (europium and terbium) nanorods as (i) fluorescent labeling in cell biology and (ii) pro-angiogenic agent, which could be used as alternative strategies for the treatment of cardiovascular and different limb ischemia diseases. We are not presenting a comprehensive review of these fields but, rather, to exemplify of the main applications.

2. General Properties of Lanthanides (Brief Description)

A group of 15 transition metals from lanthanum (Z=57) to lutetium (Z=71) in group-III of periodic table are known as rare earth (RE) or lanthanides (Ln) or lanthanoids. The symbol Ln, not assigned to any particular element, is commonly used to designate the lanthanides or rare earth elements as a class. Originally, lanthanide series were known as rare-earth, not because they are rare, but because at one time they were thought to be rare as they were difficult to identify from one another, difficult to extract from their corresponding ores and difficult to separate from each other. Now-a-days, these elements are not known as rare-earth due to their normal occurrence. They are f-block elements except lutetium (d-block element). The lanthanide series is named after lanthanum and the lanthanides are abbreviated to Ln. The lanthanide consists of 14 elements: lanthanum (La), cerium (Ce), praseodymium (Pr), neodymium (Nd), promethium (Pm), samarium (Sm), europium (Eu), gadolinium (Gd), terbium (Tb), dysprosium (Dy), holmium (Ho), erbium (Er), thulium (Tm), ytterbium (Yb), lutetium (Lu). The lanthanides have the general electronic configuration $[Xe]4f^n5d^16s^2$ with n = 0 (La) to 14 (Lu). Readers who are interested to know about the properties of rare earth elements in detail can refer to the following books, articles or reviews or the websites [21, 45-48, 49 Beatty, 2007 #464, 50-55]. Now-a-days chemists are paying more attentions to the studies of chemical, biological, medical and environmental applications of lanthanide elements to develop rare-earth/lanthanide industry. In this context, the two most important properties of lanthanide nanoparticles are fluoresence and pro-angiogenic properties.

3. Biomedical Nanotechnology: Definition and Application

The ‘Nãnos’, a Greek word meaning "dwarf" is used in the metric system to refers to 10^{-9} or one-billionth. Thus a nanometer is 10-9 or one billionth of a meter. Nanoscience and nanotechnology, a branch of applied science and technology is devoted to understand, create, design and use material structures, devices and systems at the atomic, molecular, or macromolecular range (~1-100 nanometers) with fundamentally new properties and functions [22, 56-58].

There are many reasons why scientists with diverse interests and backgrounds have converged in their interest to work with and understand material properties on a nanoscale. One of the fundamental reason is that the dimension of nanoscale devices is similar to cellular components such as DNA and proteins [22-26], therefore tools developed through nanotechnology may be utilized to detect or monitor several diseases at the molecular level [15, 27, 28]. For example, hemoglobin, the molecule that carries oxygen in red blood cells, is approximately 5 nanometers in diameter. The width of a DNA molecule is approximately 2.5 nm. The dimensions of most proteins are in the range of 1.0 to 15.0 or 20.0 nm, and the width of cell membranes is in the range of 6–10 nm [23, 59].

Therefore, these nanoparticles can easily enter the cells after and before functionalization, depending upon the chemical nature of nanoparticles due to their small size compared to human cells (one hundred to ten thousand times smaller than human cells). Therefore, nanoscale devices/nanoparticles can readily interact with biomolecules on both the surface of cells and inside of cells [60]. As they have easy access to the many parts of the body, they have the potential to detect disease and deliver the drug to the malignant cells with better therapeutic efficacy using targeting molecule linked to the nanoparticles.

4. Development of Lanthanide Compounds (Background)

The chemistry of the rare earth metals has been slow to develop compare to that of other metals in periodic table. Weissman first reported the luminescence properties of lanthanide-centered coordination compounds in 1942 [61]. He observed characteristic line luminescence from f-f transitions of trivalent europium during the absorption of radiation (sun is a source of light) with the wavelengths in the range 320-440 nm by organic part of Eu^{III} complexes. The first well-characterized organometallic complexes of the lanthanide, the tris(cyclopentadienyl) derivatives Cp3Ln, were synthesized by Wilkinson and Birmingham in 1954 [62]. Due to the intrinsic instability of these organometallic compounds towards moisture and oxygen, further development of this new area of organometallic chemistry was hampered. Again the slow initial development of the organometallic chemistry of the rare earth metals was the belief that these compounds were ionic and represented merely trivalent versions of alkali and alkaline earth metal organometallic species [63]. After two decades, the availability of relatively more sophisticated experimental and analytical techniques made the

rigorous exclusion of traces of air and moisture during preparation and characterization possible in the 1970s. Further development of organolanthanides was observed in the late 1970s and early 1980s and it shows a rich and interesting chemistry, such as catalytic alkene hydrogenation [64, 65] and polymerization [66, 67] at very high rates [68, 69] and reactivity towards the C-H bonds of arenes, alkenes and alkanes [70, 71]. Up to the early 1970s organo rare-earth metal chemistry had been limited to π-bonded organometallic compounds, such as tris(cyclopentadienyl) [62] tris(indenyl) [72] and cyclooctatetraene [73] complexes.

Few years back, the work in this field has shown a departure from organolanthanides chemistry to lanthanide salt/chelate chemistry which have been used in diverse biomedical applications, namely time-resolved fluorometric assays and immunoassays using the optical properties of lanthanide (especially Eu & Tb) salts and their chelates [3-11]. Some of the applications of examples lanthanide salt/chelate chemistry, in brief are described below:

5. Application of Lanthanide Salt and Chelates in Biologgy and Medicine

In general, lanthanide chelates in biomedical studies contain an organic chromophore (conjugated π-system or metallic part of the molecule responsible for its color). Selvin et al introduced three prototypical luminescent probes which contain organic chromophore, acting as an antenna or sensitizer, absorbing the excitation light and transferring the energy to lanthanide ion (Fig.1.a-c) [46].These probes have been used as detection agents to replace the conventional fluorescent probes or radioactive probes [74, 75].

Optical properties of europium (Eu) and terbium (Tb) salts and their chelates have been used in diverse biomedical applications, namely time-resolved fluorometric assays, magnetic resonance imaging (MRI) and immunoassays [3-11, 49, 76, 77]. For examples, Yuan et al summarized the recent developments of lanthanide complex-based fluorescence labels and their applications in time-resolved fluorescence bioassays [78]. The luminescence properties of trivalent lanthanide ions have been used for the applications of lighting displays, solar energy, lasers, optical telecommunications, biotechnology, medical diagnostics, bio-imaging and various other fields [45, 79, 80]. Mathis et al. developed a homogeneous assay method based on the long-lived fluorescence of rare earth cryptates and amplification by non-radiative energy transfer for immunoassays [81]]. Synthesis, characterization, and application of Eu(III), Tb(III), Sm(III), and Dy(III) lanthanide chelate nanoparticle labels have been used long life time fluorescent label in a heterogeneous sandwich-type fluoroimmunoassay for human prostate-sppecific antigen(PSA) [82]. Huhtinen et al also introduced the possibility of using europium(III)-labeled 68 nm particles coated with monoclonal antibodies or streptavidine (SA) to detect prostate-specific antigen [83]. Siitari et described an immunoassay of hepatitis B surface antigen (HBsAg) based on time-resolved (TR) fluorescence using a lanthanide (Eu, Tb, Sm, Dy) chelate as label having a long fluorescent lifetime [84]. Jaras et al developed ENSAM (Europium Nanoparticles for Signal enhancement of Antibody Microarrays) based on two nanomaterials (polystyrene and

nanoporous silicon), incorporated with europium chelate (β -diketone) and coated with streptavidin in order to improve the sensitivity of antibody microarray assays [85].

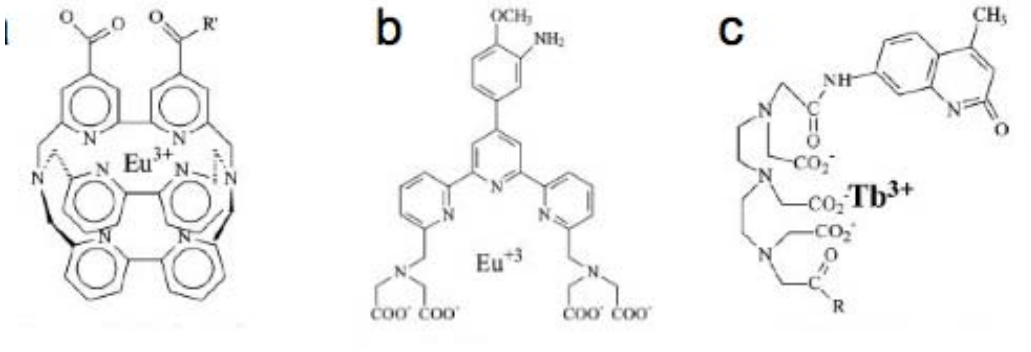

Figure1. Structure of representative lanthanide (Eu & Tb) chelates. For (a) cryptates and (b) terpyridine, the chelate and antena are logically same entity. For (c) DTPA-cis124, the complex contains a DTPA chelate and a cis 124 antena. Reprinted, with permission from [46]. Selvin et al.,Principles and biophysical applications of lanthanide-based probes. *Annual Review of Biophysics and Biomolecular Structure* 2002, **31:**275-302 © 2002 by Annual Reviews www.annualreviews.org).

Magnetic resonance imaging (MRI) is one of the most important and prominent technique in diagnostic clinical medicine and biomedical research. Gadolinium(III) is the dominant starting material for contrast agent design biomedical research but other lanthanide ions (europium, dysprosium) are also being increasingly investigated as alternatives to gadolinium(iii) within laboratory conditions [77]. Paramagnetic lanthanide complexes as PARACEST agents for medical imaging based upon the chemical shift saturation transfer (CEST) mechanism has been well demonstrated by woods et al in a special issue of Chem. Soc. Review [86]. Readers who are interested to know about the medicinal use of lanthanide elements in MRI in detail can refer to the following books, articles or reviews [49, 76, 77].

5.1. Forensic Applications

Allred et al introduced a lipid-specific europium-bioconjugate method for the detection of latent fingerprints using the unique properties of europium (large Stokes shift and long luminescence lifetime) [87]. Considering the all factors such as applicability of this new method to porous and smooth surface, basis of covalent interaction with lipid, absence of chlorofluorocarbon as solvent, cost, faster etc imply that this approach will become a major fingerprint detection method. They also demonstrated that this method would be applicable to the chemistry of DNA profiling.

In another study, the luminescence property of europium-beta-diketone chelates, produced by the interaction of Eu^{3+} ions with aryl-beta-diketones as fluorescent dyes was applied for the detection of cyanoacrylate developed fingerprints on human skin [88]. Emission spectra of europium with narrow band (10 nm) at 614 nm as a result of an intramolecular energy transfer was used for this study.

5.2. Detection of DNA Hybridization and Protein Expression

DNA hybridization is one of the powerful methods for the detection of specific nucleic acids sequences, which is required for the analysis of gene expression profile. Several groups have been demonstrated for the detection of DNA hybridization based on the luminescence properties of europium labeled probes [89-93]. Rintamaki et al reported the detection of streptococcus pneumoniae DNA by using polymerase chain reaction (PCR) with the help of time-resolved fluorescence (TRF) of the Europium-labelled probes [90].

In another study, Nojima et al developed a lanthanide (europium) fluorescent intercalator that specifically binds to double stranded DNA [89]. They have demonstrated the detection of double stranded DNA (dsDNA) immobilized on a solid surface using a fluorescent intercalator consists of naphthalene diimide derivative moiety and two fluorescent tetradentate p-diketone-Eu^{3+} chelates. This compound selectively binds to only dsDNA, and the binding to single stranded DNA (ssDNA) is negligible.

Komiyama et al demonstrated the sequence-specific and hydrolytic scission of DNA and RNA using lanthanide complex-oligoDNA hybrids [94]. They have found that the cerium(IV) ion is the most active as to DNA scission, whereas the europium(III), thulium(III), and lutetium(III) ions are the most effective for RNA scission.

Franz et al reported that peptide sequences with a 40-fold higher affinity for Tb^{3+} ions and significantly brighter luminescence intensity compared with existing peptides [95]. They have found that incorporation of an lanthanide binding tags (LBT) onto ubiquitin as a prototype fusion protien allows the use of powerful protein-visualization techniques, which include rapid luminescence detection of LBT-tagged proteins in SDS-PAGE gels, as well as determination of protein concentrations in complex mixtures. The LBT strategy is a new alternative for expressing fluorescent fusion proteins by routine molecular biological techniques.

5.3. Heparin Determination

Heparin (Hep), a highly-sulfated glycosaminoglycan has the highest negative charge density of any known biological molecule. Hep and its derivatives with an average molecular weight 15,000 have various biological activities such as anticoagulant, antilipemic, antithrombotic, immunoregulatory, antiphlogistic and antianaphylactic activities. It is widely used in many clinical procedures[96].Therefore, the Hep level in the patients' blood needs to be carefully accurately monitored during surgery and recovery. Wei et al developed a very simple, practical and a new spectrofluorimetric method for determination of trace amount of heparin (Hep) using lomefloxacin (LOM)-terbium ion (Tb^{3+}) as a fluorescent probe (where LOM is one kind of antibacterial containing α-carbonyl carboxylic acid configuration is an ideal ligand Tb^{3+} ion), in the physiological buffer solution of pH 8.7 [96]. The emission wavelength of Tb^{3+} is λ = 545 nm was used for this study. The linear range for the determination of Hep was 0.6-2.0 μg/ml and the detection limit was 45.22 ng/ml. This method developed by Wei et al is very simple, practical and relatively free of interference

from coexisting substances and it can be successfully applied to assess Hep in biological samples.

5.4. Staining the Nucleolus of Cells

It is well established that nucleoli are nuclear sites of ribosomal RNA transcription, processing, and ribosome assembly [3, 97]. Studies of nucleoli and nucleolus-related processes sometimes require the visualization of nucleoli. Techniques such as silver nitrate staining [98], employment of antibodies against a certain component of the nucleolus [99], commercial nucleolar stain "SYTO RNA-Select" [100] have been used for nuclear staining for the visualization of nucleoli. In this context, Yu et al has reported the selective staining the nucleolus of NIH 3T3, HeLa, and HDF cells using a cationic europium(III) complex $[EuL]^{3+}$ [3]. The europium complex, $[EuL]^{3+}$ (controlled alkylation of the trans-disubstituted cyclen diamide gives the desired ligand, L,) can be used both in live cell and fixed cell imaging, giving an average intracellular concentration on the order of 0.5 M. They have demonstrated that lanthanide complexes have the advantage of a long luminescence lifetime, large Stokes shift, and relatively high quantum yield compared to common organic fluorescent dyes and semiconductor quantum dots (QDs). These results suggest that europium complex will be suitable for use in selective cell staining experiments and amenable to examination by time-resolved microscopy.

However, there are some problems about the application of lanthanide salts and chelates, for example lanthanide ions are toxic and a sensitization process of lanthanide metal ion luminescence is needed via the antenna effect (vide supra) [52, 101, 102]. Therefore they are not welcome for diagnostic purpose in biomedical application due to their toxic effect. In this context, inorganic lanthanide nanoparticles/nanorods have raised new possibilities for the ultrasensitive and multiplexed imaging of molecular targets in living cells and animal models. In last few years, lanthanide-based inorganic fluorescents, especially Eu- and Tb-phosphate/oxides/hydroxide nanoparticles, have attracted a great deal of attention in medicine and cell biology [21, 38-40, 103]. Some of the applications of lanthanide (Eu & Tb) nanorods/nanoparticles are described below:

6. Lanthanide (Eu & Tb) Nanorods/Nanoparticles in Nanobiotechnology

6.1. Synthesis

Since this book chapter will mainly focus on the application of lanthanide, (especially europium and terbium) nanopartcicles in biomedical application, therefore it is important to describe, in brief, the synthesis of oxide, hydroxide and phosphate lanthanide (Eu & Tb) nanorods/nanomaterials. The chemical, physical, optical properties and reactivity, as well as the catalytic activity, of lanthanide nanoparticles can be dramatically enhanced when the particle size is reduced to nanometer scale from bulk size. The synthesis of lanthanide

nanoparticles (europium and terbium) is mainly classified in to two groups: (a) chemical method and (b) physical method. Readers who are interested to know the synthesis of europium and terbium nanoparticles in detail can refer to the following articles, reviews or books [104, 105].

6.1.1. Chemical Methods

Various low-dimensional nanostructures, such as nanowires, nanotubes, nanosheets, and fullerene-like nanoparticles have been selectively synthesized from rare-earth compounds (hydroxides, nitrates, fluorides) based on a facile hydrothermal method. Wang and Li et al have selectively synthesized various low-dimensional nanostructures such as nanoparticles, nanowires, nanorods, nanotubes,nanosheets and fullerene like nanoparticles using facile hydrothermal method[106-110]. Lanthanide (especially Eu and Tb) doped nanomaterials or lanthanide naoparticles (oxides, hydroxides, phosphates) were synthesized by hydrothermal methods [82, 105, 106, 111-123]. For example, Wang et al developed a hydrothermal method for the synthesis of rhabdophane rare earth phosphate nanorods [115] lathanide hydroxide and synthesis of Eu or Tb doped Lu_2O_3 square nanosheets were prepared by hydrothermal method [106, 116]. Fang et al has been developed for the systematic synthesis of lanthanide orthophosphate crystals with different crystalline phases and morphologies using a simple hydrothermal method [105]. Yan et al demonstrated the synthesis of phase-pure and single-crystalline monoclinic, hexagonal, and tetragonal one-dimensional LnPO4 nanostructures of different aspect ratios by hydrothermal method [118]. Yan and Zhang et al developed a hydrothermal method for the synthesis of hexagonal LnPO4·nH2O (Ln=La, Ce, Pr, Nd, Sm, Eu, Gd) and orthorhombic LnPO4·nH2O (Ln=Tb, Dy) one-dimensional nanomaterials [119, 120]. Tang et al introduce a template assited hydrothermal route for the synthesis of $Tb(OH)_3$ nanotubes [123]. A facile, surfactant-assisted, hydrothermal approach has been developed by Bu et al to synthesize lanthanide phosphate single-crystalline nanowires/nanorods with smooth surface, uniform diameter, and good crystallinity [122]. Cao et al have been successfully synthesized $LaPO_4$ and $CePO_4$ nanorods/nanowires with controlled aspect ratios using a hydrothermal microemulsion method under mild conditions [124]. Xu et al developed a method for the synthesis of multiple fluorescent labeling of silica nanoparticles with lanthanide chelates by microemulsion method [125]. Wang et al demonstrated synthesis of luminescent Ca1-xF2+x:Eux nanoparticles by a chemical co-precipitation method in an ethanol solution [126]. A series of rare earth hydroxide and oxide nanoparticles have been prepared by precipitation method with alcohol as the dispersive and protective reagent by Dong et al [127]. 2-40 nm of Eu_2O_3 nanocrystals synthesis was introduced by Wakefield et al using a colloidal precipitation route [128]. Nunez et al proposed a ionic liquid based synthesis of luminescent lanthanide fluoride nanoparticles[129].

6.1.2. Physical Methods

Physical methods for the synthesis of lathnide nanoparticles/nanorods involve microwave irradiation methods, sonchemical methods, etc. [22, 38-40, 130-135]. For example, Patra et al introduced a microwave approach for the synthesis of rhabdophane-type lanthanide orthophosphate (Ln = La, Ce, Nd, Sm, Eu, Gd and Tb) nanorods under solvothermal conditions [131]. Panda et al described the microwave synthesis and optical properties of

uniform nanorods and nanoplates of rare earth oxides. Patra et al reported the sonochemical preparation and characterization of Eu_2O_3 and Tb_2O_3 and doped in and coated on silica and alumina nanoparticles [132]. In another study, Zhu et al demonstrated a facile sonochemical synthesis of single-crystalline europium fluorine with novel nanostructure [133]. Pol et al also introduced the synthesis of europium oxide nanorods by ultrasound irradiation [135].

6.2. Characterization of Lanthanide Nanorods / Nanoparticles

The most common characterization techniques used for the characterization of lanthanide nanomaterials involve x-ray diffraction (XRD: in order to find out the crystalline nature, geometry or shape of a compound) method [112-115, 117, 119, 120, 127, 131, 134], scanning electron microscope (SEM: is a method for high-resolution imaging of surfaces of nanomaterials) [105, 128], transmission electron microscopy (TEM is used to characterize the microstructure of materials with very high spatial resolution) [113, 115, 119, 120, 127, 131, 134], high resolution transmission electron microscopy (HRTEM: is an imaging mode of the transmission electron microscope (TEM) that allows the imaging of the crystallographic structure of a sample/nanomaterial at an atomic scale. Because of its high resolution, it is an invaluable tool to study nanoscale properties of crystalline material such as semiconductors and metals) [105, 111, 112, 115, 117, 119, 120, 131, 134], absorption spectroscopy(techniques employing the interaction of electromagnetic radiation with nanomaterials) [105, 111, 115, 123, 128], luminescence spectroscopy (related to three spectroscopic techniques: Molecular fluorescence spectroscopy, Molecular phosphorescence spectroscopy and Chemiluminescence spectroscopy) [38, 39, 105, 111-113, 115, 117, 123, 128, 131], UV-vis absorption spectroscopy (is the measurement of the wavelength and intensity of absorption of near-ultraviolet and visible light by a sample) [113, 127, 134], Fourier transform infrared (FTIR is most useful for identifying chemicals that are either organic or inorganic in solid ,liquid or gaseous state. It can be utilized to quantitate some components of an unknown mixture.) [119, 120, 127, 131], Raman spectroscopy (is a spectroscopic technique used in condensed matter physics and chemistry to study vibrational, rotational, and other low-frequency modes in a system) [131], Cofocal microscopy (The technique is applicable to all fluorescence microscopy for biomedical applications) [38, 39], upconversion spectra (used for ultrafast fluorescence measurements) [117], and X-ray photoelectron spectroscopy (XPS is a quantitative spectroscopic technique that measures the elemental composition, empirical formula, chemical state and electronic state of the elements that exist within a material) etc.[115, 131].

7. Application of $LnPO_4.H_2O$ (Ln = Eu, Tb) Nanorods in Cell Biology

It is important to point out that fluorescence labeling of molecules is a standard technique in biomedical technology. One of the fundamental goals in biology is to understand the complex spatiotemporal interplay of biomolecules from the cellular to the integrative level. To study these interactions, researchers commonly use fluorescent labeling for both *in vivo* cellular imaging and *in vitro* assay detection [15, 39, 136]. In this context, one of the fastest developing and most exciting interfaces of nanotechnology is the use of inorganic quantum dots or fluorescent nanoparticles in cell biology. In addition, the ability to make such nanoparticles and then target these particles to specific biomolecules has led to promising applications in cellular labeling, deep-tissue imaging, and assay labeling, and also as efficient fluorescence resonance energy transfer (FRET) donors [39].

Conventionally organic dyes (Fluorescein, Texas Red™, Lissamine Rhodamine B, and Tetramethylrhodamine), fluorescent proteins (Green fluorescent protein, GFP), lanthanide chelates, which are still the most commonly used fluorescent labels as they have some advantages such as (i) they can be very small, (ii) highly water soluble (at high salt concentrations), (iii) the ease of their usage and (iv) the existence of standard protocols for their bioconjugation [8, 76, 137]. However, these conventionally used fluorescent labels, have several disadvantages de to their intrinsic properties such as broad spectral features, short lifetime (a fluorophore which is excited by a photon will drop to the ground state with a certain probability based on the decay rates through a number of different (radiative and/or nonradiative) decay pathways), low photobleaching thresholds, poor photo chemical stability and potential toxicity to the cells [137].

On the other hand, inorganic fluorescent nanoparticles have several unique optical and electronic properties such as size- and composition-tunable emission from visible to infrared wavelengths, long life time, a large stokes shift, symmetric emission spectrum, large absorption coefficients across a wide spectral range, simultaneous excitation of multiple fluorescent colors, very high levels of brightness, high resistance to photobleaching, and an exceptional resistance to photo- and chemical degradation [15-18, 29, 46, 138-140].

In this context, compare to the traditional organic fluorescent dyes/materials, the lanthanide compounds have several advantages: (1) Long lifetime. Lanthanide compound, mainly of europium and terbium, have long fluorescent lifetimes longer than several hundreds microseconds, whereas traditional organic reagents have several nano seconds [5, 89]; (2) Large Stokes shift. In most case, the lanthanide compounds are excited by UV absorption, and emit light of wavelength longer than 500 nm. The emission peaks of Eu, Sm, Tb, and Dy complexes are 615 nm, 643 nm, 545 nm, and 574 nm, respectively [5, 89]; (3) The fluorescent peak profiles are sharp: The half-widths are 10nm – 20 nm. It is known that the fluorescence is based on the energy-transfer from the ligand to the central lanthanide metal ion [5, 89]; (4) Lanthanide compounds, especially hydroxide and phosphates of europium and terbium are not toxic to endothelial cells [38-40, 130].

7.1. Synthesis of $Lnpo_4.H_2O$ Nanords

Recently our group has reported the synthesis, characterization of inorganic lanthanide phosphate nanorods ($LnPO_4.H_2O$ where Ln = Eu, Tb) and demonstrated that these nanorods retain their fluorescent properties after internalization into human umbilical vein endothelial cells (HUVEC), 786-O cells (RCC: renal carcinoma cells) [38, 39]. Therefore these nanorods can be used as novel fluorescent label in cell biology. Patra et al synthesized $LnPO_4.H_2O$ (Ln = La, Ce, Nd, Sm, Eu, Gd, Tb & Er) nanorods/nanoparticle by the interaction of aqueous solution of $NH_4H_2PO_4$ and aqueous solution of $Ln(NO_3)_3$ in a round-bottomed flask on a domestic microwave oven (DMO) using microwave irradiations as follows:

$$Ln(NO_3)_3 + NH_4H_2PO_4 + H_2O + \text{MW-Heating} \longrightarrow LnPO_4.H_2O \quad \text{(i)}$$

7.2. Advantage of Microwave Heating

The microwave-assisted products are obtained pure, in high yields, and are structurally uniform and well-crystallized. The method does not need high temperatures (though local high temperatures are obtained), high pressures, catalyst, templates, surfactants, vacuum conditions or preprocessing. It is simple, fast, clean, efficient, economically cheap, nontoxic. The MW technique is considered to be ecologically friendly for the following reasons: (a) the speed of chemical reactions is enhanced with minimal energy output and thus the heating energy is very focused; in contrast, the use of a heating plate wastes more energy; (b) 2.45-GHz radiation is not harmful; and (c) the solvents used, such as water and ethanol, efficiently absorb MW radiation and are also considered environmentally friendly[39].

7.3. Characterization of $Lnpo_4.H_2O$ Nanords

These nanorods were characterized by several physico-chemical analysis such as powder X-ray diffraction, BET measurements, low resolution transmission electron microscopy, high resolution transmission electron microscopy, selected area electron diffraction, thermogravimetric analysis, differential scanning calorimetry, infrared spectroscopy, Raman spectroscopy, X-ray photoelectron spectroscopy, and photoluminescence spectroscopy [131]. The experimental conditions for the synthesis of $LnPO_4.H_2O$ nanoparticles/nanorods and selected data (XRD, TEM, BET) are shown in Table-1 [131]. According to the TEM experiments, it is found from Fig.2 that the as-synthesized $EuPO_4.H_2O$ products consisted of nanorods (6 to 8 nm in diameter and 100 to 300 nm long), and $TbPO_4.H_2O$ products were a mixture of two types rods in micrometer sizes (small rods 0.5 to 1.5 μm long and 6 to 8 nm wide, and bigger rods 1.1 to 2.2 μm long and 80 to 130 nm wide) [38, 131].

Table-1: Experimental conditions of microwave -assisted synthesis of different lanthanide ortho phosphate [$Ln(PO)_4.nH_2O$] and their physico-chemical characterizations.

Entry No.	Lanthanide nitrate $Ln(NO_3)_3$	[b]Lanthanide ortho phosphate $LnPO_4.nH_2O$	Yield of the product (wt.%)	BET surface area (m^2g^{-1})	XRD	TEM		
					JCPDS No.	Length (nm)	Width (nm)	Morphology
1.	$La(NO_3)_3$	$LaPO_4.0.5H_2O$	98.3	127	46-1439	70-180	6-9	nanorods
2.	$Ce(NO_3)_3$	$CePO_4.H_2O$	99.1	114	35-0614	130-240	8-9	nanorods
3.	$Nd(NO_3)_3$	$NdPO_4.0.5H_2O$	95.3	110	34-0535	210-350	7-9	nanorods
4.	$Sm(NO_3)_3$	$SmPO_4.0.5H_2O$	99.8	112	34-0537	70-790	8-9	nanorods
5.	$Eu(NO_3)_3$	$EuPO_4.H_2O$	97.3	105	20-1044	70-180	6-9	nanorods
6.	$Gd(NO_3)_3$	$GdPO_4.H_2O$	99.3	110	39-0232	100-300	6-7	nanorods
7.	$Tb(NO_3)_3$	$TbPO_4.H_2O$	98.4	86	20-1244	1.1-2.2 μm	80-130	nanorods
						0.5-1.5 μm	6-8	nanowires
8	$Er(NO_3)_3$	$ErPO_4.0.3H_2O$	98.2	90	20-0391	20-100		Nanoparticles

Experimental conditions, Yield, BET surface area, XRD and TEM of rhabdophane type LnPO4.nH2O synthesized using Ln(NO3)3 and NH4H2PO4 under microwave irradiation.Reaction Conditions: Microwave heating a mixture of 20 rn1 0.05 (M) of an aqueous solution of lanthanide(III)nitrate and 20 rnl 0.05 (M) of an aqueous solution of NH4H2PO4. The pH of the solution 1.8- 2.2, time = 20 min, bEDX analysis gives a Ln/P/O atomic ratio of ~ 1: 1 :4 to 1: 1:4.5, in agreement with the LnPO4.nH2O. All as-prepared samples are well crystallined (confirmed by XRD). Adopted from [Ref. No.]. Reproduced by permission of The Royal Society of Chemistry (RSC) on behalf of the Centre National de la Recherche Scientifique (CNRS) and http://dx.doi.org/10.1039/b415693e. Patra et al. Microwave approach for the synthesis of rhabdophane-type lanthanide orthophosphate (Ln= La, Ce, Nd, Sm, Eu, Gd and Tb) nanorods under solvothermal conditions. New Journal of Chemistry, 2005, 29, 733-739. Patra et al. © Royal Society of Chemistry 2008.

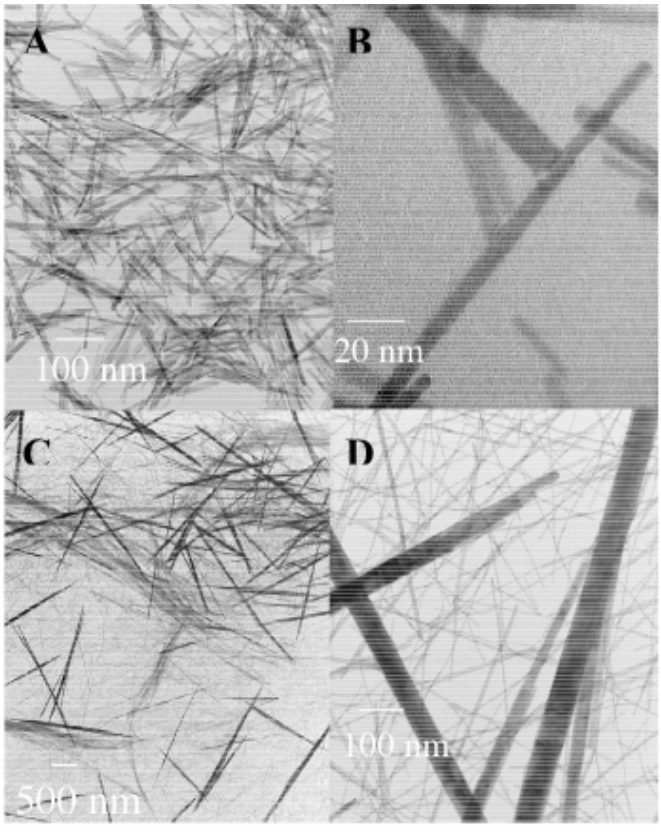

Figure 2. TEM images of as-synthesized (A-B) EuPO4·H2O nanorods and (C-D) TbPO4·H2O nanorods with different magnifications, respectively. Reprinted with the permission from [38], Patra et al. Inorganic phosphate nanorods are a novel fluorescent label in cell biology. J Nanobiotechnology 2006, 4. doi:10.1186/1477-3155-4-11. © 2006 Patra et al; licensee BioMed Central Ltd.

7.4. Fluorescence Spectroscopy of HUVEC and 786-O cells treated with LnPO4.H2O Nanords

The excitation and emission spectra of $EuPO_4.H_2O$ and $TbPO_4.H_2O$ nanorods are presented in Fig.3(A-D). The most intense emission peak $EuPO_4.H_2O$ was observed at 588 nm during the excitation at 393 nm (Fig. 3A). Again, the most prominent emission peak of $TbPO_4.H_2O$ was observed at 543 nm (Fig. 3D) during the excitation at 378 nm (Fig. 3C).

In order to measure the fluorescence activity of these $LnPO_4.H_2O$ (Ln = Eu &Tb) nanorods remain unchanged inside the cell, 786-O cells and HUVEC cells were incubated for 24 hours with these nanorods at various concentrations (0-100 μg/mL). After extensive washing with phosphate buffered saline (PBS), the cells were trypsinized and re-dispersed in PBS and finally the emission (fluorescence) spectra were recorded. (Fig.4.A-B) We have found that with increasing concentrations of $LnPO_4.H_2O$ nanorods (0 to 100 μ g/ml), the fluorescence intensity from curve -a to curve -c/d of Fig.4.A-B increases which indirectly prove the internalization of these nanorods inside the 786-O and HUVEC cells and increasing the rate of nanorod accumulation with increasing concentration.

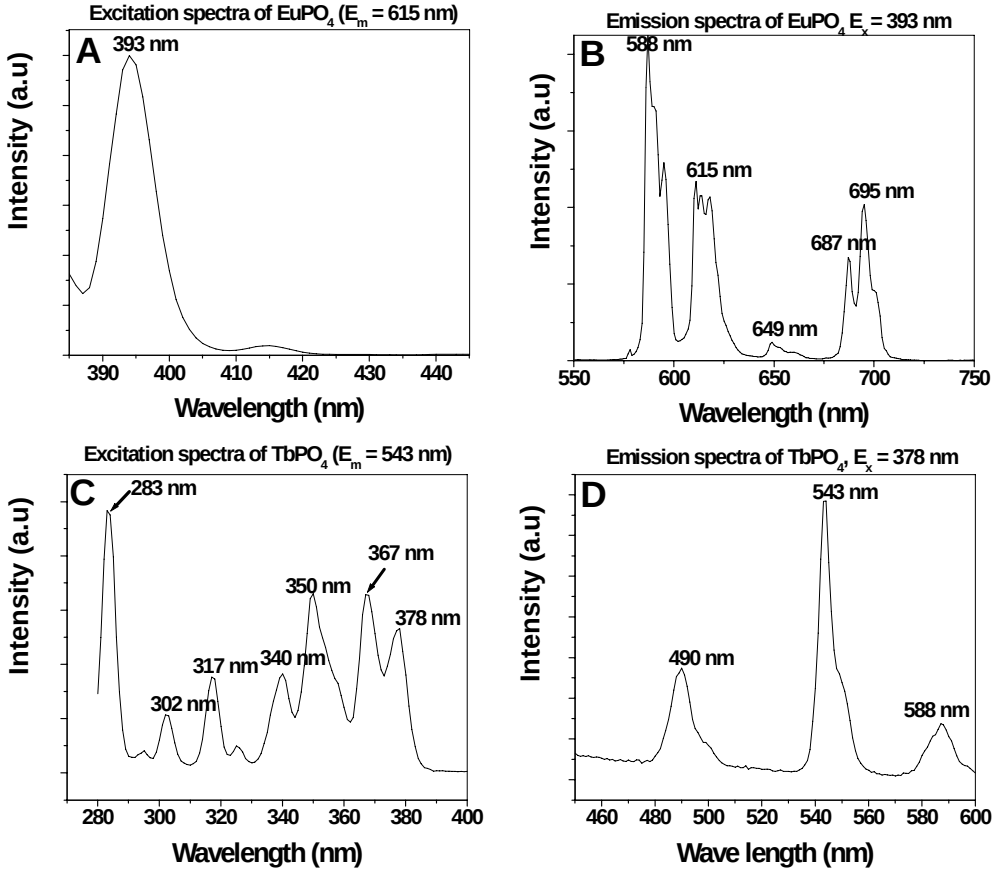

Figure 3. Excitation (A,C) and emission spectra (B,D) of as-synthesized EuPO4·H2O, TbPO4·H2O nanorods. Reprinted with the permission from [38], Patra et al. Inorganic phosphate nanorods are a novel fluorescent label in cell biology. *J Nanobiotechnology* 2006, 4. doi:10.1186/1477-3155-4-11. © 2006 Patra et al; licensee BioMed Central Ltd.

7.5. Internalization of $Lnpo_4.H_2O$ Nanorods in HUVEC and 786-O Cells

The internalization of LnPO4.H2O nanorods into 786-O and HUVEC cells were determined by several techniques such as differential interference contrast (DIC) microscopy, confocal microscopy, and transmission electron microscopy (TEM) [38]. In order to find out the effect of nanorods on cells, it is very important to detect the localization (nucleaus, cytoplasom or cell surface) of these nanorods in cells. TEM images in Fig.5. (A-F) indicate the direct proof of internalization of LnPO4.H2O nanorods into HUVEC cells. Interestingly, both EuPO4.H2O and TbPO4.H2O nanorods remain unchanged their morphology after internalization into the cytoplasm of the cell. The exact nature of the cytoplasmic vesicles is still unknown to us, but it appears that nanorods internalize in double-membrane layered early endosomelike compartments away from the nucleus or late endosomelike structures close to the nucleus.

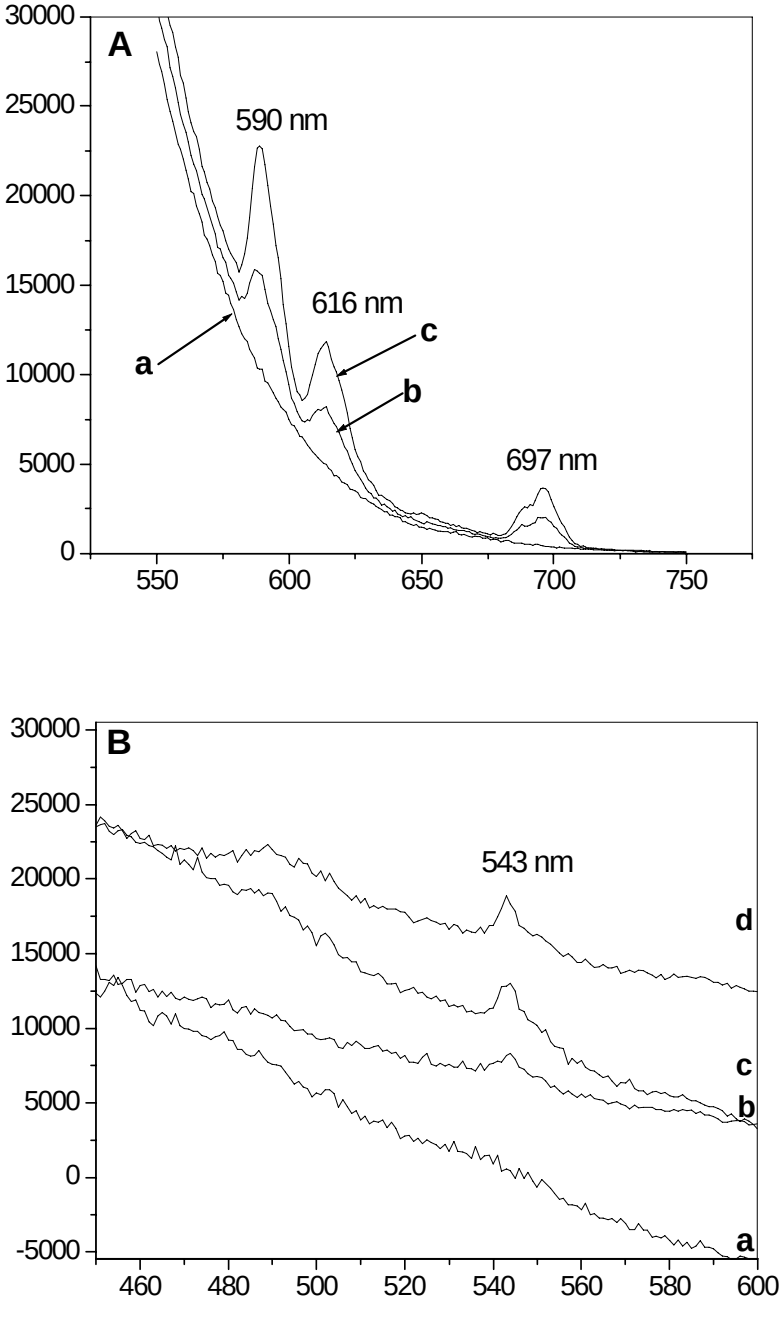

Figure 4. Emission spectra of (A) EuPO4·H2O nanorods loaded inside 786-O cells treated at various concentrations (a = 0 μg/ml, b = 50 μg/ml, c = 100 μg/ml), (B) TbPO4·H2O nanorods loaded inside HUVEC cells treated at various concentrations (a = 0 μg/ml, b = 20 μg/ml, c = 50 μg/ml, d = 100 μg/ml). Reprinted with the permission from [38], Patra et al. Inorganic phosphate nanorods are a novel fluorescent label in cell biology. *J Nanobiotechnology* 2006, 4. doi:10.1186/1477-3155-4-11. © 2006 Patra et al; licensee BioMed Central Ltd.

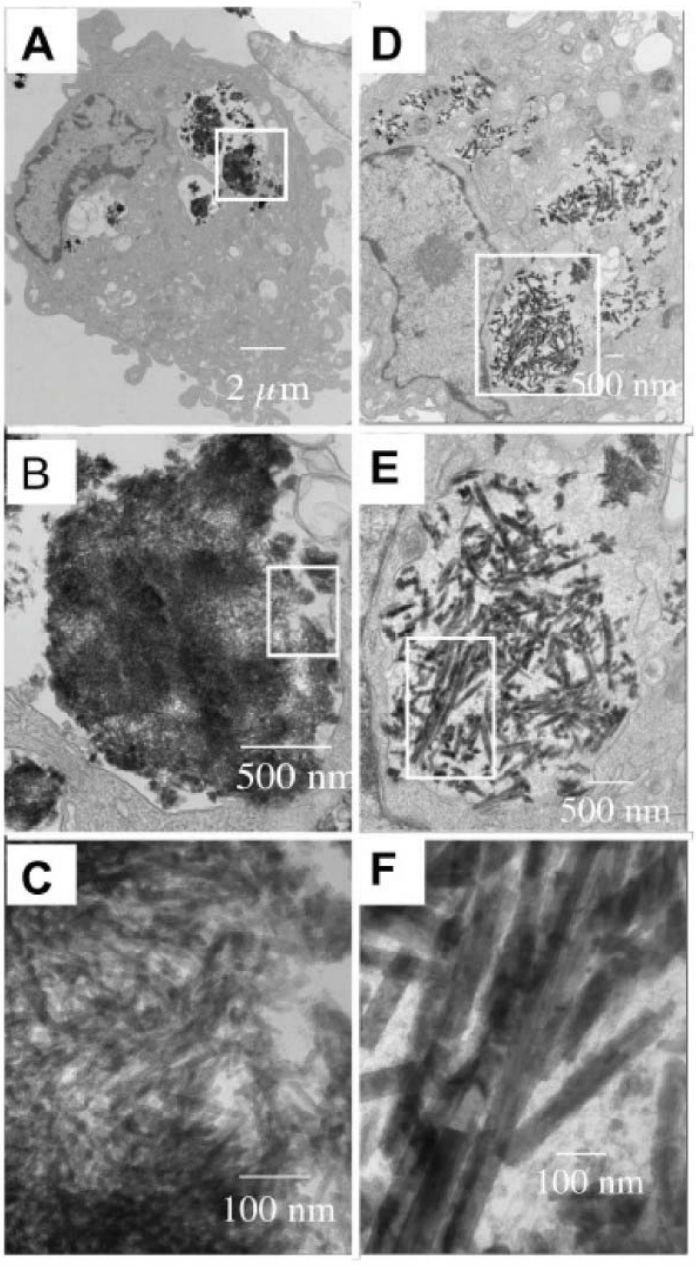

Figure 5. Fluorescent LnPO4·H2O nanorods were visualized by TEM inside the cytoplasmic compartments of HUVEC. (A-C) EuPO4·H2O nanorods and (D-F) TbPO4·H2O nanorodsare observed inside the HUVEC with increasing magnifications. B was the enlarge picture of white block in A, C was the enlarge picture of white block in B. Similarly, E was the enlarge picture of white block in D and F was the enlarge picture of white block in E. Reprinted with the permission from [38], Patra et al. Inorganic phosphate nanorods are a novel fluorescent label in cell biology. *J Nanobiotechnology* 2006, 4. doi:10.1186/1477-3155-4-11. © 2006 Patra et al; licensee BioMed Central Ltd.

7.6. Confocal Microscopy of HUVEC and 786-O Cells Treated with $Lnpo_4 \cdot H_2O$

After incubating HUVEC and 786-O cells with LnPO4·H2O (Ln= Eu & Tb) nanorods on glass cover slips and fixing the cells with freshly prepared 4% paraformaldehyde the plates were examined the fluorescence properties with confocal microscopy [39]. Two-dimensional, confocal fluorescence microscopy images were collected through the use of an LSM 510 confocal laser scan microscope (Carl Zeiss) with an argon ion laser excitations at 364 and 488 nm for Eu and Tb, respectively). The red and green fluorescence emissions were collected through a 601- and 505-nm long-pass filter for EuPO4.H2O and TbPO4.H2O nanorods, respectively and shown in Fig. 6 (A-J).

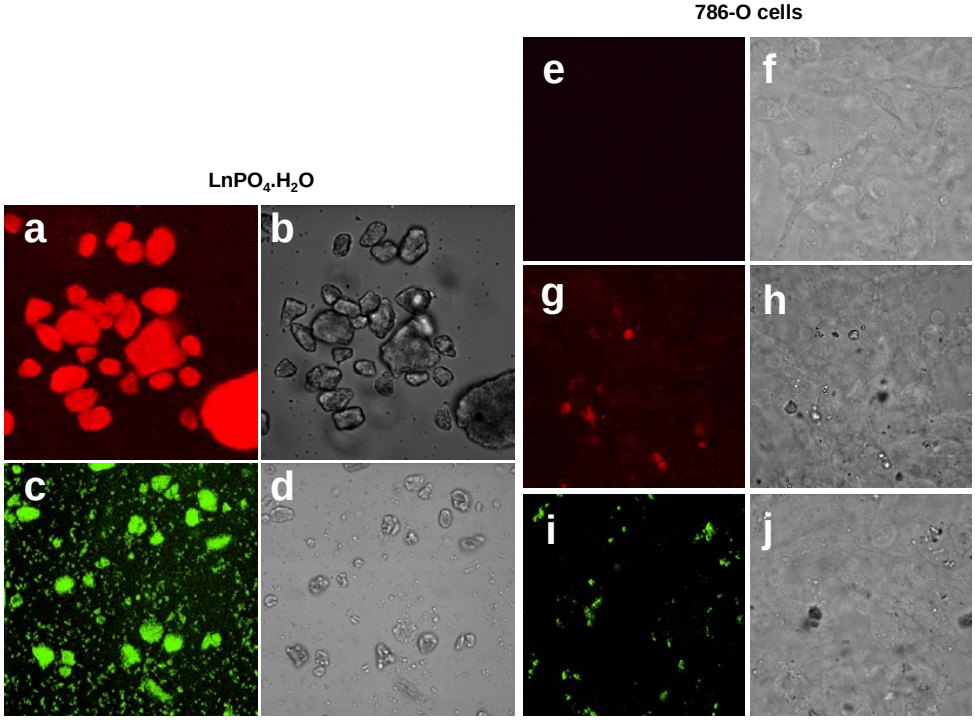

Figure 6. Fluorescence (A, C, E, G, and I) and corresponding phase images (B, D, F, H, and J) of LnPO4 · H2O nanorods (A–D), control untreated 786-O cells (E, F), and 786-O cells treated with LnPO4 · H2O nanorods (G–J): red fluorescence (A) and corresponding phase images (B) of EuPO4 · H2O nanorods can be observed, along with green fluorescence (C) and corresponding phase images (D) of TbPO4 · H2O nanorods. (E, F), control 786-O cells with no treatment, no fluorescence (E), and no nanoparticles (F). (G, H), 786-O cells treated with EuPO4 · H2O nanorods and red fluorescence are visible in (G) due to the presence of Eu+3 ions; and nanoparticles are visible in the corresponding phase image (H). (I, J), 786-O cells treated with TbPO4 · H2O nanorods and green fluorescence are visible in (I) because of the presence of Tb+3 ions, and nanoparticles are visible in the corresponding phase image (J). Reprinted with permission from [39], Patra et al. Lanthanide phosphate nanorods as inorganic fluorescent labels in cell biology research. *Clinical Chemistry* 2007, **53:**2029-2031.Doi:10.1373/clinchem.2007.091207. ©2007 American Association for Clinical Chemistry, Inc.

A red and green fluorescence (Fig. 6.A) were observed in Fig.6.A and Fig.6.C due to $EuPO_4.H_2O$ and $TbPO_4.H_2O$ nanorods, respectively and their corresponding phase images were found in Fig. 6.B and Fig.6.D indicating the presence of particles. Fig.6.E indicates the confocal image of control 786-O cell without nanorods and it does not show any fluorescence even no auto-fluorescence was observed. However, Fig.6.G shows the significant red fluorescence of 786-O cells due to presence of $EuPO_4.H_2O$ nanorods inside the cells. Similarly, a prominent green fluorescence (Fig.6.I) was observed due to presence of $TbPO_4.H_2O$ nanorods inside the cells [39]. Our inorganic fluorescent label method is a simple tool for examining the cellular compartments of living cells as these nanorods are non-toxic to endothelial cells (toxicity discussed later). Fluorescent nanorods may enable improved detection of malignant tumor cells. These results indicate that these fluorescent nanorods can internalize in cells, which in turn can be visualized by microscopy. Therefore, these nanorods offer useful and alternative inorganic fluorescent probes for targeting various molecules in living cells. These resulst suggest that this technique might be used for live-cell imaging, a requisite analytical tool in most cell biology experiments and a routine procedure in neurobiology, developmental biology, pharmacology, and several other related biomedical research fields [39].

7.8. *In Vitro* Toxicity (Cell viability test, Cell Proliferation and Apoptosis assay)

As we have observed the distinct fluorescence activity of $LnPO_4.H_2O$ upon cellular internalization, therefore before going to apply these nanorods as fluorescent label in cell biology, *in vitro* toxicity measurement is a topic of considerable importance. It is reported that exposure to certain nanomaterials and metallic salts of lanthanides might lead to adverse biological effects, this appears to dependent upon the chemical and physical properties of the material [17, 36, 37, 41, 42, 141].

Initially, to observe viability, HUVEC cells were incubated with 50 μg/mL of $LnPO_4.H_2O$ nanorods for 24–48 hours. There was no difference in cell death between untreated control cells (no treatment) and nanorod-treated HUVEC cells as assessed by trypan blue. These results clearly indicate a biocompatibility between the nanorods and the cells. We have investigated the *in vitro* toxicity using [^{3}H]-thymidine incorporation assays (cell proliferation assay) on HUVEC cells and found them to be non-toxic up to 100 μg/mL [38]. However, they are acting as pro-angiogenic agent (discussed later)[40].

In order to investigate whether uptake of these nanorods induce apoptosis, we have done two type of apoptosis assay name (i) flow cytometry method using Annexin V-FITC and (ii) TUNEL assay (dUTP nick-end labeling). In both cases we have observed that $LnPO_4{\cdot}H_2O$ nanorods are nontoxic to endothelial cells [38].

Fig.7. illustrates the results of TUNEL assay of HUVEC cells treated with nanorods where red color nuclei (TMR red –stained) in first column indicates the apoptotic cells, blue color in second column indicates the nuclei stained with DAPI (4'-6-Diamidino-2-phenylindole) and third column indicates the merge pictures of first and second column. Red color nuclei in Fig. 7.A indicate the apoptotic cells in presence of ~2.5 mM camptothecin,

served as positive inducer. There is no presence of red nuclei in control HUVEC cells as expected. No red nuclei (TMR red-stained) of HUVEC cells treated with nanorods in Fig. 7.C & D were detected indicating the absence of apoptotic cells. These results clearly indicate that these nanorods were not toxic to endothelial cells. We have first time demonstrated the in vitro toxicity experiments using nanorods in cell biology research.

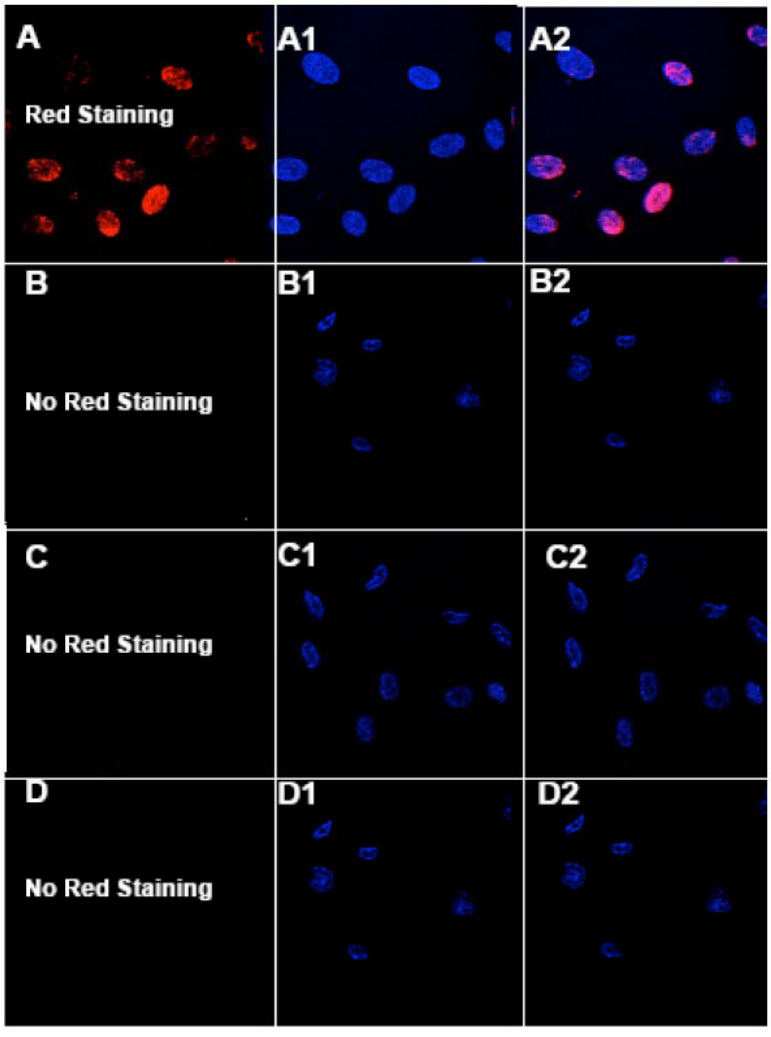

Figure 7. TUNEL assay apoptosis of HUVEC. First row: positive control experiment, second row: untreated control experiment, third row: HUVEC treated with EuPO4·H2O at 50 μg/ml for 20 h of incubation at 37°C and fourth row: HUVEC treated with TbPO4·H2O at 50 μg/ml for 24 h of incubation at 37°C. TUNEL assay apoptosis of HUVEC using camptothecin (4 h incubation at 37°C) as positive inducer (First row). A: TMR red -stained nuclei of HUVEc appear in red color due to presence of apoptotic cells, A1: The DAPI-stained nuclei appear in blue and A2: merged picture of A and A1. First Column: The nuclei of HUVEC were stained with TMR red (B-D), red staining was not observed due to absence of no apoptotic cells. Second column: The DAPI-stained nuclei appear in blue (B1-D1), and Third column: merged picture of first and second column (B2-D2). Reprinted with the permission from [38], Patra et al. Inorganic phosphate nanorods are a novel fluorescent label in cell biology. *J Nanobiotechnology* 2006, 4. doi:10.1186/1477-3155-4-11. © 2006 Patra et al; licensee BioMed Central Ltd.

8. Europium Oxide Nanoparticles in an Immunoassay for Atrazine

Synthesis and surface functionalization of nanoparticles is an important area of research in nanotechnology [142]. The basic application of surface functionalization of nanoparticles is to enhance the overall performance of nanoparticles for targeted delivery of DNA, drugs, proteins, antibodies etc. Functionalization of metal oxide nanoparticles enables their use in biological applications via modification of surface properties[143]. In general, metal oxide nanoparticles have no affinity to bind drug molecules/proteins/DNA due to absence of free reactive functional groups such as hydroxyl (-OH), amino (-NH2), mercapto (-SH) on the surface of these nanoparticles. Therefore, functionalization of the surface of the nanoparticles is one of the key step in drug delivery. In this context, Feng et al and his co-workers have demonstrated the microwave assisted functionalization of europium oxide (Eu2O3) nanoparticles, used as fluorescent label in an immunoassay for atrazine [144]. Direct coating of nanoparticles with Si-containing matrix may provide the best way to preserve the optical properties of Eu2O3 nanoparticles and to provide biologically functional groups at the same time. Therefore, they have demonstrated the functionalization of Eu2O3 nanoparticles using 3-amino-propyl trimethoxy silane (APTMS), which provides the free reactive -NH2 amino group for conjugation with drugs (atrazine) (Fig.8) and investigated their efficacy in a model immunoassay. The application of the functionalized nanoparticles in competitive immunoassay foratrazine is presented schematically in Fig.9. This method is very simple and rapid method for functionalization of the metal oxide nanoparticles. The application of this material to an immunoassay for atrzine showed promise as a simplified competitive assay with little reduction sensitivity. In another study they have developed a method for coating Eu:Gd2O3 particles with proteins and described the use of these particles as phosphores for the visualizaion of protein micropatterns where avidin-biotin specific binding was used as a model system [103].

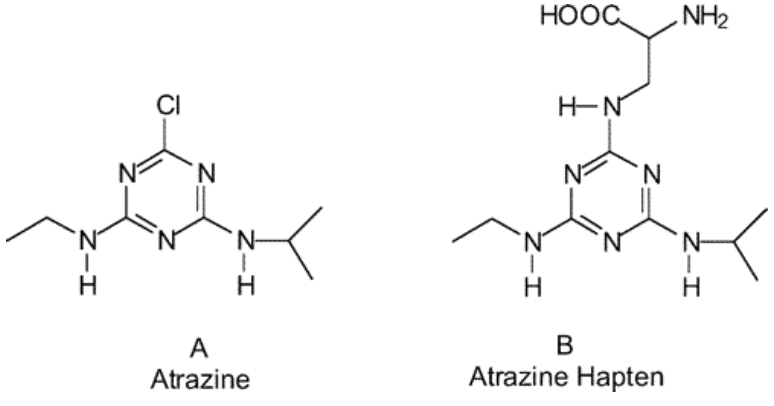

Figure 8. (A) and (B) atrazine and derivative used for conjugation. Reprinted with the permission from [144], Feng et al. Functionalized europium oxide nanoparticles used as a fluorescent label in an immunoassay for atrazine. *Analytical Chemistry* 2003, 75:5282-5286. DOI: 10.1021/ac034063m S0003-2700(03)04063-0. ©2003 American Chemical society.

However, inorganic lanthanide nanoparticles have raised new possibilities for the ultrasensitive and multiplexed imaging of molecular targets in living cells, animal models, and possibly in human subjects. Lanthanide-based inorganic fluorescents, especially Eu- and Tb-phosphate/oxides/hydroxide nanoparticles, have attracted a great deal of attention in medicine and cell biology [38, 39].

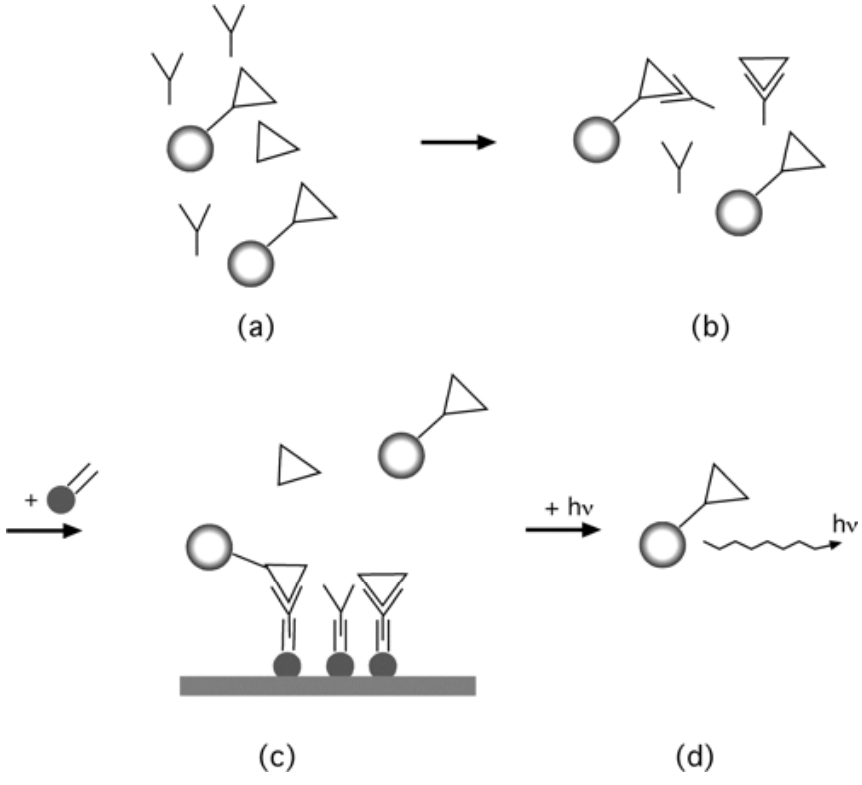

Figure 9. Schematic presentation of the competitive assay using magnetic separation. The assay was carried out as follows: (a) the atrazine-derivatized europium particles (O-), the free atrazine in the sample (), and the monoclonal anti-atrazine antibody (Y) are added together and (b) allowed to react. (c) Magnetic beads coated with anti-mouse antibody are then added. Free antibody, antibody bound to free analyte (-Y), and antibody bound to the atrazine-derivatized europium particles are all removed from the solution, leaving only atrazine-derivatized europium particles in solution. (d) The solution is then measured for fluorescence. If the analyte concentration is low, then most of the atrazine-derivatized europium particles will be bound to anti-atrazine antibody and subsequently to the magnetic beads and removed from solution; thus, the fluorescence of the solution will be low. If the analyte concentration is high, then the anti-atrazine antibody will be bound to the free analyte. When the magnetic beads are applied, very little atrazine-derived antibody will be removed from solution, since most of the antibody is bound to free atrazine; thus, the fluorescence of the solution will be high. This format results in a calibration curve in which the concentration of free analyte in the sample is directly proportional to the amount of fluorescence detected in the solution. Reprinted with the permission from [144], Feng et al. Functionalized europium oxide nanoparticles used as a fluorescent label in an immunoassay for atrazine. *Analytical Chemistry* 2003, 75:5282-5286. DOI: 10.1021/ac034063m S0003-2700(03)04063-0. ©2003 American Chemical society.

9. Angiogenesis By $Eu^{iii}(Oh)_3$ Nanorods

It is now well established tha angiogenesis is the process of formation of new capillaries from preexisting blood vessels [145] and it is a complex process involving both pro-angiogenic and anti-angiogenic factors. The process of angiogenesis consists of several steps, which include the stimulation of endothelial cells by growth factors, degradation of the extracellular matrix by proteolytic enzymes, migration and proliferation of endothelial cells, and, ultimately, capillary tube formation [146]. Endothelial cell migration and proliferation are critical steps in the angiogenic process [147]. Angiogenesis plays an essential role in physiological processes such as embryonic development, the menstrual cycle, and in pathologic conditions (e.g. wound healing, tumor growth and metastasis, rheumatoid arthritis, proliferative diabetic retinopathy, atherosclerosis, and post ischemic vascularization of the myocardium) [145, 148-153]. However, the most important objective of angiogenesis is to induce or stimulate vessel growth in patients with conditions characterized by insufficient blood flow, such as ischemic heart disease and peripheral vascular diseases. Ischemic heart disease is the most common cause of death in United States as well as several countries around the world [154, 155]. According to 'Morbidity and Mortality Weekly Report' (Feb 21, 1997), in 1994, a total of 481,458 persons died as a result of ischemic heart disease (IHD), which comprises two thirds of all heart disease - the leading cause of death in the United States. The development of drugs that stimulate revascularization of ischemic tissues remains an exciting but unrealized goal in cardiovascular therapeutics.

A number strategies including prevention through diet, exercise, and lipid-lowering drugs and medical intervention via angioplasty, stent placement, surgery, and pro-angiogenic factors such as vascular endothelial growth factor A (VEGF-A) and basic fibroblast growth factor (bFGF) [149, 150, 152, 156], used to enhance blood flow in ischemic tissues via formation of collateral blood vessels have also been associated with pathological angiogenesis, thrombosis, fibrosis and/or the proliferation of tumor cells [156-158]. The latter observation warrants that the development of novel pro-angiogenic as well as anti-angiogenic molecules is very important step in biomedical research (especially ischemic heart disease and peripheral vascular diseases) where nanotechnology (a multidisciplinary field, which covers a vast and diverse array of devices derived from engineering, biology, physics and chemistry) can play a pivotal role. Earlier reports suggest that transition and lanthanide elements have important role in biology and medicine [3, 38, 39, 44, 49, 102, 159-165]. With a view to understanding the biological impact of lanthanide metals, we have investigated the pro-angiogenic properties of europium(III) hydroxide nanorods [$Eu^{III}(OH)_3$] by several *in vitro* analyses and also by *in vivo* CAM (chick chorioallantoic membrane) assays [40]. Therefore, we strongly believe that the pro-angiogenic properties of [$Eu^{III}(OH)_3$] nanorods can be used to develop new treatment strategies for cardiovascular ischemic and peripheral vascular diseases, or limb ischemia-related diseases in near future.

The pro-angiogenic properties of $Eu^{III}(OH)_3$ nanorods was investigated by several *in vitro* assays and CAM assay (*in vivo* model) which are summarized below.

9.1. Synthesis, Characterization and Internalization of $Eu^{iii}(OH)_3$ Nanorods

$Eu^{III}(OH)_3$ nanorods were prepared by microwave heating a mixture of an aqueous solution containing Europium(III)nitrate and aq.NH_4OH at atmospheric pressure in an open reflux system [40]. The nanorods were characterized by several analytical tools such as X-ray diffraction (XRD), Thermo-gravimetric (TG) and Differential Scanning Calorimetric (DSC) Analysis, Transmission electron microscopy (TEM) study, fluorescence spectroscopy (FS), confocal microscopy etc in order to evaluate the crystal structure, morphology and chemical nature [40]. We prepare [$Eu^{III}(OH)_3$] nanorods suspension solution in sterile TE (tris- EDTA) buffer and use only freshly prepared suspension in TE buffer for all cell culture experiments and CAM assay. Internalization and colocalization of these nanorods inside the cells was investigated by several techniques such as FS, differential interference contrast (DIC) microscopy, confocal microscopy, and transmission electron microscopy (TEM).

9.2. Cell Viablity, Apoptosis Assay and [^{3}H]Thymidine Incorporation Assay

Before applying these nanorods *in vitro*, we have decided to check their toxicity to endothelial cells (HUVEC) by several *in vitro* assays. However we have first tested the viability of HUVEC cells treated with $Eu^{III}(OH)_3$ nanorods at different concentrations from 20-100 μg /mL and incubated for 24-48 hrs to observe apoptosis. Both in the untreated control and in the nanorod treated samples HUVEC remained equally viable, as assessed by Trypan Blue exclusion assay (data not shown). This indicated that these nanorods were biocompatible and did not affect cell viability. According to tunnel-based apoptosis (dUTP nick-end labeling) assay (as described before) the red colored nuclei were not observed when the HUVEC cells were incubated with 50 μg /mL indicating no induction of apoptosis in presence of these nanorods. However, there was ~10% of the nuclei stained red when treated with nanorods at 100 μg/mL compared to control untreated cells. We also determined the *in vitro* toxicity of these nanorods by performing [^{3}H]thymidine incorporation assay in HUVEC [38-40, 153]. Endothelial cell proliferation is one of the critical steps in angiogenesis [145, 153, 166]. In order to determine whether our [$Eu^{III}(OH)_3$] nanorods can stimulate the endothelial cells, we have performed [^{3}H]-thymidine incorporation assay for HUVECs treated with these nanorods in dose dependent and time dependent way (Fig. 10a). We have found that these nanorods promote a dose-dependent increase in endothelial cell proliferation when used at a concentration of 20-50 μg/ml as compared to that of untreated controls. However, less cell proliferation was observed when nanorods concentration was 100 μg/ml (Fig.10a). At the same time we have carried out the [^{3}H]-thymidine incorporation assay to endothelial cells incubated with amorphous europium hydroxide and oxide materials and observed no significant proliferation. Even we did not found any significant change in endothelial cell proliferation by the treatment of other lanthanide [Neodymium (Nd), Samarium (Sm), Gadolinium (Gd) and Terbium (Tb)] hydroxide nanoparticles under identical experimental conditions. As expected, HUVECs treated with VEGF (10 ng/ml) have shown increased proliferation in similar fashion (Fig.10.a). Hence, our results clearly show that $Eu^{III}(OH)_3$

nanorods, although inorganic material, function like other proangiogenic cytokines such as VEGF.

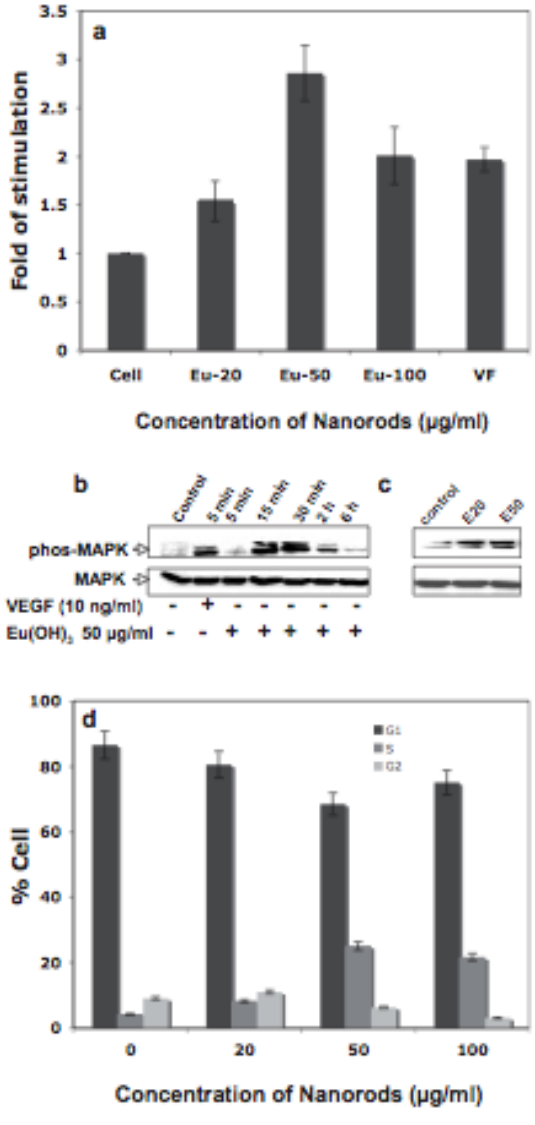

Figure 10. a) Effect of EuIII(OH)3 nanorods [Eu-20, Eu-50, Eu-100 indicates 20, 50, and 100 lgmL–1, respectively, and VF = VEGF (10 ng mL–1)] on HUVECs, observed by cell proliferation assay, represented as fold stimulation. b) Western blot analysis for phosphomapkinase (phos-MAPK) and total mapkinase from lysate of i) untreated control HUVECs, and HU-VECs treated with ii) EuIII(OH)3 nanorods of 50 lgmL–1 between 5 min to 6 h, and iii) VEGF (10 ng mL–1) for 5 min. c) HUVECs treated with Eu-III(OH)3 nanorods at different concentrations for 24 h. d) Cell-cycle analysis of HUVECs treated with EuIII(OH)3 nanorods (0–100 lgmL–1). The data are statistically significant where $p \leq 0.05$ [(mean $\bar{\gamma}$ one standard deviation) of three separate experiments performed in triplicates]. See main text for further explanation of cell cycle classification. Reprinted with the permission from [40], Patra et al. Pro-angiogenic properties of europium(III) hydroxide nanorods. Advanced Materials 2008, 20:753-756. DOI: 0.1002/adma.200701611.© 2006 Patra et al; Wiley-VCH Verlag GmbH & Co.KGaA.

9.3. Mapkinase Phosphorylation

Mitogen-activated protein kinase (MAPK) activation is one of the key important signaling for the angiogenesis, demonstrating by several groups including our group [167-172]. To further confirm the results obtained from cell proliferation assay, western blot analysis for phospho-MAPK of HUVEC treated with and without $Eu^{III}(OH)_3$ nanorods were performed in a dose-dependant (20-50 μg/mL) (Fig.10.c) and time dependant fashion (5min - 6h) (Fig.10.b). As a positive control, HUVEC cells were treated with vascular endothelial growth factor (VEGF) at a concentration of 10 ng/ml for 5 min [173]. Western blot analysis for phospho-MAPK of HUVEC treated with and without $Eu^{III}(OH)_3$ nanorods between 15 min 30 min is comparable to VEGF treated 5 min sample. Again, with increasing the concentration of $Eu^{III}(OH)_3$ nanorods (20-50 μg/ml), mapkinase phosphorylation was increased and reached maximum at 50 μg/ml. These results support the cell proliferation analysis data where we got maximum proliferation at50 μg/ml concentration. The mechanism of up-regulation of phospho-mapkinase by nanorods is currently unknown and a subject of future investigation.

9.4. Cell Cycle Assay

To investigate the mechanism of HUVEC cell proliferation in the presence of EuIII(OH)3 nanorods, we have performed cell cycle analysis. The cell cycle in eukaryotes is broadly classified into four phases, G1-preparation of the chromosomes for replication, S-synthesis of DNA and centrosomes, G2-preparation for mitosis and M-mitosis; the cell dividing into two daughter cells each with a complete set of genes [174, 175]. Therefore, it is expected that the proliferation of HUVEC cells should be reflected in cell cycles where higher population would be expected in the S-phase and fewer population in the G1-phase. [176] Cell cycle analysis using PI staining in HUVEC cells revealed a significant increase in the percentage of cells in S-phase when treated with 50 μg/ml of EuIII(OH)3 nanorods as compared with that of untreated control cells (Fig.10.d). Conversely, percentage of cells in the S-phase decreased at a concentration of 100 μg/ml of EuIII(OH)3 nanorods. These cell cycle data further supports the results obtained from thymidine incorporation assay and MAPK activation assay.

9.5. Chick Chorioallantoic Membrane (CAM) Assay (*In Vivo* Model)

In order to determine the in vivo relevance of our in vitro findings we performed CAM assays to measure nanoparticle-induced angiogenesis. Chick eggs were maintained in a humidified 39 ^{0}C incubator (Lyon Electric, CA). Pellets containing 0.5% methylcellulose, plus recombinant human VEGF-A (50 ng, positive control) or water (negative control) or TE (diluent control) or 50uL of nanoparticles at various concentrations were placed onto the CAM's of separate 10-day-old chick pathogen-free embryos (SPAFAS; Charles River Laboratories, Wilmington, MA). The CAM's were exposed by cutting a small window in the

egg shell to facilitate application of the relevant substances. CAMs were imaged on Day 13 either following fixation and excision or with real time live imaging using a digital camera (Canon Supershot6) attached to a Zeiss stereomicroscope. Angiogenesis was quantified by counting branch points arising from tertiary vessels from a minimum of 10 specimens from three separate experiments.

Fig.11.a and Fig.11.b illustrate negative control experiment and positive control experiment where CAMs were treated with only TE (tris-EDTA) buffer solution and VEGF, respectively. As expected, we have observed vascular sprouting when CAMs have been treated with pro-angiogenic stimulus VEGF (50 ng) (Fig. 9b). $Eu^{III}(OH)_3$ nanorods in different concentrations (1μg and 10μg) induced significant angiogenesis (Fig.11.c-d) compared to control CAMs without nanorods. White arrows mark the matured vascular sprouting in presence of these nanorods. The quantitative data for the angiogenesis assay (CAM assay) using nimrods were also shown in Fig.11.e as a histogram. The formation of vascular sprouting as observed by CAM assay in the presence of Euro $^{III}(OH)_3$ nimrods directly suggest that these inorganic nimrods have unique pro-angiogenic properties like VEGF.

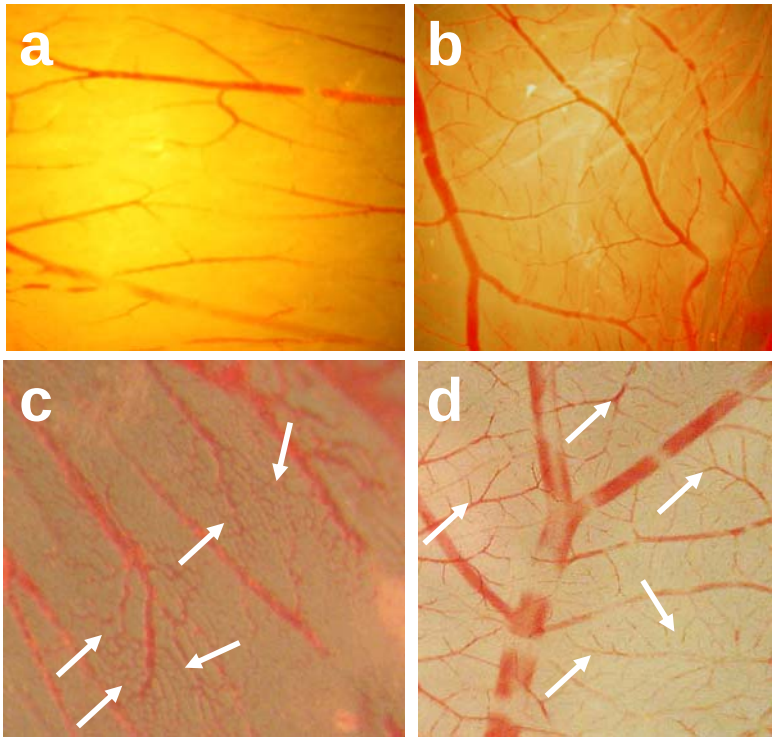

Figure 11. (a-d) Chick CAM assays treated with a) TE (tris-EDTA; tris-ethylenediaminetetraacetate) buffer, b) VEGF (50 ng), c,d) 1 and 10 ng of nanorods, respectively, in TE buffer at higher magnification. Magnification for (a,b,d) = x1.6. Magnification for (c) = x 4.

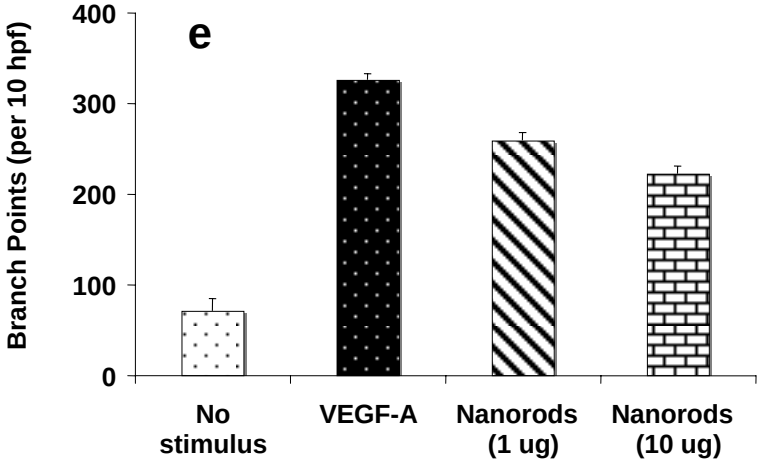

Figure 11e). Angiogenesis was quantified by counting branch points arising from tertiary vessels from a minimum of ten specimens from three separate experiments. hpf: high power field. Reprinted with the permission from [40], Patra et al. Pro-angiogenic properties of europium(III) hydroxide nanorods. *Advanced Materials* 2008, 20:753-756. DOI: 10.1002/adma.200701611.© 2006 Patra et al; Wiley-VCH Verlag GmbH & Co.KGaA.

9.6. Plausible Mechanism for Nanorods Induced Angiogenesis

Formation of reactive oxygen species (ROS) plays an important role in angiogenesis demonstrated by several researchers [177-182]. Therefore we investigated the formation of ROS in nanorods induced angiogenesis in HUVEC cells (Fig.12.a-I). A weaker green fluorescence was observed in control untreated HUVEC cells due to formation of endogenous ROS (Fig. 12.a-c). The green fluorescence as seen in Figure 12(d-f) indicates that the production of ROS inside HUVECs induced with 100 μM of tert-butyl hydroperoxide (TBHP) for 1h served as a positive inducer. Figure 12(g-i) and Figure 12(j-l) indicate the generation of ROS in the presence of $Eu^{III}(OH)_3$ nanorods at the concentrations of 20 and 50 μg/ml, respectively, suggesting nanorods induce angiogenesis most likely due to increased production of ROS.

Other than our above-mentioned *in vitro* and *in vivo* investigations we have carried out some other in vivo experiments. For example, the nude mice ear model showed the formation of new blood vessels in the nanorods treated mice ear compared to vehicle (tris-EDTA) treated control ears. (unpublished data)The detailed *in vivo* toxicity experiments on C57BL6 mice did not show any biochemical or hematological toxicity after peritoneal injection. However, the efficacy of these nanorods in promoting angiogenesis in the mammalian heart and its safety with *in vivo* use has not been established. The data obtained from this study may provide the basis for the development of novel therapeutics for patients who otherwise have non-revascularizable ischemic heart disease.

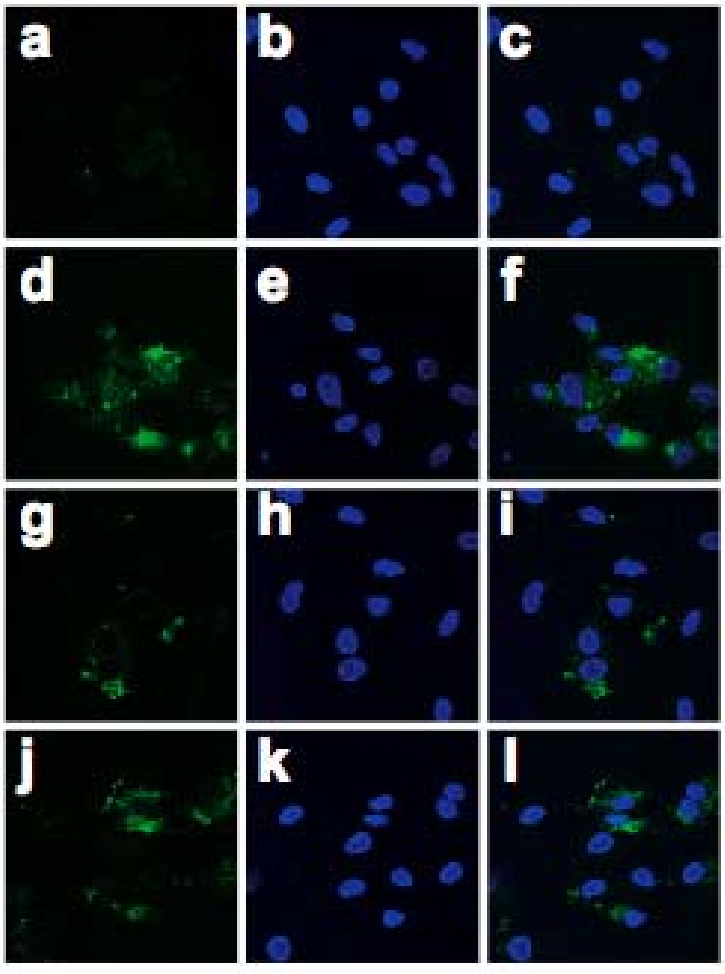

Figure 12. ROS are produced during the endothelial cell proliferation in the presence of EuIII(OH)3 nanorods at different concentrations. a–c) Control, untreated HUVECs. d–f) HUVECs treated with 100 lM mL–1 of *tert*-butyl hydroperoxide as a positive ROS inducer. g–l) HUVECs treated with 20 lg mL–1 (g–i) and 50 lg mL–1 (j–l) of EuIII(OH)3 nanorods. Reprinted with the permission from [40], Patra et al. Pro-angiogenic properties of europium(III) hydroxide nanorods. *Advanced Materials* 2008, 20:753-756. DOI: 10.1002/adma.200701611.© 2006 Patra et al; Wiley-VCH Verlag GmbH & Co.KGaA.

10. Therapeutic Application Lanthanide Nanoparticles

Before discussion application of lanthanides in therapy we should inform readers who are interested to know about the biological/medicinal use of lanthanide elements in detail can refer to the following books, articles or reviews [12, 45, 49, 76, 183-197]. Inorganic and bioinorganic chemistry have made important contributions to bio-medical science and human health care in the past half century. Now-a-days, metal-containing imaging agents are extensively used in therapeutics, which constitute a multi-billion dollar industry[198].

Lanthanide ions are trivalent metallic cations (Ln^{3+}) and it can interact with different types of biologically important proteins including G protein-coupled receptors, ion channels [186-189]. The strong interactions of Ln^{3+} ions with these protein molecules are due to the sharing of biologically important properties with divalent calcium ions (Ca^{2+}). The Ln^{3+} ions have strong affinity to Ca^{2+} sites on biological molecules due to variety of similarity to Ca^{2+} ions with respect to ionic radii, coordination chemistry, and affinity for the oxygen donor groups underlies their strong interaction with Ca2+-binding sites on a wide range of proteins. Hence lanthanides ions can act as either Ca^{2+} inhibitors or probes on biological molecules [190-194].

Blockade of current through single calcium channels and T-type calcium channels by trivalent lanthanide cations are well established [195, 196]. Time-resolved fluorometry is a technology that exploits the unique fluorescence properties of lanthanide chelates. Lanthanide-based luminescent assays, a highly sensitive assay, have been used for different types of ligand-receptor interactions [186-189].

Fricker et al demonstrated the therapeutic application of lanthanides in his review [43]. Lanthanide compounds for therapeutic and diagnostic applications have been also described elaborately by Thompson and Bünzli et al [44, 76]. Recent report by Chen et suggested that rare earth nanoparticles prevent retinal degeneration induced by intracellular peroxides [185].

Storr et al described the recent advances in medicinal inorganic chemistry pertaining to the use of multifunctional ligands that target specific tissues, membrane receptors, or endogenous molecules, including enzymes [184]. The application of Eu_2O_3, known as inorganic red phosphor nanoparticles labels in an immunoassay yields very good sensitivity in an immunoassay for atrazine (sub-parts-per-billion detection limit) without optimization of the detection system [144].

11. Conclusion

The low cost synthesis method (especially microwave method) and unique properties of lanthanides (Eu &Tb) nanorods/nanoparticles make them very attractive in varieties of applications in biomedical nanotechnology. The shrap spectral features, size dependent emission wavelengths, photostability, large stokes shift, Improved signal brightness and long life time (several hundreds microseconds) of lanthanide-based nanoparticles are promising for their implementation in multiplexed detection schemes. Various applications of lathanide compounds/chelates/nanoparticles/nanorods in biomedical technology have been described in this book chapter. The pro-angiogenic properties of europium(III) hydroxide nanorods could be used to develop new treatment strategies for cardiovascular ischemic and peripheral vascular diseases, the most common cause of death in United States as well as several countries around the world. Recent discoveries in the synthesis of inorganic nanoparticles, especially lanthanide elements opens up a new route for biological imaging, drug delivery and therapeutic agents. These areas represent some of the most recent and still relatively unexplored themes in nanotechnology that might be exciting and fruitful topics of study for the community interested in 'metals in medicine.

12. Abbreviations

bFGF: Basic fibroblast growth factor
CAM: Chick chorioallantoic membrane)
DIC: Differential interference contrast
DMO: Domestic Microwave Oven
DSC: Differential scanning calorimetry
Eu: Europium
FS: Fluoresence spectroscopy
HBsAg: Hepatitis B surface antigen
HRTEM: High resolution transmission electron microscopy
HUVEC: Human umbilical vein endothelial cells
IR Spectroscopy: Infrared spectroscopy
LBT: Lanthanide binding tags
$LnPO_4.H_2O$: Lanthanide phosphate (Ln = lanthanide)
LRTEM: Low resolution transmission electron microscopy
MAPK: Mitogen-activated protein kinase
MRI: Magnetic resonance imaging
PCR: Polymerase chain reaction
PS: Photoluminescence spectroscopy
PSA: Prostate-specific antigen
RCC:Renal carcinoma cells (786-O cells)
ROS: Reactive oxygen species
RS: Raman spectroscopy
SA: Streptavidine
SAED: Selected area electron diffraction
Tb: Terbium
TBHP: Tert-butyl hydroperoxide
TEM: Transmission Electron Microscopy
TGA: Thermogravimetric analysis
TRF: Time-resolved fluorescence (TRF)
VEGF-A: Vascular endothelial growth factor A
XPS: X-ray photoelectron spectroscopy
XRD: X-ray diffraction

Acknowledgement

This work was partly supported by NIH grants CA78383, HL70567, a grant from the American Cancer Society to D. Mukhopadhyay and a developmental grant from Haem-malignancy program at Mayo Clinic (RAF-20P) and CLL-global foundation grant to P. Mukherjee and also partly supported by UOFM-MEDICA#5CA and UOFM-MEDICA# 5P1, a grant from‘Minneasota Partnership for translational Nanotechnology in Cancer’ to D. Mukhopadhyay and P.Mukherjee, respectively.

References

[1] Xu AW, Gao Y, Liu HQ. The preparation, characterization, and their photocatalytic activities of rare-earth-doped TiO2 nanoparticles. *Journal of Catalysis* 2002, 207:151-157.

[2] Wu GS, Zhang LD, Cheng BC, Xie T, Yuan XY. Synthesis of Eu2O3 nanotube arrays through a facile sol-gel template approach. *Journal of the American Chemical Society* 2004, 126:5976-5977.

[3] Yu JH, Parker D, Pal R, Poole RA, Cann MJ. A europium complex that selectively stains nucleoli of cells. *Journal of the American Chemical Society* 2006, 128:2294-2299.

[4] Lim MJ, Patton WF, Lopez MF, Spofford KH, Shojaee N, Shepro D. A luminescent europium complex for the sensitive detection of proteins and nucleic acids immobilized on membrane supports. *Analytical Biochemistry* 1997, 245:184-195.

[5] Yuan JL, Wang GL, Majima K, Matsumoto K. Synthesis of a terbium fluorescent chelate and its application to time-resolved fluoroimmunoassay. *Analytical Chemistry* 2001, 73:1869-1876.

[6] Scorilas A, Bjartell A, Lilja H, Moller C, Diamandis EP. Streptavidin-polyvinylamine conjugates labeled with a europium chelate: Applications in immunoassay, immunohistochemistry, and microarrays. *Clinical Chemistry* 2000, 46:1450-1455.

[7] Qin QP, Lovgren T, Pettersson K. Development of highly fluorescent detection reagents for the construction of ultrasensitive immunoassays. *Analytical Chemistry* 2001, 73:1521-1529.

[8] Ye ZQ, Tan MQ, Wang GL, Yuan JL. Novel fluorescent europium chelate-doped silica nanoparticles: preparation, characterization and time-resolved fluorometric application. *Journal of Materials Chemistry* 2004, 14:851-856.

[9] Hai XD, Tan MQ, Wang G, Ye ZQ, Yuan JL, Matsumoto K. Preparation and a time-resolved fluoroimmunoassay application of new europium fluorescent nanoparticles. *Analytical Sciences* 2004, 20:245-246.

[10] Nichkova M, Dosev D, Gee SJ, Hammock BD, Kennedy IM. Microarray immunoassay for phenoxybenzoic acid using polymer encapsulated Eu : Gd2O3 nanoparticles as fluorescent labels. *Analytical Chemistry* 2005, 77:6864-6873.

[11] Nichkova M, Dosev D, Perron R, Gee SJ, Hammock BD, Kennedy IM. Eu3+-doped Gd2O3 nanoparticles as reporters for optical detection and visualization of antibodies patterned by microcontact printing. *Analytical and Bioanalytical Chemistry* 2006, 384:631-637.

[12] Sudnick DR, Horrocks Jr. WD. Lanthanide ion probes of structure in biology. Environmentally sensitive fine structure in laser-induced terbium(III) luminescence. *Biochimica et biophysica acta* 1979, 578:135-144.

[13] Alivisatos AP. Semiconductor nanocrystals as fluorescent biological labels. *Abstracts of Papers of the American Chemical Society* 1999, 218:U296-U296.

[14] Bruchez M, Moronne M, Gin P, Weiss S, Alivisatos AP. Semiconductor nanocrystals as fluorescent biological labels. *Science* 1998, 281:2013-2016.

[15] Medintz IL, Uyeda HT, Goldman ER, Mattoussi H. Quantum dot bioconjugates for imaging, labelling and sensing. *Nature Materials* 2005, 4:435-446.
[16] Gao XH, Cui YY, Levenson RM, Chung LWK, Nie SM. In vivo cancer targeting and imaging with semiconductor quantum dots. *Nature Biotechnology* 2004, 22:969-976.
[17] Gao XH, Yang LL, Petros JA, Marshal FF, Simons JW, Nie SM. In vivo molecular and cellular imaging with quantum dots. *Current Opinion in Biotechnology* 2005, 16:63-72.
[18] Parak WJ, Gerion D, Pellegrino T, Zanchet D, Micheel C, Williams SC, Boudreau R, Le Gros MA, Larabell CA, Alivisatos AP. Biological applications of colloidal nanocrystals. *Nanotechnology* 2003, 14:R15-R27.
[19] Jain KK. Nanotechnology in clinical laboratory diagnostics. *Clinica Chimica Acta* 2005, 358:37-54.
[20] Salata OV. Applications of nanoparticles in biology and medicine. *J Nanobiotechnology* 2004, doi:10.1186/1477-3155-2-3. .
[21] Dosev D, Nichkova M, Kennedy IM. Inorganic lanthanide nanophosphors in biotechnology. *Journal of Nanoscience and Nanotechnology* 2008, 8:1052-1067.
[22] Patra CR, Bhattacharya R, Mukhopadhyay D, Mukherjee P. Application of gold Nanoparticles for targeted therapy in cancer. *J Biomed Nanotechnol* 2008.
[23] Thrall JH. Nanotechnology and medicine. *Radiology* 2004, 230:315-318.
[24] Bertozzi CR. National Institutes of Health (U.S.). Medical Arts and Photography Branch. Chemistry in living systems new tools for probing the glycome. [Bethesda, Md.: National Institutes of Health, 2005.
[25] Prescher JA, Bertozzi CR. Chemistry in living systems. *Nature Chemical Biology* 2005, 1:13-21.
[26] Winter JO: *Nanoparticles and anowires for cellular engineering.* Wenheim, Germany: Wiley VHC; 2006.
[27] El-Sayed IH, Huang XH, El-Sayed MA. Surface plasmon resonance scattering and absorption of anti-EGFR antibody conjugated gold nanoparticles in cancer diagnostics: Applications in oral cancer. *Nano Letters* 2005, 5:829-834.
[28] Dubertret B, Calame M, Libchaber AJ. Single-mismatch detection using gold-quenched fluorescent oligonucleotides. *Nature Biotechnology* 2001, 19:680-681.
[29] Alivisatos P. The use of nanocrystals in biological detection. *Nature Biotechnology* 2004, 22:47-52.
[30] Voura EB, Jaiswal JK, Mattoussi H, Simon SM. Tracking metastatic tumor cell extravasation with quantum dot nanocrystals and fluorescence emission-scanning microscopy. *Nature Medicine* 2004, 10:993-998.
[31] Michalet X, Pinaud FF, Bentolila LA, Tsay JM, Doose S, Li JJ, Sundaresan G, Wu AM, Gambhir SS, Weiss S. Quantum dots for live cells, in vivo imaging, and diagnostics. *Science* 2005, 307:538-544.
[32] Casci T. How the butterfly got its spots. *Nature Reviews Genetics* 2001, 2:911-911.
[33] Chan WCW, Nie SM. Quantum dot bioconjugates for ultrasensitive nonisotopic detection. *Science* 1998, 281:2016-2018.
[34] Han MY, Gao XH, Su JZ, Nie S. Quantum-dot-tagged microbeads for multiplexed optical coding of biomolecules. *Nature Biotechnology* 2001, 19:631-635.

[35] Rosenthal SJ. Bar-coding biomolecules with fluorescent nanocrystals. *Nature Biotechnology* 2001, 19:621-622.
[36] Jaiswal JK, Mattoussi H, Mauro JM, Simon SM. Long-term multiple color imaging of live cells using quantum dot bioconjugates. *Nature Biotechnology* 2003, 21:47-51.
[37] Derfus AM, Chan WCW, Bhatia SN. Probing the cytotoxicity of semiconductor quantum dots. *Nano Letters* 2004, 4:11-18.
[38] Patra CR, Bhattacharya R, Patra S, Basu S, Mukherjee P, Mukhopadhyay D. Inorganic phosphate nanorods are a novel fluorescent label in cell biology. *J Nanobiotechnology* 2006, 4.
[39] Patra CR, Bhattacharya R, Patra S, Basu S, Mukherjee P, Mukhopadhyay D. Lanthanide phosphate nanorods as inorganic fluorescent labels in cell biology research. *Clinical Chemistry* 2007, 53:2029-2031.
[40] Patra CR, Bhattacharya R, Patra S, Vlahakis NE, Gabashvili A, Koltypin Y, Gedanken A, Mukherjee P, Mukhopadhyay D. Pro-angiogenic properties of europium(III) hydroxide nanorods. *Advanced Materials* 2008, 20:753-+.
[41] Shimada H, Nagano M, Funakoshi T, Kojima S. Pulmonary toxicity of systemic terbium chloride in mice. *Journal of Toxicology and Environmental Health* 1996, 48:81-92.
[42] Ogawa Y, Suzuki S, Naito K, Saito M, Kamata E, Hirose A, Ono A, Kaneko T, Chiba M, Inaba Yea. Toxicity study of europium chloride in rats. *J-Environ-Pathol-Toxicol-Oncol* 1995, 14:1-19.
[43] Fricker SP. The therapeutic application of lanthanides. *Chemical Society Reviews* 2006, 35:524-533.
[44] Thompson KH, Orvig C. Editorial: Lanthanide compounds for therapeutic and diagnostic applications. *Chemical Society Reviews* 2006, 35:499-499.
[45] Ellis KJ. The lanthanide elements in biochemistry, biology and medicine. *Inorganic Perspectives in Biology and Medicine* 1977, 1:101-135.
[46] Selvin PR. Principles and biophysical applications of lanthanide-based probes. *Annual Review of Biophysics and Biomolecular Structure* 2002, 31:275-302.
[47] Evans CH. *Biochemistry of the lanthanides* New York: Plenum Press; 1990.
[48] Smentek L, Wybourne BG. *Optical spectroscopy of lanthanides; magnetic and hyperfine interactions.* Florida: CRC Press/ Taylor & Francis; 2007.
[49] Authors. Lanthanides in medicine special issue. *Chem Soc Rev* 2006, 35:493-576.
[50] Bentor Y. http://www.chemicalelements.com/groups/rareearth.html.
[51] Kagan HB, Namy JL. *Lanthanides: Chemistry and Use in Organic Synthesis.* Berlin Springer-Verlag; 1999.
[52] Turro C, Fu PKL, Bradley PM. *Lanthanide Ions as Luminescent Probes of Proteins and Nucleic Acids.* New York: Marcel Dekker; 2003.
[53] KREBS RE. *LANTHANIDE SERIES (RARE-EARTH ELEMENTS).* Westport, CT: GREENWOOD PRESS 1998.
[54] webelements: http://www.webelements.com/webelements/scholar.
[55] Wikipedia: http://en.wikipedia.org/wiki/Lanthanide.
[56] Craighead H. *Applications: Biological, medical and health.* Boston: Kluwer Academic Publishers; 2000.

[57] Nanoword.net: http://www.nanoword.net/library/def/bldefnano.htm.
[58] http://en.wikipedia.org/wiki/Nanotechnology
[59] Freitas RA. *Molecular transport and sortation.* Austin, Texus Landes Bioscience; 1999.
[60] http://nano.cancer.gov/resource_center/nano_critical.asp#why
[61] Weissman SI. Intramolecular Energy Transfer The Fluorescence of Complexes of Europium. *J Chem Phys* 1942, 10:214.
[62] Wilkinson G, Birmingham JM. Cyclopentadienyl compounds of Sc, Y, La, Ce and some lanthanide elements. *JACS* 1954, 76:6210.
[63] Dissertations: dissertations.ub.rug.nl/FILES/faculties/science/2006/v.f.quiroga.norambue/01_c1.pdf. DISSERTATIONS University of Groningen, 2006.
[64] Evans WJ, Bloom I, Hunter WE, Atwood JL. Organolanthanide hydride chemistry. 3. Reactivity of low-valent samarium with unsaturated hydrocarbons leading to a structurally characterized samarium hydride complex. *JACS* 1983, 105:1401.
[65] Ye C, Qian C, Yang X. Studies on organolanthanide complexes : XXXV. Sythesis and reactivity of new organo rare earth hydridesand references therein. *J Organomet Chem* 1991, 407:329.
[66] Ballard DGHC, A.; Holton, J.; McMeeking, J.; Pearce, R. Alkyl bridged complexes of the group 3A and lanthanoid metals as homogeneous ethylene polymerisation catalysts *J ChemSoc, Chem Commun* 1978:994.
[67] Jeske G, Lauke H, Mauermann H, Schumann H, Marks TJ. Highly reactive organolanthanides. Systematic routes to and olefin chemistry of early and late bis(pentamethylcyclopentadienyl) 4f hydrocarbyl and hydride complexes *J Am Chem Soc* 1985, 107:8091.
[68] Kobayashi T, Sakakura T, Hayashi T, Yumura M, Tanaka M: *ChemLett* 1992:1158.
[69] Jeske G, Schock LE, Swepston PN, Schumann H, Marks TJ. Highly reactive organolanthanides. Systematic routes to and olefin chemistry of early and late bis(pentamethylcyclopentadienyl) 4f hydrocarbyl and hydride complexes *J Am Chem Soc* 1985, 107:8103.
[70] Watson PL. Selective Hydrocarbon Activation. Principles and Progress. Weinheim: VCH Publishers; 1990.
[71] Rothwell IP. Selective Hydrocarbon Activation. Principles and Progress. Weinheim: VCH Publishers; 1990.
[72] Gysling MTaHJ. A New Series of Organolanthanides: Ln(indenyl). *J Am Chem Soc* 1969 91:3175-3178.
[73] Hedaya E, Krull IS, Miller RD, Kent ME, D'Angelo PFD, Schissel P. Flash vacuum pyrolysis. VI. Cyclobutadieneiron tricarbonyl. *J Am Chem Soc* 1969, 91:6880 - 6881.
[74] Zhang J, Campbell RE, Ting AY, Tsien RY. Creating new fluorescent probes for cell biology. *Nature Reviews Molecular Cell Biology* 2002, 3:906-918.
[75] Zhang J, Campbell RE, Ting AY, Tsien RY. Creating new fluorescent probes for cell biology (vol 3, pg 906, 2002). *Nature Reviews Molecular Cell Biology* 2003, 4:-.
[76] Bünzli J-CG. *Luminescent Lanthanide Probes as Diagnostic and Therapeutic Tools.* New York: Marcel Dekker Inc.; 2004.

[77] Bottrill M, Nicholas LK, Long NJ. Lanthanides in magnetic resonance imaging. *Chemical Society Reviews* 2006, 35:557-571.

[78] 78. Yuan JL, Wang GL. Lanthanide complex-based fluorescence label for time-resolved fluorescence bioassay. *Journal of Fluorescence* 2005, 15:559-568.

[79] Werts MHV. Making sense of lanthanide luminescence. *Science Progress* 2005.

[80] Pandya S, Yu JH, Parker D. Engineering emissive europium and terbium complexes for molecular imaging and sensing. *Dalton Transactions* 2006:2757-2766.

[81] Mathis G. Rare earth cryptates: A new type of fluorescent label and new homogeneous assay methods in biology. *Immuno-Analyse et Biologie Specialisee* 1996, 11:355-360.

[82] Huhtinen P, Kivela M, Kuronen O, Hagren V, Takalo H, Tenhu H, Lovgren T, Harma H. Synthesis, characterization, and application of Eu(III), Tb(III), Sm(III), and Dy(III) lanthanide chelate nanoparticle labels. *Analytical Chemistry* 2005, 77:2643-2648.

[83] Huhtinen P, Soukka T, Lovgren T, Harma H. Immunoassay of total prostate-specific antigen using europium(III) nanoparticle labels and streptavidin-biotin technology. *Journal of Immunological Methods* 2004, 294:111-122.

[84] Siitari H, Hemmilä I, Soini E, Lövgren T, Koistinen V. Detection of hepatitis B surface antigen using time-resolved fluoroimmunoassay. *Nature* 1983, 20:258-260.

[85] Jaras K, Tajudin AA, Ressine A, Soukka T, Marko-Varga G, Bjartell A, Malm J, Laurell T, Lilja H. ENSAM: Europium Nanoparticles for Signal enhancement of Antibody Microarrays on nanoporous silicon. *Journal of Proteome Research* 2008, 7:1308-1314.

[86] Woods M, Donald EWC, Sherry AD. Paramagnetic lanthanide complexes as PARACEST agents for medical imaging. *Chemical Society Reviews* 2006, 35:500-511.

[87] Allred CE, Menzel ER. A novel europium-bioconjugate method for latent fingerprint detection. *Forensic Science International* 1997, 85:83-94.

[88] Wilkinson DA, Watkin JE. Europium Aryl-Beta-Diketone Complexes as Fluorescent Dyes for the Detection of Cyanoacrylate Developed Fingerprints on Human Skin. *Forensic Science International* 1993, 60:67-79.

[89] Nojima T, Kondoh Y, Takenaka S, Ichihara T, Takagi M, Tashiro H, Matsumoto K. Detection of DNA hybridization by use of a lanthanide fluorescent intercalator that specifically binds to double stranded DNA. *Nucleic Acids Research Supplement No 1* 2001, 1:105-106.

[90] Rintamaki S, Saukkoriipi A, Salo P, Takala A, Leinonen M. Detection of Streptococcus pneumoniae DNA by using polymerase chain reaction and microwell hybridization with Europium-labelled probes. *Journal of Microbiological Methods* 2002, 50:313-318.

[91] Saha AK, Kross K, Kloszewski ED, Black CDV, Desai V, Snow RA, Toner JL, Upson DA. Time-Resolved Fluorescence of a New Europium - Chelate Complex - Highly Sensitive Detection of Protein and DNA Samples. *Abstracts of Papers of the American Chemical Society* 1993, 206:412-ORGN.

[92] Saha AK, Kross K, Kloszewski ED, Upson DA, Toner JL, Snow RA, Black CDV, Desai VC. Time-Resolved Fluorescence of a New Europium Chelate Complex - Demonstration of Highly Sensitive Detection of Protein and DNA Samples. *Journal of the American Chemical Society* 1993, 115:11032-11033.

[93] Yoshikawa K, Yuan JL, Matsumoto K, Kimura H. Time-resolved fluorometric detection of DNA using a tetradentate beta-diketonate europium chelate as a label. *Analytical Sciences* 1999, 15:121-124.

[94] Komiyama M. Sequence-Specific and Hydrolytic Scission of DNA and Rna by Lanthanide Complex-Oligodna Hybrids. *Journal of Biochemistry* 1995, 118:665-670.

[95] Franz KJ, Nitz M, Imperiali B. Lanthanide-binding tags as versatile protein coexpression probes. *Chembiochem* 2003, 4:265-271.

[96] Wei W, Wang HJ, Jiang CQ. Spectrofluorimetric determination of trace heparin using lomefloxacin-terbium probe. *Spectrochimica Acta Part a-Molecular and Biomolecular Spectroscopy* 2006, 63:241-246.

[97] Yusupov MM, Yusupova GZ, Baucom A, Lieberman K, Earnest TN, Cate JHD, Noller HF. Crystal structure of the ribosome at 5.5 angstrom resolution. *Science* 2001, 292:883-896.

[98] Derenzini M. The AgNORs. *Micron* 2000 31:117-120.

[99] Dean KA, von Ahsen O, Gorlich D, Fried HM. Signal recognition particle protein 19 is imported into the nucleus by importin 8 (RanBP8) and transportin. *Journal of Cell Science* 2001, 114:3479-3485.

[100] Root DD. In situ molecular association of dystrophin with actin revealed by sensitized emission immuno-resonance energy transfer. *Proceedings of the National Academy of Sciences of the United States of America* 1997, 94:5685-5690.

[101] Bulman RA. Metal Ions in Biological Systems. New York Marcel Dekker Inc.; 2003.

[102] Sigel RKO. *Metal Ions in Biological Systems.* New York: Marcel Dekker Inc; 2003.

[103] Dosev D, Nichkova M, Liu MZ, Guo B, Liu GY, Hammock BD, Kennedy IM. Application of luminescent Eu : Gd2O3 nanoparticles to the visualization of protein micropatterns. *Journal of Biomedical Optics* 2005, 10:-.

[104] Wang X, Zhuang J, Peng Q, Li YD. A general strategy for nanocrystal synthesis. *Nature* 2005, 437:121-124.

[105] Fang YP, Xu AW, Song RQ, Zhang HX, You LP, Yu JC, Liu HQ. Systematic synthesis and characterization of single-crystal lanthanide orthophosphate nanowires. *Journal of the American Chemical Society* 2003, 125:16025-16034.

[106] Wang X, Li YD. Synthesis and characterization of lanthanide hydroxide single-crystal nanowires. *Angewandte Chemie-International Edition* 2002, 41:4790-4793.

[107] Wang X, Li YD. Rare-earth-compound nanowires, nanotubes, and fullerene-like nanoparticles: Synthesis, characterization, and properties. *Chemistry-a European Journal* 2003, 9:5627-5635.

[108] Wang X, Li YD. Fullerene-like rare-earth nanoparticles. *Angewandte Chemie-International Edition* 2003, 42:3497-3500.

[109] Wang X, Zhuang J, Peng Q, Li YD. Hydrothermal synthesis of rare-earth fluoride nanocrystals. *Inorganic Chemistry* 2006, 45:6661-6665.

[110] Wang JY, Jin AZ, Bai YZ, Ji H, Jin CS. Etching of CVD diamond thick films by rare-earth compound ink. *Journal of Inorganic Materials* 2002, 17:172-174.

[111] Bazzi R, Flores-Gonzalez MA, Louis C, Lebbou K, Dujardin C, Brenier A, Zhang W, Tillement O, Bernstein E, Perriat P. Synthesis and luminescent properties of sub-5-nm lanthanide oxides nanoparticles. *Journal of Luminescence* 2003, 102:445-450.

[112] Fan X, Pi D, Wang F, Qiu J, Wang M. Hydrothermal Synthesis and Luminescence Behavior of Lanthanide-Doped GdF3 Nanoparticles. *IEEE TRANSACTIONS ON NANOTECHNOLOGY* 2006, 5:123-128.

[113] Riwotzki K, Haase M. Wet-Chemical Synthesis of Doped Colloidal Nanoparticles: YVO4:Ln (Ln = Eu, Sm, Dy). *J Phys Chem B* 1998, 102 10129 -10135.

[114] Ascencio J, Canizal G. Synthesis and characterization of rare-earth nanoparticles. In *Microscopy and Microanalysis; Texas, USA*. 2003

[115] Wang XJ, Gao MY. A facile route for preparing rhabdophane rare earth phosphate nanorods. *Journal of Materials Chemistry* 2006, 16:1360-1365.

[116] Wang JC, Liu Q, Liu QF. Synthesis and luminescence properties of Eu or Tb doped Lu2O3 square nanosheets. *Optical Materials* 2007, 29:593-597.

[117] Anh T, Benalloul P, Barthou C, Giang LT, Vu N, Minh LQ. Luminescence, Energy Transfer, and Upconversion Mechanisms of Y2O3 Nanomaterials Doped with Eu3+, Tb3+, Tm3+,Er3+, and Yb3+ Ions. *Journal of Nanomaterials* 2007, 20077:10 pages.

[118] Yan RX, Sun XM, Wang X, Peng Q, Li YD. Crystal structures, anisotropic growth, and optical properties: Controlled synthesis of lanthanide orthophosphate one-dimensional nanomaterials. *Chemistry-a European Journal* 2005, 11:2183-2195.

[119] Yan ZG, Zhang YW, You LP, Si R, Yan CH. General synthesis and characterization of monocrystalline 1D-nanomaterials of hexagonal and orthorhombic lanthanide orthophosphate hydrate. *Journal of Crystal Growth* 2004, 262:408-414.

[120] Zhang YW, Yan ZG, You LP, Si R, Yan CH. General synthesis and characterization of monocrystalline lanthanide orthophosphate nanowires. *European Journal of Inorganic Chemistry* 2003:4099-4104.

[121] Härmä H, Graf C, Hänninen P. Synthesis and characterization of core-shell europium(III)-silica nanoparticles. *J Nanoparticle Res* 2008, 10.1007/s11051-008-9380-5.

[122] Bu WB, Hua ZL, Zhang LX, Chen HR, Huang WM, Shi JL. Surfactant-assisted synthesis of lanthanide phosphates single-crystalline nanowires/nanorods. *Journal of Materials Research* 2004, 19:2807-2811.

[123] Tang Q, Shen JM, Zhou WJ, Zhang W, Yu WC, Qian YT. Preparation, characterization and optical properties of terbium oxide nanotubes. *Journal of Materials Chemistry* 2003, 13:3103-3106.

[124] Cao MH, Hu CW, Wu QY, Guo CX, Qi YJ, Wang EB. Controlled synthesis of LaPO4 and CePO4 nanorods/nanowires. *Nanotechnology* 2005, 16:282-286.

[125] Xu Y, Li QG. Multiple fluorescent labeling of silica nanoparticles with lanthanide chelates for highly sensitive time-resolved Immunofluorometric assays. *Clinical Chemistry* 2007, 53:1503-1510.

[126] Wang F, Fan XP, Pi DP, Wang MQ. Synthesis and luminescence behavior of Eu3+-doped CaF2 nanoparticles. *Solid State Communications* 2005, 133:775-779.

[127] Dong X, Hong G. Preparation of Rare Earth Hydroxide and Oxide Nanoparticle by Precipitation Method. *J Mater Sci Technol, Vol21 No4, 2005* 2005, 21.

[128] Wakefield G, Keron HA, Dobson PJ, Hutchison JL. Synthesis and properties of sub-50-nm europium oxide nanoparticles. *Journal of Colloid and Interface Science* 1999, 215:179-182.

[129] Nunez NO, Ocana M. An ionic liquid based synthesis method for uniform luminescent lanthanide fluoride nanoparticles. *Nanotechnology* 2007, 18:.

[130] Patra CR, Mukherjee P, Bhattacharya R, Mukhopadhyay D, Vlahakis NE. Rare Earth Nanoparticles. . USA; 2007.

[131] Patra CR, Alexandra G, Patra S, Jacob DS, Gedanken A, Landau A, Gofer Y. Microwave approach for the synthesis of rhabdophane-type lanthanide orthophosphate (Ln = La, Ce, Nd, Sm, Eu, Gd and Tb) nanorods under solvothermal conditions. *New Journal of Chemistry* 2005, 29:733-739.

[132] Patra A, Sominska E, Ramesh S, Koltypin Y, Zhong Z, Minti H, Reisfeld R, Gedanken A. Sonochemical preparation and characterization of Eu2O3 and Tb2O3 doped in and coated on silica and alumina nanoparticles. *Journal of Physical Chemistry B* 1999, 103:3361-3365.

[133] Zhu L, Liu XM, Meng J, Cao XQ. Facile sonochemical synthesis of single-crystalline europium fluorine with novel nanostructure. *Crystal Growth & Design* 2007, 7:2505-2511.

[134] Panda AB, Glaspell G, El-Shall MS. Microwave synthesis and optical properties of uniform nanorods and nanoplates of rare earth oxides. *Journal of Physical Chemistry C* 2007, 111:1861-1864.

[135] Pol VG, Palchik O, Gedanken A, Felner I. Synthesis of europium oxide nanorods by ultrasound irradiation. *Journal of Physical Chemistry B* 2002, 106:9737-9743.

[136] Miyawaki A. Visualization of the spatial and temporal dynamics of intracellular signaling. *Developmental Cell* 2003, 4:295-305.

[137] Wang F, Tan WB, Zhang Y, Fan XP, Wang MQ. Luminescent nanomaterials for biological labelling. *Nanotechnology* 2006, 17:R1-R13.

[138] Murphy CJ. Optical sensing with quantum dots. *Analytical Chemistry* 2002, 74:520A-526A.

[139] Niemeyer CM. Nanoparticles, proteins, and nucleic acids: Biotechnology meets materials science. *Angewandte Chemie-International Edition* 2001, 40:4128-4158.

[140] Rabbani E, Hurley I. Energy transfer hybridization assay using intercalators and lanthanide metals. 1999.

[141] Hirano S, Suzuki KT. Exposure, Metabolism, and Toxicity of Rare Earths and Related Compounds. *Environmental Health Perspectives Supplements* 1996 , 104:85-95.

[142] Baraton M-I. *Synthesis, Functionalization and Surface Treatment of Nanoparticles (Hardcover).* CA: American Scientific Publishers 2002.

[143] Koh I. Functionalization of nanoparticles for biological applications. University of Maryland, College Park, Department of Chemical and Biomolecular Engineering; 2005.

[144] Feng J, Shan GM, Maquieira A, Koivunen ME, Guo B, Hammock BD, Kennedy IM. Functionalized europium oxide nanoparticles used as a fluorescent label in an immunoassay for atrazine. *Analytical Chemistry* 2003, 75:5282-5286.

[145] Risau W. Mechanisms of angiogenesis. *Nature* 1997, 386:671-674.

[146] Chavakis E, Dimmeler S. Regulation of endothelial cell survival and apoptosis during angiogenesis. *Arteriosclerosis Thrombosis and Vascular Biology* 2002, 22:887-893.

[147] Yancopoulos GD, Davis S, Gale NW, Rudge JS, Wiegand SJ, Holash J. Vascular-specific growth factors and blood vessel formation. *Nature* 2000, 407:242-248.

[148] Isner JM, Losordo DW. Therapeutic angiogenesis for heart failure. *Nature Medicine* 1999, 5:491-492.

[149] Folkman J. Clinical-Applications of Angiogenesis Research. *Journal of Acquired Immune Deficiency Syndromes and Human Retrovirology* 1993, 6:686-686.

[150] Folkman J. Diagnostic and Therapeutic Applications of Angiogenesis Research. *Comptes Rendus De L Academie Des Sciences Serie Iii-Sciences De La Vie-Life Sciences* 1993, 316:914-918.

[151] Dardik R, Loscalzo J, Eskaraev R, Inbal A. Molecular mechanisms underlying the proangiogenic effect of factor XIII. *Arteriosclerosis Thrombosis and Vascular Biology* 2005, 25:526-532.

[152] Folkman J. Angiogenesis in Cancer, Vascular, Rheumatoid and Other Disease. *Nature Medicine* 1995, 1:27-31.

[153] Basu S, Nagy JA, Pal S, Vasile E, Eckelhoefer IA, Bliss VS, Manseau EJ, Dasgupta PS, Dvorak HF, Mukhopadhyay D. The neurotransmitter dopamine inhibits angiogenesis induced by vascular permeability factor/vascular endothelial growth factor. *Nature Medicine* 2001, 7:569-574.

[154] Huston SL, Lengerich EJ, Conlisk E, Passaro K. Trends in ischemic heart disease death rates for blacks and whites United States, 1981-1995 (Reprinted from MMWR, vol 47, pg 945-949, 1998). *Jama-Journal of the American Medical Association* 1999, 281:28-29.

[155] Jones DW, Chambless LE, Folsom AR, Heiss G, Hutchinson RG, Sharrett AR, Szklo M, Taylor HA. Risk factors for coronary heart disease in African Americans - The Atherosclerosis Risk in Communities Study, 1987-1997. *Archives of Internal Medicine* 2002, 162:2565-2571.

[156] Ferrara N, Gerber HP, LeCouter J. The biology of VEGF and its receptors. *Nature Medicine* 2003, 9:669-676.

[157] Claffey KP, Brown LF, delAguila LF, Tognazzi K, Yeo KT, Manseau EJ, Dvorak HF. Expression of vascular permeability factor vascular endothelial growth factor by melanoma cells increases tumor growth, angiogenesis, and experimental metastasis. *Cancer Research* 1996, 56:172-181.

[158] Straume O, Akslen LA. Importance of vascular phenotype by basic fibroblast growth factor, and influence of the angiogenic factors basic fibroblast growth factor/fibroblast growth factor receptor-1 and ephrin-A1/EphA2 on melanoma progression. *American Journal of Pathology* 2002, 160:1009-1019.

[159] Sun HZ, Chen R, Che CM. Metals in biology and medicine. *Progress in Chemistry* 2002, 14:257-262.

[160] Carell T. The 16(th) symposium on role of metals in biological reactions, biology and medicine (SRM2006) - Abstracts - June 1-June 2, 2006, Sanjo Conference Hall, Tokyo, Japan. *Yakugaku Zasshi-Journal of the Pharmaceutical Society of Japan* 2006, 126:-.

[161] Anon. The 15th Symposium on Role of Metals in Biological Reactions, Biology and Medicine - June 9-June 10, 2005 - Senri Life Science Center - Osaka, Japan - Abstracts. *Yakugaku Zasshi-Journal of the Pharmaceutical Society of Japan* 2005, 125:23-+.

[162] Sigel H, Sigel A. Metal ions in environment and biology. *Journal of the Indian Chemical Society* 2000, 77:501-509.

[163] Sigel A, Sigel H. *Metal Complexes in Tumor Diagnosis and as Anticancer Agents.* New York: Marcel Dekker; 2004.

[164] Collery P. *Metal Ions in Biology and Medicine.* Neuherberg/Munich, Germany: John Libbey eurotext; 1998.

[165] Misra SN, Gagnani MA, Devi I, Shukla RS. Biological and clinical aspects of lanthanide coordination compounds. *Bioinorganic Chemistry and Applications* 2004, 2:155-192.

[166] Coultas L, Chawengsaksophak K, Rossant J. Endothelial cells and VEGF in vascular development. *Nature* 2005, 438:937-945.

[167] Zeng HY, Dvorak HF, Mukhopadhyay D. Vascular permeability factor (VPF)/vascular endothelial growth factor (VEGF) receptor-1 down-modulates VPF/VEGF receptor-2-mediated endothelial cell proliferation, but not migration, through phosphatidylinositol 3-kinase-dependent pathways. *Journal of Biological Chemistry* 2001, 276:26969-26979.

[168] Zeng HY, Sanyal S, Mukhopadhyay D. Tyrosine residues 951 and 1059 of vascular endothelial growth factor receptor-2 (KDR) are essential for vascular permeability factor/vascular endothelial growth factor-induced endothelium migration and proliferation, respectively. *Journal of Biological Chemistry* 2001, 276:32714-32719.

[169] Zeng HY, Zhao DZ, Yang SP, Datta K, Mukhopadhyay D. Heterotrimeric G alpha(q)/G alpha(11) proteins function upstream of vascular endothelial growth factor (VEGF) receptor-2 (KDR) phosphorylation in vascular permeability factor/VEGF signaling. *Journal of Biological Chemistry* 2003, 278:20738-20745.

[170] Milanini J, Vinals F, Pouyssegur J, Pages G. p42/p44 MAP kinase module plays a key role in the transcriptional regulation of the vascular endothelial growth factor gene in fibroblasts. *Journal of Biological Chemistry* 1998, 273:18165-18172.

[171] Mavria G, Vercoulen Y, Yeo M, Paterson H, Karasarides M, Marais R, Bird D, Marshall CJ. ERK-MAPK signaling opposes Rho-kinase to promote endothelial cell survival and sprouting during angiogenesis. *Cancer Cell* 2006, 9:33-44.

[172] Rajashekhar G, Suckow M, Kamocka M, Rosen E, Clauss M. The p38 MAPK signaling pathway contributes to tumor-induced angiogenesis. *Faseb Journal* 2007, 21:A747-A747.

[173] Bhattacharya R, Mukherjee P, Xiong Z, Atala A, Soker S, Mukhopadhyay D. Gold nanoparticles inhibit VEGF165-induced proliferation of HUVEC cells. *Nano Letters* 2004, 4:2479-2481.

[174] Teer JK, Dutta A. *Regulation of S Phase.* Berlin, Heidelberg, New York: Springer; (2006).

[175] Ewen ME. *Cell Cycle Control.* Berlin: Springer-Verlag; 1998

[176] Bhattacharya R, Decker NK, Hughes DA, Mukherjee P, Shah V, McNiven MA, Mukhopadhyay D. Regulatory role of dynamin-2 in VEGFR-2/KDR-mediated endothelial signaling. *Faseb Journal* 2005, 19:1692-+.

[177] Ushio-Fukai M. Redox signaling in angiogenesis: Role of NADPH oxidase. *Cardiovascular Research* 2006, 71:226-235.

[178] Ushio-Fukai M. Reactive oxygen species as mediators of angiogenesis. *Faseb Journal* 2006, 20:A21-A21.

[179] Ushio-Fukai M, Alexander RW. Reactive oxygen species as mediators of angiogenesis signaling - Role of NAD(P)H oxidase. *Molecular and Cellular Biochemistry* 2004, 264:85-97.

[180] Ebrahimian TG, Heymes C, You D, Blanc-Brude O, Mees B, Waeckel L, Duriez M, Vilar J, Brandes RP, Levy BI, et al. NADPH oxidase-derived overproduction of reactive oxygen species impairs postischemic neovascularization in mice with type 1 diabetes. *American Journal of Pathology* 2006, 169:719-728.

[181] Datla SR, Jiang F, Dusting GJ. Nox4-type NADPH oxidase mediates the angiogenic response of human endothelial cells in vitro. *Faseb Journal* 2007, 21:A526-A526.

[182] Nickoloff SJ, Greene AS. Reactive oxygen species augment the angiogenic response in rat skeletal muscle. *Faseb Journal* 2006, 20:A709-A709.

[183] Gschneidner Jr KA, Bünzli J-CG, Pecharsky VK. *Handbook on the Physics and Chemistry of Rare Earths* NORTH-HOLLAND: Elsevier.

[184] Storr T, Thompson KH, Orvig C. Design of targeting ligands in medicinal inorganic chemistry. *Chemical Society Reviews* 2006, 35:534-544.

[185] Chen JP, Patil S, Seal S, McGinnis JF. Rare earth nanoparticles prevent retinal degeneration induced by intracellular peroxides. *Nature Nanotechnology* 2006, 1:142-150.

[186] Labrecque J, Anastassov V, Lau G, Darkes M, Mosi R, Fricker SP. The development of an europium-GTP assay to quantitate chemokine antagonist interactions for CXCR4 and CCR5. *Assay and Drug Development Technologies* 2005, 3:637-648.

[187] Handl HL, Vagner J, Yamamura HI, Hruby VJ, Gillies RJ. Lanthanide-based time-resolved fluorescence of in cyto ligand-receptor interactions. *Analytical Biochemistry* 2004, 330:242-250.

[188] Engströma M, Närvänenb A, Savolaa JM, Wurster S. Assessing activation of the human neuropeptide FF2 receptor with a non-radioactive GTP binding assay. *Peptides* 2004, 25:2099-2104.

[189] Handl HL, Gillies RJ. Lanthanide-based luminescent assaysfor ligand-receptor interactions. *Life Sci* 2005, 77:361-371.

[190] Evans CH. *Chemical properties of biochemical relevance.* New York: Plenum Press; 1990.

[191] Dos Remedios CG. Lanthanide ion probes of calcium-binding sites on cellular membranes. *Cell Calcium* 1981, 2:29-51.

[192] Nieboer E. *The lanthanide ions as structural probes in biological and model systems.* Berlin: Springer Berlin / Heidelberg; 1975.

[193] Williams RJP. *The chemistry of lanthanide ions in solution and in biological systems.* Berlin: Springer Berlin / Heidelberg; 1982.

[194] Enyeart JJ, Xu L, Enyeart JA. Dual actions of lanthanides on ACTH-inhibited leak K+ channels. *American Journal of Physiology-Endocrinology and Metabolism* 2002, 282:E1255-E1266.

[195] Lansman JB. Blockade of current through single calcium channels by trivalent lanthanide cations. *J Gen Physiol* 1990, 95:679-696.

[196] Mlinar B, Enyeart JJ. Block of Current through T-Type Calcium Channels by Trivalent Metal-Cations and Nickel in Neural Rat and Human-Cells. *Journal of Physiology-London* 1993, 469:639-652.

[197] Horrocks WD. *Lanthanide ion probes of biomolecular structure.* New York: Elsevier; 1982.

[198] Cohen SM. New approaches for medicinal applications of bioinorganic chemistry. *Current Opinion in Chemical Biology* 2007, 11:115-120.

In: Clinical Chemistry Research
Editors: Brian H. Mitchem and Charles L. Sharnham
ISBN 978-1-60692-517-1

Chapter IV

Identification and Analysis of Effective Components in Animal Biofluids Following Administration of Natural Medicines

Chenggang Huang[1*], Chunhui Ma[1], Yihong Tang[1] and Yuanyuan Zhang[2]

[1] Shanghai Institute of Material Medica, Shanghai Institutes for Biological Sciences, Shanghai, P. R. China

[2] Department of Microbiology and Microbial Engineering, School of Life Sciences, Fudan University, Shanghai, P. R. China

Abstract

Natural medicines play their biological and pharmacological roles after orally administered, based upon their effective substances including both the original components in the natural medicines absorbed and their metabolites. These effective substances can only be identified when chemical structures of these components and their metabolites are revealed, and corresponding pharmacological experiments have been carried out. Identification and analysis of the effective components following oral administration of natural medicines in animal biofluids are of great importance both to understand how these natural medicines exert their biological effects, and to improve methods for quality control in production of natural medicines. However, advances in the field have seldom been reviewed. Based on research experience of our group for dozens of years and corresponding literature, we will review on the identification and analysis of effective components following orally administration of natural medicines in animal

* Prof. Chenggang Huang, 555 Zuchongzhi Rd, Zhangjiang, Pudong, Shanghai 201203, P. R. China,Tel: +86-21-50806716, Fax: +86-21-50806716, Email: cgsimm@126.com

biolfuids, mainly in blood and urine. First, we will address the biological and pharmacological significances of identification and analysis of effective components of natural medicines. Then, we will describe, in detail, the commonly used methods and procedures for identification and analysis of effective components of natural medicines. These methods and procedures include how to prepare natural medicines for oral administration, how to choose appropriate animals, how to administer natural medicines, how to collect blood and urine samples of animals, how to prepare samples for identification, and how to identify and analyse chemical structures of effective components. Finally, we wish to provide the potential future prospects in the field.

Keywords: Natural Medicine, Traditional Chinese Medicine, Effective Constitutes, Medicated Biofluids, Serum, Urine

1. Introduction

Effective components in natural medicines are responsible for their therapeutic effects and of great importance in quality control. Phytochemitry method is the routine way for screening effective components in natural medicines and its analysis process is summarized below. Firstly, pure compounds and fractions were extracted from natural medicines by separation means. Then, pharmacological tests are carried out to determine the bioactivity of these pure compounds and fractions，respectively. Although the phytochemitry method is very straightforward and objective, some disadvantages have been found. For example, there are hundreds or even thousands of compounds contained in one herb. It is extremely difficult to isolate and identify chemical structures and clear the therapeutic mechanism of every compound by common technologies at the present. The components of natural medicines are very complicated and many of the compounds can not get into blood circulation by oral administration. Only those compounds which can be absorbed into blood and reach target organ are able to exert bioactive effects. Moreover, some components are changed by gastrointestinal or liver metabolism, therefore, the actual effective components are not always the components in original natural medicines. It has been reported that many compounds whose pharmacological effects has been demonstrated by in vitro experiments show no or different bioactive activities in vivo. Wang *et al* demonstrated Agrimony decoction showed strong anti-tumor activities in vitro while its medicated serum had no anti-tumor effects [1]. Iwama *et al* also found Minor Radix Bulpleri decoction but not its medicated serum had mitogenic effects in vitro [2]. On the contrary, Wang *et al* demonstrated that *Sophora Flavescens Ait* decoction and medicated serum had obvious anti-tumor effects in serum pharmacological experiments [1]. Medicated serum showed even higher inhibition rates on tumor cells than decoction, which suggested that metabolites from the transformation of some components in original medicine had stronger anti-tumor activities.

Therefore, the actual effective components are not always the components in original natural medicines. The real bioactive components might be the metabolites from the transformation of some components in original medicines by absorption and metabolism *in vivo*. However, it is still unclear that how these original constitutes will be metabolized. So, it is of great importance to screen effective components which include the original components,

metabolites by gastrointestinal tract, and metabolites by other organs after being absorbed. Thus, Dr. Xinsheng Yao put forward a new strategy of in vivo direct effective substances of natural medicines research [3]. In vivo direct effective substances of natural medicines are composed of some original components and some metabolites. Not all of the components of natural medicines are effective substances. Only those which can be absorbed into blood can possibly have pharmacological effects. His new strategy for screening bioactive components is very straightforward and helpful to discover the real active components in natural medicines.

Serum pharmacochemistry, proposed by Tashiro Shinichi in 1980s, is a serum pharmacological screening strategy to discover the real bioactive components in natural medicines [4]. It has been widely approved and attracts much attention of many famous experts. The method of serum pharmacochemistry utilizes the physiology of animal to separate the bioactive components of natural medicines into blood of animals, and then extract and identify these bioactive components in the blood subsequently by common techniques. This method put enough consideration to metabolism of natural medicines, which can give much information of transformation and changes of effective components in vivo. Its objects are mainly focused on small molecules absorbed into blood and metabolites of natural medicines. Yoshihiro *et al* screened active compounds in medicated serum of the Gancao-Fuzi decoction and Artemisia Capillatis by high performance liquid chromatography (HPLC) method [5，6]. Wang *et al* carried out a lot of fruitful research on natural medicines by the serum pharmacochemistry [7]. They identified effective substances of granule of Liuwei Dihuang and some single folium after investigating their original constitutes and metabolites. They systematically reviewed application of serum pharmacochemistry method in research of natural medicines which put solid foundation for development of serum pharmacochemistry. But serum pharmacochemistry also has some unavoidable deficiencies which obviously limited its application in pharmacological screening. For example, it is very difficult to detect some substance in medicated serum even by LC-MS because their concentrations are very low in serum. It is also hard to obtain enough serum to carry out pharmacological evaluation and structural identification since it will cause injury to animals to get blood.

In Recent years, we isolate, enrich, analyze and identify original compounds and metabolites of natural medicines in medicated urine. The correlation between effective components and their pharmacological effects were also investigated. This chapter reviewed some aspects on how to identify effective substances in medicated biofluids (serum and urine) and determine the metabolic process and parameters after orally administering natural medicines and prescriptions.

The routine process for analysis of multi-constituents in animal biofluids following administration of natural medicines is to quantitatively determine or qualitatively identify the natural compounds absorbed and their metabolites in the biofluids. Several problems should be unavoidably considered in this procedure. For example, how to prepare the natural medicine samples? What kinds of the experimental animals and drug administration methods can be used? How to collect and dispose the biofluids (blood and urine) containing drugs? How to analyze natural constituents in the biofluids? These questions are the most vital to be concerned. In this chapter, we will discuss them in detail.

2. The Natural Medicine Sample Preparation

Sample preparation is the first step to carry out our research which is the fundamental base for the whole study. Generally, there are two kinds of sample preparation methods according to the purity of the natural medicine used in the experiments, the pure natural compounds, and the crude natural medicine extracts. The pure natural compounds are preferred in western countries. But for the traditional Chinese medicines, crude natural medicine extracts have been more frequently used in China. These two kinds of sample preparation methods are both of great importance in research.

2.1. The Pure Natural Compounds

The formation for oral administration can be prepared by simply mixing the pure compounds with sodium carboxymethylcellulose (CMC-Na) solution, deionized water or *β*-cyclodextrin. For example, pure natural compound mangiferin was isolated, from *Anemarrhena asphodeloides* Bge in our lab. Then, this compound was blended with sodium carboxymethylcellulose and distilled water to prepare the suspension for oral administration [8]. Our research group also used sodium carboxymethyl cellulose water solution to prepare the oral administration formula of calycosin-7-O-β-D-glucopyranoside for male Sprague-Dawley (SD) rats [9].

Deionized water is a good solvent for intravenous administration. In quantitative determination of saikosaponin in rat plasma, saikosaponin was dissolved in the deionized water for intravenous administration to SD rats after fasting [10]. Similarly, Xu *et al* dissolved natural compound Sal B in deionized water, and orally administered to normal and antibiotic-treated rats [11]. In the contribution of Qian *et al*, pure compound Rg3 was dissolved in *β*-cyclodextrin and sonicated, then diluted by adding saline to the solution for the intravenous administration to SD rats [12].

Since properties of pure compounds are certain to be detected and stable, sample preparation methods can be easily selected according to their physical properties

2.2. The Crude Natural Medicine Extracts

The literatures on preparations of crude natural medicine extracts sample are much less than those of pure natural compounds, probably because of the low concentration of target compounds in biofluids samples and difficulty for detection. The crude natural medicines extracts include extracts of the single natural medicine and of the herb formulas. They were usually prepared by following several common steps. Firstly, extract natural medicines with proper solvents. Then, filter extracts. Finally, evaporate extracts in vacuum. This procedure is in accordance with the conventional method of extracting traditional Chinese medicine. In this procedure, the quality stability of the extracts is guaranteed by the establishment of the corresponding quality control indicators. In our lab, we prepared the Rhizoma Anemarrhenae decoction in the following methods [13]. The mixture of Rhizoma Anemarrhenae was

extracted with water twice, and filtered. The filtrate was collected and concentrated by rotary vaporization under reduced pressure. In order to obtain the Yin-Zhi-Ku decoction, the herbal materials were extracted twice by refluxing in water, filtered, concentrated, and lyophilized [14, 15].

Many different kinds of constituents are in the final extracts obtained by the method above, which will make concentrations of the active constituents very low. Technologies like liquid–liquid extraction (LLE) and different kinds of chromatography are often employed in order to get rid of these interfering constituents. Our research group developed the isolation methods of active fractions by macroporous resin column technique from Huangbai-Zhimu drug pair. At first, the mixture of Huangbai and Zhimu was extracted by reflux with ethanol, filtered and concentrated to dryness under reduced pressure. The residue was divided into two subfractions by D101 macroporous resin eluted with different proportion of ethanol and water. One of the subfractions was the final extract for oral administration to rats [16]. There are many similar reports. He *et al* prepared their sample fractions by macroporous resin and silica gel columns in the following procedures [17]. Fresh rhizomes were cut into pieces and refluxed with ethanol. After evaporated under vacuum, the residue was then recovered with distilled water and subjected to D101 resin and silica gel column. Eluted by the different concentration of ethanol and $CHCl_3$–MeOH–H_2O solvent system respectively, the fractions containing the target constituents were obtained. Liquid-liquid extraction, macroporous resin column and polyamide chromatography column techniques were also employed by other researchers, like Zhou *et al*, Lai *et al* and Qiu *et al* in their experiments to get the active fractions for further administration [18-20].

No matter what kind of sample preparation methods are used, there are two common steps in sample preparation procedures. One is to select proper experimental animals and drug administration methods. The other is to collect and dispose medicated biofluids. When addressing the next two steps in section 2.2 and 2.3, we will not elaborate them by subtitles of different kind of sample preparation methods.

3. The Proper Experimental Animals and Drug Administration

The most popular animals used are rats and mice since they are cheap and easy to operate [21-23]. Rats are used as the experimental animals at most of time, such as in the contributions of Wang *et al*, Ye *et al*, Tang *et al* and Ma *et al* [8-10, 13-16, 24]. Mice are also widely used. But they can not provide as much blood as rats. Wang *et al* and Xiong *et al* used mice as the experimental animals in their experiments [25, 26]. Moreover, other animal models such as dogs [27], pigs [28], rabbits [29, 30], and horses [31] are also chosen when needed.

Oral administration, intravenous and intraperitoneal injections are the most common methods of drug administration. Oral administration was the most popular administration method under the guidance of traditional Chinese medicine theories in China, such as the studies on the magiferin, calycosin-7-O-β-D-glucopyranoside, huangbai-zhimu drug pair and Yi-Zhi-Ku decoction [8, 9, 13-16, 24]. Other researchers like Xu *et al*, Si *et al*, Wen *et al* and

Cao *et al* all gave their natural medicines to animals by oral administration [21-23, 27]. When the saikosaponin was determined in rat plasma, the intravenous injection administration method was used [10]. Yang *et al*, Ma *et al*, Wang *et al* and Xiong *et al* used intravenous and intraperitoneal injections in their experiments [25, 26, 32, 33]. In addition, there were some other ways for the medicine administration, such as intramuscular injection, subcutaneous injection, nasal sprays and transdermal delivery system. For example, Huang *et al* administered palmatine to the canine by intramuscular injection in order to determine the palmatine content in canine plasma [34]. Badeau *et al* used subcutaneous injection when they quantitatively determined the genistein fatty acid esters in monkey plasma [35]. Jung *et al* applied nasal sprays for administration of proliposomes of nicotine to rats [36]; Batchelder *et al* gave the major catechins and caffeine from extract of Camellia sinensis to animals by transdermal delivery system [37].

4. Medicated Biofluids Collection and Disposal

4.1. Medicated Biofluids Collection

Animals should be kept in a controlled environment for at least 3 days before experiments. They are fed with standard laboratory food and water. Before the test, they are fasted overnight but with access to water. Then a proper dose of natural medicines are administered. After a certain period of time, blood and urine can be collected for further detection.

4.1.1. The Blood Collection

Blood collection has great influence on further detection. If large amount of blood is expected, the animal will unavoidably be executed. Abdominal aorta and arteria carotis are the best place to collect large amount of blood. When carrying out research of identification of major alkaloids and steroidal saponins in rat serum by HPLC-DAD-MS/MS technique, we opened the rat abdomen and collected the blood from the abdominal aorta in order to get as much blood as possible [16]. By the same way, Moon *et al* obtained the rat blood from the abdominal aorta, too [38]. For most of the big animals, like pigs, dogs or horses, arteria carotis is a good place to collect blood. For example, Yang *et al* obtained the pig blood samples from the arteria carotis after the last dosing [39]. If little amount of blood is enough, the tail vein, vena orbitalis and leg vein will be the proper positions. When quantitatively determined calycosin-7-O-β-D-glucopyranoside, geniposide, saikosaponin and mangiferin in rat plasma, Ye *et al*, Tang *et al* and Wang *et al* all collected the rat plasma from the tail vein because of the advantages of easiness to operation, without slaughter to the animals and repetitious time's collection in our lab [8-10, 15]. Murugaiyah *et al* also withdrew rat blood from the tail vein after dose administration [40]. In addition, Ying *et al* acquired the rat blood from the vena orbitalis [41]. Cao *et al* collected the dog blood samples from the foreleg vein after administration [27].

4.1.2. The Urine Collection

The collection of urine is simpler than that of blood. Almost all the operations are carried out in the metabolism cages. The metabolic cage is developed to have a control of total intake of feed and water and the excretion of urine and feces. We all used metabolism cages to collect animal urine in our lab. For example, Ma *et al* obtained the urine sample by metabolism cages when they wanted to identify the major xanthones and steroidal saponins in rat urine by HPLC-MS/MS technique following oral administration of Rhizoma Anemarrhenae decoction [13]. Wang *et al* obtained the rat urine samples in the same way. In that experiment, they identified and determined four metabolites of mangiferin in rat urine [24]. In order to determine the content of geniposide in rat urine after oral administration of the traditional Chinese medicinal prescription Yin-Zhi-Ku decoction, we collected urine samples by metabolism cages until 96 hours after dosing [14]. There are also many examples in other research groups. For instance, Kuwayama *et al* obtained urine by metabolism cages when they studied on the analysis of amphetamine-type stimulants and their metabolites in urine [42]. The contributions of some other scientists like Ge *et al*, Yang *et al* and Roig *et al* are also good examples [43-45].

4.2. Medicated Biofluids Disposal

Some measures should be immediately taken to dispose the biofluids after they are collected. Blood acquired from animals should be transferred into the heparinized tubes and centrifuged. Plasma samples should be kept at 4 °C for further use. Otherwise, in order to prevent from rotting, the urine collected should be kept at -20 °C or -80 °C.

There are many endogenous components (mostly proteins) in animal blood and urine which shows great influences on the further identification or analysis of the natural medicine constituents and their metabolites in biofluids. They should be eliminated as completely as possible from biofluids. This step is the most important one of the whole research. It is closely correlated with . Generally, four kinds of methods can be used to remove proteins.

4.2.1. Removal of Proteins by Precipitators or Denaturants

The suitable precipitators or denaturants, like organic solvents, neutral salts or acids, can make the protein dehydrate or form the indissoluble salts, which can remove proteins from medicated biofluids. For example, acetonitrile-acetic acid was added into the biofluids as precipitator or denaturant to remove the proteins after the sample collection and necessary predisposition such as centrifugation. After another centrifugation for a few minutes, the supernatant was transferred into a clean test tube and evaporated to dryness in water bath under a stream of nitrogen. The residue was reconstituted in methanol and then centrifuged, and finally the supernatant could be analyzed by HPLC [8]. In order to quantitative analyze of five active constituents in rat plasma, Xu *et al* pipetted an aliquot of plasma into plastics centrifuge tubes with addition of methanol (containing 0.1% formic acid) to precipitate protein [21]. Zhang *et al* selected methanol and acetonitrile as the denaturants for deproteinization [46]. Joo *et al* tested various solutions such as perchloric acid,

trichloroacetic acid, methanol and acetonitrile, to get an optimal condition for deproteinization of rat plasma [47].

4.2.2. Removal of Proteins by Organic Solvents Extraction

Most of the molecules absorbed into the biofluids or their metabolites produced *in vivo* can be easily dissolved in the high polar organic solvents such as methanol or ethanol, while proteins in the biofluids can not be got through of these organic solvents. Extraction with methanol or ethanol can efficiently separate the proteins and the interested molecules in biofluids. In the research of Huangbai-Zhimu drug pair, we mixed all the serum samples, and froze them to a dry powder. Then the dry powder was sonicated three times with methanol. After evaporated under reduced pressure to remove methanol, the sample for HPLC-DAD-MS/MS analysis was obtained [16]. Similarly, in the contribution of Yang *et al*, they also used this method to treat the blood samples and obtainedgood results [39].

Liquid-liquid extraction can be used to extract the non-polar or weak-polar constituents from the aqueous solutions. The organic layers can be evaporated to dryness under stream of nitrogen. Then the residues are dissolved in proper solvent for the high performance liquid chromatography analysis. Zhang *et al* tested deproteinization by liquid-liquid extraction with different organic solvents including dichloromethane-isopropanol, N-hexane-dichloromethane-isopropanol and chloroform [46]. Dai *et al* used ether, ethyl acetate, ethyl acetate-isopropanol and n-hexane-dichloromethane-isopropanol as solvents in liquid-liquid extraction operation to remove protein [47].

4.2.3. Removal of Proteins by Solid Phase Extraction (SPE)

Solid phase extraction (SPE) plays more and more important roles in sample preparation. Many problems associated with liquid-liquid extraction can be prevented with the help of SPE, such as incomplete phase separations, less-than-quantitative recoveries, use of breakable glassware, and disposal of large quantities of organic solvents. SPE is more efficient than liquid-liquid extraction. It yields quantitative extractions that are easy to perform rapidly and automatically. Solvent use and lab time can be significantly reduced. There are several kinds of SPE cartridge, such as reversed phase SPE, normal phase SPE, and ion exchange SPE (anion and cation exchange SPE). There are five common steps in SPE procedure. The first is to select the proper SPE tube or disk. The second is to condition the SPE tube or disk. The third is to add the sample. The fourth is to wash the packing. The last one is to elute the target compounds. SPE has been widely used in biofluids analysis. We selected solid-phase extraction to treat the rat blood samples, in order to carry on pharmacokinetic study of geniposide in rat serum. The procedures in detail were as the following. C_{18} cartridges were conditioned before use by means of methanol and triple-distilled water. Rat serum with geniposide and paeoniflorin was transferred into an SPE column cartridge. Columns with absorbed geniposide were washed with distilled water first. Then the compounds were eluted with methanol under low vacuum. After the resulting solution evaporated to dryness *in vacuo*, the evaporated residue was dissolved in the mobile phase and could be injected into HPLC for analysis [15]. We also used the SPE method to dispose urine samples, and the similar specific procedures were applied [9, 14]. Many of other scholars, like Tang *et al*, Liang *et al*, Wang *et al*, Zhang *et al*, Wang *et al*, Han *et al* and

Lai *et al* all used SPE to remove proteins from plasma and urine samples [10, 19, 48-53]. The SPE technique has been become very popular in this field in the past decades which will still play important roles in the future.

We often synthetically apply some of the deproteinization methods in the experiments to acquire the best results. Organic solvents and SPE are used together to remove the protein in rat serum. The plasma sample was first diluted with methanol in phosphate buffer. After vortex mixing and centrifugation, the supernatant was transferred to a HLB cartridge preconditioned by sequential washing with methanol and phosphate buffer. The cartridge was washed with water first. After the eluent evaporated to dryness under a gentle stream of nitrogen, the residue was redissolved in methanol, and was injected into the HPLC system for analysis [54].

4.2.4. The Pure Compounds Isolated from Biofluids

The best way to completely avoid the interference from the endogenous proteins is to isolate pure interest compounds directly from the biofluids. This method also has advantages in structural elucidation. Many technologies such as nuclear magnetic resonance spectra, infared spectra, ultraviolet spectra, and some related chemical methods can be easily used with this method to obtain the precise structure of the compounds. If we do not isolate the pure compounds from the biofluids, it will be only tentative for us to identify the constituents just by the HPLC-DAD-MSn technique. We isolated four metabolites from the rat urine by the liquid-liquid extraction and chromatography column techniques. By the NMR and mass spectra, their structures were precisely elucidated [24]. The procedures were as follows. The collected urine samples were concentrated to dryness. The residue was suspended in methanol and deposited for few hours. The supernatant was removed and evaporated to dryness. Then the residue was dissolved in water and partitioned with n-butanol three times. The n-butanol layer was subjected to D101 macroporous resin chromatography column and eluted with H2O-EtOH solvent stepwise. The eluting fractions were further subjected to Sephadex LH-20 with a MeOH-H2O system, and then the eluted fractions were combined and subjected to a silica gel chromatography column, sephadex LH-20 and semi-preparative HPLC to give 1,3,7-trihydroxyxanthone, 1,3,6,7-tetrahydroxy- xanthone, 1,3,6-trihydroxy methoxyxanthone and 1,7-dihydroxyxanthone.

5. Analysis of Medicated Biofluids

After finishing pretreatment procedures, the biofluids samples will be analyzed by separation techniques, such as HPLC with ultraviolet detector [55-58], fluorescence detector [59], optical emission detector [60], high performance liquid chromatography-mass spectrometry (LC-MS) [61-64], and gas chromatography with mass spectrometry [65] or flame ionization detector [66]. As we know, crude medicine extracts are complex mixtures containing up to hundreds or even thousands of different compounds. The large numbers and low concentrations of compounds in crude medicine extracts make the analysis and identification of bioactive components in biofluids obtained from animal after administrated crude medicine extracts extremely difficult. So, there are many differences in the methods of

analysis and identification between the medicated biofluids with pure compounds and crude medicine extracts. How to efficiently solve these problems is the key procedure in the whole research process. In this section, we will elaborate the analysis methods of medicated biofluids according to two before-mentioned natural medicine sample preparation methods.

5.1 Analysis of Pure Compounds

Compared with crude medicine extracts, pure compounds has the advantage of rapid efficiency, small volume and easy to administer. Usually, it presents high concentration in biofluids which will make the analysis comparably easy to carry out. In this kind of research process, the quantitative determination and qualitative identification are the two popular aspects for analysis of pure compounds.

5.1.1 Qualitative Identification

Generally, there are three kinds of methods for qualitative identification. The first is by the standard pure compound; the second is by HPLC-MS^n analysis; the third is by nuclear magnet resonance (NMR) spectrum, ultraviolet absorbance (UV) spectrum, Infrared (IR) spectrum, mass (MS) spectrum and other chemical ways. The proper choice of identification methods is mainly based on whether the standard compound are present and whether the interest compounds can be isolated from biofluids.

5.1.1.1 Qualitative Identification by the Standard Sample Compounds

In the research process, we can apply this method for qualitative identification if the standard sample compound is provided. For example, when determined the saikosaponin in rat plasma, we purchased saikosaponin as the standard sample and by the comparison of the retain time, the peak of saikosaponin in plasma HPLC chromatograms were assigned (see Fig. 1) [10]. With the same manner, in our research group, Ye *et al* determined calycosin-7-O-*β*-D-gluco-pyranoside in rat plasma (see Fig. 2) [9]. Furthermore, there are many other scientists used this kind of method, like Qian *et al*, Wang *et al*, Huang *et al* and Ying *et al* [12, 25, 34, 41].

5.1.1.2 Qualitative Identification by HPLC-Ms^n

HPLC-MS^n had been proved to be a modern powerful tool for the identification of substances in biofluids due to its high sensitivity and specificity. In addition, MS^n technique also provides rich structural information of analytes of interest. Wittig *et al* used the SRM experiments identify the quercetin glucuronides in human plasma by high-performance liquid chromatography–tandem mass spectrometry technology [67]. Song *et al* analyzed ten metabolites of lobeline in the rat urine by liquid chromatography–tandem mass spectrometry [68]. Ge *et al* identified the amygdalin and six its major metabolites in rat urine by LC–MS/MS technology [43]. Han *et al* studied dauricine and eight its metabolites in rat urine by liquid chromatography–tandem mass spectrometry [69]. These researches are the good examples for qualitative identification by HPLC-MS^n technique.

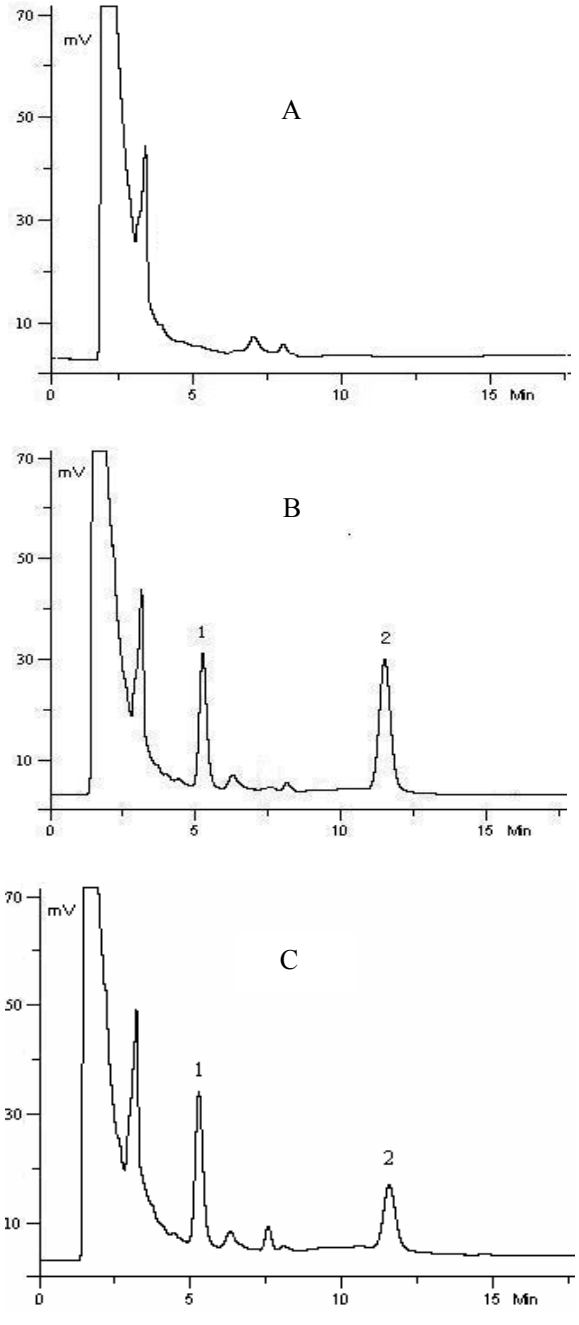

Figure 1. Chromatograms of : (A) blank rat plasma; (B) rat plasma sample spiked with SSa and I.S.; (C) plasma sample from a rat following intravenous dose of SSa. 1. jujuboside A (I.S.) 2. SSa

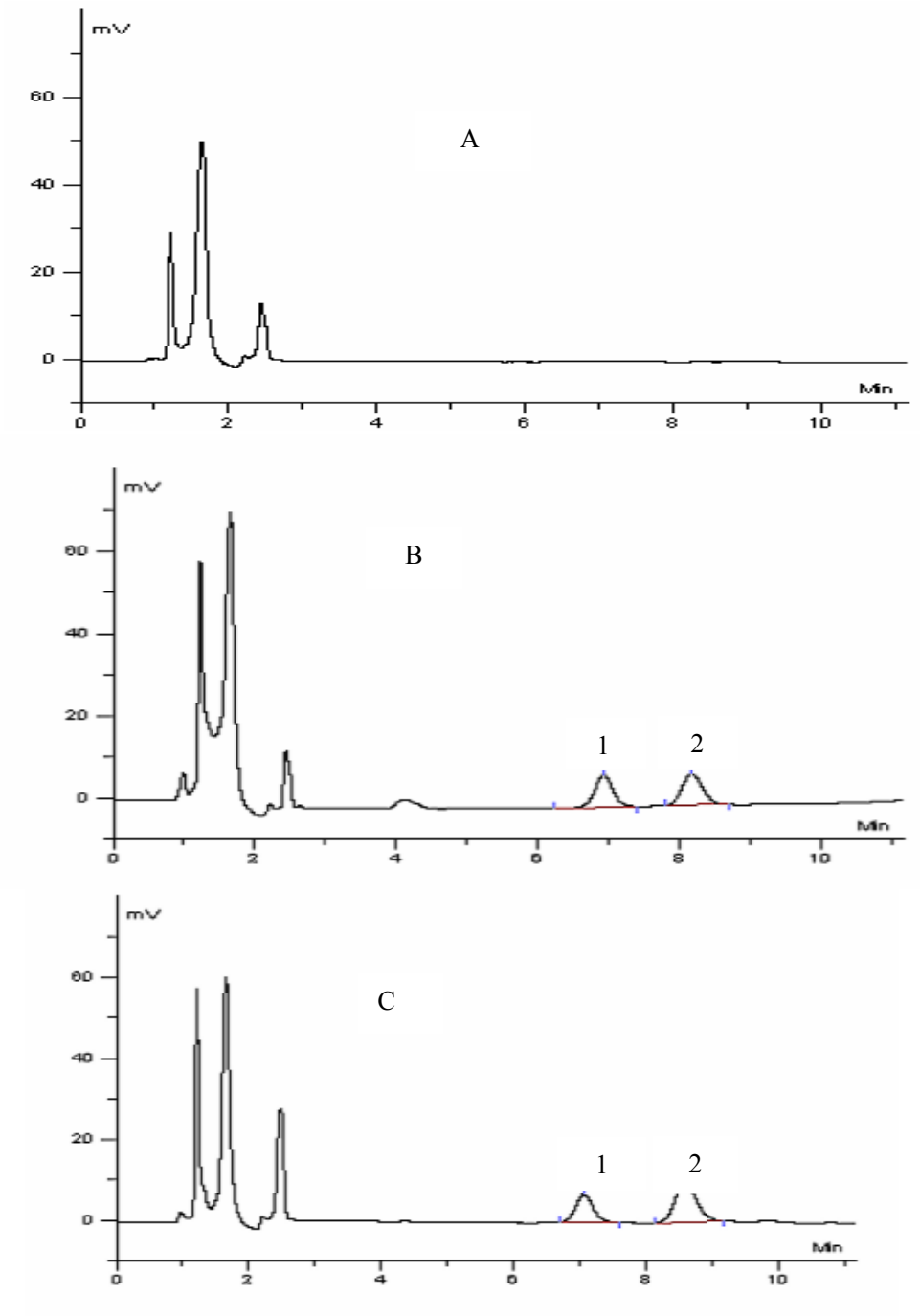

Figure 2. Chromatograms for the analysis of calycosin-7-O-β-D-glucopyranoside in rat plasma. (A) Chromatogram of a blank rat plasma sample. (B) Chromatogram of a plasma sample from rat spiked with IS after oral administration of calycosin-7-O-β-D-glucopyranoside. (C) Chromatogram of a blank plasma sample spiked with calycosin-7-O-β-Dglucopyranoside and IS. 1. calycosin-7-O-β-D-glucopyranoside 2. I.S.

5.1.1.3 Qualitative Identification by Spectrums

Besides the HPLC-MS^n technique, the phytochemical structural elucidation techniques, such as NMR, UV, IR, MS spectra and related chemical techniques can also be used for qualitative identification in the event of the deficiency of the standard pure compound. However, the pure interest compounds isolated from the biofluids were required in these techniques. For example, we successfully isolated four metabolites of mangiferin in the rat urine. By the NMR and MS analysis, the structures of these four metabolites were precisely determined as 1,3,7-trihydroxyxanthone, 1,3,6,7-tetrahydro-xyxanthone, 1,3,6-trihydroxy-7-methoxyxanthone and 1,7-dihydroxy xanthone, and the possible metabolic pathways for mangiferin was also deduced (see Fig. 3). In addition, Moon *et al* determined the structure of quercetin 3-O-*β*-D-glucuronide as an antioxidative metabolite in rat plasma after oral administration of quercetin [70]. Houghton *et al* isolated several C_{18} neutral steroids from the urine of the male horse and identified their structures [71].

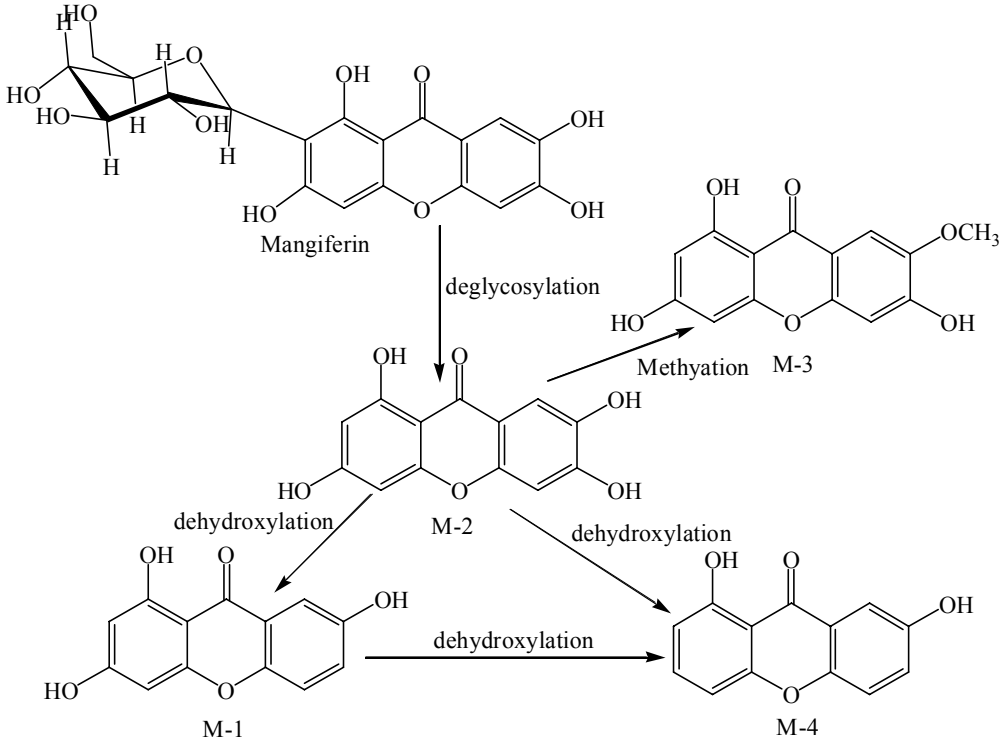

Figure 3. Structure of mangiferin metabolites and possible metabolic pathways for their production.

5.1.2 Quantitative Determination

In the quantitative analysis, assay validation is a critical procedure which demonstrates that the performance characteristics of the newly developed method were suitable and reliable for the intended applications. So the high pure standard samples are required for the assay validation. The criteria used to validate the method for quantification of multiple analytes from plasma should not be compromised for each analyte in accuracy, precision, selectivity, sensitivity, reproducibility, and stability. Each analyte should be tested to ensure no cross-interference from the other analytes. In our research group, a plenty of work has been done in the recent years. For example, based on the necessary validation for the assay method, we determined saikosaponin in rat plasma, and then successfully obtained the concentration-time profile of saikosaponin in plasma after single intravenous administration of saikosaponin to rats (see Fig. 4) [10]. In the same way, we also determined calycosin-7-O-*β*-D-glucopyranoside in rat plasma, and obtained its mean plasma concentration-time profile of calycosin-7-O-*β*-D-glucopyranoside after an oral dose to rat (see Fig. 5) [9]. Many other scientists, like Qian *et al*, Wang *et al*, Huang *et al* and Ying *et al* have also done much of this kind of work and obtained the good results [12, 25, 34, 41].

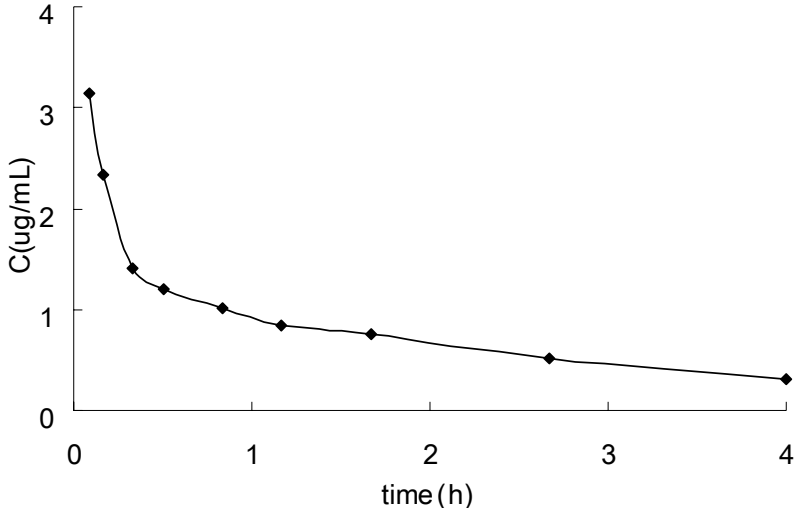

Figure 4. Mean concentration-time profile of SSa in plasma after single intravenous administration of SSa to rats. Each data point represents the mean of four animals.

5.2 Analysis of Crude Natural Medicine Extracts

The crude natural medicine includes single natural medicine, the herb formulas and fractions. The medicine preparation method for administration is in accordance with those of the traditional Chinese formulas. Development of the analysis methods for the crude natural medicine extracts is in great importance.

5.2.1 Qualitative Identification

There are three kinds of methods same as the pure compounds provided for the analysis of crude natural medicine extracts in biofluids, and some contributions have been done on the qualitative identification of crude natural medicine extracts in biofluids using the first and second methods. However, for the third one, no research paper is reported to our knowledge until now, probably because of the lower concentrations of the interest compounds in the biofluids and the difficulty to acquire plenty of biofluids to isolate the interest compounds.

5.2.1.1 Qualitative Identification by the Standard Sample Compound

The lower concentration of the interest compounds makes the detection extremely difficult. In this research process, strict pretreatment experiments were required to enhance the interest compounds concentration in the biofluids. Furthermore, the advanced mass technology, such as single reaction monitoring (SRM), multiple reaction monitoring (MRM), will be used to help scientists find the target compounds in the biofluids. For example, we identified four bioactive substances in the duck serum after oral administration of *Sophora flavescens* extracts by LC-MS technology. The identification was mainly based on comparison of the chromatographic properties of interest peaks with those of the standard pure compound. Furthermore, the MS of the peak also gave the additional information. The TIC chromatogram in positive mode of duck serum after administrated of *S. flavescens* extract and MS spectra of the four identified compounds were shown in Fig. 5 and 6, respectively. By the similar way, Lai *et al* assigned four flavonol peaks in the HPLC chromatograms of rat plasma and urine after oral administration of *Abelmoschus manihot* extract [19]. Pan *et al* identified five absorbed and metabolic components in rat plasma after oral administration of 'Shuangdan' granule by HPLC–DAD–ESI-MS/MS [72].

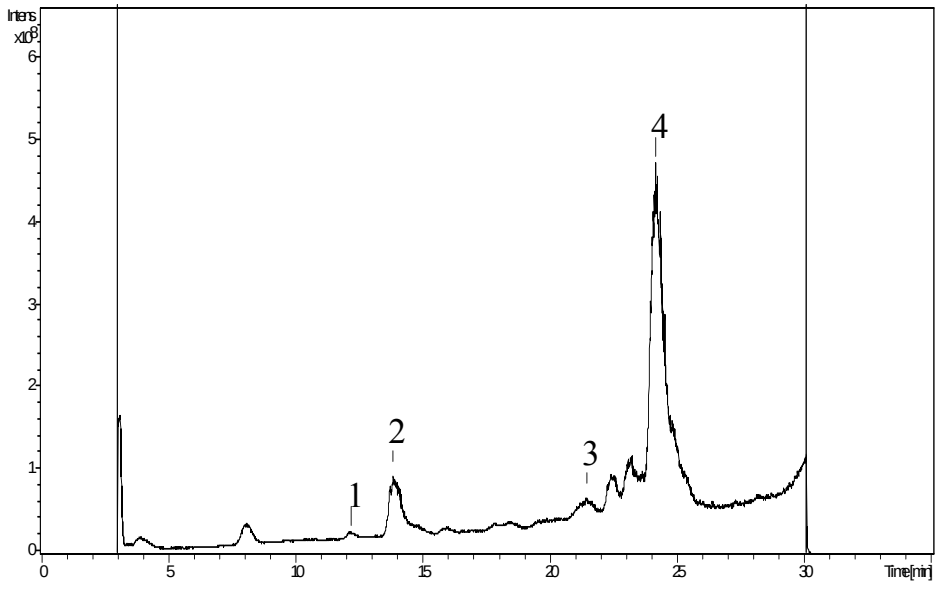

Figure 5. TIC chromatogram in positive mode of duck serum after administrated of S. flavescens extract.

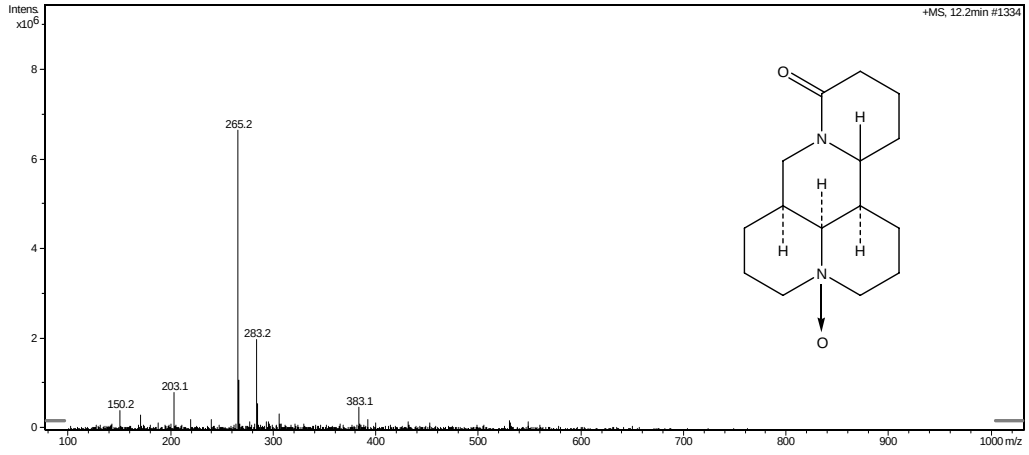

Oxymatrine (**1**)

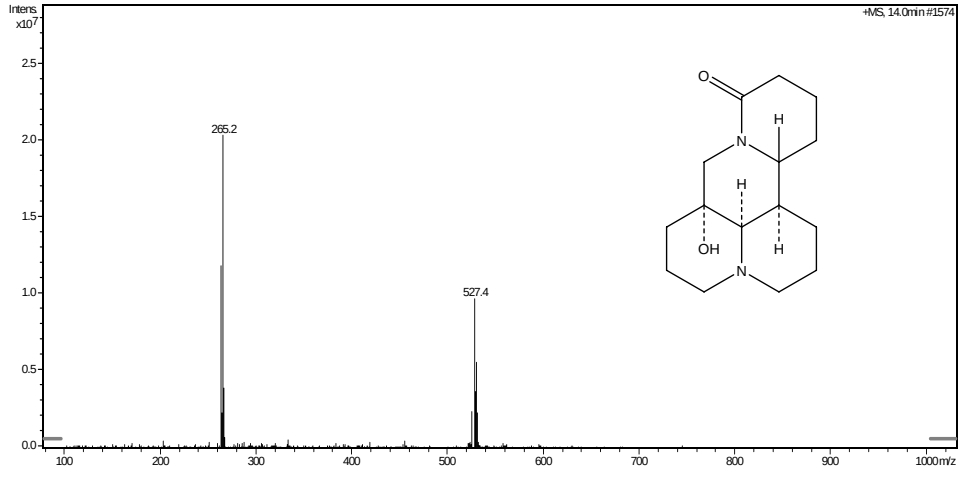

Sophoranol (**2**)

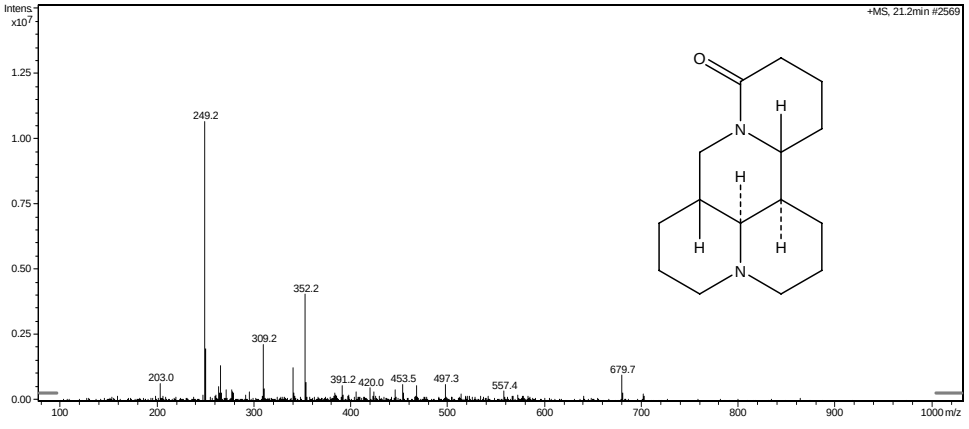

Sophoridine (**3**)

Figure 6. Continued on next page.

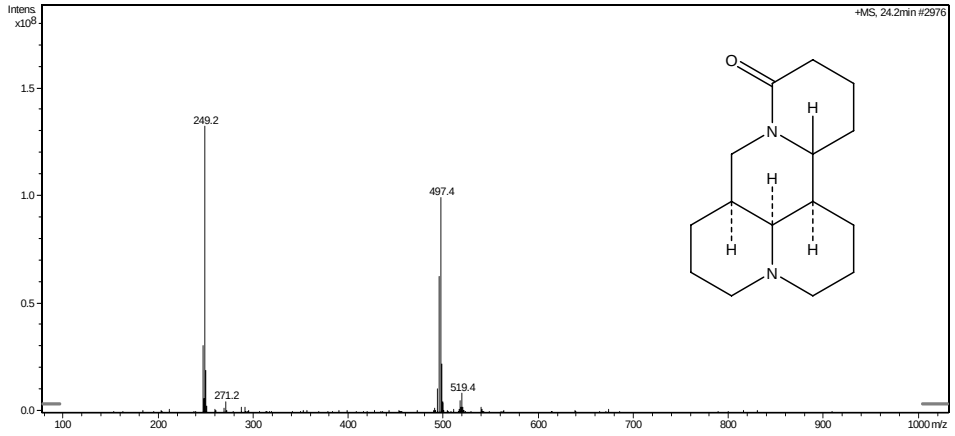

Matrine (**4**)

Figure 6. MS spectra of the four identified compounds in positive mode.

5.2.1.2 Qualitative Identification by HPLC-Ms^n

HPLC-MS^n will be a powerful technique to identify the constituents absorbed into the biofluids and their metabolites. In our research group, Ma *et al* successfully identify four alkaloids and five steroidal saponins including magnoflorine, menisperine, palmatine, berberine, timosaponin N or timosaponin E1, timosaponin D, timosaponin BIII or anemarsaponin C or xilingsaponin B, timosaponin BII and timosaponin AIII in rat serum by HPLC-DAD-MS/MS method following oral administration of Huangbai-Zhimu herb-pair Extract. The TIC chromatogram, the CID spectra and the proposed mechanistic pathways for fragments formed in MS^2 of the representative magnoflorine (alkaloid) and timosaponin D (steroidal saponin) are shown in Fig. 7-9, scheme 1 and 2, respectively [16]. They also identified four xanthones and seven steroidal saponins in rat urine by HPLC-MS/MS technology following oral administration of Rhizoma Anemarrhenae decoction [13]. They were neomangiferin, Glucuronide and monomethyl conjugate of mangiferin, mangiferin, monomethyl conjugate of mangiferin, Dimethyl conjugate of mangiferin, timosaponin N or timosaponin E1, timosaponin BII, timosaponin BIII Anemarrhenasaponin I or Anemarrhenasaponin II, timosaponin AII and timosaponin AIII. The peaks of these eleven compounds were all presented in the TIC chromatogram (see Fig. 10). The proposed mechanistic pathways for fragments formed in MS^2 were also deduced. The CID and the fragments deduction of the representative neomangiferin (xanthone) and timosaponin BII (steroidal saponins) were shown in Fig. 11, 12 and scheme 3, 4, respectively. By now, only a small amount of literatures related to this kind of research were published, in which Yang *et al* identified nine constituents of Buyang Huanwu decoction in pig serum using combined HPLC–DAD–MS techniques [39].

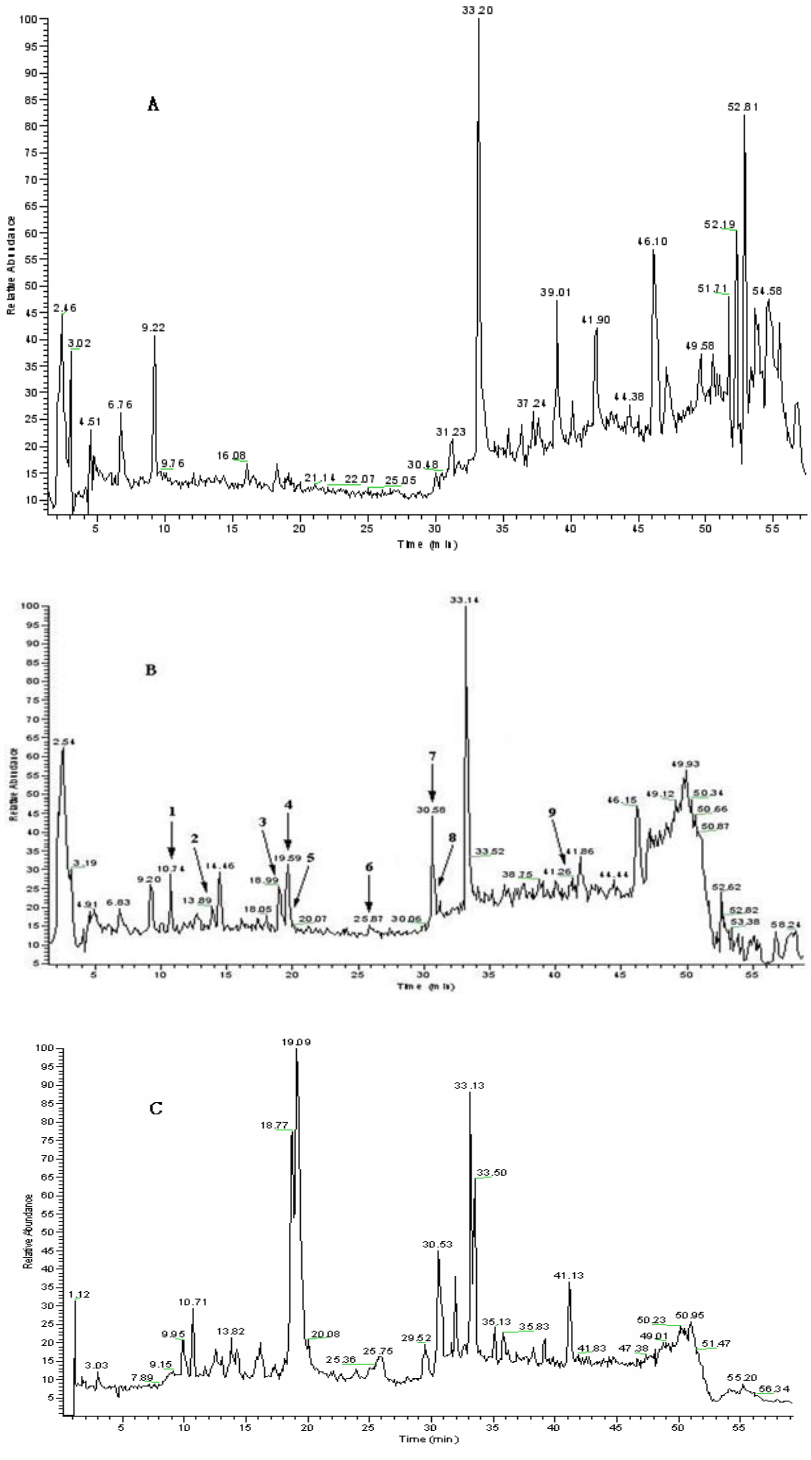

Figure 7. MS total ion current chromatograms of blank rat serum (A), the serum sample after oral administration of HBZMHP extract (B) and HBZMHP extract (C); Labelled chromatographic peaks were identified by mass spectrometry as follows: magnoflorine (1), menisperine (2), palmatine (3), berberine (4), timosaponin N or timosaponin E1 (5), timosaponin D (6), timosaponin BIII or anemarsaponin C or xilingsaponin B (7) timosaponin BII (8) and timosaponin AIII (9).

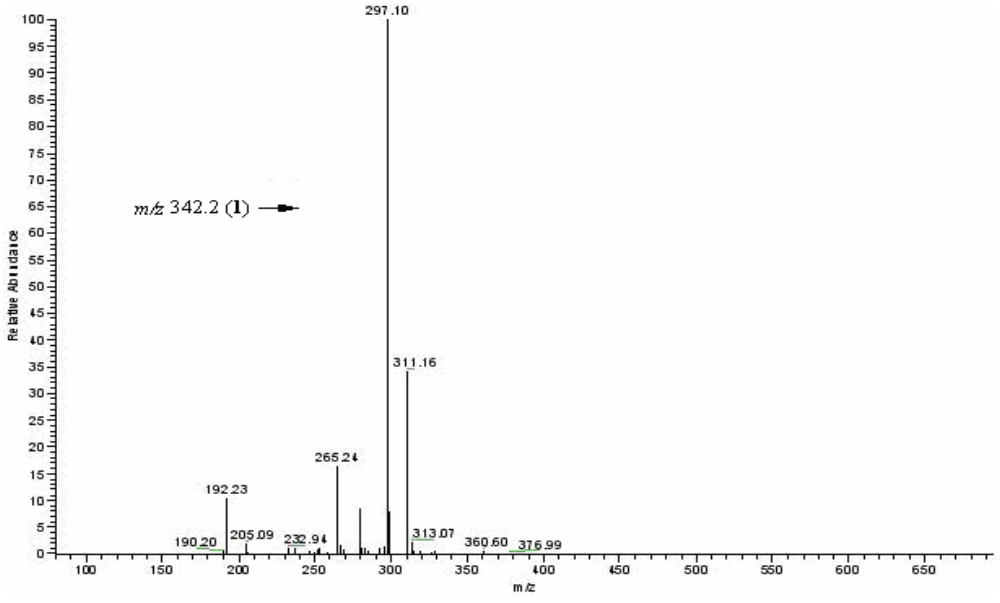

Figure 8. CID spectrum of the ion at m/z 342.2 of magnoflorine.

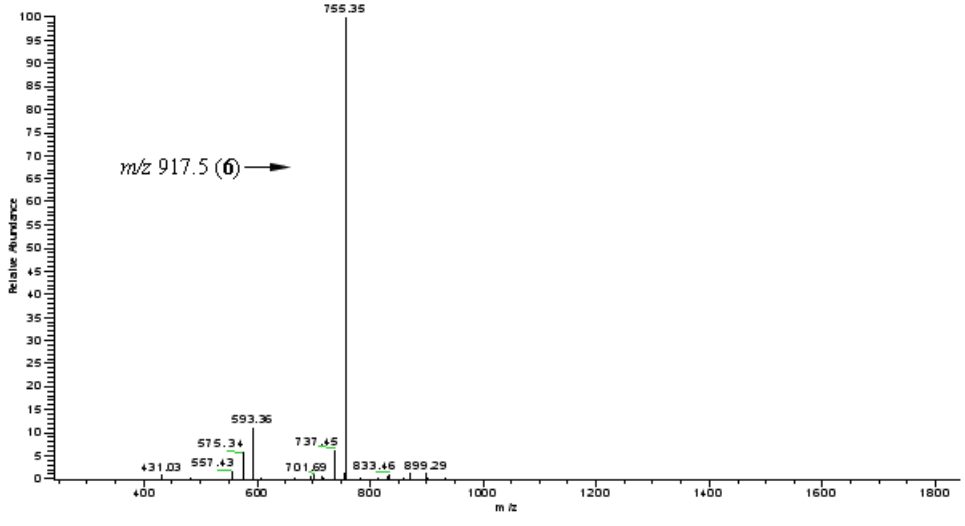

Figure 9. CID spectrum of the ion at m/z 342.2 of timosaponin D.

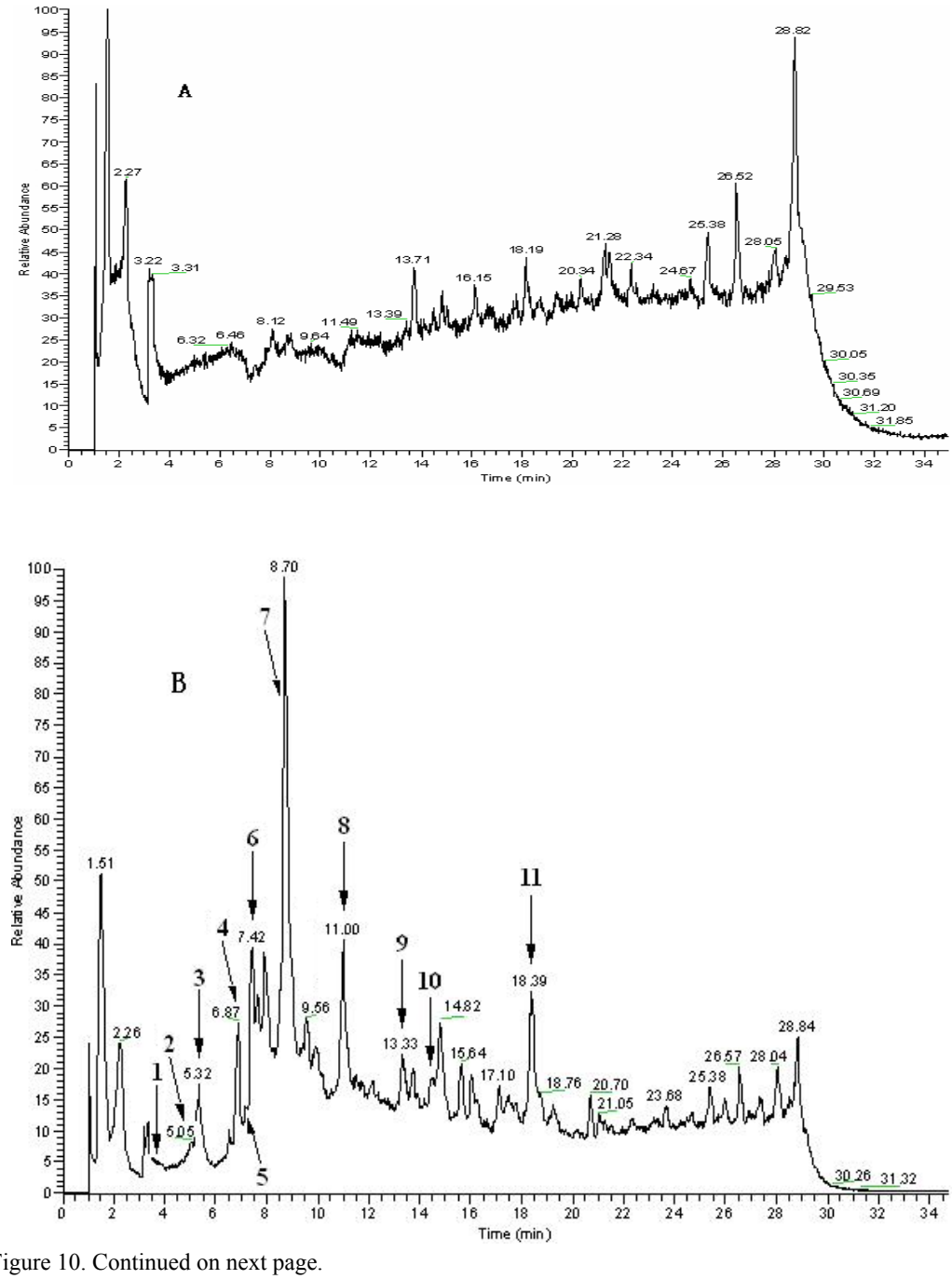

Figure 10. Continued on next page.

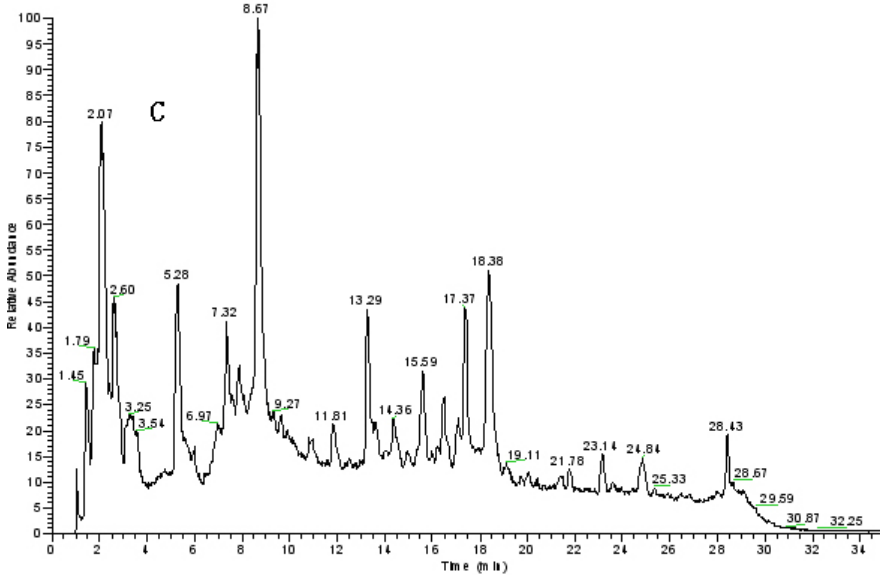

Figure 10. MS total ion current chromatograms of blank rat urine (A), the urine sample collected after oral administration of Rhizoma Anemarrhenae decoction (B) and Rhizoma Anemarrhenae decoction (C). Labelled chromatographic peaks were identified by mass spectrometry as follows: neomangiferin (1), glucuronide and monomethyl conjugate of mangiferin (2), mangiferin (3), monomethyl conjugate of mangiferin (4), dimethyl conjugate of mangiferin (5), timosaponin N or timosaponin E1 (6), timosaponin BII (7), timosaponin BIII or anemarsaponin C or xilingsaponin B (8) anemarrhenasaponin I or anemarrhenasaponin II (9), timosaponin AII (10) and timosaponin AIII (11).

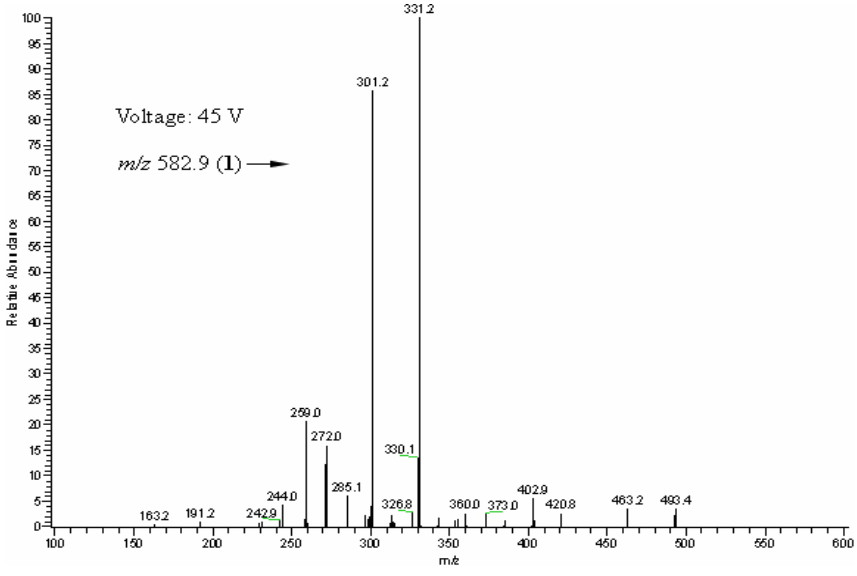

Figure 11. CID spectrum of the ion at m/z 342.2 of neomangiferin.

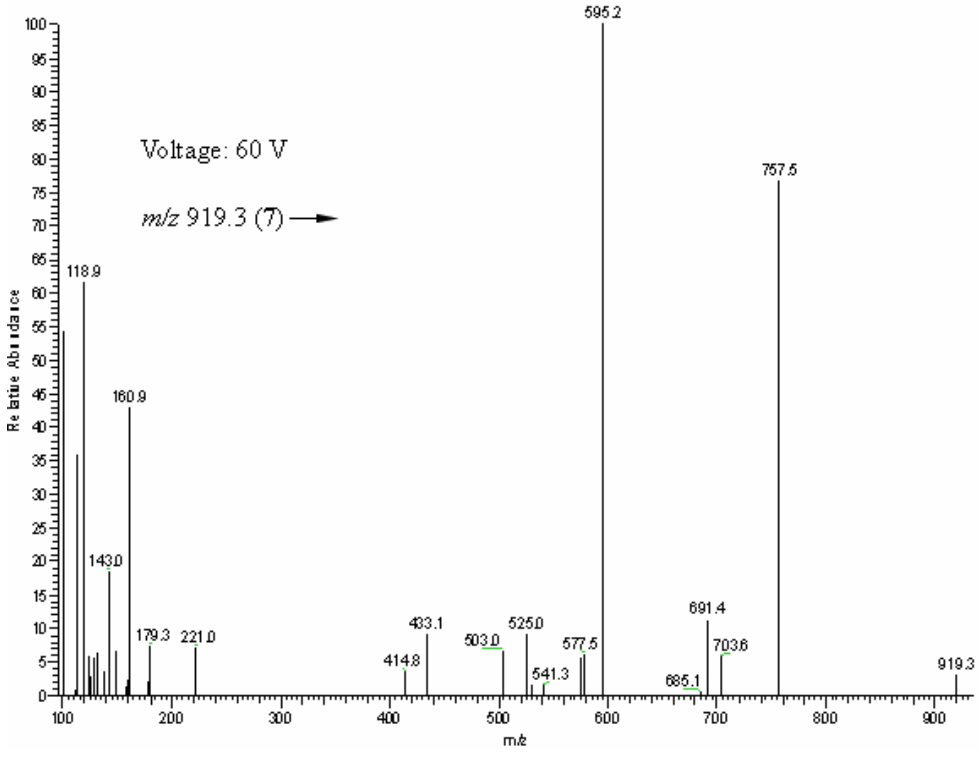

Figure 12. CID spectrum of the ion at m/z 342.2 of timosaponin BII.

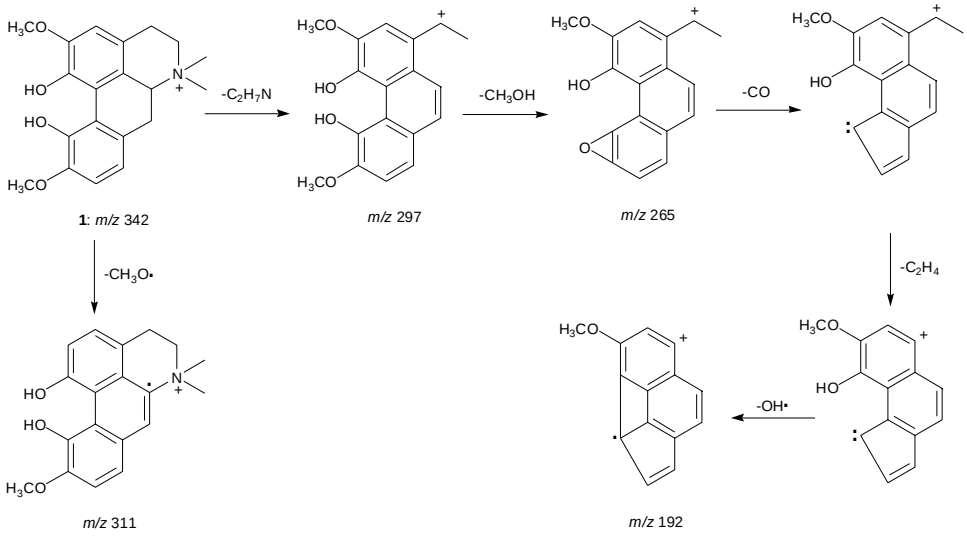

Scheme 1. Proposed mechanistic pathway for fragments formed in MS^2 of magnoflorine.

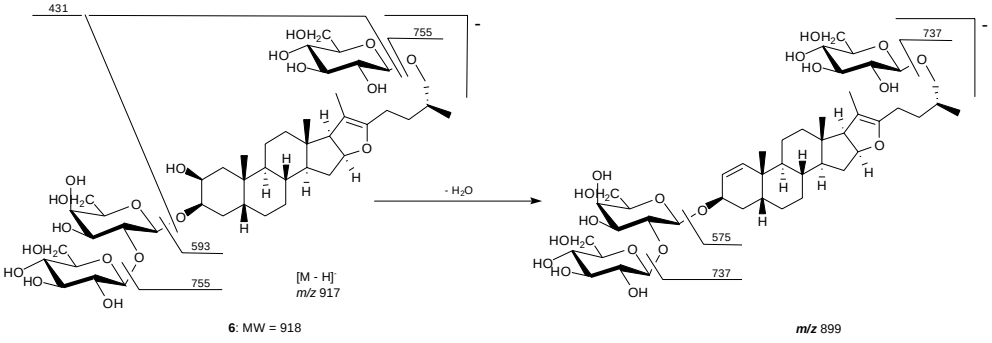

Scheme 2. Proposed mechanistic pathway for fragments formed in MS2 of timosaponin D.

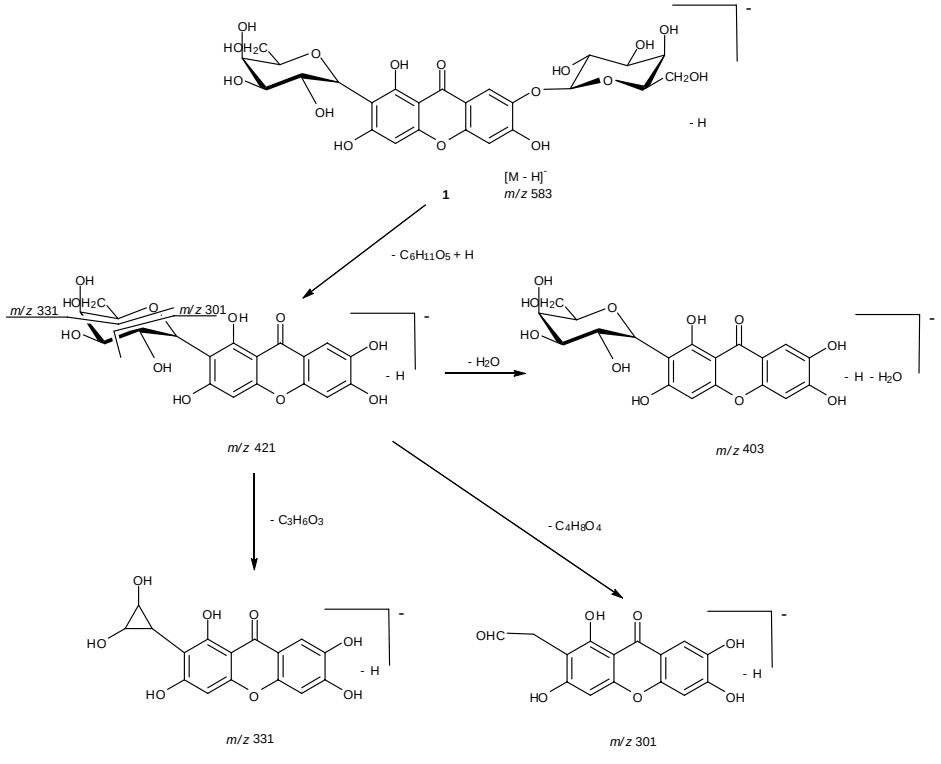

Scheme 3. Proposed mechanistic pathway for fragments formed in MS2 of neomangiferin.

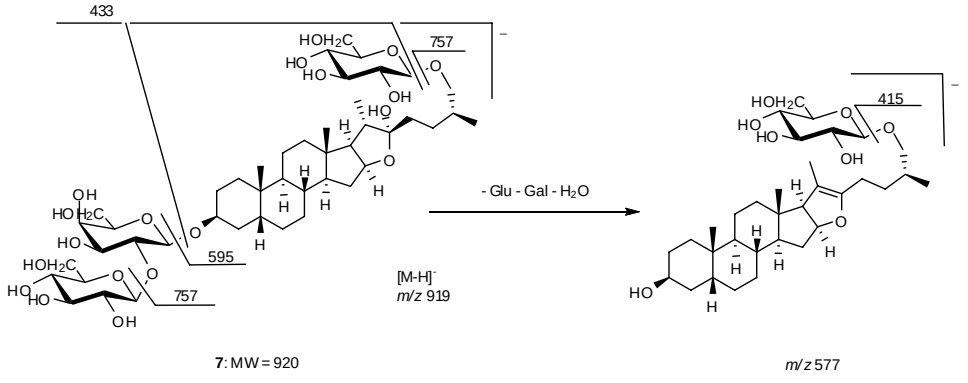

Scheme 4. Proposed mechanistic pathway for fragments formed in MS2 of timosaponin BII .

5.2.2 Quantitative Determination

The quantitative determination methods for the medicated biofluids obtained form the animal after administrated crude natural medicine extracts have no much difference with those for pure natural compounds, even though the concentration of interest compounds are comparably low. The standard compounds and the validation of the method for quantification are both of necessaries. Great contributions have been dong in this kind of research. In our research group, Ye *et al* determined the geniposide in rat serum and urine respectively, after oral administration of traditional Chinese medicinal preparation Yin-Zhi-Ku decoction. They successfully acquired the Serum concentration-time curve of geniposide (see Fig. 13) [15] and the profile of cumulative excretion of geniposide into urine (see Fig. 14) [14]. Lai *et al* determined four flavonols in rat plasma and urine after oral administration of *Abelmoschus manihot* extract [19]. Si *et al* studied the pharmacokinetic of isoferulic acid in rat plasma by high-performance liquid chromatography after oral administration of isoferulic acid and Rhizoma Cimicifugae extract [22]. Wen *et al* simultaneously determined calycosin-7-O-*β*-d-glucoside, ononin, astragaloside IV, astragaloside I and ferulic acid in rat plasma after oral administration of Danggui Buxue Tang extract for their pharmacokinetic studies by liquid chromatography–mass spectrometry [23]. Cao *et al* studied the pharmacokinetic of bufadienolides in dog's plasma after administration of Liu-Shen-Wan by high performance liquid chromatography time-of-flight mass spectrometry [27]. Yu *et al* Simultaneously analyzed five ginsenosides in rabbit plasma using solid-phase extraction and HPLC/MS technique after intravenous administration of 'SHENMAI' injection [30].

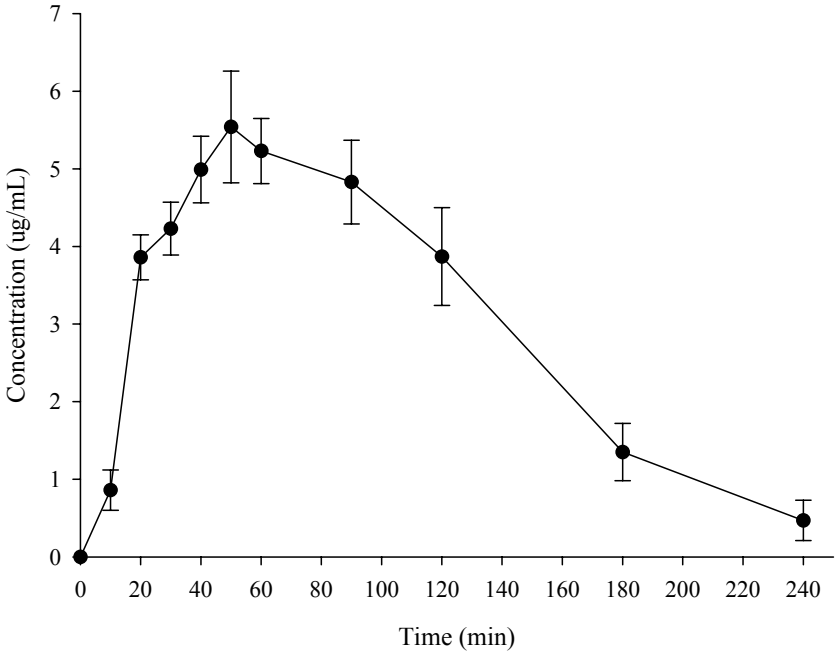

Figure 13. Serum concentration-time curve of geniposide in rats after oral administration of YZK (at a dose containing 310 mg/kg geniposide). Each point and bar represent the mean ±SD (n=5).

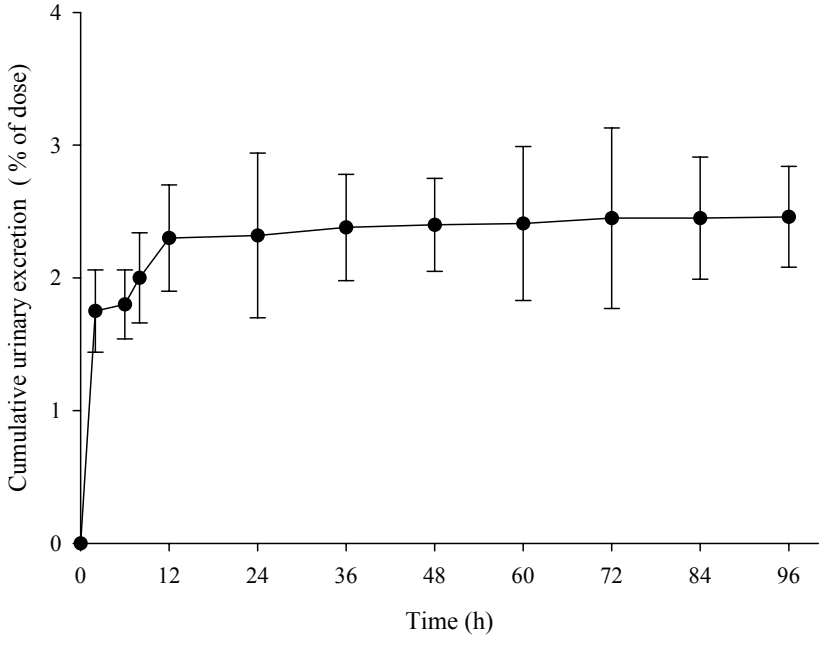

Figure 14. Profile of cumulative excretion of geniposide into urine after oral administration of the YZK decoction.

6. Conclusion

For most of natural medicines by oral administration, compounds absorbed into blood circulation will be excreted into urine finally. Most of compounds and metabolites of natural medicines can be detected in urine. We analyzed and identified compounds in urine which can indirectly gave us valuable information on effective substances of natural medicines. Effective substances concentrations in urine are higher than in serum since they are concentrated in the production of urine. HPLC-MS has high separation ability, high sensitivity, high selectivity, and high specificity, which is especially good at identifying trace components in biofluids [73, 74]. This technique is employed to analyze these compounds which are sensitive and reliable.

Most of previous studies on natural medicines metabolism research focused on pure component. Reports on metabolites structures and pharmacological screenings were very limited. Since the concentrations of original components and metabolites are low in the medicated serum, it is difficult to enrich and identify them by serum pharmacological method. We orally administered natural medicines to animals, enriched and isolated original components and metabolites in urine, carried out pharmacological screening, and identified their structures. By this method, active compounds can be identified. This method has several advantages. First, detected compounds in urine are all absorbed which possibly have pharmacological effects. Secondly, the concentrations of effective components in urine are higher than in serum, which makes it possible to detect most of components in urine. Finally, in contrast to serum pharmacological method, enough amount of urine sample for enriching and isolating effective components can be easily obtained since it will not cause injury to animals to get urine. The present research model separates the possible bioactive components from the numerous compositions in natural medicines and makes the determination of effective components more easily. It reduces the scale of screening and excludes those components which are existed in natural medicines, but can not be absorbed. Obviously, this research method can increase hit rate of identifying active compounds and is an important supplement to phytochemistry method and serum pharmacochemistry method.

The main aim of analyzing multi-constitutes of natural medicines in vivo is to elucidate effective components of natural medicines. Thus, analyzing and identifying structures of possibly effective substances are not enough for this aim. Possibly effective components must be largely enriched, isolated, and then screened by pharmacological experiments. Therefore, effective substances in natural medicines and their mechanisms of pharmacological effects can be elucidated by the systemic study. The metabolism pathway of some components can also be illustrated. Some lead compounds or pure compounds may be found for new drug development by the study.

There are still some technical difficulties though many advances have been made on in vivo multi-constitutes analysis. For example, to enrich and isolate effective components with enough purity is a prerequisite to carry on pharmacological screening and identification. It is still very difficult to enrich and isolate effective components in medicated serum or urine until now. Some endogenous constitutes in medicated biofluids will cause serious interference in pharmacological experiments. Effective approaches must be employed to reduce interference. Furthermore, the relationship of original components and their

metabolites should be cleared, which will elucidate metabolism procedure, and also provide information for large preparation of effective metabolites. With the development of novel analysis technologies, sample pretreatment technologies, and pharmacological screening technologies, these difficulties will be solved gradually. Therefore, in vivo multi-constitutes of natural medicines analysis and pharmacological screening will become an effective and promising research method to identify effective substances of natural medicines in the future.

References

[1] Wang, L. Q., She, S. C., Li, Y. K., Li, Y. (1995). Anti-tumor effects of Kushan and Xianhecao with serum pharmacology. *Chinese Journal of Traditional Chinese Medicines and Pharmacy*, 2, 19-21.

[2] Iwama, H., Amagaya, S., Oqihara, Y. (1987). Effect of Shassaikoto'A Japanese and Chinese herbal medical mixture, on the mitogenic activity of lipopolysaccharide: a new pharamacological testing method. *Journal of Ethnopharmacology*, 211, 45-53.

[3] Qiu, F., Yao, X. S. (1999). New thinking of in vivo direct effextive substances basis research. *Pharmacology and clinics of Chinese Material medica*, 15, 1-2.

[4] 田代真一. (1988). 血清藥理理學と血清藥化學—

漢方の藥理學から始まった藥物血中濃度測定の新しい世界[J]. *TDM研究*, 5, 54-565.

[5] Yoshihiro, K., Tetsuro, S. (1989). Components of Chinese Traditional prescription" KANZOBUSIT-O" in rat portal blood after oral administration. *Shoyakugaku Zasshi*, 43, 199-203.

[6] Yoshihiro, K., Wang, X. J., Junko, S. (1994). Pharmacological properities of galenical preparations (Ⅸ Ⅹ) Pharmacokinetics studyof 6,7-dimethylesculetin in rats. *Journal of traditional medicine*, 11, 176-180.

[7] Wang, X. J., Zhang, N., Sun, H., Sun, W. J. (2004). Preliminary Study on Serum Pharmacochemistry of Liu Wei Di Huang Wan. *Chinese Journal of Natural Medicines*, 2, 219-222.

[8] Wang, H., Ye G., Tang, Y. H., Zhu H. Y., Ma, R. R., Sun, Z. L. & Huang, C. G. (2006). High-performance liquid chromatographic method for the determination of mangiferin in rat plasma and urine. *Biomedical Chromatography*, 20, 1304-1308.

[9] Ye, G., Ma, R. R., Li, Z. H. Wang, H., Zhu, H. Y., Sun Z. L. & Huang, C. G. (2007). Determination of calycosin-7-O-*β*-D-glucopyranoside in rat plasma and urine by HPLC. *Biomedical Chromatography*, 21, 762-767.

[10] Tang, Y. H., Zhang, Y. Y., Zhu, H. Y., & Huang, C. G. (2007). A high-performance liquid chromatographic method for saikosaponin a quantification in rat plasma. *Biomedical Chromatography*, 21, 458-462.

[11] Xu, M., Guo, H., Han, J., Sun, S. F., Liu, A. H., Wang, B. R., Ma, X. C., Liu, P. Qiao, X., Zhang, Z. C. & Guo, D. A. (2007). Structural characterization of metabolites of salvianolic acid B from Salvia miltiorrhiza in normal and antibiotic-treated rats by

liquid chromatography–mass spectrometry. *Journal of Chromatography B*, 858, 184-198.

[12] Qian, T. X., Cai, Z. W., Wong, R. N. S., Mak, N. K., & Jiang, Z. H. (2005). In vivo rat metabolism and pharmacokinetic studies of ginsenoside Rg3. *Journal of Chromatography B*, 2005, 816, 223-232.

[13] Ma, C. H., Wang, L. X., Tang, Y. H., Fan, M. S., Xiao, H. B., & Huang, C. G. Identification of major xanthones and steroidal saponins in rat urine by liquid chromatography–atmospheric pressure chemical ionization mass spectrometry technology following oral administration of Rhizoma Anemarrhenae decoction. *Biomedical Chromatography*, published online.

[14] Ye, G., Zhu, H. Y., Zhao, H. L., Xu, B. & Huang, C. G. (2006). Determination of Geniposide in Rat Urine after Oral Administration of the Traditional Chinese Medicinal Preparation Yin-Zhi-Ku Decoction by High-Performance Liquid Chromatography. *Journal of Chromatographic Science*, 44, 1-4.

[15] Ye G., Zhu, H. Y., Zhao, H. L., Xu, B. & Huang, C. G. (2006). HPLC method for the determination and pharmacokinetic studies on geniposide in rat serum after oral administration of traditional Chinese medicinal preparation Yin-Zhi-Ku decoction. *Biomedical Chromatography*, 20, 743-747.

[16] Ma, C. H., Fan, M. S., Tang, Y. H., Li, Z. X., Sun, Z. L., Ye G. & Huang, C. G. Identification of major alkaloids and steroidal saponins in rat serum by HPLC-diode array detection-MS/MS following oral administration of Huangbai-Zhimu herb-pair Extract, *Biomedical Chromatography*, published online.

[17] He, X. J., Qiao, A. M., Wang, X. L., Liu, B., Jiang, M. M., Su, L. N. & Yao, X. S. (2006). Structural identification of methyl protodioscin metabolites in rats' urine and their antiproliferative activities against human tumor cell lines. *Steroids*. 71, 828-833.

[18] Zhou, D. Y., Xing, R., Xu, Q., Xue, X. Y., Zhang, F. F. & Liang, X. M. (2008). Polymethoxylated flavones metabolites in rat plasma after the consumption of Fructus aurantii extract: Analysis by liquid chromatography/electrospray ion trap mass spectrometry. *Journal of Pharmaceutical and Biomedical Analysis*, 46, 543-549.

[19] Lai, X. Y., Zhao, Y. Y., Liang, H., Bai, Y. J., Wang B. & Guo D. (2007). SPE-HPLC method for the determination of four flavonols in rat plasma and urine after oral administration of *Abelmoschus manihot* extract. *Journal of Chromatography B*, 852, 107-114.

[20] Qiu, P. H., Ai, C. C., Lin, L., Wu, J. Z. & Ye, F. Q. (2007). Simultaneous determination of selenium and arsenic contents in different extracts of Radix Astragali by enhancement effect of ethanol in hydride generation-inductively coupled plasma-atomic emission spectrometry. *Microchemical Journal*, 87, 1-5.

[21] Xu, F. G., Liu, Y., Zhang, Z. J., Song, R., Dong, H. J. & Tian, Y. (2008). Rapid simultaneous quantification of five active constituents in rat plasma by high-performance liquid chromatography/tandem mass spectrometry after oral administration of Da-Cheng-Qi decoction. *Journal of Pharmaceutical and Biomedical Analysis*, 47, 586-595.

[22] Si, D. D., Sun, X. H., Qi, D. D., Chen, X. H. & Bi, K. H. (2008). Determination and pharmacokinetics of isoferulic acid in rat plasma by high-performance liquid

chromatography after oral administration of isoferulic acid and Rhizoma Cimicifugae extract. *Journal of Pharmaceutical and Biomedical Analysis*, 47, 140-145.

[23] Wen, X. D., Qi, L. W., Li, P., Bao, K. D., Yan, X. W., Yi, L. & Li, C. Y. (2008). Simultaneous determination of calycosin-7-O-β-d-glucoside, ononin, astragaloside IV, astragaloside I and ferulic acid in rat plasma after oral administration of Danggui Buxue Tang extract for their pharmacokinetic studies by liquid chromatography–mass spectrometry. *Journal of Chromatography B*, 865, 99-105.

[24] Wang, H., Ye, G., Ma, C. H., Tang, Y. H., Fan, M. S., Li, Z. X. & Huang, C. G. (2007). Identification and determination of four metabolites of mangiferin in rat urine. *Journal of Pharmaceutical and Biomedical Analysis*, 45, 793–798.

[25] Wang, Z., Wang, H., Rhie, J. L. K., Covey, J. M., Liang, P., Wang, S. Y., Wang, C., Hu, Y. X., Prasad, G., Nan, L., Hill, D. L. & Zhang, R. W. Determination of desoxyepothilone B in nude mice plasma by liquid–liquid extraction and reversed-phase high-performance liquid chromatography. *Journal of Pharmaceutical and Biomedical Analysis*. 42, 272-276.

[26] Xiong, F., Wang, H., Cheng, J. & Zhu, J. B. (2006). Determination of scutellarin in mouse plasma and different tissues by high-performance liquid chromatography. *Journal of Chromatography B*, 835, 114-118.

[27] Cao Y., Zhao, L. L., Liang, Q. L., Bi, K. S., Wang, Y. M. & Luo, G. A. (2007). Study of the determination and pharmacokinetics of bufadienolides in dog's plasma after administration of Liu-Shen-Wan by high performance liquid chromatography time-of-flight mass spectrometry. *Journal of Chromatography B*, 853, 227-233.

[28] Garcés, A., Zerzaňová, A., Kučera, R., Barrón, D., & Barbosa, J. (2006). Determination of a series of quinolones in pig plasma using solid-phase extraction and liquid chromatography coupled with mass spectrometric detection: Application to pharmacokinetic studies. *Journal of Chromatography A*, 1137, 22-29.

[29] Zhang, X., Sun, Y. G., Cheng, M. C., Wang, Y. Q., Xiao, H. B. & Liang, X. M. (2007). Simultaneous quantification of three isoflavonoid glycosides in rabbit plasma after oral administration of Astragalus mongholicus extract by high-performance liquid chromatography coupled with electrospray ionization tandem mass spectrometry. *Analytica Chimica Acta*, 602, 252-258.

[30] Yu, K., Ma, Y. H., Shao, Q., Qu, H. B. & Cheng, Y. Y. (2007). Simultaneously determination of five ginsenosides in rabbit plasma using solid-phase extraction and HPLC/MS technique after intravenous administration of 'SHENMAI' injection. *Journal of Pharmaceutical and Biomedical Analysis*, 44, 532-539.

[31] Songsermsakul, P., Sontag, G., Cichna-Markl, M., Zentek, J. & Razzazi-Fazeli, E. (2006). Determination of zearalenone and its metabolites in urine, plasma and faeces of horses by HPLC–APCI–MS. *Journal of Chromatography B*, 843, 252-261.

[32] Yang, X. N., Wang, Y. J., Liu, Y. S. & Tang, X. (2008). Pharmacokinetics of salvianolic acids after intravenous injection, with and without Panax quinquefolium protopanaxadiol saponins, in rats. *Journal of Ethnopharmacology*, 117, 408-414.

[33] Ma, G., Jiang, X. H., Chen, Z., Ren, J. Li, C. R. & Liu, T. M. (2007). Simultaneous determination of vitexin-4″-O-glucoside and vitexin-2″-O-rhamnoside from hawthorn leaves flavonoids in rat plasma by HPLC method and its application to

pharmacokinetic studies. *Journal of Pharmaceutical and Biomedical Analysis*, 44, 243-249.

[34] Huang, J. M., Wang, G. Q., Jin, Y. E., Shen, T. & Weng, Y. E. (2007). Determination of palmatine in canine plasma by liquid chromatography–tandem mass spectrometry with solid-phase extraction. *Journal of Chromatography B*, 854, 279-285.

[35] Badeau, M., Tikkanen, M. J., Appt, S. E., Adlercreutz, H., Clarkson, T. B., Hoikkala, A., Wähälä, K. & Mikkola, T. S. (2005). Determination of plasma genistein fatty acid esters following administration of genistein or genistein 4′7-O-dioleate in monkeys. *Biochimica et Biophysica Acta (BBA) - Molecular and Cell Biology of Lipids*, 1738, 115-120.

[36] Jung, B. H., Chung, B. C., Chung, S. J., Lee, M. H. & Shim, C. K. (2000). Prolonged delivery of nicotine in rats via nasal administration of proliposomes. *Journal of Controlled Release*, 66, 73-79.

[37] Batchelder, R. J., Calder, R. J., Thomas, C. P. & Heard, C. M. (2004). In vitro transdermal delivery of the major catechins and caffeine from extract of Camellia sinensis. *International Journal of Pharmaceutics*, 283, 45-51.

[38] Moon, J. H., Tsushida, T. J., Nakahara, K. & Terao, J. J. (2001). Identification of quercetin 3-O-β-D-glucuronide as an antioxidative metabolite in rat plasma after oral administration of quercetin. *Free Radical Biology and Medicine*, 30, 1274-1285.

[39] Yang, D. H., Cai, S. Q., Liu, H. Y., Guo, X. X., Li, C. L. Shang, M. Y., Wang, X. & Zhao, Y. Y. (2006). On-line identification of the constituents of Buyang Huanwu decoction in pig serum using combined HPLC–DAD–MS techniques. *Journal of Chromatography B*, 831, 288-302.

[40] Murugaiyah, V. & Chan, Q. L. (2007). Analysis of lignans from Phyllanthus niruri L. in plasma using a simple HPLC method with fluorescence detection and its application in a pharmacokinetic study. *Journal of Chromatography B*, 852, 138-144.

[41] Ying, X. X., Gao, S., Zhu, W. L., Bi, Y. J., Qin, F., Li, X. Q. & Li, F. M. (2007). High-performance liquid chromatographic determination and pharmacokinetic study of vitexin-2″-O-rhamnoside in rat plasma after intravenous administration. *Journal of Pharmaceutical and Biomedical Analysis*, 44, 802-806.

[42] Kuwayama, K., Inoue, H., Kanamori, T., Tsujikawa, K., Miyaguchi, H., Iwata, Y. T. Miyauchi, S. & Kamo, N. (2008). Analysis of amphetamine-type stimulants and their metabolites in plasma, urine and bile by liquid chromatography with a strong cation-exchange column-tandem mass spectrometry. *Journal of Chromatography B*, 867, 78-83.

[43] Ge, B. Y., Chen, H. X., Han, F. M. & Chen, Y. (2007). Identification of amygdalin and its major metabolites in rat urine by LC–MS/MS. *Journal of Chromatography B*, 857, 281-286.

[44] Yang, G. J., Liu, P., Qu, X. L., Xu, M. J., Qu, Q. S., Wang, C. Y., Hu, X. Y., Wang, Z. Y. (2007). The simultaneous separation and determination of six flavonoids and troxerutin in rat urine and chicken plasma by reversed-phase high-performance liquid chromatography with ultraviolet–visible detection. *Journal of Chromatography B*, 856, 222-228.

[45] Roig, M., Segura, J. & Ventura, R. (2007). Quantitation of 17β-nandrolone metabolites in boar and horse urine by gas chromatography–mass spectrometry. *Analytica Chimica Acta*, 586, 184-195.

[46] Zhang, L., Liu, W., Zhang, R., Wang, Z. W., Shen, Z. D., Chen, X. H. & Bi, K. H. (2008). Pharmacokinetic study of matrine, oxymatrine and oxysophocarpine in rat plasma after oral administration of Sophora flavescens Ait. extract by liquid chromatography tandem mass spectrometry. *Journal of Pharmaceutical and Biomedical Analysis*, Available online.

[47] Joo, K. M., Park, C. W., Jeong, H. J., Lee, S. J. & Chang, I. S. (2008). Simultaneous determination of two Amadori compounds in Korean red ginseng (Panax ginseng) extracts and rat plasma by high-performance anion-exchange chromatography with pulsed amperometric detection. *Journal of Chromatography B*, 865, 159-166.

[48] Dai, J. N., Chen, X. H., Cheng, W. M., Liu, X., Fan, X., Shen Z. D. & Bi, K. H. (2008). A sensitive liquid chromatography–mass spectrometry method for simultaneous determination of two active chromones from Saposhnikovia root in rat plasma and urine. *Journal of Chromatography B*, 868, 13-19.

[49] Liang, Y., Liu, A. J., Qin, S., Sun, J. H., Yang, M., Li, P. & Guo, D. A. (2008). Simultaneous determination and pharmacokinetics of five bufadienolides in rat plasma after oral administration of Chansu extract by SPE-HPLC method. *Journal of Pharmaceutical and Biomedical Analysis*, 46, 442-448.

[50] Wang, X. J., Sun, W. J., Sun, H., Lv, H., Wu, Z. M., Wang, P., Liu, L. & Cao, H. X. (2008). Analysis of the constituents in the rat plasma after oral administration of Yin Chen Hao Tang by UPLC/Q-TOF-MS/MS. *Journal of Pharmaceutical and Biomedical Analysis*, 46, 477-490.

[51] Zhang, Y. S., Zhang, Q. Y., Li, L. Y., Wang, B., Zhao, Y. Y. & Guo, D. A. Simultaneous determination and pharmacokinetic studies of dihydromyricetin and myricetin in rat plasma by HPLC-DAD after oral administration of Ampelopsis grossedentata decoction. *Journal of Chromatography B*, 860, 4-9.

[52] Wang, X. Y., Zhao, T., Gao, X. Y., Dan, M., Zhou, M. M. & Jia, W. Simultaneous determination of 17 ginsenosides in rat urine by ultra performance liquid chromatography–mass spectrometry with solid-phase extraction. *Analytica Chimica Acta*, 594, 265-273.

[53] Han, F. M., Peng, Z. H., Song, W., Zhang, H. M., Zhu, M. M. & Chen, Y. (2007). Identification of dauricine and its metabolites in rat urine by liquid chromatography–tandem mass spectrometry. *Journal of Chromatography B*, 854, 1-7.

[54] Tang, Y. H., Zhu, H. Y., Zhang Y. Y. & Huang, C. G. (2006). Determination of human plasma protein binding of baicalin by ultrafiltration and high-performance liquid chromatography. *Biomedical Chromatography*, 20, 1116-1119.

[55] Thomas, B. F., Zeisel, S. H., Busby, M. G., Hill, J. M., Mitchell, R. A., Scheffler, N. M., Brown, S. S., Bloeden, L. T., Dix, K. J. & Jeffcoat, A. R. Quantitative analysis of the principle soy isoflavones genistein, daidzein and glycitein, and their primary conjugated metabolites in human plasma and urine using reversed-phase high-performance liquid chromatography with ultraviolet detection. *Journal of Chromatography B: Biomedical Sciences and Applications*, 760, 191-205.

[56] Liang, Y. Liu, A. H., Qin, S., Sun, J. H., Yang, M., Li, P. & Guo, D. A. (2008). Simultaneous determination and pharmacokinetics of five bufadienolides in rat plasma after oral administration of Chansu extract by SPE-HPLC method. *Journal of Pharmaceutical and Biomedical Analysis*, 46, 442-448.

[57] Zhang, Y. S., Zhang, Q. Y., Li, L. Y., Wang, B., Zhao, Y. Y. & Guo, D. E. (2007). Simultaneous determination and pharmacokinetic studies of dihydromyricetin and myricetin in rat plasma by HPLC-DAD after oral administration of Ampelopsis grossedentata decoction. *Journal of Chromatography B*, 860, 4-9.

[58] Xia, Y. F., Dai, Y., Wang, Q. & Liang, Z. D. (2007). Determination of scopoletin in rat plasma by high performance liquid chromatographic method with UV detection and its application to a pharmacokinetic study. *Journal of Chromatography B*, 857, 332-336.

[59] Frank, M. P. & Powers, R. W. (2007). Simple and rapid quantitative high-performance liquid chromatographic analysis of plasma amino acids. *Journal of Chromatography B*, 852, 646-649.

[60] Trevizan, L. C., Silva, F. V., Nogueira, A. R. A. & Nóbrega, J. A. (2007). Evaluation of a rapid semi-quantitative analysis approach using inductively coupled plasma optical emission spectrometry with axial viewing. *Microchemical Journal*, 86, 60-64.

[61] Deng, Y. T., Liao, Q. F., Li, S. H., Bi, K. S., Pan, B. Y. & Xie, Z. Y. (2008). Simultaneous determination of berberine, palmatine and jatrorrhizine by liquid chromatography–tandem mass spectrometry in rat plasma and its application in a pharmacokinetic study after oral administration of coptis–evodia herb couple. *Journal of Chromatography B*, 863, 195-205.

[62] Zhao, Y. Sun, Y. & Li, C. Simultaneous Determination of Ginkgo Flavonoids and Terpenoids in Plasma: Ammonium Formate in LC Mobile Phase Enhancing Electrospray Ionization Efficiency and Capacity. *Journal of the American Society for Mass Spectrometry*, 19, 445-449.

[63] Yu, S., Pang, X. Y., Deng, Y. X., Liu, L., Liang, Y. Liu, X. D., Xie, L., Wang, G. J. Wang, X. T. (2007). A sensitive and specific liquid chromatography mass spectrometry method for simultaneous determination of berberine, palmatine, coptisine, epiberberine and jatrorrhizine from Coptidis Rhizoma in rat plasma. *International Journal of Mass Spectrometry*, 268, 30-37.

[64] Xu, W., Luo, H., Zhang, Y. P., Shan, L., Li, H. Y., Yang, M., Liu, R. H. & Zhang, W. D. (2007). Simultaneous determination of five main active bufadienolides of Chan Su in rat plasma by liquid chromatography tandem mass spectrometry. *Journal of Chromatography B*, 859, 157-163.

[65] Leis, H. J., Fauler, G., Raspotnig, G. & Windischhofer, W. Quantitative analysis of morphine in human plasma by gas chromatography–negative ion chemical ionization mass spectrometry. *Journal of Chromatography B: Biomedical Sciences and Applications*, 744, 113-119.

[66] Tvrzická, E., Vecka, M., Staňková, B. & Žák, A. (2002). Analysis of fatty acids in plasma lipoproteins by gas chromatography–flame ionization detection: Quantitative aspects. *Analytica Chimica Acta*, 465, 337-350.

[67] Wittig, J., Herderich, M., Graefe, E. U. & Veit, M. (2001). Identification of quercetin glucuronides in human plasma by high-performance liquid chromatography–tandem

mass spectrometry. *Journal of Chromatography B: Biomedical Sciences and Applications*, 753, 237-243.

[68] Song, W., Peng, Z. H., Ge, B. Y., Han, F. M. & Chen, Y. (2008). Identification of metabolites of lobeline in the rat urine by liquid chromatography–tandem mass spectrometry. *International Journal of Mass Spectrometry*, 269, 131-137.

[69] Han, F. M., Peng, Z. H., Song, W., Zhang, H. M., Zhu, M. M. & Chen, Y. Identification of dauricine and its metabolites in rat urine by liquid chromatography–tandem mass spectrometry. *Journal of Chromatography B*, 854, 1-7.

[70] Moon, J. H., Tsushida, T., Nakahara, K. & Terao, J. Identification of quercetin 3-O-β-D-glucuronide as an antioxidative metabolite in rat plasma after oral administration of quercetin. *Free Radical Biology and Medicine*, 30, 1274-1285.

[71] Houghton, E., Tealea P. & Dumasiaa, M. C. (2007). Studies related to the origin of C18 neutral steroids isolated from extracts of urine from the male horse: The identification of urinary 19-oic acids and their decarboxylation to produce estr-4-en-17β-ol-3-one (19-nortestosterone) and estr-4-ene-3,17-dione (19-norandrost- 4-ene-3,17-dione) during sample processing. *Analytica Chimica Acta*, 586, 196-207.

[72] Pan, J. Y. & Cheng, Y. Y. (2006). Identification and analysis of absorbed and metabolic components in rat plasma after oral administration of 'Shuangdan' granule by HPLC–DAD–SI-MS/MS. *Journal of Pharmaceutical and Biomedical Analysis*, 42, 565-572.

[73] Lee, M. S. & Kerns, E. H. (1999). LC/MS Applications in drug development. *Mass Spectrometry Reviews*, 18, 87-279.

[74] Xu, L. L., An, R. & Wang, X. H. (2006). Application of LC-MS in analysis of traditional Chinese medicines. *Chinese Traditional Patent Medicine*, 28, 239-245.

In: Clinical Chemistry Research
Editors: Brian H. Mitchem and Charles L. Sharnham
ISBN 978-1-60692-517-1

Chapter V

Frontiers of Molecular Technologies in Noninvasive Prenatal Diagnosis

Sherry Sze Yee Ho[1], Sonia Baig [1], Sukumar Ponnusamy[1] and Mahesh Choolani [1*]

[1]Department of Obstetrics & Gynaecology, Yong Loo Lin School of Medicine, National University of Singapore, Singapore

Introduction

Current methods of prenatal diagnosis for chromosomal and single gene disorders involve invasive procedures such as amniocentesis, chorion villus sampling or fetal blood sampling to obtain fetal genetic material for cytogenetic and/or molecular analysis. These procedures involve a 1-4% risk of miscarriage that is unacceptable to some couples. Invasive prenatal diagnosis can cause a psychological burden on pregnant women. The anxiety about the invasive nature of the procedure and the attendant risk of fetal loss of a wanted pregnancy can cause emotional stress (Beeson and Golbus, 1979; Weinman and Johnston, 1988; Kowalcek, 2007). Missed diagnosis of handicapping congenital diseases occurs in at-risk women who reject invasive prenatal diagnosis due to the risk of fetal loss or morbidity (Chitty, 1998). Noninvasive and accurate prenatal diagnosis that does not carry any risk of procedural-related fetal loss is therefore desirable to at-risk pregnant women. The presence of cell-free fetal DNA/RNA circulating in the maternal blood offers an alternative source of fetal genetic material for prenatal diagnosis. Fetal DNA is readily detected in maternal plasma and serum (Bianchi and Lo 2001; Lo and Poon 2003; Birch et al., 2005; Galbiati et al., 2005). The estimated 3-6% fetal DNA in maternal plasma (Lo et al., 1997) can be detected in as early as 5 gestational weeks (Rijnders et al., 2003). In theory, fetal DNA sequences that differ from maternal DNA sequences can be identified in maternal plasma,

* A/P Mahesh Choolani (PhD, MRCOG), Department of Obstetrics and Gynaecology, National University Hospital, 5 Lower Kent Ridge Road, Singapore 119074, Tel: 67724279; Fax: 67794753, Email: obgmac@nus.edu.sg

thus allowing noninvasive prenatal testing of paternally-inherited genetic diseases. However, enrichment and detection of fetal sequences is hindered by the high amounts of background maternal sequences. The detection of fetal DNA sequences is therefore, dependent on the sensitivity of the assay and the amount of fetal sequences. Using innovative strategies and state-of-the-art technologies, researchers had overcome many technical challenges by the development of many potential noninvasive tests with significant clinical applications.

Results in Real-Time

Polymerase chain reaction (PCR) was invented in 1983 by Nobel laureate, Kary Mullis to amplify specific regions of a DNA strand exponentially, detecting small amounts of DNA template with high sensitivity. Since then, PCR-based technologies such as real-time PCR were developed to improve sensitivity and specificity. Unlike conventional PCR where the detection of amplicon is end-point, real-time PCR detects and quantifies the amount of amplicons generated "live" during PCR. This technique is similar to conventional PCR except that additional non-sequence specific intercalating double-stranded DNA dyes (SYBR Green) or sequence-specific fluorescence-labeled probes (TaqMan probes, molecular beacons, scorpion primers and probes) are used as reporters to reflect the quantity of amplicons. The emitted fluorescence is detected by a combined thermal cycler/fluorescence detector with the ability to monitor the progress of individual PCR reactions. SYBR Green was the first fluorescence detector to be used in real-time PCR. Although it is inexpensive, easy to use and relatively sensitive, it binds to any double-stranded DNA and is not specific. This results in misdiagnosis and overestimation of the amount of targeted DNA as SYBR Green binds to all double-stranded DNA in a PCR reaction. Specificity is essential in noninvasive prenatal diagnosis as the target fetal sequences exist in small amounts within the high background of maternal DNA in the maternal plasma (mean, 35.8 copies of fetal DNA/ (1019) copies of maternal DNA per ml maternal plasma, Galbiati et al., 2005). Sequence-specific probes such as TaqMan and molecular beacons are thus preferred. These molecular hybridisation probes rely on Fluorescence Resonance Energy Transfer (FRET) which is based on the 5'-nuclease assay. FRET is a distance-dependent interaction between the electronic excited states of two dye molecules, the quencher (Q) and the reporter (R) (Figures 1, 2). In close proximity of each other, excitation is transferred from the reporter molecule to the quencher molecule without emission of a photon. The reporter and quencher molecules are located at the 5' and 3' ends of the molecular hybridisation probe respectively. This dual-labeled fluorogenic hybridisation probe is included in addition to the two amplification primers normally used in conventional PCR and is complementary to the target sequences. During the extension phase of PCR in the TaqMan system, the 5' to 3' exonuclease activity of the Taq DNA polymerase cleaves the reporter molecule from the TaqMan probe, releasing it from the quencher. Photons are emitted and the resulting fluorescent emission from the reporter molecule is captured by the charge coupled device camera. These fluorescence measurements are performed without opening the PCR tube and thus, risk of carry-over contamination is reduced. In addition to the ease of automation, real-time PCR is less cumbersome than conventional PCR as end-point analyses such as gel or capillary

electrophoresis are not required. An alternative variation to linear hydrolysis probes such as TaqMan is the molecular beacon. Molecular beacons are short segments of single-stranded DNA containing R and Q molecules but FRET only occurs when the Q molecule is directly adjacent to the R molecule. These hybridisation probes are structured as "hairpins" when "free" in solution to allow R and Q molecules to be in close proximity. During hybridisation of the molecular beacon and extension of the target sequences in PCR, the hairpin structure of the molecular beacon denatures, separating the R and Q molecules and FRET cannot occur. This results in the emission of photons from the R molecule. The advantage of using molecular beacons over TaqMan probes is that molecular beacons remain intact during the amplification process and will rebind to the target sequences in every cycle for signal measurement (Figure 2). A Scorpion is a specific probe sequence that is held in a hairpin loop conformation by complementary stem sequences on the 5' and 3' sides of the probe similar to a molecular beacon. The reporter molecule attached to the 5'-end is quenched by the quencher molecule on the 3'-end by FRET. However, unlike TaqMan probes and molecular beacons which probe by bimolecular mechanisms, a Scorpion probe by unimolecular mechanism as the primers and probes are linked together. With its unimolecular mechanism, Scorpions give a more intense signal than either of the two probe systems under fast cycling condition (Thelwell et al., 2000).

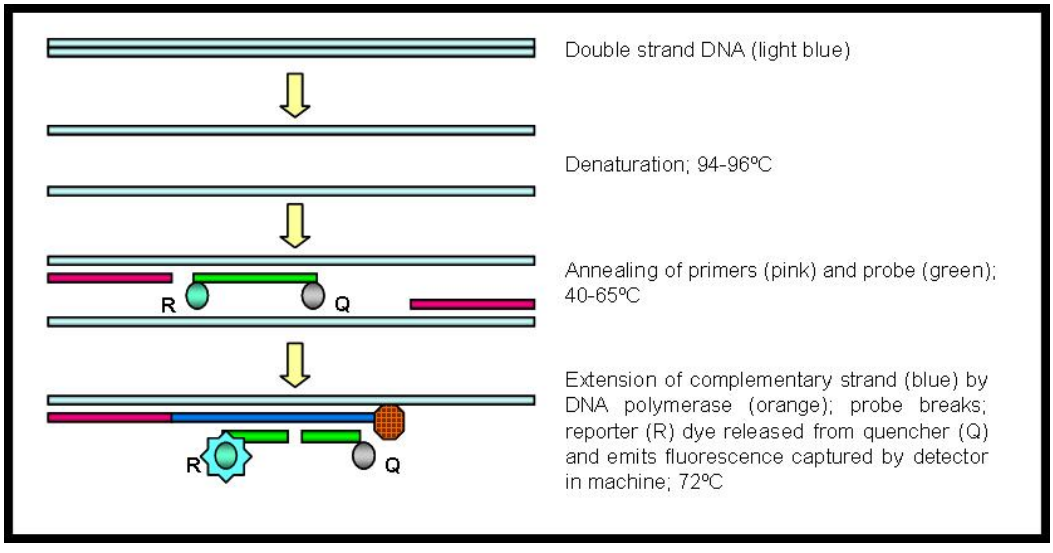

Figure 1 Real-time PCR using TaqMan system.

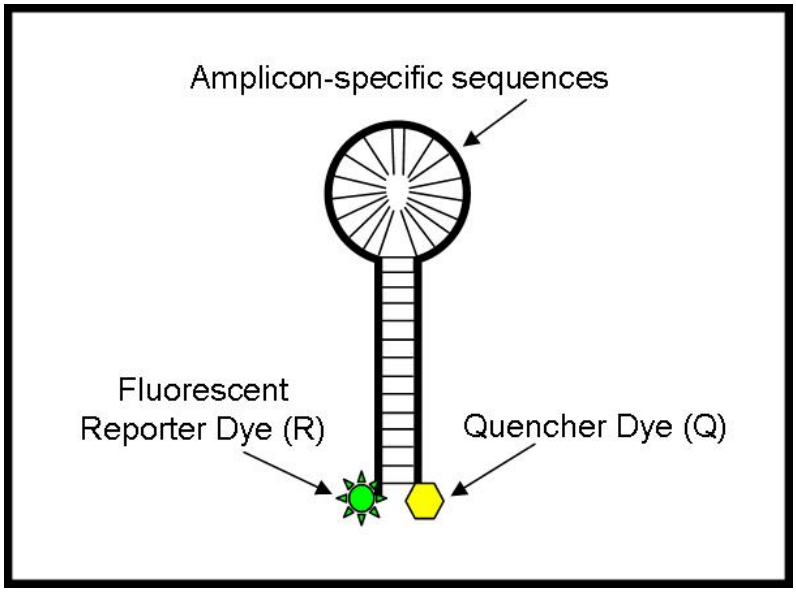

Figure 2 Hairpin conformation of a molecular beacon.

Girl or Boy?

Real-time PCR was instrumental in the detection and quantitation of Y-chromosome-specific DNA sequences (*SRY*) in maternal plasma throughout pregnancy in many studies. The use of real-time PCR to detect and quantify fetal *SRY* sequences in the maternal plasma was first demonstrated by Dennis Lo and colleagues in 1998 (Lo et al., 1998a). The amount of fetal DNA was estimated to be 3.4 - 6.2% of total DNA in the maternal plasma throughout pregnancy. Since then, fetal *SRY* sequences could be detected and quantified in as early as 5 gestational weeks in many studies using real-time PCR (Birch et al., 2005; Galbiati et al., 2005). The overall 87-100% sensitivity with 100% specificity was observed when in real-time PCR amplification of Y-specific sequences (*SRY, DYS14, DYZ3, DAZ*) in maternal plasma of pregnancies carrying male fetuses (Avent and Chitty, 2006; Vainer et al., 2008). The use of multi-copy *DYS14* and *DAZ* sequences instead of single-copy *SRY* improves the sensitivity of real-time PCR (Zimmermann et al., 2005; Purwosunu et al., 2008; Vainer et al., 2008). Targeting multi-copy *DYS14* sequences of *TSPY* allowed the detection of fetal DNA in maternal plasma in as early as 4 weeks' gestation (Illanes et al., 2007). A recent large-scale study to compare the efficiencies of predicting fetal gender using real-time PCR targeting *DYS14* and *SRY* assays were performed on 145 plasma samples from healthy pregnant women (11-12 gestational weeks). The efficiencies of *DYS14* and *SRY* assays were found to be 97.9% and 80% respectively, indicating that the multi-copy *DYS14* assay as the best approach for early fetal gender assessment as it is more sensitive, accurate and efficient than using the single-copy *SRY* assay (Picchiassi et al., 2008).

The high sensitivities and specificities of real-time PCR to noninvasively determine fetal gender result in its implementation into routine clinical practice for pregnancies at risk of sex-linked disorders. Sex-linked disorders such as haemophilia, Fragile X and Duchenne Muscular Dystrophy (DMD) occur only in males and therefore, early determination of fetal gender can exclude unnecessary invasive testing of female fetuses (Norbury and Norbury, 2008; Bustamante-Aragones et al., 2008).

Fetal gender determination is also useful in the clinical management of pregnancies at risk of congenital adrenal hyperplasia (CAH). CAH individuals have high levels of androgens and as a result, female fetuses in CAH-affected pregnancies exhibit varying degrees of virilisation and can develop ambiguous genitalia from as early as 8 gestational weeks. Administration of steroid dexamethasone in pregnancies with female fetuses suppresses the hypothalamic-pituitary-adrenal axis and prevents virilisation. The determination of fetal gender in pregnancies at risk of CAH enables early cessation or avoidance of steroid treatment in all male fetuses (Rijnders et al., 2001; Chiu et al., 2002a).

The application of real-time PCR extends to monitoring mothers in pregnancy-related pathological complications such as pre-term labour and preeclampsia (PE). Using quantitative real-time PCR of Y-chromosome-specific sequences, the concentrations of fetal DNA in the maternal plasma in normal pregnancies throughout gestation provide a comparative set of standard values (Lo et al., 1998a; Farina et al., 2002; Chan et al., 2003; Birch et al., 2005). When compared with plasma samples obtained from women with various complications of pregnancy, including PE, pre-term labour, invasive placenta, aneuploidies, hyperemesis gravidarum and fetal growth restriction, a significant increase in the number of copies of fetal DNA was observed. These elevations are useful as noninvasive prognostic markers to monitor and manage adverse pregnancy outcomes (Leung et al., 1998; Lo et al., 1999; Zhong et al., 2000; Pertl and Bianchi, 2001; Leung et al., 2001; Zhong et al., 2001; Zhong et al., 2002; Swinkels et al., 2002; Sekizawa et al., 2003; Shimada et al., 2004; Tjoa et al., 2004; Farina et al., 2004; Levine et al., 2004; Bauer et al., 2006; Alberry et al., 2009). Unfortunately, as the detection and quantitation of fetal sequences from the maternal plasma using real-time PCR is dependent on the presence of male-specific DNA sequences, this strategy is applicable only to pregnancies of male fetuses (50% of all pregnancies) (Hyett et al., 2005). As such, quantitative fluorescence PCR (QF-PCR) of X chromosome short tandem repeats was used to detect female fetal DNA from maternal plasma (Tang et al., 1999a; Pertl et al., 2000; Vecchione et al., 2008).

The most extensive clinical application of real-time PCR in noninvasive prenatal diagnosis is to assess whether the fetus is at risk of HDFN (haemolytic disease of the fetus and newborn) (Lo et al., 1998b; Finning et al., 2002; Brojer et al., 2005; Minon et al., 2008; Avent, 2008). The fetus of a sensitized RhD-negative mother and a father who is heterozygous for the D antigen has a 50% chance of being RhD positive and at risk of alloimmune intrauterine haemolysis, leading to fetal anaemia and death (Choolani et al., 2006). Determination of fetal RHD status can permit early intervention either by in utero transfusion by cordocentesis or administration of prophylactic anti-D during pregnancy. These clinical measures will prevent alloimmunization caused by fetomaternal haemorrhage during the third trimester of pregnancy. The screening of HDFN to identify at risk mothers during pregnancy includes monitoring levels of maternal anti-blood group-specific antibodies

(anti-D and anti-c). The detection of elevated levels of anti-D in D-negative mothers leads to fetal Rh genotyping. This will avoid unnecessary antenatal prophylaxis of RhD-negative fetuses in RhD-negative mothers and allow early antenatal prophylaxis in affected mothers. However, invasive procedures such as amniocentesis and chorionic villus sampling are required to obtain fetal DNA for analysis. Besides a procedural-related risk of miscarriage, these invasive procedures might further sensitize the mother against fetal Rhesus antigens. Noninvasive detection of fetal RhD sequences in maternal plasma using real-time PCR will eliminate such procedural-related risks. The diagnostic accuracy of large-scale noninvasive fetal RhD determination using real-time PCR was more than 99% (Rouillac-Le Sciellour et al., 2004; Van der Schoot et al., 2006; 2008). The International Blood Group Reference Laboratory (IBGRL) currently offers molecular tests for fetal Rh genotyping. However, similar to fetal gender determination, the use of Y-chromosome-specific sequences as positive control to demonstrate the presence of detectable fetal DNA is limited to pregnancies involving male fetuses. The absence of a positive control that is applicable in all pregnancies regardless of fetal gender limits Rh testing. As fetal sequences may be undetected due to low concentrations or loss of fetal DNA during sample processing, false-negatives may result, leading to misdiagnosis. A positive control that is gender-independent will eliminate false negatives. These positive controls should contain fetal-specific sequences that are polymorphic to enable discrimination between fetal and maternal DNA sequences. Studies exploring the use of genetic polymorphisms such as epigenetic sequences and single nucleotide polymorphisms (SNPs) can be developed into universal fetal DNA markers. Chim et al. (2005) described hypomethylated *maspin* (SERPINB5) gene as the first universal marker for quantitative and qualitative applications of fetal DNA in maternal plasma. In the study, DNA isolated from paired placental tissues and maternal blood samples was bisulfite-converted for DNA sequencing of the *maspin* gene promoter (Frommer et al., 1992). Bisulfite converts unmethylated cytosine into uracil while leaving methylated cytosine unchanged (Herman et al., 1996). The methylation status of the *maspin* promoter in the placental tissues and maternal blood cells were found to be hypomethylated (U-maspin) and densely methylated (M-maspin) respectively. The concentrations of U-maspin and M-maspin promoter DNA sequences were quantified in maternal plasma from preeclamptic and nonpreeclamptic pregnancies by real-time quantitative methylation-specific PCR (Chim et al., 2005). The maternal plasma concentration of unmethylated maspin sequences was elevated by a median of 5.7 times in preeclamptic pregnancies compared with nonpreeclamptic pregnancies. Hypomethylated maspin sequences allowed the measurement of fetal DNA concentrations in pregnancy-associated disorders, irrespective of fetal gender and genetic polymorphisms. The ease of use, sensitivity, published assays, and ability to automate and thus avoid contamination issues were factors influencing the use of real-time PCR.

Being Selective to be Specific

The vast amounts of maternal DNA sequences present a major problem in noninvasive prenatal diagnosis as it obscures the detection and analysis of fetal-specific sequences in the

maternal plasma. Strategies using allele-specific PCR (ASPCR) to selectively amplify target fetal-specific sequences had been developed. ASPCR was reportedly capable of detecting more than 5 copies of target allele in the presence of up to approximately 100 000 copies of the background allele without interference from the background sequence (Nasis et al., 2004). However, a low quantity of target allele and reduced PCR efficacy resulting from stringent PCR conditions in ASPCR require a high number of amplification cycles. This increased in the number of PCR cycles lead to high levels of nonspecific amplification, interfering with detection of target alleles. The addition of replication accessory proteins (thermostable proteins) to ASPCR would suppress potential false-positive results caused by high amounts of wild-type allele (background) by destabilizing mismatched primers and inhibit amplification of wild-type allele. As such, Nasis et al. (2004) combined replication accessory proteins from Pfx System with Taq polymerase (without 3'-exonuclease proofreading activity) and TaqMaster PCR Enhancer. This additive was found to decrease the formation of primer-dimer artifacts. Primer-dimer artifacts are known to reduce PCR efficacy as they compete with the target amplicon, thus reducing the yield. These modifications were implemented in ASPCR to detect paternally-inherited cystic fibrosis D1152H mutation in the maternal plasma of a pregnant carrier at 11 gestational weeks (Nasis et al., 2004).

ASPCR was commonly used in real-time PCR with allele-specific primers and a fluorescent probe. Using primers and a probe specific for a deletion in codon 41/42 (-CTTT) in the beta-globin gene, Chiu et al. (2002) excluded fetal inheritance of paternally-inherited codon 41/42 mutation in 2 out of 8 pregnancies at risk of beta-thalassaemia major noninvasively using maternal plasma (Chiu et al., 2002b).

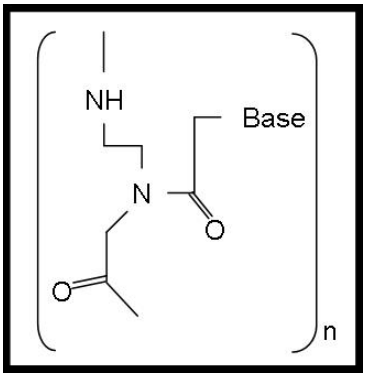

Figure 3 Chemical structure of a peptide nucleic acid (PNA).

Besides selective amplification of target fetal alleles, strategies to suppress amplification of maternal alleles using a peptide-nucleic-acid (PNA) clamp were also explored. PNA is an artificially synthesized polymer similar to DNA or RNA. In PNAs, the ribose phosphate backbone is replaced with a polyamide backbone of repeating units of N-(2-aminoethyl)-glycine linked by peptide bones (Figure 3). The various purine and pyrimidine bases are connected to the backbone by methylene carbonyl bonds. There are no charged phosphate groups in the backbone of PNA and binding between PNA-DNA strands is stronger than between DNA-DNA strands due to the lack of electrostatic repulsion. PNA oligomers thus show greater specificity in binding to complementary DNAs forming PNA-DNA strands with

much higher thermal stability than corresponding DNA-DNA strands. In addition, PNA-DNA strands are more susceptible to destablization when single base pair mismatches are present. Thus, there is preferential amplification of the PNA-free target DNA strand than the wild-type PNA-DNA strand in maternal plasma due to the suppression of amplification by PNA. Allele-specific real-time PCR with prior PNA-clamp PCR can therefore, selectively suppress the amplification of normal wild-type (background) allele.

Size Matters

The use of size fractionation in the enrichment of cell-free fetal DNA from cell-free maternal DNA in the maternal plasma was based on observations that the majority (>99%) of fetal-derived DNA molecules in the maternal circulation were shorter (<313 bp in length) than the maternal-derived DNA molecules (Chan et al., 2004). Agarose gel electrophoresis of extracted total cell-free DNA followed by excision of the gel slice containing approximately 100-300 bp for DNA isolation can enrich cell-free fetal DNA from maternal DNA (Li et al., 2004). Many researchers combined different strategies to improve sensitivity and specificity. With a selective enrichment of fetal DNA species by size fractionation in addition to PNA-clamp PCR before allele-specific real-time PCR, paternally-inherited fetal mutant alleles for were readily detected (Li et al., 2008a). With this strategy, β-thalassaemia mutations from size-fractionated DNA from maternal plasma can be detected (Li et al., 2005). Thirty-two maternal plasma DNA samples from pregnant women at risk of β-thalassaemia were analysed for the presence or absence of 4 common β-thalassaemia mutations that were paternally-inherited (*IVSI*-1, *IVSI*-6, *IVSI*-110, codon 39). Of the 32 maternal plasma samples that were analysed, 6 (86%) of 7 cases with the IVSI-1 mutation, 4 (100%) of 4 with the IVSI-6 mutation, 5 (100%) of 5 with the IVSI-110 mutation, and 13 (81%) of 16 with the codon 39 mutation were correctly identified. One false-positive test result was scored for the IVSI-1 mutation. Two cases with the codon 39 mutation were classified as uncertain and 1 case was excluded due to lack of a diagnostic test results at the time of analysis. The combined use of size fractionation, PNA clamps and fluorescence-based detection in allele-specific real-time PCR achieved an overall sensitivity of 100% and specificity of 93.8%, with classified cases removed. The usefulness of PNA-clamps was further demonstrated in a recent study by Galbiati and colleagues. PNA-mediated enriched PCR of maternal plasma was used in combination with microelectronic microchip analysis, direct sequencing and pyrosequencing to detect 7 frequent β-globin gene mutations in 41 pregnancies (9-12 gestational weeks) at risk of beta-thalassaemia. Results were completely concordant in the microchip analysis while >96% accuracy was achieved in direct sequencing and pyrosequencing (Galbiati et al., 2008).

The effect of size fractionation of cell-free DNA on the detection of paternally inherited SNPs was examined when using either the homogeneous MassEXTEND (hME) or the single allele base extension reaction (SABER) assay for the Matrix-assisted laser desorption/ionization time of flight mass spectrometry (MALDI-TOF MS) analysis. Size fractionation led to increase in the sensitivity of hME and not SABER. This improvement in hME is attributable to the increased concentration of fetal DNA sequences relative to

maternal cell-free DNA sequences in the size-fractionated preparation. The use of size fractionation also gave clearer mass spectra signals although it did not lead to an increase in the sensitivity of detection in SABER (Li et al., 2006a). In a separate study, the combination of size fractionation and MALDI-TOF MS lead to a more precise detection of the fetal G1138A mutation in the maternal plasma of two pregnant women affected with achondroplasia (Li et al., 2007). Subsequently, MALDI-TOF MS hME was also used to detect paternally inherited SNP alleles in size-fractionated maternal plasma DNA. Allele-specific MALDI-TOF MS SABER was also used to detect fetal KEL1 gene in maternal plasma from KEL1-negative pregnant women with 94% accuracy (Li et al., 2008b).

All about Mass

Matrix-assisted laser desorption/ionization time of flight mass spectrometry (MALDI-TOF MS) is a powerful tool in SNP genotyping, quantitative DNA analysis, detection of insertions and deletions (indels) associated with microsatellite repeat instability (MSI) and short tandem repeats, gene expression analysis, DNA and RNA sequencing and DNA methylation analysis (Tang et al., 1999b; Tolson and Nicholson, 1998; Ragoussis et al., 2006). MALDI-TOF MS with a resolution of approximately 100 times higher than capillary sequencing for DNA analysis is effective in detecting paternally-inherited SNPs from maternal plasma for noninvasive prenatal diagnosis. Sensitivities of MALDI-TOF MS and TaqMan real-time PCR in detecting fetal-specific sequences in maternal plasma were compared and found to be comparable at 95% and 93% respectively (Li et al., 2006b). However, with the low quantity of fetal DNA in maternal plasma at approximately 20 copies per ml of maternal plasma in the first trimester, MALDI-TOF MS is a preferred alternative to real-time PCR for the detection and analysis of cell-free fetal DNA in maternal plasma (Ding and Lo, 2006).

Two amplification steps enhanced the high sensitivity and specificity of MALDI-TOF MS. DNA is first amplified by PCR, followed by an additional linear amplification step called base extension reaction (hME or SABER). In hME, base extension reaction is performed with an extension primer designed to anneal to regions immediately upstream of the mutation site. Both mutant and wild-type alleles are interrogated by the base extension primer which is being extended by adding a mixture of 2',3'-dideoxynucleoside triphosphates and deoxynucleotide triphosphates (dNTPs) (Tang et al., 1999b). In SABER, primer extension was restricted to the fetal-specific allele of interest by the addition of a single species of dideoxynucleoside triphosphate (ddNTP) without any dNTP (Ding et al., 2004). Therefore, depending on the specific mutation introduced and the ddNTP/dNTP mixtures used, either one or two bases are added to the extension primer, producing two extension products from the wild-type DNA and the mutant DNA. MALDI-TOF MS was then used to discriminate between the single nucleotide differences by the determination of the unique molecular mass of the target amplicons containing the interrogated SNP.

The detection sensitivities of standard base extension in hME and single allele base extension reaction in SABER were compared by MS analysis of fetal inheritance of the four most common Southeast Asian β-thalassaemia mutations (CD 41/41-CTTT, IVS2 654 (C →

T), nt - 28 (A → G), and CD 17 (A → T) in maternal plasma by Ding and colleagues in 2004. Maternal plasma samples from 12 pregnancies (7-21 gestational weeks) at risk of β-thalassaemia major were analysed. Among the 12 at risk pregnancies, 11 pregnancies involved couples where both parents carried different β-thalassaemia mutations. While hME gave two false-negatives, the detection of paternal mutation in all six maternal plasma samples by SABER was completely concordant with the fetal genotype. The protocols of hME and SABER are similar, involving PCR amplification of the paternally inherited fetal allele and the maternal background alleles from maternal plasma, followed by a base extension reaction before MS analysis. The primary difference of SABER from hME is that a different base extension step that is restricted to the allele of interest to improve sensitivity is used. SABER was thus able to specifically detect fetal alleles instead of both fetal and maternal alleles (Ding et al., 2008).

The usefulness of SABER is not limited to detecting fetal-specific SNP alleles in the maternal plasma. With the low amounts of fetal DNA (3-6%, Lo et al., 1998a) in the maternal plasma, fetal sequences may not be detectable due to the low concentrations or loss of fetal DNA during sample processing. These false-negative results may lead to misdiagnosis without the use of internal positive controls. As such, a SNP panel was developed using SABER to serve as internal positive controls to detect fetal DNA in maternal plasma (Chow et al., 2007). The SNP panel consists of 9 SNPs that were selected from the RealSNP^{TM} Assay Database (www.realsnp.com, Sequenom) for a minor allele frequency of ≥35%. hME was used to determine the fetal and maternal genotypes while SABER was used to detect fetal-specific SNP alleles from the maternal plasma. Fetal-specific SNP alleles were detected in 36 out of 41 maternal plasma samples where the fetal genotype was informative. There were no false-positives and the SABER assays were able to detect at least one of the informative SNPs in all of the cases when the 9 SNPs were applied as a panel.

Universal fetal epigenetic markers can be developed for maternal plasma detection and hypomethylated maspin (SERPINB5) DNA is the first universal marker for fetal DNA in maternal plasma. Methylation status of maspin gene, a tumour suppressor gene expressed in the placenta, was explored using real-time quantitative methylation-specific PCR and MALDI-TOF MS (Chim et al., 2005). The methylation status of maspin gene promoter in paired placental tissues and maternal blood cells from pregnant women was analysed using bisulfite sequencing and found to be hypomethylated and densely methylated respectively. SNP genotyping using MALDI-TOF MS within the unmethylated maspin sequences in maternal plasma demonstrated that these sequences originated from the fetus. As maspin gene is located on chromosome 18, the allelic ratio for placenta-derived hypomethylated maspin in maternal plasma is useful for noninvasive detection of fetal trisomy 18 (Tong et al., 2006). Using a similar strategy to develop a noninvasive detection test for trisomy 21, Chim et al. (2008) went on to search for placental DNA-methylation markers on chromosome 21. Methylation-sensitive single nucleotide primer extension (Ms-SNuPE) followed by MALDI-TOF MS was used for high-throughput and cost-effective screening of CpG islands containing differentially methylated CpG sites in the placenta and maternal blood cells. Twenty-two CpG islands encompassing 255 CpG sites located on chromosome 21 were identified as potential candidates for development of circulating markers of fetal DNA. Of these, two novel fetal-DNA markers, U-PDE9A and U-CGI137 that are pregnancy-specific in

maternal plasma were shown to clear within 24 h postpartum. As these CpG islands that showed epigenetic differences between samples of placenta and maternal blood cells are located on chromosome 21, they are potential markers for noninvasive prenatal diagnosis of Down syndrome, either by the analysis of epigenetic allelic ratios or by direct comparison with a placenta-specific DNA methylation marker on a reference chromosome (Chim et al., 2008).

Besides exploring epigenetic differences in genomic DNA of placental tissues and maternal blood cells, differences in gene-expression patterns between placental tissues and maternal blood cells were also explored. Microarray-based strategy to identify placental mRNA that would be detectable in maternal plasma was developed (Tsui et al., 2004). PLAC4 mRNA, which is transcribed from chromosome 21 and expressed by the placenta, showed the highest absolute level of expression in the placenta and the largest relative difference in expression levels between the placenta and maternal blood cells. The determination of allelic ratio of a SNP rs8130833 in PLAC4 mRNA by MALDI-TOF MS hME in maternal plasma identified fetal trisomy 21 with a sensitivity of 90% and a specificity of 96.5% in ten cases of trisomy 21, demonstrating the potentials of using MALDI-TOF MS to measure plasma RNA-SNP allelic ratio as indicators of fetal aneuploidy status (Lo et al., 2007a).

Back to Real-Time in Digital

Digital PCR was first described in 1997 by Kalinina and colleagues by monitoring PCR in volumes of 10 nl in glass microcapillaries using FRET (TaqMan) assay (Kalinina et al., 1997). The assay was shown to be able to detect single starting template molecules in dilutions of genomic DNA and results suggest that it may be feasible to determine the number of template molecules in a sample by counting the number of positive PCRs in a set of replicate reactions using terminally diluted sample. Dennis Lo and colleagues were the first to utilise digital PCR for prenatal diagnosis of fetal aneuploidies (Lo et al., 2007b). Similar to the study described by Kalinina et al., PCR was set up to amplify extracted DNA that had been diluted to a concentration of one template molecule per reaction well except that 96-well and 384-well reaction plates were used in this study. Each reaction well could contain zero, one or more template molecules based on Poisson distribution. The number of positive and informative wells in a digital PCR run would then be counted. Two digital PCR methods, a polymorphic-dependent (digital RNA SNP) and a polymorphic-independent (digital relative chromosome dosage) were developed. Digital RNA SNP was used to determine allelic imbalance in the ratio of polymorphic alleles of an A/G SNP, rs8130833, located on PLAC4. As described earlier, PLAC4 is a placenta-expressed transcript located on chromosome 21. For an euploid fetus with heterozygous rs8130833, the A and G alleles would be equally represented in the fetal genome as 1:1 while a fetus with trisomy 21 would present with a ratio of 2:1 or 1:2. This ratio was determined by digital RNA SNP real-time PCR that targets A and G PLAC4 alleles and by using the sequential probability ratio test (SPRT), euploidy or aneuploidy could be classified depending on the degree of allelic imbalance. In cases where SPRT failed classification, additional 384-well plates were

analysed until the aggregated data become classifiable by SPRT. Computer stimulation and empirical validation confirmed the high accuracy of the disease classification algorithm by SPRT. Digital RNA SNP was applied on plasma RNA samples from nine women carrying euploid fetuses and four women carrying trisomy 21 fetuses and all cases were correctly classified. A second method named digital relative chromosome dosage (RCD) is polymorphic-independent and was used to assess whether the total copy number of chromosome 21 in a sample containing fetal DNA is overrepresented with respect to a reference chromosome. In this method, digital PCR analysis was used to determine chromosome dosage by calculating the proportion between nonpolymorphic loci on chromosome 21 (chr21) and a reference chromosome, chromosome 1 (chr1) in a sample. A fetus with trisomy 21 will therefore, exhibit a ratio of 3:2 in chr21:chr1 ratio while an euploid sample will exhibit a ratio of 2:2. Even without elaborate instrumentation, digital RCD allows the detection of trisomy 21 in samples containing 25% fetal DNA. The advantage of digital RCD over digital RNA SNP is that it is polymorphic-independent and measurements can still be conducted if the fetus is homozygous for the analysed SNP. The principles of digital RCD and digital RNA SNP bring about the development of digital relative mutation dosage (RMD) approach for monogenic diseases such as beta-thalassaemia. Digital real-time PCR assays were developed to discriminiate between mutant and wild-type alleles, and their allelic ratios were analysed using SPRT to determine whether an allelic imbalance is present. To enrich fetal DNA molecules that are shorter than maternal DNA fragments in maternal plasma, digital nucleic acid size selection (NASS) was developed. In this duplex digital PCR, two forward primers and one reverse primer were designed to amplify a short target region that overlaps with a long amplicon. When a DNA molecule with the same length as the expected long amplicon was amplified, both long and short amplicons were produced. When a DNA molecule is shorter than the expected long amplicon, only the short target region is amplified. The resulting long and short amplicons were detected by specific hybridisation probes or extension primers where only short amplicons were counted to obtain a higher effective fetal DNA fraction for digital RMD analysis. With this combined digital NASS/ RMD approach in digital PCR, locus-specific enrichment of fetal DNA can be performed without additional enrichment steps or extra volumes of maternal plasma for precise allelic discrimination and subsequent analysis of allelic imbalance (Lun et al., 2008a).

The novel nanofluidic biochip (Fluidigm, South San Francisco, CA) enhance the clinical applicability of using digital PCR for noninvasive prenatal diagnosis. The nanofluidic biochip utilises integrated channels and valves that partition mixtures of sample and reagents into 765 nanolitre volume reaction chambers. DNA molecules in each mixture are randomly partitioned into the 765 chambers of each panel. The chip is then thermocycled and imaged on Fluidigm's BioMark real-time PCR system and the positive chambers that originally contained 1 or more molecules can be counted by the digital array analysis software (Dube et al., 2008). With the advent of digital PCR, the concentrations of cell-free fetal DNA in maternal plasma can be precisely measured. Lun et al. (2008b) explored the variations of microfluidics digital PCR, real-time PCR and mass spectrometry in estimating the concentrations of male DNA in artificial mixtures of male and female DNA. The imprecisions of microfluidics digital PCR and nondigital real-time PCR are compared by measuring male fetal DNA in maternal plasma. Microfluidics digital PCR showed the least

quantitative bias for measuring the fractional concentration of male DNA and had a lower imprecision and higher clinical sensitivity than nondigital real-time PCR. The median fractional concentration of fetal DNA in maternal plasma was found to be 2-fold higher than previously reported for all 3 trimesters of pregnancy when microfluidics digital PCR was used. This suggests that the noninvasive detection of Down syndrome using fetal DNA from maternal plasma is technically more feasible than previously assumed with a decrement by a factor of ~4 in the number of analysed molecules required to diagnose Down syndrome (Lun et al., 2008b).

Digital PCR can also be applied to bisulfite-converted DNA for single-molecule high-resolution DNA methylation analysis and for increased sensitivity DNA methylation detection. Weisenberger et al. (2008) developed digital bisulfite genomic sequencing to efficiently determine single-base pair DNA methylation patterns on single-molecule DNA templates without an interim cloning step. Digital MethyLight was used to identify single-molecule, cancer-specific DNA hypermethylation events in the CpG islands of RUNX3, CLDN5 and FOXE1 present in the plasma samples from breast cancer patients (Weisenberger et al., 2008). The applications of digital PCR can thus be extended to the analysis of placenta-specific DNA methylation markers located on chromosomes 18 and 21 that were identified in previous placenta-specific methylation studies. The complementation of new technologies and strategies will allow clinical implementation of noninvasive prenatal diagnosis using cell-free nucleic acids in the maternal circulation.

References

Alberry M, Maddocks D, Hadi M, Metawi H, Hunt L, Abdel-Fattah S, Avent N, Soothill P. (2009) Quantification of cell free fetal DNA in maternal plasma in normal pregnancies and in pregnancies with placental dysfunction. *Am J Obstet Gynecol*, 200, 98.e1-6.

Avent N, Chitty L. (2006) Non-invasive diagnosis of fetal sex; utilisation of free fetal DNA in maternal plasma and ultrasound. *Prenat Diagn*, 26, 598-603.

Avent N. (2008) RHD genotyping from maternal plasma: guidelines and technical challenges. *Methods Mol Biol*, 444, 185-201.

Bauer M, Hutterer G, Eder M, Majer S, Leshane E, Johnson K, Peter I, Bianchi D, Pertl B. (2006) A prospective analysis of cell-free fetal DNA concentration in maternal plasma as an indicator for adverse pregnancy outcome. *Prenat Diagn*, 26, 831-836.

Beeson D, Golbus M. (1979) Anxiety engendered by amniocentesis. *Birth Defects*, 15, 191-197.

Bianchi D, Lo Y. (2001) Fetomaternal cellular and plasma DNA trafficking: the Yin and the Yang. *Ann N Y Acad Sci*, 945, 119-131.

Birch L, English C, O'Donoghue K, Barigye O, Fisk N, Keer J. (2005) Accurate and robust quantification of circulating fetal and total DNA in maternal plasma from 5 to 41 weeks of gestation. *Clin Chem*, 51, 312-320.

Brojer E, Zupanska B, Guz K, Orziñska A, Kaliñska A. (2005) Noninvasive determination of fetal RHD status by examination of cell-free DNA in maternal plasma. *Transfusion,* 45, 1473-80.

Bustamante-Aragones A, Rodriguez de Alba M, Gonzalez-Gonzalez C, Trujillo-Tiebas M, Diego-Alvarez D, Vallespin E, Plaza J, Ayuso C, Ramos C. (2008) Foetal sex determination in maternal blood from the seventh week of gestation and its role in diagnosing haemophilia in the foetuses of female carriers. *Haemophilia*, 14, 593-598.

Chan L, Leung T, Chan K, Tai H, Lau T, Wong E, Lo Y. (2003) Serial analysis of fetal DNA concentrations in maternal plasma in late pregnancy. *Clin Chem*, 49, 678-680.

Chan K, Zhang J, Hui A, Wong N, Lau T, Leung T, Lo K, Huang D, Lo Y. (2004) Size distributions of maternal and fetal DNA in maternal plasma. *Clin Chem*, 50, 88-92.

Chim S, Tong Y, Chiu R, Lau T, Leung T, Chan L, Oudejans C, Ding C, Lo Y. (2005) Detection of the placental epigenetic signature of the maspin gene in maternal plasma. *Proc Natl Acad Sci USA*, 102, 14753-14758.

Chim S, Jin S, Lee T, Lun F, Lee W, Chan L, Jin Y, Yang N, Tong Y, Leung T, Lau T, Ding C, Chiu R, Lo Y. (2008) Systematic search for placental DNA-methylation markers on chromosome 21: toward a maternal plasma-based epigenetic test for fetal trisomy 21. *Clin Chem*, 54, 500-511.

Chitty L. (1998) Antenatal screening for aneuploidy. *Curr Opin Obstet Gynecol*, 10, 91-96.

Chiu R, Lau T, Cheung P, Gong Z, Leung T, Lo Y. (2002a) Noninvasive prenatal exclusion of congenital adrenal hyperplasia by maternal plasma analysis: a feasibility study. *Clin Chem*, 48, 778-780.

Chiu R, Lau T, Leung T, Chow C, Chui H, Lo Y. (2002b) Prenatal exclusion of β thalassaemia major by examination of maternal plasma. *Lancet*, 360, 998-1000.

Choolani M, Bennett PR, Rodeck CH. Rhesus and other fetomaternal incompatibilities. (2006) In: Rimoin DL, Connor JM, Pyeritz RE, Korf B (eds). *Emery and Rimoin's Principles and Practice of Medical Genetics (5th edition)*. Churchill Livingstone, Philadelphia, USA, 2, 1727-1738.

Chow C, Chiu R, Tsui N, Ding C, Lau T, Leung T, Lo Y. (2007) Mass spectrometric detection of an SNP panel as an internal positive control for fetal DNA analysis in maternal plasma. *Clin Chem*, 53, 141-142.

Ding C, Chiu R, Lau T, Leung T, Chan L, Chan A, Charoenkwan P, Ng I, Law H, Ma E, Xu X, Wanapirak C, Sanguansermsri T, Liao C, Ai M, Chui D, Cantor C, Lo Y. (2004) MS analysis of single-nucleotide differences in circulating nucleic acids: applications to noninvasive prenatal diagnosis. *Proc Natl Acad Sci USA*, 101, 10762-10767.

Ding C, Lo Y. (2006) MALDI-TOF mass spectrometry for quantitative, specific, and sensitive analysis of DNA and RNA. *Ann NY Acad Sci*, 1075, 282-287.

Ding C. (2008) MALDI-TOF mass spectrometry for analyzing cell-free fetal DNA in maternal plasma. *Methods Mol Biol*, 444, 253-267.

Dube S, Qin J, Ramakrishnan R. (2008) Mathematical analysis of copy number variation in a DNA sample using digital PCR on a nanofluidic device. *PLoS ONE*, 3, e2876.

Farina A, Caramelli E, Concu M, Sekizawa A, Ruggeri R, Bovicelli L, Rizzo N, Carinci P. (2002) Testing normality of fetal DNA concentration in maternal plasma at 10-12 completed weeks' gestation: a preliminary approach to a new marker for genetic screening. *Prenat Diagn*, 22, 148-152.

Farina A, Sekizawa A, Sugito Y, Iwasaki M, Jimbo M, Saito H, Okai T. (2004) Fetal DNA in maternal plasma as a screening variable for preeclampsia. A preliminary nonparametric analysis of detection rate in low-risk nonsymptomatic patients. *Prenat Diagn*, 24, 83-86.

Finning K, Martin P, Soothill P, Avent N. (2002) Prediction of fetal D status from maternal plasma: introduction of a new noninvasive fetal RHD genotyping service. *Transfusion*, 42, 1079-1085.

Frommer M, McDonald L, Millar D, Collis C, Watt F, Grigg G, Molloy P, Paul C. (1992) A genomic sequencing protocol that yields a positive display of 5-methylcytosine residues in individual DNA strands. *Proc Natl Acad Sci USA*, 89, 1827-1831.

Galbiati S, Smid M, Gambini D, Ferrari A, Restagno G, Viora E, Campogrande M, Bastonero S, Pagliano M, Calza S, Ferrari M, Cremonsi L. (2005) Fetal DNA detection in maternal plasma throughout gestation. *Hum Genet*, 117, 243-248.

Galbiati S, Foglieni B, Travi M, Curcio C, Restagno G, Sbaiz L, Smid M, Pasi F, Ferrari A, Ferrari M, Cremonesi L. (2008) Peptide-nucleic acid-mediated enriched polymerase chain reaction as a key point for non-invasive prenatal diagnosis of beta-thalassemia. *Haematologica*, 93, 610-614.

Herman J, Graff J, Myöhänen S, Nelkin B, Baylin S. (1996) Methylation-specific PCR: a novel PCR assay for methylation status of CpG islands. *Proc Natl Acad Sci USA*, 93, 9821-9826.

Hyett J, Gardener G, Stojilkovic-Mikic T, Finning K, Martin P, Rodeck C, Chitty L. (2005) Reduction in diagnostic and therapeutic interventions by non-invasive determination of fetal sex in early pregnancy. *Prenat Diagn*, 25, 1111-1116.

Illanes S, Denbow M, Kailasam C, Finning K, Soothill P. (2007) Early detection of cell-free fetal DNA in maternal plasma. *Early Hum Dev*, 9, 563-566.

Kalinina O, Lebedeva I, Brown J, Silver J. (1997) Nanoliter scale PCR with TaqMan detection. *Nucleic Acids Res*, 25, 1999-2004.

Kowalcek I. (2007) Stress and anxiety associated with prenatal diagnosis. *Best Pract Res Clin Obstet and Gynaecol*, 21, 221-228.

Leung T, Zhang J, Lau T, Hjelm N, Lo Y. (1998) Maternal plasma fetal DNA as a marker for preterm labour. *Lancet*, 352, 1904-1905.

Leung T, Zhang J, Lau T, Chan L, Lo Y. (2001) Increased maternal plasma fetal DNA concentrations in women who eventually develop preeclampsia. *Clin Chem*, 47, 137-139.

Levine R, Qian C, Leshane E, Yu K, England L, Schisterman E, Wataganara T, Romero R, Bianchi D. (2004) Two-stage elevation of cell-free fetal DNA in maternal sera before onset of preeclampsia. *Am J Obstet Gynecol*, 190, 707-713.

Li Y, Zimmermann B, Rusterholz C, Kang A, Holzgreve W, Hahn S. (2004) Size separation of circulatory DNA in maternal plasma permits ready detection of fetal DNA polymorphisms. *Clin Chem*, 50, 1002-1011.

Li Y, Di Naro E, Vitucci A, Zimmermann B, Holzgreve W, Hahn S. (2005) Detection of paternally inherited fetal point mutations for β-thalassemia using size-fractionated cell-free DNA in maternal plasma. *JAMA*, 293, 843-849.

Li Y, Wenzel F, Holzgreve W, Hahn S. (2006a) Genotyping fetal paternally inherited SNPs by MALDI-TOF MS using cell-free fetal DNA in maternal plasma: influence of size fractionation. *Electrophoresis*, 27, 3889-3896.

Li Y, Holzgreve W, Kiefer V, Hahn S. (2006b) MALDI-TOF mass spectrometry compared with real-time PCR for detection of fetal cell-free DNA in maternal plasma. *Clin Chem*, 52, 2311-2312.

Li Y, Page-Christiaens G, Gille J, Holzgreve W, Hahn S. (2007) Non-invasive prenatal detection of achondroplasia in size-fractionated cell-free DNA by MALDI-TOF MS assay. *Prenat Diagn*, 27, 11-17.

Li Y, Holzgreve W, Hahn S. (2008a) Size fractionation of cell-free DNA in maternal plasma and its application in noninvasive detection of fetal single gene point mutations. *Methods Mol Biol*, 444, 239-251.

Li Y, Finning K, Daniels G, Hahn S, Zhong XY, Holzgreve W. (2008b) Noninvasive genotyping fetal Kell blood group (KEL1) using cell-free fetal DNA in maternal plasma by MALDI-TOF mass spectrometry. *Prenat Diagn*, 28, 203-208.

Lo Y, Corbetta N, Chamberlain P, Rai V, Sargent I, Redman C, Wainscoat J. (1997) Presence of fetal DNA in maternal plasma and serum. *Lancet*, 350, 485-487.

Lo Y, Tein M, Lau T, Haines C, Leung T, Poon P, Wainscoat J, Johnson P, Chang A, Hjelm N. (1998a) Quantitative analysis of fetal DNA in maternal plasma and serum: implications for noninvasive prenatal diagnosis. *Am J Hum Genet*, 62, 768-775.

Lo Y, Hjelm N, Fidler C, Sargent I, Murphy M, Chamberlain P, Poon P, Redman C, Wainscoat J. (1998b) Prenatal diagnosis of fetal RhD status by molecular analysis of maternal plasma. *N Engl J Med*, 339, 1734-1738.

Lo Y, Lau T, Zhang J, Leung T, Chang A, Hjelm N, Elmes R, Bianchi D. (1999) Increased fetal DNA concentrations in the plasma of pregnant women carrying fetuses with trisomy 21. *Clin Chem*, 45, 1747-1751.

Lo Y, Poon L. (2003) The ins and outs of fetal DNA in maternal plasma. *Lancet*, 361, 193-194.

Lo Y, Tsui N, Chiu R, Lau T, Leung T, Heung M, Gerovassili A, Jin Y, Nicolaides K, Cantor C, Ding C. (2007a) Plasma placental RNA allelic ratio permits noninvasive prenatal chromosomal aneuploidy detection. *Nat Med*, 13, 218-223.

Lo Y, Lun F, Chan K, Tsui N, Chong K, Lau T, Leung T, Zee B, Cantor C, Chiu R. (2007b) Digital PCR for the molecular detection of fetal chromosomal aneuploidy. *Proc Natl Acad Sci USA*, 104, 13116-13121.

Lun F, Tsui N, Chan K, Leung T, Lau T, Charoenkwan P, Chow K, Lo W, Wanapirak C, Sanquansermsri T, Cantor C, Chiu R, Lo Y. (2008a) Noninvasive prenatal diagnosis of monogenic diseases by digital size selection and relative mutation dosage on DNA in maternal plasma. *Proc Natl Acad Sci USA*, 105, 19920-19925.

Lun F, Chiu R, Chan K, Leung T, Lau T, Lo Y. (2008b) Microfluidics digital PCR reveals a higher than expected fraction of fetal DNA in maternal plasma. *Clin Chem*, 54, 1664-1672.

Minon J, Gerard C, Senterre J, Schaaps J, Foidart J. (2008) Routine fetal RHD genotyping with maternal plasma: a four-year experience in Belgium. *Transfusion,* 48, 373-381.

Nasis O, Thompson S, Hong T, Sherwood M, Radcliffe S, Jackson L, Otevrel T. (2004) Improvement in sensitivity of allele-specific PCR facilitates reliable noninvasive prenatal detection of cystic fibrosis. *Clin Chem*, 50, 694-701.

Norbury G & Norbury C. (2008) Non-invasive prenatal diagnosis of single gene disorders: How close are we? *Semin Fetal Neonatal Med*, 13, 76-83.

Pertl B, Sekizawa A, Samura O, Orescovic I, Rahaim P, Bianchi D. (2000) Detection of male and female fetal DNA in maternal plasma by multiplex fluorescent polymerase chain reaction amplification of short tandem repeats. *Hum Genet*, 106, 45-49.

Pertl B, Bianchi D. (2001) Fetal DNA in maternal plasma: emerging clinical applications. *Obstet Gynecol*, 98, 483-490.

Picchiassi E, Coata G, Fanetti A, Centra A, Pennacchi L, Di Renzo G. (2008) The best approach for early prediction of fetal gender by using free fetal DNA from maternal plasma. *Prenat Diagn*, 28, 525-530.

Purwosunu Y, Sekizawa A, Okai T. (2008) Detection and quantification of fetal DNA in maternal plasma by using LightCycler technology. *Methods Mol Biol*, 444, 231-238.

Ragoussis J, Elvidge G, Kaur K, Colella S. (2006) Matrix-assisted laser desorption/ionisation, time-of-flight mass spectrometry in genomics research. *PLoS Genet,* 2, e100.

Rijnders R, van der Schoot C, Bossers B, De Vroode M, Christiaens G. (2001) Fetal sex determination from maternal plasma in pregnancies at risk for congenital adrenal hyperplasia. *Obstet Gynecol*, 98, 374-378.

Rijnders R, van der Luijt R, Peters E, Goeree J, van der Schoot C, Ploos Van Amstel J, Christiaens G. (2003) Earliest gestational age for fetal sexing in cell-free maternal plasma. *Prenat Diagn*, 23, 1042-1044.

Rouillac-Le Sciellour C, Puillandre P, Gillot R, Baulard C, Metral S, Le Van Kim C, Cartron JP, Colin Y, Brossard Y. (2004) Large-scale pre-diagnosis study of fetal RHD genotyping by PCR on plasma DNA from RhD-negative pregnant women. *Mol Diagn*, 8, 23-31.

Sekizawa A, Jimbo M, Saito H, Iwasaki M, Matsuoka R, Okai T, Farina A. (2003) Cell-free fetal DNA in the plasma of pregnant women with severe fetal growth restriction. *Am J Obstet Gynecol*, 188, 480-484.

Shimada K, Murakami K, Shozu M, Segawa T, Sumitani H, Inoue M. (2004) Sex-determining region Y levels in maternal plasma: Evaluation in abnormal pregnancy. J Obstet Gynaecol Res, 30, 148-154.

Swinkels D, de Kok J, Hendriks J, Wiegerinck E, Zusterzeel P, Steegers E. (2002) Hemolysis, elevated liver enzymes, and low platelet count (HELLP) syndrome as a complication of preeclampsia in pregnant women increases the amount of cell-free fetal and maternal DNA in maternal plasma and serum. *Clin Chem*, 48, 650-653.

Tang N, Leung T, Zhang J, Lau T, Lo Y. (1999a) Detection of fetal-derived paternally inherited X-chromosome polymorphisms in maternal plasma. *Clin Chem*, 45, 2033-2035.

Tang K, Fu D, Julien D, Braun A, Cantor C, Köster H. (1999b) Chip-based genotyping by mass spectrometry. *Proc Natl Acad Sci USA*, 96, 10016-10020.

Thelwell N, Millington S, Solinas A, Booth J, Brown T. (2000) Mode of action and application of Scorpion primers to mutation detection. *Nucleic Acids Res,* 28, 3752-3761.

Tjoa M, Oudejans C, van Vugt J, Blankenstein M, van Wijk I. (2004) Markers for presymptomatic prediction of preeclampsia and intrauterine growth restriction. *Hypertens Pregnancy*, 23, 171-189.

Tolson D, Nicholson N. (1998) Sequencing RNA by a combination of exonuclease digestion and uridine specific chemical cleavage using MALDI-TOF. *Nucleic Acids Res*, 26, 446-451.

Tsui N, Chim S, Chiu R, Lau T, Ng E, Leung T, Tong Y, Chan K, Lo Y. (2004) Systematic micro-array based identification of placental mRNA in maternal plasma: towards non-invasive prenatal gene expression profiling. *J Med Genet*, 41, 461-467.

Vainer O, Katokhin A, Kustov S, Vlassov V, Laktionov P. (2008) A new Y chromosome marker for noninvasive fetal gender determination. *Ann N Y Acad Sci*, 1137, 157-161.

Van der Schoot C, Soussan A, Koelewijn J, Bonsel G, Paget-Christiaens L, de Haas M. (2006) Non-invasive antenatal RHD typing. *Transfus Clin Biol*, 13, 53-57.

Van der Schoot C, Hahn S, Chitty L. (2008) Non-invasive prenatal diagnosis and determination of fetal Rh status. *Semin Fetal Neonatal Med*, 13, 63-68.

Vecchione G, Tomaiuolo M, Sarno M, Colaizzo D, Petraroli R, Matteo M, Greco P, Grandone E, Margaglione M. (2008) Fetal sex identification in maternal plasma by means of short tandem repeats on chromosome X. *Ann N Y Acad Sci*, 1137, 148-156.

Weinman J, Johnston M. (1988) Stressful medical procedures: analysis of the effects of the psychological intervention and of the stressfulness of the procedures. *In Maes* S (eds). *Topics in Health Psychology* Chichester, J. Wiley, 205-218.

Weisenberger D, Trinh B, Campan M, Sharma S, Long T, Ananthnarayan S, Liang G, Esteva F, Hortobagyi G, McCormick F, Jones P, Laird P. (2008) DNA methylation analysis by digital bisulfite genomic sequencing and digital MethyLight. *Nucleic Acids Res*, 36, 4689-4698.

Zhong X, Burk M, Troeger C, Jackson L, Holzgreve W, Hahn S. (2000) Fetal DNA in maternal plasma is elevated in pregnancies with aneuploid fetuses. *Prenat Diagn*, 20, 795-798.

Zhong X, Holzgreve W, Hahn S. (2001) Circulatory fetal and maternal DNA in pregnancies at risk and those affected by preeclampsia. Ann N Y *Acad Sci,* 945, 138-140.

Zhong X, Holzgreve W, Hahn S. (2002) The levels of circulatory cell free fetal DNA in maternal plasma are elevated prior to the onset of preeclampsia. *Hypertens Pregnancy*, *21*, 77-83.

Zimmermann B, El-Sheikhah A, Nicolaides K, Holzgreve W, Hahn S. (2005) Optimized real-time quantitative PCR measurement of male fetal DNA in maternal plasma. *Clin Chem*, *51*, 1598-1604.

In: Clinical Chemistry Research ISBN 978-1-60692-517-1
Editors: Brian H. Mitchem and Charles L. Sharnham

Chapter VI

Polymeric Nanoparticles as Carrier Systems: How Does the Material and Surface Charge Affect Cellular Uptake?

***Anna Musyanovych*[*1] , *Katharina Landfester*[1] *and Volker Mailänder*[2]**
[1] Max Planck Institute for Polymer Research, Mainz, Germany
Institute of Organic Chemistry III – Macromolecular Chemistry
and Organic Materials, University of Ulm, Ulm, Germany.
[2] Internal Medicine III, Johann-Gutenberg-University Clinic, Mainz, Germany
Institute for Clinical Transfusion Medicine and Immunogenetics Ulm,
Department of Transfusion Medicine, University of Ulm, Ulm, Germany.

Abstract

In recent years, polymeric nanoparticles have emerged as a powerful tool in bio-related fields. Their application in the diagnostics and drug delivery systems is a rapidly advancing research area. A detailed understanding of particle-cell interaction is essential and of immense interest in order to create a specific carrier for each particular application need. Changes in the structural and functional properties of the particle, namely chemical composition, surface charge and morphology, can significantly affect particle-cell interaction. In this chapter, we consider the cellular uptake of nanoparticles as a function of several parameters, such as polymeric material (polystyrene- or polyester-based), surfactant type (nonionic versus ionic), surface charge sign (cationic versus anionic), surface groups' density, and type of cell line. Furthermore, the influence of surface charge sign on the uptake mechanism of polystyrene particles was studied on the example of HeLa cells. The particle uptake efficiency was evaluated as a function of different factors (e.g. temperature, presence of drugs, etc.) known to inhibit the endocytosis.

* E-mail: musyanov@mpip-mainz.mpg.de Tel.: +49(0)6131 379-248 Fax: +49(0)6131 379-370

1. Introduction

Polymeric particles in the sub-micrometer size range are extensively utilized in biomedical applications[1-8]. Their main advantages over the others nanoparticular systems such as liposomes, micelles, etc., are their increased colloidal stability, their chemical resistance, and their simple formulation procedures. A growing interest in the development of nanoparticles as specific carriers for therapeutic, contrasting or imaging agents is generally focused on their tissue permeability. The drugs encapsulated inside a nanoparticle can be efficiently protected against enzymatic and hydrolytic degradation. Understanding the interactions of nanoparticles with cells and establishing the effects that influence the intracellular uptake of the nanoparticles are the crucial tasks for improving the delivery of bioactive agents.

Over the past decades, the cellular uptake of various polymeric micro- and nanoparticles, prepared from natural or synthetic polymers has been extensively described in the literature. Unfortunately most studies were carried out in different systems of synthesis and therefore it is hard to compare these studies among each other. Recent studies demonstrate that the rate and extent of particle uptake can be influenced by many factors: i) concentration of nanoparticles in the medium[9, 10]; ii) incubation time and temperature[9, 11]; iii) cells type and density[12]; iv) encapsulated drug; v) polymer material[13]; vi) size and surface characteristics of the particles[11, 14]; vii) etc., which determines the particle adsorption/adhesion to and interaction with the living cells.

Müller et al.[15] studied the uptake of negatively charged polystyrene particles with different sizes (100, 200, and 500 nm) and different surface hydrophobicity in HL60 cells. The authors reported that hydrophobic particles were taken up more efficiently in the cells compared to the hydrophilic ones. An increase in cellular uptake was also observed with increasing particle size. Uptake studies of polystyrene particles (50, 100, 200, 500, and 1000 nm) in Caco-2 cells were reported by Win and Feng[10]. All of the particles were negatively charged in the range of -18 to -37 mV. However, in contrast to Müller et.al.[15] the obtained results show that the uptake of particles decreases with the increase of the particle size. The exception were the 50 nm particles, which showed the lowest uptake efficiency, indicating therefore that there may be a limit below which the particle size does not play a significant role in the uptake mechanism. Such particles are treated by the cell as other macromolecules that either required a specific receptor for internalization or a channel. The explanation for the contrary results in the uptake of the same size particles reported by Müller et al.[15] and Win and Feng[10] could be related to the difference in the cell type used in their studies. A size- and cell type-dependent particle uptake was reported by Zauner et al.[12]. The authors used different sized negatively charged polystyrene particles (20 nm, 93 nm, 220 nm, 560 nm, and 1010 nm) for in vitro uptake studies in six different cell lines (HUVEC, ECV 304, HNX 14C, KLN 205, HepG2 and Hepa 1-6). It was found that different cell types have different cut-off values for the size of particles that can be taken up, although the particles in the size range of 100-220 nm were taken up by all cell lines efficiently. The uptake and distribution of colored polystyrene microspheres of much bigger sizes (0.75 μm, 2 μm, and 4.5 μm) were studied in intestinal lymphoid tissues[16]. Particles of all sizes were found in Peyer's patches; however, the density of 0.75 μm microspheres was higher as compared with

the other particles. The interaction of polystyrene particles with the inflamed tissue of experimental model colitis as a function of particle size was studied by Lamprecht et. al.[17]. Particles used for the studies had an average diameter of 100 nm, 1000 nm, and 10 μm and possessed a negatively charged surface. A higher deposition rate was observed for smaller particles. Furthermore, it was proposed that particles possessing negative charge may adhere more readily to inflamed tissues, especially in the stomach[18], which contain high concentrations of positively charged proteins incorporated into the cell membrane, and therefore the affinity to negatively charged substances increases.

The effect of the particle material was studied for example for biodegradable fluorescent PLGA and polystyrene nanoparticles (500 nm) by Pietzonka et al.[13]. From the obtained uptake results in Caco-2 cells the authors concluded that both particle types were not taken up by Caco-2 monolayers and explain these results with the physical properties of the particles such as size, surface charge, and hydrophobicity. Several authors have extensively reviewed this subject[19-21].

Although it is known that the size and the surface properties of the nanoparticles play a key role in a cellular uptake[22], more detailed studies are lacking which could clarify the uptake behavior of nanoparticles as a function of polymer nature and surface charge. Moreover, the variety in the analytical methods and experimental models that have been used to investigate the particle uptake results in difficulties to compare the data obtained from different systems. Also the studied material is not always well characterized. The commercially available polymer latex particles, which are commonly used for the cellular uptake study, have different physical properties depending on the type of surfactant and initiator employed during the polymerization process, components that are not given in the data sheet and are treated as proprietary information by most suppliers.

The current chapter focuses on studies of the nanoparticle cellular uptake as a function of several parameters, including polymer and surfactant type (nonionic versus ionic), surface charge (cationic versus anionic), surface groups' density, and the effect of the cell type. Experiments were performed using non-biodegradable carboxyl- or amino-functionalized polystyrene and biocompatible and biodegradable poly(L-lactide) (PLLA), poly(ε-caprolactone) (PCL), and poly(D,L-lactide-co-glycolide) 50:50 (PLGA) latex particles. The uptake experiments were performed without using any (toxic) transfection agent. As cell lines we chose HeLa as an adherent cell line which is well established in cell culture labs, mesenchymal stem cells for their potential in regenerative medicine, KG1a as model for CD34+ hematopoetic stem cells and Jurkat as model for T cells. Furthermore, in order to determine whether the route of uptake depends on the nanoparticles surface characteristics, negatively and positively charged polystyrene particles of the same size were used for uptake experiments in HeLa cells in the presence of different inhibitors in order to obtain information about the uptake mechanism.

All analyzed nanoparticles presented here were synthesized using the miniemulsion process. "Miniemulsion" generally implies a method that allows one to create small stable droplets in a continuous phase by applying high shear stress[23]. Under high shear, e.g. ultrasonication, the broadly distributed macrodroplets are broken into narrowly distributed, defined small nanodroplets in the size range between 50 and 500 nm. The size of the droplets mainly depends on the type and the amount of the emulsifier used in the particular system.

Polystyrene particles were prepared by free-radical polymerization of the monomer(s) within nanodroplets (Scheme 1)[24, 25]. This type of heterophase polymerization enables to functionalize the nanoparticles surface in a controlled manner. The combination of emulsion/solvent evaporation method and miniemulsion technique was applied in order to obtain biodegradable polyester-based nanoparticles from preformed polymer prior to the emulsification process (Scheme 2)[26].

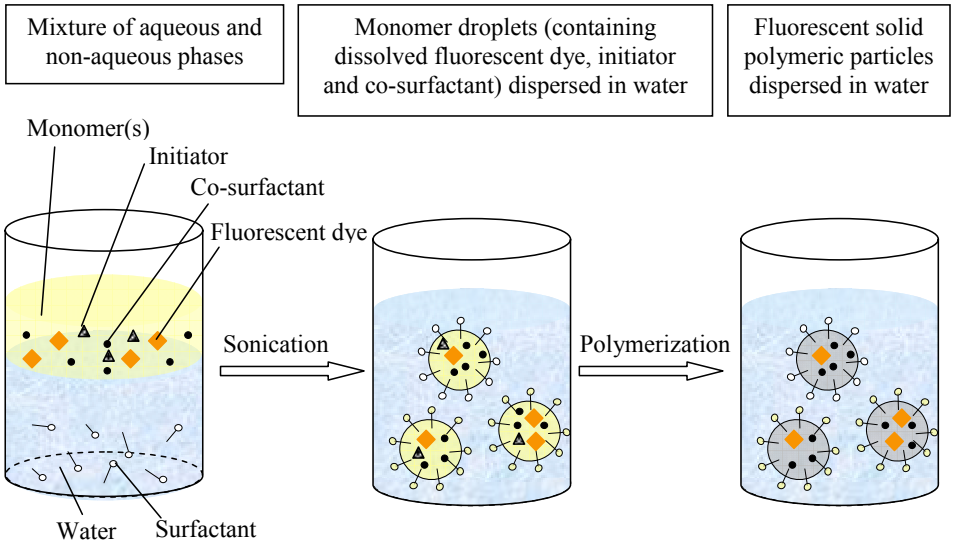

Scheme 1. Synthesis of polystyrene-based nanoparticles via the miniemulsion process.

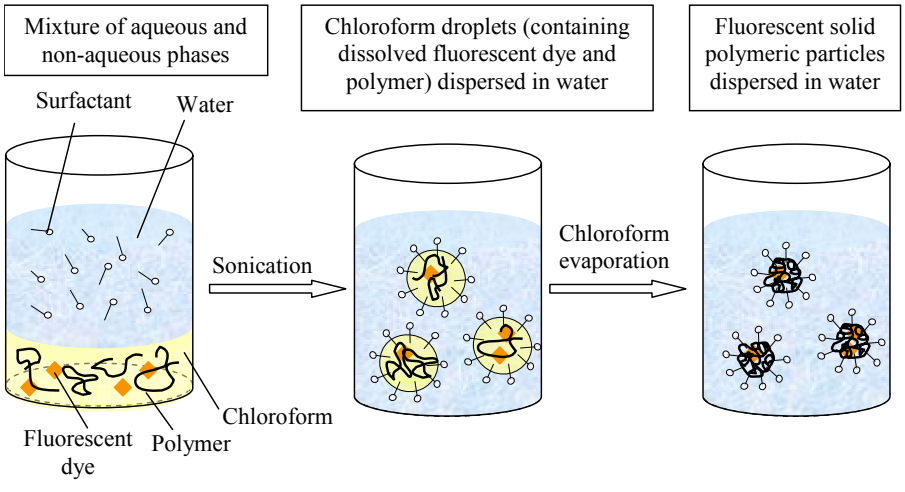

Scheme 2. Formation of biodegradable nanoparticles from preformed polymer via the miniemulsion process.

An encapsulated hydrophobic fluorescent dye (i.e. N-(2,6-diisopropylphenyl)-perylene-3,4-dicarbonacidimide (PMI)) was used as a model marker in order to study the entrapment efficiency and diffusion yield out of the particle.

2. Polystyrene Nanoparticles

2.1. Synthesis and Characterization

Initial experiments were carried out to synthesize pure polystyrene particles and particles composed of polystyrene and functional comonomers, i.e. negatively charged acrylic acid and positively charged aminoethyl methacrylate. Depending on the type and amount of comonomer used during polymerization, the particle surface is comprised of long or short chains of the hydrophilic segments of the copolymer between styrene and functionalized monomer. Moreover, performing the polymerization with different surfactants (non-ionic or ionic) will results in polymeric particles which exhibit an additional steric layer or electrostatic barrier around the particle surface.

In order to prevent polymerization of the hydrophilic monomer in the water phase and to avoid the presence of the hydrophilic groups originated from the initiator, the polymerization was started by using the hydrophobic initiator V-59. Latex particles were synthesized either in the presence of low molecular weight ionic surfactants, i.e. SDS and CTMA, or a non-ionic polymeric surfactant, i.e. Lutensol AT50. Their chemical structures are shown in Figure 1. In Table 1, the analytical characteristics of functionalized particles are summarized.

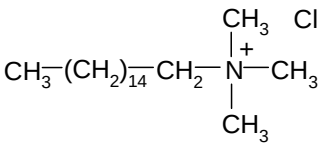

Cetyltrimethylammonium chloride

(CTMA-Cl)

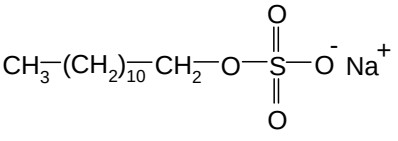

Sodium dodecyl sulfate

(SDS)

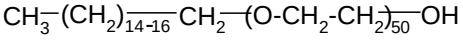

(Lutensol AT50)

Figure 1. Chemical structures of the surfactants used for particle preparation.

It can be seen, that the particles stabilized with Lutensol AT50 are slightly bigger in size compared to those obtained with ionic surfactant. However, this difference is not significant regarding the uptake mechanism of particles, as it has been shown earlier that no size-dependent changes for particles within a diameter range of 100-200 nm[12, 27] can be observed. The particle size of the carboxyl functionalized latexes stabilized with SDS is

relatively constant till 10 wt% of added acrylic acid. At higher amounts of acrylic acid, the diameter sharply increased reaching an average value of 140 nm. The increase in particle size with the increase of the acrylic acid amount can be explained by the formation of a "hairy" layer around the particle, which is mainly composed of hydrophilic polyacrylic acid units. The size of amine functionalized particles is not strongly dependent on the initial amount of functional monomer and was in the range between 110 and 130 nm. More detailed information regarding the polymerization mechanism can be found in ref.[24].

Table 1. Characteristics of the fluorescent polystyrene-based latex particles. The total amount of monomer(s) used during the polymerization corresponds to 6 g.

Sample Name	Functional comonomer		Surfactant type	D_h, nm	ζ, mV	PMI, $mg/g_{polymer}$
	Type	Amount, g (wt%)*				
L0	Acrylic acid	0 (0)	Lutensol AT50	217	-12	0.29
AL1		0.06 (1)		185	- 32	0.19
AL2		0.12 (2)		160	- 44	0.27
AL3		0.18 (3)		168	- 46	0.31
S0		0 (0)	SDS	101	-58	0.28
VS1		0.06 (1)		99	-50	0.43
VS2		0.12 (2)		98	-59	0.40
VS3		0.18 (3)		100	-62	0.40
VS5		0.30 (5)		97	-64	0.49
VS10		0.60 (10)		103	-51	0.48
VS15		0.90 (15)		148	-42	0.37
VS20		1.80 (20)		150	-59	0.44
NL1	AEMH	0.06 (1)	Lutensol AT50	175	-8	0.18
NL2		0.12 (2)		162	-2	0.27
NL3		0.18 (3)		154	5	0.37
NL5		0.30 (5)		160	27	0.33
NL10		0.60 (10)		155	29	0.35
NL15		0.90 (15)		143	32	0.21
NL20		1.80 (20)		119	36	0.36
C0		0.06 (0)	CTMA-Cl	110	45	0.35
NC1		0.12 (1)		114	48	0.36
NC2		0.18 (2)		118	45	0.32
NC3		0.30 (3)		113	45	0.37
NC5		0.60 (5)		127	51	0.39
NC10		0.90 (10)		133	54	0.36
NC15		1.80 (15)		134	57	0.33
NC20		0.06 (20)		126	52	0.32

* - related to the total amount of monomer(s) used in the polymerization.

Electron microscopy studies of fluorescent polystyrene-based nanoparticles revealed their regular, spherical, and smooth shape without any visible defects. TEM images of polySt-polyAA latexes obtained with 1 and 3 wt% AA and different surfactants are presented in Figure 2.

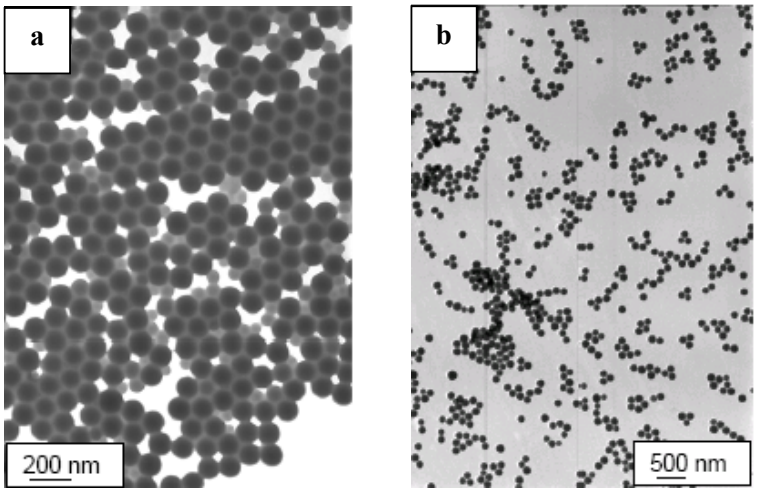

Figure 2. TEM images of carboxyl functionalized polystyrene particles stabilized with non-ionic and ionic surfactant: a - with 3 wt% of acrylic acid (sample AL1), b - with 1 wt% of acrylic acid (sample VS1). (Image (a) is taken from ref.[24], Figure 4a. Copyright American Chemical Society. Reproduced with permission).

The amount of carboxyl and amino groups, which are present on the particle surface, was quantitatively determined by a polyelectrolyte titration. This method is based on the interaction between oppositely charged groups on the particle surface and polyelectrolyte chain[28, 29]. The density of carboxyl and the number of amino groups on the particle surface are presented in Table 2.

Table 2. Surface charge characteristics of functionalized polystyrene latex samples.

Sample Name	Amount of COO^- groups per		Sample Name	Amount of NH_3^+ groups per	
	particle	nm^2		particle	nm^2
AL1	30275	0.28	NL1	9883	0.10
AL2	53857	0.67	NL2	13679	0.17
AL3	98835	1.12	NL3	19126	0.26
			NL5	40545	0.50
			NL10	70761	0.94
			NL15	74291	1.16
			NL20	59851	1.35
VS1	5864	0.19	NC1	3265	0.08
VS2	9266	0.31	NC2	4809	0.11
VS3	12275	0.39	NC3	4811	0.12
VS5	11847	0.40	NC5	9623	0.19
VS10	21733	0.66	NC10	17218	0.31
VS15	150844	2.19	NC15	29319	0.52
VS20	317821	4.48	NC20	34895	0.70

Comparing the titration data for polySt-polyAA samples, it can be seen that an average surface charge density of the carboxyl groups prepared with a non-ionic surfactant is considerably higher than that with an anionic one if the same amount of acrylic acid was used. The same trend was found for the polySt-polyAEMH samples. It can be also seen that the dense monolayer of carboxylic groups 0.68 nm^2 per COOH[30] (1.47 groups per nm^2) on the particles prepared with non-ionic surfactant was almost achieved with 3 wt% of acrylic acid, and more than 10 wt% of acrylic acid was required in the case of anionically stabilized particles.

2.2. In Vitro Cellular Uptake of Polystyrene-Based Nanoparticles

For all types of polystyrene particles described in the current chapter, the averaged cell viability was observed to be around 96%±2 after incubation for 24 h, i.e. cell viability was not significantly affected after nanoparticle incubation. Even the high density of surface functional groups, independently from the charge nature, did not show any effect on the cell viability. A quantitative evaluation of particle uptake was performed by FACS experiments, counting the number of cells with incorporated fluorescent particles and normalizing the amount of nanoparticle uptake according to the amount of PMI per particle. To evaluate the difference between the particle surface characterizations (surfactant type and surface charge density), fluorescent carboxyl- and amino-functionalized polystyrene particles were incubated with HeLa cells. The comparison of cellular uptake for each nanoparticle type is presented in Figure 3.

The results shown in Figure 3 demonstrate that the particle charge and functional groups density as well as a type of surfactant affect the cellular uptake efficiency. The amount of polystyrene particles taken up by HeLa cells after 24 h was observed to be higher in the case of non-ionically (Lutensol AT50) stabilized particles. An increase of fluorescence intensity is found especially in cells that have been exposed to amino-functionalized latex particles.

For particles stabilized with an ionic surfactant, the uptake of polySt-polyAEMH particles stays on the plateau value till 5 wt% of AEMH and then gradually increases with increasing amount of surface amino groups' density. Comparing the uptake data with the surface amino groups' density for amino-functionalized particles synthesized in the presence of Lutensol AT50 and CTMA-Cl one can see that in both cases a significant difference in the uptake is achieved when the amount of surface amino groups' was around 0.2 groups per nm^2. In the case of the non-ionic Lutensol AT50 and the cationic CTMA-Cl stabilized particles it corresponds to sample NL2 (0.17 NH_2 per nm^2) and NC5 (0.19 NH_2 per nm^2), respectively.

In contrast to amino functionalized particles, the uptake of carboxyl functionalized ones shows a slight increase in fluorescent intensity till the concentration of carboxyl groups reaches the monolayer density (1.47 COOH per nm^2). At higher densities of carboxyl groups, the uptake efficiency was inhibited. This inhibition has to be attributed to the swollen ("hairy") layer of polyacrylic acid chains on the particle surface that results in the hydrodynamic barrier between the particle and the cell membrane.

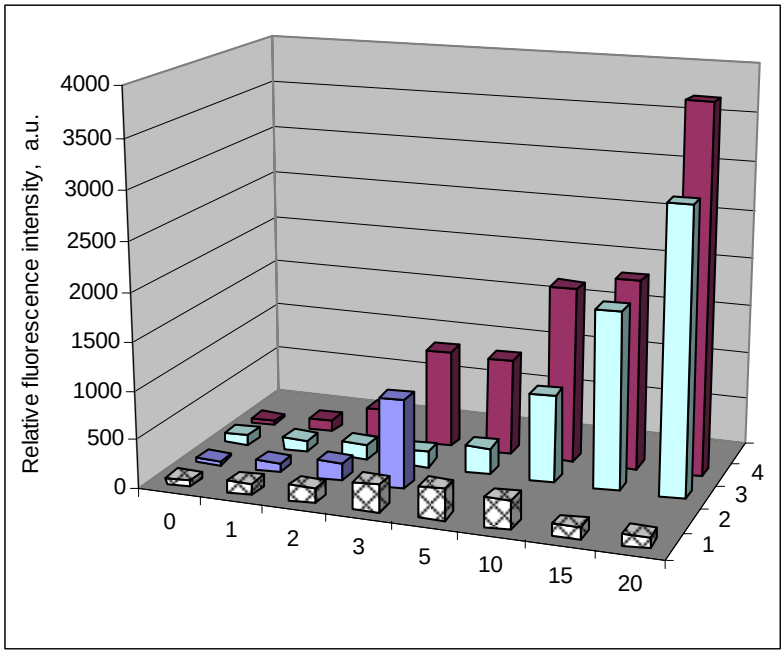

Figure 3. Uptake of fluorescent carboxyl- and amino-functionalized polystyrene particles in HeLa cells incubated for 24 h: (1: VS0-20; 2: AL0-3; 3: NC0-20; 4: NL0-20). Each bar corresponds to the normalized fluorescent intensity (nFL) and represents a mean value of the triplicate sample measurements.

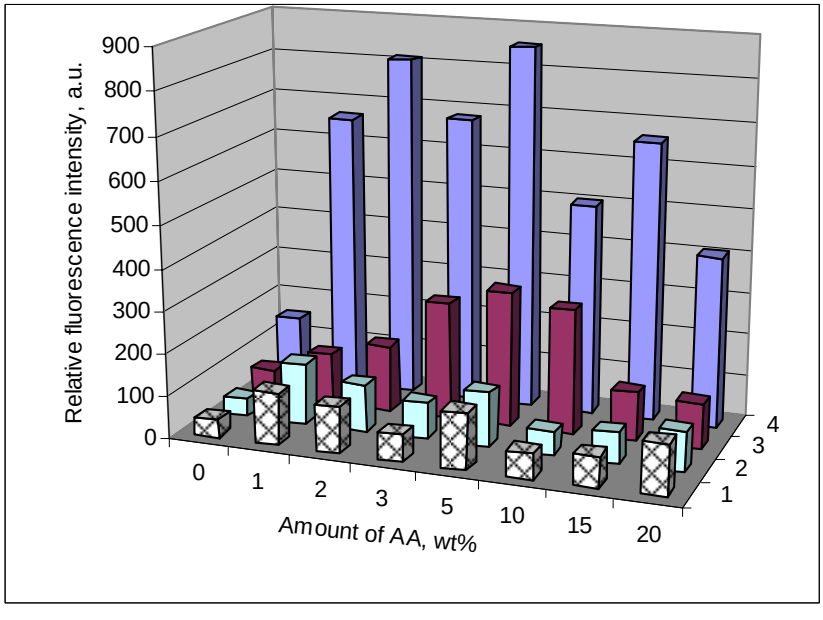

Figure 4. Uptake of fluorescent carboxyl-functionalized polystyrene particles stabilized with SDS in different cell lines incubated for 24 h with: (1: Jurkat; 2: KG1a; 3: HeLa; 4: MSC). Each bar corresponds to the normalized fluorescent intensity (nFL) and represents a mean value of the triplicate sample measurements.

In the next set of experiments the effect of particle surface charge and density was evaluated from the uptake experiments in different cell lines, such as Jurkat, KG1a, MSC, and HeLa. The experiments were carried out with amino and carboxyl functionalized particles synthesized in the presence of ionic surfactants. The obtained results are summarized in Figures 4 and 5 for polySt-AA and polySt-AEMH particles, respectively.

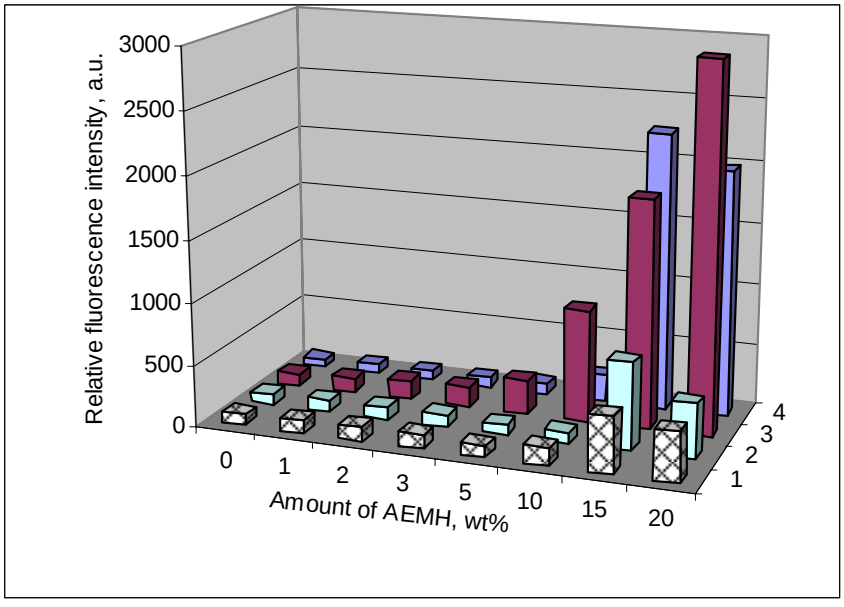

Figure 5. Uptake of fluorescent amino-functionalized polystyrene particles stabilized with CTMA-Cl in different cell lines incubated for 24 h with: (1: Jurkat; 2: KG1a; 3: HeLa; 4: MSC). Each bar corresponds to the normalized fluorescent intensity (nFL) and represents a mean value of the triplicate sample measurements.

It is apparent that the positively charged amino functionalized particles were taken up to a much greater extent than carboxyl-functionalized ones, independently from the cell type. This fact is expected knowing that the cell membrane possess a negative charge, and therefore the adhesion and subsequent internalization by endocytosis of positively charged nanoparticles inside the cell is favored for cationic nanoparticles. Similar results were also obtained with polylactide-based nanoparticles[31]. Regarding to the cell lines, amino-functionalized particles were taken up more efficiently by adherent MSC and HeLa cells (based on the FACS data). It is interesting to note, that although all particles possess approximately the same zeta-potential value, the increase in the uptake was observed only with a particles having high density of the surface amino groups. In the case of MSC and HeLa cells this amount corresponds to 0.31 groups per nm^2 and for Jurkat and KG1a cell lines it is 0.52 groups per nm^2. These findings indicate, that not the overall particle charge influences uptake, but the density of the charged groups which are strongly (covalently) bonded onto the particle surface are the main driving force in the uptake kinetics.

Carboxylated particles showed a clear uptake dependency only with HeLa cells. Particles with a lower density of carboxylic groups (up to 10 wt%) were taken up more efficiently,

compared to the highly charged ones. In the case of Jurkat or KG1a cell lines, even after 24 h incubation time, the particles appear not to be adsorbed onto the cell. A relatively high but not a systematic uptake/adsorption of particles was observed for MSC cells.

The location of the particles (exrtracellular or intracellular) was studied by CLSM measurements (see Figure 6 and 7 for HeLa and Jurkat cells, respectively). In these pictures the particles are shown in green as the incorporated dye (PMI) is emitting in the green part of the visible spectrum. The confocal fluorescent microscope defines an optical section of about 500 nm thickness (axial resolution) by focusing the laser light and selectively only collecting the light from this plane by passing the light through a pinhole. This avoids nearly all of the signals from below and above the focus plane of the objective Therefore the cell membrane is detected as a line surrounding the cytoplasm and not – as would be in conventional fluorescent microscopy – as a filled cell body. Other cellular structures like e.g. the cell nucleus are not fluorescently labeled. The lateral resolution is around 200 nm with an optimal setup of the CLSM.

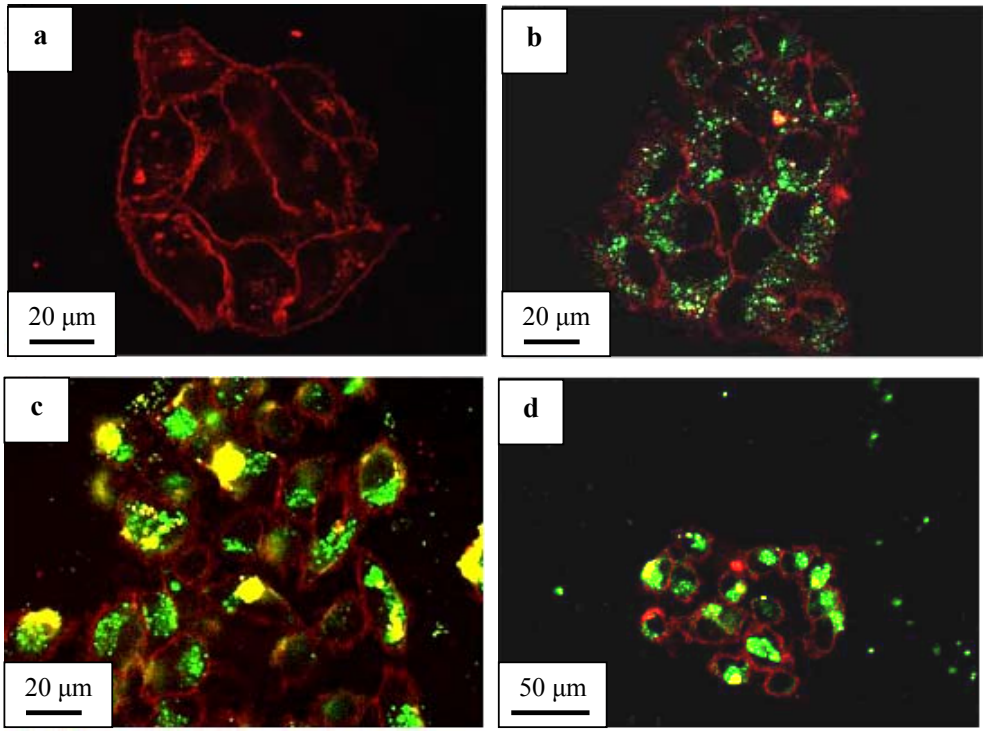

Figure 6. CLSM images of HeLa cells incubated for 24 h with amino functionalized polystyrene particles prepared in the presence of cationic surfactant (CTMA-Cl): a - cells without particles (control sample); b - NC3; c - NC15; d - NC20. The cell membrane has been stained by a red fluorescent dye (RH414).

Positively charged particles with low concentration of amino functionalized monomer (up to 5 wt%) were accumulated exclusively inside the cell, whereas particles with higher amounts of surface amino groups were found not only inside the cell but also attached to the cell membrane in the form of particle aggregates. No particles could be observed inside the

nucleus. The localization of negatively charged particles exhibit similar trends. With HeLa cells, the particles were taken up nearly uniformly by all cells. In Jurkat and KG1a cells the fluorescent signal was mainly restricted to cell membrane. In general, the rate of internalization of amino compared to carboxyl functionalized particles was approximately doubled, which correlates well with the FACS results.

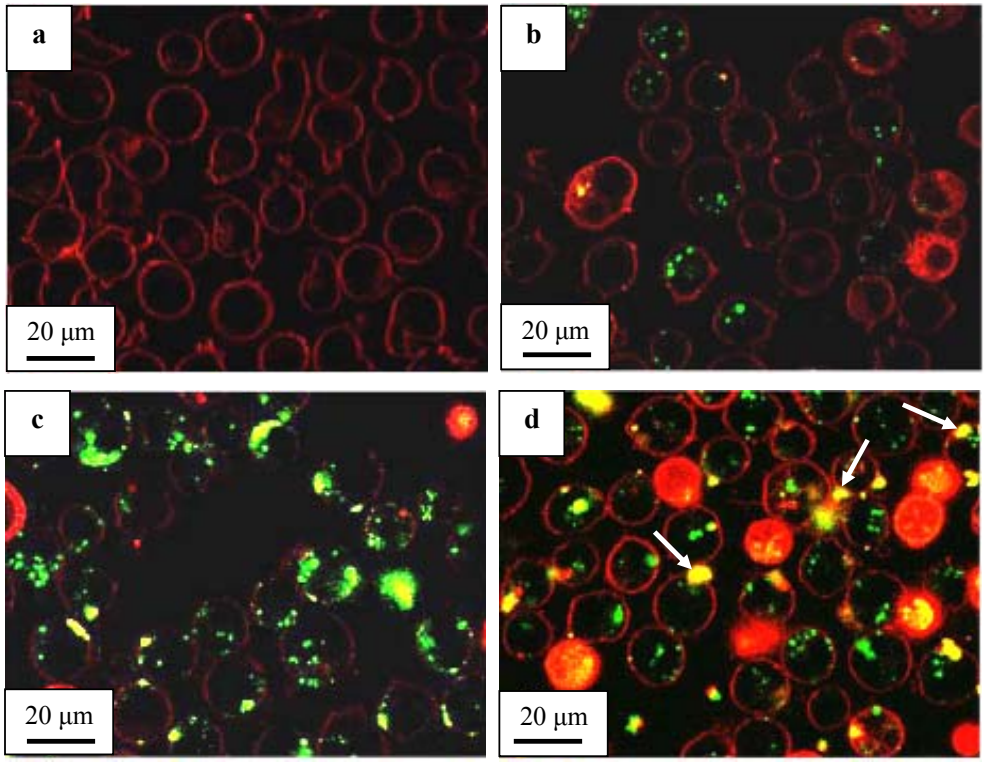

Figure 7. CLSM images of Jurkat cells incubated for 24 h with amino functionalized polystyrene particles prepared in the presence of cationic surfactant (CTMA-Cl): a - cells without particles (control sample); b - NC3; c - NC15; d - NC20. The cell membrane has been stained by a red fluorescent dye (RH414). Overlay of red and green fluorescence is depicted in yellow (arrow).

Electron microscopic studies were performed in order to visualize the location of the particles on a nanoscale range (Figure 8). The TEM images reveal that for HeLa cells (Figure 8a) the majority of the internationalized particles were located in the lysosomes of the cells and were therefore most likely taken up by an endocytotic pathway. In the case of Jurkat cells and KG1a, the particles are mostly observed near the cell membrane (Figure 8b for Jurkat cells).

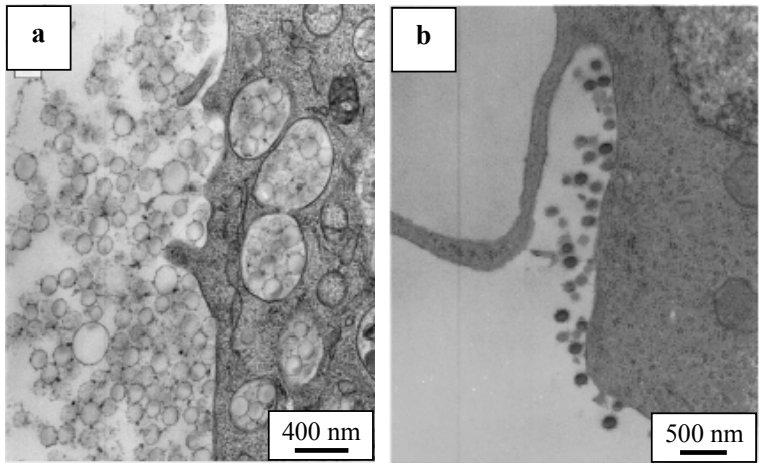

Figure 8. TEM images of: a - HeLa cells incubated for 24 h with amino-functionalized particles (sample NC3) and b - Jurkat cells incubated for 24 h with carboxyl-functionalized particles (sample VS20).

2.3. In Vitro Cellular Uptake of Polystyrene-Based Nanoparticles in the Presence of Inhibitors[32].

There are several pathways for supramolecular aggregates to enter the cells. Besides the phagocytic processes of specialized cell types (macrophages, dendritic cells) other cell types usually show different routes of uptake that are summarized as endocytotic pathways. Although it is generally assumed that particles in the size range of several till some hundreds nanometers have the ability to enter cells encapsulated in membrane vesicles, the mechanism of uptake and intracellular trafficking of the nanoparticles has been addressed only very recently[27, 31, 33-35]. Biologically active molecules and viruses[36-38] were used in order to study the mechanisms of endocytosis. Hereby, the distinct routes of uptake were identified. First indication that the uptake of extracellular material is not simply a budding of vesicles from the cell membrane was found by electron microscopy, as TEM showed that one type of these endocytotic vesicles was surrounded by a specific molecular machinery, i.e. a clathrin coated pit. Diverse receptors are known to be involved in endocytosis for specific cargoes[39], some of them concentrating in clathrin-rich or lipid raft regions. They signal through the membrane if a ligand has been bound and may thus trigger their internalization process[38]. For many years, numerous research groups have broadened our knowledge about the influence of different inhibitors on nanoparticles uptake. In most papers the examined nanoparticles were generally characterized in terms of their size, but not by the nature and density of charged groups, which impedes the comparison between different papers.

The influence of the charge (positively and negatively charge) of the nanoparticles on the uptake mechanisms was studied and if more than one endocytotic pathway is involved. The experiments were carried out with HeLa cells and the particle uptake efficiency was evaluated as a function of different factors (e.g. temperature, presence of drugs, etc.) known

to inhibit the endocytosis. Both test-particles (NC5 and S0) were of the same size, and therefore the difference in the uptake mechanism should mainly depend on the surface characteristics of the particles. The incubation time was limited to 1 h in order to prevent the activation of another endocytotic pathways by blocking one route of uptake[31, 40] For example Damke et al.[41] reported on dynamin-defective HeLa cells, which were able to internalize transferrin by a clathrin-independent pinocytotic pathway.

2.3.1. Effect of Temperature

Since all known endocytotic pathways are energy dependent, cooling of the cell culture to 4 °C should inhibit the process of uptake. Incubation at 4 °C resulted in an inhibition of endocytosis of about 60% (Figure 9)[32] which is comparable with the results of similar systems described in the literature[33].

2.3.2. Effect of Dynamin

Dynamin is known to be involved in clathrin and caveolin mediated endocytosis and also plays a role in some lipid raft-mediated processes[39]. The specific inhibitor dynasore was used to inhibit dynamin without affecting cell viability[42]. In the presence of dynasore, the endocytosis of the positively and negatively charged polystyrene particles was strongly inhibited indicating that uptake of these nanoparticles is highly dependent on dynamin (Figure 9)[32]. For the negatively charged particles, uptake inhibition was less pronounced but still significant.

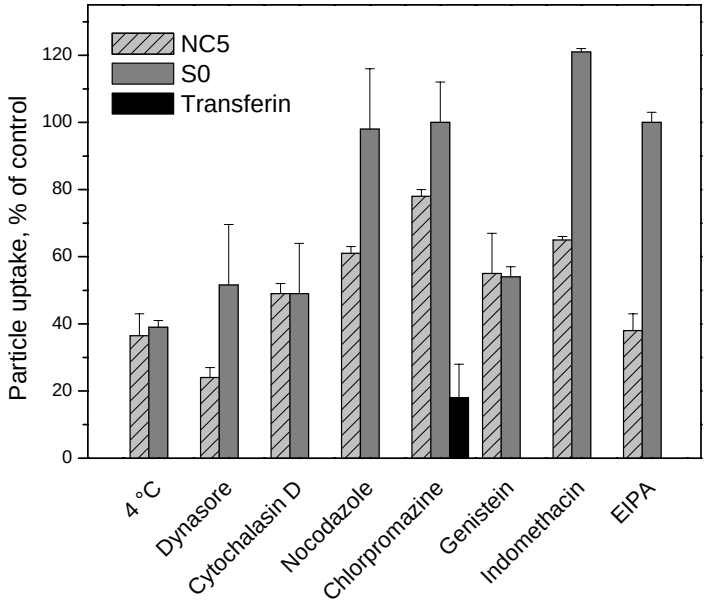

Figure 9. Uptake of positively and negatively charged polystyrene particles (or fluorescein-transferrin) into HeLa cells under different inhibitory conditions. HeLa cells were preincubated 30 min with the respective drugs and particle uptake within 1 h was determined by flow cytometry. Alternatively, cells were preincubated at 4 °C and particle incubation was done at 4 °C, too. Mean values and standard deviations of 2-3 independent triplicate experiments are given.

2.3.3. Effect of F-Actin and Microtubules

The cytoskeleton comprising actin, tubulin and intermediate filaments (e.g. vimentin) has a prominent role in endocytosis and trafficking of endocytotic vesicles. The function of F-actin can be inhibited by cytochalasin D. As shown in Figure 9, cytochalasin D strongly inhibited the endocytosis of the negatively and positively charged nanoparticles demonstrating that nanoparticle internalization is highly dependent on F-actin.

Microtubules which are also known to be involved in the uptake, can be disrupted by nocodazole[43]. While negatively and positively charged nanoparticles showed an analogous behavior under the previous conditions, here the surface charge made a difference (Figure 9): Nocodazole inhibited only the uptake of positively charged particles, whereas negatively charged particles were endocytosed as well as the control sample without any inhibitors.

In comparison to the control without the inibitor where nanoparticles are found in the cell (Figure 10b), confocal laser scanning microscopy shows that the positively charged particles in the presence of nocodazole are mainly co-localized with the membrane dye (Figure 10a) which indicates that they are either not endocytosed or, more likely, that the intracellular trafficking of the early endosomes was inhibited by the drug and the particles are trapped in endosomes that are located close to the inner side of the cell membrane. Electron microscopy revealed that particles were either not yet fully taken up in the presence of nocodazole or they remained close to the cell membrane (Figure 10c).

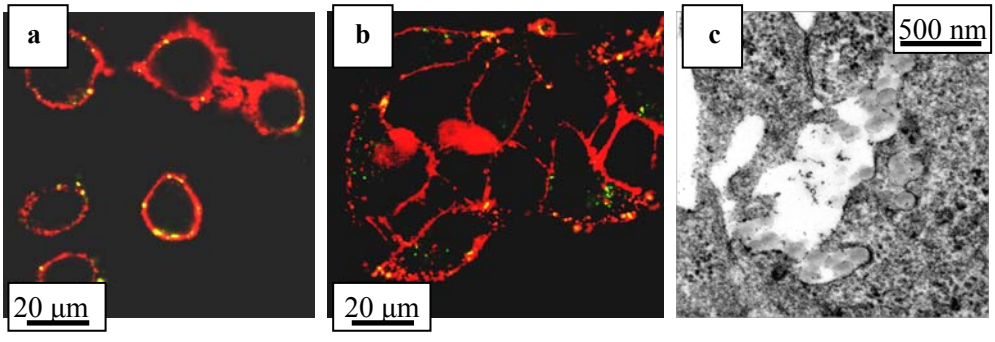

Figure 10. HeLa cells after 1 h incubation with positively charged particles (green) in the presence of nocodazole (a and c) or as a positive control without any drugs (b). The cell membrane has been stained by a red fluorescent dye (RH414). Co-localization of particles and cell membrane is shown in yellow. Particles were detected as not yet endocytosed by the cell and remained near the outer membrane (c: TEM image). (Taken from ref.[32], Figure 5. Copyright Wiley-VCH Verlag GmbH & Co. KGaA. Reproduced with permission).

2.3.4 Effect of the Clathrin Pathway and Contribution of Micropinocytosis

Chlorpromazine is known to inhibit clathrin assembly and disassembly[37]. As shown in Figure 9, the presence of this inhibitor resulted in a 20% uptake decrease of positively charged particles and was without a significant effect in the case of negatively charged particles. The participation of the clathrin pathway could also be confirmed by transmission

electron microscopy (TEM). As shown in Figure 11b, empty clathrin-coated pits are well visible in TEM images, whereas particles in clathrin-coated pits or vesicles were never seen. On the contrary, a situation like shown in Figure 8a has often been observed, where protrusions of the plasma membrane seem to extend from the cell membrane with a cluster of nanoparticles located between these protrusions. Also note that there is an abundance of intracellularly located nanoparticles just inside the cytoplasm in endocytotic vesicles that could be interpreted as nanoparticles that have just been endocytosed. Furthermore the clathrin-coated pit itself is a more rigid structure forming an endosomal invagination with a maximum diameter of 100 to 150 nm. Therefore, only uptake of single nanoparticles should be observed when the clathrin pathway is the predominating uptake mechanism while in Figure 8a and most of the other TEM observations several nanoparticles seemed to be endocytosed simultaneously.

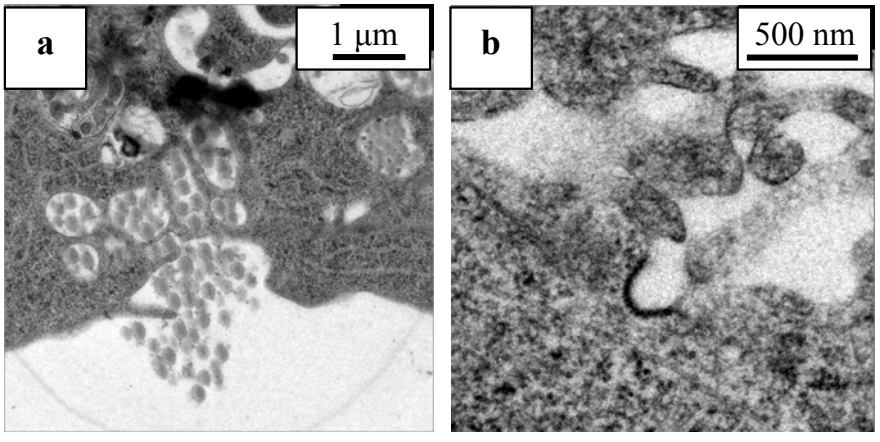

Figure 11. TEM images of HeLa cells incubated with positively charged polystyrene nanoparticles: a - HeLa cell during endocytosis of nanoparticles; b - clathrin-coated pit at the membrane of a HeLa cell. (Taken from ref.[32], Figure 7. Copyright Wiley-VCH Verlag GmbH & Co. KGaA. Reproduced with permission).

It could be concluded that the clathrin pathway plays only a minor role during the uptake of positively charged particles and does not participate in the uptake of negatively charged particles in our setup. In line with this finding Harush-Frenkel et al.[31] also suggested a charge-dependent mechanism involving clathrin for positively charged particles but not for negatively charged ones. However, other groups report conflicting data in the literature related to the topic of clathrin participation during endocytosis of nanoparticles. Some authors state that clathrin is partly implied[33, 44], while others show a clearly clathrin-independent pathway[45].

The contribution of macropinocytosis to the uptake of the nanoparticles could be studied by using EIPA which specifically inhibits the Na^+/H^+ pump located in membranes [46, 47]. It was found that EIPA has an inhibitory effect on the endocytosis of positively charged particles while uptake of negatively charged nanoparticles remained unaffected (Figure 9).

Further evidence that macropinocytosis is involved in particle uptake was found by electron microscopy, where different macropinocytic stages were seen frequently (Figure 11).

2.3.5 Lipid Raft-Associated Proteins are involved in Particle Uptake

A variety of receptors is associated with lipid rafts[48-50] and a receptor-associated tyrosine specific protein kinase is reported to be involved in lipid raft-dependent endocytosis[51, 52]. Genistein is a specific inhibitor of the receptor-associated tyrosine specific protein kinase and it was a powerful inhibitor for endocytosis of both types of nanoparticles (Figure 9) leading to the conclusion that participation of lipid raft-associated receptors in the endocytosis of the particles is very probable.

Furthermore the uptake of positively charged particles was reduced to about 60% by indomethacin (Figure 9) which is a known inhibitor of cyclooxygenases[36, 53] Indomethacin shows inhibition of folate receptor uptake and recycling which is caveolin- and thereby lipid raft-dependent[51, 54]. Interestingly indomethacin did not have an effect on the uptake of negatively charged nanoparticles, indicating again that the uptake depends on the surface charge.

In summary, it was shown[32] that the uptake of polymeric nanoparticles of either positive or negative surface charge is energy-dependent and involves dynamin and F-actin. Positively charged nanoparticles showed that their uptake only partially depends on the clathrin pathway, on microtubules, and an active cyclooxygenase, having no effect in endocytosis of negatively charged ones. Also macropinocytosis seems to be not an important mechanism for negatively charged nanoparticles.

3. Polyester Nanoparticles[26]

3.1. Synthesis and Characterization

Biodegradable fluorescent polyester nanoparticles with a narrow size distribution were formulated from the preformed polymers by the emulsification/solvent evaporation process combined with the miniemulsion technique (see Scheme 2). Three different types of polymers such as poly(L-lactide) (PLLA), poly(ε-caprolactone) (PCL), and poly(D,L-lactide-co-glycolide) 50:50 (PLGA) were used for the formulation process. The stabilization of the final particles was achieved by using the anionic surfactant SDS. TEM and high resolution SEM were employed in visualization of the polymeric nanoparticles morphology. As an example, the PLLA particles stabilized by SDS are presented in Figure 12. All particles have a spherical shape and demonstrate low size polydispersity. Slightly deformed particles visible on SEM image are due to the polymer melting under an electron beam. In order to examine the effect of surface charge on the uptake behavior, the SDS molecules were partially exchanged with Lutensol AT50 by repetitive centrifugation/redispersion[26] and positively charged PLLA particles were formulated in the presence of CTMA-Cl. The characterization data of the used particles are summarized in Table 3.

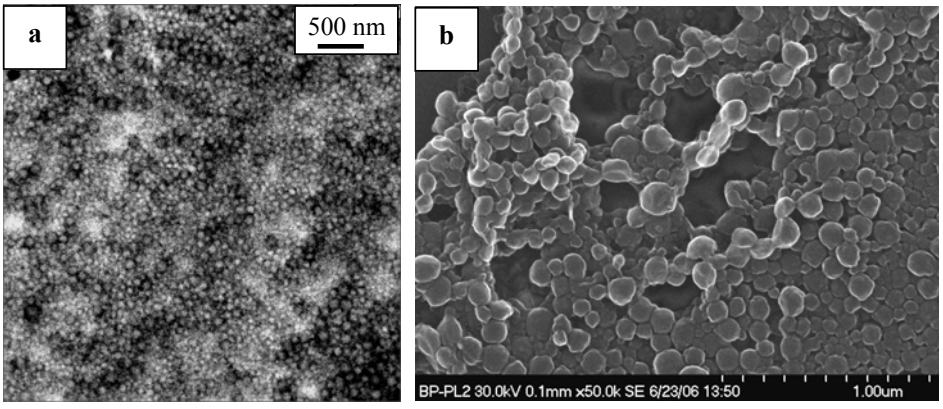

Figure 12. Poly(L-lactide) nanoparticles stabilized by SDS: a- TEM and b- high resolution SEM images. (Taken from ref.[26], Figure 1. Copyright Wiley-VCH Verlag GmbH & Co. KGaA. Reproduced with permission).

Table 3. Characteristics of the fluorescent biodegradable polyester nanoparticles.

	Sample Name						
	PLLA-SDS	PLLA-Lut	PLLA-CT	PCL-SDS	PCL-Lut	PLGA-SDS	PLGA-Lut
Polymer type	poly(L-lactide)			poly(ε-caprolactone)		poly(D,L-lactide-co-glycolide)	
Polymer M_w, g/mole	101 700			≈115 000[b)]		≈15 000[b)]	
Surfactant type	SDS	Lutensol AT50	CTMA-Cl	SDS	Lutensol AT50	SDS	Lutensol AT50
D_h, nm	121	151	144	165	206	76	110
PDI[a)]	0.09	0.07	0.03	0.14	0.11	0.13	0.06
ζ, mV	- 52	- 23	+ 55	- 54	- 22	- 51	- 32

[a)] - polydispersity index (PDI); [b)] - for these polymers M_w was calculated from the gel permeation chromatography (GPC) analysis.

After exchange of the surfactant from SDS to Lutensol AT50, the particle size slightly increases, which is in agreement with sterical conformations caused by the adsorption of the high molecular weight Lutensol molecules onto the particle surface. From the zeta potential values it could be determined that approximately half of the SDS amount was exchanged by the non-ionic surfactant.

3.2. In Vitro Cellular Uptake of Polyester Nanoparticles

Uptake studies were performed with Jurkat and HeLa cells using the fluorescent polymeric particles of PLLA, PCL, and PLGA which were stabilized with either the anionic

SDS or the non-ionic Lutensol AT50. Within 24 h, none of the particles was cytotoxic, as quantified via 7-AAD-staining with HeLa cell vitalities of more than 98%±2 (not shown). For both cell lines, the uptake patterns of the various particle variants were similar (Figure 13).

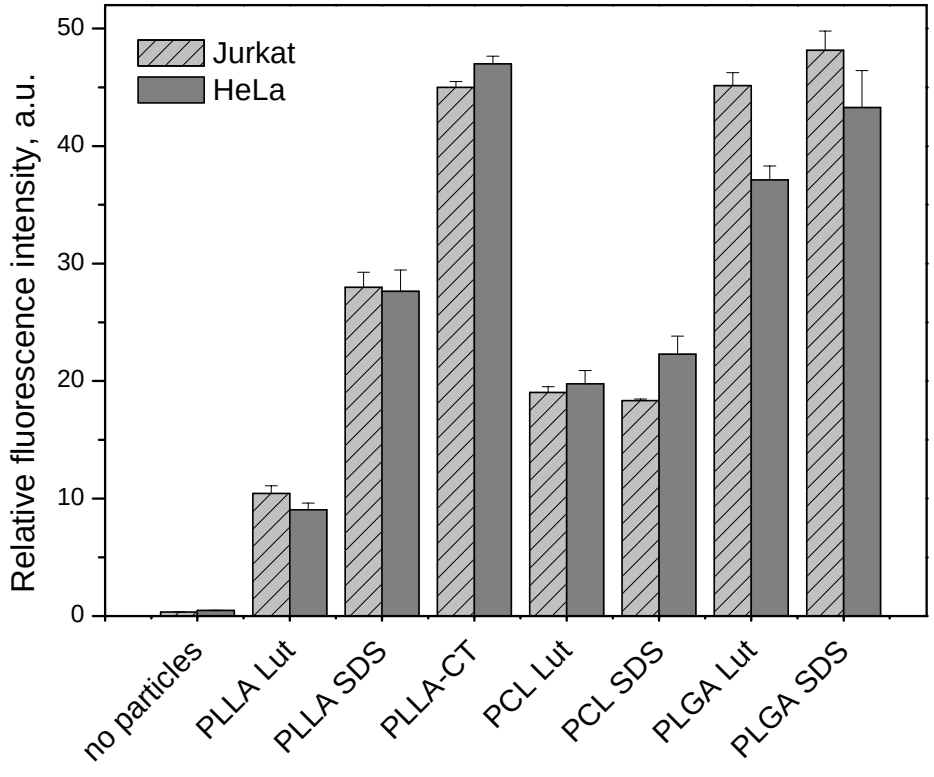

Figure 13. Uptake of biodegradable fluorescent nanoparticles in Jurkat and HeLa cells. Results are expressed as arithmetic mean and standard deviation of triplicates. Differences between the uptake of particles with Lutensol AT50 versus SDS variants were noted for PLLA particles in both cell lines.

The uptake of PLLA and PCL particles was slightly lower as compared to the PLGA nanoparticles, which may be due to the smaller PLGA particle size or higher hydrophilicity of the polymer. However, according to our previous studies performed with the PLLA and PCL particles formulated of different molecular weight polymers[26], no significant influence on the uptake was observed, although the surface hydrophobicity of the particles formed from long polymeric chains expected to be higher to those made of a low molecular weight polymers.

The surfactant located on the surface of the nanoparticles influenced the cellular uptake in a consistent manner with the exception of PCL particle uptake in Jurkat cells. Anionically stabilized SDS particle variants were taken up to a greater extent than Lutensol AT50 analogues (non-ionically stabilized) in most cases. This effect was most pronounced for PLLA particle uptake, whereas it was much weaker for PLGA and PCL particle uptake. Similar results were obtained for polystyrene nanoparticles, where the introduction of negatively charged carboxylic groups led to a better uptake of the nanoparticles (see Figure 3,

lines 1 and 2). Since the cell membrane is also negatively charged, it is likely that a protein adsorption on the particles' surface leads to a modification of the particles and therefore an increased uptake[25, 55]. Furthermore, due to the negatively charged cell membrane the highest uptake values were found for positively charged PLLA particles. However, it is worth to mention that after 24 h of incubation with PLLA-CTMA particles about 50% of cells were detected as apoptotic. This effect was not observed with polystyrene particles. It can be hypothesized that the amount of CTMA-Cl molecules internalized into the cells is responsible for their vitality. According to the formulation process, the CTMA-Cl molecules are physically adsorbed onto the polystyrene or PLLA particles surface. However, keeping in mind that the molecules of poly(L-lactide) are negatively charged (due to the presence of carboxylic group in the end of the polymeric chain) it can be assumed that the interaction between the CTMA-Cl molecules and PLLA particle's surface is much stronger compared to the inert polystyrene surface. As a result, the probability for CTMA-Cl molecules to be internalized into the cell together with a PLLA particle and not being desorbed during the uptake process is higher compared to that for polystyrene particles.

The intracellular location of the nanoparticles versus adherence on the cell surface was confirmed by confocal laser scanning microscopy (CLSM). Figure 14 shows images of Jurkat and HeLa cells after 24 h of incubation with the respective types of polymeric particles stabilized with Lutensol AT50. Images after uptake of SDS variants showed similar results (not shown). The fluorescence signals were usually detected in the cytoplasm, less frequently on the cell membrane and never in the nucleus as identified by the overlay with the transmitted light channel or by TEM studies (Figure 15).

Particles (green) adherent to the cell membrane (in red) will give a signal in the same pixel of the image as these small lateral differences cannot be resolved by CLSM given the lateral resolution of around 200 nm in confocal microscopy. Therefore a yellow signal caused by an overlay of green and red fluorescence signals is obtained like in Figure 14b (arrow). The staining patterns are similar in Jurkat and HeLa cells. Bright spots indicate particle clusters located in cell compartments like endosomes and lysosomes as shown in other studies[55] and in TEM images (Figure 15). PLLA-Lut particles, which appear as bright spots in TEM, are found in the vicinity of cells and intracellularly. A couple of filopodia-like membrane extensions are visible, which seem to enclose the particles. In most cases, multiple particles are localized in endosomes of varying sizes. These are up to several micrometers in diameter, but some individual particles seem to have escaped from those compartments (arrows in Figure 15). Win and Feng[10] reported the nuclear uptake of vitamin E TPGS-coated PLGA particles of ~ 200 nm size into Caco-2 cells. This is contradictory to our results, where never particles located in the nucleus, neither during CLSM nor during TEM imaging, were detected.

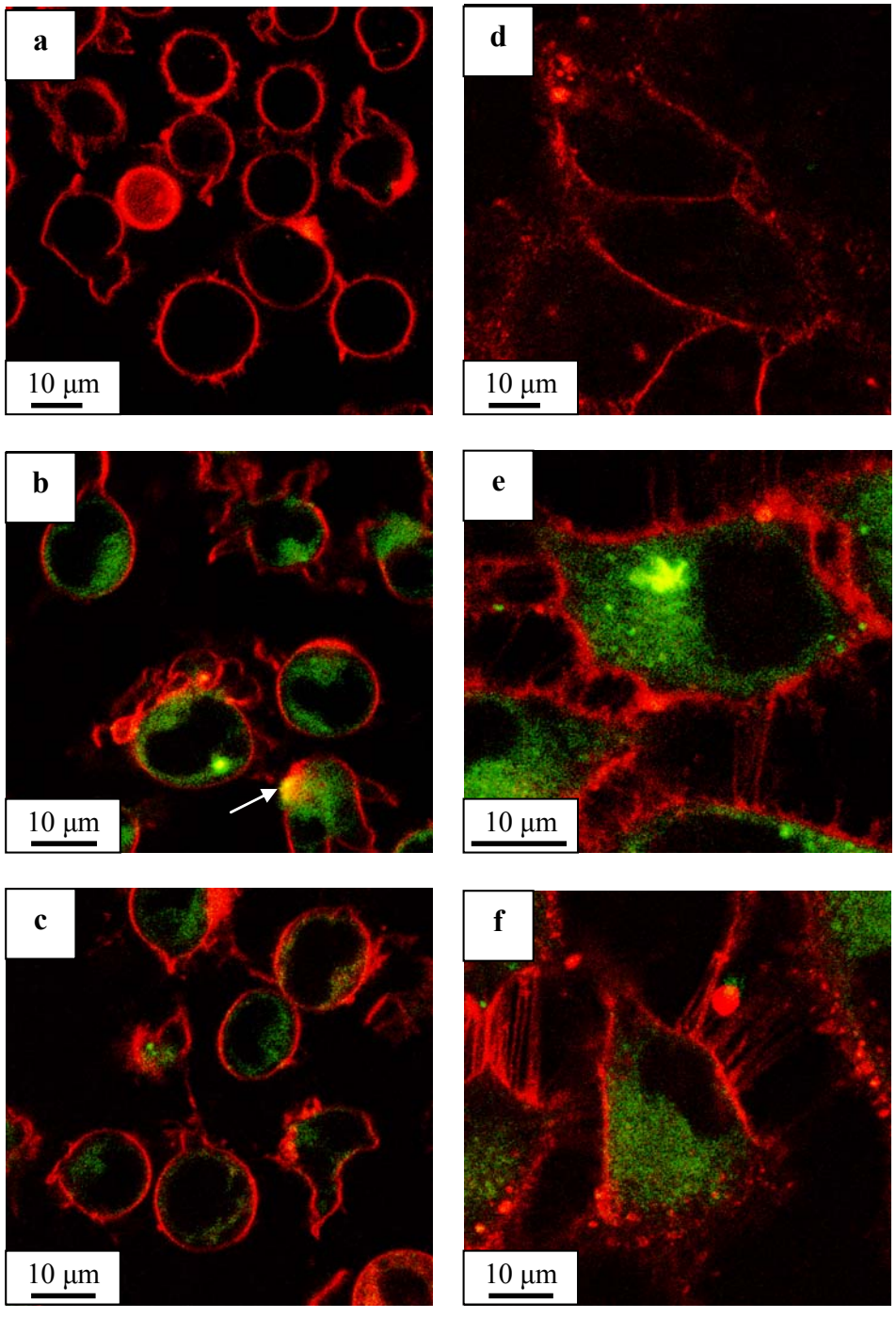

Figure 14. CLSM images of Jurkat (a-c) and HeLa (d-f) cells: a, d - are negative controls. The other images were taken after 24 h incubation with the respective types of polymeric particles (bright spots) stabilized with Lutensol AT50: b, e - PCL-Lut; c, f - PLGA-Lut. The particles contain PMI as green fluorescent dye and the cell membranes are stained red with RH414. (Taken from ref.[26], Figure 5. Copyright Wiley-VCH Verlag GmbH & Co. KGaA. Reproduced with permission).

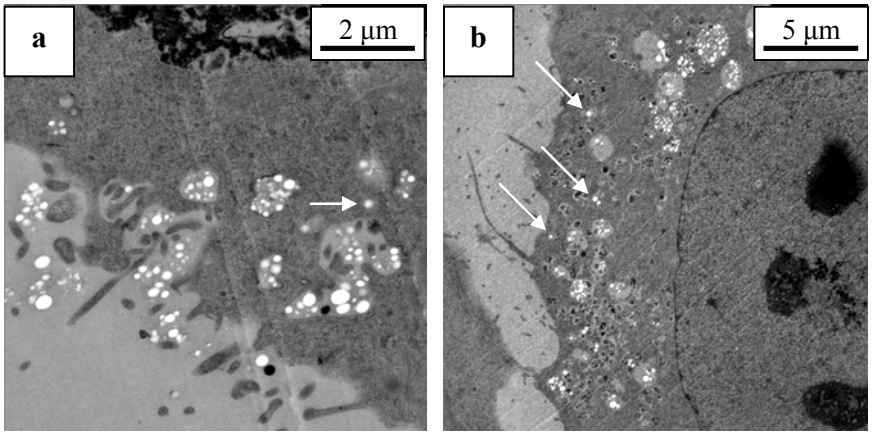

Figure 15. TEM images of HeLa cells incubated 24 h with PLLA-Lut particles. Arrows indicate particles which seem to have escaped from endosomal compartments. (Taken from ref.[26], Figure 6. Copyright Wiley-VCH Verlag GmbH & Co. KGaA. Reproduced with permission).

In summary, the results of this study demonstrate that the biodegradable PLLA, PCL and PLGA particles in the size range of 80 - 206 nm were efficiently taken up by Jurkat and HeLa cells. The cellular uptake is mainly influenced by the type of surfactant (ionic or non-ionic) which is present on the particles' surface and polymer characteristics (hydrophobicity, crystallinity, etc.) used for the particle formation.

4. Conclusion

Polymeric nanoparticles for drug delivery can be produced from different materials in a variety of synthetic processes. Depending on the formulation strategy used for their preparation, particles of different size, composition and physicochemical properties can be obtained. Besides the particle size, the particle surface characteristics play a crucial role in the cellular uptake process. It is important to bear in mind that an interplay of hydrophobic and hydrophilic interactions are of relevance: although, for example, polystyrene itself is a hydrophobic material, the surface of polystyrene nanoparticles dispersed in an aqueous phase exhibit more hydrophilic character, mainly due to the presence of amphiphilic surfactant molecules on the particle surface and/or residual ionic groups from the decomposed initiator. Moreover, if the synthesis of polystyrene particles was performed in the presence of any comonomer having a functional hydrophilic group, one may expect that this group will be located on the particle surface and thus influence the properties of the particle. As discussed above, the zeta-potential value will affect the adsorption rate of the particles to the cell membrane, however, the increase in the uptake was observed only with particles having a certain density of the covalently bonded surface functional (charged) groups. Furthermore, the nanoparticles made of different materials may not show the same uptake behavior. The results presented in the current chapter show that the polyester particles were taken up by the HeLa and Jurkat cells to a slightly lower extent in comparison with the polystyrene particles stabilized with the same amount of a corresponding surfactant. Knowing that the polyester

particles are less stable than polystyrene, the difference in polymer characteristics such as crystallinity/hardness could be the explanation for this phenomenon. A thorough understanding of the particle – cell biological interactions along with the uptake mechanism allow to control these interactions. This makes it feasible to avoid or enhance the uptake, as well as to target the nanoparticles to subcellular compartments. With more characterization and knowledge of the factors that affect the uptake of polymeric nanoparticles, the vision of creating a specific carrier with desired properties for each particular application need, will soon become a reality.

Acknowledgments

This research was supported by the German Research Foundation (DFG). The authors thank Julia Schmitz-Wienke, Martin Dass, Anita Höcherl, Dr. Myriam Lorenz, and Dr. Verena Holzapfel for their help in synthetic, microscopic, and cell uptake experiments.

5. References

[1] Moghimi, S. M., Hunter, A. C. & Murray, J. C. (2005). Nanomedicine: Current status and future prospects. *FASEB J.,* 19, 311-330.

[2] Allemann, E., Leroux, J. C. & Gurny, R. (1998). Polymeric nano- and microparticles for the oral delivery of peptides and peptidomimetics. *Adv. Drug Deliv. Rev.,* 34, 171-189.

[3] Panyam, J. & Labhasetwar, V. (2003). Biodegradable nanoparticles for drug and gene delivery to cells and tissue. *Adv. Drug Deliv. Rev.,* 55, 329-347.

[4] Matuszewski, L., Persigehl, T., Wall, A., Sehwindt, W., Tombach, B., Fobker, M., Poremba, C., Ebert, W., Heindel, W. & Bremer, C. (2005). Cell tagging with clinically approved iron oxides: Feasibility and effect of lipofection, particle size, and surface coating on labeling efficiency. *Radiology,* 235, 155-161.

[5] Gupta, A. K. & Curtis, A. S. G. (2004). Surface modified superparamagnetic nanoparticles for drug delivery: Interaction studies with human fibroblasts in culture. *J. Mater. Sci. Mater. Med.*, 15, 493-496.

[6] Shenoy, D. B., Chawla, J. S. & Amiji, M. M. (2005). Biodegradable polymeric nanoparticles for tumor-selective tamoxifen delivery: In vitro and in vivo studies. *Mat. Res. Soc. Symp. Proc.,* 845, 369-373.

[7] Cegnar, M., Premzl, A., Zavašnik-Bergant, V., Kristl, J. & Kos, J. (2004). Poly(lactide-co-glycolide) nanoparticles as a carrier system for delivering cysteine protease inhibitor cystatin into tumor cells. *Exp. Cell Res.,* 301, 223-231.

[8] Delie, F. & Blanco-Príeto, M. J. (2005). Polymeric particulates to improve oral bioavailability of peptide drugs. *Molecules,* 10, 65-80.

[9] Davda, J. & Labhasetwar, V. (2002). Characterization of nanoparticle uptake by endothelial cells. *Int. J. Pharm.,* 233, 51-59.

[10] Win, K. Y. & Feng, S.-S. (2005). Effects of particle size and surface coating on cellular uptake of polymeric nanoparticles for oral delivery of anticancer drugs. *Biomaterials*, 26, 2713-2722.

[11] Desai, M. P., Labhasetwar, V., Walter, E., Levy, R. J. & Amidon, G. L. (1997). The mechanism of uptake of biodegradable microparticles in Caco-2 cells is size dependent. *Pharm. Res.,* 14, 1568-1573.

[12] Zauner, W., Farrow, N. A. & Haines, A. M. R. (2001). In vitro uptake of polystyrene microspheres: effect of particle size, cell line and cell density. *J. Control. Release,* 71, 39-51.

[13] Pietzonka, P., Rothen-Rutishauser, B., Langguth, P., Wunderli-Allenspach, H., Walter, E. & Merkle, H. P. (2002). Transfer of lipophilic markers from PLGA and polystyrene nanoparticles to Caco-2 monolayers mimics particle uptake. *Pharm. Res.*, 19, 595-601.

[14] Eldridge, J. H., Hammond, C. J., Meulbroek, J. A., Staas, J. K., Gilley, R. M. & Tice, T. R. (1990). Controlled vaccine release in the gut-associated lymphoid tissues. I. Orally administered biodegradable microspheres target the peyer's patches. *J. Control. Release,* 11, 205-214.

[15] Müller, R. H., Rühl, D., Lück, M. & Paulke, B.-R. (1997). Influence of Fluorescent Labelling of Polystyrene Particles on Phagocytic Uptake, Surface Hydrophobicity, and Plasma Protein Adsorption. *Pharm. Res.,* 14, 18-24.

[16] Hoshi, S., Uchino, A., Kusanagi, K. I., Ihara, T. & Ueda, S. (1999). Uptake of orally administered polystyrene latex and poly(D,L-lactic/glycolic acid) microspheres into intestinal lymphoid tissues in chickens. *Vet. Immunol. Immunopathol.,* 70, 33-42.

[17] Lamprecht, A., Schäfer, U. & Lehr, C. M. (2001). Size-dependent bioadhesion of micro- and nanoparticulate carriers to the inflamed colonic mucosa. *Pharm. Res.,* 18, 788-793.

[18] Nagashima, R. (1981). Mechanisms of action of sucralfate. *J. Clin. Gastroenterol.,* 3, 117-127.

[19] Kreuter, J. (1991). Peroral administration of nanoparticles. *Adv. Drug Deliv. Rev.*, 7, 71-86.

[20] Florence, A. T. (1997). The oral absorption of micro- and nanoparticulates: Neither exceptional nor unusual. *Pharm. Res.,* 14, 259-266.

[21] Delie, F. (1998). Evaluation of nano- and microparticle uptake by the gastrointestinal tract. *Adv. Drug Deliv. Rev.,* 34, 221-233.

[22] Wilhelm, C., Billotey, C., Roger, J., Pons, J. N., Bacri, J.-C. & Gazeau, F. (2003). Intracellular uptake of anionic superparamagnetic nanoparticles as a function of their surface coating *Biomaterials,* 24, 1001-1011.

[23] Landfester, K. (2006). Synthesis of colloidal particles in miniemulsions. *Annu. Rev. Mater. Res.,* 36, 231-279.

[24] Musyanovych, A., Rossmanith, R., Tontsch, C. & Landfester, K. (2007). Effect of Hydrophilic Comonomer and Surfactant Type on the Colloidal Stability and Size Distribution of Carboxyl- and Amino-Functionalized Polystyrene Particles Prepared by Miniemulsion Polymerization. *Langmuir,* 23, 5367-5376.

[25] Holzapfel, V., Musyanovych, A., Landfester, K., Lorenz, M. R. & Mailänder, V. (2005). Preparation of fluorescent carboxyl and amino functionalized polystyrene

particles by miniemulsion polymerization as markers for cells. *Macromol. Chem. Phys*., 206, 2440-2449.

[26] Musyanovych, A., Schmitz-Wienke, J., Mailänder, V., Walther, P. & Landfester, K. (2008). Preparation of biodegradable polymer nanoparticles by miniemulsion technique and their cell interactions. *Macromol. Biosci.,* 8, 127-139.

[27] Rejman, J., Oberle, V., Zuhorn, I. S. & Hoekstra, D. (2004). Size-dependent internalization of particles via the pathways of clathrin- and caveolae-mediated endocytosis. *Biochem. J.,* 377, 159–169.

[28] Müller, R. H. (1996). Zetapotential und Partikelladung in der Laborpraxis: Einführung in die Theorie, praktische Messdurchführung, Dateninterpretation, Stuttgart: Wiss. Verl.-Ges.

[29] Lagaly, G., Schulz, O. & Zimehl, R. (1997). Dispersionen und Emulsionen : eine Einführung in die Kolloidik feinverteilter Stoffe einschließlich der Tonminerale, Darmstadt: Steinkopff.

[30] Vorwerg, L. & Gilbert, R. G. (2000). Electrosteric Stabilization with Poly(Acrylic) Acid in Emulsion Polymerization: Effect on Kinetics and Secondary Particle Formation. *Macromolecules,* 33, 6693-6703.

[31] Harush-Frenkel, O., Debotton, N., Benita, S. & Altschuler, Y. (2007). Targeting of nanoparticles to the clathrin-mediated endocytic pathway. *Biochem. Biophys. Res. Commun.,* 353, 26-32.

[32] Dausend, J., Musyanovych, A., Dass, M., Walther, P., Schrezenmeier, H., Landfester, K. & Mailänder, V. (2008). Uptake mechanism of oppositely charged fluorescent nanoparticles in HeLa cells. *Macromol. Biosci.,* 8, 1135-1143.

[33] Panyam, J., Zhou, W. Z., Prabha, S., Sahoo, S. K. & Labhasetwar, V. (2002). Rapid endo-lysosomal escape of poly(DL-lactide-co-glycolide) nanoparticles: Implications for drug and gene delivery. *FASEB J.,* 16, 1217-1226.

[34] Rabinovitch, M. (1995). Professional and non-professional phagocytes: An introduction. *Trends in Cell Biology,* 5, 85-87.

[35] Lai, S. K., Hida, K., Man, S. T., Chen, C., Machamer, C., Schroer, T. A. & Hanes, J. (2007). Privileged delivery of polymer nanoparticles to the perinuclear region of live cells via a non-clathrin, non-degradative pathway. *Biomaterials,* 28, 2876-2884.

[36] Llorente, A., Van Deurs, B., Garred, O., Eker, P. & Sandvig, K. (2000). Apical endocytosis of ricin in MDCK cells is regulated by the cyclooxygenase pathway. *J. Cell Sci.,* 113, 1213-1221.

[37] Stuart, A. D. & Brown, T. D. K. (2006). Entry of feline calicivirus is dependent on clathrin-mediated endocytosis and acidification in endosomes. *J. Virology,* 80, 7500-7509.

[38] Szymkiewicz, I., Shupliakov, O. & Dikic, I. (2004). Cargo- and compartment-selective endocytic scaffold proteins. *Biochem. J.,* 383, 1-11.

[39] Kirkham, M. & Parton, R. G. (2005). Clathrin-independent endocytosis: new insights into caveolae and non-caveolar lipid raft carriers. *Biochim. Biophys. Acta,* 1746, 349-363.

[40] Conner, S. D. & Schmid, S. L. (2003). Regulated portals of entry into the cell. *Nature,* 422, 37-44.

[41] Damke, H., Baba, T., Van Der Bliek, A. M. & Schmid, S. L. (1995). Clathrin-independent pinocytosis is induced in cells overexpressing a temperature-sensitive mutant of dynamin. *J. Cell Biol.*, 131, 69-80.

[42] Macia, E., Ehrlich, M., Massol, R., Boucrot, E., Brunner, C. & Kirchhausen, T. (2006). Dynasore, a Cell-Permeable Inhibitor of Dynamin. *Dev. Cell,* 10, 839-850.

[43] Hasegawa, S., Hirashima, N. & Nakanishi, M. (2001). Microtubule involvement in the intracellular dynamics for gene trasnfection mediated by cationic liposomes. *Gene Ther.,* 8, 1669-1673.

[44] Qaddoumi, M. G., Gukasyan, H. J., Davda, J., Labhasetwar, V., Kim, K. J. & Lee, V. H. L. (2003). Clathrin and caveolin-1 expression in primary pigmented rabbit conjunctival epithelial cells: Role in PLGA nanoparticle endocytosis. *Mol. Vis.*, 9, 559-568.

[45] des Rieux, A., Fievez, V., Theate, I., Mast, J., Preat, V. & Schneider, Y. J. (2007). An improved in vitro model of human intestinal follicle-associated epithelium to study nanoparticle transport by M cells. *Eur. J. Pharm. Sci.*, 30, 380-391.

[46] Gekle, M., Freudinger, R. & Mildenberger, S. (2001). Inhibition of Na+-H+ exchanger-3 interferes with apical receptor-mediated endocytosis via vesicle fusion. *J. Physiol.*, 531, 619-629.

[47] Gekle, M., Drumm, K., Mildenberger, S., Freudinger, R., Gaßner, B. & Silbernagl, S. (1999). Inhibition of Na+-H+ exchange impairs receptor-mediated albumin endocytosis in renal proximal tubule-derived epithelial cells from opossum. *J. Physiol*., 520, 709-721.

[48] Nichols, B. (2003). Caveosomes and endocytosis of lipid rafts. *J. Cell Sci.*, 116, 4707-4714.

[49] Puri, V., Watanabe, R., Singh, R. D., Dominguez, M., Brown, J. C., Wheatley, C. L., Marks, D. L. & Pagano, R. E. (2001). Clathrin-dependent and -independent internalization of plasma membrane sphingolipids initiates two Golgi targeting pathways. *J. Cell Biol.,* 154, 535-547.

[50] Simons, K. & Toomre, D. (2000). Lipid rafts and signal transduction. *Nat. Rev. Mol. Cell Biol.,* 1, 31-39.

[51] Mineo, C. & Anderson, R. G. W. (2001). Potocytosis. Histochem. *Cell Biol.*, 116, 109-118.

[52] Tuma, P. L. & Hubbard, A. L. (2003). Transcytosis: Crossing cellular barriers. *Physiol. Rev.*, 83, 871-932.

[53] McNeill, J. R. & Jurgens, T. M. (2006). A systematic review of mechanisms by which natural products of plant origin evoke vasodilatation. *Can. J. Physiol. Pharmacol.,* 84, 803-821.

[54] Anderson, R. G. W. (1998). The caveolae membrane system. *Ann. Rev. Biochem.,* 67, 199-225.

[55] Lorenz, M. R., Holzapfel, V., Musyanovych, A., Nothelfer, K., Walther, P., Frank, H., Landfester, K., Schrezenmeier, H. & Mailänder, V. (2006). Uptake of functionalized, fluorescent-labeled polymeric particles in different cell lines and stem cells. *Biomaterials,* 27, 2820-2828.

In: Clinical Chemistry Research ISBN 978-1-60692-517-1
Editors: Brian H. Mitchem and Charles L. Sharnham

Chapter VII

The Role of 1, 25 Dihydroxy-Vitamin D3 in Immunity to Infectious Disease.

Michael Eisenhut
Paediatric Department, Luton & Dunstable Hospital NHS Trust, United Kingdom

Abstract

Cells of the monocyte/macrophage and lymphoid lineages express receptors for 1, 25-dihydroxy-vitamin D3 (calcitriol). While this vitamin has been shown to promote differentiation of monocyte precursors to monocytes/macrophages and formation of antimicrobial peptides by this cell population, it has been shown to inhibit effector function of both T-and B lymphocytes. This is related to a reduction of accumulation of mRNA for IL-1 alpha, tumor necrosis factor alpha, IL-2 and IFN gamma, interference with T helper cell function reducing induction of immunoglobulin production by B cells and promotion of T-suppressor cells. In HIV infection in vitro studies suggest promotion of HIV replication by calcitriol, while genetic linkage studies suggest an association of dysfunctional vitamin D receptor genotypes and progression of HIV related immunodeficiency. Immunological effects cannot explain the higher risk of active tuberculosis in patients with low serum vitamin D levels evident from a meta-analysis of observational studies and the higher risk may be related to the reduction in production of antimycobacterial peptides. Future studies need to explore the potential of vitamin D supplementation in treatment and prevention of mycobacterium tuberculosis infection and its impact on the course of HIV infection and on the immunological and related functional long-term impact of viral lower respiratory tract infections.

1. Introduction

Historical background of investigations into the role of vitamin D in regulation of immunity.

The first indication of a role of vitamin D in regulation of function of cells of the immune system was provided by the discovery of effects of vitamin D on promyelocytes causing

suppression of their proliferation and causing differentiation into monocytes (Abe et al.1981, Tanaka et al. 1982) and the subsequent detection of vitamin D receptors on monocytes and activated lymphocytes (Provvedini et al. 1983, Bhalla et al. 1983). Just prior to these reports an anephric patient with sarcoidosis was described who had hypercalcemia and an elevated 1,25 dihydroxy vitamin D3 (calcitriol) level (Barbour et al. 1981). This led to the finding of the ability of sarcoid lymphnode homogenates and alveolar macrophages to activate 25-hydroxy-vitamin D by 1-hydroxylation (Adams et al. 1983, Mason et al. 1984), confirming the ability of this cell population to produce calcitriol. Early animal experiments into the role of calcitriol revealed its dichotomous role by demonstration of an impaired delayed hypersensitivity response to dinitrobenzene under conditions of vitamin D deficiency (Yang et al. 1993a) but a suppression of response by calcitriol (Yang et al. 1993b).

2. 1,25 Dihydroxy Cholecalciferol as Regulator of Cell Mediated Immunity

2.1. Regulation of Monocyte Function

Early experiments showed that in a myelo-monocytic murine cell line calcitriol enhances the gamma interferon induced expression of the class II major histocompatibility complex antigens, which mediate antigen presentation to lymphocytes. The modulation of gamma-interferon induced antigen presentation by calciferol suggested that the hormone might promote antigen presentation by monocytes (Manolagas et al. 1985). Experiments by other groups using human monocytes however showed that calcitriol consistently and specifically reduced HLA-DR and CD4 expression while CD14 and class I HLA antigen expression were unaffected (Rigby et al. 1990). This was achieved at a concentration of 10 nmol/l (physiological levels about 0.12 nmol/l). Expression of Fcgamma receptors I-III on monocytes was variably modulated by calcitriol but no differences in antibody-dependent cell cytotoxicity were observed. The ability of monocytes to induce antigen-dependent T-cell proliferation was markedly reduced by calcitriol pre-treatment. This suggested differences in effects on murine versus human monocytic cells.

Calcitriol was furthermore found to promote hydrogen peroxide and heat shock protein production in some experiments. Other experiments in human monocytes showed that calcitriol at a concentration of 10 nmol/l significantly inhibited the production of interleukin-1 alpha, interleukin-6 and tumor necrosis factor alpha but not interleukin-1 beta without affecting the superoxide burst response (Mueller et al. 1992) Vitamin D deficiency has also been associated with a reduced ability of phagocytosis (Bar-Shavit et al. 1981). Some of the effects of calcitriol may be related to its ability to promote the differentiation of myeloid precursors toward the macrophage/dendritic cell phenotype and its ability to stall the more distal maturation of these cells (Penna et al. 2000, Adorini 2003). It has been proposed that the maintenance of dendritic cells in a relatively immature state attenuates T-cell proliferation (Adams et al. 2007). Effects on macrophage function were associated with concentrations of calcitriol 10 to 100 times higher than physiological blood levels. Calcitriol concentrations in

the microenvironment may however be higher than those in the circulation and 70 times physiological levels have been observed in cell cultures.

2.2. Regulation of T-Cell Mediated Immunity

In contrast to resting monocytes resting peripheral $CD4^+$ T cells express low concentrations of calcitriol receptors. In vitro activation of $CD4^+$ T cells with mitogenic lectins such as phytohemagglutinin and concanavalin A caused an up to five fold increase in the expression of the calcitriol receptor (Provvedini et al.1983, Bhalla et al. 1983, Mahon et al. 2003). $CD8^+$ T cells express the highest number of vitamin D receptors whether activated or not. Calcitriol is an inhibitor of T-cell proliferation as well as of interleukin 2 and 5, interferon gamma production in Th1 cells. It increased IL-4 production in Th2 cells. It also increased granulocyte/monocyte –colony stimulating factor production in peripheral blood mononuclear cells. Influence on interferon gamma production is hereby concentration dependent with concentrations in PHA activated PBMC of 1-100 picomol/l stimulating interferon gamma production and inhibition occurring at concentrations above 10 nmol/l (Manolagas et al. 1989). Calcitriol inhibited antigen-or alloantigen-induced proliferation of murine spleen T cells but not that induced by lectin. In the human calcitriol inhibits lymphocyte proliferation regardless of the activating signal. Calcitriol hereby did not affect the RNA synthesis required for entry of T-cells into early G1 from G0, it specifically inhibited RNA synthesis necessary for T cells to progress from early to late G1, which enables T cells to initiate DNA synthesis. The anti-proliferative effects of calcitriol occurred after the calcium sensitive phase of T-cell activation (Rigby et al. 1988). One mechanism is the suppression of interleukin-1 production by monocytes. The calcitriol mediated suppression of IL-1 production reduced membrane associated IL-1 which provides the mitogenic signal for T-cells and hereby reduces T-cell proliferation (Manolagas et al. 1989). In the model of the human mixed lymphocyte reaction calcitriol was shown to prevent the generation of cytotoxic T cells and enhanced suppressor cell activity at concentrations of 0.1 to 10 nmol/l (Meehan et al.1992).

2.3. Regulation of B-Cell Mediated Immunity by 1,25 Dihydroxy Cholecalciferol

Calcitriol reduced levels of IgG and IgM in in vitro cultures of lectin-stimulated mononuclear cells, which was paralleled by a decrease in the number of IgG, IgM and IgA – secreting cells. This effect seemed to depend on the presence of macrophages and T-cells (Mueller et al. 1996). The regulation of immunoglobulin production has hereby been shown to be due to indirect effects on T-cells rather than direct action of the hormone on B-cells (Lemire et al. 2006)

3. Vitamin D Deficiency and Susceptibility to Active Tuberculosis

3.1. Background

Historical data suggested the successful use of calciferol inducing or supplementing treatment in patients with tuberculosis during the pre-chemotherapy era (Macrae et al.1946, Dowling et al. 1946). Anecdotal evidence suggested successful treatment of tuberculosis patients with vitamin D containing cod liver oil in the middle of the 19th century (Davies 1985). Sunlight exposure which induces vitamin D production in skin cells was found to be successful in treatment of lupus vulgaris (tuberculosis of the skin) with a 95% success rate, a principle for which the Nobel prize was awarded to Finsen in 1903 (Zasloff 2006).

Once it emerged that calcitriol is an important immunoregulator, which is modulating components of cellular immunity, researchers explored its role in antituberculous immunity because it is known that antituberculous immunity is based on cell populations like activated macrophages known to be key-factors in anti-mycobacterial immune defence.

3.2. In Vitro Studies

3.2.1. Changes in Cytokine Production to Mycobacterium Tuberculosis in Response to Vitamin D.

Initial in vitro experiments investigating the role of vitamin D_3 -metabolites found that out of all metabolites investigated only calcitriol reduced the proliferation of *M. tuberculosis* in human monocytes at a concentration of 100 micromol/l. The underlying mechanisms involved increased production of hydrogen peroxide and tumor necrosis factor (Cohen et al. 1986, Rook et al. 1986). The investigators noted that gamma interferon enhanced the capacity of monocytes to produce calcitriol by augmentation of the 25(OH) D_3-1-hydroxylase activity (Rook et al.1986). Subsequent investigations found that calcitriol suppressed IL-12p40 and IFN-gamma production in response to live *M. tuberculosis* in human peripheral blood mononuclear cells (PBMC) with a maximum suppression at a concentration of 100 nmol/l. In *M. tuberculosis* culture filtrate antigen stimulated cultures of PBMC addition of calcitriol suppressed IL-8, IL-6 and IL-10 production indicating a reduction of Th1 cytokines and the associated immune response which develops when the innate immunity fails to eradicate the pathogen (Vidyarani et al. 2007).

3.2.2. Induction of Antimicrobial Peptides by Vitamin D.

Initial investigations showed that in conjunction with an unknown factor present in serum calcitriol caused a threefold slowing of intra-macrophageal bacillary replication from a generation time of a mean of 23.5 hours to a mean of 71.8 hours in human macrophages (Crowle et al. 1987). This was achieved at a concentration of calcitriol of 4 microgram/ml as opposed to 2.6 to 7.0×10^{-5} microgram/ml in the normal circulating range. It is not clear what concentrations are achieved locally in tuberculous granulomas where macrophages may act on each other through a paracrine pathway of calcitriol production. The antimycobacterial

mechanism was found to involve the induction of expression of multiple antimicrobial peptides mediated by the vitamin D receptor complex in keratinocytes, monocytes and neutrophils (Wang et al. 2004). An important antimicrobial peptide induced by calcitriol in phagocytes found to kill mycobacterium tuberculosis within phagocytic vacuoles is LL-37, which is also chemoattractant for monocytes and macrophages (Liu et al. 2006).

Recent work indicated that interaction of pathogen-associated molecular patterns shed from the cell wall of *mycobacterium tuberculosis* interact with the toll like receptor 2/1 dimer pair on the macrophage triggering upregulation of expression of both the CYP 2761 (25(OH) D_3-1-hydroxylase) and vitamin D receptor. This permits the macrophage to internalise serum vitamin D binding protein-bound 25 hydroxy vitamin D from the extracellular fluid by facilitated endocytosis, where it becomes substrate for the upregulated CYP 2761. Calcitriol then transactivates the endogenous defensive gene, cathelicidin and thus leads to expression of LL-37 leading to killing of intracellular *mycobacterium tuberculosis*. Extracellular 25-hydroxy vitamin D was hereby as or more effective than equimolar concentrations of calcitriol in inducing LL-37 production despite its much lower affinity to vitamin D receptor (Adams et al. 2007). Calcitriol induced antimicrobial activity was completely inhibited in the presence of small interfering RNA against mRNA of LL-37 (cathelicidin) (Liu et al. 2007). This proved that in the human monocytic cell line THP-1 anti-microbial peptide LL-37 induction was the only mechanism of antimycobacterial activity. Application of a single dose of oral vitamin D in a double blind randomised controlled trial in 192 adults resulted in an increased ability of participants whole blood to restrict BCG-lux luminescence in vitro (Martineau et al. 2007). The 24-hour luminescence ratio was 20.4% lower for individuals allocated to vitamin D compared with those allocated to placebo (0.57 vs 0.71 respectively; 95% CI for difference, 0.01-0.25; p=0.03). The sized of the effect observed probably explains why in a small trial (n=8) of UV-B induced increase (approximately doubling) of serum Vitamin D levels no effect on BCG-lux luminescence was observed (Yesudian et al. 2008).

3.2.3. Role of Free Radicals in Calcitriol Induced Antimycobacterial Immune Defence

A key study in a human macrophage-like cell line HL-60_{hca} found that calcitriol stimulated expression of nitric oxide synthetase-2 mRNA and generation of nitric oxide at physiological concentrations (1nmol/l). Incubation with a nitric oxide synthase inhibitor reduced growth inhibition by calcitriol in vitro (Rockett et al. 1998). Human promonocytic cell lines and human peripheral blood, monocyte-derived macrophages infected with *M. tuberculosis* alone or incubated with vitamin D3 alone produced little or undetectable amounts of superoxide anion. In contrast, exposure of M. tuberculosis-infected cells to calcitriol led to significant production of superoxide anions and this response was eliminated by inhibitors of phosphatidylinositol 3-kinase via its effect on the phagocytic NADPH oxidase (Sly et al. 2001). Reactive oxygen intermediate scavengers also abrogated calcitriol induced antimycobacterial activity. *M. tuberculosis* infection acted to prime cells to respond to vitamin D3 and this priming was specific for viable *M. tuberculosis*, since it was not observed in cells that had ingested either dead bacilli or latex beads.

3.3. Data from Animal Models of Tuberculosis

Important for the interpretation of rodent models of tuberculosis is the fact that antimicrobial immune defence in macrophages in mice was found to depend heavily on nitric oxide and the gene encoding a dominant antituberculotic antimicrobial peptide LL-37 (cathelicidin) in mice does not contain a vitamin D receptor binding site. An explanation brought forward for the differences in antimicrobial mechanisms was the fact that mice are nocturnally active as opposed to humans who are adapted to living in sunlight (Zasloff 2006).

3.4. Epidemiological Data in Humans

3.4.1. Vitamin D Levels in Patients with Mycobacterium Tuberculosis Infection.

Early epidemiological studies suggested that increased vitamin D levels were associated with a reduced development of active tuberculosis from latent disease and less extensive pulmonary disease in patients with pulmonary tuberculosis (Davies et al. 1985 b, Grange et al. 1985).

A meta-analysis of seven observational studies investigating the relationship of low vitamin D levels and active tuberculosis found a summary effect size of 0.68 (95% CI of 0.43 to 0.93) meaning that overall serum vitamin D levels were 0.68 standard deviations lower in people with tuberculosis compared to controls (Nnoaham et al. 2008). A study conducted in African immigrants in Australia using gamma interferon release assay to exclude patients with latent mycobacterium tuberculosis infection from the control group showed that 25-hydroxy vitamin D levels were significantly lower in participants with latent mycobacterium tuberculosis infection compared to uninfected controls (37.3 versus 54.6 nmol/l; $p=0.007$) and in patients with active tuberculosis/ past tuberculosis versus people with latent mycobacterium tuberculosis infection (16.1 versus 54.6 nmol/l; $p<0.001$) (Gibney et al. 2008). A central role of vitamin D status in immune defence against tuberculosis explains the seasonal increase in incidence of active tuberculosis (Chan 1999). The low post winter trough levels of vitamin D, which may be caused by reduced stimulation of vitamin D synthesis by sunlight in the skin, might result in impaired cellular immunity, which, after a latent period, leads to the reactivation of dormant mycobacterial infection (Douglas et al. 1998, Chan 1999). Against an influence of reduced sunlight exposure and reduced nutritional intake of vitamin D in the low vitamin D levels found in patients with tuberculosis is the finding of a prospective study conducted in London, United Kingdom with 178 patients with tuberculosis and 130 contacts. Sunlight exposure and nutritional intake of vitamin D was not higher in controls. Tuberculosis patients as opposed to controls showed no seasonal variation of serum 25-hydroxycholecalciferol levels (Sita-Lumsden et al. 2007). This led to the conclusion by the authors that in patients with tuberculosis metabolism and uptake of vitamin D is abnormal.

3.4.2. Vitamin D Receptor Gene Polymorphisms

A systematic review of eight studies investigated the association of vitamin D receptor polymorphisms TaqI and FokI and pulmonary tuberculosis. FokI is a polymorphism at the translation initiation start site of the vitamin D receptor gene and results in two version of the vitamin D receptor protein, which differ in length by three amino acids. The short version, the *F* allele, is more active. The TaqI restriction fragment length polymorphism involves regulation of expression and there is some evidence that the haplotype BAt containing the 't' allele of the TaqI polymorphism appears to display higher levels of mRNA expression than the haplotype (paT) containing the 'T' allele, although evidence for functionality is weak and inconclusive. Meta-analysis revealed that overall comparison of tt versus TT showed an OR (95% CI) of 1.00(0.59-1.70) and Tt versus TT of 0.95 (0.8-1.14) of developing pulmonary tuberculosis. For ff versus FF genotype the OR (95% CI) was 1.12 (0.67-1.86) and for Ff versus FF 0.99 (0.81-1.22) for developing pulmonary tuberculosis (Lewis et al. 2005). The results did not allow the conclusion that there was an association of the genotypes investigated and pulmonary tuberculosis. This was attributed to all studies being underpowered. One study included in this meta-analysis found that sputum culture conversion was faster among participants with the Tt genotype, compared with the TT genotype. An increased probability of culture conversion during TB treatment was independently associated with the Tt genotype (age- and sex-adjusted relative risk, 4.28; 95% confidence interval, 1.88-9.75; p=0.001) (Roth et al. 2004).

In patients with smear positive pulmonary tuberculosis in South Africa another group found that both Tt and TT genotypes were associated with a shorter time to sputum smear negativity on antituberculous treatment compared to patients with the tt genotype (Babb et al. 2007).

Not included in the meta-analysis was a study in Native South Americans, which showed that individuals with the TT genotype were 42 times less likely (OR=0.42; 95% CI: 0.21, 0.83, p=0.007) than those with at least one copy of t to have a positive tuberculin skin test (wheal size > 5 mm diameter).indicating that individuals with at least one copy of the Taq1 t allele are better able to mount an appropriate cell-mediated immune response to *M. tuberculosis* exposure (Wilbur et al. 2007). Above listed studies investigated polymorphisms in the 3' untranslated regions of the vitamin D receptor gene. Subsequently conducted studies concentrated on the 5' regulatory region of the vitamin D receptor gene namely Cdx-2 and A1012G which influence the expression of vitamin D receptor directly rather than being merely in dysequilibrium with relevant regions. A significantly decreased frequency of Cdx-2 G allele (p=0.016) and G/G genotype (p=0.01) and an increased frequency of A-A haplotype (A allele of Cdx-2 and A allele of A1012G) (p=0.015) were observed in patients with pulmonary tuberculosis compared to healthy controls in Chennai, South India (Selvaraj et al. 2008).

3.5. Treatment of Tuberculosis with Vitamin D

A systematic review identified 14 prospective clinical studies in which vitamin D had been administered to patients with pulmonary tuberculosis (Martineau et al. 2007). Three

studies were randomised controlled trials (RCT's) and the others case series. None of the RCT's which had between 23 and 60 participants demonstrated a therapeutic response.

A study conducted in Indonesia in patients with moderately advanced pulmonary tuberculosis demonstrated that patients given vitamin D had a higher rate of sputum conversion and an increased radiological improvement compared with the placebo group (Nursyam et al. 2006).

3.6. Directions for Future Research

To elucidate the cause of the lack of seasonal variability of 25- hydroxyl vitamin D levels in tuberculosis patients further studies need to compare vitamin D binding protein levels and function of 25 hydroxylase active in monocytes of tuberculosis patients with that of controls. To adequately power a study on vitamin D receptor polymorphisms it was calculated that 2000 cases and controls are required to have 80% power to detect an OR of 1.4 associated with the ff genotype assuming a type I error rate of 0.01 (Lewis et al. 2005).

A focus for future research needs to be the effects of adjuvant treatment of patients with active tuberculosis with calcitriol. Mouse models are, because of the different immunological and antimicrobial response to calcitriol, not suitable for preliminary experiments. Such studies in humans need to be double blind, placebo controlled and adequately powered and include monitoring of uptake of medication by directly observed treatment and regular checks of plasma levels to monitor absorption.

4. Influence of 1,25 Dihydroxy Cholecalciferol on Human Immunodeficiency Virus –1 multiplication

4.1. In Vitro Studies

With the acknowledgement that functions of the key cells involved in replication of HIV like $CD4^+$ T-cells and monocytes are regulated by calciferol the interaction of vitamin D levels and immunity and viral replication in HIV infection became subject of research (Villamor 2006). Most studies addressing the interaction of calcitriol and HIV investigated HIV replication in cultures of human peripheral blood monocytes and cell lines including pro-monocytic, promyelocytic and myeloblastic cell lines HeLa, U937, Cos-1, HL-60 and A3.5 and found that at concentrations between 12 pM to 240 nmol/l including physiological levels of 0.12 nmol/l and pre-incubation calcitriol increased HIV replication (Locardi et al. 1990, Kitano et al.1990, Skolnik et al.1991, Kizaki et al.1993, Nevado et al. 2007). The opposite was shown in one study where calcitriol suppressed HIV replication (Connor et al.1991).

Calcitriol was found to upregulate chemokine receptor 4 (CXCR4) on U937 cell lines. By this effect it was found to enhance viral replication (Biswas et al. 1998). Calcitriol induced changes in CD4 receptor numbers did not correlate with changes in HIV replication (Skolnik et al. 1991, Kizaki et al.1993). This study confirmed earlier reports on the ability of

calcitriol to upregulate CXCR4 mRNA in the promyelocytic cell line HL-60. Recent experiments in HeLa, U937 and Cos-1 cells revealed that the vitamin D receptor is able to stimulate HIV-1 long terminal repeat transactivation increasing HIV gene expression (Nevado et al. 2007).

4.2. Data from Studies in Humans

4.2.1. HIV-1 Infection and Vitamin D Status

A comparison of plasma 25-hydroxyvitamin D levels in adolescents (14-23 years) with HIV infection (n=238) with controls (n=121) revealed no significant difference (Stephensen et al. 2006). This observation confirmed the results of most previous studies (Villamor 2006). This is in contrast to studies investigating levels of calcitriol, which was shown to be consistently lower in patients with HIV-1 infection with lower levels in patients with symptomatic immunodeficiency (Haug et al.1994). Calcitriol concentrations below 25 pg/ml were associated with a significantly shorter survival time than those with normal concentrations after adjustment for CD4+ cell counts. A proposed explanation is that increased tumor necrosis factor (TNF) concentrations in patients with AIDS can block the stimulatory effect of parathyroid hormone on the renal 1-alpha-hydroxylase. TNF-α appears to downregulate PTH receptors and impair protein kinase C activity and cAMP response after PTH stimulation. This is supported by the finding of a strong negative correlation of TNF and calcitriol levels in HIV infected patients in one study (Haug et al. 1998) and neopterin levels as a marker of activation of macrophages in another ($r=-0.55$, $p<0.001$, Haug et al. 1994). Alternative explanations brought forward are increased utilisation for maturation and proliferation of T lymphocytes during HIV infection or the effects of antiretroviral drugs. The proteinase inhibitor ritonavir has been shown in vitro to inhibit both the 1-alpha-hydroxylase as well as the 25-hydroxylase (Villamor 2006).

4.2.2. Vitamin D Receptor Polymorphisms

The first study investigating polymorphisms of the gene encoding the vitamin D receptor studied the restriction fragment length polymorphism corresponding to the BsmI restriction enzyme in the 3'untranslated region of the vitamin D receptor gene in 185 white HIV sero-positive injecting drug users. It found that a higher proportion of the vitamin D receptor-BB genotype was found in patients with <200 CD4 cells/microliter ($p=0.009$, OR: 2.4 95% CI 1.3-4.7) as well as faster progression to AIDS and to a CD4 cell < 200 cells/microliter. There were no significant differences in vitamin D receptor genotype frequencies between patients and healthy, white HIV-1 seronegative blood donors suggesting that BsmI locus polymorphisms are not associated with risk of HIV infection (Barber et al. 2001).

Like for tuberculosis an association between AIDS disease progression rates and the Fok I polymorphisms of the vitamin D receptor gene was investigated. Patients heterozygous at the Fok I polymorphism were over-represented in the group of patients that showed a drop in CD4 cell count to below 200 /microliter (52% of progressors versus 36% of non-progressors, $p=0.037$; RR=1.44 (95% CI: 1.02-2.03). Mean time to AIDS CDC-1993 was shorter for those with Ff genotype than for those with FF and ff genoypes (non-Ff genotype patients), (log

rank test p=0.035; Cox hazard ratio for Ff versus non-Ff = 1.53 (95% CI: 1.0-2.23), p=0.047). In addition the drop in CD4 cell count to below 200/microl was reached faster in Ff carriers than in non-Ff patients (log rank test p=0.015; Cox hazard ratio for Ff versus non-Ff = 1.77 (95% CI: 1.12-2.8), p= 0.014) (Nieto et al. 2004).

A recent epidemiological study investigated the association of vitamin D receptor polymorphisms and susceptibility to HIV-1 infection in injection drug users (De la Torre et al. 2008).

The study found an association with protection against infection for the G-A-T-G-L haplotye (OR (95% CI 0.22-0.72; p=0.0025).This haplotype contains the 3' UTR rs 1544410-G allele. It has also been described that the exon 2 polymorphism rs10735810-T allele produces a low transactivation capacity of the vitamin D receptor protein, which could prevent normal vitamin D receptor function.

The high HIV disease progression rates associated with certain vitamin D receptor polymorphisms could be interpreted as showing that persons, who carry these genotypes have a reduced response to the immunesuppressive actions of vitamin D and allow the activation of Th1 cells.

4.3. Directions for Future Research

In view of the strong in vitro evidence for increased HIV replication in response to calcitriol future studies need to investigate whether vitamin D supplementation in HIV infected persons not on antiretroviral treatment (e.g. long term non- or slow progressors) and with vitamin D deficiency show an increase in viral load and deterioration of immune function with calcitriol supplementation and whether this is associated with an increase in Th1 response.

5. Role Of 1,25 Dihydroxy Cholecalciferol in other Infections

5.1. Animal Models

Calcitriol did not have any effect on the susceptibility to *Herpes simplex virus* or *Candida albicans* infections in the mouse model. The number of mice in the treatment groups however was too small (n=10) to exclude a significant effect (Cantorna et al. 1998). Vitamin D receptor knock-out mice showed an increased granulomatous inflammatory response to *Schistosoma mansoni* infection (Cantorna et al. 2004).

In the mouse model calcitriol treatment of *Leishmania major* infected macrophages demonstrated a vitamin D receptor dependent inhibition of macrophage killing activitiy. Further analysis showed that this was a result of decreased production of nitric oxide by calcitriol-treated macrophages due to vitamin D receptor-dependent up-regulation of arginase I expression, which overrides NO production by NOS-2 (Ehrchen et al. 2007). In the

abdominal septicemia rat model subcutaneous administration of calcitriol resulted in better maintenance of platelet counts compared to controls (Moller et al. 2007).

5.2. Studies in Humans

5.2.1. Association of Vitamin D Levels with Frequency and Severity of Respiratory Tract Infections

Serum vitamin D levels in young Finnish men serving on a military base were measured and frequency of respiratory tract infections recorded prospectively. Subjects with serum 25 hydroxy vitamin D concentrations of <40 nmol/l had significantly (p=0.004) more days of absence from duty due to respiratory tract infection compared to subjects with higher levels (Laaksi et al. 2007). The reason for hospitalisation in children with rickets was significantly more often a lower respiratory tract infection compared to children without and hospitalisation was prolonged (Najada et al. 2004). Clinical vitamin D deficiency was associated with a 13-fold increased risk of pneumonia in Ethiopian children less than 5 years of age (Muhe et al. 1997).

Subclinical vitamin D deficiency was a significant independent risk factor for severe acute lower respiratory tract infection in children < 5 years of age in India (Wayse et al. 2004). In multivariate analysis, factors associated with significantly lower odds ratio for having severe acute lower respiratory infection (WHO definition) included a serum 25 hydroxy vitamin D level of > 22.5 nmol/l (OR: 0.09; 95% CI 0.03-0.24; p<0.001).

5.2.2. Vitamin D receptor polymorphisms

5.2.2.1. Viral Bronchiolitis

In a recent epidemiological study conducted in Canada researchers found that the FokI *ff* genotype of the vitamin D receptor was associated with an adjusted relative odds of hospitalisation with a viral lower respiratory tract infection (82 % due to respiratory syncytial virus) seven times that of the FokI *FF* genotype (Roth et al. 2008). The *f* allele translates a vitamin D receptor protein that is longer than that translated by the *F* allele and has decreased rates of transcription of vitamin D receptor RNA (Jurutka et al. 2000). In peripheral blood mononuclear cell cultures, the concentration of calcitriol required to cause 50% growth inhibition was directly related to the number of *f* alleles, and in vitro lympho-proliferation caused by exposure to mycobacterial antigen was more likely to be inhibited by calcitriol if the cells expressed the *FF* genotype (Colin et al. 2000, Selvaraj et al. 2004).

5.2.2.2. Extrapulmonary Infections

Investigation of associations of polymorphism at codon 352 revealed that patients with a specific genotype were significantly underrepresented among patients with persistent hepatitis B infection but not in subjects with clinical malaria compared with the other genotypes (Bellamy et al. 1999).

6. Conclusion

1, 25 dihydroxy-vitamin D3 has powerful immunomodulatory effects on cell-mediated immunity with impact on immune defence to a wide spectrum of pathogens.

The in vitro data on induction of antimicrobial peptides against *mycobacterium tuberculosis* together with epidemiological data clearly demonstrate the key role of vitamin D in anti-mycobacterial immune defence. Because of differences in immunological response and regulation of antimicrobial peptide release mouse models cannot be used to represent humans.

Future studies need to investigate the importance of calcitriol in immune defence against intracellular pathogens dwelling in human macrophages like *Leishmania* species and *Trypanosoma cruzi.* The role of vitamin D in HIV infection is not clear and requires intervention studies to clarify whether calcitriol deficiency is only a consequence of HIV infection through immune activation or has also a role in increasing HIV replication and deterioration of HIV induced immunodeficiency in humans in vivo. In vitro results suggest the opposite. Adequately powered prospective epidemiological studies need to explore the association of vitamin D status with frequency and severity of viral respiratory tract infections. Such investigations need to take into account its potential to influence immunological processes involved in the pathogenesis of hyperreactive airway disease like asthma and reduced alveolar fluid clearance in pneumonia and septicemia and of mucosal oedema and hypersecretion in the airways in allergic and non-allergic inflammation (Eisenhut 2006).

References

Abe, E., Miyaura, C., Sakagami, H., Takeda, M., Konno, K., Yamazaki, T., Yoshiki, S., Suda, T. (1981). Differentiation of mouse myeloid leukaemia cells induced by 1 alpha, 25 –dihydroxyvitamin D3. *Proc. Natl. Acad. Sci. USA* 78: 4990-4994.

Adams, J.S., Liu, P.T., Chuu, R., Modlin, R.L., Hewison, M.. (2007) Vitamin D in defense of the human immune response. *Ann. N.Y. Acad. Sci.* 1117:94-105.

Adams, J.S., Sharma, O.P., Gacad, M.A., Singer, F.R. (1983). Metabolism of 25-hydroxyvitamin D3 by cultured pulmonary alveolar macrophages in sarcoidosis. *J. Clin. Invest.* 72: 1856-1860.

Adorini, L.(2003). Tolerogenic dendritic cells induced by vitamin D receptor ligands enhance regulatory T cells inhibiting autoimmune diabetes. *Ann. N.Y .Acad., Sci*. 987: 258-261.

Babb, C., Van der Merwe, L., Beyers, N., Pheiffer, C., Walzl, G., Duncan, K., Van Helden, P., Hoal, E.G. (2007). Vitamin D receptor gene polymorphisms and sputum conversion time in pulmonary tuberculosis patients. *Tuberculosis* 87: 295-302.

Barber, Y., Rubio, C., Fernandez, E., Rubio, M., Fibla, J. (2001). Host genetic background at CCR5 chemokine receptor and vitamin D receptor loci and human immunodeficiency virus (HIV) type disease progression among HIV seropositive injection drug users. *J. Infect. Dis.* 184, 1279-1288

Barbour, G.L., Coburn, J.W., Slatopolosky, E., Norman, A.W., Horst, R.L. (1981). Hypercalcemia in an anephric patient with sarcoidosis: evidence for extrarenal generation of 1,25-dihydroxyvitamin D. *N.E.J.M.* 305: 440-443.

Bar-Shavit, Z., Noff, D., Edelstein, S., Meyer, M., Shibolet, S., Goldman, R (1981). 1, 25-Dihydroxyvitamin D3 and the regulation of macrophage function. *Calcif. Tissue Int.* 33: 673-676.

Bellamy, R., Ruwende, C., Corrah, T., McAdam, K.P.W.J., Thursz, M., Whittle, H.C., Hill, A.V.S. (1999). Tuberculosis and chronic hepatitis B virus infection in Africans and variation in the vitamin D receptor gene. *J. Infect. Dis.*179:721-724.

Bhalla, A.K., Amento, E.P., Clemens, T.L., Holick, M.F., Krane, S.M. (1983). Specific high-affinity receptors for 1,25-dihydroxyvitamin D3 in human peripheral blood mononuclear cells: presence in monocytes and induction in T lymphocytes following activation. *J. Clin. Endo. Metab.* 57: 1308-1310.

Biswas, P., Mengozzi, M., Mantelli, B., Delfanti, F., Brambilla, A., Vicenzi, E., Poli, G. (1998). 1,25-dihydroxyvitamin D3 upregulates functional CXCR4 human immunodeficiency virus type 1 coreceptors in U-937 minus clones: NF-kappaB-independent enhancement of viral replication. *J.Virol.* 72: 8380-8383.

Cantorna, M., Hullett, D.A., Redaelli, C., Brandt, C.R., Curtis, R., Humpal-Winter, J., Sollinger, H.W., Deluca, H,F. (1998).1,25 dihydroxyvitamin D3 prolongs graft survival without compromising host resistance to infection or bone mineral density. *Experimental Transplantation* 66: 828-831.

Cantorna, M.T., Zhu, Y., Froicu, M., Wittke, A. (2004). Vitamin D status, 1,25-dihydroxyvitamin D3, and the immune system. *Am. J. Clin. Nutr.* 80 (suppl): 1717S-1720S.

Chan, T.Y.K. (1999). Seasonal variations in vitamin-D status and the incidence of tuberculosis in different countries. *Respiration* 66:196.

Cohen, M.S., Mesler, D.E., Snipes, R.G., Gray, T. (1986). 1, 25 dihydroxyvitamin D3 activates secretion of hydrogenperoxide by human monocytes. *J Immunol* 136: 1049-1053.

Colin, E.M., Weel, A.E., Uitterlinden, A.G., Buurman, C.J., Birkenhaeger, J.C., Pols, H.A., van Leeuwen, J.P. (2000). Consequences of vitamin D receptor gene polymorphisms for growth inhibition of cultured human peripheral blood mononuclear cells by 1, 25-dihydroxyvitamin D3. *Clin. Endocrinol. (Oxf)* 52:211-216**.**

Connor, R.I., Rigby, W.F.C. (1991). 1 α, 25-dihydroxyvitamin D3 inhibits productive infection of human monocytes by HIV-1. *Biochem. Biophys. Res. Commun.*176: 852-859.

Crowle, A.J., Ross, E.J, May, M.H. (1987). Inhibition by 1,25 $(OH)_2$—Vitamin D_3 of the multiplication of virulent tubercle bacilli in cultured human macrophages. *Infection Immun.* 55: 2945-2950.

Davies, P.D.O. (1985). A possible ling between vitamin D deficiency and impaired host defence to Mycobacterium tuberculosis. *Tubercle* 66: 301-306.

Davies, P.D.O., Brown, R.C., Woodhead, J.S. (1985). Vitamin D and calcium homeostasis in the tuberculous patient before treatment. *Thorax* 40:187.

De la Torre, M.S., Torres, C., Nieto, G., Vergara, S., Carrero, A.J., Macias, J., Pineda, J.A., Caruz, A., Fibla, J. (2008). Vitamin D receptor gene haplotypes and susceptibility to HIV-1 infection in injection drug users. *J. Infect. Dis.*197: 405-410.

Douglas, A.S., Ali, S., Bakhshi, S.S. (1998). Does vitamin D deficiency account for ethnic differences in tuberculosis seasonality in the UK. *Ethnicity & Health* 3: 247-253.

Dowling, G.B., Prosser-Thomas, E.W. (1946) Treatment of lupus vulgaris with calciferol. *Lancet* 1:919-922.

Ehrchen, J., Helming, L., Varga, G., Pasche, B., Loser, K., Gunzer, M., Sunderkoetter, C., Sorg, C., Roth, J., Lengeling, A. (2007). Vitamin D receptor signalling contributes to susceptibility to infection with *Leishmania major*. *F.A.S.E.B. J.* 21: 3208-3218.

Eisenhut, M. (2006). Changes in ion transport in inflammatory disease. *J. Inflamm.* 3: 5.

Gibney, K.B., MacGregor, L., Leder, K., Torresi, J., Marshall, C., Ebeling, P.R., Biggs, B.-A. (2008).Vitamin D deficiency is associated with tuberculosis and latent tuberculosis infection in immigrants from Sub-Saharan Africa. *Clin. Infect. Dis.* 46:443-446.

Grange, J.M., Davies, P.D.O., Brown, R.C., Woodhead, J.S., Kardjito, T. (1985).A study of vitamin D levels in Indonesian patient s with untreated pulmonary tuberculosis. *Tubercle* 66: 187.

Haug, C., Mueller, F., Aukrust, P., Froland, S.S. (1994).Subnormal serum concentration of 1, 25-vitamin D in human immunodeficiency virus infection: correlation with degree of immune deficiency and survival. *J. Infect. Dis,* 169: 889-893.

Haug, C.J., Aukrust, P., Haug, E., Morkrid, L., Mueller, F., Froland, S.S. (1998). Severe deficiency of 1,25-dihydroxyvitamin D3 in human immunodeficiency virus infection: association with immunological hyperactivity and only minor changes in calcium homeostasis. *J. Clin. Endocrinol. Metab.* 83: 3832-3838.

Jurutka, P.W., Remus, L.S., Whitfield, G.K., Thompson, P.D., Hsieh, J.C., Zitzer, H., Tavakkoli, P., Galligan, M.A., Dang, H.T., Haussler, C.A., Haussler, M.R. (2000). The polymorphic N terminus in human vitamin D receptor isoforms influences transcriptional activity by modulating interaction with transcription factor II B. *Mol. Endocrinol.* 14: 401-420.

Kitano, K., Baldwin, G.C., Raines, M.A., Golde, D.W.(1990). Differentiating agents facilitate infection of myeloid leukaemia cell lines by monocytotropic HIV-1 strains. *Blood* 76:1980-1988.

Kizaki, M., Ikeda, Y., Simon, K.J., Nanjo, M., Koeffler, H.P. (1993). Effect of 1, 25-dihydroxyvitamin D3 and its analogs on human immunodeficiency virus infection in monocytes/macrophages. *Leukemia* 7: 1525-1530.

Laaksi, I., Ruohola, J.-P., Tuohimaa, P., Auvinen, A., Haataja, R., Pihlajamaeki, H., Ylikomi, T. (2007). An association of serum vitamin D concentrations <40 nmol/lol/l with acute respiratory tract infection in young Finnish men. *Am. J. Clin. Nutr.* 86: 714-717.

Lemire, J.M., Adams, J.S., Sakai, R., Jordan, S.C. (2006).1 alpha 25- dihydroxy vitamin D3 suppresses proliferation and immunoglobulin production by normal human peripheral blood mononuclear cells. *J. Clin. Invest.* 74: 657-661.

Lewis, S.J., Baker, I., Davey-Smith, G. (2005). Meta-analysis of vitamin D receptor polymorphisms and pulmonary tuberculosis risk. *Int. J. Tuberc. Lung Dis.* 9: 1174-1177.

Liu, P.T., Stenger, S., Li, H., Wenzel, L., Tan, B.H., Krutzik, S.R., Ochoa, M.T., Schauber, J., Wu, K., Meinken, C., Kamen, D.L., Wagner, M., Bals, R., Stein-Meyer, **A.,** Zuegel, U., Gallo, R.L., Eisenberg, D., Hewison, M., Hollis, B.W., Adams, J.S., Bloom, B.R., Modlin, R.L. (2006). Toll-like receptor triggering of a vitamin D-mediated human antimicrobial response. *Science* 311: 1770-1773.

Liu, P.T., Stenger, S., Tang, D.H., Modlin, R.L. (2007). Cutting edge: Vitamin D mediated human antimicrobial activity against Mycobacterium tuberculosis is independent on the induction of cathelicidin. *J. Immunol.*179: 2060-2063.

Locardi, C., Petrini, C., Boccoli, G., Testa U, Dieffenbach C, Butto S, Belardelli F. (1990). Increased human immunodeficiency virus (HIV) expression in chronically infected U937 cells upon in vitro differentiation by hydroxyvitamin D3: roles of interferon and tumor necrosis factor in regulation of HIV production. *J. Virol.* 64: 5874-5882.

Macrae, D.E. (1946). Calciferol treatment of lupus vulgaris. *Br. J. Dermatol.* 58:333-338.

Mahon, B.D., Wittke, A., Weaver, V., Cantorna, M.T. (2003). The targets of vitamin D depend on the differentiation and activation status of CD4-positive T cells. *J. Cell. Biochem.* 89: 922-932.

Manolagas, S.C., Hustmyer, F.G., Yu, X.-P. (1989). 1, 25-dihydroxyvitamin D_3 and the immune system. *Proc. Soc. Exp. Biol. Med.*191: 238-245.

Manolagas, S.C., Provvedini, D.M., Tsoukas, C.D. (1985). Interactions of 1, 25-dihydroxyvitamin D_3 and the immune system. *Molec. Cell. Endocrinol.* 43:113-122.

Martineau, A.R., Honecker, F.U., Wilkinson, R.J., Griffiths, C.J. (2007). Vitamin D in the treatment of pulmonary tuberculosis. *J. Steroid Biochem. Molec. Biol* .103: 793-798.

Martineau, A.R., Wilkinson, R.J., Wilkinson, K.A., Newton, S.M., Kampmann, B., Hall, B.M., Packe, G.E., Davidson, R.N., Eldridge, S.M., Maunsell, Z.J., Rainbow, S.J., Berry, J.L., Griffiths, C.J. (2007). A single dose of vitamin D enhances immunity to mycobacteria. *Am. J. Respir. Crit. Care Med.* 176: 208-213.

Mason, R.S., Frankel, T., Chan, Y., Lissner, D., Posen, S. (1984). Vitamin D conversion by sarcoid lymph node homogenate. *Ann. Intern. Med.*100: 59-61.

Meehan, M.A., Kerman, R.H., Lemire, J.M. (1992). 1,25-dihydroxyvitamin D3 enhances the generation of non-specific suppressor cells while inhibiting the induction of cytotoxic cells in a human MLR. *Cell. Immunol.* 140: 400-409.

Moller, S., Laigaard, F., Olgaard, K., Hemmingen, C. (2007). Effect of 1,25-dihydroxy-vitamin D3 in experimental sepsis. *Int. J. Med. Sci.* 4: 190-195.

Mueller, K., Bendtzen, K. (1996). 1, 25-dihydroxyvitamin D_3 as a natural regulator of human immune functions. *J. Investig. Dermatol. Sympos. Proceedings* 1: 68-71.

Mueller, K., Haahr, P.M., Diamant, M., Rieneck, K., Kharazmi, A., Bendtzen, K.(1992). 1,25-dihydroxyvitamin D3 inhibits cytokine production by human blood monocytes at the post-transcriptional level. *Cytokine* 4: 506-512.

Muhe, L., Lulseged, S., Mason, K.E., Simoes, E.A.F. (1997). Case-control study of the role of nutritional rickets in the risk of developing pneumonia in Ethiopian children. *Lancet* 349: 1801-1804.

Najada, A.S., Habashneh, M.S., Khader, M.(2004). The frequency of nutritional rickets among hospitalised infants and its relation to respiratory diseases. *Trop. Paed.* 50: 364-368.

Nevado, J., Tenbaum, S.P., Castillo, A.J., Sanchez-Pacheco, A., Aranda, A. (2007). Activation of the human immunodeficiency virus type 1 long terminal repeat by 1α 25-dihydroxy vitamin D3. *J. Molec. Endocrinol.* 38: 587-601.

Nieto, G., Barber, Y., Rubio, M.C., Rubio, M., Fibla, J. (2004). Association between AIDS disease progression rates and the Fok-I polymorphism of the vitamin D receptor gene in a cohort of HIV-1 seropositive patients. *J. Steroid Biochem. Molec. Biol.* 89-90: 199-207.

Nnoaham, K.E., Clarke, A. (2008). Low serum vitamin D levels and tuberculosis: a systematic review and meta-analysis. *Internat. J. Epidemiol.* 37: 113-119.

Nursyam, E.W., Amin, Z., Rumende, C.M. (2006). The effect of vitamin D as supplementary treatment in patients with moderately advanced pulmonary tuberculous lesion. *Acta Med. Indones.* 38: 3-5.

Penna, G., Adorini, L.(2000). 1-alpha, 25 –dihydroxy vitamin D3 inhibits differentiation, maturation, activation, and survival of dendritic cells leading to impairment alloreactive T-cell activation. *J. Immunol.* 164: 2405-2411.

Provvedini, D.M., Tsoukas, C.D., Deftos, L.J., Manolagas, S.C. (1983). 1, 25-dihydroxyvitamin D3 receptors in human leukocytes. *Science* 221: 1181-1183.

Rigby, W.F.C. (1988). The immunobiology of vitamin D. *Immunology today* 9: 54-58.

Rigby, W.F.C., Waugh, M., Graziano, R.F. (1990). Regulation of human monocyte HLA-DR and CD4 antigen expression, and antigen presentation by 1,25-dihydroxyvitamin D3. *Blood* 76: 189-197.

Rockett, K.A., Brookes, R., Udalova, I., Vidal, V., Hill, A.V.S., Kwiatkowski, D. (1998). 1-25-dihydroxyvitamin D3 induces nitric oxide synthase and suppresses growth of Mycobacterium tuberculosis in a human macrophage-like cell line. *Infect Immun* 66: 5314-5321.

Rook, G.A.W., Steele, J., Fraher, L., Barker, S., Karmali, R., O'Riordan, J., Stanford, J. (1986). Vitamin D_3, gamma interferon, and control of proliferation of Mycobacterium tuberculosis by human monocytes. *Immunology* 57: 159-163.

Roth, D.E., Jones, A.B., Prosser, C., Robinson, J.L., Vohra, S. (2008). Vitamin D receptor polymorphisms and the risk of acute lower respiratory tract infection in early childhood. *J. Infect. Dis.* 197: 676-680.

Roth, D.E., Soto, G., Arenas, F., Bautista, C.T., Ortiz, J., Rodriguez, R., Cabrera, L., Gilman, R.H. (2004). Association between vitamin D receptor gene polymorphisms and response to treatment of pulmonary tuberculosis. *J. Infect. Dis.* 190: 920-927.

Selvaraj, P., Alagarasu,K., Harishankar, M., Vidyarani, M., Narayanan, P.R. (2008). Regulatory region polymorphisms of vitamin D receptor gene in pulmonary tuberculosis patients and normal healthy subjects of south India. *Internat. J. Immunogenetics* 35: 251-254.

Selvaraj, P., Chandra, G., Jawahar, M.S., Rani, M.V., Rajeshwari, D.N., Narayanan, P.R. (2004). Regulatory role of vitamin D receptor gene variants of BsmI, ApaI, TaqI, and FokI polymorphisms on macrophage phagocytosis and lymphoproliferative response to mycobacterium tuberculosis antigen in pulmonary tuberculosis. *J. Clin. Immunol.* 24: 523-532.

Sita-Lumsden, A., Lapthorn, G., Swaminathan, R., Milburn, H.J. (2007). Reactivation of tuberculosis and vitamin D deficiency: the contribution of diet and exposure to sunlight. *Thorax* 62: 1003-1007.

Skolnik, P.R., Jahn, B., Wang, M.Z., Rota, T.R., Hirsch, M.S., Krane, S.M. (1991). Enhancement of human immunodeficiency virus 1 replication in monocytes by 1, 25-dihydroxycholecalciferol. *Proc, Natl, Acad. Sci.* USA 88: 6632-6636.

Sly, L.M., Lopez, M., Nauseef, W.M., Reiner, N.E.(2001). 1 alpha, 25-dihydroxyvitamin D3-induced monocyte antimycobacterial activity is regulated by phosphatidylinositol 3-inase and mediated by the NADPH-dependent phagocyte oxidase. *J. Biol. Chem.* 276: 35482-35493.

Stephensen, C.B., Marquis, G.S., Kruzich, L. A., Douglas, S.D., Aldrovandi, G.M., Wilson, C.M. (2006). Vitamin D status in adolescents and young adults with HIV infection. *Am. J. Clin. Nutr.* 83:1135-1141.

Tanaka, H., Abe, E., Miyaura, C., Kuribayashi, T., Konno, K., Nishii, Y., Suda, T.(1982).1 alpha 25-Dihydroxycholecalciferol and a human myeloid leukaemia cell line (HL-60). The presence of a cytosol receptor and induction of differentiation . *Biochem. J.* 204: 713-719.

Vidyarani, M., Selvaraj, P., Jawahar, M.S., Narayanan, P.R.(2007). 1,25 dihydroxyvitamin D3 modulated cytokine response in pulmonary tuberculosis. *Cytokine* 40:128-134.

Villamor, E. (2006). A potential role for vitamin D on HIV infection. *Nutr. Rev.* 64: 226-233.

Wang, T.T., Nestel, F.P., Bourdeau, V., Nagai, Y., Wang, Q., Liao, J., Tavera-Mendoza, L., Lin, R., Hanrahan, J.H., Mader, S., White, J.H. (2004). Cutting edge: 1,25-dihydroxyvitamin D3 is a direct inducer of antimicrobial peptide gene expression. *J. Immunol.*173: 2909-2912.

Wayse, V., Yousafzai, A., Mogale, K., Filteau, S. (2004). Association of subclinical vitamin D deficiency with severe acute lower respiratory infection in Indian children under 5 years . *Eur. J. Clin. Nutr.* 58: 563-567.

Wilbur, A.K., Kubatko, L.S., Hurtado, A.M., Hill, K.R., Stone, A.C. (2007). Vitamin D receptor gene polymorphisms and susceptibility M. tuberculosis in native Paraguayans. *Tuberculosis* 87: 329-337.

Yang, S., Smith, C., De Luca, H.F. (1993). 1 alpha 25-Dihydroxyvitamin D3 , and 19—nor-1 alpha, 25-dihydroxy vitamin D2 suppress immunoglobulin production and thymic lymphocyte proliferation in vivo. *Biochim. Biophys. Acta* 1158: 279-286.

Yang, S., Smith, C., Prahl, J.M., Luo, X., De Luca, H.F.(1993). Vitamin D deficiency suppresses cell-mediated immunity in vivo. *Arch. Biochem. Biophys.* 303: 98-106.

Yesudian, P.D., Berry, J.L., Wiles, S., Hoyle, S., Young, D.B., Haylett, K., Rhodes, L.E., Davies, P. (2008). The effect of ultraviolet B-induced vitamin D levels on host resistance to Mycobacterium tuberculosis: a pilot study in immigrant Asian adults living in the United Kingdom.*Photodermatology, Photoimmunology& Photomedicine* 24: 97-98.

Zasloff, M. (2006). Fighting infections with vitamin D. *Nature Medicine* 12: 388-390.

In: Clinical Chemistry Research
Editors: Brian H. Mitchem and Charles L. Sharnham
ISBN 978-1-60692-517-1

Chapter VIII

Generation and Analysis of Disease-Specific Mouse Models by Clinical Chemical Screening

Bernhard Aigner*, Birgit Rathkolb and Eckhard Wolf
Institute of Molecular Animal Breeding and Biotechnology, and
Laboratory for Functional Genome Analysis (LAFUGA),
Ludwig-Maximilians-Universität, Munich, Germany

Abstract

Animal models are required for studying the pathobiology of diseases as well as for the development and evaluation of therapeutic strategies. Specific mouse models for known genetic diseases are generated by reverse genetics strategies using genetic engineering techniques which result in defined alterations of the mouse genome. Standardized clinical chemical analysis contributes to the determination of the exact phenotype of the animal models. However, the resulting phenotypes of the mutant mice cannot be predicted and do not always mirror the respective human disease. A complementary strategy is to generate new alleles by random mutagenesis and to screen for clinically relevant phenotypes. The underlying mutations are then identified by forward genetics strategies and lead to the identification of genes/alleles which may have counterparts relevant for human diseases. Novel disease models were derived from phenotype-driven large-scale ethylnitrosourea (ENU) mouse mutagenesis projects which started a decade ago by using clinical chemical parameters in high-throughput screens. Offspring of chemically mutagenized mice were analyzed in order to detect phenotypic variants with defects of various organ systems or changes in metabolic pathways. Breeding of the affected mice and screening of the offspring confirmed the transmission of the altered phenotype to subsequent generations, thereby revealing a mutation as cause for the aberrant phenotype. The subsequent in-depth genotypic and phenotypic analysis of mutant lines

* Institute of Molecular Animal Breeding and Biotechnology, Hackerstr. 27, D-85764 Oberschleißheim, Germany, Phone: +49 89 218078420, Fax:+49 89 218078422, E-mail: b.aigner@gen.vetmed.uni-muenchen.de

showing alterations in clinical chemical parameters produced novel models for the biomedical research.

Introduction

Genome sequencing projects provided the complete genomic sequences of human and other mammalian organisms. The functional analysis of genes and pathways requires a high number of animal models. Mice are the primary models in biomedical research. Novel animal models for human diseases are produced using both gene-driven and phenotype-driven methods (Figure 1). These two complementary strategies already provided a high number of interesting new mouse mutants. The reverse genetics approach uses transgenic mice which are generated with the gene of interest by various genetic engineering techniques leading to the non-homologous or homologous recombination of the host genome. The transgenic mice are subsequently analyzed for the resulting phenotype. Analogously, mice derived from embryonic stem cells with induced mutations in chosen genes (Skarnes et al. 2004) (http://www.genetrap.org) are established as novel animal models by comprehensive phenotypic analysis. As the resulting phenotypes of the transgenic mice cannot be predicted and do not always mirror the respective human disease, closing the phenotype gap in animal models is currently done by using phenotype-driven strategies. The forward genetics approach uses spontaneous or induced phenotypic alterations of clinical relevance and subsequently detects the causative mutation. Therefore, genome-wide random mutagenesis of mice and the screen for clinically relevant phenotypes in the offspring are carried out followed by the establishment and subsequent genotypic analysis of mutant lines (Silver 1995; Peters et al. 2007). Analogous approaches are the phenotypic examination of independent and combined crosses of inbred mouse strains, and the subsequent genome-wide search for genetic polymorphisms by linkage analysis which control the examined phenotype (Churchill et al. 2004). In addition, already existing mouse populations like heterogeneous stock mice are phenotypically examined and analyzed by high-resolution whole-genome association studies for genetic polymorphisms influencing the selected quantitative phenotypic traits (Valdar et al. 2006). New mouse models which are established by using both gene-driven and phenotype-driven strategies are available from various resource centers (Strivens and Eppig 2004; Davisson 2006) (http://www.informatics.jax.org/imsr).

In humans, most inherited metabolic disorders lead directly or indirectly via altered organ functions to changes of diagnostic laboratory parameters (Greiling and Gressner 1995). Identification of mutant mice derived from gene- and/or phenotype-driven approaches showing similar clinical chemical deviations provide novel appropriate animal models for the detection of the causative mutation and the pathologic consequences thereof. As homeostasis of clinical chemical parameters is regulated by polygenic factors, quantitative trait loci (QTL) affecting chosen parameters and eventually influencing disease susceptibility are revealed using mouse models which show considerable differences in the parameters in question. The diagnostic impact of clinical chemical parameters for specific pathologic alterations has been described in mice (Loeb and Quimby 1999; Rathkolb et al. 2000a; Klempt et al. 2006a).

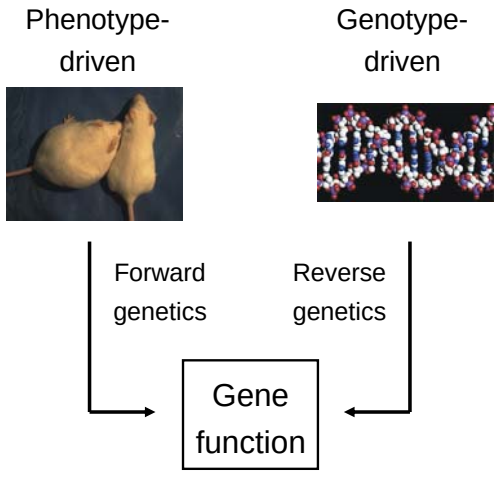

Figure 1. Generation of novel mouse mutants for the biomedical research using two complementary strategies. The gene-driven approach works with transgenic animal models. The mice are generated with the gene of interest by various genetic engineering techniques and subsequently analyzed for the resulting phenotype. The phenotype-driven approach searches for spontaneous or induced phenotypic alterations of clinical relevance and subsequently detects the causative mutation in the mice.

Standardized Clinical Chemical Analysis of the Mouse

Understanding mammalian genetic systems requires the overcoming of challenges in the phenotyping of mouse models (Brown et al. 2006). Clinical chemical analysis of the mouse uses laboratory diagnostic procedures suitable to detect defects of various organ systems, changes in metabolic pathways and hematological disorders. The methods are automated routine procedures according to the techniques carried out with human samples which allow the high-throughput screening of a large number of mice for a broad spectrum of clinical chemical parameters in blood and urine, including substrates, proteins, electrolytes and enzymes, as well as hematological parameters such as red and white blood cell counts (Loeb and Quimby 1999). Mouse husbandry, blood collection, sample preparation and sample analysis are standardized for obtaining valid and reproducible results (Rathkolb et al. 2000a, 2000b; Klempt et al. 2006a).

Experimental Procedures

The limiting factor for the clinical chemical analysis in mice is the volume of the blood sample. The total blood volume corresponds to 7.5% of the body weight of the mouse. Up to 15% of the total blood volume can be removed once without causing significant alterations. For repeated sampling, 10%, 7.5% and 1% of the total blood volume can be removed every two weeks, every week and each day, respectively (Morton et al. 1993; Suckow et al. 2001). Different blood collection procedures are described for the mouse. Blood collection by

retroorbital sinus puncture under short-term general anesthesia results in the collection of a large sample volume, the absence of marked hemolysis, the achievement of reproducible examination results and the possibility of repeated collection at the same site. Thus, it is recommended for the clinical chemical screen. For the general clinical chemical screen, fasting of the mice, e.g. by food withdrawal overnight, is not recommended. From three-month-old mice, 300 µl blood is collected in Li-heparin treated tubes to obtain 130 µl plasma and additional 50 µl blood is collected in EDTA-coated tubes.

The clinical chemical parameters of blood plasma samples are automatically analyzed using appropriate routine procedures (Table 1). In our screen, an Olympus AU400 autoanalyzer (Olympus, Hamburg, Germany) and the adapted reagents for human samples from Olympus (Hamburg, Germany) are used. Calibration and quality control are performed according to the manufacturer's protocols. The clinical chemical analysis is carried out in 130 µl plasma diluted with the same volume of deionised water to the total volume of 260 µl and includes the following 19 parameters in their linear measurement range: substrates: cholesterol, creatinine, glucose, triglycerides, urea, uric acid; proteins: total protein, ferritin, transferrin; electrolytes: calcium, chloride, inorganic phosphorus, potassium, sodium; enzyme activities: alanine aminotransferase (EC 2.6.1.2), aspartate aminotransferase (EC 2.6.1.1), alkaline phosphatase (EC 3.1.3.1), α-amylase (EC 3.2.1.1), creatine kinase (EC 2.7.3.2).

Analysis of the hematological parameters is done using an Animal Blood Counter (Scil, Viernheim, Germany) validated by the manufacturer for the analysis of mouse blood. In 50 µl EDTA-treated blood, the following hematological parameters are directly measured: red blood cells: hemoglobin, mean corpuscular volume (MCV), red blood cell count (RBC); white blood cells: white blood cell count (WBC), platelets. Additional hematological parameters are calculated using the parameters measured.

The clinical chemical screen which was established for the Munich ENU mouse mutagenesis project, is based on three steps. The largely automated high-throughput primary screen allows the efficient analysis of a large number of mice for a broad range of alterations in various organ systems and metabolic pathways. Automated high-throughput secondary screens are established for the confirmation of defined organ defects and the comprehensive analysis of tissue-specific profiles on subsequent blood samples. The tertiary screen is not carried out as high-throughput screen but consists of more specific and complex in-depth examinations of a relatively small number of mice for the detailed characterization of particular interesting disease phenotypes. This may be glucose tolerance test, blood gas measurement, differential white blood cell count, and urinary protein electrophoresis. Thus, the screen is suitable to detect a plethora of diverse defects in organ systems and metabolic pathways. Parameter selection may be adapted according to the aim of the proposed project (Klempt et al. 2006a).

Table 1. Common clinical chemical plasma parameters established for the analysis of the mouse.

Parameter	Assay	Unit[1]	Linear range[2]
Alanine aminotransferase (EC 2.6.1.2)	IFCC, GSCC[3]	µkat/l	0.05-8.33
		U/l	3-500
Alkaline phosphatase (EC 3.1.3.1)	Orthophosphoric-monoester-phosphorhydrolase	µkat/l	0.08-25
		U/l	5-1500
α-Amylase (EC 3.2.1.1)	α-1,4-glucan-4- glucanohydrolase	µkat/l	0.08-25
		U/l	5-1500
Aspartate aminotransferase (EC 2.6.1.1)	IFCC, GSCC[3]	µkat/l	0.05-16.7
		U/l	3-1000
Calcium	Arsenazo III	mmol/l	1-4
Chloride	Target value ISE indirect	mmol/l	50-200
Cholesterol	Cholesteroloxidase peroxidase (CHOD-PAP)	mmol/l	0.64-18
		mg/dl	25-700
Creatine kinase (EC 2.7.3.2)	IFCC, GSCC[3]	µkat/l	0.17-33.4
		U/l	10-2000
Creatinine	Jaffé	µmol/l	18-2200
		mg/dl	0.2-25
Ferritin	Latex agglutination	µg/l	8-450
Glucose	Hexokinase	mmol/l	0.6-45
		mg/dl	10-800
Phosphorus, inorganic	Complex formation with molybdate	mmol/l	0.32-6.4
Potassium	Target value ISE indirect	mmol/l	1-10
Sodium	Target value ISE indirect	mmol/l	50-200
Total protein	Biuret	g/dl	3-12
Transferrin	Turbidimetric end point	mg/dl	75-750
Triglcerides	Glycerolphosphateoxidase peroxidase (GPO-PAP)	mmol/l	0.11-11.4
		mg/dl	10-1000
Urea	Glutamate dehydrogenase (GLDH)	mmol/l	0.8-50
		mg/dl	5-300
Uric acid	Uricase, Peroxidase (POD), N-ethyl-N-(2-hydroxy-3-sulfopropyl)-3-methylaniline (TOOS), 4-aminophenazone	µmol/l mg/dl	11.9-1487 0.2-25

[1] The SI unit of the parameter is given in the first line in the cases where two units are listed.

[2] Linear measurement range for the Olympus AU400 autoanalyzer (Olympus, Hamburg, Germany) and the adapted reagents for human samples according to the manufacturer.

[3] Assay based on the recommendations of the International Federation for Clinical Chemistry and the German Society for Clinical Chemistry.

Standardization

Multiple factors influence the outcome of the phenotypic analysis of the mouse. Effective standardization of the mouse husbandry including the abiotic and biotic environmental factors is carried out for the achievement of valid and reproducible results of the clinical chemical screen. Standardization of mouse husbandry has been extensively reviewed (Hedrich and Bullock 2004, and references therein). Mouse husbandry is done under a continuously controlled specific pathogen-free (SPF) hygiene standard according to the recommendations of the Federation of European Laboratory Animal Science Associations (FELASA) (Nicklas et al. 2002) (http://www.felasa.eu).

Former phenotype assessment protocols like SHIRPA included the analysis of few basal biochemical parameters (Rogers et al. 1997). Comprehensive phenotypic examination as well as standardization of the phenotypic analysis for obtaining valid and reproducible results were greatly improved by establishing specialized mouse phenotyping centers which use defined standard operating procedures (SOPs) (Table 2) (http://www.interphenome.org). The aim of the centers is the characterization of mouse models for human diseases to understand molecular mechanisms of human disorders and to develop new therapies. The specialized mouse phenotyping centers develop and offer the standardized and comprehensive phenotypic analysis of mouse mutants from various sources (e.g. transgenics, knockout mice, mutants from mutagenesis screens like ENU). As an example, the German Mouse Clinic (GMC) (Gailus-Durner et al. 2005) (http://www.mouseclinic.de) was established evolving from the Munich ENU mouse mutagenesis project. It offers the examination of more than 240 parameters. The screens in the German Mouse Clinic are designated to the areas of allergy, behavior, cardiovascular analysis, clinical chemistry, dysmorphology with special emphasis on bone and cartilage development, energy metabolism, immunology, lung function, molecular phenotyping, neurology and pain perception, steroid metabolism, vision, and pathology.

Table 2. Mouse phenome databases containing protocols and results of clinical chemical analyses (according to http://www.interphenome.org).

Database	URL
EMPReSS	http://empress.har.mrc.ac.uk
Ensembl	http://www.ensembl.org
EuroPhenome	http://www.europhenome.eu
IMSR (International Mouse Strain Resource)	http://www.informatics.jax.org/imsr/index.jsp
Mouse Genome Informatics (MGI)	http://www.informatics.jax.org
Mouse Phenome Database (MPD)	http://aretha.jax.org/pub-cgi/phenome/mpdcgi?rtn=docs/home
Omic Space	http://omicspace.riken.jp
RIKEN GSC	http://www.gsc.riken.jp/Mouse/main.htm

Various projects published SOPs for the clinical chemical analysis and data obtained by using these SOPs (Table 2) (Paigen and Eppig 2000; Mouse Phenotype Database Integration Consortium 2007) (http://www.interphenome.org). The Mouse Genome Database (MGD) serves as an integration point for mouse genomic and biological data (Strivens and Eppig 2004). In Europe, EUMORPHIA was a project funded by the European Commission. The work carried out was EMPReSS (European Mouse Phenotyping Resource of Standardized Screens) (Brown et al. 2005; Green et al. 2005), a database of SOPs for standardized screens to characterize the mouse phenotype, EuroPhenome (Mallon et al. 2008), an online database to hold phenome data obtained from the EMPReSS SOPs, and EUMODIC (European Mouse Disease Clinic), the generation of the phenome data on several hundred mutant mouse lines using the EMPReSS SOPs (Mouse Phenotype Database Integration Consortium 2007). EMPReSS contains SOPs for the clinical chemical and hematological analysis including animal husbandry and diet, blood collection, blood sample handling and analytical tests. Clinical chemical and hematological data of selected inbred strains (129Sv, BALB/c, C3H, C57BL/6) are stored in the EuroPhenome phenotyping resource allowing the assessment of inter-strain, -gender and -laboratory variation of the tests.

Outcome of the Analysis

Prerequisite to the detection of phenotypic alterations in mutant mice is the determination of the physiologic values in the genetic background used in each project. By examining a sufficient number of control mice, the 95% range of the values is defined to be the reference range thereby eliminating outlier data. The 95% range covers the data range including two standard deviations above and below the mean if Gaussian distribution of the data occurs for the parameter in question (Loeb and Quimby 1999).

The published clinical chemical data from various projects (Table 2) (Mouse Phenotype Database Integration Consortium 2007) (http://www.interphenome.org) are of great value for the choice of the appropriate mouse strain according to the aims of the proposed project. Analysis of selected inbred strains (129Sv, BALB/c, C3H, C57BL/6) in the German Mouse Clinic showed considerable differences in the values of the clinical chemical and hematological parameters (Table 3). Interaction of unrecognized laboratory-specific factors in mouse genotype, husbandry and experimental procedure may lead to significant deviations in the results of highly standardized analyses of clinical chemical and hematological parameters (Champy et al. 2004, 2008; Klempt et al. 2006b). As the great number of critical variables can not be completely standardized between different laboratories, analysis of a sufficient number of controls is necessary for each project (Loeb and Quimby 1999).

Table 3. Physiologic values (mean±SD) of clinical chemical plasma parameters in 12-week-old inbred mice (n=15 per strain and sex).

	Males				Females			
Parameter (Unit)	129SvJ	BALB/cAnPt	C3HeB/FeJ	C57BL/6J	129SvJ	BALB/cAnPt	C3HeB/FeJ	C57BL/6J
Cholesterol (mg/dl)	123±11^{C}	103±5	174±11^{C}	96±13	98±9^{C}	81±6^{A}	130±21^{C}	73±9
Creatinine (mg/dl)	0.30±0.02^{C}	0.30±0.03^{C}	0.29±0.03^{C}	0.39±0.03	0.32±0.02^{B}	0.28±0.03^{C}	0.31±0.03^{B}	0.34±0.03
Glucose (mg/dl)	171±26^{C}	73±20	196±19^{C}	67±19	166±20^{C}	90±21	165±20^{C}	79±34
Triglycerides (mg/dl)	217±55^{C}	195±30^{B}	303±59^{C}	153±32	149±31^{C}	146±28^{C}	272±109^{C}	83±28
Urea (mg/dl)	66±8	51±6^{C}	50±8^{C}	72±9	62±8^{A}	44±6^{C}	42±10^{C}	70±12
Uric acid (mg/dl)	1.5±0.4	1.4±0.7	1.5±0.7	1.3±0.9	1.1±0.5	3.2±1.6^{A}	1.5±0.6	1.9±1.8
Ferritin (µg/l)	36±4^{C}	55±8^{C}	54±8^{C}	72±13	39±4^{C}	73±16^{C}	75±13^{C}	118±30
Total protein (g/dl)	5.3±0.4^{A}	5.4±0.2^{A}	5.7±0.3	5.6±0.2	5.1±0.3^{B}	5.3±0.2	5.5±0.2	5.4±0.2
Transferrin (mg/dl)	152±6^{C}	161±4^{C}	183±5^{C}	144±5	155±4^{C}	164±4^{C}	182±5^{C}	147±4
Calcium (mmol/l)	1.9±0.1^{C}	2.0±0.1^{C}	2.3±0.1^{A}	2.3±0.1	2.0±0.0^{C}	2.0±0.1^{C}	2.4±0.0^{C}	2.2±0.1
Chloride (mmol/l)	110±3.5^{C}	114±1.1^{C}	112±1.2^{C}	117±2.3	109±2.0^{C}	115±1.7^{C}	114±1.5^{C}	119±3.2
Phosphorus (mmol/l)	1.4±0.1^{C}	1.6±0.3^{C}	1.9±0.2	2.0±0.3	1.4±0.2^{C}	1.5±0.1^{A}	1.7±0.4	1.7±0.2
Potassium (mmol/l)	4.6±0.4^{C}	4.3±0.3^{B}	4.3±0.2^{C}	3.9±0.3	5.0±0.4^{C}	4.8±0.6^{C}	3.9±0.2	3.7±0.3
Sodium (mmol/l)	152±5.1^{C}	161±1.5^{C}	157±1.3^{C}	166±2.1	149±2.2^{C}	160±1.5^{C}	156±1.4^{C}	163±2.3
ALT (U/l)	13±5^{B}	26±12	16±4	19±6	13±5^{B}	25±12	15±4^{A}	27±17
ALP (U/l)	nd	156±9	163±29	150±12	nd	177±23	214±34^{A}	187±39
Amylase (U/l)	2674±224	2786±237	2466±161	2626±345	2535±191^{B}	2500±168^{B}	2068±132^{C}	3587±1351
AST (U/l)	22±7^{A}	41±13	23±5^{A}	37±23	24±5^{C}	62±27^{B}	32±10	38±12
CK (U/l)	50±49^{A}	171±127	69±55	233±313	41±25^{C}	216±156^{A}	110±96	113±53
Hemoglobin (g/dl)	18.1±0.9^{C}	17.2±1.8^{B}	15.5±0.5	15.4±1.4	16.6±0.9^{C}	15.4±2.6	15.3±0.4	15.1±0.8
MCV (fl)	48.7±0.5^{C}	47.6±0.7^{C}	49.6±0.5^{C}	45.4±0.9	50.1±0.4^{C}	48.7±0.8^{C}	50.8±0.7^{C}	45.1±1.0
RBC ($\times 10^{6}$/µl)	11.5±0.6^{C}	11.3±1.2^{A}	10.0±0.4	10.3±0.9	10.1±0.5	9.8±1.7	9.8±0.3^{A}	10.1±0.5
WBC ($\times 10^{3}$/µl)	6.1±1.1	5.1±1.4	6.3±1.3	5.8±1.4	6.3±0.8^{C}	4.0±1.8	5.4±1.2^{B}	3.9±1.4
Platelets ($\times 10^{3}$/µl)	562±50^{C}	739±64^{A}	704±52^{B}	860±165	549±49^{C}	579±159^{C}	660±87^{C}	887±128

nd, not determined. t-test of the values compared to C57BL/6J: ^{A} $p < 0.05$, ^{B} $p < 0.01$, ^{C} $p < 0.001$.

Clinical Chemical Phenotyping to Define Novel Mouse Models

Spontaneous and induced mouse mutants show a large variation in clinical chemical and hematological values. The clinical chemical screen allows not only the accurate and efficient examination of the expected effects but also the discovery of additional, more subtle consequences of particular genetic modifications, e.g. in knockout mice without obvious phenotypic alterations. Furthermore, in-depth clinical chemical examinations contribute to the understanding of the pathomechanisms in mouse models with interesting disease phenotypes. In the following, the impact of overall and specialized clinical chemical analyses of mice derived from gene-driven as well as phenotype-driven projects is shown on various examples.

In humans, increased bone fragility, fractures and osteoporosis are main symptoms of the inherited disorder Osteogenesis imperfecta. A novel ENU-induced mouse model was derived from the dysmorphology screen for dominant mutations in the Munich ENU mouse mutagenesis project. The heterozygous mutants exhibited reduced bone mass, multiple fractures and early lethality. The causal gene in the mutant mice was mapped to chromosome 11 by linkage analysis, and a C-terminal frameshift mutation was identified in the collagen type I, alpha 1 (*Col1a1*) gene. The subsequent examination of the mice included clinical chemical analysis which specifically concentrated on parameters of the bone turnover. Compared to wild-type controls, increased levels of alkaline phosphatase, tartrate-resistent acid phosphatase 5b and osteocalcin as well as of the hormones parathyroid hormone and calcitonin were detected in the heterozygous mutants. Thus, the metabolic bone turnover was elevated in the heterozygous mutants. These analyses contributed to the phenotypic description of a new model for Osteogenesis imperfecta (Lisse et al. 2008).

The four dickkopf (*Dkk*) genes encode a small family of secreted *Wnt* antagonists and show regionalized expression during vertebrate embryogenesis. Dickkopf3 (*Dkk3*) appears as a divergent member of the *Dkk* family and its function is poorly understood. Using genetic engineering techniques, *Dkk3* deficient mice were generated by targeted disruption. *Dkk3* knockout mice were viable and fertile. Overall phenotypic analysis showed no major alterations in organ morphology and physiology. Therefore, they were phenotypically analyzed in the German Mouse Clinic including the overall clinical chemical and hematological examination. In this screen, increased hemoglobin and hematocrit levels were observed. Mean corpuscular volume (MCV) and mean corpuscular hemoglobin (MCH) were increased, whereas mean corpuscular hemoglobin concentration (MCHC) was decreased. The proposed function of *Dkk3* in thyroid hormone metabolism was not supported as mutant mice were euthyroid. Instead, novel phenotypes were observed for the subsequent description of the *Dkk3* gene function (Barrantes et al. 2006).

Mutations in the hemochromatosis (*Hfe*) gene result in hereditary hemochromatosis (HH) which is characterized by increased duodenal iron absorption. As there is no known physiologic pathway for iron excretion, this results in tissue iron overload. *Hfe* knockout mice as well as mice harboring the orthologous *Hfe* disease mutation of human patients recapitulate the human HH phenotype. Specific clinical chemical analysis of the iron metabolism in the *Hfe* mutants observed increased liver iron levels, normal serum iron and

ferritin levels and decreased unsaturated iron binding capacity (UIBC). For the further functional analysis of *Hfe*, tissue-specific *Hfe* knockout mice were generated by using the *Cre*/*loxP* technology. Mice with efficient deletion of *Hfe* in crypt- and villi-enterocytes were examined for iron metabolism parameters. They maintained physiologic iron metabolism with wild-type hepatic iron levels, normal serum iron and ferritin levels and unaltered unsaturated iron binding capacity (UIBC). This demonstrated that intestinal *Hfe* is dispensable for the physiologic control of systemic iron homeostasis under steady state conditions thereby excluding a direct role for duodenal *Hfe* in the pathogenesis of HH (Vujic et al. 2007).

The *Notch* signaling pathway is an evolutionarily conserved transduction pathway involved in embryonic patterning and regulation of cell fates during development. Delta1 (*Dll1*) is one of the ligands of the *Notch* receptors. Homozygous *Dll1* knockout mice die during embryonic development. Heterozygous *Dll1* knockout mice were phenotyped including the overall clinical chemical screen. Compared to wild-type controls, they showed alterations in metabolites and electrolytes relevant for kidney function. Subsequently, a genetic screen for modifiers of the *Dll1*-dependent *Notch* signaling in the mouse was carried out. Heterozygous *Dll1* knockout mice were used for a phenotype-driven modifier screen by crossing them to ENU-mutagenized mice. The offspring were subsequently phenotyped including the analysis of clinical chemical parameters. New mutant lines were generated, and five of them are novel tools for studying the role of *Dll1*-dependent *Notch* signaling in kidney and liver function as well as cholesterol and iron metabolism (Rubio-Aliaga et al. 2007).

Generation of Novel Mouse Models by Phenotype-Driven ENU Mouse Mutagenesis Projects

Random chemical mutagenesis and subsequent screening for clinically relevant phenotypes without *a priori* assumptions is a powerful approach to derive novel mouse models for biomedical research. The alkylating agent N-ethyl-N-nitrosourea (ENU) is currently the most powerful mutagen for the production of mutant mice. ENU shows mutagenic action on premeiotic spermatogonial stem cells. This allows the production of a large number of randomly mutant offspring from treated males. Compared to other mutagenesis methods, ENU predominantly induces point mutations thereby leading to allelic series for the functional analysis of genes (Stanford et al. 2001). Mutations induced by ENU are not tagged molecularly as it is the case in other random mutagenesis projects e.g. using gene traps. This is initially a disadvantage as the causative mutations have to be analyzed by linkage analysis. However, the availability of point mutations is important for the detailed functional analysis of genes. The function of a given gene cannot be described by analyzing only one mutant allele, but multiple alleles of the same gene are necessary for this goal (Hrabé de Angelis et al. 2007).

After mating the ENU mutagenized males to wild-type females, specific pathologic states are identified in the offspring by appropriate routine procedures which allow the screening of large numbers of mice for a broad spectrum of parameters. Phenotypic screens in major ENU mouse mutagenesis projects often include allergy, behaviour, clinical chemistry,

dysmorphology, immunology as well as other screens with a high number of test parameters. However, also smaller laboratories efficiently set up specialized projects. Screening profiles of clinical chemical blood parameters were established in order to detect phenotypic variants with defects of various organ systems or changes in metabolic pathways. Thus, the ENU mouse mutagenesis projects established during the last ten years serve as platforms for the systematic, genome-wide, large-scale production and analysis of mouse mutants as a model system for inherited human diseases, thereby facilitating the identification and functional characterization of genes which are relevant for the prevention, diagnosis, and therapy of diseases (Hrabé de Angelis et al. 2007). Mutant lines with the causative mutation already identified are successfully used in different areas of biomedical research (Hrabé de Angelis et al. 2000; Nolan et al. 2000).

ENU mouse mutagenesis projects include following parts: genome-wide random mutagenesis of founder males, breeding of G1 and G3 offspring according to a defined breeding scheme, phenotypic screening of G1 and G3 offspring for alterations, confirmation cross to confirm a mutation as cause for the phenotypic alteration, generation of a mutant line inheriting the altered phenotype, chromosomal mapping of the mutation by linkage analysis, identification of the causal mutation, and in-depth phenotyping of the mutant line (Aigner et al. 2008, and references therein). As a representative example for the basic strategy of other projects, in the Munich ENU mouse mutagenesis project ten-week-old inbred C3H male mice were injected intraperitoneally with ENU. The screen for dominant mutations was performed on G1 animals which were derived by mating of mutagenized G0 males to wild-type females. G1 males which did not show an abnormal phenotype in the screen for dominant mutations, were mated to wild-type females to produce G2 daughters which were then mated to their fathers. The resulting G3 mice were used for the screen for recessive mutations (Figure 2A). Breeding of the phenotypically affected mice and screening of the offspring confirmed the transmission of the altered phenotype to subsequent generations, thereby revealing a mutation as cause for the aberrant phenotype. Inheritance of observed abnormal phenotypes in G1 mice was tested in G2 offspring from the mating of the affected G1 mouse exhibiting the altered phenotype and wild-type mice. Inheritance of observed abnormal phenotypes in the G3 mice was tested on G4 intercross or G4 × G3 backcross offspring in the inbred genetic background (Figure 2B). ENU mouse mutagenesis projects are done on different inbred genetic backgrounds (BALB/c, C3H, C57BL/6). The chemically mutagenized mice are subsequently mated with mice of the same or of different inbred strains.

Using similar mutagenesis protocols and various inbred strains, studies of different chromosomal regions of ENU-mutagenized mice with different molecular genetic methods observed one mutation in 100,000 bp and one mutation in 1.0-2.5 Mbp (Aigner et al. 2008, and references therein). After confirming the inheritance of the mutant phenotype to the subsequent generations, backcross of the phenotypic mutant animal to wild-type mice leads to the loss of non-causative mutations. After ten backcross generations, 20 cM of the originally mutagenized genomic DNA remains which harbours about 25 mutations including the causative mutation (Silver 1995). Considering only a small number of the more than 1000 mutations per animal as potentially functional by causing phenotypic consequences, at least the very most part of them except of the causative mutation is segregated (Russ et al. 2002; Keays et al. 2006).

A

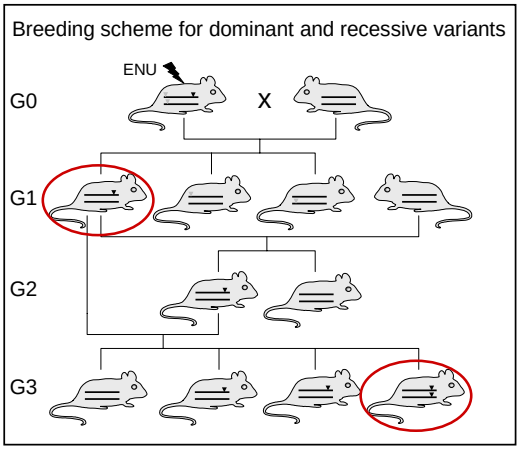

B

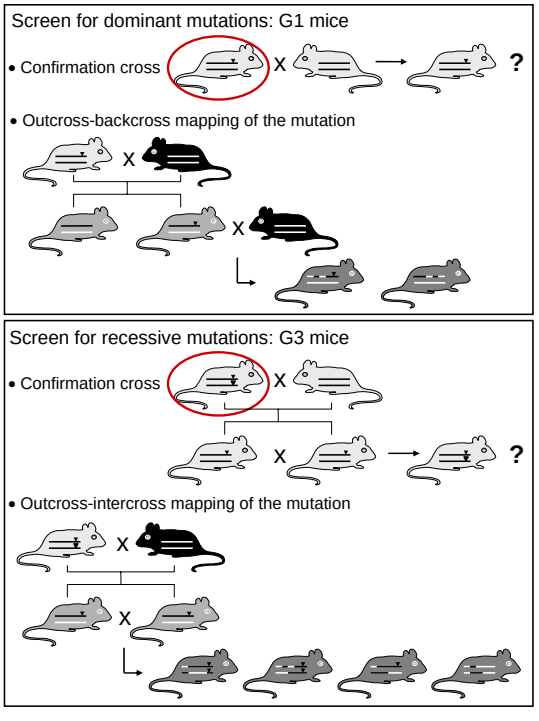

Figure 2. Generation of novel disease models in phenotype-driven ENU mouse mutagenesis projects. (A) After treatment of male mice with ENU, defined mating schemes produce the G1 and G3 offspring, which are phenotypically examined for alterations e.g. by clinical chemical analysis. Mice with phenotypic alterations of clinical relevance (variants) presumably habour a causative dominant (G1) or recessive (G3) mutation (in circles). (B) Phenotypic G1 and G3 variants (in circles) are mated to test the inheritance of the altered phenotype caused by dominant or recessive mutations, respectively. The chromosomal position of the causative mutation is identified by linkage analysis which is subsequently followed by candidate gene analysis. Black triangle: ENU-induced mutation causing an altered phenotype; light triangles: non-causative ENU-induced mutations.

The establishment of lines showing the mutant phenotype indicates the penetrance of the mutant phenotype and the number of segregating mutations causing the mutant phenotype. The underlying mutation is then identified by forward genetics strategies. The examination of the chromosomal position of the causative mutation is carried out by linkage analysis (Figure 2B). Briefly, phenotypic mutants harbouring the mutation are bred to wild-type mice of a second inbred strain, the resulting hybrid offspring are analyzed for the abnormal phenotype of the parent and hybrid mutants are backcrossed to wild-type mice of the second inbred strain (for dominant mutations) or intercrossed (for recessive mutations). The resulting offspring are again analyzed for the abnormal phenotype of the parent, thereby dividing them into phenotypically mutant and non-mutant animals. Genome-wide linkage analysis of the genomic DNA samples using polymorphic markers subsequently reveals the chromosomal position of the mutation. Further linkage analysis on the determined chromosomal site and candidate gene analysis including sequencing techniques are then performed in order to identify the causative mutation (Silver 1995). The probability that a confounding mutation is linked to a sequenced mutation in a determined chromosomal region with a length of 5 Mb was calculated to be low ($p < 0.05$). In total, most mutant phenotypes are effectively monogenic (Keays et al. 2006, 2007).

The functional proof that a mutation which lies in the correct genomic interval is responsible for the phenotype may be carried out by demonstrating that the affected protein is absent or inactive, by rescuing the phenotype via introduction of a wild-type copy of the gene using reverse genetics methods, or by performing complementation tests with another mutant allele (Caspary and Anderson 2006). The mutants may carry loss-of-function, dominant negative, hypomorphic or gain-of-function alleles of the affected genes.

Clinical Chemical Screening in ENU Projects

Several public ENU mouse mutagenesis projects used clinical chemical screening parameters for the generation of novel disease models (Table 4). In the Munich ENU mouse mutagenesis project, a screening profile of clinical chemical parameters was established for the analysis of offspring of chemically mutagenized mice on the inbred C3HeB/FeJ (C3H) genetic background. Screening of more than 20,000 G1 and G3 mice for dominant and recessive mutations led to the establishment of about 100 mutant lines with deviations of various plasma substrates, proteins, electrolytes and enzyme activities, and/or hematological parameters (Klempt et al. 2006a).

In addition to the clinical chemistry screen in the Munich ENU project, a systematic clinical chemistry analysis has been described to date in another ENU mouse mutagenesis program (Nolan et al. 2000). The appearance of lines exhibiting altered plasma parameter values was reported on a different genetic background (BALB/c × C3H) (Hough et al. 2002). Specific plasma parameters were described for their successful use in other phenotype-driven ENU mouse mutagenesis projects (Table 4), e.g. diabetes models were established by screen for hyperglycemia (Aigner et al. 2008).

Search for defined phenotypes in published chemically induced (ENU) mutants (as of 23.02.2009) of the “phenotypes and alleles” database in the Mouse Genome Informatics

website (http://www.informatics.jax.org/searches/allele_form.shtml) revealed 1948 alleles and 1607 genes/markers. Of them, 194 alleles and 165 genes/markers were described with phenotypes influencing homeostasis or metabolism, whereas 182 alleles and 146 genes/markers were described with phenotypes influencing the hematopoietic system. In total, 344 alleles and 291 genes/markers show alterations in homeostasis or metabolism and/or the hematopoietic system.

Table 4. Major public ENU mouse mutagenesis projects using clinical chemical screening parameters.

ENU project	URL
Baylor College of Medicine, Houston, USA	http://www.mouse-genome.bcm.tmc.edu
Helmholtz-Zentrum, München, Germany	http://www.helmholtz-muenchen.de/en/ieg/
Jackson Laboratory, Bar Harbor, USA	http://pga.jax.org
MRC, Harwell, UK	http://www.mgu.har.mrc.ac.uk
RIKEN GSC, Yokohama, Japan	http://www.gsc.riken.go.jp/Mouse
University of Toronto, Toronto, Canada	http://www.cmhd.ca

ENU-Induced Mouse Models for Selected Disorders by Clinical Chemical Screen of the Munich ENU Project

The clinical chemical screen of the Munich ENU mouse mutagenesis project especially focused on the analysis of the plasma levels of cholesterol, glucose and urea to produce novel models for the biomedical research in the fields of atherosclerosis and cardiovascular disease, diabetes, and nephropathies.

Plasma Cholesterol as Screening Parameter

Development of atherosclerotic cardiovascular disease is influenced by dyslipidemia including increased values of the normal proportion of low density lipoprotein cholesterol (LDL-C) and high density lipoprotein cholesterol (HDL-C). Beneath a subset of rare monogenic forms, pathologic cholesterol levels often occur as a polygenic and multifactorial disorder. Humans show predominantly LDL-C and are sensitive to diet-induced elevations of LDL-C. In contrast, mice exhibit high amounts of HDL-C and a low LDL-C level (Loeb and Quimby 1999). Therefore, instead of acting as model to enlighten the pathogenesis of human cardiovascular diseases, mice are the animal model of choice to search for additional alleles influencing the plasma lipoprotein cholesterol homeostasis.

Determination of the physiologic plasma cholesterol range in male and female C3H controls resulted in total cholesterol levels of 132±15 (mean ± standard deviation) and

109±17 mg/dl, respectively. The 95% range of the values covered the data range including two standard deviations above and below the mean which indicated the Gaussian distribution of the data. Thus, hypercholesterolemia was defined in our test for male and female mice showing values above the cut-off level of 160 and 140 mg/dl, respectively, whereas hypocholesterolemia was defined for male and female mice showing values below the cut-off levels of 100 and 75 mg/dl, respectively.

Hypercholesterolemic and hypocholesterolemic variants derived from the phenotype screening of the G1 and G3 mice were subsequently mated for the analysis of the inheritance of the altered cholesterol phenotype (Mohr et al. 2004; Aigner et al. 2007b). Using the mice with hypercholesterolemia, nine males of the 43 offspring producing phenotypic variants transmitted hypercholesterolemia to the subsequent generations which led to six and three mutant lines harboring dominant and recessive mutations, respectively. The male and female phenotypic mutants of the nine lines showed mean plasma total cholesterol levels between 170 and 230 mg/dl and between 150 and 200 mg/dl, respectively. In five of the nine lines, a high phenotypic penetrance of hypercholesterolemia was observed, whereas the other four lines showed an incomplete penetrance of various degrees.

Using the mice with hypocholesterolemia, 12 hypocholesterolemic lines harboring dominant mutations and three hypocholesterolemic lines harboring recessive mutations were established. The male and female phenotypic mutants of the 15 lines showed mean plasma total cholesterol levels between 62 and 95 mg/dl and between 53 and 68 mg/dl, respectively. A high phenotypic penetrance of hypocholesterolemia was observed in 13 of the 15 lines.

The majority of the hypercholesterolemia and hypocholesterolemia lines showed no obvious deviations in the additional clinical chemistry plasma parameters measured and also appeared normal in the general clinical examination. Thus, most lines harbor mutations in genes which do not cause altered plasma cholesterol levels secondary to preceding alterations in other metabolic pathways, but primarily and selectively influence the plasma cholesterol homeostasis. In summary, we successfully established a novel panel of ENU-derived mutant mouse lines for their subsequent use in the identification of alleles influencing the plasma cholesterol homeostasis in humans and other species (Mohr et al. 2004; Aigner et al. 2007b).

Plasma Glucose as Screening Parameter

Determination of the physiologic plasma glucose range in male and female C3H controls resulted in levels of 128±47 (mean ± standard deviation) and 123±47 mg/dl, respectively. Using plasma glucose as parameter in the screen for dominant mutations, we found hyperglycemia (276 and 335 mg/dl) in the male G1 mouse no. 20016135 (Herbach et al. 2007; Aigner et al. 2008). Mating revealed the inheritance of the abnormal phenotype to the G2 offspring leading to the mutant line GLS004. The line GLS004 was bred for more than ten generations without losing the abnormal phenotype. Genome-wide linkage analysis of the mutation using a single nucleotide polymorphism (SNP) marker assay resulted in the strong linkage of the mutation to the marker rs13479566 of chromosome 7. Candidate gene examination of insulin 2 (*Ins2*) in the mutant mice observed a T→A transversion in the *Ins2*

gene at nt 1903 in exon 3, which leads to the amino acid exchange C95S and loss of the A6-A11 intrachain disulfide bond. Therefore, the line was designated Munich *Ins2*^{C95S}.

From one month of age onwards, blood glucose levels of heterozygous Munich *Ins2*^{C95S} mutant mice were significantly increased as compared to controls. The fasted and postprandial serum insulin levels of the heterozygous mutants were indistinguishable from those of wild-type littermates. However, serum insulin levels after glucose challenge, pancreatic insulin content and homeostasis model assessment (HOMA) beta cell indices of heterozygous mutants were significantly lower than those of wild-type littermates. Initial blood glucose decrease during insulin tolerance test was lower and HOMA insulin resistance indices were significantly higher in mutant mice. The total islet volume, the volume density of beta cells in the islets and the total beta cell volume of heterozygous male mutants were significantly reduced, as compared to wild-type mice. Electron microscopy of the beta cells of male mutants showed virtually no secretory insulin granules, the endoplasmatic reticulum was severely enlarged and mitochondria appeared swollen. In total, we established a novel diabetes mouse model which represents an excellent tool for studying the mechanisms of beta cell dysfunction and death, and for therapeutic intervention studies (Herbach et al. 2007).

Plasma Urea as Screening Parameter

Kidney diseases lead to the failure of urinary excretion of metabolism products. In our study, urea levels in plasma from male and female C3H controls corresponded to 48±11 (mean ± standard deviation) and 41±11 mg/dl, respectively. The values within the 95% range were defined to be physiologic thereby eliminating outlier data. Thus, pathologic plasma urea levels were defined in our test for both male and female mice showing values above the cut-off level of 70 mg/dl in two measurements within a three-week interval.

We identified 44 animals consistently exhibiting increased plasma urea concentrations (Aigner et al. 2007a). Transmission analysis of the altered phenotype of 23 mice to subsequent generations led to the establishment of five mutant lines. One and four mutant lines were derived from the screen for dominant and recessive mutations, respectively. Both sexes were affected in the lines. The phenotypic mutants of the five lines showed mean plasma urea levels between 83 and 106 mg/dl, respectively. A suitable phenotypic penetrance of the pathologic urea levels above 50% was observed in all five lines which facilitates effective phenotypic and molecular genetic analyses. The five lines were bred for multiple generations without losing the abnormal phenotype.

Urinary urea levels were decreased in the mutants of the five lines. In addition, most mutants showed increased plasma and decreased urinary creatinine levels. Pathological investigation of kidneys from the five mutant lines revealed a broad spectrum of alterations, ranging from no macroscopic and light microscopic kidney alterations to decreased kidney-to-body weight ratio, dilation of the renal pelvis and severe glomerular lesions.

Linkage analysis of the chromosomal site of the mutation was already carried out in two lines with recessive mutations. The examination revealed a strong linkage of the mutation to a defined single chromosomal site on chromosome 2 at 132 Mb (Mouse genome build 36.1) in one line and on chromosome 7 at 115 Mb in the other line (Aigner et al. 2007a). The

ongoing work in the five nephropathy models includes the linkage analysis of the causative mutation in the other three lines, the identification of the causative mutation in the linked chromosomal region, and the further in-depth analysis of the altered phenotype.

Conclusion

Different mouse strains show a large variation in clinical chemical and hematological values. Standard operating procedures (SOPs) were published for the standardized clinical chemical analysis. Data derived from selected inbred strains may be used as reference values. Mouse disease models derived from both gene-driven and phenotype-driven projects were comprehensively analyzed for clinical chemical and hematological parameters both as overall screen thereby using high-throughput techniques as well as in-depth pathway-specific screens. This led to the description of novel animal models for prominent human health problems. In addition, ENU mouse mutagenesis projects generated novel mutant animal models with primary alterations in clinical chemical and/or hematological parameters for their subsequent use in biomedical research. Further phenotypic and genetic analyses promote the integrated evaluation of the mammalian genome function and represent an important contribution to the development of systems biology of complex organisms.

Acknowledgments

This work was supported by the German Human Genome Project (DHGP) and the National Genome Research Network (NGFN) (EW).

References

[1] Aigner B, Rathkolb B, Herbach N, Kemter E, Schessl C, Klaften M, Klempt M, Hrabé de Angelis M, Wanke R, Wolf E (2007a) Screening for increased plasma urea levels in a large-scale ENU mouse mutagenesis project reveals kidney disease models. *Am J Physiol Renal Physio*l 292, F1560-F1567

[2] Aigner B, Rathkolb B, Mohr M, Klempt M, Hrabé de Angelis M, Wolf E (2007b) Generation of ENU-induced mouse mutants with hypocholesterolemia: novel tools for dissecting plasma lipoprotein homeostasis. *Lipids* 42, 731-737

[3] Aigner B, Rathkolb B, Herbach N, Hrabé de Angelis M, Wanke R, Wolf E (2008) Diabetes models by screen for hyperglycemia in phenotype-driven ENU mouse mutagenesis projects. *Am J Physiol Endocrinol Metab* 294, E232-E240

[4] Barrantes IB, Montero-Pedrazuela A, Guadano-Ferraz A, Obregon MJ, Martinez dM, Gailus-Durner V, Fuchs H, Franz TJ, Kalaydjiev S, Klempt M, Holter S, Rathkolb B, Reinhard C, Morreale dE, Bernal J, Busch DH, Wurst W, Wolf E, Schulz H, Shtrom S,

Greiner E, Hrabé de Angelis M, Westphal H, Niehrs C (2006) Generation and characterization of dickkopf3 mutant mice. *Mol Cell Biol* 26, 2317-2326

[5] Brown SD, Chambon P, Hrabé de Angelis M, Eumorphia Consortium (2005) EMPReSS: standardized phenotype screens for functional annotation of the mouse genome. *Nat Genet* 37, 1155

[6] Brown SD, Hancock JM, Gates H (2006) Understanding mammalian genetic systems: the challenge of phenotyping in the mouse. *PLoS Genet* 2, e118

[7] Caspary T, Anderson KV (2006) Uncovering the uncharacterized and unexpected: unbiased phenotype-driven screens in the mouse. *Dev Dyn* 235, 2412-2423

[8] Champy MF, Selloum M, Piard L, Zeitler V, Caradec C, Chambon P, Auwerx J (2004) Mouse functional genomics requires standardization of mouse handling and housing conditions. *Mamm Genome* 15, 768-783

[9] Champy MF, Selloum M, Zeitler V, Caradec C, Jung B, Rousseau S, Pouilly L, Sorg T, Auwerx J (2008) Genetic background determines metabolic phenotypes in the mouse. *Mamm Genome*, 19, 318-331

[10] Churchill GA, Airey DC, Allayee H, Angel JM, Attie AD, Beatty J, Beavis WD, Belknap JK, Bennett B, Berrettini W, Bleich A, Bogue M, Broman KW, Buck KJ, Buckler E, Burmeister M, Chesler EJ, Cheverud JM, Clapcote S, Cook MN, Cox RD, Crabbe JC, Crusio WE, Darvasi A, Deschepper CF, Doerge RW, Farber CR, Forejt J, Gaile D, Garlow SJ, Geiger H, Gershenfeld H, Gordon T, Gu J, Gu W, de Haan G, Hayes NL, Heller C, Himmelbauer H, Hitzemann R, Hunter K, Hsu HC, Iraqi FA, Ivandic B, Jacob HJ, Jansen RC, Jepsen KJ, Johnson DK, Johnson TE, Kempermann G, Kendziorski C, Kotb M, Kooy RF, Llamas B, Lammert F, Lassalle JM, Lowenstein PR, Lu L, Lusis A, Manly KF, Marcucio R, Matthews D, Medrano JF, Miller DR, Mittleman G, Mock BA, Mogil JS, Montagutelli X, Morahan G, Morris DG, Mott R, Nadeau JH, Nagase H, Nowakowski RS, O'Hara BF, Osadchuk AV, Page GP, Paigen B, Paigen K, Palmer AA, Pan HJ, Peltonen-Palotie L, Peirce J, Pomp D, Pravenec M, Prows DR, Qi Z, Reeves RH, Roder J, Rosen GD, Schadt EE, Schalkwyk LC, Seltzer Z, Shimomura K, Shou S, Sillanpaa MJ, Siracusa LD, Snoeck HW, Spearow JL, Svenson K, Tarantino LM, Threadgill D, Toth LA, Valdar W, de Villena FP, Warden C, Whatley S, Williams RW, Wiltshire T, Yi N, Zhang D, Zhang M, Zou F (2004) The Collaborative Cross, a community resource for the genetic analysis of complex traits. *Nat Gene*t 36, 1133-1137

[11] Davisson M (2006) FIMRe: Federation of International Mouse Resources: global networking of resource centers. *Mamm Genome* 17, 363-364

[12] Gailus-Durner V, Fuchs H, Becker L, Bolle I, Brielmeier M, Calzada-Wack J, Elvert R, Ehrhardt N, Dalke C, Franz TJ, Grundner-Culemann E, Hammelbacher S, Holter SM, Holzlwimmer G, Horsch M, Javaheri A, Kalaydjiev SV, Klempt M, Kling E, Kunder S, Lengger C, Lisse T, Mijalski T, Naton B, Pedersen V, Prehn C, Przemeck G, Racz I, Reinhard C, Reitmeir P, Schneider I, Schrewe A, Steinkamp R, Zybill C, Adamski J, Beckers J, Behrendt H, Favor J, Graw J, Heldmaier G, Hofler H, Ivandic B, Katus H, Kirchhof P, Klingenspor M, Klopstock T, Lengeling A, Muller W, Ohl F, Ollert M, Quintanilla-Martinez L, Schmidt J, Schulz H, Wolf E, Wurst W, Zimmer A, Busch DH,

Hrabé de Angelis M (2005) Introducing the German Mouse Clinic: open access platform for standardized phenotyping. *Nat Methods* 2, 403-404

[13] Green EC, Gkoutos GV, Lad HV, Blake A, Weekes J, Hancock JM (2005) EMPReSS: European mouse phenotyping resource for standardized screens. *Bioinformatics* 21, 2930-2931

[14] Greiling H, Gressner AM (1995) *Lehrbuch der Klinischen Chemie und Pathobiochemie.* Schattauer, Stuttgart

[15] Hedrich HJ, Bullock G (2004) *The laboratory mouse*. Elsevier Academic Press, London

[16] Herbach N, Rathkolb B, Kemter E, Pichl L, Klaften M, Hrabé de Angelis M, Halban PA, Wolf E, Aigner B, Wanke R (2007) Dominant-negative effects of a novel mutated Ins2 allele causes early-onset diabetes and severe beta-cell loss in Munich $Ins2^{C95S}$ mutant mice. *Diabetes* 56, 1268-1276

[17] Hough TA, Nolan PM, Tsipouri V, Toye AA, Gray IC, Goldsworthy M, Moir L, Cox RD, Clements S, Glenister PH, Wood J, Selley RL, Strivens MA, Vizor L, McCormack SL, Peters J, Fisher EM, Spurr N, Rastan S, Martin JE, Brown SD, Hunter AJ (2002) Novel phenotypes identified by plasma biochemical screening in the mouse. *Mamm Genome* 13, 595-602

[18] Hrabé de Angelis M, Flaswinkel H, Fuchs H, Rathkolb B, Soewarto D, Marschall S, Heffner S, Pargent W, Wuensch K, Jung M, Reis A, Richter T, Alessandrini F, Jakob T, Fuchs E, Kolb H, Kremmer E, Schaeble K, Rollinski B, Roscher A, Peters C, Meitinger T, Strom T, Steckler T, Holsboer F, Klopstock T, Gekeler F, Schindewolf C, Jung T, Avraham K, Behrendt H, Ring J, Zimmer A, Schughart K, Pfeffer K, Wolf E, Balling R (2000) Genome-wide, large-scale production of mutant mice by ENU mutagenesis. *Nat Genet* 25, 444-447

[19] Hrabé de Angelis M, Michel D, Wagner S, Becker S, Beckers J (2007) Chemical mutagenesis in mice. In: *The mouse in biomedical research - v.1. History, wild mice, and genetics*, edited by Fox JG, Barthold SW, Davisson MT, Newcomer CE, Quimby FW, Smith AL. Academic Press, Burlington, p. 225-260

[20] Keays DA, Clark TG, Flint J (2006) Estimating the number of coding mutations in genotypic- and phenotypic-driven N-ethyl-N-nitrosourea (ENU) screens. *Mamm Genome* 17, 230-238

[21] Keays DA, Clark TG, Campbell TG, Broxholme J, Valdar W (2007) Estimating the number of coding mutations in genotypic and phenotypic driven N-ethyl-N-nitrosourea (ENU) screens: revisited. *Mamm Genome* 18, 123-124

[22] Klempt M, Rathkolb B, Aigner B, Wolf E (2006a) Clinical chemical screen. In: *Standards of mouse model phenotyping*, edited by Hrabé de Angelis M, Chambon P, Brown S. Wiley-VCH, Weinheim, p. 87-107

[23] Klempt M, Rathkolb B, Fuchs E, Hrabé de Angelis M, Wolf E, Aigner B (2006b) Genotype-specific environmental impact on the variance of blood values in inbred and F1 hybrid mice. *Mamm Genome* 17, 93-102

[24] Lisse TS, Thiele F, Fuchs H, Hans W, Przemeck GK, Abe K, Rathkolb B, Quintanilla-Martinez L, Hoelzlwimmer G, Helfrich M, Wolf E, Ralston SH, Hrabé de Angelis M

(2008) ER stress-mediated apoptosis in a new mouse model of Osteogenesis imperfecta. *PLoS Genet* 4, e7

[25] Loeb WF, Quimby FW (1999) *The clinical chemistry of laboratory animals*. Taylor & Francis, Philadelphia

[26] Mallon AM, Blake A, Hancock JM (2008) EuroPhenome and EMPReSS: online mouse phenotyping resource. *Nucleic Acids Res* 36, D715-D718

[27] Mohr M, Klempt M, Rathkolb B, Hrabé de Angelis M, Wolf E, Aigner B (2004) Hypercholesterolemia in ENU-induced mouse mutants. *J Lipid Res* 45, 2132-2137

[28] Morton DB, Abbot D, Barclay R, Close BS, Ewbank R, Gask D, Heath M, Mattic S, Poole T, Seamer J, Southee J, Thompson A, Trussell B, West C, Jennings M (1993) Removal of blood from laboratory mammals and birds. First report of the BVA/FRAME/RSPCA/UFAW Joint Working Group on Refinement. *Lab Anim* 27, 1-22

[29] Mouse Phenotype Database Integration Consortium (2007) Integration of mouse phenome data resources. *Mamm Genome* 18, 157-163

[30] Nicklas W, Baneux P, Boot R, Decelle T, Deeny AA, Fumanelli M, Illgen-Wilcke B (2002) Recommendations for the health monitoring of rodent and rabbit colonies in breeding and experimental units. *Lab Anim* 36, 20-42

[31] Nolan PM, Peters J, Strivens M, Rogers D, Hagan J, Spurr N, Gray IC, Vizor L, Brooker D, Whitehill E, Washbourne R, Hough T, Greenaway S, Hewitt M, Liu X, McCormack S, Pickford K, Selley R, Wells C, Tymowska-Lalanne Z, Roby P, Glenister P, Thornton C, Thaung C, Stevenson JA, Arkell R, Mburu P, Hardisty R, Kiernan A, Erven A, Steel KP, Voegeling S, Guenet JL, Nickols C, Sadri R, Nasse M, Isaacs A, Davies K, Browne M, Fisher EM, Martin J, Rastan S, Brown SD, Hunter J (2000) A systematic, genome-wide, phenotype-driven mutagenesis programme for gene function studies in the mouse. *Nat Genet* 25, 440-443

[32] Paigen K, Eppig JT (2000) A mouse phenome project. *Mamm Genome* 11, 715-717

[33] Peters LL, Robledo RF, Bult CJ, Churchill GA, Paigen BJ, Svenson KL (2007) The mouse as a model for human biology: a resource guide for complex trait analysis. *Nat Rev Genet* 8, 58-69

[34] Rathkolb B, Decker T, Fuchs E, Soewarto D, Fella C, Heffner S, Pargent W, Wanke R, Balling R, Hrabé de Angelis M, Kolb HJ, Wolf E (2000a) The clinical-chemical screen in the Munich ENU Mouse Mutagenesis Project: screening for clinically relevant phenotypes. *Mamm Genome* 11, 543-546

[35] Rathkolb B, Fuchs E, Kolb HJ, Renner-Muller I, Krebs O, Balling R, Hrabé de Angelis M, Wolf E (2000b) Large-scale N-ethyl-N-nitrosourea mutagenesis of mice - from phenotypes to genes. *Exp Physiol* 85, 635-644

[36] Rogers DC, Fisher EM, Brown SD, Peters J, Hunter AJ, Martin JE (1997) Behavioral and functional analysis of mouse phenotype: SHIRPA, a proposed protocol for comprehensive phenotype assessment. *Mamm Genome* 8, 711-713

[37] Rubio-Aliaga I, Soewarto D, Wagner S, Klaften M, Fuchs H, Kalaydjiev S, Busch DH, Klempt M, Rathkolb B, Wolf E, Abe K, Zeiser S, Przemeck GK, Beckers J, Hrabé de Angelis M (2007) A genetic screen for modifiers of the delta1-dependent notch signaling function in the mouse. *Genetics* 175, 1451-1463

[38] Russ A, Stumm G, Augustin M, Sedlmeier R, Wattler S, Nehls M (2002) Random mutagenesis in the mouse as a tool in drug discovery. *Drug Discov Today* 7, 1175-1183

[39] Silver LM (1995) *Mouse genetics: concepts and applications*. Oxford University Press, New York

[40] Skarnes WC, von Melchner H, Wurst W, Hicks G, Nord AS, Cox T, Young SG, Ruiz P, Soriano P, Tessier-Lavigne M, Conklin BR, Stanford WL, Rossant J (2004) A public gene trap resource for mouse functional genomics. *Nat Genet* 36, 543-544

[41] Stanford WL, Cohn JB, Cordes SP (2001) Gene-trap mutagenesis: past, present and beyond. *Nat Rev Genet* 2, 756-768

[42] Strivens M, Eppig JT (2004) Visualizing the laboratory mouse: capturing phenotype information. *Genetica* 122, 89-97

[43] Suckow MA, Danneman P, Brayton C (2001) *The laboratory mouse*. CRC Press, Boca Raton

[44] Valdar W, Solberg LC, Gauguier D, Burnett S, Klenerman P, Cookson WO, Taylor MS, Rawlins JN, Mott R, Flint J (2006) Genome-wide genetic association of complex traits in heterogeneous stock mice. *Nat Genet* 38, 879-887

[45] Vujic SM, Kiss J, Herrmann T, Kessler R, Stolte J, Galy B, Rathkolb B, Wolf E, Stremmel W, Hentze MW, Muckenthaler MU (2007) Physiologic systemic iron metabolism in mice deficient for duodenal Hfe. *Blood* 109, 4511-4517

In: Clinical Chemistry Research
Editors: Brian H. Mitchem and Charles L. Sharnham
ISBN 978-1-60692-517-1

Chapter IX

Gene Therapy of Congenital Diseases: Applications, Problems and Prospects

Jixin Yang and Jiexiong Feng*
Department of Pediatric Surgery, Tongji Hospital,
Huazhong University of Science and Technology, Wuhan, China.

Abstract

Congenital diseases refer to the pathologic changes that ascribe to the solitude or cooperative factors of heredity, poison or drugs, infection and environment, before or at birth. The onset of congenital diseases can either be found immediately after birth, or in the growth process of children, or even after adult. There are several kinds of pathologic changes of congenital diseases: malformation, chromosomal abnormality and genic abnormality, etc. Gene therapy is a new technology developed in last two decades, and traditional gene therapy is to introduce exogenous DNA or RNA segments into target cells or tissues, or to retrieve and repair gene defects. In recent years, this technology, besides above-mentioned, has expanded to skipping or silencing virulence genes, enhancement of antivirulence genes, and regulation of cell functions by using cytokine genes, etc. Although still in a primitive stage, now gene therapy is widely used in the management of congenital diseases. In this article, we reviewed some representative preclinical and clinical gene therapies, in the aspects of gene targets, vectors, routes and opportunity of administration, as well as side-effects, to analyze the key points and research highlights in gene therapy of congenital diseases and prospect for possible approaches and potential applications in future.

Keywords: Congenital Disease, Gene Therapy, Hereditary Disease

* Jiexiong Feng, MD, PhD, Department of Pediatric Surgery, Tongji Hospital, Huazhong University of Science and Technology, Wuhan 430030, China (Tel: 86-27-83663808; Email: fengjiexiong@126.com)

Introduction

The past medical view of a congenital disease was considered as "a group of uncommon disease which is caused by chromosome or gene abnormality and mainly happened in children"*(1)*, which might had been right 30 years ago, with the approval of gene drugs in clinical trials by FDA since 1990 and accomplishment of genomic sequencing by 2004, people began to realize sufficiently that owing to the importance of genes interacting with the other factors such as poison or drugs, infection and environment, the risk of a certain congenital disease may be higher in a specific group of people than the others. Along with the revealing of the mystery of genome, the concept of gene therapy expanded to a broader area and in almost every stage of growth and development-- from the neonatal period onwards to adulthood. Congenital diseases include most of the hereditary mono/polygenic diseases, birth defects and congenital intrauterine infections. Theoretically, repair for defective genes is the only thorough therapy for monogenic diseases, and gene transfer for viral infection could also gain more significant effect compared with traditional antiviral drugs. Nowadays, gene therapy includes: ① Introducing exogenous DNA or RNA segments into target cells or tissues. ② Retrieving and repairing gene defects. ③ Skipping or silencing virulence genes. ④ Regulation of cell functions by using cytokine genes to enhance or inhibit immune system indirectly. ⑤ Specifically killing pathological cells by exogenous gene expression. And the ultimate destination is to transfer exogenous gene into patients' body to ensure efficient and appropriate expression to cure congenital diseases*(2)*. In this article, we reviewed some preclinical and clinical gene therapy, in the aspects of gene targets, vectors, routes and opportunity of administration, to analyze the key points and research highlights in gene therapy of congenital diseases and prospect for possible approaches and potential applications in future.

1. Development and Advancement of Gene Therapy of Congenital Diseases Sorted by Target Organ / Tissue / Cell / Virus

1.1. Respiratory Epithelia

The study of gene therapy of cystic fibrosis is one of the early researches in congenital lung diseases, it is known that gene therapy is performed in the CFTR gene of epithelia of respiratory tract in adenovirus, AAV or liposome vectors in vivo *(3,4)*.In the early researches, gene therapy was performed in adult animal model *(5,6)*, but in the adults, access to the deficient cell population was limited to the time after disease onset, and a significant level of organ and cell-directed gene transfer has been difficult to achieve *(7)*. Then, fetoscopic gene therapy was developed *(8)*, which was applied before the onset, and the trial showed a fetoscopic therapy could attain a high level of organ-specific gene transfer to the fetal lung late in gestation in the model of fetal sheep. In 2004, a clinical multicenter, double blind and

placebo-controlled trial— "Repeated adeno-associated virus serotype 2 aerosol-mediated cystic fibrosis transmembrane regulator gene(tgAAVCF) transfer to the lungs of patients with cystic fibrosis" was completed at phase Ⅱ, it resulted in encouraging trends in improvement in pulmonary function in patients with CF and mild lung disease, and confirmed the safety and good tolerability of the repeated doses of aerosolized tgAAVCF gene therapy *(9)*. In 2007, United Kingdom cystic fibrosis gene therapy consortium carried out a multidose trial to research the safety dose, timing of CT scanning, using computed tomography as a surrogate outcome measure *(10)*, and the trial is still in progress.

α_1-antitrypsin(α_1-AT) deficiency is a fatal hereditary disease most common in Caucasians, and leads to pulmonary emphysema and liver disease *(11)*. The disease is inherited in an autosomal recessive fashion; several mutations have been identified that result in either absent or severely low levels of circulating protein. Plasma-derived α_1-AT intravenous administration is a traditional treatment, but it is costly and has a short half-life, and frequent administration is necessary *(12)*, especially, it needs to be purified from human serum. Therefore, gene therapy is considered to be efficient and convenient. At beginning, α_1-AT gene in liposome or Ad vectors was transduced into animal models in variety of routes, including injection into muscles *(13)*, tail vein, portal vein and directly into liver, infusion into biliary duct *(14)*, or implantation of genetically modified myoblasts *(15)*. In 2000, patients with α_1-AT deficiency received in vivo clinical trial, in a topical route— liposome-α_1-AT complex which was given in nostril, and protein was detected, with a higher level than other routes of administration *(16)*, and levels of the pro-inflammatory cytokine, IL-8, were decreased in the treated nostril, this anti-inflammatory effect was not observed in intravenous trials. Development of gene therapy of α_1-AT deficiency strongly suggests that administration routes can be different and may lead to different expression level of the transferred α_1-AT gene.

1.2. Muscle

Duchenne muscular dystrophy(DMD) is a fatal X-linked recessive hereditary disease, and it is induced by DMD gene which encodes the dystrphin *(17)*. Mini dystrphin gene(6.3 to 6.4kb) was cloned from the genome of patients with Becker muscular dystrophy(BMD) and transduced into DMD model. It could significantly improve muscular motive function *(18)*. Later, RNAi based technologies consummated the gene therapy, antisense oligonucleotides and siRNA were transfected into muscular cell, which transformed frameshift mutation(FSM) into nonframeshift mutation(NFSM) and deleted abnormal terminator caused by NFSM *(19)*. In recent years, body-wide gene therapy of Duchenne muscular dystrophy in the mdx mouse models has been researched, systemic delivery of the AAV/8 vector resulted in effective body-wide colonization, significant recovery of the functional properties in vivo, and a lower creatine kinase serum level, suggesting an overall decrease in muscle wasting *(20)*, it provided solid bases for a systemic use of AAV-mediated antisense RNA expression for the treatment of DMD.

1.3. Myocardial Tissue

Dilated cardiomyopathy(DCM) is a compound myocardial disease which has both hereditary and nonhereditary factors, δ- sarcoglycan gene was considered to induce DCM in the hamster model of T0-2 DCM (21,22). Recombinant adeno-associated virus/8(rAAV/8) mediated δ- sarcoglycan was injected directly into the thoracic cavity, and its expression was found in several types of myocardial cells, which obviously ameliorated the heart function (23).The rAAV is demonstrated to have no harm in some associated studies (24). Monocyte chemoattractant protein-1(MCP-1) and macrophage inflammatory protein-1alpha (MIP-1α) were found to have close relationship with DCM (25), and transfection of MCP-1 inhibiting gene 7ND(cDNA 50μg) before induction of experimental autoimmune myocarditis(EAM) could significantly reduce the pathologic changes of EAM (26). Phospholamban(PLN) is a crucial sarcoplasmic reticulum membrane protein expressed in myocardial cells, it can inhibit Ca^{2+}-ATPase of sarcoplasmic reticulum and aggravate heart failure (27), according to this discovery, the reduction of PLN mRNA could relatively increase the activity of sarcoplasmic reticulum (28).

1.4. Liver

Ornithine transcarbamylase(OTC) deficiency is a X-linked inborn error of urea synthesis. Before gene therapy, the clinical outcome was poor, and the prognosis was rather bad, either in internal or surgical treatments *(29,30)*. After the finding of the mutation of ornithine transcarbamylase locus, and the cloning of the gene *(31)*, the vector E1-E4-deleted Ad/5 containing OTC cDNA was used to perform in liver directed gene therapy in vivo, in the Spf/Y mice *(32-34)*. Clinically stable adults with partial OTC deficiency were given gene transfer in a pilot trial *(35)*, the vector containing OTC cDNA was infused into the right hepatic artery at a dose of $6x10^{11}$ particles per kilogram, but an 18-year-old OTC deficient patient died of systemic inflammatory response syndrome, intravascular coagulation and MODS 98h after gene transfer, while the 17 first subjects was noted to have altered mental status and jaundice *(36)*. This incidence resulted in a pause of gene therapy of OTCD, and called attention to the other clinical trials to consider the problem of safety. Further studies of the safety of Ad/5 vectors are still under research.

Familial hypercholesterolemia(FH) is an autosomal dominant hereditary disease, it can cause the hereditary occlusive vascular disease, severe hypercholesteremia, and atherosclerosis. FH is closely related with the deletion of gene encoding LDL receptor in the liver *(37)*. Pakkanen TM transduced retrovirus and adenovirus-mediated LDL receptor gene into hepatocytes isolated from the Watanabe Heritable hyperlipidemic(WHHL) rabbit liver, and administrated the cells back into the portal vein of rabbits *(38)*. This ex vivo trial demonstrated the reduction of the level of LDL, and increasing of HDL in the serum. Clinical trials using LDL gene therapy had satisfactory initiatory outcome, concentration of LDL in the serum of the patients with FH could increase rapidly and persistently in a stable level, and the patients have better reaction to statin therapy*(39)*. Further researches discovered that apolipoprotein B is an important structural protein on the surface of atherogenic lipoproteins

such as remnant very-low-density lipoprotein and low-density lipoprotein and facilitates the clearance of these particles from the circulation by binding to the low-density lipoprotein receptor, and its antisense oligonucleotide could lower LDL cholesterol in hyperlipidemic mice without causing hepatic steatosis*(40)*. ISIS 301012 is an antisense oligonucleotide that inhibits apolipoprotein B production by binding directly to and reducing the expression of apolipoprotein B messenger RNA, and it is the first agent to enter clinical trials utilizing an antisense mechanism for reducing the production of apolipoprotein B *(41)*. In a clinical trial, ISIS 301012 in the dose of 50-400mg administered weekly via subcutaneous injection for 4 weeks reduced apolipoprotein B by 14.3-47.4% and low-density lipoprotein cholesterol by 5.9-40% at 55 days, and the most frequent adverse event was spontaneous hemolysis at the injection-site *(42)*. Further studies are ongoing to verify its safety, efficacy, and position of therapy in the dyslipidemic patients.

Phenylketonuria(PKU) is a kind of autosomal recessive disease caused by deficiency of phenylalanine hydroxylase(PAH) in liver, which plays an important role in phenylalanine metabolism. Dietary restriction treatment is imperative, but it still has some shortcomings *(43)*. Instead, after the sensitive mutation in PAH gene was found in the year 2006 *(44,45)*, the advantages of gene therapy is emerging. Ding Z and Jin-OK Choi utilized recombinant AAV/8 pseudotyped vector-mediated PAH-cDNA to transfer into PKU model mice, the concentration of Phe reduced to normal level, the fur of the mice returned from brown to black, and the activity of PAH extracted from liver is back to normal *(46,47)*. Harding C.O also demonstrated the feasibility of complete correction of hyperphenylalaninemia following liver-directed, recombinant AAV2/8 vector-mediated gene therapy in murine phenylketonuria *(48)*. However, clinical trial has not been performed yet; it is not known now whether it is possible to replace the dietary treatment and whether it can be united with the replacement therapy of BH4.

1.5. Kidney

Gene therapy research of congenital renal diseases is relatively less, Alport's syndrome (AS) and autosomal recessive polycystic kidney disease(ARPKD) are two hotspots in this area.

AS is a hereditary nephritic disease caused by the defect of collagenⅣ in the GBM, and the target gene COL4A5 mutation was demonstrated to be the reason *(49)*. COL4A5 is difficult to enter podocytes through the GBM, Heikkila et al infused adenovirus mediated COL4A5 gene for persistent 2-12 hours, and successfully introduced the COL4A5 into renal glomerular cells *(50)*, and later they used this technology in the model of canis familiaris with Alport's syndrome, and surprisingly found COL4A5 gene expressed in renal glomerulus—CollagenⅣ A3, A4 and A5. Now they are trying hard to implement the therapy in clinical trials.

Autosomal dominant polycystic kidney disease(ADPKD) originally is not an ideal disease for gene therapy, as the gene therapy is mainly limited in the treatment of autosomal recessive or X-linked hereditary disease. Richer et al injected antisense c-myc ODN into autosomal recessive polycystic kidney disease(ARPKD) model repeatedly for 20 days, and

found the growth rate of renal cysts reduced, the number of cysts became less, and renal function recovered to some extent than before *(51)*. However, as the crucial point of the etiology that leads to terminal stage of renal failure is not the formation of cysts, but the lost of normal renal tubular cells. So to explore the the target gene that can inhibit the growth of renal cysts and the proliferation of tubular cells could be a new highlight.

1.6. $CD34^+$ Periphery Blood Stem Cells, Lymphocytes and $CD34^+$ Cells

The research of severe combined immunodeficiency(SCID) and X-linked SCID are the hottest and the most often to be debated. Studies of gene correction of ADA deficient SCID date back to 1990, and the researches initially targeted peripheral blood mononuclear cells rather than bone marrow stem cells. In 1995, a retrovirus mediated vector was used to transduce patient T cells, and after expansion, the T cells were returned to the patients *(52)*. The early successful gene therapy in SCID infants was contrasted by a report of ineffectiveness in teenage patients *(53)*, because of the limitation of the capacity for elder patients to produce T cells. In spite that preteen patients with X-linked SCID were reported to have no cytoreductive conditioning in infancy with T cell depleted bone marrow transplantation, they could be chronically ill for a long time, due to graft-versus-host diseases *(54)*. And unexpected lymphoproliferative complications following gene therapy occurred in one of the gene therapy trials for SCID-X1. Four infants developed lymphoproliferative disorders, with rapid expansion of a limited number of T cell clones, and prompt chemotherapy was used to successfully induce remission, however, one patient relapsed and subsequently died following allogeneic stem cell transplantation. *(55,56)*. When newly developed molecular technologies identified where the genome vector integration had occurred in the expanded cells, the site mapped close to a known T cell proto-oncogene, LMO2 in the case above *(56)*. Thus, unanticipated vector mediated oncogene activation seems to have precipitated leukaemogenesis, but a number of other factors may have been relevant in these patients. In the context of lymphopaenia, gene corrected cells have a notable proliferation advantage and this combined with reduced immune surveillance in SCID patients, which may have allowed abnormal clones to escape challenge and become leukaemogenic. There is also a possibility that in SCID-X1 the nature of the γc transgene, with its central role in T cell development and function, is important, although suggestions that vector mediated expression of common γc may directly cause leukaemogenesis have been controversial. *(57,58)*. In general, gene therapy has shown to be the most valuable to mismatched stem cell transplantation for infants, if the problems of safeguards can be managed to solve, we could have prospects, that gene therapy should offer therapeutic benefit in a range of blood and immune system disorders in future.

1.7. Multiple Target Cells

Hereditary hemophilia is a group of hemorrhagic disease caused by congenital single gene defect of clotting factors: FⅧ, FⅨ or FⅪ, and it has three types: Hemophilia A, B and

C. Currently replacement therapy such as repeated i.v injections of FⅧ concentrates derived from either human plasma or recombinant clotting factors is the main treatment for hemophiliacs *(59,60)*, thus for more than 75% patients, replacement therapy is not available, while the Hemophilia is an excellent candidate disease for the application of gene therapy (61). In the early stage, fibroblasts and keratinocytes were selected to be the targets *(62)*, and leucovirus, RV and rAAV vectors were used to integrate FⅧ and FⅨ cDNA to these target cells *(63,64)*, the primary gene therapy targets for hemophilia to date have been the liver, and cells outside liver, such as hematopoietic stem cells, muscle, bone marrow stromal cells and blood out-growth endothelial cells(BOECs), and these lead to increased level of plasma FⅧ or FⅨ *(65-67)*,with the use of new vectors such as recombinant lentivirus, miniadenovirus to reduce the side effect caused by the repeated doses of vectors *(68-70)*. Further researches are still ongoing, a recent pilot research demonstrated that targeting FIX expression in platelets could form a FIX storage pool in platelets, and the stored FIX was functional and could be released by agonist-induced stimulation, targeting FIX expression in platelets could be a new strategy in gene therapy for hemophilia B in which the stored FIX might be protected from FIX inhibitory antibodies. Release of FIX at the site of vascular injury would increase the local concentration of FIX and achieve effective hemostasis in hemophilia B even in patients with FIX inhibitory antibodies *(66,71-73)*, and the new target—platelet and FⅧ inhibitor could be the next hotspot in future researches.

1.8. Viruses

According to a serial of epidemiologic studies and clinical researches, rotavirus(RV) is considered to be the main etiology of Biliary Atresia(BA)—a common congenital disease in clinic, and a successful animal model of BA was replicated *(74-77)*. All of these researches made the relationship of RV infection and BA become a new hotspot in the research of etiology for BA *(78)*. In 2002, Déctor MA used the technology of RNA interference to study the role of RV-VP4 in RV infection, and the results showed specific siRNA could inhibit the expression of VP4, and the infection rate reduced, which meant the importance of VP4 in RV infection *(79)*. Two years later, American scientists transfected liposome-mediated siRNA into RV infected cells, and discovered the expression of NSP1, NSP2, NSP4, VP4 and VP7 were crucial roles in RV replication, installation of viral particles and formation of RV outer capsid, which could be silenced by siRNA, thus there were no viral particle formation and the other viral protein expressions were down regulated *(80,81)*. If this new RNAi technology can be united with the in utero gene therapy to localize siRNA precisely in fetus who is infected by RV in uterine, these studies may become the first light of morning in altering the current status in the treatment of BA, especially for the types that can not be surgically treated.

Table1. Overview of Gene Therapy of Congenital Disease

Target	Disease	Gene	Gene drugs	Route	Vector
Respiratory epithelia	CF	CFTR	cDNA	in vivo	Ad AAV Liposome
	α1-AT deficiency	α_1-AT	cDNA	ex vivo	liposome Ad
Muscle	DMD	DMD	Mini dystrphin gene antisense oligonucleotide siRNA	in vivo	AAV/8 liposome liposome
Myocardial tissue	DCM	δ- sarcoglycan MCP-1 and MIP-1α	cDNA antisense oligonucleotide	in vivo	rAAV liposome
Liver	OTC deficiency	OTC	cDNA	ex vivo	Ad/5
	FH	LDL receptor	cDNA	ex vivo	RV Ad
		apolipoprotein B	ISIS 301012	in vivo	liposome
	PKU	PAH	cDNA	in vivo	rAAV/8
Kidney	AS	COL4A5	cDNA	in vivo	Ad
	ARPKD	pkd1 and pkd2	antisense c-myc ODN	in vivo	liposome
Lymphocytes and CD34$^+$ cells	SCID	ADA	cDNA	ex vivo	RV
CD34+ cells	X-linked SCID	γc	cDNA	in vivo	RV
Multiple Target cells	Hemophilia A	FⅧ	cDNA	ex vivo	RV/rAAV
	Hemophilia B	FⅨ	cDNA	ex vivo	RV/Leucovirus/ rAAV recombinant lentivirus miniAd
Rotavirus	BA	RV mRNA	siRNA	in vivo	liposome
Hepatitis B Virus	Congenital HBV infection	HBV mRNA	siRNA	in vivo	liposome
		interferon gene	cDNA	in vivo	Ad

Vertical transmission of HBV from a mother to a fetus is a main route of HBV infection. Traditional antiviral drugs have similar mechanism, they can not kill viruses that are in incubation or non-replication period, and can induce drug fast strains, and even more, can elevate virulence *(82)*.Congenital HBV infection can cause serious clinical manifestations, and the gene therapy for HBV infection now has great advancement. C.M Ahamed et al transduced interferon gene into specific tissues to maintain locally stable concentration of interferon, which reduced adverse side effects *(83)*. Hammerhead and hairpin ribozymes were based on the antisense oligonucleotide RNA technology, several hammerhead ribozymes were successfully used in deactivation of HBV RNA, at the target sequences with poly(A) and core area of HBV tail *(84,85)*. In 2003, in Hamasaki`s ex vivo trial, siRNA is transfected aiming directly at HBV synthesis, and significantly inhibited HBV replication and reduced mRNA(3.5kb) *(86)*. Giladi et al transfected specific siRNA into HepG2.2.15 containing HBV gene and injected siRNA into mouse tail vein, both ex vivo and in vivo trials showed reduction of HBV protein expression and DNA replication *(87)*. A new breakthrough came from Shlomai's research, he inserted green fluorescent protein(GFP) into HBV genome to break the activity of core protein and polymerase to stop replication of virus, and then he introduced specific siRNA into HBV, the result showed RNAi effect still existed, which demonstrated its antiviral effect was not dependent on viral replication *(88)*. If further preclinical study can testify the safety and efficiency of RNAi technology, it can be widely used in the antiviral treatment.

We summarized the abovementioned in table 1 in brief.

2. Development of Vectors in Gene Therapy of Congenital Diseases

Generally, vectors are divided into two main types: nonviral and viral-based vectors--either of these two has its own advantages and shortcomings. Gene transfer mediated by viral vectoers is called transduction, while by the nonviral called transfection.

2.1. Viral Vectors

According to Edelstein's investigation *(89)*, viral vectors have been used in approximate 70% of the clinical trials until 2004. Viruses were considered to be efficient in transducing cells, however, the safety concerns regarding the use of viruses in humans make nonviral delivery system an attractive alternative, but fairly speaking, nonviral vectors are inefficient at transferring genes. Most of clinical gene therapies for hereditary monogenic diseases were using retrovirus as a vector, while the fact is, retrovirus has low transduction and infection rate, and the insertion or integration position is randomized, which has the potential risk of insertion mutation or malignant transformation of cells (90). The lentiviral vector system was developed, which can be integrated into cleavage cells and noncleavage ones, and has higher transduction rate in lymphocytes and stem cells, which made the scientists great interested in it (91, 92). To overcome the shortcomings of viral vectors, adenovirus mediated vector was

also redesigned and reformed: more safer and efficient vectors, such as gutless, target and replicative adenovirus, are developed, which could carry more gene information, and have less adverse cytotoxicity and immunogenicity *(93, 94)*. AAV was considered to be nonpathogenic and have numerous target hosts, which could transduce cells in all phases of cell cycle, and could be inserted into chromosomes, or out of them with the concatemer DNA form to express proteins stably and for a long duration. The AAV showed significant advantages in gene therapy of hereditary disorders and infectious diseases, and also in cancers, autoimmune diseases, organ-transplantations and tissue engineering *(95)*. Recent researches demonstrated AAV/8 to be the most effective vector for gene delivery to muscles and heart*(96)*.

Table 2. Vectors of Gene Transfer

Vectors	Advantages	Disadvantages
Retrovirus	Well characterized; stable and persistent insertion	Poor infection efficiency; unavailable to nondivided cells
Adenovirus	Noncytopathic; high infection efficiency; available to nondividing cells	threatening immune system; short term episomal expression
Adeno-associated virus	Noncytopathic;broad infectivity; available to nondividing cells	Limited integration; short term expression
Lentivirus	Persistently infection to nondividing cells; high viral titres	Safety concerns of HIV derivation
Liposome	Noncytopathic; noncytotoxic	Poor transfection efficiency

2.2. Nonviral Vectors

As aforementioned about nonviral gene transfer strategy, compared with viral vectors, the nonviral gene delivery is still in its infant stage, including “Naked DNA” and cationic lipids(liposomes), both of which do not result in integration of the transgene. The Naked DNA delivery system is the simplest gene transfer system. In 1990, Wolff and colleagues demonstrated Naked plasmid DNA encoding a viral antigen could generate antiviral response by the injection into skeletal muscles *(97)*, and this new therapeutic modality was call “DNA vaccine”, to be considered as a novel and potential treatment for curing infective diseases. “Gene gun” and electroporation enhanced the efficiency of gene transfer; they were based on physical methods, the DNA penetrated cell membrane and into endosome or lysosome, or directly into nucleus. It was reported that intramuscular injection of plasmid DNA followed by electroporation results in an impressive level of gene expression *(98)*, but in clinical trial, it is administrated most often in muscle. Further studies should focus on the mechanism of cellular uptake of Naked DNA in vitro to promote clinical breakthrough. Cationic-lipid-DNA complex(termed lipoplex) has been utilized in clinical trials of Cystic Frbrosis*(3,4)*, which is proven to be safe at low doses and administration localized *(99)*. According to current researches, the fate of plasmid DNA after it reaches the nucleus is understood little, especially about how the gene express shut off, and why the duration in cells is shot. With the

unanswered questions, scientists are now engaging in the "switch system" of lipoplex, and some preclinical trials are ongoing.

The advantages and disadvantages of vectors are summarized in table 2.

3. Prospects

3.1. Minimize the Adverse Side Effects

It is unrealistic to avoid or eliminate side effects of gene therapy, as it is an exogenous insertion, and how to turn the "switch" on or off will definitely be a highlight in further studies. We presume that an ideal model of gene transfer switch system should consist of an unexpressive integrated gene and an exogenous promoter which could be controlled by patients' drug intake(figure 1). To restrict the excessive expression, the drug should be eliminated automatically by human body or can be combined with another drug with a receptor which is competitive with the promoter.

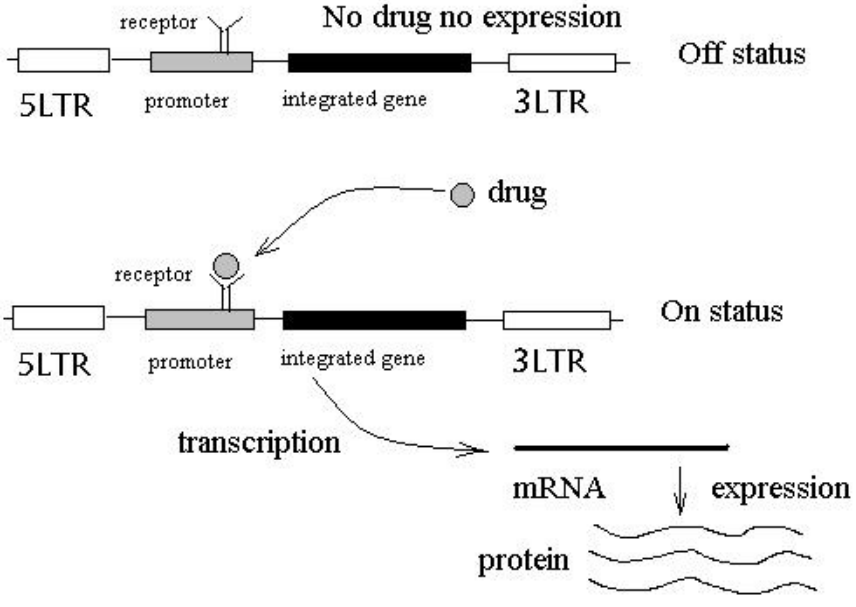

Figure 1. An ideal model of gene transfer system. The therapeutic gene and its promoter with a specific receptor is transduced into targets. If there is no specific drug taken by patients to combine with the receptor, the promoter does not work, thus the therapeutic gene does not express protein. Once the drug combined with the receptor and activated the promoter to start the integrated gene expression, protein can be expressed immediately.

We summarized the associated researches, and listed following possible approaches we may achieve: (1) Develop novel vectors with less cytotoxicity and genotoxicity to ensure the safety. It needs onward exploration of bioengineering to design or discover new vectors, advanced and prompt test facility to decide when is the right time to start or pause gene

therapy. (2) Define the safe integration site and locus. As aforementioned, the main limitation of gene transfer is that we can not often control the precise insertion position in the genome, thus it sometimes may result in certain unexpected effects, such as cell canceration, even when affecting the neighboring cellular genes,. In molecular insertion site analysis, we can use the transgene as a tag to identify neighboring cellular sequences, which is a powerful tool for precise localization *(100)*. Besides finding specific sites, other new biochemistry findings may contribute to our exploration, RNAi technology is a classic example, which changed our sight from "insertion" or "addition" to "silencing" or "skipping", derived technology can always become our innovation and evocation. (3) Localize the gene therapy to reduce cell exposure to vectors and restrict vector integration with unexpected cells. An example of localized gene therapy of fetoscopic technology is mentioned above *(8)*, the lung-specific gene transfer is an early pilot trial, which may give us a hint that the earlier and more precise treatment, the better effect.

3.2. Higher Efficiency of Transduction or Transfection

Besides the development of new vectors and gene items, specific molecular adhesion technology is an ideal ally with gene therapy. In chemotherapy, the immunoliposome, which refers to the liposomes that are connected with antibodies or receptors, had been a stable drug carrier, and the union of antigen and antibody is utilized to target specific cells or organs *(101)*. Illuminated by this means, receptor-liposome-plasmid complex could be used in gene transfer, and we conclude the research of double or even triple targeting strategy could be a new focus in future.

3.3. Drug Combination

Like the gene therapy, pharmacogenetics is also a newborn and uprising science since 1990s, which focuses on individual variation dependent administration, gene mutation of drug-metabolizing enzyme and protein transport, and receptors are its molecular foundation. It emphasizes the importance of individual mutation of gene structure and chooses the most proper drugs and doses *(102)*. As the above-mentioned, some congenital diseases still need traditional drugs to perform replacement or antiviral treatment that gene therapy to date can not displace completely. However, until now, no thorough studies have done to explore the pharmacogenentical utilization in the area of gene drugs. We consider that the individual dependent administration is important to patients with congenital diseases who need supportive drugs and gene therapy, as it has the potential to ensure the best efficiency and minimal toxicity for both traditional and gene drugs.

3.4. Gene Therapy of Polygenic Diseases

Different from monogenic diseases, polygenic disorders have two or more allelomorphic gene mutations, each of which has tiny contribution to hereditary character called minor gene and together to form a phenotype termed additive effect. Environmental factors can also influence the mobility. To date, more complex diseases could be explained by polygenic disorders, e.g. allergic rhinitis, asthma, simple obesity, idiopathetic dwarfism and idiopathetic sexual precosity, etc. Some of the candidates of predisposing genes are now conclusive, which make treatment always more complex and individualized than monogenic diseases. According to recent studies, aiming directly at different predisposing genes together to perform multigene therapy could be an ideal strategy. In gene therapy of asthma, for example, according to the pathogenesis—imbalanced differentiation of CD_4^+ T-cell to Th1/Th2-- and the close correlation mediator such as IL-2, IL-4, IL-5, IL-12, IL-18, IFN-r, GATA-3 and C-Maf, genes expressing IL-12, IL-18, IL-4 and IFN-r mediated by recombinant adenovirus were transferred to OVA mouse T cells *(103-105)*, siRNA expressing vectors specific to $CD40^+$ were administrated into $CD40^+$ cells, all of the above could reduce allergic responses and also attenuate asthma *(106)*. These researches hint that we have more gene target options to choose in treating polygenic disorders and a union therapy of different genes specific to the predisposing genes in each individual should be a proper choice. We may conclude, this is a possible tendency in treatment of polygenic disorders.

4. Summary

So far we have reviewed some applications, found some problems and discussed some potential approaches. With the development of molecular biology and bioengineering, advanced delivering system, precise targets and gene switch control can be improved. Once these barriers to success are cleared by further experiments, the potential of gene therapy will emerge onwards, and we believe that it is not beyond our ability to achieve success.

References

[1] Theodore Friedmann, Richard Roblin. Gene Therapy for Human Genetic Disease? *Science,* 1972;175:949 –55.

[2] Selkirk SM. Gene therapy in clinical medicine. Postgrad. *Med,* 2004;80:560–70.

[3] Rosenfeld MA, Yoshimura BC, Trapnell BC, Yoneyama K, Rosenthal ER, Dalemans W, et al. In vivo transfer of the human cystic fibrosis transmembrane conductance regulator gene to the airway epithelium. *Cell,* 1992;68:143–55.

[4] Rich DP, Couture LA, Cardoza LM, Guiggio VM, Armentano D, Espino PC, et al. Development and analysis of recombinant adenovirus for gene therapy of cystic fibrosis. *Hum Gene Ther* 1993;4:461–76.

[5] Grubb BR, Pickles RJ, Ye H, Yankaskas JR, Vick RN, Engelhardt JF, et al. Inefficient gene transfer by adenovirus vector to cystic fibrosis airway epithelium of mice and humans. *Nature* 1994;371:802–6.

[6] Colledge WH, Evans MJ. Cystic fibrosis gene therapy. *British Medical Bulletin* 1995;51:82–90.

[7] Crystal RG, McElvaney NG, Rosenfeld MA, Chu CS, Mastrangeli A, Hay JG, et al. Administration of an adenovirus containing the human CFTR cDNA to the respiratory tract of individuals with cystic fibrosis. *Nat Genet* 1994;8:42–51.

[8] Sylvester KG, Yang EY, Cass DL, Crombleholme TM, Adzick NS. Fetoscopic Gene Therapy for Congenital Lung Disease. *J Pediatr Surg* 1997;32:964–9.

[9] Moss RB, Rodman D, Spencer LT, Aitken ML, Zeitlin PL, Waltz D, et al. Repeated adeno-associated virus serotype 2 aerosol-mediated cystic fibrosis transmembrane regulator gene transfer to the lungs of patients with cystic fibrosis. *Chest* 2004;125:509–21.

[10] Aziz ZA. United Kingdom Cystic Fibrosis Gene Therapy Consortium Multidose Trial--The Proposed Use of Computed Tomography. *Proc Am Thorac Soc* 2007;4:355–8.

[11] Coakley RJ, Taggart C, O'Neill S, McElvaney NG. Alpha1-antitrypsin deficiency: biological answers to clinical questions. *Am J Med Sci* 2001;321:33–41.

[12] Pierce JA. Alpha1-antitrypsin augmentation therapy. *Chest* 1997;112:872–4.

[13] Song S, Morgan M, Ellis T, Poirier A, Chesnut K, Wang J, et al. Sustained secretion of human alpha-1-antitrypsin from murine muscle transduced with adeno-associated virus vectors. *Proc Natl Acad Sci USA* 1998;95:14384–8.

[14] Kay MA, Graham F, Leland F, Woo SL. Therapeutic serum concentrations of human alpha-1-antitrypsin after adenoviral-mediated gene transfer into mouse hepatocytes. *Hepatol* 1995;21:815–9.

[15] Bou-Gharios G, Wells DJ, Lu QL, Morgan JE, Partridge T. Differential expression and secretion of alpha1 anti-trypsin between direct DNA injection and implantation of transfected myoblast. *Gene Ther* 1999;6:1021–9.

[16] Brigham KL, Lane KB, Meyrick B, Stecenko AA, Strack S, Cannon DR, et al. Transfection of nasal mucosa with a normal α_1-antitrypsin gene in α_1-antitrypsin-deficient subjects: comparison with protein therapy. *Hum Gene Ther* 2000;11:1023–32.

[17] Keoning M, Hoffman EP, Bertelson CJ, Monaco AP, Feener C, Kunkel LM. Complete cloning of the Duchenne muscular dystrophy (DMD) cDNA and preliminary genomic organization of the DMD gene in normal and effected individuals. *Cell* 1987;50:509–17.

[18] Deconick N, Ragot T, Marechal G, Perricaudet M, Gillis JM. Functional protection of dystrophic mouse(mds) muscles after adenovirus-mediated transfer of truncated dystrophin cDNAs. *Proc Natl Acad Sci* 1996;93:3570–4.

[19] Pramono ZA, Takeshima Y, Alimsardjono H, Ishii A, Takeda S, Matsuo M. Induction of exon skipping of the dystrophin transcript in lymphoblastoid cells by transfecting an antisense oligodeoxynucleotide complementary to an exon recognition sequence. *Biochem Biophys Res Commun,* 1996;226:445–9.

[20] Denti MA, Rosa A, D`Anton G, Sthandier O, De Angelis FG, Nicoletti C, et al. Body-wide gene therapy of Duchenne muscular dystrophy in the mdx mouse model. *Proc Natl Acad Sci USA* 2006;103:3758–63.

[21] Tsubata S, Bowles KR, Vatta M, Zintz C, Titus J, Muhonen L, et a1. Mutations in the human delta sarcoglycan gene in familial and sporadic dilated cardiomyopathy. *J Clin Invest* 2000;106:655–62

[22] Sakamoto A, Ono K, Abe M, Jasmin G, Eki T, Murakami Y, et al. Both hypertrophic and dilated cardiomyopathies are caused by mutation of the same gene, delta sarcoglycan, in hamster: an animal model of disrupted dystrophin aasociated glycoprotein complex. *Proc Natl Acad Sci USA* 1997;94:13873–8.

[23] Kawada T, Nakazawa M, Nakauchi S, Yamazaki K, Shimamoto R, Urabe M, et al. Rescue of hereditary form of dilated cardiomyopathy by rAAV- mediated somatic gene therapy: amelioration of morphological findings, sarcolemmal permeability, cardiac performances, and the prognosis of TO- 2 hamsters. *Proc Natl Acad Sci USA* 2002;99:901–6.

[24] Svensson EC, Marshall DJ, Woodard K, Lin H, Jiang F, Chu L, et al. Efficient and stable transduction of cardiomyocytes after intramyocardial injection or intracoronary perfusion with recombinant adeno-associated virus vectors. *Circulation* 1999;99:201–5.

[25] Kobayashi M, Nakamura K, Kusano KF, Nakamura Y, Ohta-Oqo K, Naqase S, et a1. Expression of monocyte chemoattractant protein-1 in idiopathic dilated cardiomyopathy. *Int J Cardiol* 2007;27:1–3.

[26] Goser S, Ottl R, Brodner A, Dengler TJ, Torzewski J, Egashira K, et al. Critical role for monocyte chemoattractant protein-1 and macrophage inflammatory protein-1alpha in induction of experimental autoimmune myocarditis and effective anti-monocyte chemoattractant protein-1 gene therapy. *Circulation 2005*;112:3400–7.

[27] Maclennan DH, Toyofuku T, Kimura Y. Sites of regulatory interaction between calcium ATPase and phospholamban. *Basic Res Cardiol* l997;92:l1–5.

[28] Haghighi K, Gregory KN, Kranias EG. Sarcoplasmic reticulum Ca-ATPase-phospholamban interaction and dilated cardiomyopathy. Biochem Biophys *Res Commun* 2004;322:1214–22.

[29] Maestri NE , Brusilow SW, Clissold DB, Bassett SS. Long - term treatment of girls with ornithine transcarbamylase deficiency. *N Engl J Med* 1996;335:855–9.

[30] Ensenauer R ,Tuchman M, El-Youssef M, Kotagal S, Ishitani MB, Matern D, et al. Management and outcome of neonatal-onset ornithine transcarbamylase deficiency following liver transplantation at 60 days of life. *Mol Genet Metab* 2005;84:363–6.

[31] Arn PH, Hauser ER, Thomas GH, Herman G, Hess D, Brusilow SW. Hyperammonemia in women with a mutation at the ornithine carbamoyltransferase locus. *N Engl J Med* 1990;322:1652–5.

[32] Raper SE, Wilson JM, Yudkoff M, Robinson MB, Ye X, Batshaw ML. Developing adenoviral-mediated in vivo gene therapy for ornithine transcarbamylase deficiency. *J Inher. Metab Dis* 1998;21:119–37.

[33] Ye X, Robinson MB, Batshaw ML, Furth EE, Smith I, Wilson JM. Prolonged metabolic correction in adult ornithine transcarbamylase-deficient mice with adenoviral vectors. *J Biol Chem* 1996;271:3639–46.

[34] Gao GP, Yang Y, Wilson JM. Biology of adenovirus vectors with E1 and E4 deletions for liver-directed gene therapy. *J Virol* 1996;70:8934–43.

[35] Raper SE, Haskal ZJ, Ye X, Pugh C, Furth EE, Gao GP, Wilson JM. Selective gene transfer into the liver of nonhuman primates with E1-deleted, E2A-defective, or E1-E4 deleted recombinant adenoviruses. *Hum Gene Ther* 1998;9:671–9.

[36] Raper SE, Chirmule N, Lee FS, Wivel NA, Baqq A, Gao GP, et al. Fatal systemic inflammatory response syndrome in a ornithine transcarbamylase deficient patient following adenoviral gene transfer. *Mol Genet Metab* 2003;80:148–58.

[37] Das, HK, Leff T, Breslow JL. Cell type-specific expression of the human apoB gene is controlled by two cis-acting regulatory regions. *J Biol Chem* 1988;263:11452–8.

[38] Pakkanen TM, Laitinen M, Hippelainen M, Kallionpaa H, Letholainen P, Leppanen P, et al. Enhanced plasma cholesterol lowering effect of retrovirus-mediated LDL receptor gene transfer to WHHL rabbit liver after improved surgical technique and stimulation of hepatocyte proliferation by combined partial liver resection and thymidine kinase-ganciclovir treatment. *Gene Ther* 1999;6:34–41.

[39] Raal FJ, Pilcher G, Rubinsztein DC, Linqenhel A, Utermann G. Statin therapy in a kindred with both apolipoprotein B and low density lipoprotein receptor gene defects. *Atherosclerosis* 1997;129:97–102.

[40] Crooke RM, Graham MJ, Lemonidis KM, Whipple CP, Koo S, Perera RJ. An apolipoprotein B antisense oligonucleotide lowers LDL cholesterol in hyperlipidemic mice without causing hepatic steatosis. *J Lipid Res* 2005;46:872–84.

[41] Matthew K Ito. ISIS 301012 Gene Therapy for Hypercholesterolemia: Sense, Antisense, or Nonsense? *Ann Pharmac* 2007;41:1669–78.

[42] Kastelein JJ, Wedel MK, Baker BF, Su J, Bradley JD, Yu RZ, et al. Potent Reduction of Apolipoprotein B and Low-Density Lipoprotein Cholesterol by Short-Term Administration of an Antisense Inhibitor of Apolipoprotein B. *Circulation* 2006;114:1729–35.

[43] Hvas AM, Nexo E, Nielsen JB. Vitamin B12 and vitamin B6 supplementation is needed among adults with phenylketonuria(PKU). *J Inherit Metab Dis* 2006;29:47–53.

[44] Kim SW, Jung J. Structural and functional analysis of mutations of the human phenylalanine hydroxylase gene. *Clin Chim Acta* 2006;365:279–87.

[45] Stojiljkovic M, Jovanovic J. Molecular and phenotypic characteristics of patients with phenylketonuria in Serbia and Montenegro. *Clin Genet*, 2006, 70(2): 151–5.

[46] Ding Z, Georgiev P, Thony B. Administration-route and gender-independent long-tern therapeutic correction of phenylketonuria(PKU) in a mouse model by recombinant adeno-associated virus 8 pseudotyped vector-mediated gene transfer. *Gene Ther* 2006;13: 587–93.

[47] Choi JO, Park JW, Oh HJ, Kyung IS, Park HY, Jung SC. Gene therapy for phenylketonuria mouse model using pseudotyped adeno-associated virus vector. *FASEB J* 2007; 21:870.

[48] Harding CO, Gillingham MB, Hamman K, Clark H, Geobel-Daqhiqhi E, Bird A, et al. Complete correction of hyperphenylalaninemia following liver-directed, recombinant AAV2/8 vector-mediated gene therapy in murine phenylketonuria. *Gene Ther* 2006;13:457–62.

[49] Hudson B, Tryggvasob K, Sundaramoorthy M, Neilson EG. Alport`s syndrome, Goodpasture`s syndrome, and typeⅣ collagen. *N Engl J MED* 2003;348: 2534–56.

[50] Heikkila P, Tibell A, Morita T, Chen Y, Wu G, Sado Y, et al. Adenovirus-mediated transfer type Ⅳ collagen alpha5 chain cDNA into swine kidney in vivo: Deposition of the protein into the glomerular basement membrane. *Gene Ther* 2001;8:882–90.

[51] Richer J, Mata J, Iversen P, Gattone VH. c-myc antisense oligo-nucleotide treatment ameliorates murine ARPKD. *Kidney Int* 2002;61:S125–31.

[52] Blaese RM, Culver KW, Miller AD, Carter CS, Fleisher T, Clerici M, et al. T lymphocyte-directed gene therapy for ADA-SCID: initial trial results after 4 years. *Science* 1995;270:475–80.

[53] Thrasher AJ, Hacein-Bey-Abina S, GasparHB, Blanche S, Davies EG, Parsley K, et al. Failure of SCID-X1 gene therapy in older patients. *Blood* 2005;105:4255–7.

[54] Buckley RH, Schiff SE, Schiff RI, Market ML, Williams LW, Roberts JL, et al. Hematopoietic stem-cell transplantation for the treatment of severe combined immunodeficiency. *N Engl J Med* 1999;340:508–16.

[55] Hacein-Bey-Abina S, von Kalle C, Schmidt M, Le Deist F, Wulffraat N, McIntyre E, et al. A serious adverse event after successful gene therapy for X-linked severe combined immunodeficiency. *N Engl J Med* 2003;348:255–6.

[56] Hacein-Bey-Abina S, von Kalle C, Schmidt M, McCormack MP, Wulffraat N, Leboulch P, et al. LMO2-associated clonal T cell proliferation in two patients after gene therapy for SCID-X1. *Science* 2003;302:415–9.

[57] Woods NB, Bottero V, Schmidt M, von Kalle C, Verma IM. Gene therapy: therapeutic gene causing lymphoma. *Nature 2*006;440:1123

[58] Thrasher AJ, Gaspar HB, Baum C, Modlich U, Schambach A, Candotti F, et al. Gene therapy: X-SCID transgene leukaemogenicity. *Nature* 2006;443: E5–7.

[59] Gitschier J, Wood WI, Goralka TM, Wion KL, Chen EY, Eaton DH, et al. Characterization of the human factor VIII gene. *Nature* 1984;312:326–30.

[60] Van Cott KE, Velander WH. Transgenic animals as drug factories: a new source of recombinant protein therapeutics. *Expert Opin Investig Drugs* 1998;7:1683-90.

[61] Hough C, Lillicrap D. Gene therapy for hemophilia: An imperative to succeed. *J Thromb Haemost* 2005;3:1195-205.

[62] Lu DR, Zhou JM, Zheng B. Stage I clinical trial of gene therapy for hemophilia B, *Sci China B* 1993;36:1342-51.

[63] Smith TA. Gene therapy for hemophilia. Expert Opin Investig Drugs 1997;6:1685-90.

[64] Brownlee GG. Prospects for gene therapy of the hemophilia A and B. *Br Med Bull* 1995;51:91-105.

[65] Matsui H, Shibata M, Brown B, Labelle A, Hegadorn C, Andrews C, et al. Ex Vivo Gene Therapy for Hemophilia A That Enhances Safe Delivery and Sustained In Vivo Factor VIII Expression from Lentivirally Engineered Endothelial Progenitors. *Stem Cells* 2007;25:2660-9.

[66] Shi QZ, Wilcox DA, Neyrinck A, Fahs SA, Weiler H, Wells CW, et al. Factor VIII ectopically targeted to platelets is therapeutic in hemophilia A with high-titer inhibitory antibodies. *J Clin Invest* 2006;116:1974-82.

[67] Ide LM, Gangadharan B, Chiang KY, Doering CB, Spencer HT. Hematopoietic stem-cell gene therapy of hemophilia A incorporating a porcine factor VIII transgene and nonmyeloablative conditioning regimens. *Blood* 2007;110:2855-63.

[68] Gao XB, Shi D, Wang F, Lu DR, Qiu XF, Xue JL. In vitro expression of human clotting factor Ⅸ minigene mediated by miniadenoviral vector. *Clin J Virol* 2000;6:294-8.

[69] Chuah MKL, Van Damme A, Zwinnen H, Goovaerts I, Vanslembrouck V, Collen D, et al. Long-term persistence of human bone marrow stromal cell transduced with factor Ⅷ retroviral vectors and transient production of therapeutic levels of human factor Ⅷ in nonmyeloablated immunodeficient mice. *Human Gene Ther* 2000;11:729-38.

[70] Kang Y, Xie L, Tran DT, Stein CS, Hickey M, Davidson BL, et al. Persistent expression of factor VIII in vivo following nonprimate lentiviral gene transfer. *Blood* 2005;106:1552-8.

[71] Ohmori T, Mimuro J, Takano K, Madoiwa S, Kashiwakura Y, Ishiwata A, et al. Efficient expression of a transgene in platelets using simian immunodeficiency virus-based vector harboring glycoprotein Ibalpha promoter: in vivo model for platelet-targeting gene therapy. *FASEB J* 2006;20:1522–4.

[72] Shi QZ, Fahs SA, Wilcox DA. Endothelial and Platelet FVIII/VWF Expression - Divergence in Clinical Effect in Murine Models of Hemophilia A with and without FVIII Inhibitory Antibodies. *Blood* 2006;108:3286

[73] Gewirtz JE, Rauova L, Poncz M. Characterizing Factor VIII Inhibitor Resistance of Platelet-Delivered Factor VIII in the Treatment of Hemophilia A. Blood 2007;110:781.

[74] Peterson C, Biemanns D, Kuske M, Schakel K, Meyer-Junqhanel L, Mildenberger H. New aspects in a murine model for extrahepatic biliary atresia. *J Pediatr Surg* 1997;32:1190-5.

[75] Feng JX, Li MJ, Cai T, Gu WZ, Tang HF. Rotavirus induced biliary tract damage in BALB/C newborn mice. *Chinese J Pediatr Surg* 2003;24:264–7.

[76] Czech-Schmidt G, Verhagen W, Szavay P, Leonhardt J, Petersen C. Immunological gap in the infectious animal model for biliary atresia. *J Surg Res* 2001;101:62–7.

[77] Riepenhoff-Talty M, Gouvea V, Evans MJ, Svensson L, Hoffenberg E, Sokol RJ. Detection of group C rotavirus in infants with extrahepatic biliary atresia. *J Infect Dis* 1996;174:8–15.

[78] Kahn E. Biliary atresia revisited. Pediatr Dev Pathol 2004;7:109–24.

[79] Déctor MA, Romero P, López T, Arias CF. Rotavirus gene silencing by small interfering RNAs. *EMBO Rep* 2002;3:1175–80.

[80] Silvestric LS, Taraporewala ZF, Patton JT. Rotavirus replication:plus-sense templates for double-stranded RNA synthesis are made in viroplasms. *J Virol* 2004;78:7763–74.

[81] López T, Camacho M, Zayas M, Najera R, Sanchez R, Arias CF, et al. Silencing the morphogenesis of rotavirus. *J Virol* 2005;79:184–92.

[82] Masanori B. Inhibitor of HIV gene expression and Transcription. *Curr Top Med Chem* 2004;4:871–63.

[83] Iqlbal Ahamed CM, Johnson HM. Interferon gene therapy for the treatment of caner and viral infections. *Drugs Today* 2003;39:763–6.

[84] Kahn AU, Lal SK. Ribozyme: a modern tool in medicine. *J Biomed Sci* 2003;10:457–67.

[85] Alvarez-Salas LM, Benitez-Hess ML, Dipaolo JA. Advances in the development of ribozymes and antisense oligodeoxynucleotides as antiviral agents for human papillomaviruses. *Antivir Ther* 2003;8:265–78.

[86] Hamasaki K, Nakao K, Matsumoto K, Ichikawa T, Ishikawa H, Eguchi K. Shot interfering RNA-directed inhibition of hepatitis B virus replication. *FEBS Lett* 2003;543(1-3):51–4.

[87] Giladi H, Ketzinel-Gillad M, Rivkin L, Felig Y, Nussbaum O, Galun E. Small interfering RNA inhibits hepatitis B virus replication in mice. *Mol Ther* 2003;8:769–76.

[88] Shlomai A, Shaul Y. Inhibition of hepatitis B virus expression and replication by RNA interference. *Hepatology* 2003;37:764–70.

[89] Edelstein ML, Abedi, MR, Wixon, J, Edelstein RM. Gene therapy clinical trials worldwide 1989-2004-an overview. *J Gene Med* 2004;6:597–602.

[90] Sadelain M. Insertional oncogenesis in gene therapy: how much of a risk? *Gene Ther* 2004;11: 569–73.

[91] Blesch A. Lentiviral and MLV based retroviral vectors for ex vivo and in vivo gene transfer. *Methods* 2004;33:164–72

[92] Buchschacher GL Jr, Wong-Staal F. Development of lentiviral vectors for gene therapy for human diseases. *Blood* 2000;95:2499–504.

[93] Kreppel F, Kochanek S. Long-term transgene expression in proliferating cells mediated by episomally maintained high capacity adenovirus vectors. *J Virol* 2004;78:9–22.

[94] Yant SR, Ehrhardt A, Mikkelsen JG, Meuse L, Pham T, Kay MA. Transposition from a gutless adeno-transposon vector stabilizes transgene expression in vivo. *Nat Biotechnol* 2002; 20:999–1005.

[95] Gonçalves MA, van der Velde I, Knaän-Shanzer S, Valerio D, de Vries AA. Stable transduction of large DNA by high-capacity adeno-associated virus/adenovirus hybrid vectors. *Virology* 2004;321:287–96.

[96] Wang Z, Zhu T, Qiao C P. Adeno-associated virus serotype 8 efficiently delivers genes to muscle and heart. *Nat Biotechnol* 2005;23:321–8.

[97] Wolff JA, Malone RW, Williams P, Chong W, Acsadi G, Jani A, et al. Direct gene transfer into mouse muscle in vivo. *Science* 1990;247:1465–8.

[98] Rizzuto G, Cappelletti M, Maione D, Savino R, Lazzaro D, Costa P, et al. Efficient and regulated erythropoietin production by naked DNA injection and muscle electroporation. *Proc Natl Acad Sci USA* 1999;96:6417–22.

[99] Nabel GJ, Nabel EG, Yang ZY, Fox BA, Plautz GE, Gao X, et al. Direct gene transfer with DNA Cliposome complexes in melanoma: expression, biologic activity, and lack of toxicity in humans. *Proc Natl Acad Sci USA* 1993;90:11307–11.

[100] Schmidt M, Zickler P, Hoffmann G, Haas S, Wissler M, Muessig A, et al. Polyclonal long-term repopulating stem cell clones in a primate model. *Blood,* Sep 2002;100:2737– 43.

[101] Rothe A, Hosse RJ, Power BE. In vitro display technologies reveal novel biopharmaceutics. *FASEB J* 2006;20:1599–610.

[102] Gardiner SJ, Begg EJ. Pharmacogenetics, Drug-Metabolizing Enzymes, and Clinical Practice. *Pharmacol Rev* 2006;58:521–90.

[103] Behera AK, Kumar M, Lockey RF, Mohapatra SS. Adenovirus mediated interferon gamma gene therapy for allergic asthma involvement of interleukin 12 and STAT4 signaling. *Hum Gene Ther* 2002;13:1697–709.

[104] Walter DM, Wong CP, DeKruyff RH, Berry GJ, Levy S, Umetsu DT. IL-18 gene transfer by adenovirus prevents the development of reverses established allergen-induced airway hyperreactivity. *J Immunol* 2001;166:6392–8.

[105] Zavorotinskaya T, Tomkison A, Murphy JE. Treatment of experimental asthma by long-term gene therapy directed against IL-4 and IL-13. *Mol Ther* 2003;7:155–62.

[106] Suzuki M, Zhang XS, Zheng XF. Novel therapy for asthma and allergic rhinitis through gene silencing of CD40 using small interfering RNA. *Chest* 2007;132:423s.

In: Clinical Chemistry Research
Editors: Brian H. Mitchem and Charles L. Sharnham
ISBN 978-1-60692-517-1

Chapter X

Porphyrazine Anti-Tumor Agents

B.J. Vesper,[1,2] A.G.M. Barrett,[3]
B. M. Hoffman[4] and J. A. Radosevich[1,2]

[1]Center for Molecular Biology of Oral Diseases, College of Dentistry,
University of Illinois at Chicago, Chicago, IL, USA
[2]Jesse Brown VAMC, Chicago, IL, USA
[3]Department of Chemistry, Imperial College of Science,
Technology, and Medicine, London, England
[4]Department of Chemistry, Northwestern University, Evanston, IL, USA

Abstract

The tetraazaporphyrins, or porphyrazines (pzs), are an emerging class of compounds exhibiting tremendous potential for use as anti-tumor therapeutic agents and in imaging applications. Pzs are related to the porphyrins, a class of compounds widely known for the clinically used photodynamic therapy agent Photofrin. Thus, like the porphyrins, it is anticipated that the pzs will be useful as anti-tumor agents. However, while similar in structure to the porphyrins, pzs are prepared via a different synthetic route—the macrocyclization of dinitrile derivatives—that results in greater synthetic flexibility, and they have improved optical properties compared to the porphyrins. The improved chemical and physical features of the pzs gives rise to differences in their biological behavior when compared to those of the porphyrins. Therefore, the initial work in this field has focused on elucidating the structure-function relationships of the pzs. As these relationships become more clearly defined, future work will involve tailoring the structure of the pzs and/or the delivery mechanisms to more selectively target tumor cells. Herein we review the initial structure-function studies that have been carried out to date on this little-studied class of compounds and discuss possible methods for maximizing their promising biomedical potential.

Introduction

In recent years, the porphyrins, a class of macrocyclic compounds, have been widely studied for use in the detection and treatment of cancer, as well as other diseases such as rheumatoid arthritis and macular degeneration [1-3]. One area where porhyrins are of particular importance is photodynamic therapy (PDT). In PDT, a patient is given a drug which is designed to preferentially accumulate in tumor cells, after which time the site of the tumor is irradiated with visible light that activates the drug, destroying only the tumor cells. Mammalian tissue absorbs near-IR (NIR) light only weakly at wavelengths beyond the absorbance of hemoglobin, ~700 nm, and below the onset of absorbance by water, ~950 nm [4-6]; thus, the most effective PDT drugs will exhibit strong absorbance within this 700-950 nm NIR window.

Porphyrins have been found to exhibit selective tumor uptake, but they exhibit only weak absorbance beyond ~500 nm [7]. Furthermore, in the specific case of Photofrin—the most common clinically used PDT agent—the photodynamic action results from a mixture of oligomers of haematoporphyrin and protoporphyrin; this mixture is commonly referred to as haematoporphyrin derivative, or HpD [1,8]. Upon separation of HpD into its monomeric forms, however, biological activity disappears [8]; thus, the Photofrin mixture is difficult to completely characterize, and the composition is difficult to accurately reproduce. Additionally, Photofrin is not very selective for tumor tissue and usually trace amounts remain in the body for 2-3 months following treatment, resulting in the serious side effect of phototoxicity [8]. As a result of these disadvantages, interest in new alternative macrocyclic photosensitizers has shifted to the use of what may be viewed as porphyrin derivatives. These include phthalocyanines (which possess superior optical properties but limitations in solubility) [9,10], benzoporphyrins [11], chlorins and bacteriochlorins [12], and expanded porphyrins [13].

Recently, another class of porphyrin derivatives, the porphyrazines (pzs), has also been investigated as possible biomedical imaging/therapeutic agents. These compounds contain the same core structure as the phthalocyanines, but can be prepared with or without the appended benzene rings (Figure 1). The pzs are prepared by a different synthetic route than either the porphyrins or phthalocyanines, and as such, possess superior chemical flexibility and physical properties that make them excellent candidates for biomedical applications [14]. Given the structural similarities of the porphyrazines and porphyrins, it was anticipated that the biocompatibility and biodistribution of the pzs would be similar to those of porphyrins. To this end, preliminary studies have been carried out to begin to understand the biological activity of the pzs, and these studies have shown promise that the pzs may well be useful as anti-tumor agents. We herein review the work that has been completed to date, and discuss the future potential of the pzs as anti-tumor imaging and therapeutic agents.

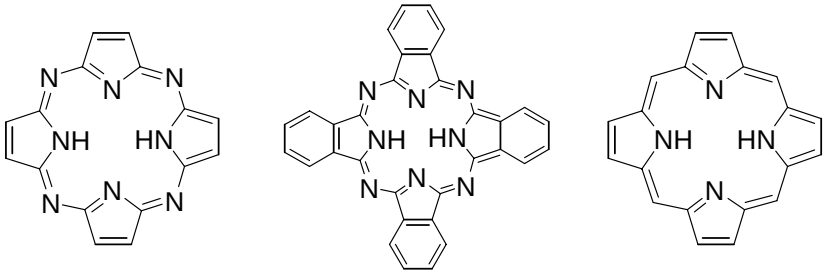

Figure 1. Basic structure of the porphyrazine, phthalocyanine, and porphryin.

The Chemical and Physical Properties of the Porphyrazines

Porphyrazines (pzs), or tetraazaporphyrins, can be viewed as porphyrinic macrocycles in which the porphyrin *meso* (CH) are replaced by *meso* nitrogen atoms linking the pyrrole rings. (For an extensive overview of the history of the porphyrazines and their syntheses and chemical/physical properties, please see the 2001 review in *Progress in Inorganic Chemistry* [14].) The synthesis and properties of the pzs are briefly discussed here as they relate to the development of pzs for biomedical applications.

Porphyrazine Synthesis

The pzs are prepared by the template cyclization of maleonitriles and/or isoindoline derivatives (Figure 2). This synthetic route allows for the straightforward synthesis of molecules with S, N, or O heteroatom groups attached to the periphery of the macrocycle core [15-23]. Such heteroatoms have strong couplings to the macrocyclic core, and as a result introduce novel electronic, optical, and chemical properties. In contrast, porphyrins are very difficult to functionalize in this way [24,25]. Pairs of maleonitriles/isoindolines can be preferentially cross-macrocyclized to generate one or more of six potential pzs of the form $M[pz(A_nB_{4-n})]$, with n = 0-4 (Figure 3). Depending upon the identities of A and B, the optical and other chemical properties of the molecules can be tuned independently of the solubility properties. Moreover, the peripheral groups of the pzs can be modified to allow for solubility in either polar or non polar media [14,26,27].

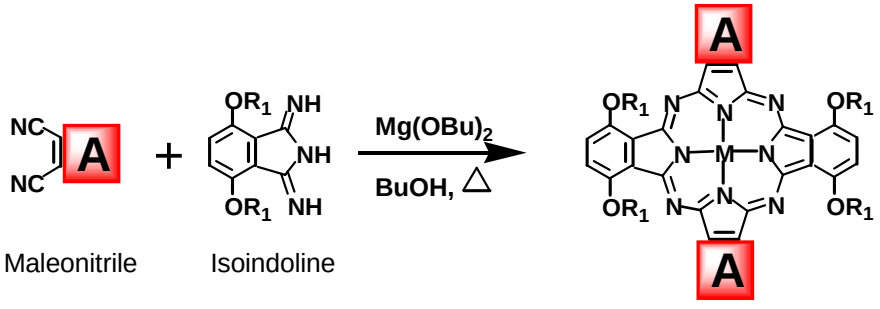

Figure 2. Example of the synthetic reaction used to prepare the pzs.

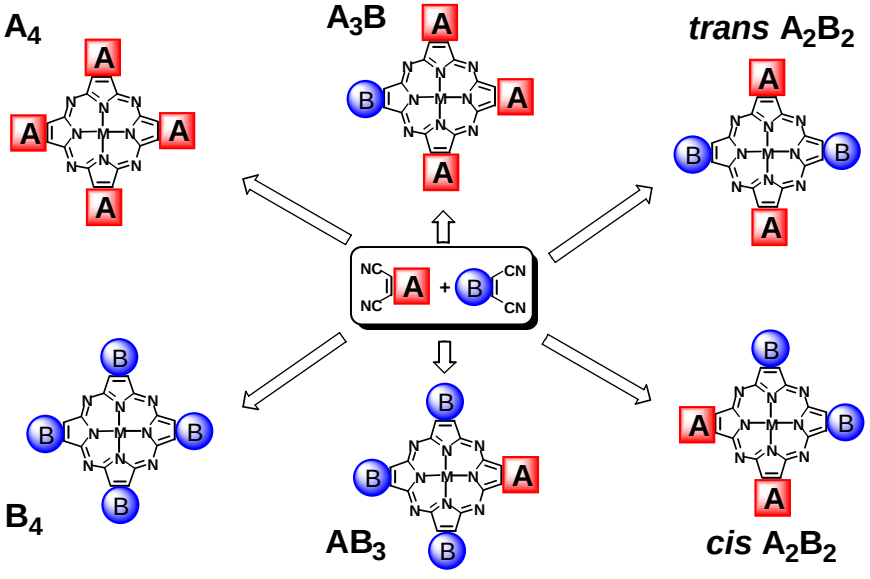

Figure 3. The six potential pz macrocycles resulting from a cross-macrocyclization reaction.

Macrocycle Properties

The photophysical properties of the pzs are intrinsically superior to the porphyrins because of the intense long-wavelength Q-band absorption and emission bands that arise due to the presence of the *meso* nitrogens. With nothing more than simple carbon-based substituents, the photophysical properties of the pzs compare favorably to those of the phthalocyanines. However, the introduction of the heteroatom peripheral substituents on the pzs results in significant red-shifts in the UV-vis spectra. Due to the enhanced optical properties of the sulfur-appended pzs, relative to pzs containing other heteroatoms [14], initial biological testing has focused primarily on pzs of the form M[pz(A_nB_{4-n})], where A represents a bis-thioether (A = [S-R]$_2$), B represents a fused β,β'-dialkoxybenzo group and M = Mg, Zn, or H_2. The R and R' groups that form the thioethers and the β,β'-dialkoxy groups, respectively, do not influence the optical properties, but may be used to modulate the physical properties and solubilities of the macrocycle.

For a given M and n, all compounds within this pz subclass possess the same basic pz structure and thus exhibit the same intrinsic absorbance and emission spectra. Table 1 shows the absorbance and emission maxima, as well as extinction coefficients, for $M[pz(A_nB_{4-n})]$ pzs with n = 2-4 and M = H_2, Mg, and Zn. Figure 4 shows typical spectra obtained in CH_2Cl_2 for the $H_2[pz(A_4)]$, $H_2[pz(A_3B)]$, and $H_2[pz(A_2B_2)]$ (i.e., free-base) pzs [14,26].

Table 1. Absorbance/emission maxima* and extinction coefficients†, where available, for selected $M[pz(A_nB_{4-n})]$ pzs, with A = $[S\text{-}R]_2$ and B = 4,7-diisopropoxybenzo, in CH_2Cl_2 [14,28,29].

	MA_4		MA_3B		MA_2B_2	
M	λ_{Abs} (ε x 10^{-3})	λ_{Em}	λ_{Abs} (ε x 10^{-3})	λ_{Em}	λ_{Abs} (ε x 10^{-3})	λ_{Em}
H_2	336 (28.8) 506 (18.2) 630 (18.2) 710 (14.1)	410 709	350 (40.7) 658 (6.6) 702 (22.4) 744 (sh)	428 800	343 (43.7) 656 (46.8) 794 (37.4)	440 827
Mg	372 670	488 706	368 676	442 744	354 667 761	447 802
Zn	378 (55.8) 672 (77.2)	435 713	362 (39.8) 618 (sh) 676 (49.0) 706 (sh)	444 754	352 (43.7) 666 (53.7) 761 (43.7)	440 795

*Absorbance and emission in nm.
†Extinction coefficients in $M^{-1}cm^{-1}$

All three H_2 pzs exhibit an intense B (Soret) band at ~350 nm (ε ~40,000 $M^{-1}cm^{-1}$), but each has a distinctly different Q-band region. For the completely symmetric $H_2[pzA_4]$ pz, a single Q-band is observed with a maximum absorption at ~710 nm (ε ~15,000 $M^{-1}cm^{-1}$). Both $H_2[pz(A_3B)]$ and $H_2[pz(A_2B_2)]$ show split Q-bands, with the former having a maximum absorption of 700 nm (ε ~25,000 $M^{-1}cm^{-1}$) and the latter having a pair of well-defined Q-bands at 654 nm and 798 nm (both with ε ~40,000 $M^{-1}cm^{-1}$), respectively. Addition of Mg or Zn to the core results in a slightly red-shifted, stronger (ε ~55,000 $M^{-1}cm^{-1}$ for Zn) Soret band at ~375 nm, and in the case of $M[pz(A_4)]$ and $M[pz(A_3B)]$, a single Q-band at ~675 nm (ε ~74,000 $M^{-1}cm^{-1}$ for $Zn[pz(A_4)]$). $M[pz(A_2B_2)]$ pzs show a split Q-band that is more red-shifted than either the $M[pz(A_4)]$ or $M[pz(A_3B)]$ pzs; but with a maximum absorbance at ~760 nm, it still lies at a lower wavelength than the $H_2[pz(A_2B_2)]$ maximum NIR absorbance.

All pzs of the $M[pz(A_nB_{4-n})]$ subclass exhibit dual fluorescence, as presented in Table 1 and shown in Figure 4 for the free-base pzs. The emission spectrum exhibits an intense luminescence in the blue, corresponding to $S_2 \rightarrow$ ground (S_0) fluorescence, and a second emission in the NIR, corresponding to $S_1 \rightarrow S_0$ fluorescence. The metallated pzs exhibit UV

fluorescence maxima at wavelengths slightly red-shifted compared to those of the equivalent H_2 pz, but exhibit a more blue-shifted NIR emission than their free-base analogues. Excitation to the blue of ~400 nm elicits both emissions; excitation to the red of ~450 nm produces only the NIR luminescence.

Previous work has shown that the singlet oxygen quantum yield (φ_Δ) for a series of M[pz(A_nB_{4-n})] pzs, where A is $[S\text{-}R]_2$ and B is a fused β,β'-dialkoxybenzo group, is also dramatically affected by the value of n and M (Table 2) [26]. For a given M (M = H_2, Mg, Zn), as the value of n increases, the singlet oxygen quantum yield decreases, independently of R [28]. A broad range of values are seen across Table 2, from low (φ_Δ = 0.007, H_2[pz(A_4)]) to high (φ_Δ = 0.370, Zn[pz(A_2B_2)]). Compounds with low values are attractive candidates as imaging agents since they absorb and fluoresce in the NIR, but do not sensitize the formation of singlet oxygen. In contrast, compounds with high singlet oxygen generation values are potential PDT agents.

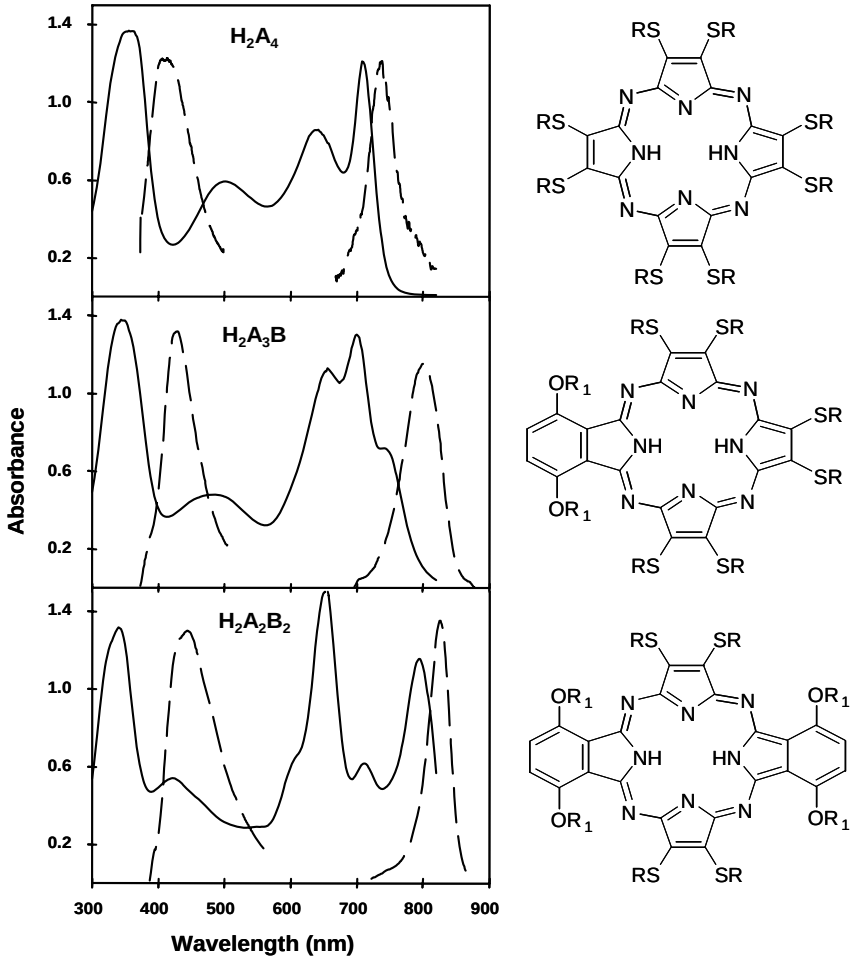

Figure 4. Absorbance (solid line) and emission (dashed line) plots for M[pz(A_nB_{4-n})] pzs, with A = $[S\text{-}R]_2$ and B = 4,7-diisopropoxybenzo, in CH_2Cl_2.

Table 2. Singlet oxygen quantum yields* for M[pz(A_nB_{4-n})] pzs, with A = [$S(CH_2CH_2O)_3H]_2$ and B = 4,7-diisopropoxybenzo, in CH_2Cl_2 [28].

M	**M**A_4 ϕ_Δ	**M**A_3B ϕ_Δ	**M**A_2B_2 ϕ_Δ
H_2	0.007	0.026	0.130
Mg	0.033	0.082	0.250
Zn	0.037	0.110	0.370

*Reference compound: α-terthienyl; ϕ_Δ = 0.67 [28].

Biocompatibility Studies of the Porphyrazines

We were the first to carry out biological studies of the pzs, with the preliminary studies being aimed primarily at developing structure-function relationships of the pzs and determining the biological activity of the pzs relative to the clinically used Photofrin. The overall goal of these studies was to determine how specific structures selectively affect biological behavior; the results of these studies would then be used to better streamline future syntheses towards preparing biologically optimized pzs. Over the past few years, our laboratory has prepared more than 250 porphyrazines, and detailed structure-function studies have been carried out and published for eleven of these pzs. In particular, the structure-function studies have focused on the subclass of the M[pz(A_nB_{4-n})] pzs where A = $[S\text{-}R]_2$ and B = fused 4,7-di-(isopropyloxy)benzo group. Each of the eleven compounds studied to date differ in the number and/or identity of R, n, and/or M (Figure 5) [29-31].[1]

Effect of Changing R

The first biological study of the pzs measured the effect that the pz substituents, or R groups, play on biological activity [31]. Specifically, the core pz structure was kept constant (H_2[pz(A_2B_2)]) while the charge of the R group was systematically varied to study neutral, negative, and positive R moieties (Pzs 1-3 in Figure 5).

Cellular uptake and toxicity studies were carried out in two cell lines: A549 (human lung adenocarcinoma cell line) and WI-38 VA13 (human embryonic fibroblast-like, virally-immortalized, normal cell line). Confocal fluorescence microscopy was used to detect cellular uptake, and all three compounds were found to localize in both tumor and normal cells.

The observed fluorescence of Pzs 2 and 3 were both quite weak, but the luminescence of Pz 1 (neutral R group) was particularly strong (Figure 6), and uptake was detected at concentrations as low as 3.1 μM. This fluorescence was observed at a much lower

[1]To aid the reader, the compounds in this chapter have been numbered sequentially 1-21. We note, however, that 1-11 were all prepared in the lab of B.M.H. and assigned the following numbers in the Master Compound Log: 1 = 16, 2 = 18, 3 = 42, 4 = 11, 5 = 4, 6 = 179, 7 = 178, 8 = 177, 9 = 176, 10 = 175, 11 = 174.

concentration than that observed for Photofrin, which was undetectable at concentrations below 25 μM. Utilizing the dual absorbance/emission of the pzs, the fluorescence of pz 1 was detected using both the blue and red emission of the compound. Co-localization studies indicated that a significant amount of Pz 1 was incorporated into the mitochondria of the tumor cells (Figure 7).

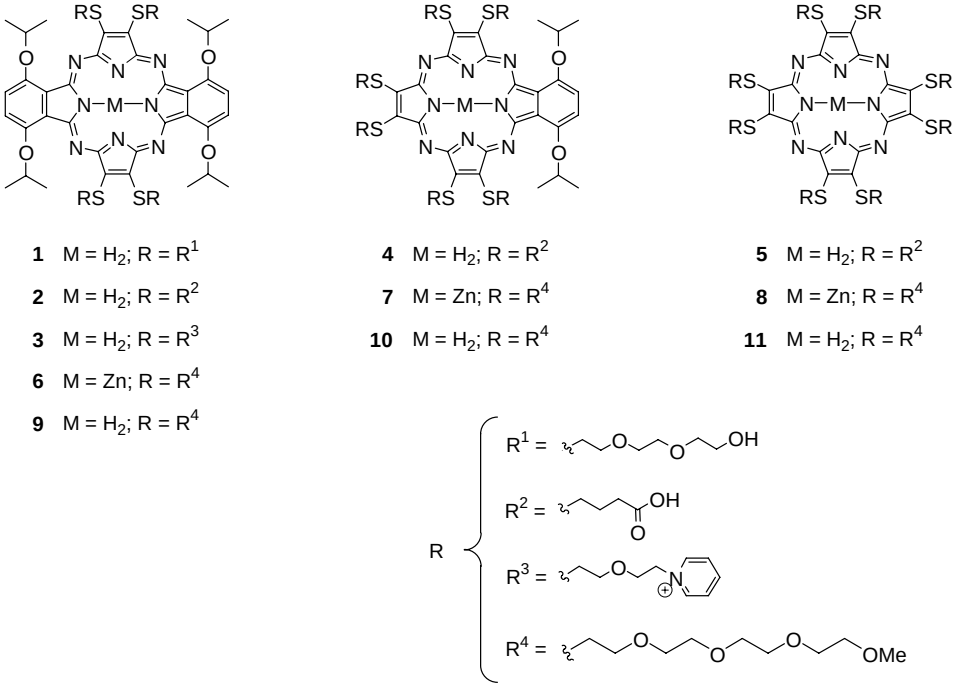

Figure 5. Chemical structures of the eleven sulfur-appended porphyrazines that have been subjected to in-depth biological studies.

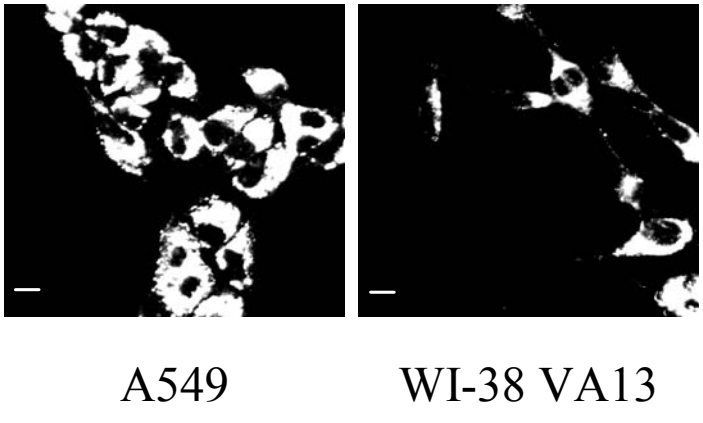

Figure 6. False-white single-photon confocal fluorescence microscopy of Pz 1 in A549 (left) tumor and WI-38 VA13 (right) normal cells treated at 50 μM. Scale bar = 10 μM. Adapted with permission from [31]. Copyright 2005 American Chemical Society.

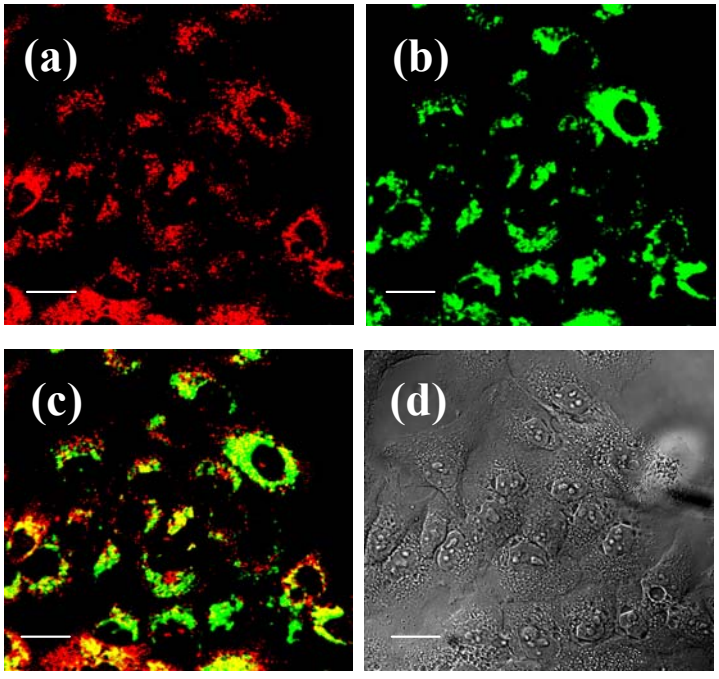

Figure 7. Intracellular co-localization of Pz 1 and MitoTracker Green in A549 cells: (a) false-red fluorescence of Pz 1; (b) false-green fluorescence of MitoTracker Green; (c) overlay, areas in yellow indicate co-localization; (d) phase contrast. Scale bar = 10 μM. Adapted with permission from [31]. Copyright 2005 American Chemical Society.

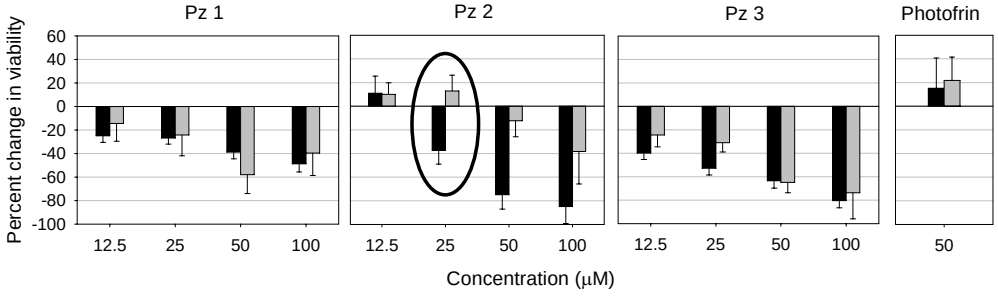

Figure 8. Dose dependency of Pzs 1-3, as measured by percent cell viability relative to DMSO control, in A549 (black bars) and WI-38 VA13 (gray bars) cells after 72 h exposure. (Note that a 0% change in cell viability indicates cells grew at the same rate as the control cells; negative values correlate to cells which grew at rates below those of the control cells.) The ellipse indicates the treatment concentration at which Pz 2 exhibited selective tumor toxicity. Adapted with permission from [31]. Copyright 2005 American Chemical Society.

Dark toxicity studies of Pzs 1, 2, and 3 revealed that the neutral and positively-charged pzs (1 and 3, respectively) were harmful to both A549 and WI-38 VA13 cells at all concentrations studied, but were more harmful to the normal cells than to the tumor cells at each treatment dose (Figure 8). Thus, despite the strong intracellular luminescence of Pz 1, neither it nor Pz 3 are likely clinical candidates due to their toxicity in normal cells. The

negatively-charged Pz 2 (R=$(CH_2)_3CO_2H$), in contrast, holds the potential to be a therapeutic agent: it was found to be selectively toxic in the A549 tumor cells at a treatment concentration of 25 μM (Figure 8). Unlike traditional PDT agents, however, none of the pzs exhibited light-induced toxicity, likely due to minor aggregation of the compounds in aqueous solution, which in turn suppressed singlet oxygen formation [31].

Effect of Changing n

The strong anti-tumor behavior observed for the anionic Pz 2 (R=$(CH_2)_3CO_2H$) led to a subsequent study of a suite of M[pz(A_nB_{4-n})] pzs utilizing the same R group and M (H_2), but n was systematically varied from 2-4 (Pzs 2, 4, and 5 in Figure 5) [30]. As with the first study, the bioactivity of the three compounds was analyzed in WI-38 VA13 normal and A549 tumor cells; the results of Pz 2 were successfully repeated. As n was increased, the number of carboxylate groups increased, corresponding to a more hydrophilic core and a greater net overall charge on the pz. This change in structure resulted in a change in biological behavior: While Pz 2 showed selective tumor killing, the dark toxicity assays of Pzs 4 and 5 (Figure 9) revealed that toxicity in both tumor and normal cells increased with increasing number of carboxylate groups and therefore negative charge (i.e., an increase in n). Again, toxicity was completely light-independent. While this was likely due to slight aggregation in aqueous media for Pzs 2 and 4, measurable light-induced toxicity was not expected for Pz 5 due to its low singlet oxygen quantum yield.

Effect of Changing M

In an effort to simultaneously increase solubility and singlet oxygen quantum yields of the pzs, a series of three Zn[pz(A_nB_{4-n})] pzs, and their corresponding free-base (H_2) analogues, were prepared with A = S[$(CH_2)_2O]_4Me$, B = fused 4,7-bis(isopropyloxy)benzo group, and n = 4, 3, or 2 (*trans*) (Pzs 6-11, Figure 5) [29]. For a given M (H_2 or Zn), as n is increased, the compounds become more hydrophilic in nature due to the increasing number of thiotetra(ethylene glycol) monomethyl ether moieties (A group). Furthermore, incorporating zinc into the core increases both solubility and singlet oxygen quantum yield. Both toxicity and cellular uptake experiments were carried out for the six compounds in A549 tumor and WI-38 VA13 cells.

Cellular dark toxicity was found to increase in a dose-dependent manner in both tumor and normal cell lines as n was decreased (Figure 10). For each concentration studied, this toxicity was generally greater in the normal cells than in the tumors, with Pz 8 being the only compound in the study that was found to be nontoxic to normal cells at concentrations above 12.5 μM. Furthermore, for a given M (Zn or H_2), cellular toxicity was generally greater upon exposure to the free-base pzs.

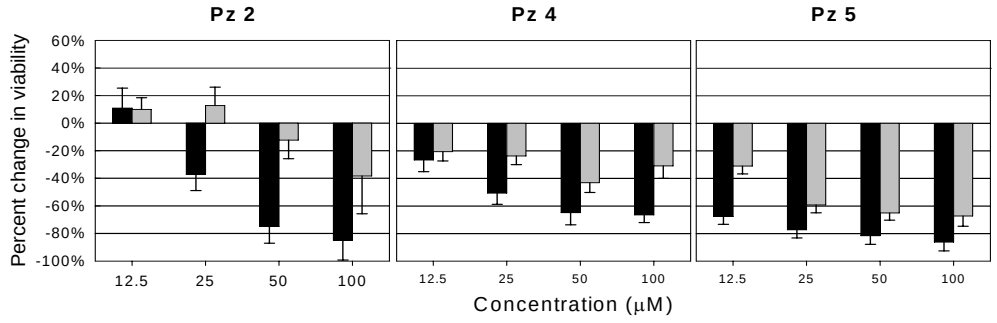

Figure 9. Dose dependency of Pzs 2, 4, and 5, as measured by percent cell viability relative to DMSO control, in A549 (black bars) and WI-38 VA13 (gray bars) cells after 72 h exposure. Adapted with permission from [30]. Copyright 2005 Elsevier B.V.

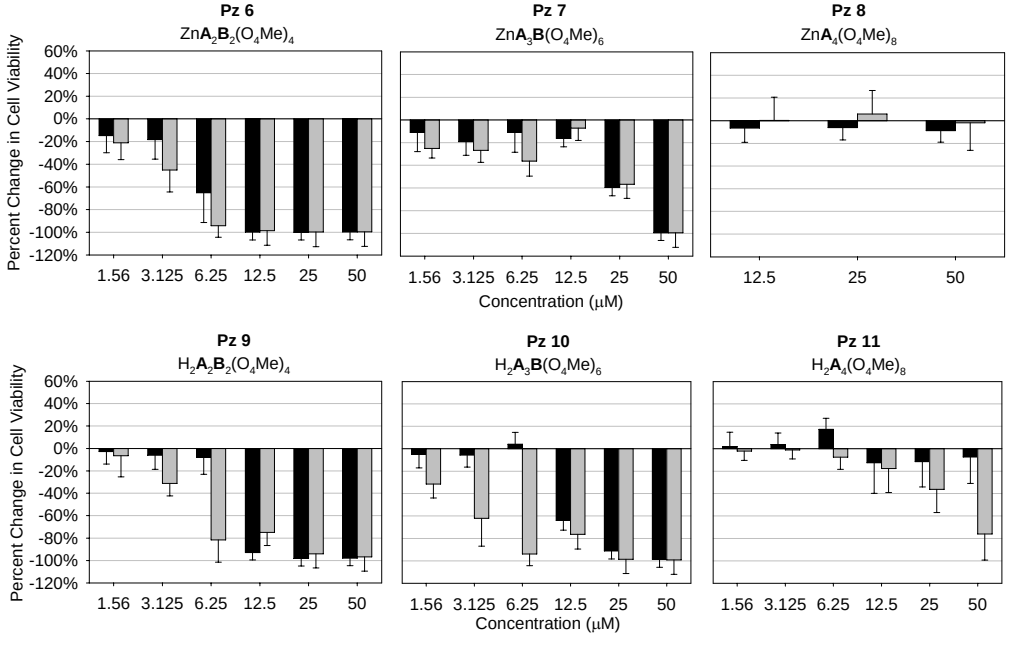

Figure 10. Dose dependency of Pzs 6-11, as measured by percent cell viability relative to DMSO control, inA549 (black bars) and WI-38 VA13 (gray bars) cells after 72 h exposure. Adapted with permission from [29]. Copyright 2008 Hindawi Publishing Corporation (open access article).

The most interesting result of the dark toxicity studies concerned Pz 11, which was found to be selectively toxic in *normal* cells. Nine different tumor cell lines (both adenocarcinomas and squamous cell carcinomas) were screened against Pz 11 and found to exhibit little-to-no dark toxicity upon treatment concentrations of 50 μM for 72 hours; in contrast, WI-38 VA13 normal cells treated under the same conditions were found to have a cell viability of only ~20%. These results suggest that Pz 11 might be a very useful diagnostic agent. For example, pathologists rely on the morphological appearance of tissue collected during biopsies to determine if a particular sample is either malignant or benign. In many cases, this determination is difficult to make, and either misdiagnosis (normal tissue diagnosed as

cancerous tissue) or undiagnosed samples (cancerous tissue diagnosed as normal tissue) can result. In situations where the diagnosis is unclear, Pz 11 could be added to a biopsy sample in culture: any normal cells would be killed, but malignant cells would remain intact. Thus, the use of a diagnostic aide such as Pz 11 would help to *biologically* differentiate tumor cells from normal cells that are not morphologically distinct.

In addition to improving the screening methods of pathologists, Pz 11 could also be used by laboratory researchers attempting to establish a new cell line derived from a human tumor. Since these cell lines originate from tumor samples of patients, it is necessary to purify the tumor cells (i.e., remove all traces of normal cells—both from within the tumor core and from the area surrounding the tumor), thus enabling the cell line to be more easily established in the laboratory. However, this purification process is very slow, laborious, and often unsuccessful, due largely in part to the difficulty in removing the normal cells. Adding Pz 11 to these samples could theoretically remove the normal cells more quickly, thereby enabling faster purification of the tumor cell line.

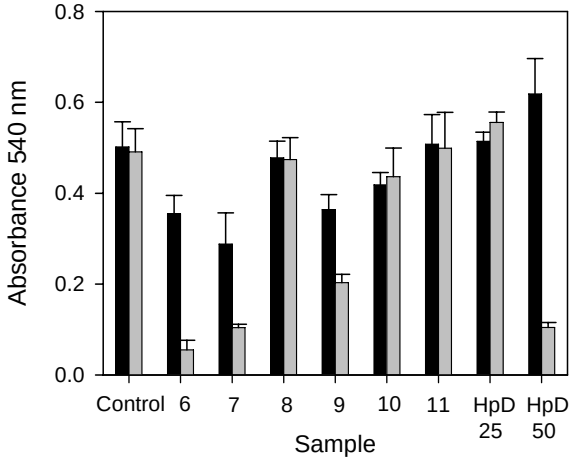

Figure 11. Light-dependent toxicity results of Pzs 6-11 in A549 cells, as measured by the 3-[4,5-dimethyl-thiazol-2-yl]-2,5-diphenyltetrazolium bromide (MTT) assay. Cells were exposed to pz (25 μM) or Photofrin (25 or 50 μM) for 4 hours, followed by white light exposure for 0 (black bars) or 10 (gray bars) minutes. Control cells were treated with an amount of DMSO equivalent to 25 μM pz. Adapted with permission from [29]. Copyright 2008 Hindawi Publishing Corporation (open access article).

Like the dark toxicity results, the light-induced toxicity experiments also generated interesting results. As anticipated, the compounds with the higher singlet oxygen yields (Pzs 6, 7, and 9) all showed enhanced cell killing upon white light treatment (Figure 11). The photosensitive effect elicited by Pz 9 suggests that the combination of the hydrophobic M[pz(A_2B_2)] core and the four hydrophilic thiotetra(ethylene glycol) monomethyl ether moieties provides the proper amphiphilicity necessary to achieve solubility in cellular environments. This contrasts with previously studied H_2[pz(A_2B_2)] pzs in which aggregation existed. Furthermore, unlike the M[pz(A_2B_2)] and Zn[pz(A_3B)] pzs, light-dependent toxicity was not observed for Pzs 8, 10, and 11 in this study. Thus, to date, photosensitive M[pz(A_4)] and H_2[pz(A_3B)] compounds have yet to be discovered. However, regardless of their

phototoxicity, these compounds may still possess selective dark toxicity and therefore may still have significant value as potential clinical anti-tumor agents.

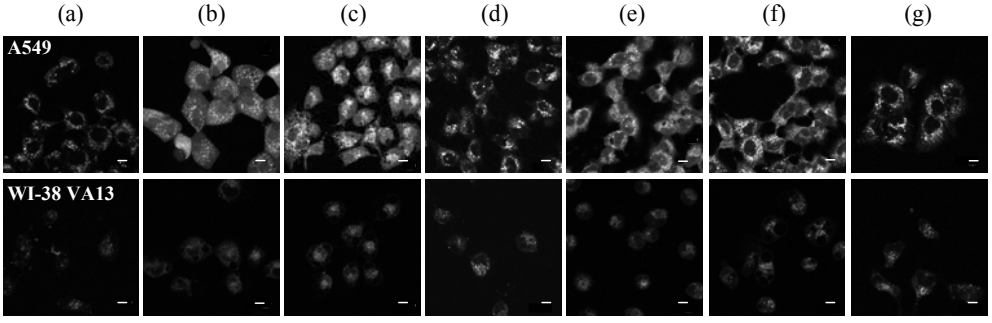

Figure 12. Cellular uptake of pzs using false-white confocal fluorescence microscopy images of A549 (top row) and WI-38 VA13 (bottom row) cells treated with 25 μM agent: (a) DMSO control, (b) Pz 6, (c) Pz 7, (d) Pz 8, (e) Pz 9, (f) Pz 10, (g) Pz 11. Scale bar = 10 μM. Adapted with permission from [29]. Copyright 2008 Hindawi Publishing Corporation (open access article).

Cellular uptake studies of Pzs 6-11 disclosed that all six compounds were preferentially incorporated in the A549 tumor cells, with the pz localizing in the cytoplasm (Figure 12). This result therefore suggests that Pz 8 may serve as a useful imaging agent, given this preferential uptake in tumor cells and the earlier observation that WI-38 VA13 normal cells are nontoxic upon exposure to Pz 8.

Future Directions

The effectiveness of a PDT or imaging agent is dependent upon the drug being preferentially incorporated into tumor cells. The structure-function studies described above for the M[pz(A_nB_{4-n})] pzs are being carried out in an effort to address this issue in the porphyrazines. By adjusting the core structure (n), the central metal ion (M), and the identity/properties of the side chains (R), one is able to adjust the hydrophobicity/hydrophilicity balance that is likely necessary for targeting tumor cells. The preliminary studies described herein have identified several such characteristics that can directly influence the biological activity of the pz. Future work will continue to build upon this knowledge of the sulfur-appended pzs, as other n, M, and R combinations will be systematically studied. As additional preclinical screening experiments are carried out, it is anticipated that a number of these compounds will be selected for future clinical trials. (Pzs 2 and 8 are early candidates, pending further studies.)

In addition to the preparation of more biologically compatible sulfur-appended pzs, future work in the field of porphyrazine anti-tumor agents will focus on both synthetic and delivery advancements. A number of other pz subclasses have recently emerged as having potential therapeutic applications [32-42]. Moreover, new breakthroughs have been reported in general porphyrazine synthetic techniques [37,43], which in turn will facilitate the

preparation and purification of future compounds. Lastly, several recent articles have attempted to improve the cellular uptake of pzs by incorporating the compounds into liposomes [44-48]. These three emerging areas in the study of pz anti-tumor agents are described in more detail below.

Emerging Pz Subclasses Exhibiting Biological Potential

While the sulfur-appended pzs have garnered much of the preliminary interest in the biological activity studies, several other pz subclasses have also been shown to be worthy of further investigation. Perhaps the most notable and well-studied subclass is the nitrogen-appended *seco*-porphyrazines. The first *seco*-pz was formed as a by-product during the synthesis of $H_2[pz(N\text{-}Me_2)_8]$: oxidation of one of the pyrrole rings resulted in the cleavage of the $R_2NC{=}CNR_2$ bond, yielding Pz 12 (Figure 13) [32]. A number of *seco*-pzs have been produced since that time [33-35], including both peripherally-metallated structures [36] (which show enhanced singlet oxygen sensitization), such as Pz 13, and water-soluble compounds, such as Pz 14, as shown in Figure 13 [37,38].

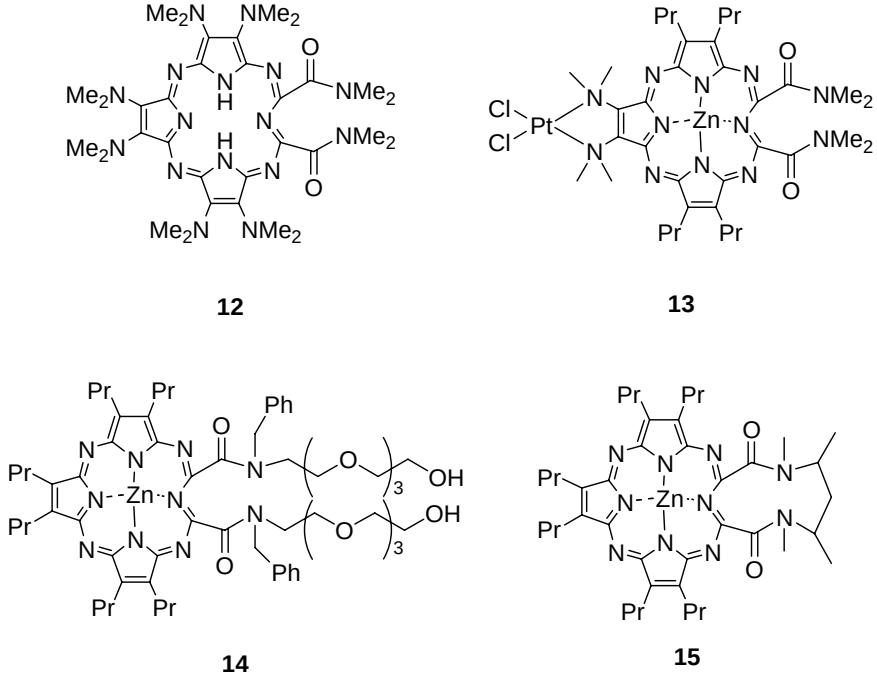

Figure 13. Selected structures of *seco*-porphyrazines.

Like Pz 13 above ($\phi_\Delta = 0.59$), many of these compounds have been found to possess very high singlet oxygen quantum yields ($\phi_\Delta \sim 0.45\text{-}0.6$), thus making them excellent candidates for PDT therapy. To date, the largest reported singlet oxygen quantum yield for a porphyrazine was an annulated seven-member ring *seco*-porphyrazine, Pz 15, with $\phi_\Delta = 0.74$ [39]. While the extremely high singlet oxygen quantum yields of the *seco*-pzs are very

promising, further biological studies are needed to realize the potential clinical relevance of this subclass of pzs.

Limited work has also been carried out on two other pz subclasses. Porphyrazine derivatives containing multifluorenyl substituents, such as Pz 16 (Figure 14), have been prepared and shown to possess photophysical properties suggesting their potential as PDT agents [40]. Similarly, a series of zinc bis(1,4-didecylbenzo)-bis(2,3-pyrido) porphyrazines, including Pz 17 (Figure 14), have been prepared; after reacting these compounds with quarternizing agents, the pzs were found to be water-soluble and exhibited a photosensitizing effect [41]. Like the *seco*-pzs, in-depth biological studies still need to be performed in order to better understand the biological activity of these two new pz subclasses.

A new subclass of boron-containing pzs has also recently been proposed for study [42]; however, the synthesis of any such compound has not yet been reported. It is believed that boron-containing pzs such as Pz 18 (Figure 14) would offer potential in both PDT and boron neutron-capture therapy applications.

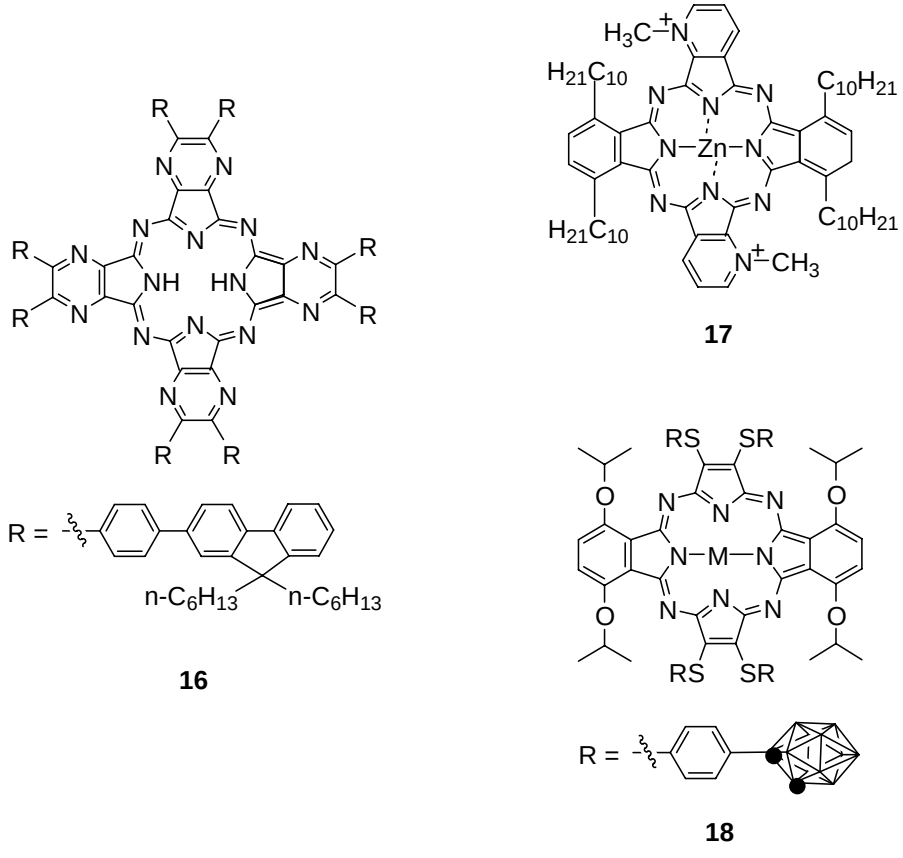

Figure 14. Selected structures of newly studied (Pzs 16 and 17) and proposed (Pz 18) subclasses of biologically active porphyrazines. For Pz 18, the cluster represents an *o*-carborane cage ($C_2B_{10}H_{12}$) with the unlabeled corners indicating a BH-unit and • indicating a CH-unit.

Synthetic Advancements

Nearly all of the pzs studied to date have been prepared via the mixed cyclization of two maleonitrile derivatives. While such compounds allow for a great amount of flexibility in tailoring the pzs for biological applications, the co-cyclization method used to prepare the compounds can result in the formation of six possible macrocycles, which then need to be separated and purified. Despite the fact that both the nature (e.g., using bulky β,β'-dialkoxybenzo groups) and the ratio of the cyclization partners can be used to favor the production of one or more isomers, isolating the desired pz is still often challenging. Recent work has therefore sought to simplify the methods by which the pzs are prepared. To this end, a one-pot synthesis has been successfully carried out to produce the nitrogen-appended Pz 19 [37]. This compound was prepared on a large scale (18.4 g) in comparatively high yield (33%) and was easily purified. Subsequent reactions led to the *seco*-pz analogue, Pz 20, a potential biological agent. Structures of Pzs 19 and 20 are shown in Figure 15. The use of the one-pot synthesis significantly reduced the amount of post-cyclization purification needed to sufficiently purify Pz 19. As more improved synthetic capabilities such as these are realized for the pzs, compounds will be produced and purified more quickly and easily, thereby facilitating the discovery of new therapeutic and imaging agents.

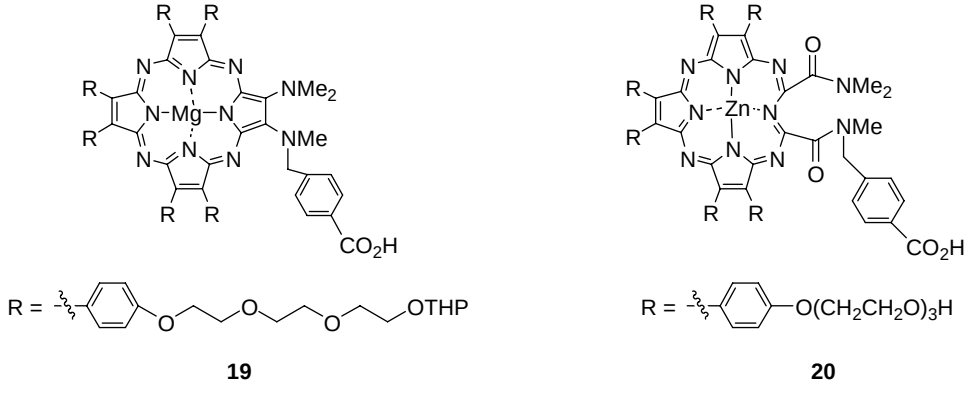

Figure 15. Porphyrazines prepared via a one-pot synthesis.

The ability to easily convert Pz 19 into the water-soluble Pz 20 addresses another shortcoming of the first-generation pz anti-tumor agents: aggregation in aqueous media. As mentioned above, many of the original sulfur-appended pzs were found to aggregate slightly in aqueous media, leading to the suppression of their singlet oxygen generation. By preparing water-soluble compounds, the pzs will be more conducive to the aqueous microenvironment of the tumor cells, thereby likely enhancing both cellular uptake and PDT applicability. Thus, significant efforts in future pz synthetic work will likely focus upon the development of water-soluble pzs for use in biological applications [43].

Pz Liposome Incorporation

In an effort to better predict future biologically active porphyrazines, recent studies have attempted to incorporate a number of pzs into liposomes [44-48]. Most notably, a series of 29 different pzs of the form $M[pz(A_nB_{4-n})]$ were studied, with A = $[S\text{-}R]_2$; B = a fused 4,7-di-(isopropyloxy)benzo group; M = H_2, Mg, or Zn; and n = 2 (*trans*), 3, or 4 [48]. The results of this study showed a strong correlation between pz structure and the ability to bind to membranes. In particular, membrane binding ability decreased as n increased, and metallated pzs resulted in stronger binding than did free-base pzs. Furthermore, R groups exhibiting a balanced amphiphilicity were found to improve membrane binding.

Thus, the most promising results were observed with $Zn[pz(A_2B_2)]$ pzs containing R groups with a balanced hydrophobicity/hydrophilicity. Pz 21 (Figure 16), with A = $S(C_2H_4O)_2H$, is one such example. The results correlate well to the structure-function studies that have been carried out to date for the sulfur-appended pzs, suggesting that liposome binding may be a useful preliminary testing method in the search for biologically active pzs [48].

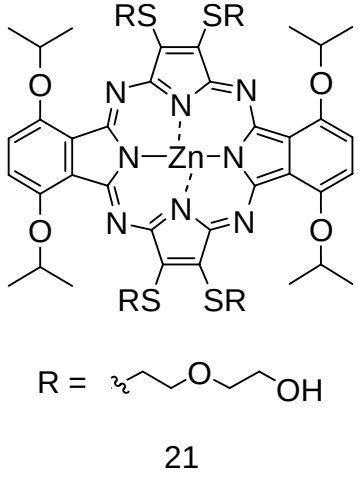

21

Figure 16. Structure of the porphyrazine found to have the strongest liposome binding constant [48].

Conclusion

The flexibility of the porphyrazines, in regards to both their ease of synthesis and the various chemical/physical properties available to them, make these compounds very attractive for imaging and therapeutic applications. Initial work has shown promise that a number of these compounds may be of potential clinical relevance. However, further studies are needed to more thoroughly elucidate the structure-function relationships of the pzs. To this end, synthetic and delivery advancements continue to unfold, and these discoveries will continue to improve our understanding of the pz biological behavior. We further note that only a small subset of pzs have to date been studied for their anti-tumor potential; many more

pzs possessing useful anti-tumor behavior likely either already exist or can be easily synthesized. Thus, the combination of the exciting results of the early pz studies and the untapped potential of this class of compounds makes the future extremely bright for the porphyrazines in the field of biological applications.

References

[1] Bonnett, R. *Rev. Contemp. Pharmaco.* 1999, *10*, 1-17.
[2] Funke, B.; Jungel, A.; Schastak, S.; Wiedemeyer, K.; Emmrich, F.; Sack, U. *Lasers Surg Med.* 2006, *38*, 866-74.
[3] Emerson, M. V.; Lauer, A. K. *BioDrugs.* 2007, *21*, 245-57.
[4] Quaresima, V.; Matcher, S. J.; Ferrari, M. *Photochem. Photobiol.* 1998, *67*, 4-14.
[5] Troy, T. L.; Page, D. L.; Sevick-Muraca, E. M. *J. Biomed. Opt.* 1996, *1*, 342-55.
[6] de Haller, E. B. *J. Biomed. Opt.* 1996, *1*, 7-17.
[7] MacDonald, I. J.; Dougherty, T. J. *J. Porphyr. Phthalocya.* 2001, *5*, 105-29.
[8] Kessel, D.; Dougherty, T. J. *Rev. Contemp. Pharmaco.* 1999, *10*, 19-24.
[9] Lui, W.; Jensen, T. J.; Fronczek, F. R.; Hammer, R. P.; Smith, K. M.; Vicente, M. G. H. *J. Med. Chem.* 2005, *48*, 1033-48.
[10] Allen, C. M.; Sharman, W. M.; Van Lier, J. E. *J. Porphyr. Phthalocya.* 2001, *5*, 161-69.
[11] Chowdhary, R. K.; Shariff, I.; Dolphin, D. J. *Pharm. Pharm. Sci.* 2003, *6*, 13-19.
[12] Lassalle, H. P.; Bezdetnaya, L.; Iani, V.; Juzeniene, A.; Guillemin, F.; Moan, J. *Photochem. Photobiol. Sci.* 2004, *3*, 999-1005.
[13] Sessler, J. L.; Seidel, D. *Angew. Chem. Int. Edit.* 2003, *42*, 5134-75.
[14] Michel, S. L. J.; Baum, S.; Barrett, A. G. M.; Hoffman, B. M. *Prog. Inorg. Chem.* 2001, *50*, 473-590.
[15] Cook, A. S.; Williams, D. B. G.; White, A. J. P.; Williams, D. J.; Lange, S. J.; Barrett, A. G. M.; Hoffman, B. M. *Angew. Chem. Int. Edit.* 1997, *36*, 760-61.
[16] Sibert, J. W.; Baumann, T. F.; Williams, D. J.; White, A. J. P.; Barrett, A. G. M.; Hoffman, B. M. *J. Am. Chem. Soc.* 1996, *118*, 10487-93.
[17] Lange, S. J.; Nie, H.; Stern, C. L.; Barrett, A. G. M.; Hoffman, B. M. *Inorg. Chem.* 1998, *37*, 6435-43.
[18] Forsyth, T. P.; Williams, D. B. G.; Montalban, A. G.; Stern, C. L.; Barrett, A. G. M.; Hoffman, B. M. *J. Org. Chem.* 1998, *63*, 331-36.
[19] Linben, T. G.; Hanack, M. *Chem. Ber.* 1994, *127*, 2051-57.
[20] Kobayashi, N.; Ashida, T.; Osa, T. *Chem. Lett.* 1992, 2031-34.
[21] Stihler, P.; Hauschel, B.; Hanack, M. *Chem. Ber.* 1997, *130*, 801-06.
[22] Leznoff, C. C.; Svirskaya, P. I.; Khouw, B.; Cerny, R. L.; Seymour, P.; Lever, A. B. P. *J. Org. Chem.* 1991, *56*, 82-90.
[23] Velázquez, C. S.; Fox, G. A.; Broderick, W. E.; Andersen, K. A.; Anderson, O. P.; Barrett, A. G. M.; Hoffman, B. M. *J. Am. Chem. Soc.* 1992, *114*, 7416-24.
[24] Sugiura, K.-I.; Kumar, M. R.; Chandrashekar, T. K.; Sakata, Y. *Chem. Lett.* 1997, 291-92.

[25] Sugiura, K.-I.; Ushiroda, K.; Johnson, M. T.; Miller, J. S.; Sakata, Y. *J. Mater. Chem.* 2000, *10*, 2507-14.
[26] Lee, S.; White, A. J. P.; Williams, D. J.; Barrett, A. G. M.; Hoffman, B. M. *J. Org. Chem.* 2001, *66*, 461-65.
[27] Ehrlich, L. A.; Skrdla, P. J.; Jarrell, W.; Sibert, J. W.; Armstrong, N. R.; Saavedra, S. S.; Barrett, A. G. M.; Hoffman, B. M. *Inorg. Chem.* 2000, *39*, 3963-69.
[28] Lee, S.; Stackow, R.; Foote, C. S.; Barrett, A. G. M.; Hoffman, B. M. *Photochem. Photobiol.* 2003, *77*, 18-21.
[29] Lee, S.; Vesper, B. J.; Zong, H.; Hammer, N. D.; Elseth, K. M.; Barrett, A. G. M.; Hoffman, B. M.; Radosevich, J. A. *Met.-Based Drugs.* 2008, *Volume 2008*, 13 pages.
[30] Vesper, B. J.; Lee, S.; Hammer, N. D.; Elseth, K. M.; Barrett, A. G. M.; Hoffman, B. M.; Radosevich, J. A. *J. Photochem. Photobiol. B.* 2006, *82*, 180-86.
[31] Hammer, N. D.; Lee, S.; Vesper, B. J.; Elseth, K. M.; Hoffman, B. M.; Barrett, A. G. M.; Radosevich, J. A. *J. Med. Chem.* 2005, *48*, 8125-33.
[32] Mani, N. S.; Beall, L. S.; White, A. J. P.; Williams, D. J.; Barrett, A. G. M.; Hoffman, B. M. *J. Chem. Soc. Chem. Commun.* 1994, 1943-4.
[33] Andersen, K.; Anderson, M.; Anderson, O. P.; Baum, S.; Baumann, T. F.; Beall, L. S.; Broderick, W. E.; Cook, A. S.; Eichhorn, D. M.; Goldberg, D.; Hope, H.; Jarrell, W.; Lange, S.
[34] J.; McCubbin, Q. J.; Mani, N. S.; Miller, T.; Montalban, A. G.; Rodriguez-Morgade, M. S.; Lee, S.; Nie, H.; Olmstead, M. M.; Sabat, M.; Sibert, J. W.; Stern, C.; White, A. J. P.; Williams, D. B. G.; Williams, D. J.; Barrett, A. G. M.; Hoffman, B. M. *J. Heterocycl. Chem.* 1998, *35*, 1013-42.
[35] Montalban, A. G.; Lange, S. J.; Beall, L. S.; Mani, N. S.; Williams, D. J.; White, A. J. P.; Barrett, A. G. M.; Hoffman, B. M. *J. Org. Chem.* 1997, *62*, 9284-89.
[36] Montalban, A. G.; Meunier, H. F.; Ostler, R. B.; Barrett, A. G. M.; Hoffman, B. M.; Rumbles, G. *J. Phys. Chem. A.* 1999, *103*, 4352-58.
[37] Sakellariou, E. G.; Montalban, A. G.; Meunier, H. G.; Rumbles, G.; Phillips, D.; Ostler, R. B.; Suhling, K.; Barrett, A. G. M.; Hoffman, B. M. *Inorg. Chem.* 2002, *41*, 2182-87.
[38] Guinchard, X.; Fuchter, M. J.; Ruggiero, A.; Duckworth, B. J.; Barrett, A. G. M.; Hoffman, B. M. *Org. Lett.* 2007, *9*, 5291-94.
[39] Sakellariou, E. G.; Montalban, A. G.; Beall, S. L.; Henderson, D.; Meunier, H. G.; Phillips, D.; Suhling, K.; Barrett, A. G. M.; Hoffman, B. M. *Tetrahedron.* 2003, *59*, 9083-90.
[40] Baum, S. M.; Trabanco, A. A.; Andres, A.; Montalban, A.; Micallef, A. S.; Zhong, C.; Meunier, H. G.; Suhling, K.; Phillips, D.; White, A. J. P.; Williams, D. J.; Barrett, A. G. M.; Hoffman, B. M. *J. Org. Chem.* 2003, *68*, 1665-70.
[41] Barker, C. A.; Zeng, X.; Bettington, S.; Batsanov, A. S.; Bryce, M. R.; Beeby, A. *Chem. Eur. J.* 2007, *13*, 6710-17.
[42] Sakamoto, K.; Ohno-Okumura, E.; Kato, T.; Watanabe, M.; Cook, M. J. *Met.-Based Drugs.* 2008, *Volume 2008*, 7 pages.
[43] Ratajski, M.; Osterloh, J.; Gabel, D. *Anti-Cancer Agents Med. Chem.* 2006, *6*, 159-66.
[44] Kemikli, N.; Ozturk, R. *Inorg. Chem. Commun.* 2008, *11*, 338-40.

[45] Ristori, S.; Salvati, A.; Martini, G.; Spalla, O.; Pietrangeli, D.; Rosa, A.; Ricciardi, G. *J. Amer. Chem. Soc.* 2007, *129*, 2728-29.

[46] Salvati, A.; Ristori, S.; Oberdisse, J.; Spalla, O.; Ricciardi, G.; Pietrangeli, D.; Giustiani, M.; Martini, G. *J. Phys. Chem. B.* 2007, *111*, 10357-64.

[47] Salvati, A.; Ristori, S.; Pietrangeli, D.; Oberdisse, J.; Calamai, L.; Martini, G.; Ricciardi, G. *Biophys. Chem.* 2007, *131*, 43-51.

[48] Sholto, A.; Lee, S.; Hoffman, B. M.; Barrett, A. G. M.; Ehrenberg, B. *Photochem. Photobiol.* 2008, *84*, 764-73.

In: Clinical Chemistry Research
Editors: Brian H. Mitchem and Charles L. Sharnham
ISBN 978-1-60692-517-1

Expert Commentary

Mass Spectrometry in Clinical Chemistry

Simone König*

Integrated Functional Genomics, Interdisciplinary Center for Clinical Research, Medical Faculty, University of Muenster, Muenster, Germany

Mass spectrometry (MS) can be viewed as the universal "balance" of the natural sciences. By measuring atomic and molecular weights it has become an essential tool for composition and structural analysis. In fact, the discovery of soft ionization techniques some 20 years ago has introduced MS to the biosciences and ultimately to clinic-associated facilities. Electrospray (ESI) and MALDI (matrix-assisted laser desorption) ionization leave biomolecules intact and allow their measurement up to very high masses. As the 2002 Nobel Price Winner John Fenn of Virginia Commonwealth University put it – elephants learned to fly. Nevertheless, MS had its place in the clinical laboratory before those discoveries with the long established coupling of gas chromatography (GC)-MS for the detection of small organic acids and metabolites. Especially for the "General-Unknown-Screening" in cases of intoxication the method has proven very useful. It is limited, however, to volatile compounds or such samples which can be derivatized to achieve that effect. The mass range of the instruments ends mostly well below 1000 Da. Therefore, liquid chromatography (LC)-MS couplings soon moved in to complement GC-MS for water-soluble and higher-molecular-weight compounds. Those two coupling techniques remain the only MS-based methods with some impact in the clinical laboratory so far. The new possibilities of investigating whole proteins or other macromolecules using MS technology have not yet found their way into clinical diagnostics. Attempts were made trying to apply SELDI (surface-enhanced laser desorption ionization) to comparative biomarker profiling of body liquids such as serum. To that end, biochips were covered with various chromatographic surfaces with the goal to simplify as well as standardize sample preparation. While some interesting reports can be

* e-mail: koenigs@uni-muenster.de

found in the literature, reproducibility seems to be a major problem which has so far effectively prevented SELDI from becoming a diagnostic tool. Reasons may be the biochips themselves whose production is an art. In addition, the biological variation introduced by the study subjects is difficult to control. A blood sample, e.g., will vary depending on the time of day it is taken, the gender and age of the person, monthly or age-dependent hormone changes, or food and drink which was consumed on a regular basis or shortly before sampling. Therefore, only drastic reproducible biological effects can be monitored in diagnostics and even then, some diagnostic markers are not very reliable as, e.g., PSA for prostate cancer. A third reason for the difficulties SELDI was experiencing was ion suppression during ionization. The effect molecules have on each other hunting for protons in the ion cloud depends on the respective make-up of the analyte and surrounding solvent system and is difficult to control. In case of large concentration differences – one major component in a bulk of minor components - this is hardly an issue for the main analyte. Minor components, however, may be effectively suppressed and become invisible in the spectrum.

In contrast to clinical diagnostics, MS has established itself very well as an essential tool in clinical research. It provides data with high sensitivity and accuracy for genomics, proteomics and metabolomics. In fact, MS-based research literally exploded as is documented in numerous new journals. As an example, whole proteomes can be identified and screened for effects due to disease or stimulation. But again, study design is very important dealing with samples of biological origin. Variation in concentration from sample to sample may be greater than technical variation. Looking at whole proteomes means to investigate snapshots of highly complex mixtures of thousands of different proteins caught at one particular point in time and space. In general, the analyst has to deal with the protein extracts of a specific number of cells or of tissue homogenates. While cell culture has the potential to supply enough material for exhaustive analysis, it has been discussed how well cells can be kept over extended periods of time without changing or contaminating them. Obtaining sufficient animal or human tissue may also prove difficult. Apart from animal rights issues, keeping and raising animals requires special, and therefore, expensive facilities. A tissue biopsy from human being is not easy to get and also does not contain too much material for further processing. Tissue and sample collection need to be highly standardized to avoid decomposition and ensure comparable results for extended periods of time. In addition, sample exchange among scientific institutions is important and the history of the analyte must be known very well. Biomolecules are highly susceptible to environmental changes and respond with, e.g., oxidation or cleavage. Particularly handling and transport steps may introduce unwanted modifications depending on the time span the sample was exposed to open air or room temperature. Therefore, biobanks are increasingly created which strive to provide state-of-the-art storage. However, well maintained storage and documentation is associated with cost and not necessarily accessible for the average scientist.

MS has reached a level of performance which causes a shift of the analytical bottleneck to sample preparation. MS does require a certain degree of purification in order to achieve reproducible results and it is these steps which, while selectively isolating one population of molecules, lose another. In an example proteome expression is considered. There the goal is to visualize the complete proteome and identify members regulated due to changes. However,

the generation of protein extracts requires homogenization, lysis and dissolvation steps so that in each procedure some information is lost, be it due to solubility or other properties. E.g., hydrophobic proteins may be lost, although the addition of detergents has expanded the soluble proteome considerably. Most of the time, “whole proteome analyses” only refer to investigations of the soluble proteome. Those can be visualized in two dimensions using gel electrophoresis. It creates maps with respect to protein isoelectric point and molecular weight. The concentration of the proteins is reflected in their staining intensity or spot size, but the dynamic range of the visualization method leaves proteins present in lower amounts invisible. More often than not, the abundant proteins are not of interest for the research project. Various authors suspect more than twelve orders of magnitude in dynamic range. Not unexpectedly, the correlation between mRNA and protein levels was shown to be insufficient to predict protein expression levels from quantitative mRNA data so that one is forced to study proteins in order to get to the essence of all efforts - function.

The wanted or unwanted separation effects are the crux of all analyses, be it small or large molecules. Nevertheless, MS is flexible enough to be adapted to complicated measurements with novel ionization or detection techniques. We may hypothesize that the impact of MS in clinical research and diagnostic will continue to grow. While for the former all suitable ionization and detection methods will be employed in any combination which solves a scientific problem, for the latter dedicated instruments and integrated system solutions will evolve. Array analysis and sample or tissue profiling seem to look the most promising applications.

Short Communications

In: Clinical Chemistry Research
Editors: Brian H. Mitchem and Charles L. Sharnham
ISBN 978-1-60692-517-1

Short Communication A

Quantitative Proteome-Disease Relationships (QPDRs) in Clinical Chemistry: Prediction of Prostate Cancer with Spectral Moments of PSA/MS Star Networks

Giulio Ferino[1,2], Giovanna Delogu[2], Gianni Podda[2], Eugenio Uriarte[1] and Humberto González-Díaz[1,2,*]

[1] Unit of Bioinformatics & Connectivity Analysis (UBICA), Institute of Industrial Pharmacy, and Department of Organic Chemistry, USC, Spain.

[2] Dipartimento Farmaco Chimico Tecnologico, Universitá degli Studi di Cagliari, Cagliari, Italia.

Abstract

The Mass Spectra (MS) of blood human proteome can be of great help in detecting diseases. In Prostate Cancer (PCa), prognostic (predictive) factors are particularly important given the marked heterogeneity of this disease at clinical, morphologic and biomolecular levels. Blood contains a treasure of previously unstudied biomarkers that could reflect the ongoing physiological state of all tissue. The serum Prostate-Specific Antigen (PSA) measurement is a very good biomarker for PCa, but the Sensitivity is somewhat low (above 62%). In this paper we propose a general strategy, based on Computational Chemistry techniques, which should improve the predictive power of PSA. Our group adapted the Shining Star graph to represent human serum-plasma-proteome MS for healthy and PCa patients. In this work we calculated different Spectral Moments of the Markov Matrix associated to the Star graph for a sample of patients.

* To whom correspondence should be addressed: Humberto González-Díaz. Faculty of Pharmacy, University of Santiago de Compostela 15782,Spain.Tel:+34-981-563100 Fax: +34-981 594912. Email: gonzalezdiazh@yahoo.es

These indices are similar to other graph parameters such as Topological Indices (TIs) or Connectivity Indices (CIs). We used these indices to create Quantitative Proteome-Disease Relationships QPDRs models in analogy to QSAR models of small drugs. The best QPDRs found model showed a sensitivity value of 89.9%. This methodology might be useful in several Bioinformatics applications based on Translational Medicine.

Keywords: Mass spectra/ Graph theory/ Complex networks/ Spectral moments/ Prostate cancer/ Prostate-specific antigen

Introduction

A blood proteome Mass Spectra (MS) represents a potential tool for the early detection of diseases [1]. Transformation of the output signal from the serum plasma MS into a graph may be a useful alternative to Prostate Cancer (PCa) MS pre-processing. This graph can be numerically drawn using numerical indices that describe the connectedness between nodes in the graph. Many authors refer to this class of indices as to Topological Indices (TIs) or Connectivity (CIs) [2-6]. The transformation of networks (a picture) into TIs or CIs (numbers) allows not only the storage, manipulation and information retrieval in computational chemistry, but also enables the search for quantitative relationships between system structure and function. However, one can consider numerous variations to this classic strategy beyond the world of small molecules and covering not only macromolecules, such as DNA and proteins, but also brain cortex, population sociology and other complex systems.

From now on we will refer to all these indices (TIs and CIs) as the CIs [7-14]. The network representation and study of CIs may help to capture not only linear but also non-linear relationships among the MS regions. The idea of the connectivity analysis applied to red blood cells metabolic components serves in some way as inspiration for this line of thinking, approaching the study of blood with CIs and graphs [14]. The CIs may improve the ability of the single biomarker to encode multi-causal information. In principle, we can represent MS information by a graph and calculate the CIs in analogy with approaches used for DNA or protein sequences [15].

In this work we adapted the Shining Star graph [16] to represent human serum-plasma-proteome MS for healthy and PCa patients. The network used in this work also incorporated as nodes the level of the Prostate Surface Antigen (PSA) for cancer and healthy patients, including benign prostatic hyperplasia patients [17]. The PSA is a very good biomarker for prostate cancer, when we try to differentiate PCa patients from control group using the dataset reported by Petricoin *et al.* [18] the PSA based model classifies correctly only the 62% of cancer patients. This methodology is new, widespread and with a great scope.

2. Materials and Methods

In Figure 1 the flowchart of this work is shown. The first step (A) was to transform the MS in order to obtain a set number used for graphic representation, see section 2.1. and 2.2. The second step (B) was to portray the MS of each patient with a Shining Randic Star [19], see section 2.3. The third and final step (C), using the Linear Discriminant Analysis, was to develop the statistical models, see section *2.4*.

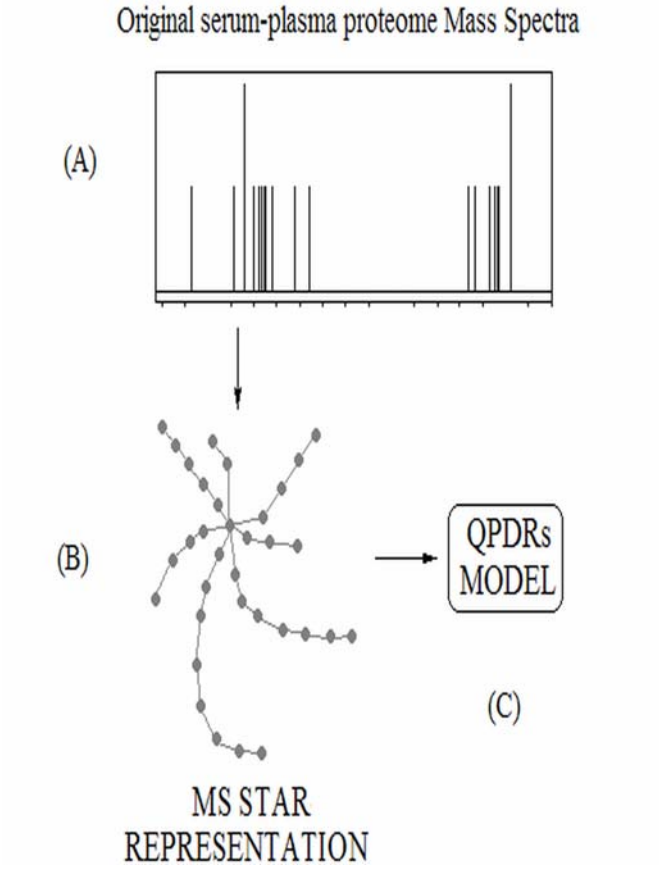

Figure 1. Work Flowchart.

2.1. Database

The database reported by Petricoin *et al.* has been used in this work [18]. It contains the MS spectra of 322 patients, classified into 4 groups according to their PSA level. The first group was formed by 190 patients with a PSA level greater than 4 (group A), the second group consisted of 63 patients with a PSA less than 1 (group B); 26 patients with a PSA level in the 4-10 range formed the third group (group C) and 43 patients with a PSA level greater than 10 the fourth group (group D). The clinical analysis has demonstrated that the healthy patients belong to the groups A and B, while the patients of the groups C and D are PCa.

2.2. Ms Data Coding

There are more than 15000 signals present in each spectrum. We have calculated the product of m/z with the corresponding intensity (I) value for each signal. By considering successive ranges of 500 values of this parameter, 31 regions have been obtained for each spectrum and the mean value within each region has been calculated, as well as the standard deviation and the standardization. The later value of I of the 31 total regions has been coded into 8 branches (B, C, D, E, F, G, H, I) depending on the weight of the region in each MS, with the aim of obtaining a graphical representation of the MS spectrum for each patient. The node corresponding to the region of PSA is represented by the letter A.

2.3. Star Graph Representations

The spectrum was represented graphically by a Shining Randic Star [19], drawn with the software *MARCH-INSIDE* [20-29]. The starting point was the classification of each region into more categories according to degrees of average intensity (B, C, D, E etc.). Afterwards, the number of regions of each type was counted and the Star graph was drawn through adding one node by region. The first node is the PSA value, represented in branch A, and 0, 1 or 2 nodes were also added in this branch depending on the PSA value = 0, 1 or 2. See Figure 2.

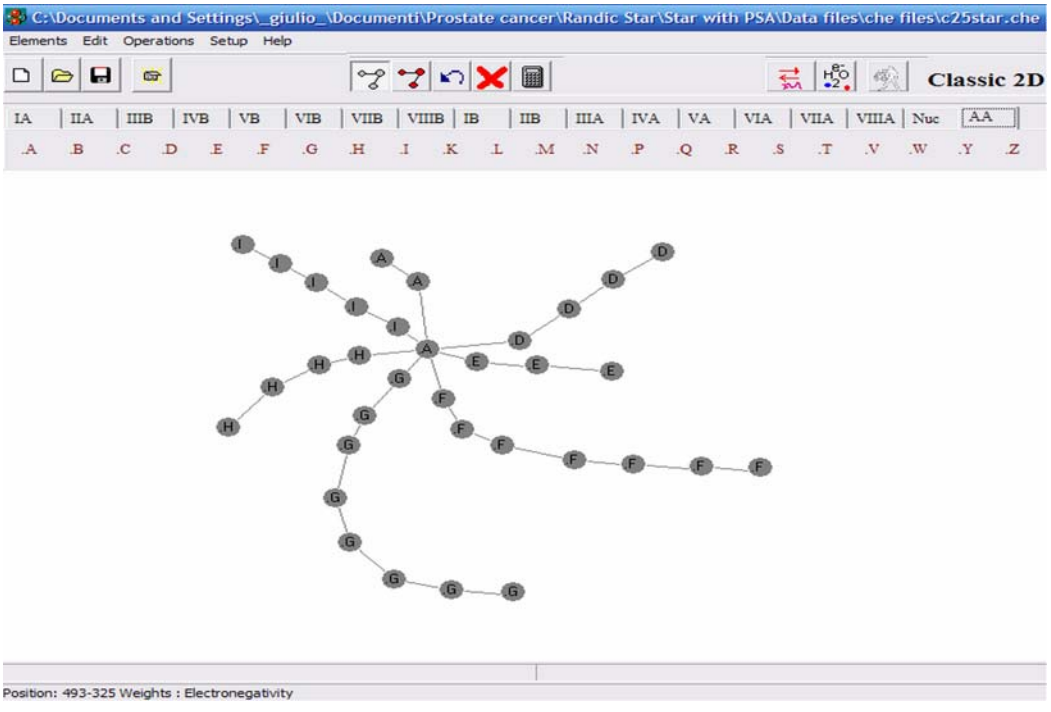

Figure 2. MARCH-INSIDE view of a Serum proteome MS Star graph.

2.4. Linear Discriminant Analysis (Lda)

The data set was divided into two series, a training series and a cross-validation series. The training series consisted of 230 patients (175 control group healthy patients and 55 PCa), while the cross-validation series contained 92 patients (78 control group healthy patients and 14 PCa). A LDA was performed using the STATISTICA package [30] to develop different classification functions capable of differentiating healthy from PCa patients. In the eq 2.1, the activity, or any given biological property, is expressed as a function of the spectral moments $\mu_k(R_i)$ of order k for every PSA region and/or MS region R_i, generated in each case. In the classification function

$$P = \sum_{i,k}^{32,5} {}^{i}b_k \cdot \mu_k(R_i) + c \quad (2.1)$$

P is the biological property, μ_k is the *k*th spectral moment, b_k are the coefficients obtained in the classification function for the spectral moment, and *c* is the intercept. The regions included 31 MS regions plus one PSA region if it is necessary. The discriminant function was obtained by using the forward-stepwise method with a minimum tolerance value of 0.01. In particular the spectral moment $\mu_0(R_{PSA})$ with order k = 0 for the PSA graph is equal to the PSA value.

3. Result and Discussion

Classification Function

Model using PSA-Moments:

$$PCa - score = 4.34 \cdot \mu_0(PSA) - 1.98 \quad (3.1)$$

$N = 322$, $R_c = 0.63$, $\lambda = 0.606$, $\chi^2 = 114.01$, $p < 0.001$

Model using PSA/MS Moments model:

$$PCa\text{-}score = 20.82 \cdot \mu_3(PSA) + 4.55 \cdot \mu_0(R_1) - 24.51 \cdot \mu_5(R_1) + 5.21 \cdot \mu_0(Total) + 16.38 \quad (3.2)$$

$N = 322$, $R_c = 0.81$, $\lambda = 0.344$, $\chi^2 = 240.95$, $p < 0.001$

N is here the number of patients included in the discriminant analysis calculation, Rc is the canonical regression coefficient, Wilk's λ is the standard statistic, used to denote the statistical significance of the discriminatory power of the current model. Its value will range from 1.0 (no discriminatory power) to 0.0 (perfect discriminatory power). The parameter χ^2 is

the Chi-squared statistic, and p is the error level [31]. The model 3.1 has 100% Specificity, its total Accuracy is 91.9%, but its Sensitivity is only 62.3%. This model has an unacceptably low predictive power for detecting a PCa patient. Main improvements are obtained when the PSA values are related to the MS. The best results are obtained by including the PSA value in the Shining Star graph (model 3.2). In this model an intimate relationship between the PSA values and the MS of the patient is originated by taking into account PSA value and MS information on the same graph. Sensitivity values reach 90.9% in training series and 92.9% in cross-validation series. For this model the Wilk's λ value is 0.344, a good result for the discriminatory power of this model. The error level p is lower than 0.05, it means that the hypothesis of groups overlapping with a 5% error can be rejected [32]. A summary of the results for the models 3.1 and 3.2 is given in Table 1.

Then we proceeded to demonstrate that the model met the basic assumptions of LDA [31]. The distribution of the residuals for all patients (raw residuals *vs.* case number) is shown in Figure 3, section (A). A double ordinate Cartesian plot of residuals (first ordinate), Leave-One-Out (LOO) residuals (second ordinate), and leverages (abscissa), defined the applicability domain of the models 3.2 as a squared area within ± 2 band for residuals and leverage threshold of h = 0.05217 [33,34]. As it can be noted in Figures 3, section (B); almost all cases used in training and validation lie within this area. Actually, some cases have a leverage value higher than the threshold, but show LOO residuals and standard residuals within the limits [35].

Table 1. Summary results for models.

Parameters	Model (3.1)	Model (3.2)
Classifications matrices		
Control group	**253** 0	**251** 2
Cancer patients	26 **43**	7 **62**
Statistic parameters in both series (%)		
Total accuracy	91.9	97.2
Specificity	100.0	99.2
Sensitivity	62.3	89.9

The bold characters refer to the number of patients that the model classifies correctly

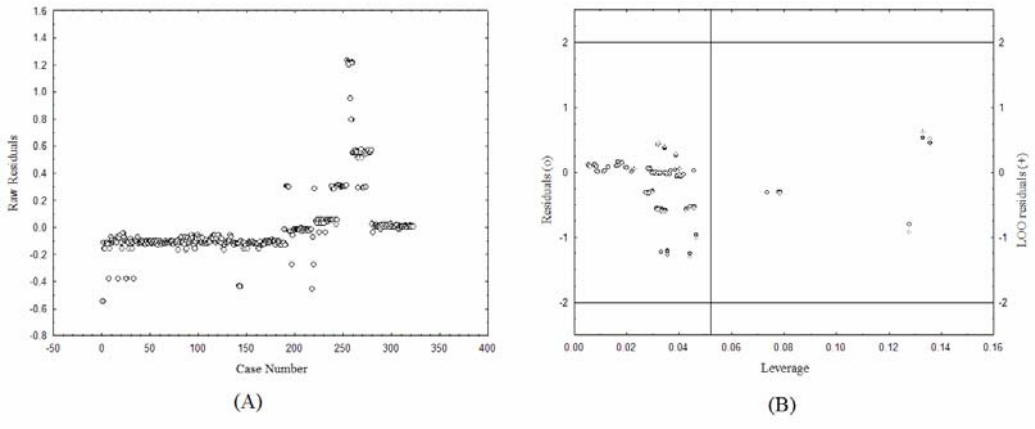

Figure 3**.** A) Scatter plot of raw residual *vs.* case number; B) Double ordinate Cartesian plot of residuals, LOO residuals and leverage for the model 3.2.

We tested the normal distribution of residual using different distribution fitting tests; the results were: Kolmogorov-Smirnov d = 0.18 with $p < 0.01$; $\chi^2 = 126.78$ with $p = 0.000$; and Shapiro-Wilks W = 0.80 and $p < 0.001$ [31]. In Figure 4, section (A), the frequency histogram is shown for normality testing. The hypothesis of normality should be rejected. However, as it is obvious in section (B), eliminating some cases (belonging to Group C) with too low residual values, normality is approached significantly. Nevertheless, the deviations from normality seem to be not severe, mainly taking into consideration certain robustness of the method to small deviations from normality. The scatter plots of square standardized residual *vs.* the respective μ_k included in the 3.2 model reveal an adequate scatter on the points without any consistent pattern, which validates the assumption of homocedasticity (*i.e.*, homogeneity of variance in variables) [36]. This important parametric assumption of LDA was represented in Figure 5.

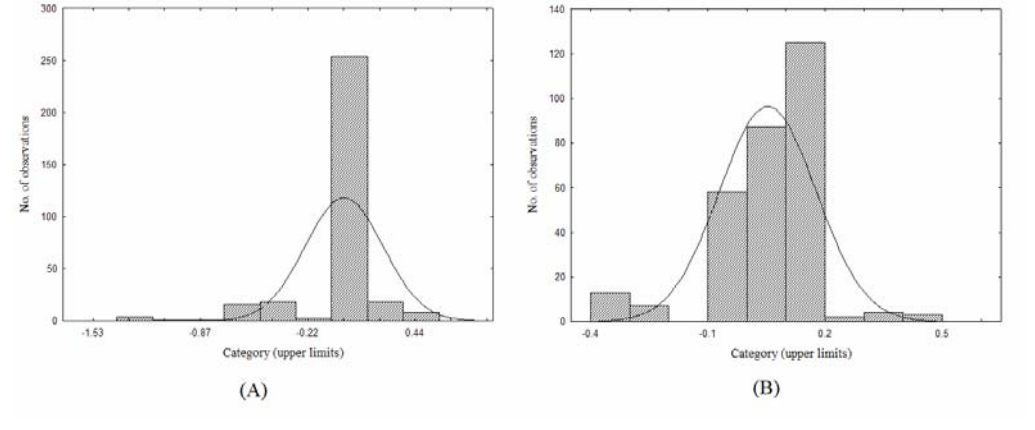

Figure 4. Analysis of the Application Domain and some Parametric Assumptions.

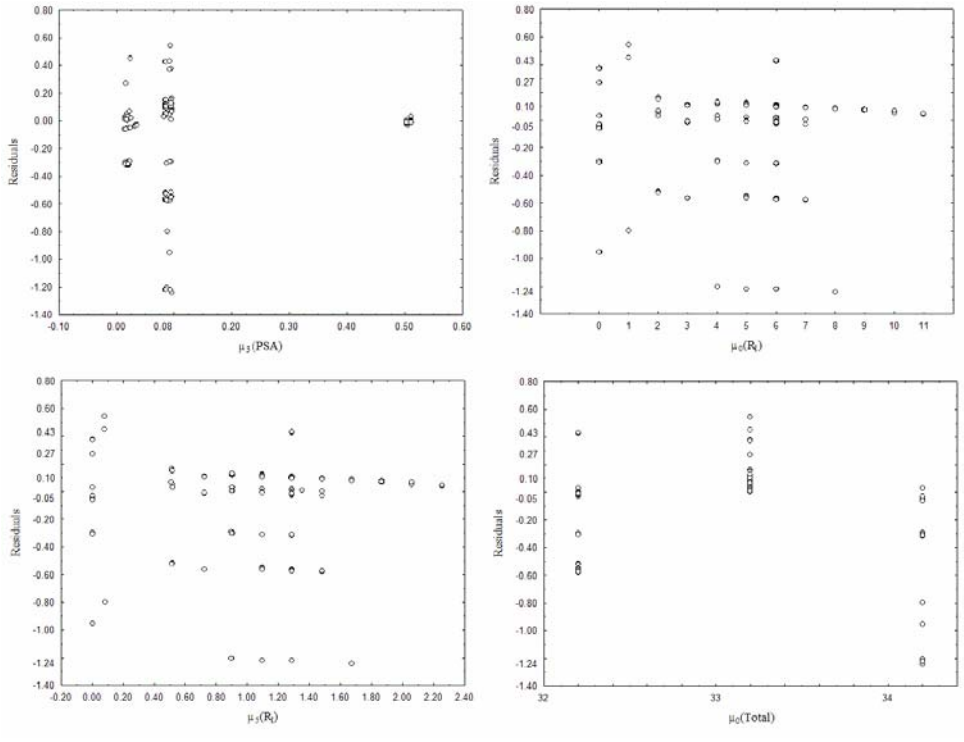

Figure 5. Normality Histograms for model 3.2.

4. Conclusion

In this work the following results were obtained. The mass spectrum of human proteome was represented by means of a method widely used to describe sequences aminoacid. The QPDRs methodology has been used to combine the Mass Spectrum with patients' PSA level, by this technique we succeeded in improving the predictive power of the PSA, increasing by 30% the sensitivity value.

Acknowledgments

Ferino, G. gratefully acknowledges a PhD scholarship from the University of Cagliari developing undergraduate research on Bioinformatics under Uriarte, E. and González-Díaz, H.'s Supervision at the University of Santiago de Compostela. González-Díaz, H. thanks "Isidro Parga Pondal" Program of Xunta de Galicia for funding a tenure-track research position at the Faculty of Pharmacy, University of Santiago de Compostela. We thanks partial financial support from grants of Xunta de Galicia (I203039ES and IB20304PR) and Ministerio de Sanidad y Consumo PI061457.

References

[1] Liotta, LA; Ferrari, M; Petricoin, EF. Clinical proteomics: written in blood. *Nature*. 2003, 425 (6961), 905.

[2] Barabasi AL. Sociology. Network theory-the emergence of the creative enterprise. *Science* New York, NY. 2005 Apr 29, 308 (5722), 639-41.

[3] Barabasi, AL; Bonabeau, E. Scale-free networks. *Scientific American*. 2003 May, 288(5), 60-9.

[4] Barabasi, AL; Oltvai, ZN. Network biology: understanding the cell's functional organization. *Nature reviews*. 2004 Feb, 5 (2), 101-13.

[5] Gonzalez-Diaz H, Vilar S, Santana L, Uriarte E. Medicinal chemistry and bioinformatics--current trends in drugs discovery with networks topological indices. *Current Topics in Medicinal Chemistry*. 2007, 7 (10), 1015-29.

[6] Balaban, AT; Basak, SC; Beteringhe, A; Mills, D; Supuran, CT. QSAR study using topological indices for inhibition of carbonic anhydrase II by sulfanilamides and Schiff bases. *Molecular diversity*. 2004, 8 (4), 401-12.

[7] Gozalbes, R; Doucet, JP; Derouin, F. Application of topological descriptors in QSAR and drug design: history and new trends. *Curr Drug Targets Infect Disord*. 2002 Mar, 2 (1), 93-102.

[8] Honey, CJ; Kotter, R; Breakspear, M; Sporns, O. Network structure of cerebral cortex shapes functional connectivity on multiple time scales. *Proc Natl Acad Sci U S A*. 2007 Jun 12, 104 (24), 10240-5.

[9] McDonald, DB. Predicting fate from early connectivity in a social network. *Proc Natl Acad Sci U S A*. 2007 Jun 26,104 (26), 10910-4.

[10] Hahn, MW; Kern, AD. Comparative genomics of centrality and essentiality in three eukaryotic protein-interaction networks. *Mol Biol Evol*. 2005 Apr, 22 (4), 803-6.

[11] Altmann, M. Reinterpreting network measures for models of disease transmission. *Social Networks.* 1993 Mar,15 (1),1-17.

[12] Bonchev, D; Buck, GA. From molecular to biological structure and back. *Journal of Chemical Inf and Model*. 2007 May-Jun, 47 (3), 909-17.

[13] Boccaletti, S; Latora, V; Moreno, Y; Chavez, M; Hwang, DU. Complex networks: Structure and dynamics. *Physics Reports*. 2006, 424, 175-308.

[14] Kauffman, KJ; Pajerowski, JD; Jamshidi, N; Palsson, BO; Edwards, JS. Description and Analysis of Metabolic Connectivity and Dynamics in the Human Red Blood Cell. *Biophysical Journal* 2002, 83, 646-62.

[15] Nandy, A; Basak, SC. Simple numerical descriptor for quantifying effect of toxic substances on DNA sequences. *J Chem Inf Comput Sci*. 2000 Jul-Aug,40 (4), 915-9.

[16] Randic´, M; Lers, N; Plavsic´, D; Basak, S; Balaban, AT. Four-color map representation of DNA or RNA sequences and their numerical characterization. *Chemical Physics Letters.* 2005, 407, 205-8.

[17] Pepe, P; Galia, A; Fraggetta, F; Grasso, G; Allegro, R; Aragona, F. Prediction by quantitative histology of pathological stage in prostate cancer. *Eur J Surg Oncol*. 2005 Apr, 31 (3), 309-13.

[18] Petricoin, EF; Ornstein, DK; Paweletz, CP; Ardekani, A; Hackett, PS; Hitt, BA et al. Serum proteomic patterns for detection of prostate cancer. *Journal of the National Cancer Institute.* 2002 October 16, 94 (20).

[19] Randic, M; Zupan, J; Vikic-Topic, D. On representation of proteins by star-like graphs. *J Mol Graph Model*. 2007 Dec 15, 290-305.

[20] González-Díaz, H; Torres-Gomez, LA; Guevara, Y; Almeida, MS; Molina, R; Castanedo, N et al. Markovian chemicals "in silico" design (MARCH-INSIDE), a promising approach for computer-aided molecular design III: 2.5D indices for the discovery of antibacterials. *J Mol Model.* 2005 Mar, 11 (2), 116-23.

[21] de Armas, RR; González-Díaz, H; Molina, R; Uriarte, E. Stochastic-based descriptors studying biopolymers biological properties: extended MARCH-INSIDE methodology describing antibacterial activity of lactoferricin derivatives. *Biopolymers.* 2005 Apr 5, 77 (5), 247-56.

[22] González-Díaz, H; Uriarte, E. Biopolymer stochastic moments. I. Modeling human rhinovirus cellular recognition with protein surface electrostatic moments. Biopolymers. 2005 Apr 5, 77(5), 296-303.

[23] Ramos de Armas, R; González-Díaz, H; Molina, R; Perez Gonzalez, M; Uriarte, E. Stochastic-based descriptors studying peptides biological properties: modeling the bitter tasting threshold of dipeptides. *Bioorg Med Chem.* 2004 Sep 15, 12 (18), 4815-22.

[24] González-Díaz, H; Sanchez, IH; Uriarte, E; Santana, L. Symmetry considerations in Markovian chemicals 'in silico' design (MARCH-INSIDE) I: central chirality codification, classification of ACE inhibitors and prediction of sigma-receptor antagonist activities. *Comput Biol Chem*. 2003 Jul, 27 (3), 217-27.

[25] Cruz-Monteagudo, M; González-Díaz, H; Borges, F; Gonzalez-Diaz, Y. Simple stochastic fingerprints towards mathematical modeling in biology and medicine. 3. ocular irritability classification model. *Bull Math Biol.* 2006 Jul 25, 1555-72.

[26] Santana, L; Uriarte, E; González-Díaz, H; Zagotto, G; Soto-Otero, R; Mendez-Alvarez, E. A QSAR model for in silico screening of MAO-A inhibitors. Prediction, synthesis, and biological assay of novel coumarins. *J Med Chem*. 2006 Feb 9, 49 (3), 1149-56.

[27] Ramos de Armas, R; González-Díaz, H; Molina, R; Uriarte E. Stochastic-based descriptors studying biopolymers biological properties: extended MARCH-INSIDE methodology describing antibacterial activity of lactoferricin derivatives. *Biopolymers*. 2005 Apr 5, 77 (5), 247-56.

[28] González-Díaz, H; Agüero, G; Cabrera, MA; Molina, R; Santana, L; Uriarte, E et al. Unified Markov thermodynamics based on stochastic forms to classify drugs considering molecular structure, partition system, and biological species: distribution of the antimicrobial G1 on rat tissues. *Bioorg Med Chem Lett.* 2005 Feb 1, 15 (3), 551-7.

[29] Ramos de Armas, R; Gonzalez-Diaz, H; Molina, R; Perez Gonzalez, M; Uriarte, E. Stochastic-based descriptors studying peptides biological properties: modeling the bitter tasting threshold of dipeptides. *Bioorg Med Chem.* 2004 Sep 15, 12 (18), 4815-22.

[30] Brzezinska, E. The QSAR analysis of tricyclic non-nucleoside inhibitors of HIV-1 reverse transcriptase. *Acta Pol Pharm.* 2003 Jan-Feb, 60 (1), 3-13.

[31] Van Waterbeemd, H. *Chemometric methods in molecular design*. New York: Wiley-VCH; 1995.

[32] Hua, S; Sun, Z. Support vector machine approach for protein subcellular localization prediction. *Bioinformatics* (Oxford, England). 2001 Aug, 17 (8), 721-8.

[33] Liu, HC; Lyu, PC; Leong, MK; Tsai, KC; Hsiue, GH. 3D-QSAR studies on PU3 analogues by comparative molecular field analysis. *Bioorg Med Chem Lett*. 2004 Feb 9, 14 (3), 731-4.

[34] Morales, AH; Perez, MA; Combes, RD; Gonzalez, MP. Quantitative structure activity relationship for the computational prediction of nitrocompounds carcinogenicity. *Toxicology.* 2006 Mar 1, 220 (1), 51-62.

[35] Gonzalez-Diaz, H; Vilar, S; Santana, L; Podda, G; Uriarte, E. On the applicability of QSAR for recognition of miRNA bioorganic structures at early stages of organism and cell development: embryo and stem cells. *Bioorg Med Chem.* 2007 Apr 1, 15 (7), 2544-50.

[36] Stewart, J; Gill; L. *Econometrics*. London: Prentice Hall; 1998.

In: Clinical Chemisty Research
Editors: Brian H. Mitchem and Charles L. Sharnham
ISBN 978-1-60692-517-1

Short Communication B

Not So Innocent - Adipocytes May Explain Racial Differences in Breast Cancer: Implications for Clinical Chemistry

Francis O. Ikpatt,[1] Errol Berman[1] and Arpad Szallasi[2*]
[1]Department of Pathology, St Barnabas Medical Center, Livingston, NJ, USA
[2]Department of Pathology, Monmouth Medical Center, Long Branch, NJ, USA

Abstract

Breast cancer is one of the most frequent malignancies in women and ranks second only to lung carcinoma among cancer deaths in adult female patients. Breast cancer is a heterogenous disease that encompasses a number of pathological entities with distinct clinical behavior. Racial differences in the biology and treatment of breast cancer are also well documented. A positive correlation between obesity and breast cancer has been established. Indeed, deregulated adipokine production from fat cells represents an important molecular basis underlying obesity-related carcinogenesis. Thus, the growth and progression of breast tumor cells is dependent both on their intrinsic malignant potential and the microenvironment they interact with.

The circulating concentrations of adiponectin, an insulin-sensitizing adipokine, correlate inversely with breast cancer development since adiponectin could potently inhibit the proliferation of both estrogen receptor-positive and estrogen receptor-negative human breast carcinoma cells.

We hypothesize that the differences in the biology of breast cancers observed in women of different races are at least partially related to differences in the secretory activity of adipocytes in the breast tissue. We review the possible role of adipokines in breast malignancies of women of various races. It is hoped that these biomarkers could identify

[*] Arpad Szallasi, Department of Pathology, Monmouth Medical Center, 300 Second Ave, Long Branch, NJ 07740. Email: ASZALLASI@SBHCS.COM, Tel: (732) 923 7360; FAX: (732) 923 7355

those women who are at increased risk for developing aggressive breast carcinomas and thus may benefit from increased surveillance and/or prophylactic intervention.

Introduction

According to the American Cancer Society, breast cancer rates have risen by 30% in the past 25 years in the developed world, due in part to increase in screening which detects the cancer in earlier stages[1]. The lifetime probability of developing breast cancer in developed countries is about 4.8%. Breast cancer is, however, a heterogenous disease that encompasses distinct pathological entities. A minor subset of breast cancers is known to arise from germline *BRCA1* mutation. Most breast cancers are, however, sporadic. Avoidable risk factors during a woman's life for developing sporadic breast cancer include becoming overweight or obese, the latter defined as a body mass index (BMI) of > or = 30.0 kg/m2. The prevalence of obesity has increased substantially over previous decades to about 20% in industrialized countries (by some estimates, in the US exceeding 60%), and a further increase is expected in the future[2-4]. Therefore a similar trend is observed in the incidence of breast cancer and obesity.

An increased concentration of estrogen from peripheral aromatization in adipose tissue partly explains the association between body mass index and the risk of post-menopausal breast cancer. Other possible mechanisms that relate obesity to cancer risk include insulin resistance and resultant chronic hyper-insulinemia, increased production of insulin-like growth factors or increased bioavailability of steroid hormones. Recently, adipose tissue-derived hormones and cytokines (so-called adipokines) such as leptin and adiponectin, as well as obesity-related inflammatory markers like the nuclear factor kappa beta (NF-kappa B) have emerged as important players in breast cancer initiation and progression[5-6].

The development of reliable gene expression arrays, real-time quantitative RT-PCR, and immunohistochemical (IHC) techniques for studying molecules have facilitated the understanding of the role of the above molecules as well as steroid hormones (including androgens and corticosteroids), fat-soluble vitamins A and D, fatty acids, and xenobiotic lipids derived from diet in the molecular events of breast cancer pathogenesis.

Although the overall incidence of breast cancer among African-American (AA) women is lower than in white American women, this cancer is more common in young premenopausal African-American women, and African-American breast cancer patients of all ages are more likely to have advanced disease at diagnosis, higher risk of recurrence, and poorer overall prognosis. Disparate characteristics of breast cancer diagnosed in African Americans as compared with Caucasians, such as more advanced stage at diagnosis and less estrogen-receptor positive, co-morbidities, and access to therapy could help explain the observed survival outcomes[7, 8].

Race-Related Differences in the Morphometry of Breast Carcinomas

Morphometric methods have been used to demonstrate the differences in the morphology between breast cancers among black and white women[9, 10]. H&E stained slides obtained from 148 Nigerian, 166 African-American and 170 Caucasian breast cancer patients were evaluated for volume-corrected mitotic index (*smi*) expressed as mitosis/mm^2, mean nuclear area (*mna*) aided by a digitizing interactive video overlay, and fraction of fields with tubular differentiation (*ftd*). Empirical distributions of, and inter-relationships between, the three features showed that there was a significant difference in the mean values among the three groups ($p<.0001$). The *smi* and *mna* values were largest for Nigerian (N), intermediate for African-American (AA), and lowest for Caucasian (C) women (*smi* N=26.5±14.7, AA=19.9±6.7, C=14.5±5.1; *mna* N=55.9±19.9, AA=47.1±12.7, C=34.3±10.3). For *smi* and *mna*, all pair wise means differed ($p<0.05$). The pattern was reversed for *ftd*, with the Nigerian cases having the smallest value (*ftd* N=17.8±17.0, AA=21.9±16.6, C=28.4±17.9). Thus, there is a significant difference in proliferative activity and degree of differentiation among Nigerian, African-American, and Caucasian women with breast cancer, even after adjusting for other confounding variables like age and stage. These differences are likely genetically programmed. These findings have also been confirmed in several other reports[11].

Race-Related Differences in the Genetics and Biology of Breast Carcinomas

Novel cancer therapies have focused on specific molecular markers present in malignant tumors. The rationale of targeted therapy relies on the knowledge of molecular mechanisms involved in carcinogenesis and their influence in clinical outcome allied to a more specific and less toxic treatment. Recent cDNA micro-array studies have demonstrated that breast cancers can be divided according to their gene expression profiles into 4 distinct subtypes: (1) basal-like tumors (ER-, HER2-), (2) tumors with amplification of *HER2/neu* (ER-/+, HER2+), (3) luminal tumors A and B (ER+, HER2-), and (4) normal breast-like cancers [8, 11]. Importantly, these subtypes have distinct prognostic and therapeutic implications. For example, basal-type breast carcinomas are high-grade with poor prognosis but respond better to conventional chemotherapy than other subtypes. Although basal-type carcinomas account for only 15-20% of all breast cancers, they are overrepresented among black women and also those with *BRCA1* germline mutation.

Factors Secreted by Adipocytes (Adipokines) are Emerging as Major Players in Breast Carcinogenesis with Race-Related Differences

Mature adipocytes, a specific mesenchymal cell type, are distributed widely throughout the body. There are two main types of mature adipocytes: white and brown. These two varieties are contained in the adipose organ in varying ratio. The relative percentage of the white and brown adipocytes in the adipose organ may vary accordingly to environmental/hormonal changes. Furthermore, they are capable of de-differentiating to less matured cells and forming proliferative-competent precursor cells like preadipocytes, adipofibroblasts, or even other forms of cells. Larger adipocytes do have a less favorable profile of cytokine secretion than smaller adipocytes. It is possible that using morphometric techniques, we may be able to demonstrate significant differences in the proportion of adipocytes in different human races and molecular subsets of breast cancers grouped according to adipokine production[12, 13].

We propose that the differences in breast cancer observed in women of different races is related not just to the degree and distribution of obesity pattern but also the type of adipocytes, their secretion profile as well as differences in receptors. Adipokines were traditionally assumed to be molecules selectively secreted from fat cells with role in regulation of energy metabolism and cardiovascular tones. They have come to be recognized as possible link between obesity and breast cancer pathogenesis. Adipokines combine positive and negative regulatory functions in cancer tumorigenesis. For example, leptins promote epithelial cell proliferation in the breast and adiponectins act as growth inhibitors of breast cancers.

Adiponectin

The circulating concentrations of adiponectin, an insulin-sensitizing adipokine, inversely correlate with breast cancer development since adiponectin could potently inhibit the proliferation of both estrogen receptor-positive and estrogen receptor-negative human breast carcinoma cells. It is possible that the protective role of obesity in pre-menopausal women is due to increased adiponectin production or activity. Administration of adiponectin significantly attenuated the mammary tumor growth in nude mice implanted with human breast carcinoma cells[12-15]. Adiponectin effects are mediated by its receptors, AdipoR1 and R2. There is an association between genetic variants of the adiponectin (ADIPOQ) and adiponectin receptor 1 (ADIPOR1) genes with breast cancer risk. Specifically, two ADIPOQ SNPs (rs2241766 and rs1501299), have been associated with circulating levels of adiponectin and increase in breast cancer risk. One ADIPOR1 SNP (rs7539542), which modulates expression of adiponectin receptor 1 mRNA, is also associated with breast cancer risk. There are findings to suggest that a cross-talk between adiponectin and estrogen receptor signaling exists in breast cancer cells and that adiponectin effects on the growth and apoptosis of breast cancer cells *in vitro* are dependent on the presence of 17-beta estradiol[16-19].

Thus, adiponectin exerts a direct growth-inhibitory effect on tumor cells by down-regulating cell proliferation and up-regulating apoptosis, and also inhibits tumor-related angiogenesis and these evidences suggest a potential therapeutic role for adiponectin in the treatment of breast cancer especially in ER- negative breast cancers observed in women of color.

Leptin

Leptin functions by stimulatory effects on the downstream cell signaling pathways of both estrogen-dependent and -independent breast cells. Cyclin *D1* may be the target gene for leptin mediated growth stimulation of breast cancer cells and molecular mechanisms involving Stat3-mediated recruitment of distinct co-activator complexes. Leptin also increases the production of E-cadherin, an intercellular adhesion molecule that is a tumor suppressor[20, 21]. Leptin and estrogen, however, synergistically increase tumor size and these changes correlated with an increase in E-cadherin. It appears that E-cadherin may paradoxically serve as a tumor enhancer when exposed to leptin and estrogen.

Leptin levels are significantly higher in black women than in white women and are also significantly higher in obese and overweight women than in normal-weight women. Further studies to evaluate relationship between molecular subsets of breast cancers and serum leptin levels/leptin receptors may yield therapeutic information[20, 21].

Hepatocyte Growth factor (HGF)

Hepatocyte growth factor (HGF)) is produced by adipocytes and HCG levels are often elevated in breast cancer patients, and particularly so in those with advanced disease. In a multivariate analysis, the HGF concentration functioned as an independent prognostic indicator[22]. HGF levels are reduced after the removal of primary tumor, suggesting that a major portion of the circulating levels was produced by the tumor itself and/or the closely associated, and excised, adipose tissue. It will be interesting to assess the racial differences of HGF in breast cancer patients of different races.

Nuclear Factor (NF)-kappa B

NF-kappa B induces aberrant cell proliferation and has anti-apoptotic properties in breast cancer cells. An inverse correlation of the level of epidermal growth factor (EGF) family of receptors (EGFR) and estrogen receptor (ER) is observed between ER- and ER + breast cancer cells. The transmission of mitogenic signal induced by EGF-EGFR interaction is mediated via activation of nuclear factor kappaB (NF-kappaB) [23].

Breast cancers in women of African descent are characterized by a more aggressive clinical behavior and increased frequency of estrogen receptor-negative immuno-phenotype.

It therefore appears that the adipocyte of Black women with breast cancers may be active secretors of NF-kappa B. This molecule is a therefore a potential therapeutic target for the subset of estrogen receptor (ER) negative (-) breast cancer cells that overproduce the epidermal growth factor (EGF) family of receptors (EGFR).

Discussion and Concluding Remarks

Breast cancer is a heterogenous disease that encompasses a number of pathological entities with distinct prognostic and therapeutic implications. Gene expression-profiling studies have demonstrated that breast cancers can be divided into four main groups, namely basal-like, luminal A and B, HER2+, and normal breast-like carcinomas. Using paraffin immunostains for estrogen and progesterone receptors (ER, PR) as well as immunohistochemical or fluorescent in situ hybridization (FISH) analysis to determine HER2/neu expression status as surrogate markers by pathologists, this classification already drives treatment decisions for newly diagnosed breast carcinoma cases.

Early detection is paramount in reducing both morbidity and mortality of breast cancer. At present, screening is routinely done by mammography at intervals that depend on the age and risk factors (e.g. family history) of the woman. Mammography is, however, both cumbersome (performed only in selected centers) and unpleasant for the patients, therefore compliance is an issue and many cancers are detected in an advanced stage. Moreover, many young women develop breast cancer well before the age when routine mammography screening begins. Clearly, an inexpensive serum marker (analogous to PSA to screen for prostate cancer in men) would be extremely useful in identifying those women who could benefit from starting mammography early.

Racial differences in the epidemiology and biology of breast cancers are well-established. Many black women appear to develop aggressive basal-like breast carcinoma at a relatively young age. Obese white women are also at increases risk, though usually at older age. There is emerging evidence that factors secreted by adipocytes may contribute to breast carcinogenesis. In the focus of attention are leptin and adiponectin, two adipokines that positively (leptin) or inversely (adiponectin) correlate with the clinical risk for developing breast cancer.

It is an attractive hypothesis that a simple serum test ran on automated chemistry analyzers that determines the secretion profile of adipocytes (e.g. circulating leptin and adiponectin levels) can identify those at-risk black and/or obese women who could benefit from vigorous mammography screening. Another promising diagnostic target produced by adipocytes is hepatocyte growth factor (HGF) that may be useful in detecting recurrent breast carcinoma.

Molecular analysis by PCR can be a helpful tool in exploring the genes involved in production of these molecules and their receptors. An understanding of the mechanisms of action of these molecules will help understand the biological differences of breast cancers in women of different races. This promises to open door for possible new therapeutic manipulations.

References

[1] National Cancer Institute, *SEER Cancer Statistics Review*, 2007. Statistics based on data, 2000-2004.

[2] Hedley AA, Ogden CL, Johnson CL, Carroll MD, Curtin LR, Flegal KM. Prevalence of overweight and obesity among US children, adolescents, and adults, 1999–2002. *JAMA* 2004; 291:2847–2850.

[3] Pischon T, Nothlings U, Boeing H. Obesity and cancer. *Proc Nutr Soc*. 2008; 67(2):128-45.

[4] Calle EE, Rodriguez C, Walker-Thurmond K, Thun MJ. Overweight, obesity, and mortality from cancer in a prospectively studied cohort of U.S. adults. *N Eng J Med* 2003; 348(17):1625-38.

[5] Renehan AG, Roberts DL, Dive C. Obesity and cancer: Pathophysiological and biological mechanisms. *Arch Physiol Biochem* 2008; 114(1):71-83.

[6] Vona-Davis L, Rose DP Adipokines as endocrine, paracrine, and autocrine factors in breast cancer risk and progression. Endocrine-Related Cancer 2007; 14 (2) 189-206.

[7] Carey LA, Perou CM, Livasy CA, et al: Race, breast cancer subtypes, and survival in the Carolina Breast Cancer Study. *JAMA* 2006; 295:2492-2502.

[8] Van't Veer LJ, Dai H, van de Vijver MJ, et al: Gene expression profiling predicts clinical outcome of breast cancer. *Nature* 2002; 415:530-536.

[9] R. Nanda, Z. Hu, X. He, M. Tretiakova, T. Grushko, F. Ikpatt, C. M. Perou and O. I. Olopade. Characterization of aggressive breast cancer in African American and Caucasian women: Patterns of gene expression in primary breast tumors. *Journal of Clinical Oncology*, 2004 ASCO Annual Meeting Proceedings (Post-Meeting Edition). Vol 22, No 14S.

[10] F. O. Ikpatt, J. J. Dignam, A. Khramtsov, T. Grushko, J. Fackenthal, L. Sveen, R. Nanda, R. Ndoma-Egba and O. I. Olopade**.** Breast tumor morphometry in relation to race reveals significant differences among Nigerians, African-Americans and Caucasian Americans. *JCO* 2004: 9567-68.

[11] Mitchell K, Carey L, Peppercorn J: Reporting of race and ethnicity in breast cancer research. *Presented at the American Society of Clinical Oncology Breast Cancer Symposium,* San Francisco, CA, September 7-8, 2007.

[12] Rose DP, Haffner SM, Baillargeon J. Adiposity, the metabolic syndrome, and breast cancer in African-American and white American women. *Endocr Rev.* 2007; 28(7):763-77.

[13] M.V. Dodson, M.E. Fernyhough[1], J.L. Vierck, G.J. Hausman. Adipocytes may not be a terminally differentiated cell type: implications for animal production. *Animal Science* 2005; 80: 239-240.

[14] Guo, Z., Hensrud, D. D., Johnson, C. M. and Jensen, M. D. Regional postprandial fatty acid metabolism in different obesity phenotypes. *Diabetes* 1999; 48**:** 1586–1592.

[15] Boudreau N & Myers C 2003 Breast cancer-induced angiogenesis: multiple mechanisms and the role of the microenvironment. *Breast Cancer Research* 2003; 5: 140–146

[16] Pfeiler GH, Buechler C, Neumeier M, Schäffler A, Schmitz G, Ortmann O, Treeck O. Adiponectin effects on human breast cancer cells are dependent on 17-beta estradiol. *Oncol Rep* 2008; 19(3):787-93.

[17] Körner A, Pazaitou-Panayiotou K, Kelesidis T, Kelesidis I, Williams CJ, Kaprara A, Bullen J, Neuwirth A, Tseleni S, Mitsiades N, Kiess W, Mantzoros CS. Total and high-molecular-weight adiponectin in breast cancer: in vitro and in vivo studies. *J Clin Endocrinol Metab* 2007; 92(3):1041-8.

[18] Yu Wang, Janice B, Lam, Karen S.L. Lam, Jing Liu, Michael C. Lam, Ruby L.C. Hoo, Donghai Wu, Garth J.S. Cooper and Aimin Xu. Adiponectin modulates the glycogen synthase kinase-3beta/beta-catenin signaling pathway and attenuates mammary tumorigenesis of MDA-MB-231 cells in nude mice. *Cancer Research* 2006; 66: 11462-11470.

[19] Kaklamani VG, Sadim M, Hsi A, Offit K, Oddoux C, Ostrer H, Ahsan H, Pasche B, Mantzoros C. Variants of the adiponectin and adiponectin receptor 1 genes and breast cancer risk. *Cancer research* 2008; 68(9):3178-84.

[20] Neeraj K. Saxena, Paula M. Vertino, Frank A. Anania, and Dipali Sharma. Leptin-induced Growth Stimulation of Breast Cancer Cells Involves Recruitment of Histone Acetyltransferases and Mediator Complex to *CYCLIN D1* Promoter via Activation of Stat3. *J. Biol. Chem* 2007; 282:13316-13325.

[21] Jen KL, Buison A, Darga L, Nelson D. The relationship between blood leptin level and bone density is specific to ethnicity and menopausal status. *J Lab Clin Med*. 2005; 146(1):18-24.

[22] Sheen-Chen SM, Liu YW, Eng HL & Chou FF. Serum levels of hepatocyte growth factor in patients with breast cancer. *Cancer Epidemiology, Biomarkers and Prevention* 2005; 14: 715–717.

[23] Biswas DK, Cruz AP, Gansberger E, Pardee AB. Epidermal growth factor-induced nuclear factor kappa B activation: A major pathway of cell-cycle progression in estrogen-receptor negative breast cancer cells. *PNAS* 2000; 97(15):8542-7.

\\

In: Clinical Chemistry Research
Editors: Brian H. Mitchem and Charles L. Sharnham
ISBN 978-1-60692-517-1

Short Communication C

Analytical Method of Allantoin Detection in Human Sera and the Clinical Significance of this Measurement

Haruhiro Muratsubaki and Keiichiro Enomoto
Department of Clinical Chemistry, Faculty of Health Sciences,
Kyorin University, Hachioji, Tokyo, Japan

Abstract

In primates, including man, purine catabolism terminates with the formation of uric acid. This is due to a lack of uricase, which catalyzes the conversion of uric acid into allantoin in most other mammals. A nonsense mutation during evolution inactivated uricase activity in humans, resulting in enhanced protection against reactive oxygen species. The loss of uric acid degradation in purine catabolism is believed to compensate for the inability of humans to synthesize vitamin C, which is a powerful antioxidant. Blood in humans contains a very low concentration of allantoin produced from the elimination of reactive oxygen species by uric acid. Therefore, the measurement of serum allantoin is a good marker for judging the degree of reactive oxygen species generation in the body. In recent years, serum allantoin has been extensively used as a marker of oxidative stress. Serum allantoin levels are reportedly increased in Down syndrome, Behçet's syndrome, Wilson disease, neonatal chronic lung disease, chronic rheumatoid arthritis, and patients undergoing hemodialysis. In this review, we will describe the analytical methods of serum allantoin measurement and their clinical significance.

Introduction

Life first appeared on the earth 35 hundred million years ago. Among the first life forms to develop were anaerobic organisms that lived quite successfully without oxygen. However,

the atmospheric oxygen level increased as new organisms that produced oxygen during photosynthesis appeared. This caused some anaerobic life forms to die out due to the oxidative action of oxygen and others to remove to anoxic environments. In time, aerobic organisms appeared that could not only protect themselves from oxygen, but could also utilize this gas.

In the present day, aerobic animals, including humans, uptake oxygen from the air and gain chemical energy (ATP) by oxidizing photosynthetic products from plants. During this process, reactive oxygen species (ROS), including superoxide anions, singlet oxygen, hydrogen peroxide, and hydroxyl radicals, are continuously generated in the body and are combated by ROS removal systems, such as superoxide dismutase, glutathione peroxidase, and catalase. Reactive oxygen species oxidize constituents that are essential for the maintenance of life, and thus can cause serious diseases. Because of their high reactivity, the half life of ROS in organisms is very short, making the direct detection of ROS very difficult. When ROS are scavenged by various constituents, metabolites of ROS scavengers are produced through antioxidation and accumulate in the body. These metabolites, so-called oxidative stress markers, are one means of examining the generation status of ROS.

Some ROS scavengers can be found in human blood. In particular, uric acid is a potent scavenger of ROS, including singlet oxygen and hydroxyl radicals [1-4]. Since humans do not have the enzyme uricase that catalyzes the conversion of uric acid into allantoin in other animals, the end product of purine catabolism is uric acid rather than allantoin. Also in contrast with other animals, humans cannot synthesize vitamin C, which is a powerful antioxidant. The loss of uric acid degradation in purine catabolism is due to an added terminal codon in the uricase gene [5], resulting in protection from ROS. In humans, this mechanism is thought to compensate for the inability to synthesize vitamin C [1, 6]. Human serum therefore contains small amounts of allantoin produced from uric acid. Here, we will describe the analytical measurement and importance of human serum allantoin as an oxidative stress marker.

Assay for Allantoin in Human Serum

Allantoin levels in the serum of laboratory animals have been measured by a colorimetric method reported by Young and Conway [7] that involves the alkaline hydrolysis of allantoin to allantoic acid, the acid hydrolysis of allantoate to glyoxylate, and the formation of the 2,4-dinitrophenylhydrazone of glyoxylate (named the Rimini-Schryver reaction) or the detection of NADH oxidation by a glyoxylate reductase reaction [8]. However, this method has both poor sensitivity and poor specificity. We recently developed a new enzymatic assay for specifically measuring the serum allantoin concentration of experimental animals, and successfully applied this method after the oral administration of purine nucleotides to rats [9]. In this method, allantoin is converted to allantoate by the action of allantoinase. Allantoate is then hydrolyzed to ureidoglycine, CO_2, and ammonia by the action of allantoate amidohydrolase. NADP-dependent glutamate dehydrogenase subsequently acts on the ammonia produced, resulting in a change in the absorbance at 340 nm due to NADPH consumption. However, this method has a poor sensitivity due to low molar extinction

coefficient of NADPH at 340 nm, and therefore cannot be used to detect serum allantoin levels in humans, who lack uricase and therefore have substantially lower serum allantoin levels than those found in other mammals.

Most human serum allantoin measurements are performed by a high performance liquid chromatography (HPLC) method [10-16]. The HPLC procedure consists of many successive steps: sample deproteination, pre-purification of allantoin by anion exchange chromatography, desiccation of the eluate, alkaline hydrolysis of allantoin to allantoic acid, acid hydrolysis of allantoic acid to glyoxylic acid, derivatization of glyoxylic acid with 2,4-dinitrophenylhydrazine, and separation of the derivative with HPLC. This process is time-consuming, complicated, and requires a large volume of sample and expensive equipment. Consequently, the HPLC method is difficult to perform on large numbers of samples. Assay methods for serum allantoin using gas chromatography/mass spectrometry [17] and capillary electrophoresis [18] have also been reported, although these methods also require expensive equipment.

To overcome these disadvantages, we recently developed a highly sensitive novel enzyme cycling method for measuring allantoin levels in human sera [19]. The scheme of our method is shown in Figure 1. The first step is allantoin hydrolysis by allantoinase, followed by the hydrolysis of allantoate by an allantoate amidohydrolase reaction, which results in ammonia production. The ammonia is then converted to NAD by NAD synthetase. This NAD is cycled between its oxidized and reduced forms in the presence of glucose dehydrogenase, diaphorase, glucose, and WST-1, producing colored WST-1 formazan that is monitored at 450 nm. Unfortunately, the allantoinase and allantoate amidohydrolase used in this method are not currently commercially available. We hope that they soon will be available, and that our enzymatic method will become commonly used for assaying human serum allantoin levels.

Clinical Significance of Allantoin Measurement

Serum allantoin levels are reported to increase in several diseases. Here, we describe the diseases that result in increased levels of serum allantoin that is formed as a consequence of the removal of ROS by uric acid. The serum allantoin levels in healthy subjects and in patients with oxidative stress–related diseases are summarized in Table I.

Down syndrome is a chromosomal disorder with three chromosomes 21 (trisomy 21), rather than the usual pair of chromosomes. The superoxide dismutase 1 (SOD1) gene residing on chromosome 21 results in excess expression of this enzyme. Thus, SOD1 activity is reportedly increased by approximately 50% in Down syndrome patients, leading to an increase in the ratio of SOD1 to the sum of catalase and glutathione peroxidase, which catalyze the conversion of hydrogen peroxide to water [20-22]. The imbalance in this ratio causes increased ROS that are removed by uric acid, resulting in increased serum allantoin levels [23].

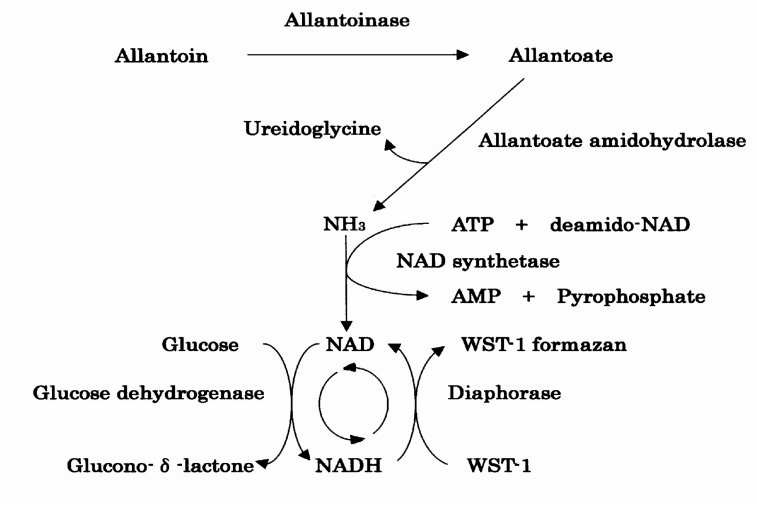

Figure 1. Reaction scheme for the enzymatic method of allantoin determination.

Behçet's disease is a chronic inflammatory disease that causes recurring aphthous stomatitis and inflammation in various organs, including the skin, vulva, and joints. Although the causes of Behçet's disease are unknown, it may an autoimmune-related disorder similar to chronic rheumatoid arthritis. Both of these inflammatory disorders can increase the number and activity of neutrophils, which when activated generate large amounts of ROS during the inflammatory response. This leads to increased serum allantoin levels in Behçet's disease [24] and chronic rheumatoid arthritis [25] as a result of the antioxidative activity of uric acid.

Plasma allantoin levels were previously reported to be significantly higher in newborns with chronic lung disease than in those without [26]. Newborn patients had severe respiratory distress syndrome and could not maintain opened pulmonary alveoli, due to the lack or insufficient production of surfactant. These patients were administered surfactant while oxygen was supplied at a continuous positive airway pressure, which led to increased ROS formation.

It has also been demonstrated that serum allantoin levels are increased in Wilson disease [27], an autosomal recessive disorder characterized by disturbed cooper metabolism. Genetic abnormalities of the copper transporter distributed mainly in the liver leads to defective incorporation of copper into apo-ceruloplasmin and the biliary excretion failure of copper. Patients with this inherited disorder have increased plasma levels of free cooper that is not bound to ceruloplasmin. The non-celuloplasmin cooper possibly causes injury by producing ROS in various tissues.

The treatment of coronary occlusion, including acute myocardial infarction, is performed by thrombolytic therapy and percutaneous coronary intervention, and results in restored blood flow into ischemic tissue. This reperfusion leads to cell membrane damage and the impairment of cellular function by ROS generated in cardiomyocytes and neutrophils. Serum allantoin levels are reportedly more increased in patients that have undergone percutaneous transluminal coronary angioplasty or thrombolytic therapies than in patients without these therapies [28].

Finally, hemodialysis is considered to cause defects in antioxidation; a decreased plasma antioxidative capacity leads to an overproduction of ROS, and serum allantoin levels are reported to increase in hemodialytic patients [16, 18, 29].

Table I. Allantoin concentration in serum from healthy subjects and from patients with oxidative stress–associated conditions.

Disorder [reference]	Subpopulation (no. of subjects)	Allantoin concentration (μM)
Down syndrome [23]	patients (16)	18.58 ± 2.27
	healthy subjects (16)	14.07 ± 1.07
Behçet's disease [24]	patients (23)	21.5 ± 11.0
	healthy subjects (21)	15.9 ± 6.9
Chronic rheumatoid arthritis [25]	patients (4)	36.1 ± 6.3
	healthy subjects (7)	18.6 ± 3.8
Neonatal chronic lung disease [26]	patients (10)	25.9 ± 9.8
	healthy subjects (9)	11.0 ± 5.7
Wilson disease [27]	patients before therapy (7)	11.0 ± 1.8
	patients after therapy (7)	4.3 ± 0.5
	healthy subjects (19)	6.5 ± 0.8
Thrombolytic therapy and percutaneous transluminal coronary angioplasty [28]	patients treated with angioplasty (8)	27.4 ± 15.2
	patients treated with thrombolysis (12)	24.6 ± 8.6
	patients without therapy (15)	15.8 ± 6.2
	healthy subjects (31)	12.6 ± 6.3
Patients undergoing hemodialysis [16]	patients (30)	27.1 ± 13.8
	healthy subjects (30)	4.76 ± 2.99

Conclusion

Oxidative stress is closely related to the above-mentioned and other diseases. It is defined as the difference between the extents of oxidative damage by ROS and the removal of ROS by various antioxidative constituents. When oxidative stress becomes excessive, proteins, lipids and DNA are oxidized. However, the measurement of generated ROS is difficult because of its very short half-life. Thus, the oxidation products of ROS scavengers in the blood or urine are frequently used as oxidative stress markers. Plasma uric acid is a mainly water-soluble antioxidant that scavenges singlet oxygen and hydroxyl radicals. We expect that the measurement of serum allantoin formed from uric acid will be performed extensively in future to determine the degree of ROS generation in various diseases.

References

[1] Ames, B.N; Cathcart, R; Schwiers, E; Hochstein, P. (1981) Uric acid provides an antioxidant defense in humans against oxidant- and radical-caused aging and cancer: a hypothesis. *Proc Natl Acad Sci U S A, 78*, 6858-6862.

[2] Kaur, H; Halliwell, B. (1990) Action of biologically-relevant oxidizing species upon uric acid. Identification of uric acid oxidation products. *Chem Biol Interact, 73*, 235-247.

[3] Becker, BF; Reinholz, N; Leipert, B; Raschke, P; Permanetter, B; Gerlach, E. (1991) Role of uric acid as an endogenous radical scavenger and antioxidant. *Chest, 100*, 176S-181S.

[4] Becker, BF. (1993) Towards the physiological function of uric acid. *Free Radic Biol Med, 14*, 615-631.

[5] Yeldandi, AV; Wang, XD; Alvares, K; Kumar, S; Rao, MS; Reddy, JK. (1990) Human urate oxidase gene: cloning and partial sequence analysis reveal a stop codon within the fifth exon. *Biochem Biophys Res Commun, 171*, 641-646.

[6] Challem, JJ; Taylor, EW. (1998) Retroviruses, ascorbate, and mutations, in the evolution of Homo sapiens. *Free Radic Biol Med, 25*, 130-132.

[7] [7] Young, EG; Conway, CF. (1942) On the estimation of allantoin by the rimini-schryver reaction. *J Biol Chem 42*, 839-853.

[8] Sumi, T; Umeda, Y; Kishi, Y; Kamimoto, F; Takahashi, K. A spectrofluorometric method for determining plasma allantoin based on the glyoxylate reductase reaction. (1976*) Anal Biochem, 75*, 563-567.

[9] Muratsubaki, H; Satake, K; Enomoto, K. (2006) Enzymatic assay of allantoin in serum using allantoinase and allantoate amidohydrolase. *Anal Biochem, 359*, 161-166.

[10] Kock, R; Delvoux, B; Greiling, H. A high-performance liquid chromatographic method for the determination of hypoxanthine, xanthine, uric acid and allantoin in serum. (1983) *Eur J Clin Chem Clin Biochem, 31*, 303-310.

[11] Grootveld, M; Halliwell, B. (1987) Measurement of allantoin and uric acid in human body fluids. A potential index of free-radical reactions in vivo? *Biochem J, 243*, 803-808.

[12] Balcells, J; Guada, JA; Peiró, JM; Parker, DS. (1992) Simultaneous determination of allantoin and oxypurines in biological fluids by high-performance liquid chromatography. *J Chromatogr, 575*, 153-157.

[13] Chen, XB; Kyle, DJ; Orskov, ER. (1993) Measurement of allantoin in urine and plasma by high-performance liquid chromatography with pre-column derivatization. *J Chromatogr, 6*17, 241-247.

[14] Lagendijk, J; Ubbink, JB; Vermaak, WJ. (1995) The determination of allantoin, a possible indicator of oxidant status, in human plasma. *J Chromatogr Sci, 33*, 186-93.

[15] Czauderna, M; Kowalczyk, J. (1997) Simultaneous measurement of allantoin, uric acid, xanthine and hypoxanthine in blood by high-performance liquid chromatography. *J Chromatogr B Biomed Sci Appl, 704*, 89-98.

[16] Kand'ár, R; Žáková, P; Mužáková, V. (2006) Monitoring of antioxidant properties of uric acid in humans for a consideration measuring of levels of allantoin in plasma by liquid chromatography. *Clin Chim Acta, 365*, 249-256.

[17] Pavitt, DV; de Fonseka, S; Al-Khalaf, N; Cam, JM; Reaveley, DA. (2002) Assay of serum allantoin in humans by gas chromatography-mass spectrometry. *Clin Chim Acta, 318*, 63-70.

[18] Caussé, E; Pradelles, A; Dirat, B; Negre-Salvayre, A; Salvayre, R. Couderc F. (2007) Simultaneous determination of allantoin, hypoxanthine, xanthine, and uric acid in serum/plasma by CE. *Electrophoresis, 28*, 381-387.

[19] Muratsubaki, H; Enomoto, K; Soejima, A; Satake, K. (2008) An enzyme cycling method for measurement of allantoin in human serum. *Anal Biochem, 378*, 65-70.

[20] Brooksbank, BW; Balázs, R. (1983) Superoxide dismutase and lipoperoxidation in Down's syndrome fetal brain. *Lancet, 1*, 881-882.

[21] De La Torre, R; Casado, A; López-Fernández, E; Carrascosa, D; Ramírez, V; Sáez, J. (1996) Overexpression of copper-zinc superoxide dismutase in trisomy 21. *Experientia, 52*, 871-873.

[22] Muchová, J; Sustrová, M; Garaiová, I; Liptáková, A; Blazícek, P; Kvasnicka, P; Pueschel, S; Duracková, Z. (2001) Influence of age on activities of antioxidant enzymes and lipid peroxidation products in erythrocytes and neutrophils of Down syndrome patients. *Free Radic Biol Med, 31*, 499-508.

[23] Zitnanova, I; Korytar, P; Aruoma, OI; Sustrova, M; Garaiova, I; Muchova, J; Kalnovicova, T; Pueschel, S; Durackova, Z. (2004) Uric acid and allantoin levels in Down syndrome: antioxidant and oxidative stress mechanisms? *Clin Chim Acta, 341*, 139-146.

[24] Yardim-Akaydin, S; Sepici, A; Ozkan, Y; Simşek, B; Sepici, V. (2006) Evaluation of allantoin levels as a new marker of oxidative stress in Behcet's disease. *Scand J Rheumatol, 35*, 61-64.

[25] Yardim-Akaydin, S; Sepici, A; Ozkan, Y; Torun, M; Simşek, B; Sepici, V. (2004) Oxidation of uric acid in rheumatoid arthritis: is allantoin a marker of oxidative stress? *Free Radic Res, 38*, 623-628.

[26] Ogihara, T; Okamoto, R; Kim, HS; Nagai, A; Morinobu, T; Moji, H; Kamegai, H; Hirano, K; Ogihara, H; Tamai, H; Mino, M. (1996) New evidence for the involvement of oxygen radicals in triggering neonatal chronic lung disease. *Pediatr Res, 39*, 117-119.

[27] Ogihara, H; Ogihara, T; Miki, M; Yasuda, H; Mino, M. (1995) Plasma copper and antioxidant status in Wilson's disease. *Pediatr Res, 37*, 219-226.

[28] Yardim-Akaydin, S; Kesimer, M; Imren, E; Sepici, A; Simşek, B; Torun, M. (2005) Urate oxidation during percutaneous transluminal coronary angioplasty and thrombolysis in patients with coronary artery disease. *Clin Chim Acta, 362*, 131-137.

[29] Sasaki, K; Motomiya, Y; Oyama, N; Hirao, Y; Okajima, E; Uji, Y; Okabe, H. (1996) Plasma allantoin in patients undergoing maintenance hemodialysis. *Nippon Jinzo Gakkai Shi, 38*, 164-170.

In: Clinical Chemistry Research
Editors: Brian H. Mitchem and Charles L. Sharnham
ISBN 978-1-60692-517-1

Short Communication D

Relationship between Serum Creatine Kinase Activity and Serum Aminotransferase Activity in Patients with Extensive Rhabdomyolysis or Myocardial Necrosis

Nadia Habal and Mark Feldman*
Department of Internal Medicine,
Texas Health Presbyterian Hospital Dallas, Dallas, TX. USA

Abstract

Background: Patients with markedly elevated serum creatine kinase (CK) activity due to muscle damage often also have increased serum aminotransferase activity (AST, ALT). However, the expected ratio of serum CK to aminotransferase activity in patients with severe muscle damage is uncertain.
Methods: We evaluated consecutive patients seen during a 6-month period who had markedly increased serum CK activity (≥ 1,000 U/L). Only patients with simultaneous measurements of CK, ALT and AST activity were included. One hundred eight patients ages of 17 to 93 years met these inclusion criteria. Their records were reviewed to ascertain the cause of the elevated CK activity.
Results: Eighty five of the study patients had rhabdomyolysis from a variety of causes to explain their marked CK elevation, while 23 had myocardial necrosis, usually from acute myocardial infarction. The median ratio of serum CK to AST activity in these 108 high-

* Mark Feldman, M.D.Chair, Department of Internal Medicine, Texas Health Presbyterian Hospital Dallas, 8200 Walnut Hill Lane, Dallas, TX 75231 214 345 7881 (phone); 214 345 5167 (fax) MarkFeldman@TexasHealth.org.

CK patients was 25:1 (interquartile range, 13 to 37:1). The median ratio of serum CK to ALT activity was 41:1 (interquartile range, 24 to 80:1). Patients with high CK activity due to rhabdomyolysis or myocardial necrosis had similar CK/AST and CK/ALT ratios.
Conclusions: In patients with a serum CK activity above 1,000 U/L, the serum CK activity should be expected to be approximately 25 times the AST activity and to be 40 times the ALT activity. These ratios can serve as guidelines when assessing high-CK patients who also have elevated serum aminotransferase activity.

Keywords: Aminotransferase, ALT, AST, skeletal muscle, rhabdomyolysis, myocardial infarction, heart, liver

Introduction

Patients with markedly increased serum creatine kinase (CK) activity are not uncommon in clinical practice. CK is highly expressed in skeletal and cardiac muscle (1). Aminotransferase enzymes (AST, ALT) are also expressed in skeletal and cardiac muscle (2-4) and some of patients with high serum CK activity also have elevated serum aminotransferase activity. Unlike CK, which is not expressed appreciably in the liver (1), AST and ALT are also expressed in the liver. Thus, it is often not clear when an elevated serum AST or ALT activity in a patient with high serum CK activity can be explained by the high CK activity per se and when another cause for the elevated aminotransferase activity, such as liver disease, needs consideration. To more fully understand relationships between serum CK and aminotransferase activities, we analyzed more than one hundred consecutive patients from our hospital who were found to have a markedly elevated serum CK activity, reflecting major skeletal or cardiac muscle injury.

Methods

Patients and Serum Samples

Between January and June 2006, our hospital's chemistry laboratory received 14,566 samples in which a measurement of serum CK activity was requested. The laboratory detected a marked elevation in serum CK activity ($\geq$ 1,000 U/L, which was more than five times the upper limit of the gender-specific reference ranges of 135 U/L for women and 170 U/L for men) in 524 (4%) of these serum samples obtained from 243 different patients. These 243 patients were eligible for the study if a simultaneous serum sample had been collected for measurement of AST and ALT. One hundred nine of them met these criteria. If a patient had more than one set of samples that met our eligibility criteria, only the initial pair of CK and AST/ALT measurements was used.

Medical records were located in 108 of the 109 patients and reviewed to establish the cause of the elevated serum CK activity. The patient whose chart could not be located was

excluded. Patients whose elevated serum CK activity was found on chart review to be due to rhabdomyolysis were further classified according to the system of Miller (5).

The median age of the study population was 58 years (range, 17-93). Males outnumbered females 2 to 1 (72 vs. 36). One sample from a woman with a serum CK activity exceeding the assay detection limit (80,000 U/L) was arbitrarily assigned a value of 80,001 U/L. One sample from a man with serum AST and ALT activity exceeding the assay detection limits (8,000 and 9,000 U/L, respectively) was arbitrarily assigned values of 8,001 and 9,001 U/L, respectively.

Statistical Analyses

Results are presented as the median and interquartile range. Differences between groups were tested for significance by the Mann Whitney U test (6). Differences between proportions were tested for significance by Fisher's exact test (7). Two-tailed probability (p) values < 0.05 were considered to be statistically significant.

Results

Diagnoses (Table 1)

Eighty five of the study patients (79%) had rhabdomyolysis as the explanation for their markedly elevated serum CK activity (Table 1). Fifty three of them were male and 32 were female. The remaining 23 patients (21%) had myocardial necrosis, in all but one case due to acute myocardial infarction (Table 1). Nineteen of them were male and 4 were female. Proportions of males and females with rhabdomyolysis or myocardial necrosis were not significantly different.

Serum Enzyme Activities

Median serum CK, AST, and ALT activities for the 108 study patients are shown in Table 2. Patients with rhabdomyolysis had lower median CK concentrations than patients with myocardial necrosis (Figure 1), but this difference did not reach statistical significance. Serum AST and ALT activities were also lower in the rhabdomyolysis patients than in the myocardial lysis patients, with the difference in serum ALT being statistically significant ($p=0.027$; Figure 1). Serum AST activity was increased above the reference range in 75% of the patients with rhabdomyolysis and in 96% of the patients with myocardial lysis ($p=0.04$). Serum ALT activity was increased above the reference range in 35% of the patients with rhabdomyolysis and in 44% of the patients with myocardial damage ($P>0.05$). Among the patients with rhabdomyolysis, serum ALT activity was increased in 25% of the men and in 53% of the women ($p=0.01$).

Table 1. Causes of elevated serum creatine kinase activity in the study cohort.

Rhabdomyolysis	**85**
Traumatic or compression	10
trauma or crush injury	4
surgical trauma	3
prolonged coma	3
Nontraumatic	75
non-exertional	68
Alcohol, drugs, toxins	36
Infection/sepsis	15
Water/electrolyte disorder	6
Inflammatory myopathy	6
Miscellaneous	5
exertional	7
Seizure	5
Hyperkinetic state	2[a]
Myocardial necrosis	**23**
Myocardial infarction [b]	22
Myopericarditis	1
TOTAL	**108**

Rhabdomyolysis cases are classified using Miller's system (5).
[a] due to alcohol withdrawal in 1 and extreme exertion/exercise in 1
[b] ST segment elevation acute myocardial infarction or acute coronary syndrome

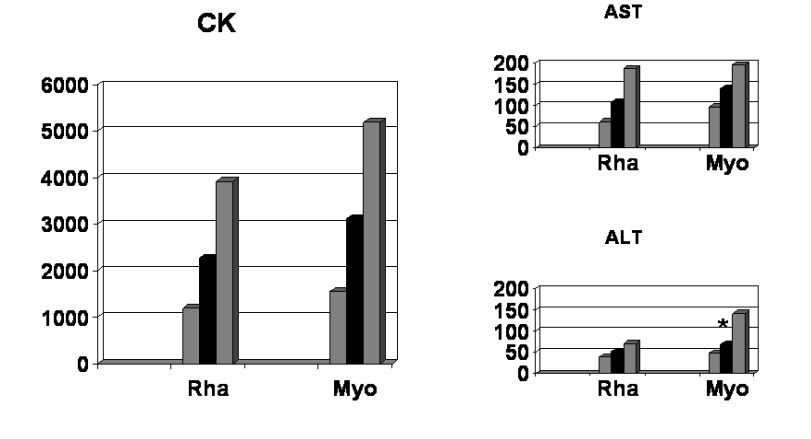

Figure 1. Median serum CK, AST, and ALT activity (U/L) in patients with rhabdomyolysis (Rha, n=85) and patients with myocardial necrosis (Myo, n=23). Median values are shown as black bars and interquartile ranges as gray bars. The difference in serum ALT between patients with rhabdomyolysis and myocardial necrosis was significant (*, p=0.027).

Serum Enzyme Activity Ratios

Median CK/AST, CK/ALT, and AST/ALT activity ratios for the entire study cohort are shown in Table 2. Median serum CK/AST and CK/ALT ratios in the patients with rhabdomyolysis were similar to the patients with myocardial necrosis (Figure 2). Likewise, median AST/ALT ratios were 1.91 in both patient groups.

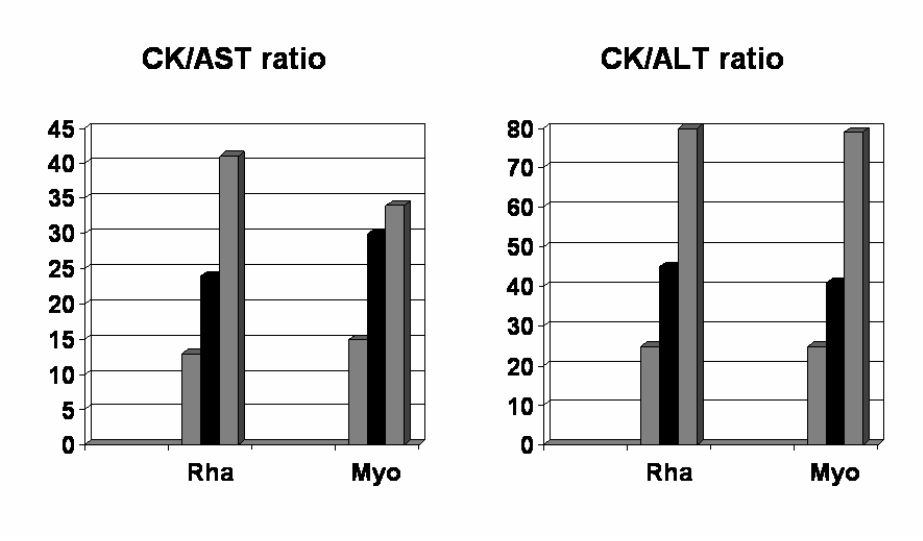

Figure 2. Median CK/AST and CK/ALT activity ratios in patients with rhabdomyolysis (Rha, n=85) and patients with myocardial necrosis (Myo, n=23). Median values are shown as black bars and interquartile ranges as gray bars. Neither of the differences between patients with rhabdomyolysis and myocardial necrosis was statistically significant.

Table 2. Median serum CK, ALT and AST activity (U/L) and ratios of CK/AST, CK/ALT, and AST/ALT in the study cohort.

CK	2,411 (1,206-4,354)
AST	110 (64-190)
ALT	54 (40-78)
CK/AST	25 (13- 37)
CK/ALT	41 (24-80)
AST/ALT	1.91 (1.32-2.92)

Values in parentheses represent interquartile ranges.
ALT, alanine aminotransferase; AST, aspartate aminotransferase; CK, creatine kinase.

Discussion

Enzymatic transamination using alanine aminotransferase (ALT) and aspartate aminotransferase (AST) was first described in skeletal muscle (2), and later in the heart, liver and other organs (3,4). Transamination reactions play a key role in intermediary metabolism by transferring an amino group from α- amino acids such as alanine or aspartic acid to α-ketoacids such as α-ketoglutaric acid.

This study documents a high prevalence of elevated serum AST and ALT activity in patients who have skeletal or cardiac muscle damage associated with high serum CK activity (≥ 1,000 U/L). Thus, measurement of serum CK activity should be considered when an otherwise unexplained elevation in serum AST or AST activity is detected on a comprehensive metabolic profile or a liver panel, as CK is not measured as a part of these panels.

The median serum CK activity in the 108 patients with high serum CK activity was 25-fold higher than the simultaneously-measured AST activity and was 40-fold higher than ALT activity. However, there was variation in CK/ALT ratio and CK/AST ratios among individual patients. Thus, a simple "correction" of the ALT or AST activity based on the level of CK activity is not feasible. However, in patients with high serum CK activity, the level of ALT or AST activity relative to the CK activity can be used as a guide in evaluating whether elevated serum AST or ALT activity can be attributed to the muscle damage. In addition to the serum CK/AST and CK/ALT activity ratios, the patient's medical and social history, medication list, physical findings and other laboratory parameters are likely to be useful in guiding the clinician to the need for additional testing for co-existent non-muscle disease.

In patients with an elevated serum ALT and/or AST activity that can be attributed to hepatic disease, a ratio of serum AST/ALT activity exceeding 2 often leads to consideration of more advanced hepatic disease caused by alcohol, non-alcoholic fatty liver, or chronic viral hepatitis (8-12). Our study demonstrated that serum AST/ALT ratios of 2 or greater also occur in nearly half of patients with rhabdomyolysis or myocardial lysis. Therefore, a serum ratio of AST to ALT activity above 2 is not specific for liver disease. Furthermore, an AST/ALT ratio above 2 is not a very sensitive method for detecting muscle lysis, as seen in this study as well as in a previous study of muscular dystrophy patients, in whom serum ALT often equaled or even exceeded AST activity (13).

Elevated serum ALT activity was twice as prevalent in women as men with high serum CK activity for unclear reasons. This gender disparity may have been, in part, due a lower serum ALT reference range in healthy women (14). Because we did not evaluate men and women with serum CK activity less than or equal to 1,000 U/L, the prevalence of elevated serum ALT and AST activity that we report here cannot be extrapolated to a population with more modest elevations in serum CK activity, in whom elevated serum aminotransferase activity would be expected to be less prevalent.

Acknowledgements

The corresponding author had full access to all of the data in the study and takes responsibility for the integrity of the data and the accuracy of the data analysis. The authors thank Guy Neel for his valuable assistance.

References

[1] Tsung SH. Creatine kinase isoenzyme patterns in human tissue obtained at surgery. Clin Chem 1976; 22: 173-175.

[2] Braunshtein, A. E., Kritsman, M.G. Formation and breakdown of amino acids by intermolecular transfer of amino groups. Nature 1937; 140: 503-504.

[3] Wroblewski F, Ladue JS. Serum glutamic pyruvic transaminase in cardiac and hepatic disease. Proc Soc Exp Biol Med 1956; 91: 569-571.

[4] Wroblewski F. The clinical significance of transaminase activities of serum. Amer J Med 1959 ; 27 : 911-923.

[5] Miller ML. Rhabdomyolysis. UpToDate Online 2007. http://www.uptodateonline.com

[6] http://elegans.swmed.edu/~leon/stats/utest.html

[7] http://www.graphpad.com/quickcalcs

[8] Nyblom H, Berggren U, Balldin J, Olsson R. High AST/ALT ratio may indicate advanced alcoholic liver disease rather than heavy drinking. Alcohol & Alcoholism. 2004; 39:336-339.

[9] Sorbi D, Boynton J, Lindor KD. The ratio of aspartate aminotransferase to alanine aminotransferase: potential value in differentiating nonalcoholic steatohepatitis from alcoholic liver disease. Amer. J. Gastroenterol. 1999; 94:1018-1022.

[10] Williams ALB, Hoofnagle JH. Ratio of serum aspartate to alanine aminotransferase in chronic hepatitis. Gastroenterology 1988; 95:734-9.

[11] Park SY, Kang KH, Park JH, et al. Clinical efficacy of AST/ALT ratio and platelet counts as predictors of degree of fibrosis in HBV infected patients without clinically evident liver cirrhosis. Korean J. Gastroenterol. 2004; 43:246-251.

[12] Angulo P, Hui JM, Marchesini G, et al. The NAFLD fibrosis Score: A noninvasive system that identifies liver fibrosis in patients with NAFLD. Hepatology 2007; 45: 846-854.

[13] Kohli R, Harris DC, Whitington, PF. Relative elevations of serum alanine and aspartate aminotransferase in muscular dystrophy. J Ped Gastroenterol Nutrit 2005; 41:121-124.

[14] Prati D, Taioli E, Zanella A, et al: Updated definitions of healthy ranges for serum alanine aminotransferase levels. Ann Int Med 2002; 137: 1-9.

[15] Reviewed by James P. Knochel, MD and Beverly Dickson, MD.

Index

A

B

C

D

E

F

G

H

I

J

K

L

M

N

O

P

Q

R

S

T

U

V

W

X

Y

Z